Concesionaria Vial Unión del Sur

Consorcio SH

Doble Calzada

Rumichaca - Pasto

Departamento de Nariño

MODELO DE CALIDAD DEL AGUA

HSE

ASESORÍA E INGENIERÍA AMBIENTAL S. A. S.

Ing. Jair Ordoñez Moncada

Ing. Martín Palacios Quevedo

JUNIO 2017

MODELO DE CALIDAD DEL AGUA

Vertimientos a Cuerpo Superficial de Agua

Proyecto Vial: Doble Calzada Rumichaca - Pasto

Tramo San Juan - Pedregal

CONCESIONARIA VIAL UNIÓN DEL SUR

Consorcio SH

Informe Técnico MP-06.038_2017

Preparación Técnica:

Martín Daniel Palacios Quevedo Ph.D. M.Sc.

Bogotá, D.C. Junio de 2017

LISTA DE DISTRIBUCIÓN

ENTIDAD	No. COPIAS
CLIENTE: GEOCOL CONSULTORES S.A.	1
CONSULTOR: QHSE Asesorías y Servicios Ambientales SAS	1
ASESOR AMBIENTAL: Martín Daniel Palacios Quevedo	1

DESCRIPCIÓN DE LAS REVISIONES

REVISIÓN	FECHA	DESCRIPCIÓN DE LA MODIFICACIÓN	OBSERVACIONES
V0	15/05/2017	Versión inicial	Creación del documento

APROBACIÓN CLIENTE			
NOMBRE	Martín Daniel Palacios Quevedo	Andrés Castro Rodriguez	Néstor Raúl Vásquez Pérez
CARGO	Ingeniero Consultor	Representante Legal QHSE	Director Proyectos GEOCOL
FECHA	Mayo 2017	Junio 2017	Junio 2017
FIRMA			
	PREPARÓ	**REVISÓ**	**APROBÓ**

APROBACIÓN CONSULTORÍA		
Elabora:	**Revisa:**	**Aprueba:**
RODRIGO MONTENEGRO CÁRDENAS	NANCY FORERO ÁVILA	MARTIN DANIEL PALACIOS QUEVEDO
Fecha: Mayo 15 de 2017	Fecha: Junio 10 de 2017	Fecha: Junio 30 de 2017
Abona:		
JAIR ORDOÑEZ MONCADA		
Fecha: Junio 30 de 2017		

TABLA DE CONTENIDO

1. Generalidades 6
1.1. Introducción 6
1.2. Objetivos 7
1.2.1. Objetivo General 7
1.2.2. Objetivos Específicos 7
1.3. Alcance 8
1.4. Marco Normativo 8
2. Revisión de Información Secundaria 13
2.1. Localización de los Puntos de Vertimientos 13
2.2. Sistema de Tratamiento de Aguas Residuales 13
2.3. Características del Aguas Residuales 14
2.4. Caracterización Hidráulica de los Tramos 15
3. Modelo Matemático Unidimensional Streeter - Phelps 23
3.1. Características Generales 23
3.2. Metodología 25
4. Capacidad de Asimilación de la Fuente Receptora 27
4.1. Modelos de Calidad del Agua 27
4.1.1. Modelo de Flujo a Pistón 27
4.1.2. Modelo de Streeter-Phelps 27
4.1.3. Modelo WASP (Water Quality Analysis Simulation Program) 28
4.1.4. Modelo QUALK2E (Q2E) 28
4.1.5. QUALK2K (Q2K) 28
4.1.6. EPD-RIV1 28
4.1.7. ADZ-QUASAR 29
4.1.8. Otros Modelos 29
4.2. Criterios de Selección del Modelo a UTILIZAR 29
4.3. Descripción de los Modelos Utilizados 30
4.3.1. ADZ QUASAR 30
4.3.1.1. Definición de Variables 30
4.3.1.2. Proceso de Modelación 31
4.3.2. Streeter-Phelps 35

4.3.2.1. Definición de Variables 35
4.3.2.2. Proceso de Modelación 36
4.4. Resultados 38
5. Conclusiones 42
6. Referencias Bibliográficas 43

LISTA DE TABLAS

Tabla 1. Norma Vertimientos a un Cuerpo de Agua Superficial 8
Tabla 2. Criterios de Calidad para la Destinación del Recurso 10
Tabla 3. Valores Límites Máximos Permisibles para Vertimientos Puntuales (Res. 631/2015) 12
Tabla 4. Ubicación General de los Puntos de Monitoreo 13
Tabla 5. Composición Típica del AR en un Proyecto Similar 14
Tabla 6. Procesos de Degradación y Transformación, según ANLA para determinantes del Grupo 1 32
Tabla 7. Tasas de Nitrificación, según ANLA 2013 33
Tabla 8. Velocidades de Sedimentación 34
Tabla 9. Factores de Asimilación considerados en la Metodología ANLA 35
Tabla 10. Relación entre la Tasa de Re-aireación y la de Desoxigenación 36
Tabla 11. Características Hidráulicas, Fisicoquímicas y Bacteriológicas de la Fuente Receptora 38
Tabla 12. Longitud de Asimilación del Vertimiento 39

LISTA DE FIGURAS

Figura 1. Localización Puntos de Vertimientos 14
Figura 2. Sección Transversal Tramo río Boquerón Aguas Arriba 15
Figura 3. Sección Transversal Tramo río Boquerón Aguas Abajo 16
Figura 4. Sección Transversal Tramo quebrada La Humeadora Aguas Arriba 17
Figura 5. Sección Transversal Tramo quebrada La Humeadora Aguas Abajo 18
Figura 6. Sección Transversal Tramo río Guaitara Aguas Arriba 19
Figura 7. Sección Transversal Tramo río Guaitara Aguas Abajo 20
Figura 8. Sección Transversal Tramo río Sapuyes Aguas Arriba 21
Figura 9. Sección Transversal Tramo río Sapuyes Aguas Abajo 22
Figura 10. Curva DOSAG o del valle de oxígeno disuelto 24
Figura 11. Diagrama de Flujo de la Metodología Típica de Modelamiento 25

LISTA DE ECUACIONES

Ecuación 1 24
Ecuación 2 24

Ecuación 3.....25
Ecuación 4.....31
Ecuación 5.....31
Ecuación 6.....32
Ecuación 7.....32
Ecuación 8.....34
Ecuación 9.....34
Ecuación 10.....35
Ecuación 11.....36
Ecuación 12.....37
Ecuación 13.....37
Ecuación 14.....37

1. Generalidades

El agua hoy y siempre ha sido considerada como uno de los elementos esenciales para el desarrollo de la vida tal como la conocemos. Por otra parte, el alto crecimiento de la población en el planeta lleva consigo un incremento proporcional en la demanda de este elemento; razón por la cual día tras día el hombre centra su preocupación en la procura de garantizar el suministro del preciado líquido a las diferentes comunidades. A la hora de garantizar el suministro de este recurso, además de requerirse en unas cantidades apropiadas, se deben considerar unas condiciones mínimas de calidad, dependiendo del uso que se le pueda dar al recurso (García, 2008).

El desarrollo de actividades dentro del proyecto Doble Calzada Rumichaca - Pasto Tramo San Juan - Pedregal, trae consigo la generación de vertimientos domésticos e industriales, los cuales se someten a un tratamiento con el objetivo de cumplir la normatividad vigente y finalmente se descargan en un cuerpo de agua cercano.

A pesar de que el agua residual generada es sometida a tratamiento, el vertimiento introduce una carga contaminante que podría afectar la calidad del agua del cuerpo receptor. En este sentido, como parte de los requerimientos exigidos para solicitar un permiso de vertimiento, es necesario realizar una modelación donde se permita conocer la capacidad de asimilación de la carga doméstica y/o industrial vertida en el cuerpo de agua.

En correlación a lo anterior y en vista de este requerimiento, en el año 2013 la Autoridad Nacional de Licencias Ambientales (ANLA) en el marco de un convenio con la Universidad Nacional de Colombia, desarrolló una metodología para el cálculo de la longitud de influencia representativa de los vertimientos. Dentro de esta metodología se destaca el planteamiento de los determinantes de calidad de agua a evaluar, para todos los sectores, incluyendo el sector de la construcción.

Con el objetivo de conocer el comportamiento de los parámetros de calidad de agua, para vertimientos generados en la construcción de vías y con miras a la obtención de permisos de vertimiento para el proyecto de la Concesionaria Vial Unión del Sur – Consorcio SH, en el presente documento se presentan los resultados de la aplicación de la metodología planteada por la ANLA. Adicionalmente, para el oxígeno disuelto se empleó el modelo Streeter y Phelps, debido a que este parámetro tiene un comportamiento diferente al de los demás parámetros planteados, dentro de los cuales se maneja el concepto de factor de asimilación.

En este documento se presentan los resultados del cálculo de la longitud de influencia de los vertimientos domésticos e industriales del proyecto, en la etapa de construcción, en el escenario más crítico que corresponde a caudal ambiental de la fuente receptora y concentraciones máximas permisibles exigidas por la normatividad vigente.

1.1. Introducción

En los diferentes países, se cuenta con entidades encargadas de regular y emitir políticas orientadas hacia la regulación de la calidad del recurso; para ello se debe estudiar con antelación las diferentes variables que hacen parte de la calidad del agua, lo que implica la realización de campañas de muestreo, que permitan conocer la concentración de los diferentes contaminantes o compuestos analizados en una corriente dada. La realización de campañas de calidad no siempre se constituye en la medida más apropiada puesto que las condiciones altamente cambiantes de la composición del agua hacen poco operativa esta alternativa. Es esta una razón por la cual se recurre a modelos

matemáticos, los cuales permiten evaluar de forma adecuada el comportamiento de la calidad del agua en una corriente natural. Adicionalmente los modelos permiten la creación de escenarios a futuro, fundamentales para la planeación y gestión apropiada de los recursos naturales.

Los modelos matemáticos habitualmente empleados para la modelación, son frecuentemente de tipo no lineal, debido a la naturaleza misma de los procesos que se pretenden emular. Las expresiones matemáticas, usualmente empleadas en la modelación de sistemas naturales son las ecuaciones diferenciales parciales, que resultan de aplicar el principio de conservación de masa, empleado en la modelación de la calidad del agua; esto implica que para la modelación matemática apropiada de la calidad del agua, se deben plantear sistemas de ecuaciones diferenciales no lineales acopladas (García, 2008).

En la aplicación de los modelos tradicionales, por tratabilidad matemática y eficiencia en los recursos computacionales, usualmente se recurre a técnicas de linealización de los sistemas de ecuaciones u omitir las no linealidades que surgen de las relaciones entre los diferentes componentes de la calidad del agua.

Hoy por hoy, a pesar de los recursos computacionales de que se dispone, modelos tradicionales y de amplia difusión en nuestro medio como el QUAL2K, AQUASIM y/o STREETER-PHELPS, entre otros; no obstante, a las innovaciones realizadas a los modelos originales, conservan como motor de búsqueda el algoritmo desarrollado en la versión original, preservando las simplificaciones hechas al modelo.

En la actualidad existen un sin número de herramientas computacionales, empleadas para modelar la calidad del agua en corrientes naturales. Producto de la complejidad que involucra la modelación de la calidad del agua, la mayoría de estas herramientas presentan limitaciones y restricciones para su implementación en la modelación (García, 2008).

Esta razón, ha impulsado el desarrollo de esta primera aproximación orientada hacia la valoración y empleo del modelo Streeter-Phepls a futuro como una herramienta adecuada para la modelación de la calidad del agua, de forma acoplada, mediante sistemas no lineales complejos.

1.2. Objetivos

1.2.1. Objetivo General

Estimar de manera objetiva y cuantitativa la capacidad que tiene los cuerpos de agua: quebrada La Humeadora, río Boquerón, río Sapuyes y río Guaitara de asimilar los vertimientos de aguas residuales tratadas mediante vertido; bajo unas condiciones climáticas, de estructura hídrica específica y bajo diferentes condiciones de caudal sobre los cuerpos de agua receptores y de carga del vertimiento en forma puntual.

1.2.2. Objetivos Específicos

- ✓ Seleccionar los indicadores de la calidad del agua a considerar en el proceso de modelación.
- ✓ Definir el modelo matemático a emplear en el proceso de modelación de los indicadores de calidad.
- ✓ Determinar la capacidad de autodepuración de la corriente modelada e indicar los impactos en el uso y calidad del agua que generan los vertimientos de agua residual en las fuentes receptoras.

1.3. Alcance

Se pretende estimar la longitud de influencia de las concentraciones de un contaminante determinado en el área de influencia del vertimiento aguas abajo del punto de vertido a autorizar sobre los cuerpos de agua siguientes: quebrada La Humeadora, río Boquerón, río Sapuyes y río Guaitara; por la Autoridad Ambiental (AA) competente, para el caso que nos ocupa la Corporación Autónoma Regional de Nariño – CORPONARIÑO.

Las actividades desarrolladas dentro de la elaboración del presente estudio son las siguientes:

Trabajo de campo,

- Prueba de trazadores y determinación de tiempos de viaje
- Campañas de aforo y muestreos de agua

Trabajo de oficina,

- Obtención y ajuste de registros hidrométricos
- Análisis Hidrológico de la fuente a modelar
- Procesamiento de la información físico-química y bacteriológica
- Selección del Modelo de Simulación a implementar
- Calibración del modelo
- Escenarios de saneamiento utilizando el modelo ya calibrado

1.4. Marco Normativo

En Colombia los usos del agua y residuos líquidos están reglamentados mediante el Decreto 1076 de 2016 y la Resolución 0631 de 2015, en donde se establecen las normas de vertimiento a un cuerpo de agua.

Tabla 1. Norma Vertimientos a un Cuerpo de Agua Superficial

PARÁMETRO	UNIDADES	ARD* con una carga menor a 625 kg/día BDO_5	ARnD**
Temperatura	°C	40	40
pH	Unidades de pH	6 a 9	6 a 9
Demanda Química de Oxígeno (DQO)	mg/L O_2	180	150
Demanda Bioquímica de Oxígeno (DBO_5)	mg/L O_2	90	50
Sólidos Suspendidos Totales (SST)	mg/L	90	50
Sólidos Sedimentables (SSED)	mL/L	5	1
Grasas y Aceites	mg/L	20	10
Compuestos Semivolátiles Fenólicos	mg/L	NE	Análisis y Reporte
Fenoles Totales	mg/L	NE	0.2
Formaldehído	mg/L	NE	Análisis y Reporte
Sustancias activas al azul de metileno (SAAM)	mg/L	Análisis y Reporte	Análisis y Reporte
Hidrocarburos Totales (HTP)	mg/L	Análisis y Reporte	10
Hidrocarburos Aromáticos Policíclicos (HAP)	mg/L	NE	Análisis y Reporte
BTEX (Benceno, Tolueno, Etilbenceno, Xileno)	mg/L	NE	Análisis y Reporte

PARÁMETRO	UNIDADES	ARD* con una carga menor a 625 kg/día BDO_5	ARnD**
Compuestos Orgánicos Halogenados Adsorbibles (AOX)	mg/L	NE	Análisis y Reporte
Ortofosfatos ($P\text{-}PO_4^{3-}$)	mg/L	Análisis y Reporte	Análisis y Reporte
Fósforo Total (P)	mg/L	Análisis y Reporte	Análisis y Reporte
Nitratos ($N\text{-}NO_3^-$)	mg/L	Análisis y Reporte	Análisis y Reporte
Nitritos ($N\text{-}NO_2^-$)	mg/L	Análisis y Reporte	Análisis y Reporte
Nitrógeno Amoniacal ($N\text{-}NH_3$)	mg/L	Análisis y Reporte	Análisis y Reporte
Nitrógeno Total (N)	mg/L	Análisis y Reporte	Análisis y Reporte
Cianuro Total (CN^-)	mg/L	NE	0.1
Cloruros (Cl^-)	mg/L	NE	250
Fluoruros (F^-)	mg/L	NE	5
Sulfatos (SO_4^{2-})	mg/L	NE	250
Sulfuros (S^{2-})	mg/L	NE	1
Aluminio (Al)	mg/L	NE	Análisis y Reporte
Antimonio (Sb)	mg/L	NE	0.3
Arsénico (As)	mg/L	NE	0.1
Bario (Ba)	mg/L	NE	1
Berilio (Be)	mg/L	NE	Análisis y Reporte
Boro (B)	mg/L	NE	Análisis y Reporte
Cadmio (Cd)	mg/L	NE	0.01
Cinc (Zn)	mg/L	NE	3
Cobalto (Co)	mg/L	NE	0.1
Cobre (Cu)	mg/L	NE	1
Cromo (Cr)	mg/L	NE	0.1
Estaño (Sn)	mg/L	NE	2
Hierro (Fe)	mg/L	NE	1
Litio (Li)	mg/L	NE	Análisis y Reporte
Manganeso (Mn)	mg/L	NE	Análisis y Reporte
Mercurio (Hg)	mg/L	NE	0.002
Molibdeno (Mo)	mg/L	NE	Análisis y Reporte
Níquel (Ni)	mg/L	NE	0.1
Plata (Ag)	mg/L	NE	0.2
Plomo (Pb)	mg/L	NE	0.1
Selenio (Se)	mg/L	NE	0.2
Titanio (T)	mg/L	NE	Análisis y Reporte
Vanadio (V)	mg/L	NE	1
Acidez Total	mg/L $CaCO_3$	NE	Análisis y Reporte
Alcalinidad Total	mg/L $CaCO_3$	NE	Análisis y Reporte
Dureza Cálcica	mg/L $CaCO_3$	NE	Análisis y Reporte
Dureza Total	mg/L $CaCO_3$	NE	Análisis y Reporte
Color Real (Medidas de Absorbancia a las siguientes longitudes de onda: 436 nm, 525 nm y 620 nm)	m^{-1}	NE	Análisis y Reporte

Fuente: * Artículo 8 y ** Artículo 15 de la Resolución 0631 de 2015. Ministerio de Ambiente y Desarrollo Sostenible

De igual forma, el Decreto 1076 de 2015 (artículos transitorios 2.2.3.3.9.2 a 2.2.3.3.9.10) establece los criterios de calidad admisibles para los diferentes usos del agua. Entre estos se encuentra el uso agrícola, pecuario, recreativo y de consumo humano, entre otros (Ver Tabla 2).

Tabla 2. Criterios de Calidad para la Destinación del Recurso

PARÁMETRO	UNIDADES	DECRETO 1076/2015 (artículos transitorios)					
		2.2.3.3.9.3	2.2.3.3.9.4	2.2.3.3.9.5	2.2.3.3.9.6	2.2.3.3.9.7	2.2.3.3.9.10
Acidez Total	mg/L CaCO3	NE	NE	NE	NE	NE	NE
Alcalinidad Total	mg/L CaCO3	NE	NE	NE	NE	NE	NE
Aluminio	mg/L	NE	NE	5.0	5	NE	NE
Antimonio	mg/L	NE	NE	NE	NE	NE	NE
Arsénico	mg/L	0,05	0,05	0,1	0,2	NE	0,1
Bario	mg/L	1	1	NE	NE	NE	0,1
Bicarbonatos	mg/L CaCO3	NE	NE	NE	NE	NE	NE
Cadmio	mg/L	0,01	0,01	0,01	0,05	NE	0,01
Calcio	mg/L	NE	NE	NE	NE	NE	NE
Carbono Orgánico Total	mg/L	NE	NE	NE	NE	NE	NE
Cianuro Total	mg/L	0,2	0,2	NE	NE	NE	0,05
Cloruros	mg/L Cl-	250	250	NE	NE	NE	NE
Cobre	mg/L	1	1	0,2	0,5	NE	0,1
Coliformes Fecales	NMP/100mL	2000	NE	NE	NE	200	NE
Coliformes Totales	NMP/100mL	20000	1000	5000	NE	1000	NE
Color Verdadero	UPC	75	20	NE	NE	NE	Ausente
Conductividad	µs/cm	NE	NE	NE	NE	NE	NE
Cromo	mg/L	0,05	0,05	0,1	1	NE	0,01 *Cromo Hexavalente
DBO5	mg/L O2	NE	NE	NE	NE	NE	NE
DQO	mg/L O2	NE	NE	NE	NE	NE	NE
Dureza Total	mg/L CaCO3	NE	NE	NE	NE	NE	NE
Fenoles Totales	mg/L	0,002	0,002	NE	NE	0,002	1 *Fenoles monohídricos
Fosfatos	mg/L P-PO4-3	NE	NE	NE	NE	NE	NE
Fósforo Inorgánico	mg/L P	NE	NE	NE	NE	NE	NE
Fósforo Orgánico	mg/L P	NE	NE	NE	NE	NE	NE
Fosforo Total	mg/L P	NE	NE	NE	NE	NE	NE
Grasas Y Aceites	mg/L	No detectable	No detectable	NE	NE	No detectable	0,01 como % de sólidos secos
Hidrocarburos Totales	mg/L	NE	NE	NE	NE	NE	NE
Hierro	mg/L	NE	NE	5	NE	NE	0,1
Magnesio	mg/L	NE	NE	NE	NE	NE	NE
Manganeso	mg/L	NE	NE	0,2	NE	NE	0,1
Material Flotante		NE	No detectable	NE	NE	No detectable	NE
Mercurio	mg/L	0,002	0,002	NE	0,01	NE	0,01
Níquel	mg/L	NE	NE	0,2	NE	NE	0,01
Nitratos	mg/L N-NO3	10	10	NE	NE	NE	NE

PARÁMETRO	UNIDADES	DECRETO 1076/2015 (artículos transitorios)					
		2.2.3.3.9.3	2.2.3.3.9.4	2.2.3.3.9.5	2.2.3.3.9.6	2.2.3.3.9.7	2.2.3.3.9.10
Nitritos	mg/L N-NO2	10	10	NE	10	NE	NE
Nitrógeno Amoniacal	mg/L N-NH3	10	1	NE	NE	NE	0,1
Nitrógeno Total	mg/L N	NE	NE	NE	NE	NE	NE
Olor		NE	NE	NE	NE	NE	Ausente
Oxígeno Disuelto	mg/L O2	NE	NE	NE	NE	70%	5
Pesticidas Organoclorados	mg/L	NE	NE	NE	NE	NE	0,001
Pesticidas Organofosforados	mg/L	NE	NE	NE	NE	NE	0,05
pH	UNIDADES	5,0-9,0	6,5-8,5	4,5-9,0	NE	5,0-9,0	6,5-9
Plomo	mg/L	0,05	0,05	5	0,1	NE	0,01
Potasio	mg/L	NE	NE	NE	NE	NE	NE
Sabor		NE	NE	NE	NE	NE	Ausente
Selenio	mg/L	0,01	0,01	0,02	NE	NE	0,01
Sodio	mg/L	NE	NE	NE	NE	NE	NE
Sólidos Disueltos Totales	mg/L	NE	NE	NE	NE	NE	NE
Sólidos Sedimentables	mL/L - h	NE	NE	NE	NE	NE	NE
Sólidos Suspendidos	mg/L	NE	NE	NE	NE	NE	NE
Sólidos Totales	mg/L	NE	NE	NE	NE	NE	NE
Sulfatos	mg/L SO4-2	400	400	NE	NE	NE	NE
Temperatura	°C	NE	NE	NE	NE	NE	NE
Tensoactivos	mg/L LAS	0,5	0,5	NE	NE	0,5	0,143
Turbiedad	NTU	NE	10	NE	NE	NE	Ausente
Zinc	mg/L	15	15	2	25	NE	0,01
Artículo 2.2.3.3.9.3: límites para consumo humano y doméstico, con tratamiento convencional							
Artículo 2.2.3.3.9.4: límites para consumo humano y doméstico, solo requiere desinfección							
Artículo 2.2.3.3.9.5: límites para uso agrícola							
Artículo 2.2.3.3.9.6: límite para uso pecuario							
Artículos 2.2.3.3.9.7: límites para fines recreativos contacto primario							
Artículos 2.2.3.3.9.10: límites para preservación de flora y fauna, en aguas dulces, frías o cálidas y en aguas marinas o estuarinas							

Fuente: Decreto 1076 de 2015. Ministerio de Ambiente y Desarrollo Sostenible

El Artículo 2.2.3.3.1.7 del Decreto 1076 del 2015, establece los parámetros mínimos que deben ser utilizados en los modelos de simulación aplicables en la ordenación del recurso hídrico, los cuales se presentan a continuación:

- DBO5: Demanda bioquímica de oxígeno a cinco (5) días.
- DQO: Demanda química de oxígeno.
- SST: Sólidos Suspendidos Totales.
- pH: Potencial del Ion hidronio, H+
- T: Temperatura.
- OD: Oxígeno disuelto.

- Q: Caudal.
- Datos Hidrobiológicos.
- Coliformes Totales y Fecales.

Igualmente, la Resolución 0631 de 2015, establece en su Capítulo VII los parámetros fisicoquímicos y sus valores límites máximos permisibles en los vertimientos puntuales de aguas residuales no domésticas para las actividades industriales, comerciales o de servicios diferentes a los del Capítulo V y VI hacia los cuerpos de aguas superficiales, a cumplirse a partir del 01 de enero del 2016.

Tabla 3. Valores Límites Máximos Permisibles para Vertimientos Puntuales (Res. 631/2015)

SST (mg/L)	DBO_5 (mg/L O_2)	DQO (mg/L O_2)	pH (unidades)
50	50	150	Entre 6-9

Fuente: Resolución 0631 de 2015, Artículo 15. Ministerio de Ambiente y Desarrollo Sostenible

2. Revisión de Información Secundaria

2.1. Localización de los Puntos de Vertimientos

El proyecto vial actualmente tiene proyectado 4 puntos de vertimientos en los cuerpos de agua: quebrada La Humeadora, río Boquerón, río Sapuyes y río Guaitara, para lo cual solicita permiso de vertimientos para la etapa de construcción de la doble calzada. Se solicita una franja de vertimiento entre 150 y 200 metros (50 m aguas arriba y 150 m aguas debajo de las coordenadas mostradas en la Tabla 4.

Tabla 4. Ubicación General de los Puntos de Monitoreo

ETAPA	ACTIVIDAD O INSTALACIÓN	UBICACIÓN			CAUDAL MINIMO DEL CUERPO DE AGUA (L/s)	FLUJO DEL VERTIMIENTO	CAUDAL A VERTER (L/s)		USOS AGUAS ABAJO
		NOMBRE	ESTE	NORTE			Industrial	Doméstico	
CONSTRUCCIÓN	Campamento 1	(V1) Río Boquerón	948589	590972	1100	Continuo	0.36	0.075	Vertimientos y riego
	Campamento 2	(V2) Q. La Humeadora	955074	597201	101.4		0.36	0.075	No se evidenciaron usos del agua
	Campamento 3 y 4	(V3) Río Guaitará	956577	600446	4935.8		0.36	0.075	No se evidenciaron usos del agua
	Campamento 5	(V4) Río Sapuyes	954849	605081	3400		0.36	0.075	Vertimientos
TOTAL							**1.44**	**0.30**	

2.2. Sistema de Tratamiento de Aguas Residuales

La disposición del agua se realiza a través del vertimiento en los cuerpos de agua enunciados, con previo tratamiento en el sistema de manejo de agua residual.

Para mayor información, se remite al lector al Capítulo 7 del EIA del proyecto vial Doble Calzada Rumichaca – Pasto Tramo San Juan – Pedregal.

Figura 1. Localización Puntos de Vertimientos

2.3. Características del Aguas Residuales

A continuación, en la Tabla 4, se presentan los resultados obtenidos para los parámetros monitoreados.

Tabla 5. Composición Típica del AR en un Proyecto Similar

PARÁMETRO	UNIDAD	VALORES REPORTADOS
Color	UPC	> 150
Cloruros	mg Cl/l	> 150
DBO	mg O_2/l	> 500
DQO	mg O_2/l	> 600
Dureza total	mg $CaCO_3$/l	50
pH	Unidad	7- 9
Sólidos disueltos	mg/l	300 – 800
Sólidos suspendidos	mg/l	100 – 200
Sulfatos	mg SO_4/l	40 – 100
Coliformes totales	NMP/100ml	900.000
Coliformes fecales	NMP/100ml	80.000
Grasas y aceites	mg/l	50- 100

Fuente: EIA del Proyecto vial Ruta del Sol - Sector I: Villeta-El Corán. 2011 – CV Helios - Informe de cumplimiento ambiental (junio – diciembre 2014), Campamento Guaduero CV Helios

2.4. Caracterización Hidráulica de los Tramos

La caracterización hidráulica de los tramos de interés para descarga fue definida a partir de inspección visual en una longitud de 300 metros, además de confirmar como usos principales actual del recurso, agrícola y pecuario, y de disposición de aguas residuales, tanto para aguas arriba como aguas abajo.

ESTACIÓN DE AFORO - Río Boqueron - Sección 1-1

COORDENADAS	
E	**N**
948,472.02	591,019.69
ALTITUD, msnm	2386
PRESIÓN, mmHg	571.50
TEMPERATURA AGUA, ºC	15.20
TEMPERATURA AMBIENTE, ºC	12.80
NUBOSIDAD, octas	6/8
HUMEDAD, %	77

PARÁMETROS HIDRÁULICOS Y GEOMÉTRICOS

Área, m^2	Velocidad, m/s	Caudal, m^3/s	Profundidad, m	Ancho, m
3.58	0.27	1.09	0.59	6.50

SECCIÓN DE AFORO

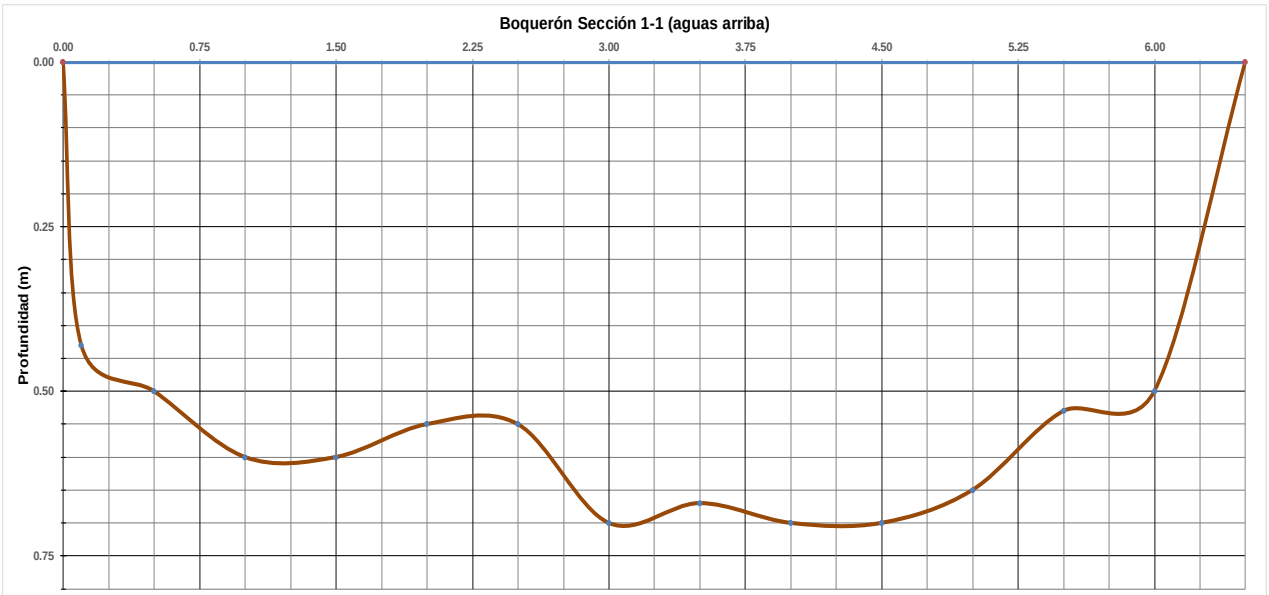

Figura 2. Sección Transversal Tramo río Boquerón Aguas Arriba

ESTACIÓN DE AFORO - Río Boqueron - Sección 2-2

COORDENADAS	
E	**N**
948,636.85	590,908.54
ALTITUD, msnm	2369
PRESIÓN, mmHg	572.66
TEMPERATURA AGUA, ºC	15.00
TEMPERATURA AMBIENTE, ºC	12.80
NUBOSIDAD, octas	6/8
HUMEDAD, %	77

PARÁMETROS HIDRÁULICOS Y GEOMÉTRICOS

Área, m^2	Velocidad, m/s	Caudal, m^3/s	Profundidad, m	Ancho, m
2.92	0.34	1.16	0.68	4.50

SECCIÓN DE AFORO

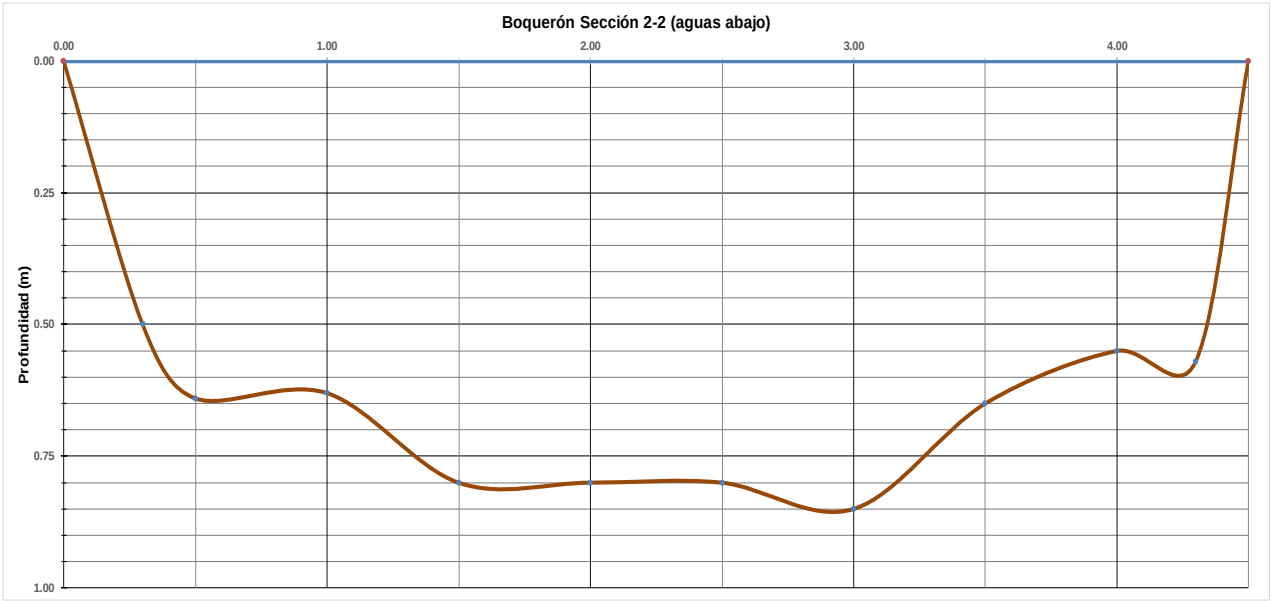

Figura 3. Sección Transversal Tramo río Boquerón Aguas Abajo

ESTACIÓN DE AFORO - Quebrada La Humeadora - Sección 1-1

COORDENADAS	
E	**N**
955,067.23	597,208.15
ALTITUD, msnm	2662
PRESIÓN, mmHg	553.08
TEMPERATURA AGUA, ºC	14.80
TEMPERATURA AMBIENTE, ºC	13.00
NUBOSIDAD, octas	4/8
HUMEDAD, %	76

PARÁMETROS HIDRÁULICOS Y GEOMÉTRICOS

Área, m^2	Velocidad, m/s	Caudal, m^3/s	Profundidad, m	Ancho, m
0.87	0.14	0.14	0.37	2.50

SECCIÓN DE AFORO

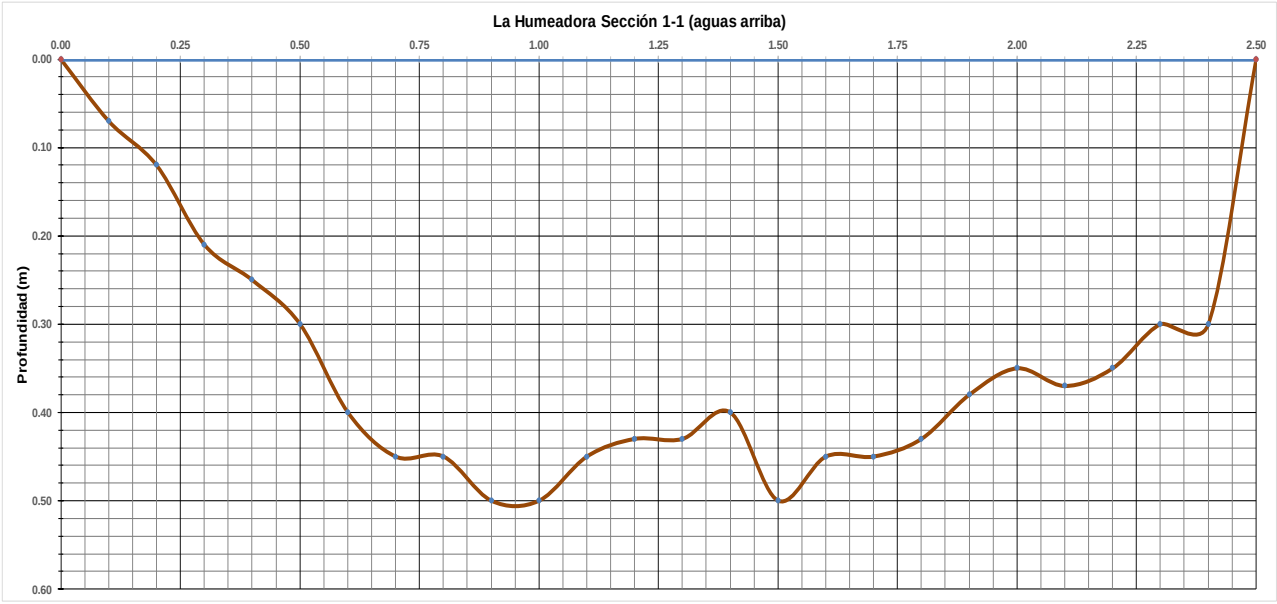

Figura 4. Sección Transversal Tramo quebrada La Humeadora Aguas Arriba

ESTACIÓN DE AFORO - Quebrada La Humeadora - Sección 2-2

COORDENADAS	
E	**N**
955,242.08	597,102.86
ALTITUD, msnm	2660
PRESIÓN, mmHg	553.22
TEMPERATURA AGUA, ºC	13.70
TEMPERATURA AMBIENTE, ºC	13.00
NUBOSIDAD, octas	4/8
HUMEDAD, %	76

PARÁMETROS HIDRÁULICOS Y GEOMÉTRICOS

Área, m^2	Velocidad, m/s	Caudal, m^3/s	Profundidad, m	Ancho, m
0.51	0.27	0.15	0.31	2.00

SECCIÓN DE AFORO

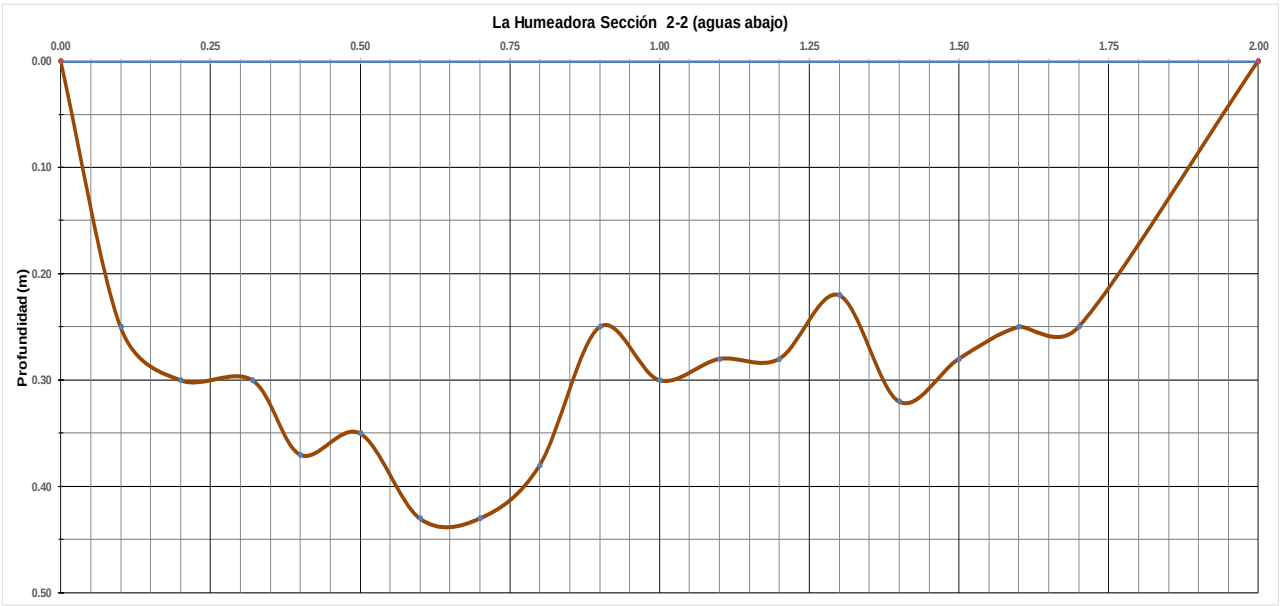

Figura 5. Sección Transversal Tramo quebrada La Humeadora Aguas Abajo

ESTACIÓN DE AFORO - Río Guaitará - Sección 1-1

COORDENADAS	
E	**N**
956,644.93	600,448.65
ALTITUD, msnm	1880
PRESIÓN, mmHg	608.15
TEMPERATURA AGUA, ºC	19.00
TEMPERATURA AMBIENTE, ºC	15.00
NUBOSIDAD, octas	2/8
HUMEDAD, %	68

PARÁMETROS HIDRÁULICOS Y GEOMÉTRICOS

Área, m^2	Velocidad, m/s	Caudal, m^3/s	Profundidad, m	Ancho, m
20.42	0.71	19.22	0.56	36.50

SECCIÓN DE AFORO

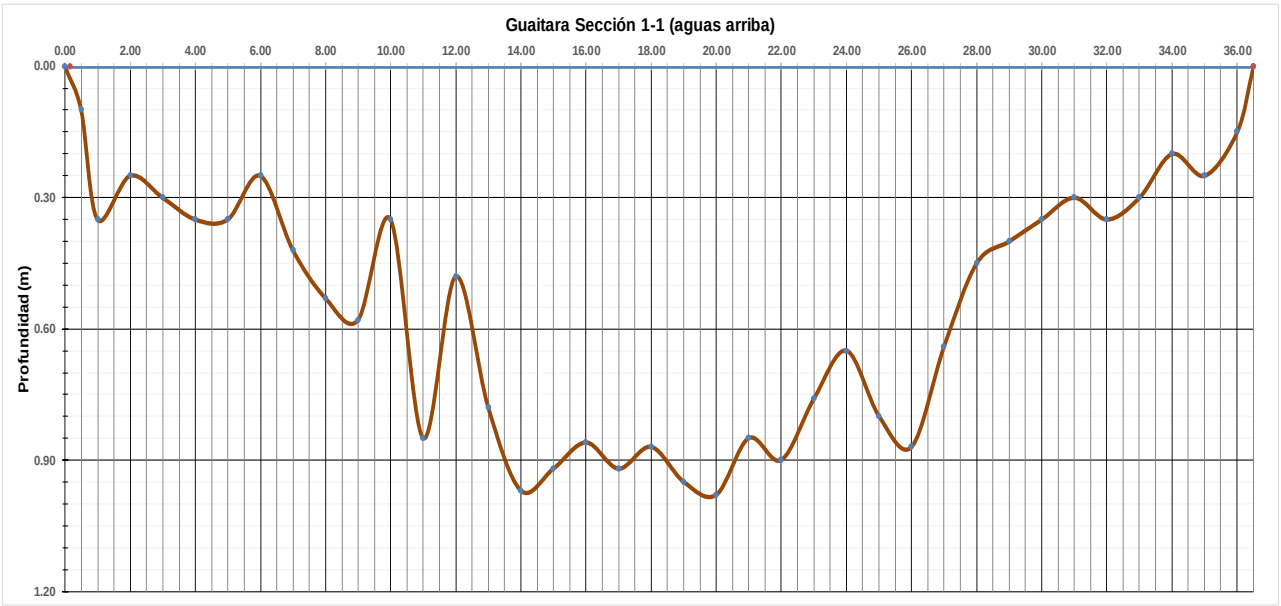

Figura 6. Sección Transversal Tramo río Guaitara Aguas Arriba

ESTACIÓN DE AFORO - Río Guaitará - Sección 2-2

COORDENADAS	
E	**N**
956,565.04	600,680.76
ALTITUD, msnm	1870
PRESIÓN, mmHg	608.88
TEMPERATURA AGUA, ºC	15.40
TEMPERATURA AMBIENTE, ºC	15.00
NUBOSIDAD, octas	2/8
HUMEDAD, %	68

PARÁMETROS HIDRÁULICOS Y GEOMÉTRICOS

Área, m^2	Velocidad, m/s	Caudal, m^3/s	Profundidad, m	Ancho, m
31.33	0.71	20.37	1.22	30.00

SECCIÓN DE AFORO

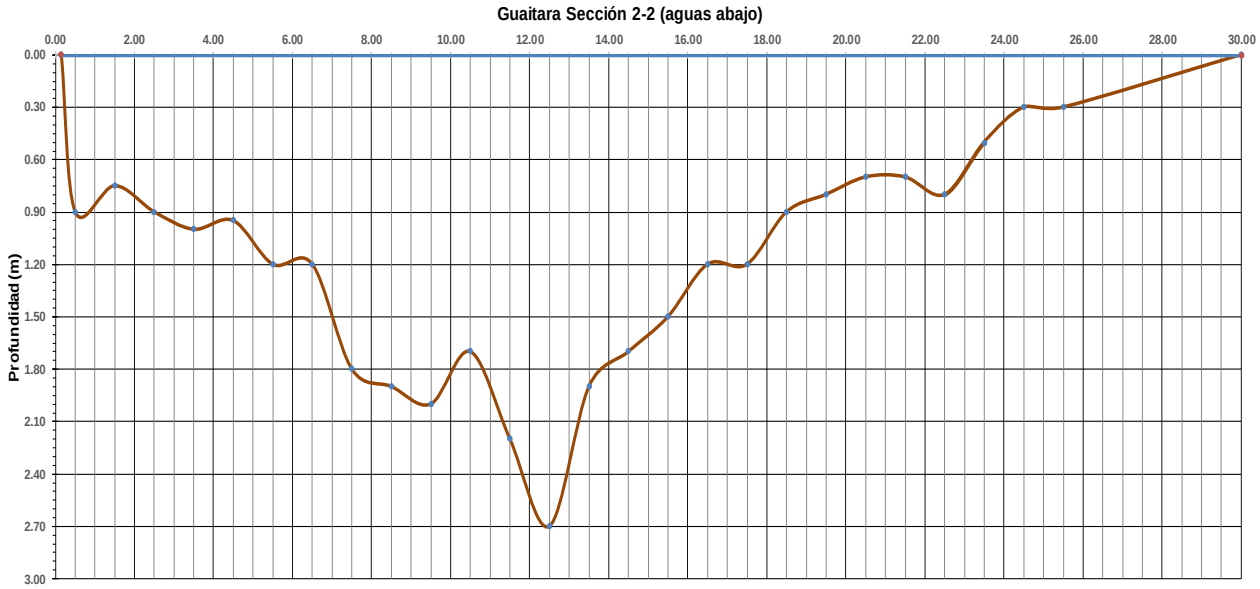

Figura 7. Sección Transversal Tramo río Guaitara Aguas Abajo

ESTACIÓN DE AFORO - Río Sapuyes - Sección 1-1

COORDENADAS	
E	**N**
954,827.67	605,159.46
ALTITUD, msnm	1830
PRESIÓN, mmHg	611.31
TEMPERATURA AGUA, ºC	16.50
TEMPERATURA AMBIENTE, ºC	14.00
NUBOSIDAD, octas	8/8
HUMEDAD, %	68

PARÁMETROS HIDRÁULICOS Y GEOMÉTRICOS

Área, m^2	Velocidad, m/s	Caudal, m^3/s	Profundidad, m	Ancho, m
7.71	0.92	5.79	0.53	12.00

SECCIÓN DE AFORO

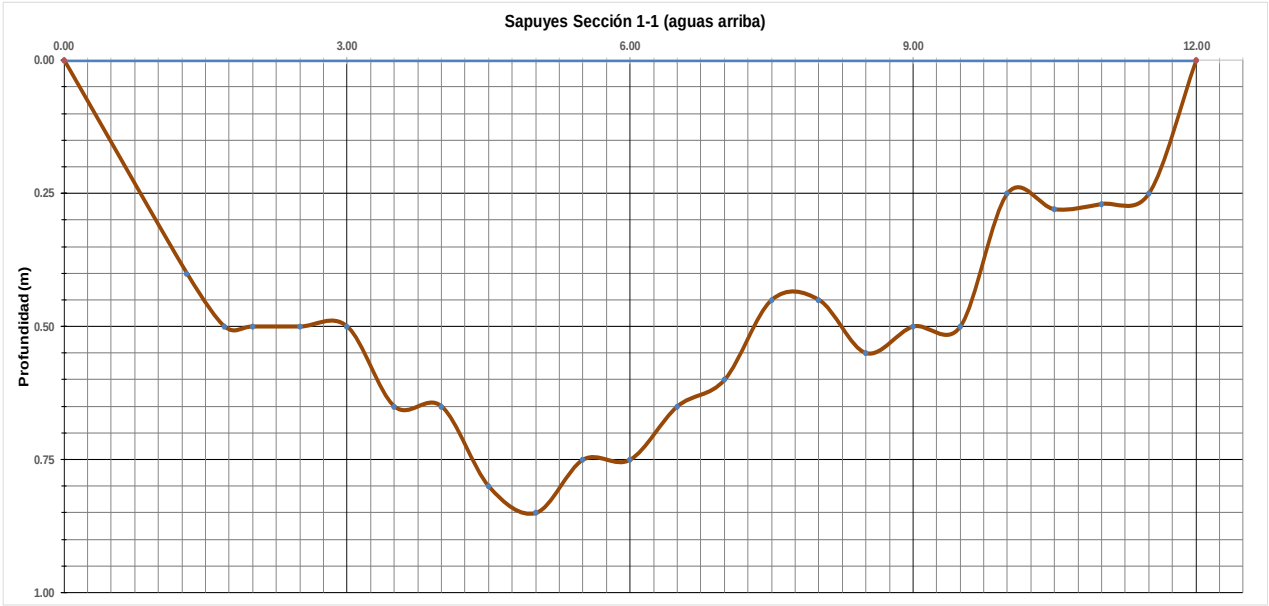

Figura 8. Sección Transversal Tramo río Sapuyes Aguas Arriba

ESTACIÓN DE AFORO - Río Sapuyes - Sección 2-2

COORDENADAS	
E	**N**
954,987.27	605,047.87
ALTITUD, msnm	1810
PRESIÓN, mmHg	612.76
TEMPERATURA AGUA, ºC	18.00
TEMPERATURA AMBIENTE, ºC	14.00
NUBOSIDAD, octas	8/8
HUMEDAD, %	68

PARÁMETROS HIDRÁULICOS Y GEOMÉTRICOS

Área, m^2	Velocidad, m/s	Caudal, m^3/s	Profundidad, m	Ancho, m
9.36	0.75	8.02	0.69	14.50

SECCIÓN DE AFORO

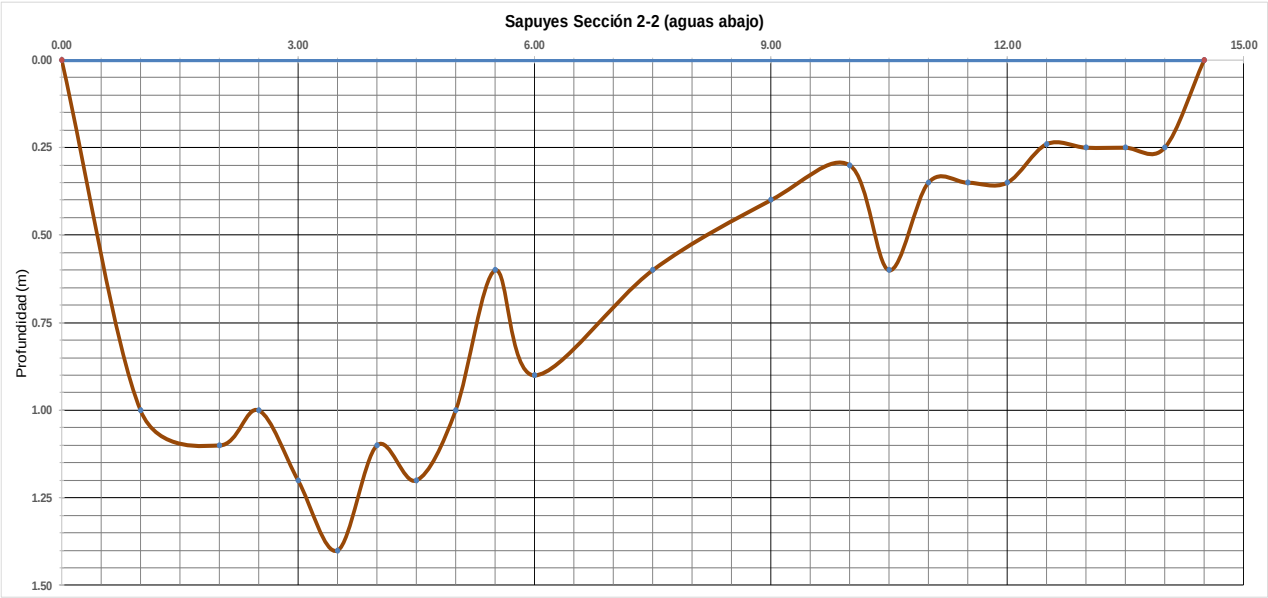

Figura 9. Sección Transversal Tramo río Sapuyes Aguas Abajo

3. Modelo Matemático Unidimensional Streeter - Phelps

Elegir un criterio para la caracterización del grado de contaminación de un río es bastante difícil ya que son muy variados los efectos que producen los diferentes tipos de contaminantes sobre las aguas. Sin embargo, la contaminación debida a la materia orgánica es a menudo la que produce un efecto más significativo sobre el sistema acuático. La fuerte demanda de oxígeno disuelto (OD), ya sea por la oxidación de la materia orgánica o inorgánica, desde la misma masa de agua o desde los sedimentos, crea problemas muy graves en todo el ecosistema acuático. El OD es el factor energético fundamental para los seres vivos. Bajas concentraciones de oxígeno producen desajustes en el ecosistema, mortalidad de peces, olores y otros efectos estéticos desagradables. En consecuencia, el OD es una de las más importantes variables del sistema acuático (Suárez, 2008).

Los primeros trabajos realizados sobre el OD se desarrollaron entre los años 1870 y 1900. Theriault (1927) ya presentaba el ensayo de la demanda bioquímica de oxígeno (DBO) y citaba las investigaciones sobre el OD en el río Támesis (Suárez, 2008).

En los Estados Unidos el mayor esfuerzo en la evaluación de la calidad de las aguas comenzó en 1912, cuando al Servicio de Salud Pública se le encomendó, por parte del Congreso, la dirección de los trabajos y estudios sobre "el saneamiento y aguas residuales, incluyendo la contaminación, directa o indirecta, en los ríos navegables y lagos de los Estados Unidos". Los estudios en el río Ohio, realizados entre 1914 y 1916, permitieron la realización del fundamental trabajo de **Harold Streeter** y **Earle Phelps** sobre la modelización matemática del OD. El trabajo incluía la aplicación de una sencilla formulación matemática de los principales procesos asociados con el oxígeno disuelto en un río (Suárez, 2008).

En este sentido, al avance del modelo contribuyeron posteriores trabajos; destacan los importantes aportes de Velz (1938, 1939, 1947, 1948), y O´Connor (1967), el cual continuó el desarrollo de las bases matemáticas y bioquímicas para el análisis del OD en corrientes y de forma más importante en sistemas estuarinos, tales como el puerto de Nueva York; los masivos y detallados esfuerzos sobre el estuario del Támesis en el Reino Unido (Departament of Scientific & Industrial Research, 1964); además de los trabajos sobre el análisis del OD en estuarios, como hicieron O´Connor (1960, 1962, 1965, 1966), Thomann (1963), y O´Connor y Mueller (1984), además de otros.

3.1. Características Generales

En definitiva, la curva que se obtiene representando la ecuación de **Streeter-Phelps** proporciona la disminución y posterior recuperación del oxígeno disuelto en el río. La degradación bioquímica comienza inmediatamente después del vertido. Puesto que la reaireación es proporcional al déficit de oxígeno disuelto, su velocidad de aporte de oxígeno va aumentando conforme el déficit va creciendo. Por último, se alcanza un punto en el cual la tasa de consumo de oxígeno se iguala a la tasa de reaireación atmosférica; la curva alcanza su mínimo. A la distancia comprendida entre el punto de vertido y este mínimo se la conoce como **distancia crítica**.

A partir del punto crítico la curva empieza a recuperarse y más abajo, el río no mostrará efecto alguno por causa del vertido. A la máxima diferencia entre el oxígeno que puede tener disuelto una masa de agua y el que tiene en realidad se denomina **déficit crítico**, el cual se corresponde con el mínimo valor de OD en el río.

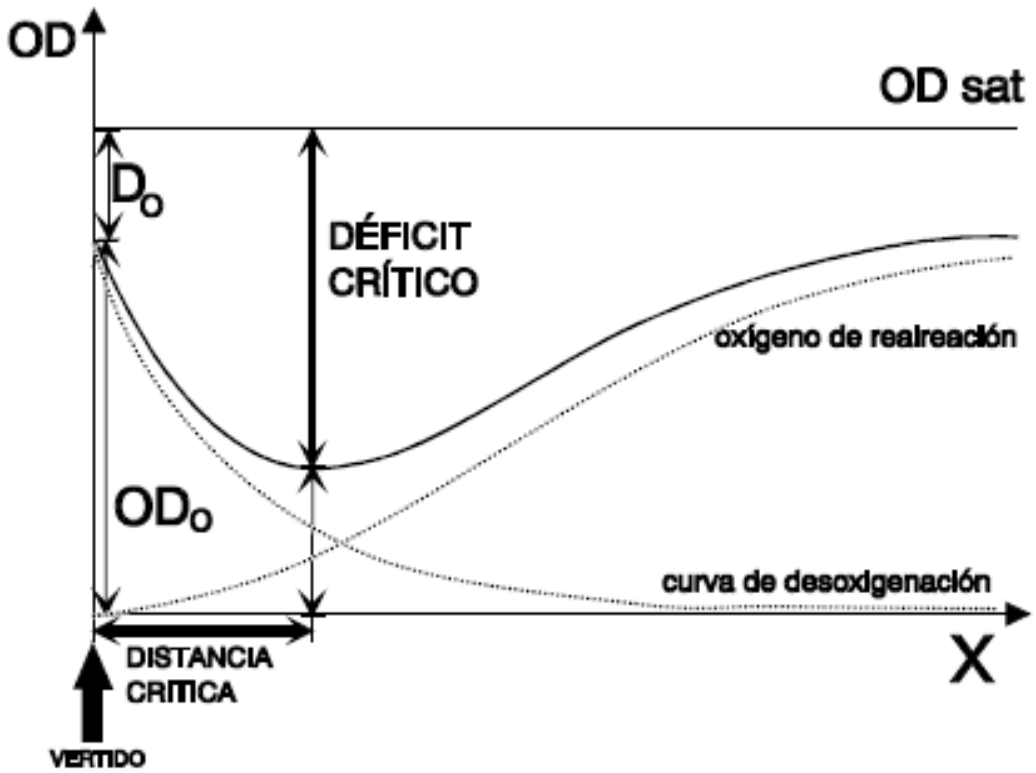

Figura 10. Curva DOSAG o del valle de oxígeno disuelto

Si la DBO última y el déficit de oxígeno en el punto inicial son ***Lo*** y ***Do***, respectivamente, la integración de la ecuación de Streeter-Phelps permite obtener los valores del **déficit de oxígeno disuelto** para cualquier punto:

$$D = \frac{K_1 \cdot L_o}{K_2 - K_1}\left(e^{-K_1 \cdot \frac{x}{U}} - e^{-K_2 \cdot \frac{x}{U}}\right) + D_o \cdot e^{-K_2 t} \qquad \textit{Ecuación 1}$$

El máximo de esta curva determina el punto del río con peores condiciones en cuanto a contenido de oxígeno disuelto (***punto crítico***). El ***déficit crítico*** en el punto crítico es importante desde el punto de vista técnico. Las normas de calidad de aguas imponen unos determinados niveles mínimos de OD para las aguas de los ríos, en función de los objetivos de calidad.

El **déficit crítico** será:

$$D_c = \frac{K_1}{K_2} \cdot L_o \cdot e^{-k_1 \cdot \frac{x_c}{U}} \qquad \textit{Ecuación 2}$$

La ***distancia crítica*** será:

$$x_c = \frac{U}{K_2 - K_1} Ln\left[\frac{K_2}{K_1}\left(1 - \frac{D_o \cdot (K_2 - K_1)}{L_o \cdot K_1}\right)\right] \qquad \textit{Ecuación 3}$$

Las tasas de las reacciones, ***K1*** y ***K2***, son valores experimentales que se obtienen por distintas medidas de laboratorio o *in situ*. Dependen de la temperatura, carga contaminante y condiciones hidráulicas. El análisis de Streeter-Phelps se centra, una vez definida la ecuación, en determinar cuáles son las condiciones más desfavorables que producen el valor más alto del déficit de oxígeno.

Estas condiciones se dan en épocas de caudal mínimo (sequía o época de estiaje) coincidiendo con altas temperaturas, que por una parte disminuyen el valor de la concentración de saturación de oxígeno y, por otra, aumentan la actividad de los organismos, por lo que la tasa de oxidación de la materia orgánica aumenta.

3.2. Metodología

La Figura 3, representa esquemáticamente la metodología aplicada para la modelación de la calidad del agua para una corriente hídrica.

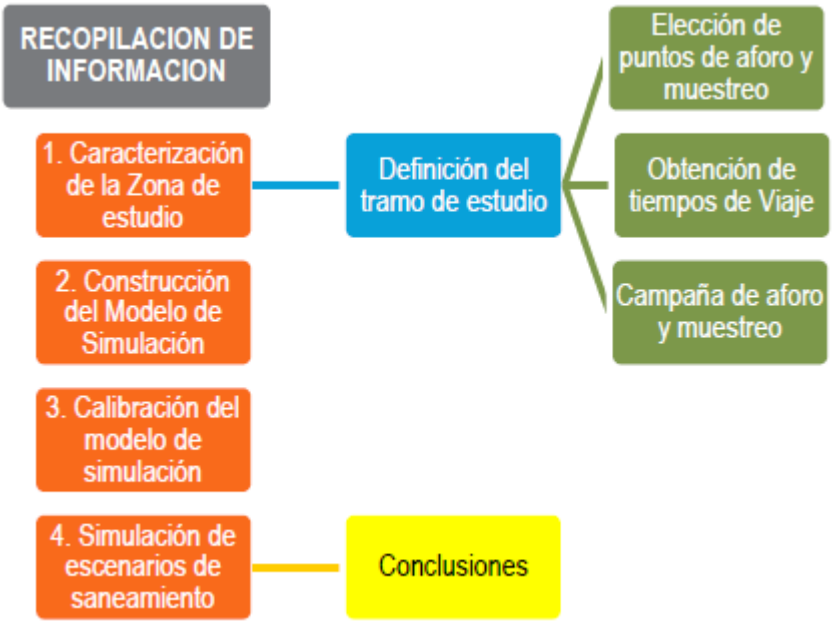

Figura 11. Diagrama de Flujo de la Metodología Típica de Modelamiento

Inicialmente se realizó la recopilación de información cartográfica con el fin de localizar la corriente principal junto a sus tributarios. A su vez, se evaluaron las diferentes estaciones a monitorear seleccionadas de acuerdo a su importancia geográfica y usos actuales (concesiones y vertimientos). Posteriormente, se georreferenciaron los puntos o secciones ya escogidos, para así determinar los tiempos de viaje de la masa de agua, cuyo fin es establecer un horario en la toma de muestras de calidad y cantidad sobre el tramo objeto de evaluación.

Definido el tramo, las secciones y los valores fisicoquímicos e hidrológicos a modelar, se construye el modelo de simulación teniéndose como objetivo, la identificación del comportamiento de los parámetros a modelar mediante el modelo de Streeter-Phelps.

Para el presente estudio, se realizó una campaña de aforo y muestreo determinada por el Cliente y QHSE SAS, esperando que esta información simule el comportamiento usual de la corriente hídrica bajo condiciones de caudales medios a bajos, sin presencia de lluvias que modifiquen el estado del líquido en su trayectoria.

Luego de ingresar los datos que requiere el modelo, se realiza el proceso de precalibración y calibración, donde se pretende aproximar los valores modelados con los valores reales tomados en la fuente hídrica, siendo esta la parte más importante en la implementación de esta herramienta.

4. Capacidad de Asimilación de la Fuente Receptora

Con el objetivo de establecer la capacidad de asimilación de los vertimientos domésticos e industriales en las fuentes receptoras, se aplicó la metodología de la ANLA (2013) la cual permite calcular la longitud de influencia de los vertimientos (Ver Anexo 1).

Esta metodología se basa en las características fisicoquímicas e hidráulicas de la fuente receptora y de los vertimientos. Para su aplicación se tiene en cuenta el escenario más crítico para el vertimiento, por lo cual se toma el caudal mínimo en la fuente receptora y se asumen las concentraciones de los determinantes evaluados iguales al límite máximo permisible, ya que en este caso se verían limitados los procesos de dispersión y asimilación de la carga, lo que representa la condición crítica para la modelación.

Según la “Metodología para la definición de la longitud de influencia de vertimientos sobre corrientes de agua superficial” (ANLA, 2013), para implementar esta metodología para todos los sectores se deberán monitorear como mínimo los siguientes determinantes de la calidad de agua sobre el cuerpo receptor: oxígeno disuelto (OD), demanda bioquímica de oxigeno (DBO), nitrógeno total (N), fosforo total (P), coliformes fecales (CF) y sólidos suspendidos totales (SST).

Estos fueron los determinantes considerados para la modelación de los vertimientos domésticos, mientras que para los vertimientos de tipo industrial se consideró el oxígeno disuelto y los sólidos suspendidos totales.

4.1. Modelos de Calidad del Agua

Existe una gran variedad de modelos de calidad de agua, con los cuales es posible establecer el comportamiento de un vertimiento en un cuerpo de agua receptor. Las principales diferencias radican en los procesos de transporte (advección, dispersión) y reacción (transformación de los determinantes de calidad de agua) que incluyen y por tanto en los supuestos que plantean. A continuación, se realiza una breve descripción de los modelos más ampliamente utilizados.

4.1.1. Modelo de Flujo a Pistón

Este modelo es la representación más sencilla, ya que no considera dentro de los procesos de transporte la dispersión, solo la advección e incluye procesos de transformación o reacción de los determinantes de calidad de agua. Así mismo, supone condiciones de flujo estable y las características geométricas e hidrológicas de las corrientes de agua constantes (Chapra, 1997 en Rojas Aguirre, 2011).

4.1.2. Modelo de Streeter-Phelps

Este modelo es uno de los más conocidos ya que permite simular de manera simplificada el comportamiento del oxígeno disuelto (OD) en un río, ante la descarga puntual de carga orgánica. Este modelo representa básicamente dos procesos: la descomposición bacterial en la fase líquida y la re-aireación (Rojas Aguirre, 2011). Adaptaciones y ampliaciones posteriores del modelo han permitido la inclusión de otros procesos como la fotosíntesis, respiración y demanda béntica de oxígeno para la determinación de otros parámetros de calidad del agua.

4.1.3. Modelo WASP (Water Quality Analysis Simulation Program)

El WASP es un programa de modelación dinámica por módulos para sistemas acuáticos que incluye la columna de agua y los bentos. El programa permite la modelación de los sistemas en 1, 2 o 3 dimensiones y para una amplia variedad de contaminantes. El modelo representa los procesos de variación temporal de advección, de dispersión, de carga de masa difusa y los intercambios de frontera o de borde.

El WASP se puede integrar a modelos hidrodinámicos y de transporte de sedimentos para determinar flujos, velocidades a profundidad, temperatura, salinidad y flujo de sedimentos. También se puede integrar a modelos hidrodinámicos y de cuencas los cuales permiten análisis multianuales ante variaciones de las condiciones meteorológicas y ambientales (USEPA, 2013).

4.1.4. Modelo QUALK2E (Q2E)

El QUAL2E es un programa para modelar la calidad de agua en ríos y corrientes. El programa permite la modelación de sistemas unidimensionales, que se pueden representar como una corriente principal con sus ramificaciones tributarias y con un flujo permanente no uniforme. El programa simula el balance de calor y de temperatura en función de la meteorología en una escala de tiempo diario.

Puede simular cargas puntuales y no puntuales, así como sumideros. Las variables de calidad de agua son simuladas en una escala de tiempo diario (USEPA, 2013).

4.1.5. QUALK2K (Q2K)

El QUAL2K es un programa para modelar la calidad de agua en ríos y corrientes, es de uso libre y representa una versión mejorada del programa de modelación QUAL2E. Además de las características del QUAL2E, señaladas en el párrafo anterior, el QUAL2K presenta, entre otros, los siguientes elementos nuevos (USEPA, 2013):

- En la segmentación del modelo, el Q2K permite dividir el sistema en segmentos de diferentes longitudes y múltiples cargas y sumideros se pueden incluir en cualquier elemento.
- Para representar el carbono orgánico, el Q2K usa dos formas de DBO de acuerdo con la velocidad de oxidación, una lenta y otra rápida.
- El Q2K calcula la anoxia reduciendo las reacciones de oxidación a cero ante niveles bajos de oxígeno. Además, la desnitrificación es modelada como una reacción de primer orden que llega a ser pronunciada ante concentraciones bajas de oxígeno.
- En los flujos de agua-sedimento el oxígeno disuelto y los nutrientes pueden ser simulados internamente en lugar de ser prescritos. El oxígeno y los flujos de nutrientes son simulados en función de la precipitación de la materia orgánica particulada.

4.1.6. EPD-RIV1

El EPD-RIV1 es un programa que simula en una dimensión la dinámica hidráulica y la calidad del agua. El modelo computacional está basado en el programa CE-QUAL-RIV1 desarrollado por la Estación Experimental de Vías Fluviales (WES, por sus siglas en inglés) de los Ingenieros de la Armada de Estados Unidos. El programa consiste de dos módulos, uno de hidrodinámica que es

comúnmente aplicado primero, y otro de calidad. El primer módulo provee la información del transporte para que el segundo módulo desarrolle las simulaciones de calidad. El módulo de calidad puede simular la interacción de 16 variables de estado, incluyendo temperatura, especies de nitrógeno (o demanda bioquímica de oxígeno nitrogenado), especies de fósforo, oxígeno disuelto, demanda de oxígeno carbonáceo (dos clases), algas, hierro, manganeso, coliformes bacterianos y dos constituyentes arbitrarios. Adicionalmente, el modelo puede simular los impactos de las macrófitas en el oxígeno disuelto y en el ciclo de nutrientes (USEPA, 2013).

4.1.7. ADZ-QUASAR

El ADZ-QUASAR es un modelo mejorado que integra las características del modelo QUASAR con las características del ADZ. El modelo QUASAR (Quality Simulation Along River Systems) proporciona herramientas cuantitativas para analizar los aspectos físicos, químicos y biológicos de sistemas de ríos complejos (Lees et al, 1998). El modelo proporciona los medios para evaluar los impactos de los contaminantes en la calidad del agua, llevar a cabo investigaciones en esos sistemas acuáticos, abordar futuros escenarios de entrada y asistir en el desarrollo de planes de manejo prácticos en los sistemas de ríos, incluyendo el establecimiento de niveles de calidad de las descargas para los objetivos de calidad del cuerpo de agua. Una aplicación típica del modelo QUASAR es el análisis de impactos en la calidad del agua resultante de los cambios en el régimen de flujo (Lees et al, 1998).

Un problema que presenta el modelo QUASAR es el uso en serie de tanques reactores continuamente agitados (CSTR, por sus siglas en inglés) para representar los procesos de advección y dispersión de contaminantes. Esta formulación en el modelo, conocida como celdas en serie, no es la más apropiada para aplicaciones que requieren predicciones de corto tiempo, tales como evaluación y predicción en tiempo real de eventos de contaminantes, ya que un número desconocido de conexiones en serie es requerido para representar la advección y dispersión observada en un tramo de río en particular (Lees et al, 1998). Para resolver este problema se integra los conceptos del modelo ADZ (Aggregated Dead-Zone) al modelo QUASAR.

El concepto de ADZ se desarrolló para representar los efectos de dispersión en las zonas muertas o zonas de almacenamiento en un tramo de un rio. Todos los procesos de dispersión que un soluto sufre en un tramo de un rio se agrupan en un término que se conoce como Tr, tiempo de residencia de la zona muerta agregada (Lees et al, 1998). En síntesis, la inclusión de los conceptos del modelo ADZ al modelo QUASAR permite representar adecuadamente el comportamiento de los solutos en las zonas de almacenamiento temporal y las zonas muertas que existen en las corrientes de agua (Rojas Aguirre, 2011).

4.1.8. Otros Modelos

En el mercado se pueden encontrar modelos integrados que permiten la modelación de alcantarillados, calidad de agua en ríos y, en muchos casos, de plantas de tratamiento de aguas residuales. Dentro de estos modelos se pueden señalar los siguientes: Integrated Catchment Simulator (ICS), Hydroworks, Synopsis, West y Simba (González Parra, 2011), CORMIX, AQUASIM, ACUATOOL, WASP, entre otros, estos pueden ser de código abierto o licenciados.

4.2. Criterios de Selección del Modelo a UTILIZAR

El principal objetivo de este trabajo es la estimación de la longitud de Influencia de los vertimientos (Liv), información requerida por la ANLA para los proyectos objeto de licenciamiento. Teniendo en

cuenta que la ANLA ha establecido una metodología clara para la determinación de la LIV, y que esta metodología ha sido desarrollada en convenio con la Universidad Nacional de Colombia, tomando como base más de quince trabajos de investigación y organizaciones internacionales, se considera que la metodología propuesta es adecuada para los objetivos y el alcance del EIA del proyecto y para la obtención del permiso de vertimiento.

4.3. Descripción de los Modelos Utilizados

A continuación, se describen los modelos empleados para el cálculo de la longitud de influencia del vertimiento, cuyo principal criterio para su determinación es la concentración estándar, es decir, la concentración del determinante en el cuerpo de agua antes del vertimiento. El comportamiento del oxígeno disuelto se modeló a través del modelo de Streeter-Phelps el cual es ampliamente aplicado para esta variable. Para los demás determinantes, se utilizó la metodología desarrollada por la ANLA la cual se basa en el modelo ADZ QUASAR.

4.3.1. ADZ QUASAR

El modelo ADZ es una representación del transporte de solutos en corrientes, considerando efectos de dispersión y advección, además representa el almacenamiento temporal y las zonas muertas presentes en las corrientes. Por su parte el modelo de calidad de agua QUASAR, considera una serie de reactores bien mezclados. El acople de los modelos ADZ y QUASAR considera fenómenos de transporte en el modelo de calidad y se incluye un término de decaimiento para incorporar el efecto de sustancias no conservativas.

Cabe resaltar que la validación de la metodología propuesta, así como la calibración del modelo que inspiró el desarrollo del trabajo de la ANLA, no se pudo realizar por dos razones fundamentales:

1. El alcance del PMAI del proyecto y de la caracterización del vertimiento y cuerpo de agua no contempló ninguna de estas actividades.

2. Validar la metodología propuesta por la ANLA implicaría la validación de más de 15 trabajos de investigadores y entidades gubernamentales sobre los cuales se apoya esta metodología.

4.3.1.1. Definición de Variables

La definición de variables y los algoritmos fueron tomados de la “Metodología para la definición de la Longitud de Influencia de Vertimientos sobre corrientes de agua superficial” de la ANLA, presentada en 2013.

En esta sección se presenta la descripción de las principales variables empleadas en el modelo ADZ-QUASAR.

W: Carga Contaminante es “la cantidad de sustancia contaminante por unidad de tiempo”. Se calcula como: **W = Q.c**, donde **Q** es el caudal vertido y **c** es la concentración de la sustancia contaminante vertida.

a: Factor de asimilación es la “razón entre la carga del contaminante a la entrada del tramo **W** y la concentración resultante aguas abajo **c** sobre el cuerpo receptor”. Es decir, **a = W / c**.

t: Tiempo medio de viaje es el "tiempo que tarda una sustancia disuelta en ser conducida por el movimiento del medio y ser dispersada". Se puede calcular como: **t = L / v**, donde **L** es la longitud del tramo y **v** es la velocidad media de la corriente correspondiente a $\mathbf{Q_0}$.

DF: Fracción Dispersiva "representa la fracción del volumen total del tramo que participa en el flujo que se considera completamente mezclada, o la fracción del tiempo de retención en el cual la sustancia disuelta es dispersada. Un valor de DF de 0 representa advección pura y de 1, dispersión pura". Se puede calcular como: $\mathbf{DF = 1 - (v / v_{max})}$.

4.3.1.2. Proceso de Modelación

Los insumos para el modelo son las características hidrológicas de la corriente de agua, las características climatológicas de la zona donde se realizará el vertimiento, las características de la calidad del agua en la corriente receptora y en el vertimiento.

Para la definición de las características hidrológicas se requirió la determinación de los caudales ambientales y de los tiempos de viaje de una partícula en la corriente de agua, en la fuente receptora.

Esta información fue obtenida en el monitoreo de campo.

En el caso de la calidad del agua del cuerpo receptor se tomó información de la campaña de muestreo realizada. Las estaciones de referencia para cada punto de vertimiento, se escogieron de acuerdo a la ubicación, tratando de tener la menor distancia entre el punto de vertimiento y el punto receptor.

En el caso de las características fisicoquímicas de los vertimientos, se tomó como referencia los límites máximos permisibles de acuerdo con la normatividad vigente de la caracterización teórica del vertimiento.

Para cada uno de los determinantes o parámetros a estimar se calculó la carga de entrada al modelo de la siguiente manera:

$$W = W_o + W_v = Q_o . c_o + Q_v . c_v \qquad \textit{Ecuación 4}$$

Dónde: **W** es la carga inicial del determinante analizado en la corriente antes del vertimiento, $\mathbf{W_v}$ es la carga del determinante analizado en el vertimiento, $\mathbf{c_0}$ es la concentración inicial del parámetro analizado en la corriente antes del vertimiento; $\mathbf{Q_v}$ es el caudal del vertimiento y $\mathbf{c_v}$ es la concentración del determinante analizado en el vertimiento.

El caudal de entrada al modelo se calcula como:

$$\mathbf{Q = Q_0 + Q_v} \qquad \textit{Ecuación 5}$$

El factor de asimilación **a**, se calcula para cada determinante, en función del tiempo medio de viaje y la fracción dispersiva, según la siguiente ecuación:

$$a = 1 + DF * Kt * e^{1-DF * Kt} * Q \qquad \textit{Ecuación 6}$$

Si se conoce el factor de asimilación **a**, se puede calcular el tiempo medio de viaje con la ecuación lineal que se presenta a continuación, la cual se puede solucionar con el método de Newton – Raphson así:

$$t_{i+1} = t_i - \frac{1 + DF.k.t_i \; Q.e^{1-DF \; k.t_i} - a}{k \; 1 + DF \; 1 - DF \; k.t_i \; Q.e^{1-DF \; k.t_i}} \qquad \textit{Ecuación 7}$$

Donde **k** es la denominación genérica de las tasas de reacción. Las tasas de reacción se estiman de acuerdo con el tipo de determinante o parámetro a analizar. De acuerdo con la metodología de la ANLA, los determinantes mínimos a analizar con el propósito de implementar la metodología son: temperatura del agua, oxígeno disuelto, DBO, NTK, fósforo total, coliformes fecales y sólidos suspendidos totales.

- Escenarios de Modelación

El escenario de modelación corresponde a las condiciones de caudal ambiental de la fuente receptora y como características de la calidad de agua, los límites máximos permisibles de acuerdo con la legislación ambiental vigente y/o la caracterización teórica asumida para el vertimiento.

- Tasas de Reacción

En la Tabla 6, se presentan las ecuaciones para el cálculo de las tasas de reacción para dichos determinantes. Existe variedad de fórmulas empíricas y analíticas propuestas por investigadores para el cálculo de las tasas de reacción, algunas de las cuales se pueden observar en las páginas 11 a 17 del documento de Metodología de la ANLA (2013).

Tabla 6. Procesos de Degradación y Transformación, según ANLA para determinantes del Grupo 1

DETERMINANTES	PROCESO	TASAS DE REACCIÓN (d^{-1})
Materia orgánica carbonácea (DBO)	Dispersión-advección, descomposición de la DBO kd, sedimentación de la materia orgánica particulada v_s	$k_r = k_d + \frac{v_s}{H}$
Nitrógeno total Kjeldahl (NTK)	Dispersión-advección, nitrificación k_n	k_n
Fósforo total	Dispersión-advección, hidrólisis k_p	k_p
Coliformes fecales	Dispersión–advección, decaimiento por muerte kb	k_b
Sólidos suspendidos totales (SST)	Dispersión–advección, velocidad de sedimentación v_{ss}	$k_s = \frac{v_{ss}}{H}$

H es la profundidad media del agua en el tramo
Fuente: ANLA, 2013

A continuación, se explican los procedimientos utilizado para el cálculo de las tasas de reacción.

A. Tasa de Nitrificación

Según la metodología de la ANLA (2013), Bansal (1976) propone una ecuación para el cálculo de la tasa de nitrificación, en función del número de Reynolds y del número de Froude. Adicionalmente, hay otra alternativa que consiste en tomar valores reportados en la literatura y fue con la cual se trabajó en el presente estudio. En la Tabla 7, se presentan las tasas de nitrificación para cuerpos de agua con diferentes profundidades.

Tabla 7. Tasas de Nitrificación, según ANLA 2013

RÍO	K_n (d^{-1})	PROFUNDIDAD (m)	REPORTADO EN
Mine Brook	8.00	0.2	Tuffey et al. (1974)
Oroua	6.70	0.25	Cooper (1986)
Waiohewa	5.90	0.3	Cooper (1986)
Speed	2.30	0.43	Gowda (1983)
Sweetwater	0.80	0.46	Cooper (1986)
Trace	2.20	0.46	Cooper (1986)
Trukee	2.40	0.51	Bansal (1976)
Grand	1.90	0.58	Bansal (1976)
Shenadoha	1.25	0.60	Deb y Bowers (1983)
Waiotapu	2.80	0.61	Cooper (1986)
Ootanaula	0.80	0.61	Cooper (1986)
Sitll	0.70	0.64	Curtis (1983)
Flint	1.53	0.66	Bansal (1976)
South Chickamauga	6.60	0.84	Cooper (1986)
Upper Mohawk	0.30	0.96	Bansal (1976)
Mud	0.50	1.00	Cooper (1986)
Big Blue	0.12	1.25	Bansal (1976)
Holston	0.23	1.30	Ruane y Krenekel (1977)
Chattahoockee	0.25	1.50	McCutcheon (1987)
Trinity	0.51	1.53	McCutcheon (1987)
Willamette	0.70	1.60	Cooper (1985)
Shenadoha	0.2	1.74	Deb y Bowers (1983)
Upper Mohawk	0.25	2.51	Bansal (1976)
Upper Mohawk	0.25	3.66	Bansal (1976)
Middle Mohawk	0.30	3.81	Bansal (1976)
Barge	0.25	3.9	Bansal (1976)
Anacostia	0.13	4.00	Sullivan y Brown (1988)
Lower Mohawk	0.30	4.25	Bansal (1976)
Seneca river	0.05	6.24	Canale et al (1995)
Ohio	0.25	8.15	Bansal (1976)

Fuente: ANLA, 2013 (tomado de Medina, 2009)

B. Velocidad de Sedimentación

Existen ecuaciones que permiten el cálculo de la velocidad de sedimentación de acuerdo a las características de los sedimentos. Como no se conoce la composición de los sedimentos que van a ser vertidos tanto para vertimientos domésticos como industriales, se adoptó la tabla de la metodología de la ANLA (2013) que presenta velocidades de sedimentación de acuerdo al tamaño de partícula (véase Tabla 8).

Tabla 8. Velocidades de Sedimentación

TIPO DE PARTÍCULA	DIÁMETRO (µM)	VELOCIDAD DE SEDIMENTACIÓN (md^{-1})
Materia orgánica particulada	1-10	0.2
	10-64	1.5
	> 64	2.3
Arcillas	2-4	0.3 – 1
Limos	10-20	3-30

C. Tasa de Decaimiento de Patógenos

De acuerdo con Chapra (1997, en ANLA, 2013) la pérdida de patógenos en corrientes superficiales puede calcularse de acuerdo con la siguiente expresión:

$$k_b = 0.8 * 1.07^{T-20} + \frac{I_0}{0.55 * SST * H} * \ 1 - e^{-0.55*SST*H} \ + F_p * \frac{v_{ss}}{H}$$ *Ecuación 8*

Donde:

T: Temperatura del agua (ºC)
I_0: Radiación solar (ly/hr)
SST: Concentración de sólidos suspendidos totales promedio en el tramo (mg/l)
H: Profundidad media del agua (m)
F_p: Fracción adsorbida de bacterias a las partículas sólidas. Valor típico: 0.7.
V_{ss}: Velocidad de sedimentación de las partículas (md^{-1})
Se puede suponer un valor típico 0,7 para F_p o calcularlo de la siguiente forma:

$$F_p = \frac{K_d SST}{1 + K_d SST}$$ *Ecuación 9*

Donde K_d es el coeficiente de partición (m^3g^{-1}).

- Factores de Asimilación

El cálculo de los factores de asimilación (**a**) se puede realizar de acuerdo con lo que se presenta en la Tabla 9.

Tabla 9. Factores de Asimilación considerados en la Metodología ANLA

DETERMINANTE	FACTOR DE ASIMILACIÓN
DBO	$a_{DBO} = \left[\left(1 + DF \cdot k_r \bar{t}_{DBO}\right) e^{(1-DF) k_r \bar{t}_{DBO}} \right] Q$
NTK	$a_{NTK} = \left[\left(1 + DF \cdot k_n \bar{t}_{NTK}\right) e^{(1-DF) k_n \bar{t}_{NTK}} \right] Q$
FÓSFORO	$a_{PT} = \left[\left(1 + DF \cdot k_p \bar{t}_{PT}\right) e^{(1-DF) k_p \bar{t}_{PT}} \right] Q$
COLIFORMES FECALES	$a_{CF} = \left[\left(1 + DF \cdot k_b' \bar{t}_{CF}\right) e^{(1-DF) k_b' \bar{t}_{CF}} \right] Q$
SST	$a_{SST} = \left[\left(1 + DF \cdot k_S \bar{t}_{SST}\right) e^{(1-DF) k_S \bar{t}_{SST}} \right] Q$ $k_S = \frac{v_{ss}}{H}$

Fuente: Modificado de ANLA, 2013

Con los resultados de tiempo medio de viaje para cada determinante se calculó la longitud de influencia de vertimientos **Liv** como:

$$\boldsymbol{Liv} = t.v \qquad \textit{Ecuación 10}$$

4.3.2. Streeter-Phelps

Es un modelo matemático que relaciona el abastecimiento de oxígeno disuelto en una corriente de agua, cuando este recibe una descarga de materia orgánica. Este modelo representa dos procesos: la re-aireación y la descomposición bacterial en la fase líquida. De acuerdo con Rojas Aguirre (2011) para la modelación del comportamiento del oxígeno disuelto ante la aplicación de una carga orgánica, es fundamental considerar dos ecuaciones: la ecuación de decaimiento de la materia orgánica y la del comportamiento del oxígeno, aguas abajo del punto de vertimiento.

4.3.2.1. Definición de Variables

D: El déficit de oxígeno es la diferencia entre el nivel actual de oxígeno en el cuerpo de agua y el oxígeno de saturación.

O_s: El oxígeno de saturación es la cantidad máxima de oxígeno que un cuerpo de agua puede tener a una temperatura determinada.

C: Es la concentración de DBO en el cuerpo de agua en mg/L.

4.3.2.2. Proceso de Modelación

Con el objetivo de establecer el comportamiento del oxígeno disuelto en el tramo de estudio de los vertimientos analizados, en primer lugar, fue necesario establecer la tasa de re-aireación y la tasa de descomposición de la DBO. A continuación, se explica el procedimiento empleado.

- Tasa de Re-aireación

De acuerdo con Rodríguez (1983) la re-aireación depende de la concentración de saturación de oxígeno (depende de la temperatura y concentración salina) y la concentración de oxígeno presente y a su vez depende de las características de la corriente como son la velocidad, profundidad, temperatura e intervalo de mezcla.

La tasa de re-aireación se determina de acuerdo con el tipo de corriente, es decir si es un rio de planicie o de alta montaña y sus condiciones hidrodinámicas. Los tramos de estudios de los cuerpos de agua receptores en este proyecto vial presentan características de ríos de montaña, por tanto, se empleó las ecuaciones propuestas por Chapra (1977) en la metodología de ANLA (2013) para este tipo de corrientes.

Cuando la corriente bajo estudio es característica de montaña (e.g. Holguín, 2003; Arenas, 2005; Gélvez y Camacho, 2008), se recomienda utilizar la siguiente expresión formulada por Tsivoglou y Neal (1976, tomado de Chapra, 1997):

$$k_a = c\frac{\Delta H}{t}$$ *Ecuación 11*

Siendo **ΔH** el cambio en la elevación de la superficie del agua en metros en un subtramo seleccionado y **t** el tiempo medio de viaje en días en el elemento, calculado como el cociente entre la longitud y la velocidad media del agua en el subtramo. La constante depende del caudal y se define de la siguiente forma:

$$c = 0.36 \text{ para } 3\ 0.028\ 0.28 \leq \leq Q\ m\ s$$
$$c = 0.177 \text{ para } 3\ 0.708\ 85 \leq \leq Q\ m\ s$$

Por su parte la tasa de desoxigenación se calculó a partir de la tasa de desoxigenación de acuerdo a las características de la corriente receptora (véase Tabla 10).

Tabla 10. Relación entre la Tasa de Re-aireación y la de Desoxigenación

CUERPO DE AGUA	RANGO DE KA/KD
Reservorio o lago pequeño	0.5 – 1.0
Curso lento, lago grande	1.0 – 2.0
Río grande y lento	1.5 – 2.0

CUERPO DE AGUA	RANGO DE KA/KD
Río grande con velocidad de flujo mediana	2.0 – 3.0
Curso rápido	3.0 – 5.0
Rápidas y caídas de agua	> 5.0

Fuente: Corporación Autónoma Regional del Valle del Cauca (s.f.)

Posteriormente, se calculó el oxígeno disuelto de saturación con la siguiente ecuación, donde T es la temperatura del agua en ºC:

$$OD_S = 14{,}61996 - 0{,}40420 * T + 0{,}00842 * T^2 - 0{,}00009 * T^3$$ *Ecuación 12*

Con la información de las tasas de aireación y de desoxigenación y con el oxígeno de saturación, además de la información de calidad de agua de la fuente receptora y los vertimientos, se procedió a la calcular la variación de la carga orgánica (expresada como DBO) en función de la distancia. Para tal fin se aplicó la siguiente ecuación:

$$DBO = DBO_o * e^{-k_d x/v}$$ *Ecuación 13*

Donde:

DBO_o: Concentración de DBO en x=0 (mg/m^3)
K_d: Tasa de descomposición de la DBO (d^{-1})
x: Distancia (m)
***v*:** Velocidad media de la fuente receptora (m/día)

Con el cálculo de la DBO se calculó el comportamiento del déficit de oxígeno a lo largo del tramo receptor (*DO*), es decir en función de la distancia, de acuerdo a la siguiente ecuación:

$$DO = \frac{K_d}{k_a - k_d} DBO_o \quad e^{-\frac{k_d x}{v}} - e^{-\frac{k_a x}{v}} + DO_o e^{-k_a x/v}$$ *Ecuación 14*

Donde:

DO_o: Déficit de oxígeno en x=0 (mg/m^3)

Finalmente, con el déficit de oxígeno ***DO*** y el oxígeno de saturación ***OD_s***, se calculó el oxígeno disuelto en la fuente receptora, ya que el oxígeno equivale a la diferencia entre el oxígeno de saturación y el déficit de oxígeno para cada punto en el tramo del río afectado por el vertimiento.

Este proceso es iterativo y termina cuando la concentración de oxígeno es igual a la concentración de oxígeno disuelto en el cuerpo de agua receptor antes del vertimiento. En otras palabras, esto equivale a la distancia donde se recuperan las condiciones de oxígeno basales.

4.4. Resultados

En esta sección se presenta el análisis de resultados de los determinantes de calidad de agua establecidos de acuerdo a la metodología de la ANLA (2013), en los vertimientos domésticos e industriales del proyecto vial Doble Calzada Rumichaca – Pasto Tramo San Juan - Pedregal. El objetivo principal de esta sección es determinar la longitud de influencia para cada determinante y vertimiento.

Las hojas de cálculo en las que se desarrolló la modelación para cada uno de los vertimientos domésticos e industriales en etapa de construcción y operación se presenta en el Anexo 2.

Adicionalmente, para realizar la modelación fue necesario conocer las características hidráulicas, fisicoquímicas y microbiológicas de cada una de las fuentes hídricas receptoras de vertimientos, tal como se presenta en la Tabla 11.

Tabla 11. Características Hidráulicas, Fisicoquímicas y Bacteriológicas de la Fuente Receptora

PARÁMETRO	UNIDAD	CUERPO RECEPTOR			
		Río Boquerón	Qda. La Humeadora	Río Guaitara	Río Sapuyes
Oxígeno Disuelto	mg/L O_2	8.1	7.8	9.2	8.4
Temperatura del agua	°C	15	13.7	15.4	18
pH		7.19	7.9	7.64	7.72
Conductividad	µS/cm	108.29	221.13	98.25	90.55
Aceites y grasas	mg/L	0.67	0.67	0.67	0.67
DBO5	mg/L O_2	5	5	5	5
DQO	mg/L O_2	20	20	20	20
Fósforo Total	mg/L P	0.062	0.062	0.062	0.062
Nitrógeno Total Kjeldahl	mg/L N	3	3	3	3
Nitrógeno Amoniacal	mg/L NH_4-N	1	1	1	1
Nitratos	mg/L NO_3-N	1.64	1.46	0.853	1.51
Nitritos	mg/L NO_2-N	0.191	0.133	0.014	0.012
Sólidos Suspendidos Totales	mg/L	46	10	88	21
Sólidos Sedimentables	mg/L	0.1	0.10	0.1	0.2
Coliformes Fecales	NMP/ 100ml	488	224	452	308
Coliformes Totales	NMP/ 100ml	5554	4250	5050	4540
Caudal	m^3/s	1.16	0.15	20.37	8.02
Profundidad media	m	0.68	0.31	1.22	0.69
Pendiente del lecho	m/m	0.07211028632	0.00831198253	0.022805049088	0.06587615283
Velocidad media	m/s	0.34	0.27	0.71	0.75
Velocidad máxima	m/s	0.44	0.35	0.92	0.98

Fuente: QHSE SAS, 2017

A continuación, en la Tabla 12, se presentan los resultados obtenidos en la modelación para los vertimientos generados en la Batería Churuyaco.

Tabla 12. Longitud de Asimilación del Vertimiento

FUENTE RECEPTORA	DISTANCIA DE ASIMILACIÓN DE CADA DETERMINANTE (m)					
	N	OD	DBO	P	SST	CF
Quebraba La Humeadora	990.61	4000	76.01	855.76	2.86	9586.50
Río Boquerón	1247.44	4000	95.71	1077.62	3.60	12071.89
Río Guaitara	2604.94	4000	199.87	2250.32	7.52	25208.94
Río Sapuyes	2751.70	4000	211.13	2377.10	7.94	26629.16

Respecto a los vertimientos y los determinantes que definen su composición se puede decir sobre el nitrógeno, que este elemento está presente en cuerpos de agua superficial y puede existir en cuatro formas diferentes: nitrógeno orgánico, amoniacal, nitritos y nitratos. Las dos primeras son las más comúnmente encontradas en agua residual sin tratar. En el tratamiento de aguas residuales domésticas se emplea el término de nitrógeno total Kjeldahl, que es la suma de nitrógeno orgánico y amoniacal y esta fracción representa aproximadamente la quinta parte de la DBO.

Este elemento sufre procesos de transformación como la nitrificación y la desnitrificación. En la nitrificación el amonio se convierte en nitrato con la ayuda de dos grupos de bacterias: las oxidantes de amonio y las oxidantes de nitrito. Por su parte en la desnitrificación el nitrato se convierte a nitrógeno gaseoso (Pérez-Peláez, *et al*., 2011).

En la nitrificación hay consumo de oxígeno, ya que las bacterias obtienen energía de la oxidación de las diferentes especies de nitrógeno. En la primera etapa de la nitrificación el amonio se transforma a nitritos:

$$NH_4^+ + 1.5O_2 \rightarrow NO_2^- + H_2O + 2H^+$$

En la segunda fase de la nitrificación, las bacterias nitrobacter oxidan los nitritos a nitratos:

$$NO_2^- + 1.5O_2 \rightarrow NO_3^-$$

De acuerdo con las reacciones anteriores el consumo de oxígeno disuelto en la etapa de nitrificación es de 4.57 gramos por cada gramo de nitrógeno (Medina, *et al*., 2008).

Según la metodología de la ANLA (2013), Bansal (1976) propone una ecuación para el cálculo de la tasa de nitrificación, en función del número de Reynolds y del número de Froude. Adicionalmente, hay otra alternativa que consiste en tomar valores reportados en la literatura y fue con la cual se trabajó en el presente estudio.

De acuerdo con Chapra (1997, en ANLA, 2013) la tasa de nitrificación está en un rango de 0.1 a 0.5 d^{-1} para aguas profundas, mientras que para aguas someras es común encontrar valores por encima de $1d^{-1}$. De esta manera con los datos de entrada según la norma vigente, se determinó para cada cuerpo receptor del vertimiento la tasa de nitrificación. En este caso, conforme a la profundidad mínima (**H_{min}**) para caudal mínimo, los cuerpos de agua receptores son someros y por tanto la tasa de nitrificación se asumió entre 2 y $10d^{-1}$.

Como se presentó en la Tabla 12, las longitudes de asimilación del vertimiento en la fuente receptora, permite establecer que este cuerpo de agua puede asimilar el nitrógeno de manera adecuada.

Respecto al oxígeno disuelto se puede decir que este es uno de los más importantes gases en los cuerpos de agua superficial y se caracteriza por su participación en diferentes procesos, en donde se consume por la actividad química y biológica. En el caso particular de las aguas residuales, dada la elevada carga orgánica el oxígeno es consumido en el proceso de degradación de la misma. Sin embargo, la concentración de oxígeno en el agua residual antes de su vertimiento depende del tipo de tratamiento al cual es sometida.

Dada su importancia en el cuerpo de agua superficial, se determinó la longitud que necesita el cuerpo de agua receptor para alcanzar las condiciones base. Aunque este cuerpo de agua requiere hasta 4.0 km, se encontró que el cuerpo de agua puede asimilar las cargas y retornar a condiciones adecuadas de concentración de oxígeno. Vale la pena mencionar que estas distancias se encuentran dentro del área de influencia del proyecto.

Por otra parte, en relación a la DBO, se debe mencionar que este es uno de los parámetros de mayor importancia en el estudio y caracterización de aguas no potables, ya que además de indicar la presencia y biodegradabilidad del material orgánico presente, es una forma de estimar la cantidad de oxígeno que requiere para estabilizar el carbono orgánico y de saber con qué rapidez el material va a ser metabolizado por las bacterias que normalmente se encuentran presentes en aguas residuales. Para este determinante, la tasa de consumo de oxígeno K_d se calculó a partir de la tasa de re-aireación o empleado la ecuación de Wright y McDonnell (1979, modificada de Bowie et al., 1985) que se presenta en la metodología de la ANLA. Según los resultados de la longitud de asimilación para este determinante, se encontró una distancia máxima de 310 m, por lo cual se puede decir que la asimilación es casi inmediata.

Otro de los determinantes de calidad de agua analizados corresponde al fósforo, el cual según Roldán y Ramírez (2008) afirman que en cuerpos de agua el fósforo se encuentra principalmente como ortofosfatos (PO_4^{3-}), cuya fuente principal son las rocas ígneas. Además, hay fuentes antrópicas como las aguas residuales domésticas, principalmente como consecuencia del uso de detergentes, y los fertilizantes.

De acuerdo con la metodología de la ANLA (2013), los procesos dominantes en la asimilación de la carga de fósforo son la dispersión, advección y la hidrólisis. La hidrólisis de fósforo es un proceso lento, por lo tanto, los principales medios de eliminación se dan a través de la mezcla. No se tienen fórmulas que permitan calcular la tasa de hidrólisis de manera rápida.

Según los resultados, se encontró longitud considerable de asimilación (hasta 4.0 km) para que se alcance la adecuada asimilación, sin embargo, es importante mencionar que estas distancias también se encuentran dentro del área de influencia del proyecto.

También es importante resaltar que estos resultados corresponden al escenario caudal mínimo de la fuente receptora y límite máxima permisible en el vertimiento, por tal razón de acuerdo al modelo aplicado, las longitudes calculadas serán menor cuando el caudal se incremente. Esto ocurrirá siempre y cuando el volumen de agua actúe diluyendo la carga que trae naturalmente el río.

Sobre los sólidos suspendidos, como su nombre lo indica se refieren a las partículas orgánicas e inorgánicas fácilmente separables del líquido por sedimentación, centrifugación o filtración. Dentro del tratamiento de aguas residuales domésticas, los sólidos suspendidos son retenidos en

sedimentadores, donde se depositan en el fondo de dichas estructuras de acuerdo a su tamaño, forma y peso. Suponiendo que las partículas tienen un diámetro entre 10 y 20 µm, y teniendo en cuenta la metodología de la ANLA (2013), se asumió que las partículas tienen una velocidad de sedimentación de 0.008 m/s.

En este caso se presentan una adecuada asimilación de los sólidos suspendidos en las fuentes receptoras, por lo que se puede decir que estos cuerpos de agua poseen las características adecuadas para dispersarlos rápidamente.

Finalmente, respecto a los coliformes fecales se puede decir que corresponden a grupos de bacterias presentes en aguas residuales. El decaimiento de estos organismos en los cuerpos de agua se produce por procesos de sedimentación, precloración, variedad de especies de algas, altos valores de pH, radiación solar, potencial de oxidación, temperatura y limitación de nutrientes.

De acuerdo con la metodología de la ANLA (2013) para este estudio en particular se consideró la dispersión, advección, sedimentación y el decaimiento por la acción de la radiación solar. Bajo esta consideración los resultados de las longitudes de asimilación de la carga de coliformes fecales en el vertimiento presentan longitudes de asimilación considerables. En este sentido es importante mencionar que se consideró que el 70% de los coliformes se adsorben a las partículas sólidas por lo que el 30% restante requiere es requiere la distancia presentada en la Tabla 12.

De igual manera el factor de asimilación de la carga podría ir cambiando en caso de que existan aportes naturales de coliformes por efecto de la escorrentía, lo cual disminuiría el factor de asimilación y por tanto la longitud de afectación del vertimiento.

5. Conclusiones

La utilización de un modelo de simulación representa un avance respecto a la aplicación de nuevas metodologías para el diagnóstico y la prevención de la contaminación del agua de los ríos.

El modelo representa adecuadamente los procesos fisicoquímicos y biológicos en el tramo de río considerado.

En las condiciones actuales, los valores de oxígeno disuelto y demanda biológica de oxígeno se encuentran dentro de valores adecuados. No se observa contaminación en los cuerpos de agua existiendo una autodepuración natural producto de las características hidráulicas del mismo.

El modelo de simulación constituye en una herramienta muy apropiada para la programación/reprogramación de un plan de monitoreo dado que la continuidad espacial de sus resultados puede advertirnos puntos críticos que no necesariamente el plan de monitoreo puede indicar.

De acuerdo con los resultados los determinantes que requieren una mayor longitud de asimilación son los coliformes fecales, el oxígeno disuelto y el fósforo. A pesar de las distancias de asimilación que demuestran en algunos casos que esta asimilación no es inmediata, se debe resaltar que las longitudes en todos los casos se encuentran dentro del área de influencia del proyecto.

Como se mencionó, es importante resaltar que estos resultados corresponden al escenario caudal mínimo de la fuente receptora y límite máximo permisible en el vertimiento, por tal razón de acuerdo al modelo aplicado, las longitudes calculadas serán menores cuando el caudal de la fuente se incremente. Esto ocurrirá siempre y cuando el volumen de agua actúe diluyendo la carga que trae naturalmente el río.

Las condiciones en las fuentes hídricas modeladas presentan condiciones de caudal permanente y semipermanente, que les permiten mantener capacidad de asimilación de la carga aportante por efecto del vertimiento de las aguas residuales tratadas. Los resultados de concentraciones obtenidas en la aplicación de los modelos de calidad del agua indican que la corriente mantiene su capacidad para asimilar del vertimiento, en condiciones de caudales críticos.

Al realizar el análisis del modelamiento y con los resultados de laboratorio obtenidos en cuanto a la calidad de agua de las fuentes y a la caracterización teórica del vertimiento (presuntiva), es evidente que el recurso cumple con los criterios establecidos en el Decreto 1076 de 2015 y que el vertimiento no afecta ninguno de ellos.

6. Referencias Bibliográficas

1. ANLA. 2013. Metodología para la definición de la Longitud de Influencia de Vertimientos sobre corrientes de agua superficial.

2. Bowie, L. G., Mills, W. B., Porcella, D. B., Campbell, C. L., Pagenkopf, J. R., & Rupp, G. L. (1985). Rates, constants, and kinetics formulations in surface water quality. Athens, Georgia: U.S. Environmental Protection Agency.

3. Brown, L. C. & Barnwell, T. 1987. The Enhanced Stream Water Quality Models QUAL2E and QUAL2E-UNCAS. Documentation and User's Manual. U.S. Environmental Protection Agency. Athens. G.A. Report EPA/600/3-87/007,189 p.

4. Camacho, L. A., Díaz-Granados, M., & Lombana, C. (2003). Diseño y desarrollo de un marco jerárquico de modelación del flujo, transporte de solutos y calidad del agua para el manejo integral del Caño Rubiales. Seminario Internacional La Hidroinformática en la Gestión Integrada de los Recursos Hídricos.

5. Camacho, L.A., Díaz-Granados, M. (2002). Metodología para la obtención de un modelo predictivo de transporte de soluto y de la calidad de agua en ríos- Caso río Bogotá. Seminario Internacional La Hidroinformática en la Gestión Integrada de los Recursos Hídricos Universidad del Valle/Instituto Cinara.

6. Chapra Steven C. Surface Water Quality Modeling, McGraw-Hill, pág 493, 1997.

7. Churchill, M.A., Elmore, H.L., and Buckingham, R.A. The prediction of stream reaeration rates. J. Sanit. Engrg. Div., ASCE, 88{4),1-46, 1962.

8. Cox, B. (2003). A review of currently available in-stream water-quality models and their applicability for simulating dissolved oxygen in lowland rivers. The Science of the total environment, 314-316, 335-377.

9. Dominguez, E. Notas de Clase, Modelación de procesos ecohidrológicos, Maestría en Hidrosistemas, Pontificia Universidad Javeriana, 2006

10. Fisher H. B., List, E. J., Koh, R. C. Y., Imberger, J. y Brooks, N. H. Mixing in Inland and Coastal Waters, Academic Press, New York, 1979.

11. García H. y Obregón N. Modelación de la Calidad del Agua en Corrientes Naturales mediante Sistemas No Lineales Acoplados, Maestría en Hidrosistemas, Pontificia Universidad Javeriana, 2008.

12. Jobson H. Modeling Water Quality in Rivers Using the Branched Lagrangian Transport Model (BLTM), USGS, 2001.

13. Jobson H., and Shoellhamer D. User Manual For a Branched Lagrangian Transport Model: U.S. Geological Survey Water-Resources Investigation Report 87-4163, pág. 80, 1987.

14. Jorgensen S. E. and Bendoricchio G. Fundamental of Ecological Modelling, Third Edition, Elsevier Science, pág. 24, 2001.

15. Kannel, P., Kanel, S., Lee, S., Lee, Y., & Gan, T. Y. (2011). A review of public domain water quality models for simulating dissolved oxygen in rivers and streams. Environmental Modeling & Assessment, 16, 183-204.

16. Kiely Gerard, Ingeniería Ambiental, Fundamentos, Entornos, Tecnología y Sistemas de Gestión, Volumen III, McGraw-Hill, pág. 1218, 1229. 1999.

17. Liu, H. 1977. Predicting Dispersion Coefficient of Streams. Joumal ofthe Environmental Engineering Division, ASCE. Vol103, No EEl.

18. Martínez A., Gálviz A., y Holguín J. Optimización de la Modelación de la Calidad del Agua del Río Cauca. Tramo: La Balsa – Anacaro, Seminario Prevención y Control de la Contaminación del Recurso Hídrico, 2007.

19. Metcalf & Eddy, Inc.1991.Wastewater Engineering: Treatment, Disposal and Reuse, 3d Ed. McGraw-Hill, New York.

20. O'Connor, D.J., and Dobbins, W.E. Mechanism of Reaeration in Natural Streams. Trans. ASCE, 123, 641-684, 1958.

21. Owens, M., Edwards, R.W., and Gibbs, J.W. Some Reaeration Studies in Streams. Int. J. Air and Water Pollution, 8, 469-486, 1964.

22. Pelletier, G., & Chapra, S. C. (2008). QUAL2Kw user manual (version 5.1). A modeling framework for simulating river and stream water quality. Olympia, Washington.

23. Refsgaard, J. C., Sluijs, J. P., Højberg, A. L., & Vanrolleghem, P. A. (2007). Uncertainty in the environmental modelling process – A framework and guidance. Environmental Modelling & Software, 22, 1543-1556.

24. Rutherford, J. C. (1994). River mixing. New York: John Wiley & Sons.

25. Ruza, J et al, “Manual para la gestión de vertidos”, Ministerio del Medio Ambiente, RESOLUCIÓN DIRECCIONAL No 008-97EM/DGAA, España, 2007.

26. Sierra R., Carlos A., “Calidad del agua – Evaluación y diagnóstico”, Editorial de la U, Medellín, 2011.

27. Shanahan P., Hense M., Koncsos L., Rauch W., Reichert P., Somlyódy, L., and Vanrollghem P. River Water Quality Modelling: III Problems of The Art, Wat. Sci. Tech, 1998.

28. Shanahan P., Borchardt D., Henze M., Rauch W., Reichert P., Somlyódy L. y Vanrolleghem P. (1998). River water quality No 1: I. Modeling Approach. Wat. Sci. Tech, 38, 245-252.

29. Suárez J., Modelos de Calidad del Agua, Master en Ingeniería del Agua, Universidad de la Coruña, 2008.

30. Thomann V., Mueller John. Principles of Surface Water Quality Modeling and Control. Harper & Row, New York, 1987

31. Universidad Politécnica de Valencia. Modelación de la calidad del agua. Departamento de ingeniería hidráulica y medio ambiente. Miguel Martín Monerris. Paula Manzal Doménech. 2000.

32. Wang, Q., Li, S., Jia, P., Qi, C., & Ding, F. (2013). A Review of Surface Water Quality Models. Retrieved from http://www.hindawi.com/journals/tswj/2013/231768/abs/

ANEXOS TÉCNICOS

ANEXO 1

METODOLOGÍA ANLA 2013

ANEXO 3

METODOLOGÍA PARA LA DEFINICIÓN DE LA LONGITUD DE INFLUENCIA DE VERTIMIENTOS SOBRE CORRIENTES DE AGUA SUPERFICIAL

AUTORIDAD NACIONAL DE LICENCIAS AMBIENTALES (ANLA)
SUBDIRECCIÓN DE INSTRUMENTOS, PERMISOS
Y TRÁMITES AMBIENTALES
ENERO DE 2013
BOGOTÁ D.C.

Contenido

1 Introducción 4
2 Definiciones 4
3 Criterios 5
3.1 Caracterización hidrológica y climatológica 5
3.2 Caracterización hidráulica 5
3.3 Caracterización de la calidad del agua y usos del agua 6
4 Metodología 6
4.1 Esquema general 6
4.2 Paso 1. Estimación del caudal ambiental 7
4.3 Paso 2. Caracterización hidráulica de la corriente 8
4.4 Paso 3. Caracterización de la calidad del agua del cuerpo receptor y del vertimiento 8
4.5 Paso 4. Cálculo de factores de asimilación y de la longitud de influencia directa 10
4.5.1 Esquema general de cálculo 10
4.5.2 Factor de asimilación por determinante 11
4.5.2.1 Estimación de tasas de reacción de determinantes convencionales de la calidad del agua 11
4.5.2.1.1 Tasa de reaireación k_a 13
4.5.2.1.2 Tasa de desoxigenación o descomposición de la DBO k_d 13
4.5.2.1.3 Tasa de nitrificación k_n 14
4.5.2.1.4 Velocidades de sedimentación v_s y v_{ss} 15
4.5.2.1.5 Tasa de decaimiento por muerte de patógenos k'_b 17
4.5.2.2 Estimación de tasas de reacción de sustancias tóxicas y metales pesados 17
4.5.2.2.1 Fracciones y coeficientes de partición 18
4.5.2.2.2 Velocidad de volatilización v_v 19
4.5.2.2.3 Otras tasas 21
4.5.2.3 Resumen de factores de asimilación 21
4.6 Paso 5. Cálculo de la carga total y recálculo de la LIV 24
5 Referencias bibliográficas 24

Lista de Figuras

Figura 1 Esquema general de la metodología en relación a la información requerida.....7
Figura 2 Velocidad de sedimentación para sedimentos no cohesivos.....16
Figura 3 Gráfica de fracción disuelta y fracción particulada versus coeficientes de partición (Chapra, 1991).....19
Figura 4 Gráfica de velocidad de volatilización contra constante de Henry (Chapra, 1991)....20

Lista de Tablas

Tabla 1 Procesos de degradación y transformación considerados en la metodología.....12
Tabla 2 Ecuaciones de reaireación para ríos de planicie.....13
Tabla 3 Tasas de nitrificación reportadas por Pauer y Auer (2009, tomado de Medina, 2009) 14
Tabla 4 Velocidades de sedimentación medidas para diferentes tipos y tamaños de partículas 15
Tabla 5 Factores de asimilación para los determinantes de calidad del agua considerados en la metodología 21

1 Introducción

En este documento se presentan los criterios y lineamientos que se deberán seguir para definir la longitud de influencia (LIV) debida a la realización de vertimientos directos de aguas residuales domésticas y/o industriales sobre cuerpos de agua superficiales en proyectos, obras o actividades sujetos a licenciamiento ambiental por parte de la Autoridad Nacional de Licencias Ambientales – ANLA. Los criterios utilizados para la definición de la LIV se refieren a aspectos hidrológicos, hidráulicos y de la calidad del agua de los cuerpos receptores; estos permitirán definir la longitud sobre la corriente receptora aguas abajo del punto de vertimiento que se considera directamente afectada por la descarga de las aguas residuales del proyecto, obra o actividad. El instrumento que se utilizará para el cálculo de dicha longitud es el factor de asimilación (UN-MAVDT, 2008; Rojas, 2011) de la corriente requerido para que esta recupere sus condiciones de calidad del agua sin vertimiento o para que se alcancen aguas abajo los objetivos y metas de calidad dispuestos por la autoridad ambiental competente. La longitud de influencia directa estimada corresponderá al tramo total sobre la corriente que deberá considerarse para la modelación de su capacidad de asimilación y sobre el cual el usuario deberá hacer seguimiento durante el desarrollo del proyecto en caso de que el permiso correspondiente sea otorgado.

2 Definiciones

Caudal ambiental (Q_{amb}): volumen de agua necesario en términos de calidad, cantidad, duración y estacionalidad para el sostenimiento de los ecosistemas acuáticos y para el desarrollo de las actividades socioeconómicas de los usuarios aguas abajo de una fuente.

Carga contaminante (W): cantidad de sustancia contaminante por unidad de tiempo. Se calcula como el producto entre el caudal vertido Q_v y la concentración de la sustancia contaminante vertida c_v,

$$W = Q_v \cdot c_v \qquad [1]$$

Factor de asimilación (a): razón entre la carga del contaminante W a la entrada del tramo y la concentración resultante aguas abajo c sobre el cuerpo receptor (Chapra, 1997),

$$a = \frac{W}{c} \qquad [2]$$

Tiempo de arribo (τ): tiempo que tarda una sustancia disuelta en ser conducida exclusivamente por el movimiento del medio solvente (advección). Se puede estimar a partir de ensayos con trazadores o aproximadamente como la razón entra la longitud del tramo L y la velocidad máxima del agua v_{max} en la sección transversal de la corriente.

$$\tau = \frac{L}{v_{max}} \qquad [3]$$

Tiempo medio de viaje ($\bar{t}$): tiempo que tarda una sustancia disuelta en ser conducida por el movimiento del medio y ser dispersada. Se puede estimar a partir de ensayos con trazadores o aproximadamente como la razón entre la longitud del tramo L y la velocidad media del agua $\bar{v}$,

$$\bar{t} = \frac{L}{\bar{v}} \qquad [4]$$

Tiempo de residencia (T_r): tiempo que tarda una sustancia disuelta en ser dispersada por efecto de las zonas muertas o almacenamiento temporal y la dispersión longitudinal de la corriente principal. Se calcula como la diferencia entre el tiempo medio de viaje y el tiempo de arribo.

$$T_r = \bar{t} - \tau \qquad [5]$$

Fracción dispersiva (*DF*): representa la fracción del volumen total del tramo que participa en el flujo que se considera completamente mezclada, o la fracción del tiempo de retención en el cual la sustancia disuelta es dispersada. Un valor de DF de 0 representa advección pura y de 1, dispersión pura. Se puede estimar a partir de ensayos con trazadores de la siguiente forma (Camacho y Lees, 2000):

$$DF = 1 - \frac{\tau}{\bar{t}} \qquad [6]$$

También se puede estimar, de manera aproximada, utilizando las velocidades medias $\bar{v}$ y máximas v_{max} del agua medidas en la sección transversal en el tramo de la corriente:

$$DF = 1 - \frac{\bar{v}}{v_{max}} \qquad [7]$$

3 Criterios

3.1 Caracterización hidrológica y climatológica

El análisis de factores de asimilación se debe hacer considerando el escenario más crítico sobre el cuerpo de agua receptor. Generalmente, este corresponde a condiciones de caudal mínimo sobre la corriente y carga máxima en el vertimiento. Para esta metodología, se define el caudal ambiental como el indicador que representa las condiciones de caudal mínimo sobre el cuerpo de agua.

También es necesaria información meteorológica como velocidad del viento, radiación solar y altitud en la zona del punto proyectado de vertimiento para la estimación de algunos parámetros en la metodología.

3.2 Caracterización hidráulica

Para la estimación de los tiempos de viaje, es necesario conocer las características hidrodinámicas de la corriente bajo condiciones de caudal mínimo o ambiental. Para este

propósito se deben determinar curvas de calibración que relacionen estas propiedades con el caudal para secciones transversales representativas sobre la corriente.

3.3 Caracterización de la calidad del agua y usos del agua

Se deben determinar las condiciones representativas de la calidad del agua de la corriente sin intervención, sobre el sitio de vertimiento propuesto. Igualmente se deben indicar las condiciones de caudal y concentración más críticas (valores máximos) del vertimiento sin tratamiento, teniendo en cuenta que para la determinación de la LIV se consideran las condiciones más desfavorables para el cuerpo receptor. También se deben conocer las metas y objetivos de calidad establecidos por la autoridad ambiental para la corriente o cuenca (si están disponibles), de acuerdo con los usos actuales y prospectivos del recurso hídrico. En caso de no contar con algunos o con la totalidad de estos estándares de calidad ambiental, se podrán utilizar los establecidos a nivel nacional o por otras organizaciones o entidades a nivel internacional.

También es necesaria una caracterización básica de los sedimentos suspendidos en la corriente receptora que consiste en su densidad y granulometría (o hidrometría).

4 Metodología

En esta sección se presenta el procedimiento que se debe seguir para estimar la distancia aguas abajo del punto de vertimiento sobre la corriente receptora que se considera directamente afectada por la descarga de aguas residuales del proyecto sujeto a licenciamiento.

4.1 Esquema general

En la Figura 1 se presenta el esquema general para implementar la metodología en relación a la información requerida para completar cada paso. Es importante señalar que toda la información necesaria para estimar la longitud de influencia directa sobre corrientes superficiales debido a vertimientos de aguas residuales se solicita en los términos de referencia para el levantamiento de la línea base y para la modelación de la capacidad de asimilación de los cuerpos receptores.

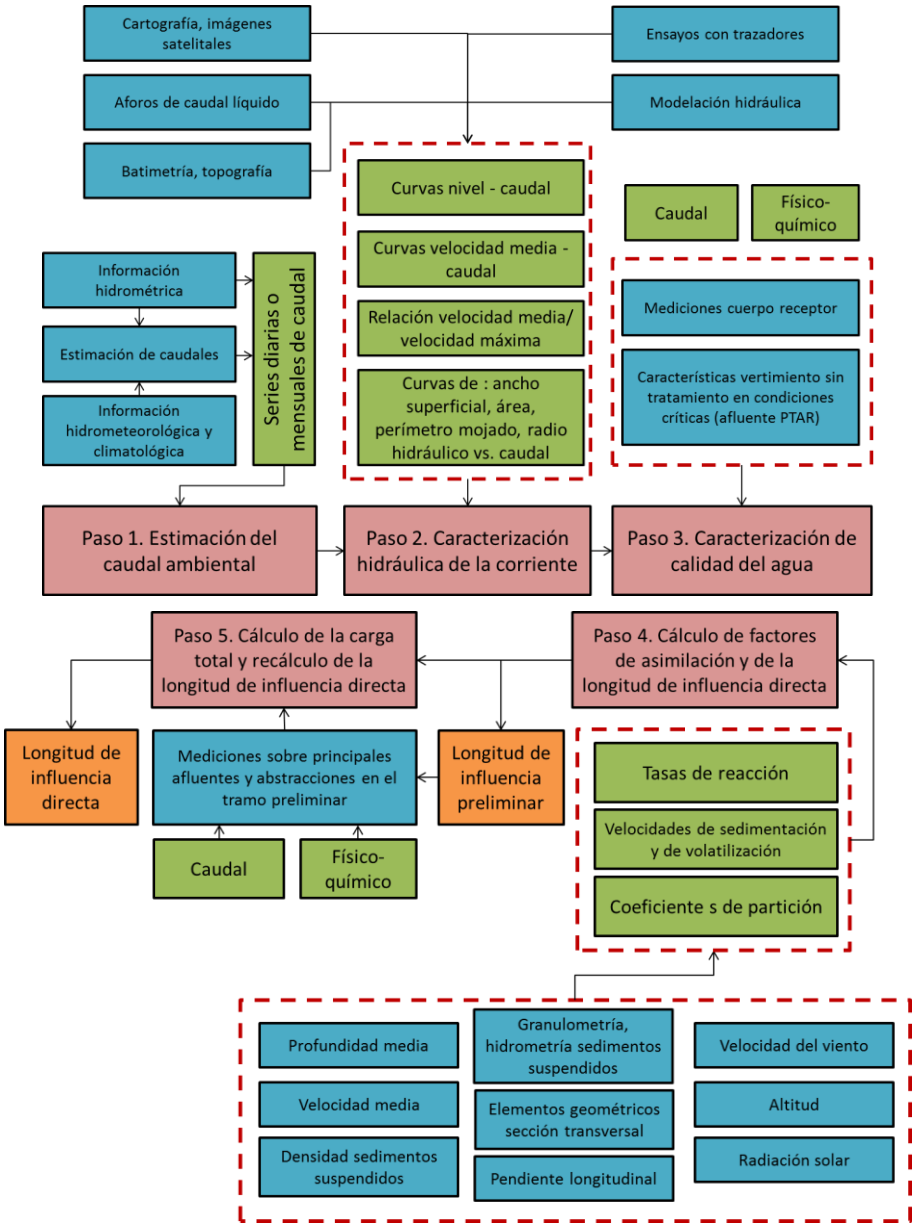

Figura 1 Esquema general de la metodología en relación a la información requerida

4.2 Paso 1. Estimación del caudal ambiental

Se deberá estimar el caudal ambiental de la corriente en el punto de vertimiento. Para la aplicación de la presente metodología, el caudal ambiental se podrá calcular de manera aproximada como el valor máximo entre el índice 7Q10 utilizando caudales medios diarios, el Q95% de la curva de duración de caudales (CDC) medios diarios y 0.25 veces el caudal medio mensual (QMM) del mes más seco. Las series de tiempo utilizadas deberán tener un período

mínimo de 10 años de información y deberán someterse previamente a análisis de homogeneidad, consistencia y llenado. En el caso que no se disponga de información a nivel diario, el caudal ambiental será el valor máximo entre el Q95% de la CDC medios mensuales y 0.25 veces el QMM del mes más seco. Si no está disponible información oficial de series de caudales, se podrán implementar métodos indirectos de estimación de caudales (técnicas de regionalización, correlaciones hidrológicas, relaciones área-precipitación-caudal, modelos de simulación hidrológica, entre otros) debidamente sustentados.

4.3 Paso 2. Caracterización hidráulica de la corriente

El cálculo de los factores de asimilación requiere la estimación del tiempo medio de viaje y del tiempo de primer arribo. Esto se puede hacer, para un rango amplio de caudales, mediante la realización de ensayos con trazadores, información de campo (aforos y levantamiento de secciones transversales representativas) o modelación hidráulica. De cualquier forma, se deben obtener las características hidrodinámicas de la corriente como la profundidad del agua, la velocidad media y la velocidad máxima. Se debe tener en cuenta que estas características varían con el caudal y dependen de la geometría de la corriente (ancho superficial, área, perímetro mojado, radio hidráulico). Por tal motivo, se debe obtener la curva de calibración en función del caudal que describa la variación del nivel del agua (medido desde el punto más bajo de la sección transversal) y la velocidad media bajo diferentes condiciones de flujo y establecer la relación entre la velocidad media y la velocidad máxima. También se deberán obtener las curvas que describan la variación de los principales elementos geométricos (ancho superficial, área, perímetro mojado, radio hidráulico) con el caudal.

Utilizando el caudal ambiental calculado en el paso 1, la curva de calibración velocidad media - caudal y la relación $v_{max}/\bar{v}$, se obtiene la velocidad media y máxima correspondiente para las condiciones de caudal mínimo o ambiental sobre la corriente. La fracción dispersiva DF se puede estimar directamente a partir de ensayos con trazadores o calcular aplicando la ecuación [7].

4.4 Paso 3. Caracterización de la calidad del agua del cuerpo receptor y del vertimiento

Para el cálculo de los factores de asimilación *requeridos* para que el cuerpo de agua receptor recupere sus condiciones de calidad de agua sin vertimiento, se debe conocer la carga contaminante a la entrada del tramo (directamente aguas abajo de la descarga) y la concentración esperada aguas abajo al final del tramo cuya longitud es el propósito de esta metodología.

Para el cálculo de la carga contaminante a la entrada del tramo se deben conocer las características promedio de calidad del agua de la corriente en el sitio de vertimiento antes de la intervención propuesta y las características de concentración y caudal máximas en el vertimiento. Las muestras de calidad del agua recogidas durante el monitoreo deben ser integradas en la sección transversal siguiendo los lineamientos establecidos por el IDEAM. Para todos los sectores, se deberán monitorear como mínimo los siguientes determinantes de la calidad del agua sobre el cuerpo receptor para propósitos de implementar esta metodología:

Grupo 1

- Temperatura del agua (°C)
- Oxígeno disuelto (mg/L O)
- DBO (mg/L O)
- NTK (mg/L N)
- Fósforo Total (mg/L P)
- Coliformes Fecales (NMP/100 mL)
- SST (mg/L)

Para el sector de hidrocarburos, se deberán medir adicionalmente los siguientes determinantes:

Grupo 2

- Fenoles totales (mg/L)
- BTEX (Benceno, Tolueno, Etilbenceno y Xileno) (mg/L)
- Hidrocarburos Aromáticos Policíclicos (HAP) (mg/L)
- Metales pesados (Arsénico, Bario, Cadmio, Plomo, Mercurio, Selenio, Cromo, Vanadio) (mg/L)

Para el sector de minería, se deberán medir, adicional a los del grupo 1, los siguientes determinantes:

Grupo 3

- Fenoles totales (mg/L)
- Metales pesados (Arsénico, Bario, Cadmio, Plomo, Mercurio, Selenio, Cromo, Cobre, Cinc) (mg/L)
- Cianuros (mg/L)

Se deberán incluir otras sustancias de interés dependiendo del tipo de proyecto. Es posible descartar algunas sustancias específicas en los sectores mencionados si se demuestra que no son relevantes según las actividades desarrolladas en el proyecto.

Adicionalmente, se deberán definir las concentraciones para los anteriores determinantes de la calidad del agua (según el sector) sobre el vertimiento sin tratamiento.

La carga a la entrada del tramo W se calculará haciendo el balance de masa entre la carga que tiene la corriente originalmente W_o antes de la descarga de las aguas residuales y la carga vertida W_v:

$$W = W_o + W_v = Q_{amb} c_o + Q_v c_v \qquad [8]$$

Siendo Q_{amb} el caudal ambiental calculado en el paso 1, c_o la concentración del determinante específico medido sobre la corriente sin intervención, Q_v el caudal máximo de vertimiento y c_v la concentración máxima esperada sin tratamiento del determinante específico en las aguas

residuales. El cálculo de la carga contaminante a la entrada del tramo se deberá hacer para todos los determinantes de calidad del agua definidos anteriormente.

La concentración esperada aguas abajo c_{est} será el valor máximo entre la condición medida sobre la corriente a la entrada del tramo y el estándar de calidad ambiental dado por la autoridad ambiental competente o según las metas y objetivos de calidad correspondientes de acuerdo con los usos actuales y prospectivos del agua en la cuenca hidrográfica (la prelación la tiene la autoridad ambiental local). Este análisis se deberá hacer para cada sustancia contaminante considerada. En caso de no contar definitivamente con un estándar de calidad ambiental (objetivo, meta de calidad) sobre el recurso hídrico para una sustancia en particular, c_{est} se tomará como la condición medida sobre la corriente a la entrada del tramo (sin contemplar el vertimiento).

4.5 Paso 4. Cálculo de factores de asimilación y de la longitud de influencia directa

4.5.1 Esquema general de cálculo

El valor del factor de asimilación correspondiente a cada determinante de calidad del agua se calcula como el cociente entre la carga contaminante a la entrada del tramo W y el valor de concentración esperada aguas abajo c_{est},

$$a_i = \frac{W_i}{c_{est\,i}} \qquad [9]$$

Donde el subíndice *i* corresponde a cada determinante de calidad del agua considerado de acuerdo con el paso 3.

Contemplando dispersión longitudinal, reacción de primer orden y estado estable, utilizando como marco el modelo ADZ-QUASAR (Lees et al., 1998), se tiene la siguiente ecuación general de balance de masa para un determinante de calidad del agua:

$$0 = \frac{1}{T_r}\left(\frac{W}{Q}e^{-k\tau} - c\right) - kc \qquad [10]$$

La concentración aguas abajo sobre el cuerpo receptor (a la salida del tramo), en función de la carga a la entrada del tramo *W*, se puede despejar y calcular como:

$$c = \frac{e^{-k\tau}}{\left(1 + kT_r\right)Q}W \qquad [11]$$

Q es el caudal a la entrada del tramo, es decir:

$$Q = Q_{amb} + Q_v \qquad [12]$$

De las expresiones [9] y [11], y teniendo en cuenta la relación entre el tiempo de residencia T_r, el tiempo medio de viaje $\bar{t}$, el tiempo de primer arribo τ y la fracción dispersiva *DF*, se puede deducir que el factor de asimilación a es:

$$a = \left[\left(1 + DF \cdot k\bar{t}\right) e^{(1-DF)k\bar{t}} \right] Q \qquad [13]$$

Si en la expresión [13] el valor de a es conocido (igual al factor de asimilación calculado con la información de calidad del agua), se tiene una ecuación con una incógnita, la cual es el tiempo medio de viaje $\bar{t}$. Esta ecuación no lineal se puede resolver iterativamente con el método de Newton – Raphson, así:

$$\bar{t}_{i+1} = \bar{t}_i - \frac{\left(1 + DF \cdot k\bar{t}_i\right) Q e^{(1-DF)k\bar{t}_i} - a}{k\left[1 + DF\left(1 - DF\right)k\bar{t}_i\right] Q e^{(1-DF)k\bar{t}_i}} \qquad [14]$$

El método se detiene cuando $\bar{t}_{i+1} \approx \bar{t}_i$. Conocido el tiempo medio de viaje, la longitud aguas abajo para la cual se alcanza el factor de asimilación definido, es decir, la longitud de influencia directa del vertimiento, se calcula utilizando la velocidad media $\bar{v}$ correspondiente a Q_{amb} como:

$$L_{IV} = \bar{t} \cdot \bar{v} \qquad [15]$$

Esta longitud se deberá calcular para cada uno de los determinantes de calidad del agua contemplados según el sector. La longitud definitiva, entendida como aquella sobre la cual existe influencia directa por parte del vertimiento, será la máxima entre todas las calculadas.

4.5.2 Factor de asimilación por determinante

El factor de asimilación en función del caudal, los parámetros de transporte y de calidad del agua, se calcula de diferente manera para cada determinante y depende de los procesos físicos, químicos y biológicos a los que está sometida cada sustancia en particular. Para el caso de las sustancias tóxicas se deben tener en cuenta sus fracciones disueltas y particuladas, las cuales están sujetas a procesos de degradación y transformación específicos. En esta sección se explicará sucintamente cómo se pueden estimar cada una de las tasas más representativas de cada determinante, así como las simplificaciones introducidas para la implementación de la presente metodología y la forma definitiva de la expresión del factor de asimilación para ser resuelta numéricamente.

4.5.2.1 Estimación de tasas de reacción de determinantes convencionales de la calidad del agua

La Tabla 1 indica los procesos de degradación y transformación considerados en la presente metodología, y las tasas de reacción que se tienen en cuenta para modelar los determinantes básicos de calidad del agua. Por simplificación, no se consideran explícitamente los procesos involucrados en la interface sedimento–agua (resuspensión, demanda béntica de oxígeno, fuentes bénticas y sedimentación de fracciones particuladas de nitrógeno y fósforo) a

excepción de la sedimentación de material particulado carbonáceo y de los SST, ni el efecto ejercido por las algas (medidas regularmente como Clorofila–a) como crecimiento y respiración.

Tabla 1 Procesos de degradación y transformación considerados en la metodología

Determinantes	Procesos	Tasas de Reacción (d^{-1})
Materia orgánica carbonácea (DBO)	Dispersión – advección, descomposición de la DBO k_d, sedimentación de la materia orgánica particulada v_s	$k_r = k_d + \frac{v_s}{H}$ (*)
Nitrógeno total Kjeldahl (NTK)	Dispersión – advección, nitrificación k_n	k_n
Fósforo total	Dispersión – advección, hidrólisis k_p	k_p
Coliformes Fecales	Dispersión – advección, decaimiento por muerte k'_b	k'_b
SST	Dispersión – advección, velocidad de sedimentación v_{ss}	$k_s = \frac{v_{ss}}{H}$ (*)
Oxígeno disuelto	Dispersión – advección, reaireación k_a, descomposición DBO k_d, nitrificación k_n	k_a, k_d, k_n

* *H* es la profundidad media del agua en el tramo

Para la estimación de las tasas de reacción, se puede acudir a valores reportados por la literatura, estudios de campo y laboratorio o a modelación matemática (calibración utilizando datos medidos en campo). Un documento base y útil para la definición inicial de las tasas de reacción mencionadas es *Rates, Constants, and Kinetics Formulations in Surface Water Quality Modeling, Second Edition* (Bowie et al., 1985) de la Agencia de Protección Ambiental de E.E.U.U. (USEPA). Para propósitos de implementar esta metodología, se recomienda el uso de valores medios o típicos encontrados en ríos con características morfológicas, hidrológicas y de calidad del agua similares a los de la corriente bajo estudio.

Existen expresiones matemáticas obtenidas empíricamente que permiten calcular algunas de las tasas mencionadas. Generalmente, la información requerida para el uso de estas ecuaciones consiste en caudales, niveles y velocidades medias, algunas otras utilizan características geométricas como área, perímetro mojado o radio hidráulico. En caso que se utilicen estas expresiones, se deben considerar las condiciones de caudal mínimo o ambiental sobre la corriente, así como tener en cuenta sus límites de aplicación. Para esta metodología, no es necesario corregir las tasas de reacción por temperatura. A continuación se presentan aproximaciones para estimar de manera preliminar algunas de las tasas de reacción antes mencionadas. En cualquier caso, el modelador tiene la facultad de asignar los valores correspondientes de acuerdo con su criterio y experiencia. Si el modelador considera el uso de otras expresiones o valores de tasas de reacción, podrá hacerlo siempre y cuando justifique plenamente su selección y fuente.

4.5.2.1.1 Tasa de reaireación k_a

Para la estimación de la tasa de reaireación, se proponen las siguientes ecuaciones de acuerdo con el tipo de corriente y sus condiciones hidrodinámicas.

Cuando la corriente bajo estudio es característica de montaña (e.g. Holguín, 2003; Arenas, 2005; Gélvez y Camacho, 2008), se recomienda utilizar la siguiente expresión formulada por Tsivoglou y Neal (1976, tomado de Chapra, 1997):

$$k_a = c\frac{\Delta H}{\bar{t}} \qquad [16]$$

Siendo ΔH el cambio en la elevación de la superficie del agua en metros en un subtramo seleccionado y $\bar{t}$ el tiempo medio de viaje en días en el elemento, calculado como el cociente entre la longitud y la velocidad media del agua en el subtramo. La constante c depende del caudal y se define de la siguiente forma:

$$c = 0.36 \text{ para } 0.028 \le Q \le 0.28 m^3/s$$

$$c = 0.177 \text{ para } 0.708 \le Q \le 85 m^3/s$$

Para el caso de ríos de planicie, se podrá seleccionar la ecuación de reaireación más apropiada de acuerdo con los rangos de profundidad y velocidad media (Chapra, 1997) establecidos en la Tabla 2, en condiciones de caudal ambiental sobre la corriente:

Tabla 2 Ecuaciones de reaireación para ríos de planicie

Parámetro	O' Connor – Dobbins	Churchill	Owens – Gibbs
Profundidad (m)	0.30 – 9.14	0.31 – 3.35	0.12 – 0.73
Velocidad media (m/s)	0.15 – 0.49	0.55 – 1.52	0.03 – 0.55
Expresiones	$k_a = 3.93\frac{U^{0.5}}{H^{1.5}}$	$k_a = 5.026\frac{U}{H^{1.67}}$	$k_a = 5.32\frac{U^{0.67}}{H^{1.85}}$

En las expresiones de la Tabla 2, H es la profundidad media del agua en metros y U es la velocidad media del flujo en m/s.

4.5.2.1.2 Tasa de desoxigenación o descomposición de la DBO k_d

Siguiendo a Thomann y Mueller (1987), los valores de k_d están aproximadamente en un rango entre 0.1 a 0.5 d^{-1} para cuerpos de agua profundos (mayores a 1.5 m) y de 0.5 a 3.0 d^{-1} para corrientes someras (profundidades menores a 1.5 m).

Una expresión propuesta por Wright y McDonnell (1979, modificada de Bowie et al., 1985) para estimar la tasa de descomposición de la DBO en función del caudal es:

$$k_d = 1.796Q^{-0.49} \qquad [17]$$

En la ecuación [17], k_d está en d^{-1} y el caudal Q en m^3/s. El rango de aplicación de esta expresión es para caudales entre 0.3 y 23 m^3/s, por encima del mayor caudal, los autores de la ecuación demostraron que k_d es independiente del caudal y los valores son consistentes con las tasas encontradas por laboratorio. En este orden de ideas, para ríos grandes, la tasa de desoxigenación encontrada en laboratorio es representativa de las condiciones de la corriente de agua. Por encima del rango de la ecuación [17], y para propósitos de esta metodología, puede suponerse un valor constante de 0.30 d^{-1} – es posible encontrar tasas aún más bajas, tal y como se indica en Bowie et al., 1985; su definición está sujeta al criterio del modelador teniendo en cuenta aspectos hidrológicos, geomorfológicos y de calidad del agua –; el máximo valor de k_d se sugiere de 3.5 d^{-1}. Para el mismo rango de caudales y como alternativa, se puede calcular la tasa de descomposición a partir del perímetro mojado P en metros como:

$$k_d = 14.597 P^{-0.84} \qquad [18]$$

Otra opción consiste en estimar directamente la tasa de remoción de DBO k_r a partir de datos medidos en campo o a partir de la literatura.

4.5.2.1.3 Tasa de nitrificación k_n

Una opción para estimar la tasa de nitrificación es a partir de únicamente parámetros hidráulicos, tal y como fue propuesto por Bansal (1976). De acuerdo con los resultados de este autor, la constante de nitrificación es función del número de Reynolds y del número de Froude, siendo la forma simplificada la que se presenta a continuación:

$$Log\left(\frac{k_n H^2}{\upsilon}\right) = -3.421 + 1.36 Log\left(\frac{\sqrt{gH^3}}{\upsilon}\right) \qquad [19]$$

En la expresión [19], H es la profundidad media del agua (m) en el tramo, g es la aceleración de la gravedad, k_n es la tasa de nitrificación (s^{-1}) y ν es la viscosidad cinemática del agua (m^2/s).

Otra alternativa es considerar valores reportados en la literatura consistentes con la corriente bajo estudio. Pauer y Auer (2009, tomado de Medina, 2009) presentan las tasas de nitrificación indicadas en la Tabla 3 para diferentes casos de estudio:

Tabla 3 Tasas de nitrificación reportadas por Pauer y Auer (2009, tomado de Medina, 2009)

Río	k_n [d^{-1}]	Profundidad (m)	Reportado en
Mine Brook	8.00	0.2	Tuffey et al. (1974)
Barge	0.25	3.9	Bansal (1976)
Upper Mohawk	0.25	3.66	Bansal (1976)
Upper Mohawk	0.30	0.96	Bansal (1976)
Upper Mohawk	0.25	2.51	Bansal (1976)
Middle Mohawk	0.30	3.81	Bansal (1976)
Lower Mohawk	0.30	4.25	Bansal (1976)
Seneca River	0.05	6.24	Canale et at. (1995), yJ.J. Pauer, M.T. Auer, (2009)
Trinity	0.51	1.53	McCutcheon (1987)
Ohio	0.25	8.15	Bansal (1976)
Flint	1.53	0.66	Bansal (1976) y O'Connor y Di Toro (1970)
Shenadoha	1.25	0.6	Deb y Bowers (1983) Deb (1985)
Shenadoha	0.2	1.74	Deb y Bowers (1983) Deb (1985)
Holston	0.23	1.3	Ruane and Krenekel (1977)
Grand	1.90	0.58	Bansal (1976) y O'Connor y Di Toro (1970)
Chattahoockee	0.25	1.5	McCutcheon (1987), Miller y Jennings (1979)
Sitll	0.70	0.64	Curtis (1983 y Maueger (1995)
Trukee	2.40	0.51	Bansal (1976) y O'Connor y Di Toro (1970)
Willamette	0.70	1.6	Dunnette y Avedovech (1983), Cooper (1985)
Anacostia	0.13	4	Sullivan y Brown (1988)
Speed	2.30	0.43	Gowda (1983)
Ootanaula	0.80	0.61	Cooper (1986)
Sweetwater	0.80	0.46	Cooper (1986)
Trace	2.20	0.46	Cooper (1986)
Mud	0.50	1	Cooper (1986)
Oroua	6.70	0.25	Cooper (1986)
Waiotapu	2.80	0.61	Cooper (1986)
Waiohewa	5.90	0.3	Cooper (1986)
Big Blue	0.12	1.25	Bansal (1976)
South Chickamauga	6.60	0.84	Cooper (1986)

Los valores de k_n generalmente están en un rango de 0.1 a 0.5 d^{-1} para aguas profundas, mientras que para aguas someras, valores por encima de 1 d^{-1} son encontrados frecuentemente (Chapra, 1997).

4.5.2.1.4 Velocidades de sedimentación v_s y v_{ss}

En cuanto a la velocidad de sedimentación de la materia orgánica particulada v_s y de los sedimentos suspendidos v_{ss}, se han encontrado los valores indicados en la Tabla 4 que varían de acuerdo con el diámetro de las partículas (Wetzel, 1975; Burns y Rosa, 1980, tomado de Chapra, 1997):

Tabla 4 Velocidades de sedimentación medidas para diferentes tipos y tamaños de partículas

Tipo de partícula	Diámetro (µm)	Velocidad de sedimentación (m d^{-1})
Carbono orgánico particulado	1-10	0.2
	10-64	1.5
	> 64	2.3
Arcilla	2-4	0.3-1
Limo	10-20	3-30

Las velocidades de sedimentación para sedimentos no cohesivos en función del tamaño de la partícula, se pueden obtener de la Figura 2 (basada en Cheng, 1997, tomado de Ji, 2008):

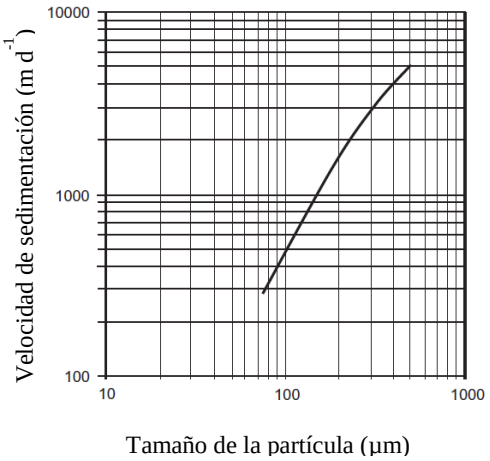

Figura 2 Velocidad de sedimentación para sedimentos no cohesivos

Para estimar la velocidad de sedimentación también se han encontrado ecuaciones empíricas de sedimentos cohesivos en función de su concentración y la intensidad de turbulencia. Un ejemplo es la expresión obtenida por Dyer et al. (2000, modificado de Ji, 2008):

$$v_{ss} = -0.243 + 0.000567S + 0.981G - 0.0934G^2 \qquad [20]$$

Siendo G el parámetro de turbulencia:

$$G = \sqrt{\frac{gUS_o}{\upsilon}} \qquad [21]$$

Donde S es la concentración de sedimentos (g/L), U es la velocidad media del agua (m/s), g es la aceleración de la gravedad (m^2/s), S_o es la pendiente longitudinal del tramo y ν es la viscosidad cinemática del agua (m^2/s).

Otra opción es estimar el valor utilizando la ley de Stokes, aunque su implementación es muy limitada puesto que supone, entre otros aspectos, flujo laminar. Thomann y Mueller (1987) proponen la siguiente forma de la ecuación:

$$v_s = 0.033634\alpha\left(\rho_s - \rho_w\right)d^2 \qquad [22]$$

Donde la velocidad de sedimentación v_s está en m d^{-1}, las densidades de la partícula ρ_s y del agua ρ_w están en g cm^{-3}, el diámetro efectivo de las partículas d está en µm y la viscosidad del agua se asume con un valor contante de 0.014 g cm^{-1} s^{-1}; α es un factor adimensional que representa el efecto de la forma de la partícula (igual a 1.0 para una esfera).

4.5.2.1.5 Tasa de decaimiento por muerte de patógenos k'_b

Siguiendo a Chapra (1997), la tasa de pérdida total de patógenos en corrientes superficiales puede calcularse de la siguiente forma:

$$k_b' = 0.8 \cdot 1.07^{T-20} + \frac{I_0}{0.55 \cdot SST \cdot H}\left(1 - e^{-0.55 \cdot SST \cdot H}\right) + F_p \frac{v_{ss}}{H} \qquad [23]$$

Siendo T la temperatura del agua (°C), I_0 la radiación solar (ly/hr), SST la concentración de sólidos suspendidos totales promedio en el tramo (mg/L), H la profundidad media del agua (m), F_p la fracción adsorbida de bacterias a las partículas sólidas y v_{ss} la velocidad de sedimentación de las partículas (m d^{-1}). Se puede suponer un valor típico de 0.7 para F_p o calcularlo de la siguiente forma:

$$F_p = \frac{K_d SST}{1 + K_d SST} \qquad [24]$$

Siendo K_d un coeficiente de partición (m^3 g^{-1}) que puede ser obtenido en laboratorio (Chapra, 1997).

4.5.2.2 Estimación de tasas de reacción de sustancias tóxicas y metales pesados

A diferencia de los determinantes convencionales de la calidad del agua, para modelar las sustancias tóxicas es muy importante distinguir sus fracciones disueltas y particuladas, ya que cada una está sometida a mecanismos que actúan selectivamente. Por ejemplo, la volatilización ocurre únicamente en la fracción disuelta mientras que la sedimentación lo hace solo sobre la fracción particulada (Chapra, 1997). Para propósitos de esta metodología, los principales mecanismos de depuración de sustancias tóxicas en la columna de agua que serán contemplados son los de advección-dispersión, adsorción y volatilización. No se tendrán en cuenta las interacciones en la interface agua-sedimento más allá de la sedimentación de las partículas sólidas. No obstante, si el modelador considera contemplar procesos de transformación adicionales como hidrólisis, oxidación, fotólisis, transformación biológica y,o bioconcentración, e incluir interacciones agua-sedimento como resuspensión y enterramiento, podrá hacerlo siempre y cuando justifique plenamente la selección de las tasas de reacción correspondientes, la modificación de las expresiones de factor de asimilación y las referencias técnicas respectivas.

4.5.2.2.1 Fracciones y coeficientes de partición

Matemáticamente, la concentración total de una sustancia tóxica *c* está separada en dos componentes:

$$c = c_d + c_p \qquad [25]$$

Siendo c_p el componente particulado y c_d el componente disuelto del contaminante. Se supone que estos componentes representan fracciones fijas de la concentración total:

$$c_d = F_d c$$
$$c_p = F_p c \qquad [26]$$

Las fracciones disuelta F_d y particulada F_p dependen del coeficiente de partición del contaminante K_d (m^3 g^{-1}) y de la concentración de *SST* (g m^{-3}) en el río. El coeficiente de partición cuantifica la tendencia que tiene el contaminante de asociarse con la materia sólida. Las fracciones se pueden calcular de la siguiente forma:

$$F_d = \frac{1}{1 + K_d SST} \qquad [27]$$

$$F_p = \frac{K_d SST}{1 + K_d SST}$$

$$F_p + F_d = 1 \qquad [28]$$

Para las sustancias tóxicas orgánicas y metales pesados, el coeficiente de partición y la velocidad de volatilización se pueden estimar a partir de información disponible en la literatura. Dos documentos básicos para este propósito son *Processes, Coefficients, and Models for Simulating Toxic Organics and Heavy Metals in Surface Waters* (Schnoor et al., 1987) y *Partition Coefficients for Metals in Surface Water, Soil, and Waste* (Allison y Allison, 2005) de la Agencia de Protección Ambiental de E.E.U.U. (USEPA). Igualmente, hay software disponible que sirve para la estimación de algunos de estos parámetros como MINTEQA2 y bases de datos disponibles en la web como http://sitem.herts.ac.uk/aeru/iupac/.

Siguiendo a Chapra (1997), el coeficiente de partición para contaminantes orgánicos se puede suponer como una función del contenido orgánico de los sólidos:

$$K_d = f_{oc} K_{oc} \qquad [29]$$

Donde K_{oc} es el coeficiente de partición del carbón orgánico y f_{oc} es la fracción en peso del carbono total en la materia sólida. El coeficiente de partición K_{oc} puede ser estimado en términos del coeficiente de partición agua-octanol K_{ow}:

$$K_{oc} = 6.17 \times 10^{-7} K_{ow} \qquad [30]$$

Por lo tanto, las ecuaciones [29] y [30] se pueden combinar para obtener, con f_{oc}=0.05:

$$K_d = 3.085 \times 10^{-8} K_{ow} \qquad [31]$$

El coeficiente de partición agua-octanol se puede obtener de la Figura 3, la cual es una recopilación de los valores obtenidos experimentalmente para diferentes grupos de tóxicos orgánicos, en forma de diagramas de cajas y bigotes.

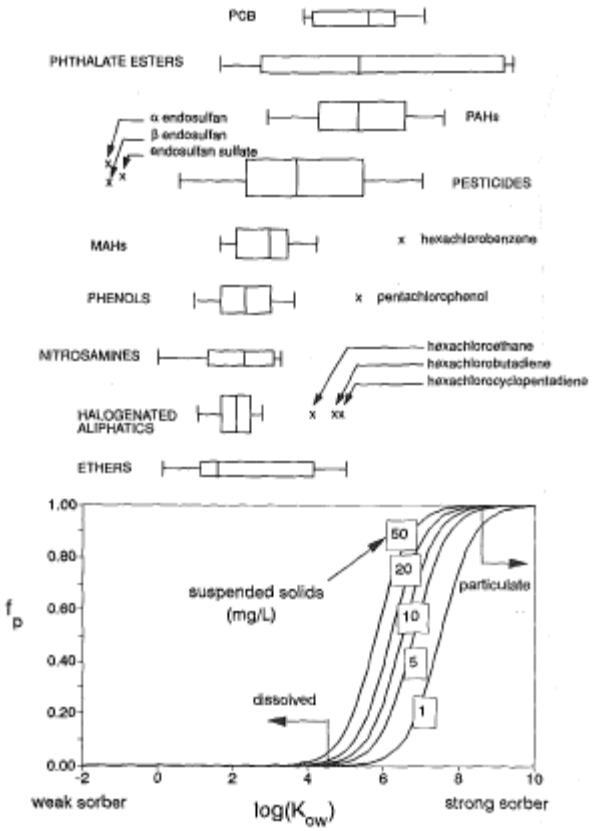

Figura 3 Gráfica de fracción disuelta y fracción particulada versus coeficientes de partición (Chapra, 1991)

4.5.2.2.2 Velocidad de volatilización v_v

Para el cálculo de la velocidad de volatilización de los contaminantes orgánicos, se deben determinar los valores de la constante de Henry H_e y los coeficientes de transferencia de lámina-líquido y lámina-gas. Utilizando la Figura 4 es posible estimar la constante H_e para los diferentes grupos de sustancias tóxicas.

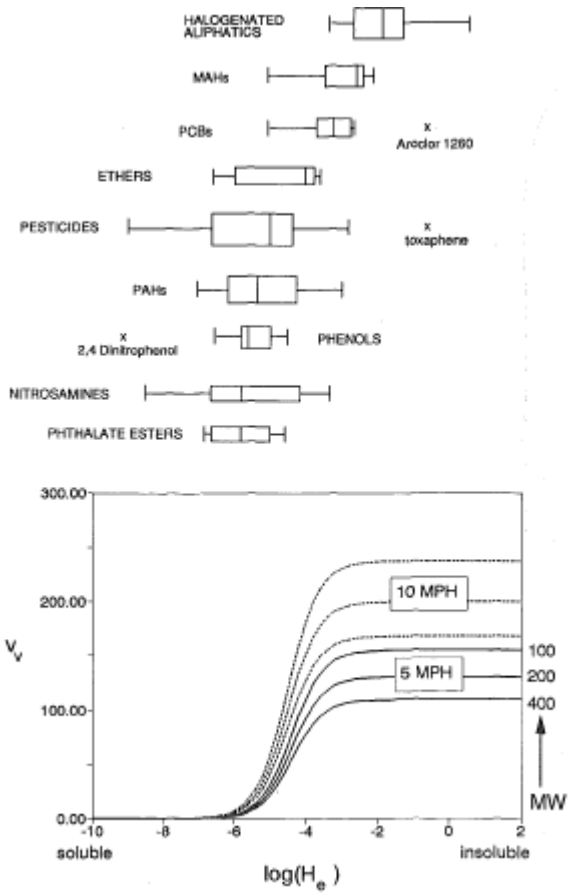

Figura 4 Gráfica de velocidad de volatilización contra constante de Henry (Chapra, 1991)

Los coeficientes de transferencia son convencionalmente estimados correlacionándolos con los procesos de transferencia comúnmente estudiados. El coeficiente de transferencia en la interfaz líquido-gas K_L está típicamente correlacionado con el transporte del vapor de agua. El coeficiente de transferencia de masa en la lámina-líquido (m yr^{-1}) puede estar relacionado con el coeficiente de transferencia de oxígeno por:

$$K_L = K_{L,O_2}\left(\frac{32}{M}\right)^{0.25} \qquad [32]$$

Donde M es el peso molecular (g mol) del componente y $K_{L,O2}$ es el coeficiente de transferencia de oxígeno. Dicho coeficiente de transferencia (reaireación) puede ser calculado a partir de las fórmulas presentadas anteriormente (ver ecuación [16] y Tabla 2) para la tasa de reaireación k_a, de la siguiente forma:

$$K_{L,O_2}(md^{-1}) = k_a H \qquad [33]$$

Siendo H la profundidad media del agua (m). Para la tasa de transferencia lámina-gas K_g en m d^{-1}, Mills et al. (1982) sugirieron:

$$K_g = 168W\left(\frac{18}{M}\right)^{0.25} \qquad [34]$$

Siendo W la velocidad del viento (m/s). La velocidad de volatilización se calcula como:

$$v_v = K_L \frac{H_e}{H_e + RT_a\left(\frac{K_L}{K_g}\right)} \qquad [35]$$

Siendo v_v la velocidad de volatilización (m yr^{-1}), R la constante de gas universal [8.206×10^{-5} atm m^3 (K mol)$^{-1}$] y T_a la temperatura absoluta del agua (K).

4.5.2.2.3 Otras tasas

Para propósitos de esta metodología, la velocidad de sedimentación de las partículas adsorbidas a los sólidos puede suponerse igual a la estimada para los *SST*.

Para el caso particular de los cianuros, se recomienda consultar el caso del río Mahoning (USEPA, 1977) y Botz y Mudder (2000).

4.5.2.3 Resumen de factores de asimilación

A partir de la ecuación general de balance de masa del modelo ADZ-QUASAR (Lees et al., 1998) y de los mecanismos de transformación considerados para la presente metodología, se presenta la Tabla 5 con el resumen de ecuaciones para los factores de asimilación de cada determinante de la calidad del agua considerado.

Tabla 5 Factores de asimilación para los determinantes de calidad del agua considerados en la metodología

Determinante	Factor de asimilación
Oxígeno disuelto (mg/L O)	$a_{OD} = \left[\frac{1 + DF \cdot k_a \bar{t}_{OD}}{e^{-k_a(1-DF)\bar{t}_{OD}} + \xi \cdot DF \cdot \bar{t}_{OD}}\right] Q$ $\xi = k_a \frac{O_s}{OD_u} - 4.57 k_n \frac{NTK}{OD_u} - k_d \frac{DBO}{OD_u}$ $O_s = \left[14.652 - 0.41022T + 0.0079910T^2 - 0.000077774T^3\right](1 - 0.1148Alt)$ T es la temperatura del agua (°C), Alt la altitud promedio del tramo (km), OD_u la concentración de oxígeno disuelto calculada a la entrada del tramo (aguas abajo del vertimiento). Las concentraciones de NTK y DBO son las definidas a la salida del tramo.
DBO (mg/L O)	$a_{DBO} = \left[\left(1 + DF \cdot k_r \bar{t}_{DBO}\right) e^{(1-DF)k_r \bar{t}_{DBO}}\right] Q$
NTK (mg/L N)	$a_{NTK} = \left[\left(1 + DF \cdot k_n \bar{t}_{NTK}\right) e^{(1-DF)k_n \bar{t}_{NTK}}\right] Q$

Fósforo Total (mg/L P)	$a_{PT} = \left[\left(1 + DF \cdot k_p \bar{t}_{PT}\right) e^{(1-DF) k_p \bar{t}_{PT}} \right] Q$
Coliformes Fecales (NMP/100 mL)	$a_{CF} = \left[\left(1 + DF \cdot k_b' \bar{t}_{CF}\right) e^{(1-DF) k_b' \bar{t}_{CF}} \right] Q$
SST (mg/L)	$a_{SST} = \left[\left(1 + DF \cdot k_S \bar{t}_{SST}\right) e^{(1-DF) k_S \bar{t}_{SST}} \right] Q$ $k_S = \frac{v_{ss}}{H}$
Fenoles (mg/L)	$a_F = \left[\left(1 + DF \cdot k_F \bar{t}_{DBO}\right) e^{(1-DF) k_F \bar{t}_{DBO}} \right] Q$ $k_F = \frac{v_{vF}}{H} F_{dF}$
Benceno (mg/L)	$a_B = \left[\left(1 + DF \cdot k_B \bar{t}_B\right) e^{(1-DF) k_B \bar{t}_B} \right] Q$ $k_B = \frac{v_{sB}}{H} F_{pB} + \frac{v_{vB}}{H} F_{dB}$
Tolueno (mg/L)	$a_T = \left[\left(1 + DF \cdot k_T \bar{t}_T\right) e^{(1-DF) k_T \bar{t}_T} \right] Q$ $k_T = \frac{v_{sT}}{H} F_{pT} + \frac{v_{vT}}{H} F_{dT}$
Etilbenceno (mg/L)	$a_E = \left[\left(1 + DF \cdot k_E \bar{t}_E\right) e^{(1-DF) k_E \bar{t}_E} \right] Q$ $k_E = \frac{v_{sE}}{H} F_{pE} + \frac{v_{vE}}{H} F_{dE}$
Xileno (mg/L)	$a_X = \left[\left(1 + DF \cdot k_X \bar{t}_X\right) e^{(1-DF) k_X \bar{t}_X} \right] Q$ $k_X = \frac{v_{sX}}{H} F_{pX} + \frac{v_{vX}}{H} F_{dX}$
HAP (mg/L)	$a_{HAP} = \left[\left(1 + DF \cdot k_{HAP} \bar{t}_{HAP}\right) e^{(1-DF) k_{HAP} \bar{t}_{HAP}} \right] Q$ $k_{HAP} = \frac{v_{sHAP}}{H} F_{pHAP} + \frac{v_{vHAP}}{H} F_{dHAP}$
Arsénico (mg/L)	$a_{As} = \left[\left(1 + DF \cdot k_{As} \bar{t}_{As}\right) e^{(1-DF) k_{As} \bar{t}_{As}} \right] Q$ $k_{As} = \frac{v_{sAs}}{H} F_{pAs}$
Bario (mg/L)	$a_{Ba} = \left[\left(1 + DF \cdot k_{Ba} \bar{t}_{Ba}\right) e^{(1-DF) k_{Ba} \bar{t}_{Ba}} \right] Q$ $k_{Ba} = \frac{v_{sBa}}{H} F_{pBa}$

Cadmio (mg/L)	$a_{Cd} = \left[\left(1 + DF \cdot k_{Cd} \bar{t}_{Cd}\right) e^{(1-DF) k_{Cd} \bar{t}_{Cd}} \right] Q$ $k_{Cd} = \frac{v_{sCd}}{H} F_{pCd}$
Plomo (mg/L)	$a_{Pb} = \left[\left(1 + DF \cdot k_{Pb} \bar{t}_{Pb}\right) e^{(1-DF) k_{Pb} \bar{t}_{Pb}} \right] Q$ $k_{Pb} = \frac{v_{sPb}}{H} F_{pPb}$
Mercurio (mg/L)	$a_{Hg} = \left[\left(1 + DF \cdot k_{Hg} \bar{t}_{Hg}\right) e^{(1-DF) k_{Hg} \bar{t}_{Hg}} \right] Q$ $k_{Hg} = \frac{v_{sHg}}{H} F_{pHg} + \frac{v_{vHg}}{H} F_{dHg}$
Selenio (mg/L)	$a_{Se} = \left[\left(1 + DF \cdot k_{Se} \bar{t}_{Se}\right) e^{(1-DF) k_{Se} \bar{t}_{Se}} \right] Q$ $k_{Se} = \frac{v_{sSe}}{H} F_{pSe}$
Cromo (mg/L)	$a_{Cr} = \left[\left(1 + DF \cdot k_{Cr} \bar{t}_{Cr}\right) e^{(1-DF) k_{Cr} \bar{t}_{Cr}} \right] Q$ $k_{Cr} = \frac{v_{sCr}}{H} F_{pCr}$
Cobre (mg/L)	$a_{Cu} = \left[\left(1 + DF \cdot k_{Cu} \bar{t}_{Cu}\right) e^{(1-DF) k_{Cu} \bar{t}_{Cu}} \right] Q$ $k_{Cu} = \frac{v_{sCu}}{H} F_{pCu}$
Cinc (mg/L)	$a_{Zn} = \left[\left(1 + DF \cdot k_{Zn} \bar{t}_{Zn}\right) e^{(1-DF) k_{Zn} \bar{t}_{Zn}} \right] Q$ $k_{Zn} = \frac{v_{sZn}}{H} F_{pZn}$
Vanadio (mg/L)	$a_{V} = \left[\left(1 + DF \cdot k_{V} \bar{t}_{V}\right) e^{(1-DF) k_{V} \bar{t}_{V}} \right] Q$ $k_{V} = \frac{v_{sV}}{H} F_{pV}$
Cianuros (mg/L)	$a_{CN} = \left[\left(1 + DF \cdot k_{CN} \bar{t}_{CN}\right) e^{(1-DF) k_{CN} \bar{t}_{CN}} \right] Q$

* Las anteriores ecuaciones son dimensionalmente homogéneas, por lo cual las unidades de las diferentes cantidades deben ser consistentes.

La determinación del tiempo medio de viaje para cada determinante se hace según se explicó en el esquema general de cálculo (ver ecuación [14]), remplazando el valor de *k* por la respectiva tasa de reacción neta que se puede obtener de la Tabla 5. La ecuación [14] no aplica para el oxígeno disuelto, cuya expresión de factor de asimilación es diferente en estructura a la de los demás determinantes considerados. La ecuación respectiva es la siguiente:

$$\bar{t}_{i+1} = \bar{t}_i - \frac{\left(1+DF\cdot k_a\cdot \bar{t}_i\right)Q\left(e^{-k_a(1-DF)\bar{t}_i}+\xi\cdot DF\cdot \bar{t}_i\right)-a\left(e^{-k_a(1-DF)\bar{t}_i}+\xi\cdot DF\cdot \bar{t}_i\right)^2}{\left[\left(e^{-k_a(1-DF)\bar{t}_i}+\xi\cdot DF\cdot \bar{t}_i\right)DF\cdot k_a-\left(1+DF\cdot k_a\cdot \bar{t}_i\right)\left(\xi\cdot DF-k_a\left(1-DF\right)e^{-k_a(1-DF)\bar{t}_i}\right)\right]Q}$$

4.6 Paso 5. Cálculo de la carga total y recálculo de la LIV

La longitud de influencia directa calculada en el paso 4 considera únicamente el efecto del vertimiento propuesto a la entrada del tramo, por lo tanto esta corresponde a una primera iteración. Aguas abajo de dicho punto ocurren generalmente afluencias o abstracciones (naturales o antrópicas) de carga o caudal que pueden afectar la calidad del agua esperada al final del tramo. Como no es posible saber *a priori* hasta qué punto se extiende la distancia de influencia, tampoco se puede definir cuáles son las principales entradas o salidas de carga contaminante aguas abajo, por lo que se requiere de una primera aproximación de dicha longitud.

Una vez encontrada la longitud de influencia preliminar (primera iteración del paso 4), se deben identificar las principales entradas y salidas en el tramo preliminar afectado directamente por el vertimiento de aguas residuales. Un criterio para seleccionar las principales afluencias o abstracciones puede ser considerar factores de dilución – razón entre el caudal vertido y el caudal de la corriente receptora – mayores a 1/10, aunque se deben tener en cuenta todos los vertimientos de aguas residuales industriales que se encuentren en esta distancia preliminar. Finalmente, la selección de elementos adicionales se define según el criterio y experiencia del modelador.

Identificadas las principales entradas y salidas a los largo del tramo de la corriente, se deberá obtener información de calidad del agua (para los determinantes considerados según el sector) y de caudales promedio anuales (estimados a partir de registros históricos, mediciones en campo o técnicas hidrológicas) sobre cada entrada y salida. Se deberá calcular la carga contaminante total sumando (o restando), a la carga contaminante *W* calculada en la primera iteración a la entrada del tramo, las cargas individuales de cada afluente o abstracción. La nueva carga a la entrada del tramo *W* será la carga total recién calculada. Con esta nueva carga, se deberá repetir la metodología utilizando los mismos valores que en la primera iteración y corregir la LIV, aunque se podrán refinar los resultados de la caracterización hidráulica (paso 2), haciendo una caracterización morfológica más detallada en el tramo preliminar acotado luego de la primera iteración.

5 Referencias bibliográficas

[1] Arenas F., G. A. 2005. Estimación experimental de la tasa de reaireación en ríos de montaña. Bogotá D.C., Tesis de Maestría. Universidad de los Andes.

[2] Bansal, M.K. 1976. Nitrification in natural systems. Journal of Water Pollution Control Federation. 48(10), pp. 2380-2393

[3] Botz, M. y Mudder, T. 2000. Modeling of natural cyanide attenuation in tailings impoundments. Mineral and Metallurgical Processing, Vol. 17, No. 4, pp. 228-233.

[4] Bowie, L. G., Mills, W. B., Porcella, D. B., Campbell, C. L., Pagenkopf, J. R., Rupp, G. L.,. 1985. Rates, constants, and kinetics formulations in surface water quality modeling. Athens, Georgia: Environmental Protection Agency.

[5] Camacho, L. A., Lees, M. 2000. Modelación de transporte de solutos en ríos bajo condiciones de flujo no permanente: un modelo conceptual integrado. XIV Seminario Nacional de Hidráulica e Hidrología

[6] Chapra, S.C. 1991. A toxicant loading concept for organic contaminants in lakes. ASCE Journal of Environmental Engineering 117(5), pp. 656-677.

[7] Chapra, S.C. 1997. Surface Water-Quality Modeling, McGraw-Hill.

[8] Gélves, R., Camacho, L. A. 2008. Metodología para determinar la tasa de reaireación por medio de trazadores volátiles en dos ríos de montaña colombianos. XXIII Congreso Latinoamericano de Hidráulica.

[9] Holguín G, J. E. 2003. Determinación de la tasa de reaireación en un río de montaña colombiano mediante el uso de trazadores. Bogotá D.C., Tesis de Maestría. Universidad de los Andes.

[10] Ji, Z.G. 2008. Hydrodynamics and water quality. Modelling Rivers, Lakes, and Estuaries, Wiley-Interscience.

[11] Lees, M.J., Camacho, L.A., Whitehead, P. 1998. Extension of the QUASAR river quality model to incorporate dead-zone mixing. Hydrology and Earth System Sciences, 2, pp. 353-365.

[12] Medina, M. P. 2009. Propuesta metodológica para la estimación de la capacidad de nitrificación de los ríos de montaña. Casos de estudio río Teusacá y río Subachoque. Bogotá, Universidad Nacional de Colombia: Tesis de Maestría.

[13] Rojas, A.F. 2011. Aplicación de factores de asimilación para la priorización de la inversión en sistemas de saneamiento hídrico en Colombia. Bogotá, Universidad Nacional de Colombia: Tesis de Maestría.

[14] Schnoor, J. L., C. Sato, D. McKetchnie, and D. Sahoo. 1987. Processes, coefficients, and models for simulating toxic organics and heavy metals in surface waters. EPA/600/3-87/015, U.S. EPA, Athens, GA, 30605.

[15] U.S. Environmental Protection Agency. 1977. Mahoning River waste load allocation study. Michigan-Ohio District Office. West Lake, Ohio.

[16] Thomann, R.V. and Mueller, J.A. 1987. Principles of surface water quality modeling and control. Addison-Wesley.

[17] UN-MAVDT, Universidad Nacional de Colombia - Ministerio de Ambiente, Vivienda y Desarrollo Territorial. 2008. Metodología para la estimación de caudales ambientales en proyectos licenciados. Bogotá: Contrato No. 0076-08 del Convenio Interadministrativo OEI-MAVDT No 004/07 de 2007.

ANEXO 2

HOJAS DE CÁLCULO DEL DESARROLLO DE LA MODELACIÓN PARA EL VERTIMIENTO

DATOS DE ENTRADA

Características de la fuente receptora

Nombre de la fuente: Río Boquerón
Coordenadas (x,y) 948636,85;590908,54
Observación

Características fisicoquímicas de la fuente receptora

Parámetro	Símbolo	Unidades	Valor	Fuente
pH	pH_0	Unidades de pH	7,19	Muestreo calidad de agua
Temperatura del agua	T_0	°C	15	Muestreo calidad de agua
Oxígeno Disuelto	OD_0	mg/L	8,1	Muestreo calidad de agua
DBO_5	DBO_0	mg O2/L	5	Muestreo calidad de agua
DQO	DQO_0	mg O2/L	20	Muestreo calidad de agua
NTK	NTK_0	mg/L	3	Muestreo calidad de agua
Fósforo total	PT_0	mg/L	0,062	Muestreo calidad de agua
Sólidos Suspendidos Totales	SST_0	mg SS/L	46	Muestreo calidad de agua
NMP Coliformes Fecales	CF_0	NMP/100ml	488	Muestreo calidad de agua

Características hidráulicas de la corriente receptora

Parámetro	Símbolo	Unidades	Valor	Fuente
Caudal minimo	Q_{amb}	m^3/s	1,1	HSEQ SAS
Profundidad media*	H_{med}	m	0,68	HSEQ SAS
Pendiente del lecho	S	%	7,21102863	HSEQ SAS
Velocidad mínima*	v_{min}	m/s		
Velocidad media*	v_{med}	m/s	0,34	HSEQ SAS
Velocidad máxima*	$v_{máx}$	m/s	0,44	HSEQ SAS
Fracción dispersiva	DF	Adim.	0,227	

Características del vertimiento de agua residual

Características fisicoquímicas del vertimiento

Parámetro	Símbolo	Unidades	Valor	Fuente
pH	pH_v	Unidades de pH	6,9	TEÓRICO
Temperatura del agua	T_v	°C	18,5	TEÓRICO
Oxígeno Disuelto	OD_v	mg/L	2,15	TEÓRICO
DBO_5	DBO_v	mg O2/L	500	TEÓRICO
DQO	DQO_v	mg O2/L	600	TEÓRICO
NTK	NTK_v	mg/L	45	TEÓRICO
Fósforo total	PT_v	mg/L	15	TEÓRICO
Sólidos Suspendidos Totales	SST_v	mg SS/L	20	TEÓRICO
NMP Coliformes Fecales	CF_v	NMP/100ml	80000	TEÓRICO

Caudal del vertimiento

Parámetro	Símbolo	Unidades	Valor	Fuente
Caudal del vertimiento	Q_v	m^3/s	0,00044	GEOCOL SAS

Datos que deben ser digitados

Datos que se calculan automáticamente

NITRÓGENO

Cálculo de la carga de entrada del tramo (W)

Caudal minimo (m^3/día)	**Qmin**	95040
Caudal del vertimiento (m3/día)	**Q_v**	38,016
Concentración en el cuerpo de agua (mg/m^3)	**NTK_0**	3000
Concentración en el vertimiento (mg/m^3)	**NTK_v**	45000
Carga de entrada (mg/día)	**W**	286830720
Velocidad media (m/día)	**v_{med}**	29376
Concentración estándar (mg/m^3)	**C_{est}**	3000
Fracción dispersiva (Adim)	**DF**	0,227

Cálculo de la tasa de nitrificación (k_n)

Profundidad H_{med} 0,68 m

K_n 1,53

Los valores de K_n generalmente están en el rango de 0.1 a 0.5 d^{-1} para aguas profundas mientras que para aguas someras valores por encima de 1d^{-1} son encontrados frecuentemente.

Río	K_n (d^{-1})	Profundidad (m)	Reportado en
Mine Brook	8.00	0.2	Tuffey et al. (1974)
Oroua	6.70	0.25	Cooper (1986)
Waiohewa	5.90	0.3	Cooper (1986)
Speed	2.30	0.43	Gowda (1983)
Sweetwater	0.80	0.46	Cooper (1986)
Trace	2.20	0.46	Cooper (1986)
Trukee	2.40	0.51	Bansal (1976)
Grand	1.90	0.58	Bansal (1976)
Shenadoha	1.25	0.60	Deb y Bowers (1983)
Waiotapu	2.80	0.61	Cooper (1986)
Ootanaula	0.80	0.61	Cooper (1986)
Sitll	0.70	0.64	Curtis (1983)
Flint	1.53	0.66	Bansal (1976)
South Chickamauga	6.60	0.84	Cooper (1986)
Upper Mohawk	0.30	0.96	Bansal (1976)
Mud	0.50	1.00	Cooper (1986)
Big Blue	0.12	1.25	Bansal (1976)
Holston	0.23	1.30	Ruane y Krenekel (1977)
Chattahoockee	0.25	1.50	McCutcheon (1987)
Trinity	0.51	1.53	McCutcheon (1987)
Willamette	0.70	1.60	Cooper (1985)
Shenadoha	0.2	1.74	Deb y Bowers (1983)
Upper Mohawk	0.25	2.51	Bansal (1976)
Upper Mohawk	0.25	3.66	Bansal (1976)
Middle Mohawk	0.30	3.81	Bansal (1976)
Barge	0.25	3.9	Bansal (1976)
Anacostia	0.13	4.00	Sullivan y Brown (1988)
Lower Mohawk	0.30	4.25	Bansal (1976)
Seneca river	0.05	6.24	Canale et al (1995)
Ohio	0.25	8.15	Bansal (1976)

$$a_{NTK} = \left[(1 + DF * K_n t_{NTK}) * e^{(1-DF)*K_n t_{NTK}}\right] * Q$$

Cálculo del factor de asimilación (a)

a_{NTK} 95610,24 m^3/día

Comprobación del cálculo de a

	a_{NTK}	101449,44	m^3/día
Insertar semilla para t_{NTK}	**t_{NTK}**	0,0424645	día
	Celda objetivo	0,061073	

Cálculo del tiempo medio de viaje para el nitrógeno (t_{NTK})

$$t_{NTK(i+1)} = t_{NTK(i)} - \frac{\left(1 + DF * k_n t_{NTK(i)}\right) * Q * e^{(1-DF)*K_n t_{NTK(i)}} - a_{NTK}}{k_n\left[1 + DF(1-DF) * k_n t_{NTK(i)}\right] * Q * e^{(1-DF)*K_n t_{NTK(i)}}}$$

Solución de la ecuación con el método de Newton-Raphson

$$X_{n+1} = X_n - \frac{f(X_n)}{f'(X_n)}$$

Tolerancia 0,0001

Iteración	X	(FX)	F'(X)	Menor a tolerancia
0		-532,224	145469,364	TODAVIA NO
1	0,0036587	1,4151047	146243,589	TODAVIA NO
2	0,003649	9,932E-06	146241,536	SOLUCION
3	0,003649	0	146241,536	SOLUCION
4	0,003649	0	146241,536	SOLUCION
5	0,003649	0	146241,536	SOLUCION
6	0,003649	0	146241,536	SOLUCION
7	0,003649	0	146241,536	SOLUCION
8	0,003649	0	146241,536	SOLUCION
9	0,003649	0	146241,536	SOLUCION
10	0,003649	0	146241,536	SOLUCION
11	0,003649	0	146241,536	SOLUCION
12	0,003649	0	146241,536	SOLUCION
13	0,003649	0	146241,536	SOLUCION
14	0,003649	0	146241,536	SOLUCION
15	0,003649	0	146241,536	SOLUCION
16	0,003649	0	146241,536	SOLUCION
17	0,003649	0	146241,536	SOLUCION
18	0,003649	0	146241,536	SOLUCION
19	0,003649	0	146241,536	SOLUCION
20	0,003649	0	146241,536	SOLUCION
21	0,003649	0	146241,536	SOLUCION
22	0,003649	0	146241,536	SOLUCION
23	0,003649	0	146241,536	SOLUCION
24	0,003649	0	146241,536	SOLUCION
25	0,003649	0	146241,536	SOLUCION
26	0,003649	0	146241,536	SOLUCION
27	0,003649	0	146241,536	SOLUCION
28	0,003649	0	146241,536	SOLUCION
29	0,003649	0	146241,536	SOLUCION
30	0,003649	0	146241,536	SOLUCION

Tiempo medio de viaje definitivo t_{NTK} 0,04246453 día

Cálculo de la longitud aguas abajo donde se alcanza el factor de asimilación (L_{IV})

L_{IV} 1247,438 m

OXÍGENO DISUELTO Y DBO

Aproximación de Streeter - Phelps

Cálculo de la carga de entrada del tramo (W)

Caudal minimo (m^3/día)	Q_{min}	95040
Caudal del vertimiento (m^3/día)	Q_v	38,016
Concentración de oxigeno en el cuerpo de agua (mg/m^3)	OD_0	8100
Concentración de oxígeno en el vertimiento (mg/m^3)	OD_v	2150
Concentración de DBO en el cuerpo de agua (mg/m^3)	DBO_0	5000
Concentración de DBO en el vertimiento (mg/m^3)	DBO_v	500.000
Concentración de oxígeno en x=0 (mg/m^3)	OD_{x0}	8098
Concentración de DBO en x=0 (mg/m^3)	DBO_{x0}	5198
Velocidad media (m/día)	v_{med}	29376

Cálculo del déficit de oxígeno

Oxígeno de saturación (mg/m^3)	OD_S	10034,19
Déficit de oxígeno en x=0 (mg/m3)	DO_{x0}	1937

Cálculo de la tasa de reaireación (k_a)

Para ríos de alta montaña

Caudal a la entrada del tramo (m^3/s)	Q	1,1
Cambio en H (m)	ΔH	0,14422057
Constante (Adim)	c	0,177
Tasa de reaireación (d^{-1})	K_a	11,817

$$k_a = c\frac{\Delta H}{t_{med}}$$

c=0.36 para 0.028≤Q≤0.28 m³/s

c=0.177 para 0.708≤Q≤85 m³/s

Para ríos de planicie

Parámetro	O`Connor-Dobbins	Churchill	Owens-Gibbs
Profundidad (m)	0.30 – 9.14	0.31 – 3.35	0.12 – 0.73
Velocidad media (m/s)	0.15 – 0.49	0.55 – 1.52	0.03 – 0.55
Expresiones	$k_a = 3.93\frac{U^{0.5}}{H^{1.5}}$	$k_a = 5.026\frac{U}{H^{1.67}}$	$k_a = 5.32\frac{U^{0.67}}{H^{1.85}}$

Elija una de las ecuaciones para el cálculo de la tasa de reaireación en un río de planicie, teniendo en cuenta la profundidad y/o velocidad medio del cuerpo de agua

Profundidad de flujo, H (m)	0,68						
Velocidad de flujo, U (m/s)	0,34	K_a	4,08666125	K_a	2,54437772	K_a	3,89351575

El río analizado es de montaña o planicie? 1

Tasa de reaireación definitiva K_a 11,8171636 d^{-1}

Cálculo de la tasa de consumo de oxígeno por degradación de DBO (k_d)

Cálculo a partir de Ka

Cuerpo de agua	Rango de $f \equiv K_a/K_d$
Reservorio o lago pequeño	0.5 – 1.0
Curso lento, lago grande	1.0 – 2.0
Rio grande y lento	1.5 – 2.0
Rio grande con velocidad de flujo mediana	2.0 – 3.0
Curso rápido	3.0 – 5.0
Rápidas y caidas de agua	> 5.0

f 3

K_d 3,93905455

Cálculo a partir de Q

K_d 1,88186623

$$k_d = 1.796Q^{-0.49}$$

Para 0.3≤Q≤23 m³/s

Tasa por degradación de DBO definitiva K_d 3,93905455

ECUACIONES

$$DO = \frac{K_d}{K_a - K_d} DBO_o\left(e^{-K_d x/U} - e^{-K_a x/U}\right) + DO_o e^{-K_a x/U}$$

$$DBO = DBO_o e^{-K_d x/U}$$

Cálculo del cambio en la concentración

x (m)	x/V_{med} (d)	DBO_5(mg/m^3)	DO	OD (mg/m^3)
0,5	0,00002	5197,57	1936,53	8097,66
2	0,00007	5196,53	1936,40	8097,79
4	0,00014	5195,13	1936,24	8097,95
8	0,00027	5192,35	1935,91	8098,28
10	0,00034	5190,96	1935,74	8098,44
30	0,00102	5177,05	1934,08	8100,11
100	0,00340	5128,69	1928,07	8106,12
213	0,00725	5051,56	1917,78	8116,41
300	0,01021	4992,97	1909,40	8124,79
400	0,01362	4926,47	1899,29	8134,90
500	0,01702	4860,85	1888,72	8145,47
600	0,02042	4796,11	1877,71	8156,48
700	0,02383	4732,22	1866,28	8167,91
800	0,02723	4669,19	1854,47	8179,71
2500	0,08510	3717,43	1616,41	8417,78
3000	0,10212	3476,36	1540,03	8494,16
3500	0,11914	3250,93	1463,41	8570,77
4000	0,13617	3040,11	1387,53	8646,66
4500	0,15319	2842,97	1313,11	8721,08
5000	0,17021	2658,61	1240,67	8793,51

GRÁFICAS DE RESULTADOS

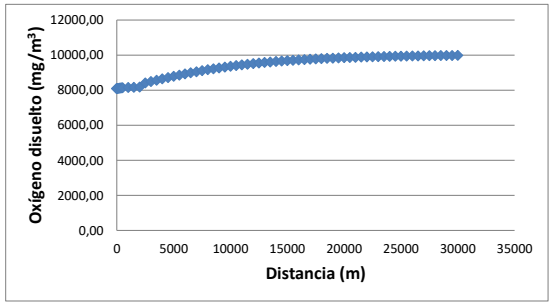

Para el oxígeno disuelto

L_{IV} 4000 m

7735

5500	0,18723	2486,21	1170,62	8863,57
6000	0,20425	2324,98	1103,21	8930,97
6500	0,22127	2174,22	1038,63	8995,56
7000	0,23829	2033,22	976,97	9057,22
7500	0,25531	1901,37	918,27	9115,92
8000	0,27233	1778,08	862,52	9171,66
8500	0,28935	1662,77	809,70	9224,49
9000	0,30637	1554,95	759,74	9274,45
9500	0,32339	1454,11	712,55	9321,63
10000	0,34041	1359,82	668,05	9366,14
10500	0,35743	1271,64	626,12	9408,07
11000	0,37446	1189,17	586,66	9447,53
11500	0,39148	1112,06	549,54	9484,64
12000	0,40850	1039,94	514,67	9519,52
12500	0,42552	972,51	481,92	9552,27
13000	0,44254	909,44	451,17	9583,01
13500	0,45956	850,47	422,33	9611,86
14000	0,47658	795,32	395,29	9638,90
14500	0,49360	743,74	369,93	9664,26
15000	0,51062	695,51	346,17	9688,02
15500	0,52764	650,41	323,91	9710,28
16000	0,54466	608,23	303,06	9731,13
16500	0,56168	568,79	283,53	9750,66
17000	0,57870	531,91	265,24	9768,94
17500	0,59572	497,41	248,13	9786,06
18000	0,61275	465,16	232,10	9802,08
18500	0,62977	434,99	217,11	9817,08
19000	0,64679	406,79	203,08	9831,11
19500	0,66381	380,41	189,94	9844,24
20000	0,68083	355,74	177,66	9856,53
20500	0,69785	332,67	166,16	9868,03
21000	0,71487	311,10	155,41	9878,78
21500	0,73189	290,92	145,35	9888,84
22000	0,74891	272,06	135,93	9898,25
22500	0,76593	254,42	127,13	9907,06
23000	0,78295	237,92	118,90	9915,29
23500	0,79997	222,49	111,19	9923,00
24000	0,81699	208,06	103,99	9930,20
24500	0,83401	194,57	97,25	9936,94
25000	0,85103	181,95	90,95	9943,24
25500	0,86806	170,15	85,05	9949,13
26000	0,88508	159,12	79,54	9954,65
26500	0,90210	148,80	74,38	9959,80
27000	0,91912	139,15	69,56	9964,62
27500	0,93614	130,13	65,05	9969,13
28000	0,95316	121,69	60,84	9973,35
28500	0,97018	113,80	56,89	9977,30
29000	0,98720	106,42	53,20	9980,98
29500	1,00422	99,52	49,75	9984,43
30000	1,02124	93,06	46,53	9987,66

Para la DBO_5

L_{IV} m

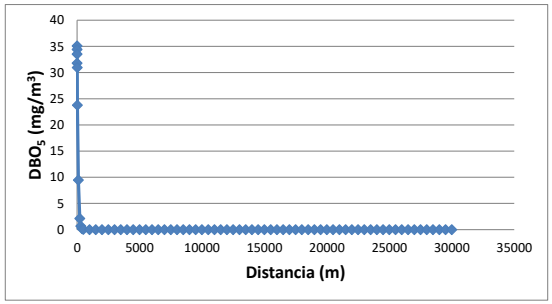

DEMANDA BIOQUÍMICA DE OXÍGENO (DBO)

Cálculo de la carga de entrada del tramo (W)

Caudal ambiental (m^3/día)	Q_{amb}	95040
Caudal del vertimiento (m^3/día)	Q_v	38,016
Concentración en el cuerpo de agua (mg/m^3)	DBO_0	5000
Concentración en el vertimiento (mg/m^3)	DBO_v	500000
Carga de entrada (mg/día)	W	494208000
Velocidad media (m/día)	v_{med}	29376
Concentración estándar (mg/m^3)	C_{est}	5000
Fracción dispersiva (Adim)	DF	0,722

$$a_{DBO} = \left[\left(1 + DF * K_d t_{DBO}\right) * e^{(1-DF)*K_d t_{DBO}}\right] * Q$$

Cálculo de la tasa de consumo de oxígeno por degradación de DBO (k_d)

K_d 3,93905455 d^{-1}

Cálculo del factor de asimilación (a)

a_{DBO} 98841,6 m^3/día

Comprobación del cálculo de a

	a_{DBO}	96302,01372	m^3/día
Insertar semilla para t_{DBO}	t_{DBO}	0,003258173	día
	Celda objetivo	0,025693496	

Cálculo del tiempo medio de viaje para la DBO (t_{DBO})

$$t_{DBO(i+1)} = t_{DBO(i)} - \frac{\left(1 + DF * k_d t_{DBO(i)}\right) * Q * e^{(1-DF)*K_d t_{DBO(i)}} - a_{DBO}}{k_d\left[1 + DF(1 - DF) * k_d t_{DBO(i)}\right] * Q * e^{(1-DF)*K_d t_{DBO(i)}}}$$

Solución de la ecuación con el método de Newton-Raphson

$$X_{n+1} = X_n - \frac{f(X_n)}{f'(X_n)}$$

Tolerancia 0,0001

Iteración	X	(FX)	F'(X)	Menor a tolerancia
0	0,014	1549,375233	384512,8983	TODAVIA NO
1	0,009970551	5,847088313	381613,742	TODAVIA NO
2	0,009955229	8,41909E-05	381602,7525	TODAVIA NO
3	0,009955228	0	381602,7523	SOLUCION
4	0,009955228	0	381602,7523	SOLUCION
5	0,009955228	0	381602,7523	SOLUCION
6	0,009955228	0	381602,7523	SOLUCION
7	0,009955228	0	381602,7523	SOLUCION
8	0,009955228	0	381602,7523	SOLUCION
9	0,009955228	0	381602,7523	SOLUCION
10	0,009955228	0	381602,7523	SOLUCION
11	0,009955228	0	381602,7523	SOLUCION
12	0,009955228	0	381602,7523	SOLUCION
13	0,009955228	0	381602,7523	SOLUCION
14	0,009955228	0	381602,7523	SOLUCION
15	0,009955228	0	381602,7523	SOLUCION
16	0,009955228	0	381602,7523	SOLUCION
17	0,009955228	0	381602,7523	SOLUCION
18	0,009955228	0	381602,7523	SOLUCION
19	0,009955228	0	381602,7523	SOLUCION
20	0,009955228	0	381602,7523	SOLUCION
21	0,009955228	0	381602,7523	SOLUCION
22	0,009955228	0	381602,7523	SOLUCION
23	0,009955228	0	381602,7523	SOLUCION
24	0,009955228	0	381602,7523	SOLUCION
25	0,009955228	0	381602,7523	SOLUCION
26	0,009955228	0	381602,7523	SOLUCION
27	0,009955228	0	381602,7523	SOLUCION
28	0,009955228	0	381602,7523	SOLUCION
29	0,009955228	0	381602,7523	SOLUCION
30	0,009955228	0	381602,7523	SOLUCION

Tiempo medio de viaje definitivo t_{DBO} 0,00325817 día

Cálculo de la longitud aguas abajo donde se alcanza el factor de asimilación (L_{IV})

L_{IV} 95,7121 m

FÓSFORO TOTAL

Cálculo de la carga de entrada del tramo (W)

Caudal ambiental (m^3/día)	Q_{amb}	95040
Caudal del vertimiento (m^3/día)	Q_v	38,016
Concentración en el cuerpo de agua (mg/m^3)	PT_0	62
Concentración en el vertimiento (mg/m^3)	PT_v	15000
Carga de entrada (mg/día)	W	6462720
Velocidad media (m/día)	v_{med}	29376
Concentración estándar (mg/m^3)	C_{est}	62
Fracción dispersiva (Adim)	DF	0,2272727

Cálculo de la tasa de hidrólisis (k_p)

K_p	6	d^{-1}

Cálculo del factor de asimilación (a)

$$a_{PT} = \left[\left(1 + DF * K_p t_{PT}\right) * e^{(1-DF)*K_p t_{PT}}\right] * Q$$

a_{PT}	104237,4194	m^3/día

Comprobación del cálculo de a

	a_{PT}	118343,16	m^3/día
Insertar semilla para t_{PT}	t_{PT}	0,0366836	
	Celda objetivo	0,1353232	

Cálculo del tiempo medio de viaje para el fósforo total (t_{PT})

$$t_{PT(i+1)} = t_{PT(i)} - \frac{\left(1 + DF * k_p t_{PT(i)}\right) * Q * e^{(1-DF)*K_p t_{PT(i)}} - a_{PT}}{k_p\left[1 + DF(1-DF) * k_p t_{PT(i)}\right] * Q * e^{(1-DF)*K_p t_{PT(i)}}}$$

Solución de la ecuación con el método de Newton-Raphson

$$X_{n+1} = X_n - \frac{f(X_n)}{f'(X_n)}$$

Tolerancia 0,0001

Iteración	X	(FX)	F'(X)	Menor a tolerancia
0		-9159,403	570468,096	TODAVIA NO
1	0,0160559	430,97389	624952,3243	TODAVIA NO
2	0,0153663	0,8418918	622512,219	TODAVIA NO
3	0,015365	3,23E-06	622507,4427	SOLUCION
4	0,015365	0	622507,4427	SOLUCION
5	0,015365	0	622507,4427	SOLUCION
6	0,015365	0	622507,4427	SOLUCION
7	0,015365	0	622507,4427	SOLUCION
8	0,015365	0	622507,4427	SOLUCION
9	0,015365	0	622507,4427	SOLUCION
10	0,015365	0	622507,4427	SOLUCION
11	0,015365	0	622507,4427	SOLUCION
12	0,015365	0	622507,4427	SOLUCION
13	0,015365	0	622507,4427	SOLUCION
14	0,015365	0	622507,4427	SOLUCION
15	0,015365	0	622507,4427	SOLUCION
16	0,015365	0	622507,4427	SOLUCION
17	0,015365	0	622507,4427	SOLUCION
18	0,015365	0	622507,4427	SOLUCION
19	0,015365	0	622507,4427	SOLUCION
20	0,015365	0	622507,4427	SOLUCION
21	0,015365	0	622507,4427	SOLUCION
22	0,015365	0	622507,4427	SOLUCION
23	0,015365	0	622507,4427	SOLUCION
24	0,015365	0	622507,4427	SOLUCION
25	0,015365	0	622507,4427	SOLUCION
26	0,015365	0	622507,4427	SOLUCION
27	0,015365	0	622507,4427	SOLUCION
28	0,015365	0	622507,4427	SOLUCION
29	0,015365	0	622507,4427	SOLUCION
30	0,015365	0	622507,4427	SOLUCION

Tiempo medio de viaje definitivo t_{PT} 0,03668362 día

Cálculo de la longitud aguas abajo donde se alcanza el factor de asimilación (L_{IV})

L_{IV} 1077,618 m

SÓLIDOS SUSPENDIDOS TOTALES

Cálculo de la carga de entrada del tramo (W)

Caudal ambiental (m^3/día)	Q_{amb}	95040
Caudal del vertimiento (m^3/día)	Q_v	38,016
Concentración en el cuerpo de agua (mg/m^3)	SST_0	46000
Concentración en el vertimiento (mg/m^3)	SST_v	20000
Carga de entrada (mg/día)	W	4,373E+09
Velocidad media (m/día)	v_{med}	29376
Concentración estándar (mg/m^3)	C_{est}	46000
Fracción dispersiva (Adim)	DF	0,227

Cálculo de la velocidad de sedimentación (v_{ss})

Tipo de partícula	Diámetro (µm)	Velocidad de sedimentación (m d^{-1})
Carbono orgánico particulado	1-10	0.2
	10-64	1.5
	> 64	2.3
Arcilla	2-4	0.3-1
Limo	10-20	3-30

v_{ss} 0,008 m/s

Cálculo de la tasa de sedimentación (k_s)

K_s 1016,470588 d-1

$$a_{SST} = \left[(1 + DF * K_s t_{SST}) * e^{(1-DF)*K_s t_{SST}}\right] * Q$$

Cálculo del factor de asimilación (a)

a_{SST} 95056,5287 m^3/día

Comprobación del cálculo de a

	a_{SST}	107652,6	m^3/día
Insertar semilla para t_{SST}	t_{SST}	0,0001226	
	Celda objetivo	0,1325114	

Cálculo del tiempo medio de viaje para los sólidos suspendidos totales (t_{SST})

Solución de la ecuación con el método de Newton-Raphson

$$t_{SST(i+1)} = t_{SST(i)} - \frac{(1 + DF * k_s t_{SST(i)}) * Q * e^{(1-DF)*K_s t_{SST(i)}} - a_{SST}}{k_s\left[1 + DF(1 - DF) * k_s t_{SST(i)}\right] * Q * e^{(1-DF)*K_s t_{SST(i)}}}$$

$$X_{n+1} = X_n - \frac{f(X_n)}{f'(X_n)}$$

Tolerancia 0,0001

Iteración	X	(FX)	F'(X)	Menor a tolerancia
0		21,487304	96644006,85	TODAVIA NO
1	-2,22E-07	0,0023025	96623295,94	TODAVIA NO
2	-2,22E-07	0	96623293,72	SOLUCION
3	-2,22E-07	0	96623293,72	SOLUCION
4	-2,22E-07	0	96623293,72	SOLUCION
5	-2,22E-07	0	96623293,72	SOLUCION
6	-2,22E-07	0	96623293,72	SOLUCION
7	-2,22E-07	0	96623293,72	SOLUCION
8	-2,22E-07	0	96623293,72	SOLUCION
9	-2,22E-07	0	96623293,72	SOLUCION
10	-2,22E-07	0	96623293,72	SOLUCION
11	-2,22E-07	0	96623293,72	SOLUCION
12	-2,22E-07	0	96623293,72	SOLUCION
13	-2,22E-07	0	96623293,72	SOLUCION
14	-2,22E-07	0	96623293,72	SOLUCION
15	-2,22E-07	0	96623293,72	SOLUCION
16	-2,22E-07	0	96623293,72	SOLUCION
17	-2,22E-07	0	96623293,72	SOLUCION
18	-2,22E-07	0	96623293,72	SOLUCION
19	-2,22E-07	0	96623293,72	SOLUCION
20	-2,22E-07	0	96623293,72	SOLUCION
21	-2,22E-07	0	96623293,72	SOLUCION
22	-2,22E-07	0	96623293,72	SOLUCION
23	-2,22E-07	0	96623293,72	SOLUCION
24	-2,22E-07	0	96623293,72	SOLUCION
25	-2,22E-07	0	96623293,72	SOLUCION
26	-2,22E-07	0	96623293,72	SOLUCION
27	-2,22E-07	0	96623293,72	SOLUCION
28	-2,22E-07	0	96623293,72	SOLUCION
29	-2,22E-07	0	96623293,72	SOLUCION
30	-2,22E-07	0	96623293,72	SOLUCION

Tiempo medio de viaje definitivo t_{SST} 0,00012259 día

Cálculo de la longitud aguas abajo donde se alcanza el factor de asimilación (L_{IV})

L_{IV} 3,6 m

COLIFORMES FECALES

Cálculo de la carga de entrada del tramo (W)

Caudal ambiental (m^3/día)	Q_{amb}	95040
Caudal del vertimiento (m3/día)	Q_v	38,016
Concentración en el cuerpo de agua (mg/m^3)	CF_0	4.880.000
Concentración en el vertimiento (mg/m^3)	CF_v	800.000.000
Carga de entrada (mg/día)	W	4,94208E+11
Velocidad media (m/día)	v_{med}	29376
Concentración estándar (mg/m^3)	C_{est}	4.880.000
Fracción dispersiva (Adim)	DF	0,227

Tasa de decaimiento por muerte de patógenos (k_b)

$$k_b = 0.8 * 1.07^{T-20} + \frac{I_0}{0.55 * SST * H} * (1 - e^{-0.55*SST*H}) + F_p * \frac{v_{ss}}{H}$$

Donde:
T: Temperatura del agua (ºC)
I_0: Radiación solar (ly/hr)
SST: Concentración de sólidos suspendidos totales promedio en el tramo (mg/l)
H: Profundidad media del agua (m)
F_p: Fracción adsorbida de bacterias a las partículas sólidas. Valor típico: 0.7.
V_{ss}: Velocidad de sedimentación de las partículas (md^{-1})

T	15	ºC
I_0	35,93	ly/hr
SST_0	46	mg/l
H	0,68	m
v_{ss}	0,008	md^{-1}

k_b	2,67062138

$$a_{CF} = \left[(1 + DF * K_s t_{CF}) * e^{(1-DF)*K_s t_{CF}}\right] * Q$$

Cálculo del factor de asimilación (a)

a_{CF}	101272,131	m^3/día

Comprobación del cálculo de a

Insertar semilla para t_{CF}

a_{CF}	277391,9049	m^3/día
t_{CF}	0,410943819	día
Celda objetivo	1,73907443	

Cálculo del tiempo medio de viaje para los coliformes totales (t_{CF})

$$t_{CF(i+1)} = t_{CF(i)} - \frac{(1 + DF * k_b t_{CF(i)}) * Q * e^{(1-DF)*K_b t_{CF(i)}} - a_{CF}}{k_b\left[1 + DF(1 - DF) * k_b t_{CF(i)}\right] * Q * e^{(1-DF)*K_b t_{CF(i)}}}$$

Solución de la ecuación con el método de Newton-Raphson

$$X_{n+1} = X_n - \frac{f(X_n)}{f'(X_n)}$$

Tolerancia 0,0001

Iteración	X	(FX)	F'(X)	Menor a tolerancia
0		-6194,115	253917,382	TODAVIA NO
1	0,024394215	195,20587	270082,275	TODAVIA NO
2	0,02367145	0,1781858	269589,352	TODAVIA NO
3	0,023670789	1,489E-07	269588,902	SOLUCION
4	0,023670789	0	269588,902	SOLUCION
5	0,023670789	0	269588,902	SOLUCION
6	0,023670789	0	269588,902	SOLUCION
7	0,023670789	0	269588,902	SOLUCION
8	0,023670789	0	269588,902	SOLUCION
9	0,023670789	0	269588,902	SOLUCION
10	0,023670789	0	269588,902	SOLUCION
11	0,023670789	0	269588,902	SOLUCION
12	0,023670789	0	269588,902	SOLUCION
13	0,023670789	0	269588,902	SOLUCION
14	0,023670789	0	269588,902	SOLUCION
15	0,023670789	0	269588,902	SOLUCION
16	0,023670789	0	269588,902	SOLUCION
17	0,023670789	0	269588,902	SOLUCION
18	0,023670789	0	269588,902	SOLUCION
19	0,023670789	0	269588,902	SOLUCION
20	0,023670789	0	269588,902	SOLUCION
21	0,023670789	0	269588,902	SOLUCION
22	0,023670789	0	269588,902	SOLUCION
23	0,023670789	0	269588,902	SOLUCION
24	0,023670789	0	269588,902	SOLUCION
25	0,023670789	0	269588,902	SOLUCION
26	0,023670789	0	269588,902	SOLUCION
27	0,023670789	0	269588,902	SOLUCION
28	0,023670789	0	269588,902	SOLUCION
29	0,023670789	0	269588,902	SOLUCION
30	0,023670789	0	269588,902	SOLUCION

Tiempo medio de viaje definitivo t_{CF} 0,411 día

Cálculo de la longitud aguas abajo donde se alcanza el factor de asimilación (L_{IV})

L_{IV} 12071,886 m

FUENTES DE INFORMACIÓN PARA CADA DETERMINANTE

En esta sección se presenta la fuente de información de los datos de entrada (recuadro rojo) para el cálculo de la longitud de asimilación de cada determinante.

Características hidráulicas de la corriente receptora

Parámetro	Símbolo	Fuente de información
Caudal mínimo	Q_{min}	QHSE SAS
Caudal medio	Q_{medio}	QHSE SAS
Caudal máximo	$Q_{máx}$	QHSE SAS
Profundidad del agua para caudal mínimo	H_{min}	QHSE SAS
Profundidad media del agua	H_{med}	QHSE SAS
Pendiente del lecho	S	QHSE SAS
Velocidad media	v_{med}	QHSE SAS
Velocidad máxima	$v_{máx}$	QHSE SAS

Nitrógeno

Parámetro	Símbolo	Fuente de información
Tasa de nitrificación	K_n	Cooper. 1986
Tolerancia	-	Criterio del profesional
Tiempo medio de viaje definitivo	t_{NTK}	Iteración

Oxígeno disuelto y DBO

Parámetro	Símbolo	Fuente de información
Cambio en H	ΔH	QHSE SAS
Constante (Adim.)	c	Modelo de Streeter y Phelps
Factor f para el cálculo de la tasa de consumo de oxígeno	f	Criterio de acuerdo a las características de la corriente receptora
Tiempo medio de viaje definitivo del oxígeno disuelto	t_{OD}	Iteración
Tiempo medio de viaje definitivo de la DBO	t_{DBO}	Iteración

Fósforo total

Parámetro	Símbolo	Fuente de información
Tasa de hidrólisis de fósforo	K_p	No aplica
Tolerancia	-	
Tiempo medio de viaje definitivo del fósforo total	t_{PT}	

Sólidos suspendido totales

Parámetro	Símbolo	Fuente de información
Tolerancia	-	Criterio del profesional
Tiempo medio de viaje definitivo de los SST	t_{SST}	Iteración
Velocidad de sedimentación	v_{ss}	ANLA. Metodología para la definición de la longitud de influencia de vertimientos sobre corrientes de agua superficial

Coliformes totales

Parámetro	Símbolo	Fuente de información
Radiación solar	I_0	No aplica
Tolerancia	-	
Tiempo medio de viaje definitivo de los coliformes totales	t_{CF}	

DATOS DE ENTRADA

Características de la fuente receptora

Nombre de la fuente: Quebrada La Humeadora
Coordenadas (x,y) 955242,08;597102,86
Observación

Características fisicoquímicas de la fuente receptora

Parámetro	Símbolo	Unidades	Valor	Fuente
pH	pH_0	Unidades de pH	7,9	Muestreo calidad de agua
Temperatura del agua	T_0	°C	13,7	Muestreo calidad de agua
Oxígeno Disuelto	OD_0	mg/L	7,8	Muestreo calidad de agua
DBO_5	DBO_0	mg O2/L	5	Muestreo calidad de agua
DQO	DQO_0	mg O2/L	20	Muestreo calidad de agua
NTK	NTK_0	mg/L	3	Muestreo calidad de agua
Fósforo total	PT_0	mg/L	0,062	Muestreo calidad de agua
Sólidos Suspendidos Totales	SST_0	mg SS/L	10	Muestreo calidad de agua
NMP Coliformes Fecales	CF_0	NMP/100ml	224	Muestreo calidad de agua

Características hidráulicas de la corriente receptora

Parámetro	Símbolo	Unidades	Valor	Fuente
Caudal minimo	Q_{amb}	m^3/s	0,1014	HSEQ SAS
Profundidad media*	H_{med}	m	0,31	HSEQ SAS
Pendiente del lecho	S	%	0,83119825	HSEQ SAS
Velocidad mínima*	v_{min}	m/s		
Velocidad media*	v_{med}	m/s	0,27	HSEQ SAS
Velocidad máxima*	$v_{máx}$	m/s	0,35	HSEQ SAS
Fracción dispersiva	DF	Adim.	0,229	

Características del vertimiento de agua residual

Características fisicoquímicas del vertimiento

Parámetro	Símbolo	Unidades	Valor	Fuente
pH	pH_v	Unidades de pH	6,9	TEÓRICO
Temperatura del agua	T_v	°C	18,5	TEÓRICO
Oxígeno Disuelto	OD_v	mg/L	2,15	TEÓRICO
DBO_5	DBO_v	mg O2/L	500	TEÓRICO
DQO	DQO_v	mg O2/L	600	TEÓRICO
NTK	NTK_v	mg/L	45	TEÓRICO
Fósforo total	PT_v	mg/L	15	TEÓRICO
Sólidos Suspendidos Totales	SST_v	mg SS/L	20	TEÓRICO
NMP Coliformes Fecales	CF_v	NMP/100ml	80000	TEÓRICO

Caudal del vertimiento

Parámetro	Símbolo	Unidades	Valor	Fuente
Caudal del vertimiento	Q_v	m^3/s	0,00044	GEOCOL SAS

Datos que deben ser digitados

Datos que se calculan automáticamente

NITRÓGENO

Cálculo de la carga de entrada del tramo (W)

Caudal minimo (m^3/día)	**Qmin**	8760,96
Caudal del vertimiento (m3/día)	**Q_v**	38,016
Concentración en el cuerpo de agua (mg/m^3)	**NTK_0**	3000
Concentración en el vertimiento (mg/m^3)	**NTK_v**	45000
Carga de entrada (mg/día)	**W**	27993600
Velocidad media (m/día)	**v_{med}**	23328
Concentración estándar (mg/m^3)	**C_{est}**	3000
Fracción dispersiva (Adim)	**DF**	0,229

Cálculo de la tasa de nitrificación (k_n)

Profundidad H_{med} 0,31 m

K_n 1,53

Los valores de K_n generalmente están en el rango de 0.1 a 0.5 d^{-1} para aguas profundas mientras que para aguas someras valores por encima de 1d^{-1} son encontrados frecuentemente.

Río	K_n (d^{-1})	Profundidad (m)	Reportado en
Mine Brook	8.00	0.2	Tuffey et al. (1974)
Oroua	6.70	0.25	Cooper (1986)
Waiohewa	5.90	0.3	Cooper (1986)
Speed	2.30	0.43	Gowda (1983)
Sweetwater	0.80	0.46	Cooper (1986)
Trace	2.20	0.46	Cooper (1986)
Trukee	2.40	0.51	Bansal (1976)
Grand	1.90	0.58	Bansal (1976)
Shenadoha	1.25	0.60	Deb y Bowers (1983)
Waiotapu	2.80	0.61	Cooper (1986)
Ootanaula	0.80	0.61	Cooper (1986)
Sitll	0.70	0.64	Curtis (1983)
Flint	1.53	0.66	Bansal (1976)
South Chickamauga	6.60	0.84	Cooper (1986)
Upper Mohawk	0.30	0.96	Bansal (1976)
Mud	0.50	1.00	Cooper (1986)
Big Blue	0.12	1.25	Bansal (1976)
Holston	0.23	1.30	Ruane y Krenekel (1977)
Chattahoockee	0.25	1.50	McCutcheon (1987)
Trinity	0.51	1.53	McCutcheon (1987)
Willamette	0.70	1.60	Cooper (1985)
Shenadoha	0.2	1.74	Deb y Bowers (1983)
Upper Mohawk	0.25	2.51	Bansal (1976)
Upper Mohawk	0.25	3.66	Bansal (1976)
Middle Mohawk	0.30	3.81	Bansal (1976)
Barge	0.25	3.9	Bansal (1976)
Anacostia	0.13	4.00	Sullivan y Brown (1988)
Lower Mohawk	0.30	4.25	Bansal (1976)
Seneca river	0.05	6.24	Canale et al (1995)
Ohio	0.25	8.15	Bansal (1976)

$$a_{NTK} = \left[(1 + DF * K_n t_{NTK}) * e^{(1-DF)*K_n t_{NTK}}\right] * Q$$

Cálculo del factor de asimilación (a)

a_{NTK} 9331,2 m^3/día

Comprobación del cálculo de a

	a_{NTK}	9388,6066	m^3/día
Insertar semilla para t_{NTK}	**t_{NTK}**	0,0424645	día
	Celda objetivo	0,0061521	

Cálculo del tiempo medio de viaje para el nitrógeno (t_{NTK})

$$t_{NTK(i+1)} = t_{NTK(i)} - \frac{\left(1 + DF * k_n t_{NTK(i)}\right) * Q * e^{(1-DF)*K_n t_{NTK(i)}} - a_{NTK}}{k_n\left[1 + DF(1-DF) * k_n t_{NTK(i)}\right] * Q * e^{(1-DF)*K_n t_{NTK(i)}}}$$

Solución de la ecuación con el método de Newton-Raphson

$$X_{n+1} = X_n - \frac{f(X_n)}{f'(X_n)}$$

Tolerancia 0,0001

Iteración	X	(FX)	F'(X)	Menor a tolerancia
0		-532,224	13462,4333	TODAVIA NO
1	0,039534	15,540639	14255,9378	TODAVIA NO
2	0,0384439	0,0122525	14233,4643	TODAVIA NO
3	0,038443	7,632E-09	14233,4465	SOLUCION
4	0,038443	0	14233,4465	SOLUCION
5	0,038443	0	14233,4465	SOLUCION
6	0,038443	0	14233,4465	SOLUCION
7	0,038443	0	14233,4465	SOLUCION
8	0,038443	0	14233,4465	SOLUCION
9	0,038443	0	14233,4465	SOLUCION
10	0,038443	0	14233,4465	SOLUCION
11	0,038443	0	14233,4465	SOLUCION
12	0,038443	0	14233,4465	SOLUCION
13	0,038443	0	14233,4465	SOLUCION
14	0,038443	0	14233,4465	SOLUCION
15	0,038443	0	14233,4465	SOLUCION
16	0,038443	0	14233,4465	SOLUCION
17	0,038443	0	14233,4465	SOLUCION
18	0,038443	0	14233,4465	SOLUCION
19	0,038443	0	14233,4465	SOLUCION
20	0,038443	0	14233,4465	SOLUCION
21	0,038443	0	14233,4465	SOLUCION
22	0,038443	0	14233,4465	SOLUCION
23	0,038443	0	14233,4465	SOLUCION
24	0,038443	0	14233,4465	SOLUCION
25	0,038443	0	14233,4465	SOLUCION
26	0,038443	0	14233,4465	SOLUCION
27	0,038443	0	14233,4465	SOLUCION
28	0,038443	0	14233,4465	SOLUCION
29	0,038443	0	14233,4465	SOLUCION
30	0,038443	0	14233,4465	SOLUCION

Tiempo medio de viaje definitivo t_{NTK} 0,04246453 día

Cálculo de la longitud aguas abajo donde se alcanza el factor de asimilación (L_{IV})

L_{IV} 990,613 m

OXÍGENO DISUELTO Y DBO

Aproximación de Streeter - Phelps

Cálculo de la carga de entrada del tramo (W)

Caudal minimo (m^3/día)	Q_{min}	8760,96
Caudal del vertimiento (m^3/día)	Q_v	38,016
Concentración de oxigeno en el cuerpo de agua (mg/m^3)	OD_0	7800
Concentración de oxígeno en el vertimiento (mg/m^3)	OD_v	2150
Concentración de DBO en el cuerpo de agua (mg/m^3)	DBO_0	5000
Concentración de DBO en el vertimiento (mg/m^3)	DBO_v	500.000
Concentración de oxígeno en x=0 (mg/m^3)	OD_{x0}	7776
Concentración de DBO en x=0 (mg/m^3)	DBO_{x0}	7139
Velocidad media (m/día)	v_{med}	23328

Cálculo del déficit de oxígeno

Oxígeno de saturación (mg/m^3)	OD_S	10331,83
Déficit de oxígeno en x=0 (mg/m3)	DO_{x0}	2556

Cálculo de la tasa de reaireación (k_a)

Para ríos de alta montaña

Caudal a la entrada del tramo (m^3/s)	Q	0,1014
Cambio en H (m)	ΔH	0,01662397
Constante (Adim)	c	0,177
Tasa de reaireación (d^{-1})	K_a	9,438

$$k_a = c\frac{\Delta H}{t_{med}}$$

c=0.36 para 0.028≤Q≤0.28 m³/s

c=0.177 para 0.708≤Q≤85 m³/s

Para ríos de planicie

Parámetro	O`Connor-Dobbins	Churchill	Owens-Gibbs
Profundidad (m)	0.30 – 9.14	0.31 – 3.35	0.12 – 0.73
Velocidad media (m/s)	0.15 – 0.49	0.55 – 1.52	0.03 – 0.55
Expresiones	$k_a = 3.93\frac{U^{0.5}}{H^{1.5}}$	$k_a = 5.026\frac{U}{H^{1.67}}$	$k_a = 5.32\frac{U^{0.67}}{H^{1.85}}$

Elija una de las ecuaciones para el cálculo de la tasa de reaireación en un río de planicie, teniendo en cuenta la profundidad y/o velocidad medio del cuerpo de agua

Profundidad de flujo, H (m)	0,31						
Velocidad de flujo, U (m/s)	0,27	K_a	11,8312843	K_a	7,50209027	K_a	14,2687898

El río analizado es de montaña o planicie? 1

Tasa de reaireación definitiva K_a 9,43784229 d^{-1}

Cálculo de la tasa de consumo de oxígeno por degradación de DBO (k_d)

Cálculo a partir de Ka

Cuerpo de agua	Rango de $f \equiv K_a/K_d$
Reservorio o lago pequeño	0.5 – 1.0
Curso lento, lago grande	1.0 – 2.0
Rio grande y lento	1.5 – 2.0
Rio grande con velocidad de flujo mediana	2.0 – 3.0
Curso rápido	3.0 – 5.0
Rápidas y caidas de agua	> 5.0

f	3
K_d	3,14594743

Cálculo a partir de Q

K_d	0,58514693

$$k_d = 1.796Q^{-0.49}$$

Para 0.3≤Q≤23 m³/s

Tasa por degradación de DBO definitiva K_d 3,14594743

ECUACIONES

$$DO = \frac{K_d}{K_a - K_d} DBO_o\left(e^{-K_d x/U} - e^{-K_a x/U}\right) + DO_o e^{-K_a x/U}$$

$$DBO = DBO_o e^{-K_d x/U}$$

Cálculo del cambio en la concentración

x (m)	x/V_{med} (d)	DBO_5(mg/m^3)	DO	OD (mg/m^3)
0,5	0,00002	7138,17	2556,21	7775,62
2	0,00009	7136,72	2556,10	7775,73
4	0,00017	7134,80	2555,96	7775,88
8	0,00034	7130,95	2555,67	7776,16
10	0,00043	7129,03	2555,52	7776,31
30	0,00129	7109,83	2554,05	7777,78
100	0,00429	7043,03	2548,60	7783,23
213	0,00913	6936,51	2538,82	7793,01
300	0,01286	6855,60	2530,51	7801,32
400	0,01715	6763,77	2520,17	7811,66
500	0,02143	6673,17	2509,04	7822,79
600	0,02572	6583,78	2497,16	7834,68
700	0,03001	6495,59	2484,57	7847,26
800	0,03429	6408,58	2471,33	7860,50
2500	0,10717	5095,62	2179,35	8152,48
3000	0,12860	4763,35	2080,70	8251,13
3500	0,15003	4452,76	1980,52	8351,31
4000	0,17147	4162,41	1880,38	8451,46
4500	0,19290	3891,00	1781,45	8550,38
5000	0,21433	3637,29	1684,64	8647,20

GRÁFICAS DE RESULTADOS

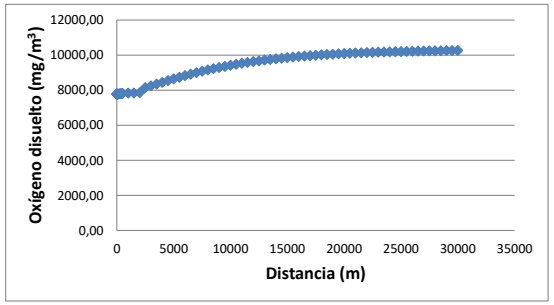

Para el oxígeno disuelto

L_{IV} 4000 m

7735

5500	0,23577	3400,11	1590,59	8741,24
6000	0,25720	3178,41	1499,79	8832,05
6500	0,27864	2971,16	1412,54	8919,30
7000	0,30007	2777,42	1329,05	9002,79
7500	0,32150	2596,32	1249,42	9082,41
8000	0,34294	2427,03	1173,70	9158,13
8500	0,36437	2268,77	1101,86	9229,97
9000	0,38580	2120,83	1033,85	9297,98
9500	0,40724	1982,54	969,57	9362,26
10000	0,42867	1853,27	908,91	9422,92
10500	0,45010	1732,43	851,73	9480,10
11000	0,47154	1619,46	797,90	9533,93
11500	0,49297	1513,87	747,27	9584,56
12000	0,51440	1415,15	699,68	9632,15
12500	0,53584	1322,88	654,99	9676,84
13000	0,55727	1236,62	613,04	9718,79
13500	0,57870	1155,98	573,69	9758,14
14000	0,60014	1080,61	536,79	9795,04
14500	0,62157	1010,15	502,20	9829,63
15000	0,64300	944,28	469,79	9862,04
15500	0,66444	882,71	439,44	9892,39
16000	0,68587	825,15	411,01	9920,82
16500	0,70730	771,35	384,39	9947,44
17000	0,72874	721,05	359,48	9972,35
17500	0,75017	674,03	336,16	9995,67
18000	0,77160	630,08	314,34	10017,49
18500	0,79304	589,00	293,93	10037,90
19000	0,81447	550,59	274,83	10057,00
19500	0,83591	514,69	256,97	10074,87
20000	0,85734	481,13	240,25	10091,58
20500	0,87877	449,76	224,63	10107,21
21000	0,90021	420,43	210,01	10121,82
21500	0,92164	393,02	196,34	10135,49
22000	0,94307	367,39	183,56	10148,28
22500	0,96451	343,43	171,60	10160,23
23000	0,98594	321,04	160,43	10171,40
23500	1,00737	300,11	149,98	10181,85
24000	1,02881	280,54	140,21	10191,63
24500	1,05024	262,24	131,07	10200,76
25000	1,07167	245,15	122,53	10209,30
25500	1,09311	229,16	114,55	10217,29
26000	1,11454	214,22	107,08	10224,75
26500	1,13597	200,25	100,10	10231,73
27000	1,15741	187,19	93,58	10238,25
27500	1,17884	174,99	87,48	10244,35
28000	1,20027	163,58	81,78	10250,06
28500	1,22171	152,91	76,45	10255,39
29000	1,24314	142,94	71,46	10260,37
29500	1,26457	133,62	66,80	10265,03
30000	1,28601	124,91	62,45	10269,38

Para la DBO_5

L_{IV} m

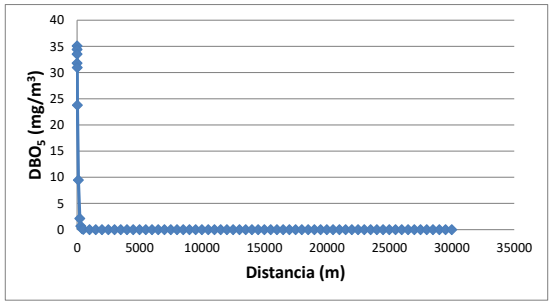

DEMANDA BIOQUÍMICA DE OXÍGENO (DBO)

Cálculo de la carga de entrada del tramo (W)

Caudal ambiental (m^3/día)	Q_{amb}	8760,96
Caudal del vertimiento (m^3/día)	Q_v	38,016
Concentración en el cuerpo de agua (mg/m^3)	DBO_0	5000
Concentración en el vertimiento (mg/m^3)	DBO_v	500000
Carga de entrada (mg/día)	W	62812800
Velocidad media (m/día)	v_{med}	23328
Concentración estándar (mg/m^3)	C_{est}	5000
Fracción dispersiva (Adim)	DF	0,722

$$a_{DBO} = \left[\left(1 + DF * K_d t_{DBO}\right) * e^{(1-DF)*K_d t_{DBO}}\right] * Q$$

Cálculo de la tasa de consumo de oxígeno por degradación de DBO (k_d)

K_d 3,14594743 d^{-1}

Cálculo del factor de asimilación (a)

a_{DBO} 12562,56 m^3/día

Comprobación del cálculo de a

	a_{DBO}	8889,387444	m^3/día
Insertar semilla para t_{DBO}	t_{DBO}	0,003258173	día
	Celda objetivo	0,292390449	

Cálculo del tiempo medio de viaje para la DBO (t_{DBO})

$$t_{DBO(i+1)} = t_{DBO(i)} - \frac{\left(1 + DF * k_d t_{DBO(i)}\right) * Q * e^{(1-DF)*K_d t_{DBO(i)}} - a_{DBO}}{k_d\left[1 + DF(1 - DF) * k_d t_{DBO(i)}\right] * Q * e^{(1-DF)*K_d t_{DBO(i)}}}$$

Solución de la ecuación con el método de Newton-Raphson

$$X_{n+1} = X_n - \frac{f(X_n)}{f'(X_n)}$$

Tolerancia 0,0001

Iteración	X	(FX)	F'(X)	Menor a tolerancia
0	0,014	-3371,939176	28269,84855	TODAVIA NO
1	0,133276874	317,1267312	33720,74487	TODAVIA NO
2	0,123872375	2,164376187	33261,34154	TODAVIA NO
3	0,123807303	0,000102825	33258,18123	TODAVIA NO
4	0,1238073	0	33258,18108	SOLUCION
5	0,1238073	0	33258,18108	SOLUCION
6	0,1238073	0	33258,18108	SOLUCION
7	0,1238073	0	33258,18108	SOLUCION
8	0,1238073	0	33258,18108	SOLUCION
9	0,1238073	0	33258,18108	SOLUCION
10	0,1238073	0	33258,18108	SOLUCION
11	0,1238073	0	33258,18108	SOLUCION
12	0,1238073	0	33258,18108	SOLUCION
13	0,1238073	0	33258,18108	SOLUCION
14	0,1238073	0	33258,18108	SOLUCION
15	0,1238073	0	33258,18108	SOLUCION
16	0,1238073	0	33258,18108	SOLUCION
17	0,1238073	0	33258,18108	SOLUCION
18	0,1238073	0	33258,18108	SOLUCION
19	0,1238073	0	33258,18108	SOLUCION
20	0,1238073	0	33258,18108	SOLUCION
21	0,1238073	0	33258,18108	SOLUCION
22	0,1238073	0	33258,18108	SOLUCION
23	0,1238073	0	33258,18108	SOLUCION
24	0,1238073	0	33258,18108	SOLUCION
25	0,1238073	0	33258,18108	SOLUCION
26	0,1238073	0	33258,18108	SOLUCION
27	0,1238073	0	33258,18108	SOLUCION
28	0,1238073	0	33258,18108	SOLUCION
29	0,1238073	0	33258,18108	SOLUCION
30	0,1238073	0	33258,18108	SOLUCION

Tiempo medio de viaje definitivo t_{DBO} 0,00325817 día

Cálculo de la longitud aguas abajo donde se alcanza el factor de asimilación (L_{IV})

L_{IV} 76,0067 m

FÓSFORO TOTAL

Cálculo de la carga de entrada del tramo (W)

Caudal ambiental (m^3/día)	Q_{amb}	8760,96
Caudal del vertimiento (m^3/día)	Q_v	38,016
Concentración en el cuerpo de agua (mg/m^3)	PT_0	62
Concentración en el vertimiento (mg/m^3)	PT_v	15000
Carga de entrada (mg/día)	W	1113419,5
Velocidad media (m/día)	v_{med}	23328
Concentración estándar (mg/m^3)	C_{est}	62
Fracción dispersiva (Adim)	DF	0,2285714

Cálculo de la tasa de hidrólisis (k_p)

K_p	6	d^{-1}

Cálculo del factor de asimilación (a)

$$a_{PT} = \left[\left(1 + DF * K_p t_{PT}\right) * e^{(1-DF)*K_p t_{PT}}\right] * Q$$

a_{PT}	17958,37935	m^3/día

Comprobación del cálculo de a

	a_{PT}	10951,895	m^3/día
Insertar semilla para t_{PT}	t_{PT}	0,0366836	
	Celda objetivo	0,3901513	

Cálculo del tiempo medio de viaje para el fósforo total (t_{PT})

$$t_{PT(i+1)} = t_{PT(i)} - \frac{\left(1 + DF * k_p t_{PT(i)}\right) * Q * e^{(1-DF)*K_p t_{PT(i)}} - a_{PT}}{k_p\left[1 + DF(1-DF) * k_p t_{PT(i)}\right] * Q * e^{(1-DF)*K_p t_{PT(i)}}}$$

Solución de la ecuación con el método de Newton-Raphson

$$X_{n+1} = X_n - \frac{f(X_n)}{f'(X_n)}$$

Tolerancia 0,0001

Iteración	X	(FX)	F'(X)	Menor a tolerancia
0		-9159,403	52793,856	TODAVIA NO
1	0,1734937	6356,9644	139482,7269	TODAVIA NO
2	0,1279185	738,37554	108353,6156	TODAVIA NO
3	0,121104	13,818882	104322,6363	TODAVIA NO
4	0,1209715	0,0050934	104245,7427	TODAVIA NO
5	0,1209714	6,912E-10	104245,7144	SOLUCION
6	0,1209714	0	104245,7144	SOLUCION
7	0,1209714	0	104245,7144	SOLUCION
8	0,1209714	0	104245,7144	SOLUCION
9	0,1209714	0	104245,7144	SOLUCION
10	0,1209714	0	104245,7144	SOLUCION
11	0,1209714	0	104245,7144	SOLUCION
12	0,1209714	0	104245,7144	SOLUCION
13	0,1209714	0	104245,7144	SOLUCION
14	0,1209714	0	104245,7144	SOLUCION
15	0,1209714	0	104245,7144	SOLUCION
16	0,1209714	0	104245,7144	SOLUCION
17	0,1209714	0	104245,7144	SOLUCION
18	0,1209714	0	104245,7144	SOLUCION
19	0,1209714	0	104245,7144	SOLUCION
20	0,1209714	0	104245,7144	SOLUCION
21	0,1209714	0	104245,7144	SOLUCION
22	0,1209714	0	104245,7144	SOLUCION
23	0,1209714	0	104245,7144	SOLUCION
24	0,1209714	0	104245,7144	SOLUCION
25	0,1209714	0	104245,7144	SOLUCION
26	0,1209714	0	104245,7144	SOLUCION
27	0,1209714	0	104245,7144	SOLUCION
28	0,1209714	0	104245,7144	SOLUCION
29	0,1209714	0	104245,7144	SOLUCION
30	0,1209714	0	104245,7144	SOLUCION

Tiempo medio de viaje definitivo t_{PT} 0,03668362 día

Cálculo de la longitud aguas abajo donde se alcanza el factor de asimilación (L_{IV})

L_{IV}	855,755	m

SÓLIDOS SUSPENDIDOS TOTALES

Cálculo de la carga de entrada del tramo (W)

Caudal ambiental (m^3/día)	Q_{amb}	8760,96
Caudal del vertimiento (m^3/día)	Q_v	38,016
Concentración en el cuerpo de agua (mg/m^3)	SST_0	10000
Concentración en el vertimiento (mg/m^3)	SST_v	20000
Carga de entrada (mg/día)	W	88369920
Velocidad media (m/día)	v_{med}	23328
Concentración estándar (mg/m^3)	C_{est}	10000
Fracción dispersiva (Adim)	DF	0,229

Cálculo de la velocidad de sedimentación (v_{ss})

Tipo de partícula	Diámetro (µm)	Velocidad de sedimentación (m d^{-1})
Carbono orgánico particulado	1-10	0.2
	10-64	1.5
	> 64	2.3
Arcilla	2-4	0.3-1
Limo	10-20	3-30

v_{ss} 0,008 m/s

Cálculo de la tasa de sedimentación (k_s)

K_s 2229,677419 d-1

$$a_{SST} = \left[(1 + DF * K_s t_{SST}) * e^{(1-DF)*K_s t_{SST}}\right] * Q$$

Cálculo del factor de asimilación (a)

a_{SST} 8836,992 m^3/día

Comprobación del cálculo de a

Insertar semilla para t_{SST}

a_{SST}	11543,113	m^3/día
t_{SST}	0,0001226	
Celda objetivo	0,3062265	

Cálculo del tiempo medio de viaje para los sólidos suspendidos totales (t_{SST})

$$t_{SST(i+1)} = t_{SST(i)} - \frac{(1 + DF * k_s t_{SST(i)}) * Q * e^{(1-DF)*K_s t_{SST(i)}} - a_{SST}}{k_s\left[1 + DF(1 - DF) * k_s t_{SST(i)}\right] * Q * e^{(1-DF)*K_s t_{SST(i)}}}$$

Solución de la ecuación con el método de Newton-Raphson

$$X_{n+1} = X_n - \frac{f(X_n)}{f'(X_n)}$$

Tolerancia 0,0001

Iteración	X	(FX)	F'(X)	Menor a tolerancia
0		-38,016	19618878,1	TODAVIA NO
1	1,938E-06	0,0779362	19699372,05	TODAVIA NO
2	1,934E-06	3,257E-07	19699207,38	SOLUCION
3	1,934E-06	0	19699207,38	SOLUCION
4	1,934E-06	0	19699207,38	SOLUCION
5	1,934E-06	0	19699207,38	SOLUCION
6	1,934E-06	0	19699207,38	SOLUCION
7	1,934E-06	0	19699207,38	SOLUCION
8	1,934E-06	0	19699207,38	SOLUCION
9	1,934E-06	0	19699207,38	SOLUCION
10	1,934E-06	0	19699207,38	SOLUCION
11	1,934E-06	0	19699207,38	SOLUCION
12	1,934E-06	0	19699207,38	SOLUCION
13	1,934E-06	0	19699207,38	SOLUCION
14	1,934E-06	0	19699207,38	SOLUCION
15	1,934E-06	0	19699207,38	SOLUCION
16	1,934E-06	0	19699207,38	SOLUCION
17	1,934E-06	0	19699207,38	SOLUCION
18	1,934E-06	0	19699207,38	SOLUCION
19	1,934E-06	0	19699207,38	SOLUCION
20	1,934E-06	0	19699207,38	SOLUCION
21	1,934E-06	0	19699207,38	SOLUCION
22	1,934E-06	0	19699207,38	SOLUCION
23	1,934E-06	0	19699207,38	SOLUCION
24	1,934E-06	0	19699207,38	SOLUCION
25	1,934E-06	0	19699207,38	SOLUCION
26	1,934E-06	0	19699207,38	SOLUCION
27	1,934E-06	0	19699207,38	SOLUCION
28	1,934E-06	0	19699207,38	SOLUCION
29	1,934E-06	0	19699207,38	SOLUCION
30	1,934E-06	0	19699207,38	SOLUCION

Tiempo medio de viaje definitivo t_{SST} 0,00012259 día

Cálculo de la longitud aguas abajo donde se alcanza el factor de asimilación (L_{IV})

L_{IV} 2,9 m

COLIFORMES FECALES

Cálculo de la carga de entrada del tramo (W)

Caudal ambiental (m^3/día)	Q_{amb}	8760,96
Caudal del vertimiento (m3/día)	Q_v	38,016
Concentración en el cuerpo de agua (mg/m^3)	CF_0	2.240.000
Concentración en el vertimiento (mg/m^3)	CF_v	800.000.000
Carga de entrada (mg/día)	W	50037350400
Velocidad media (m/día)	v_{med}	23328
Concentración estándar (mg/m^3)	C_{est}	2.240.000
Fracción dispersiva (Adim)	DF	0,229

Tasa de decaimiento por muerte de patógenos (k_b)

$$k_b = 0.8 * 1.07^{T-20} + \frac{I_0}{0.55 * SST * H} * (1 - e^{-0.55*SST*H}) + F_p * \frac{v_{ss}}{H}$$

Donde:
T: Temperatura del agua (ºC)
I_0: Radiación solar (ly/hr)
SST: Concentración de sólidos suspendidos totales promedio en el tramo (mg/l)
H: Profundidad media del agua (m)
F_p: Fracción adsorbida de bacterias a las partículas sólidas. Valor típico: 0.7.
V_{ss}: Velocidad de sedimentación de las partículas (md^{-1})

T	13,7	ºC
I_0	35,93	ly/hr
SST_0	10	mg/l
H	0,31	m
v_{ss}	0,008	md^{-1}

k_b	17,7909364

$$a_{CF} = \left[(1 + DF * K_s t_{CF}) * e^{(1-DF)*K_s t_{CF}}\right] * Q$$

Cálculo del factor de asimilación (a)

a_{CF}	22338,1029	m^3/día

Comprobación del cálculo de a

	a_{CF}	6615027,566	m^3/día
Insertar semilla para t_{CF}	t_{CF}	0,410943819	día
	Celda objetivo	295,1320219	

Cálculo del tiempo medio de viaje para los coliformes totales (t_{CF})

$$t_{CF(i+1)} = t_{CF(i)} - \frac{(1 + DF * k_b t_{CF(i)}) * Q * e^{(1-DF)*K_b t_{CF(i)}} - a_{CF}}{k_b\left[1 + DF(1 - DF) * k_b t_{CF(i)}\right] * Q * e^{(1-DF)*K_b t_{CF(i)}}}$$

Solución de la ecuación con el método de Newton-Raphson

$$X_{n+1} = X_n - \frac{f(X_n)}{f'(X_n)}$$

Tolerancia 0,0001

Iteración	X	(FX)	F'(X)	Menor a tolerancia
0		-13539,13	156542,023	TODAVIA NO
1	0,086488769	16640,502	652223,369	TODAVIA NO
2	0,060975268	3017,342	430610,634	TODAVIA NO
3	0,053968144	166,66178	383911,149	TODAVIA NO
4	0,053534028	0,592167	381186,143	TODAVIA NO
5	0,053532475	7,548E-06	381176,426	SOLUCION
6	0,053532475	0	381176,426	SOLUCION
7	0,053532475	0	381176,426	SOLUCION
8	0,053532475	0	381176,426	SOLUCION
9	0,053532475	0	381176,426	SOLUCION
10	0,053532475	0	381176,426	SOLUCION
11	0,053532475	0	381176,426	SOLUCION
12	0,053532475	0	381176,426	SOLUCION
13	0,053532475	0	381176,426	SOLUCION
14	0,053532475	0	381176,426	SOLUCION
15	0,053532475	0	381176,426	SOLUCION
16	0,053532475	0	381176,426	SOLUCION
17	0,053532475	0	381176,426	SOLUCION
18	0,053532475	0	381176,426	SOLUCION
19	0,053532475	0	381176,426	SOLUCION
20	0,053532475	0	381176,426	SOLUCION
21	0,053532475	0	381176,426	SOLUCION
22	0,053532475	0	381176,426	SOLUCION
23	0,053532475	0	381176,426	SOLUCION
24	0,053532475	0	381176,426	SOLUCION
25	0,053532475	0	381176,426	SOLUCION
26	0,053532475	0	381176,426	SOLUCION
27	0,053532475	0	381176,426	SOLUCION
28	0,053532475	0	381176,426	SOLUCION
29	0,053532475	0	381176,426	SOLUCION
30	0,053532475	0	381176,426	SOLUCION

Tiempo medio de viaje definitivo t_{CF} 0,411 día

Cálculo de la longitud aguas abajo donde se alcanza el factor de asimilación (L_{IV})

L_{IV} 9586,497 m

FUENTES DE INFORMACIÓN PARA CADA DETERMINANTE

En esta sección se presenta la fuente de información de los datos de entrada (recuadro rojo) para el cálculo de la longitud de asimilación de cada determinante.

Características hidráulicas de la corriente receptora

Parámetro	Símbolo	Fuente de información
Caudal mínimo	Q_{min}	QHSE SAS
Caudal medio	Q_{medio}	QHSE SAS
Caudal máximo	$Q_{máx}$	QHSE SAS
Profundidad del agua para caudal mínimo	H_{min}	QHSE SAS
Profundidad media del agua	H_{med}	QHSE SAS
Pendiente del lecho	S	QHSE SAS
Velocidad media	v_{med}	QHSE SAS
Velocidad máxima	$v_{máx}$	QHSE SAS

Nitrógeno

Parámetro	Símbolo	Fuente de información
Tasa de nitrificación	K_n	Cooper. 1986
Tolerancia	-	Criterio del profesional
Tiempo medio de viaje definitivo	t_{NTK}	Iteración

Oxígeno disuelto y DBO

Parámetro	Símbolo	Fuente de información
Cambio en H	ΔH	QHSE SAS
Constante (Adim.)	c	Modelo de Streeter y Phelps
Factor f para el cálculo de la tasa de consumo de oxígeno	f	Criterio de acuerdo a las características de la corriente receptora
Tiempo medio de viaje definitivo del oxígeno disuelto	t_{OD}	Iteración
Tiempo medio de viaje definitivo de la DBO	t_{DBO}	Iteración

Fósforo total

Parámetro	Símbolo	Fuente de información
Tasa de hidrólisis de fósforo	K_p	No aplica
Tolerancia	-	
Tiempo medio de viaje definitivo del fósforo total	t_{PT}	

Sólidos suspendido totales

Parámetro	Símbolo	Fuente de información
Tolerancia	-	Criterio del profesional
Tiempo medio de viaje definitivo de los SST	t_{SST}	Iteración
Velocidad de sedimentación	v_{ss}	ANLA. Metodología para la definición de la longitud de influencia de vertimientos sobre corrientes de agua superficial

Coliformes totales

Parámetro	Símbolo	Fuente de información
Radiación solar	I_0	No aplica
Tolerancia	-	
Tiempo medio de viaje definitivo de los coliformes totales	t_{CF}	

DATOS DE ENTRADA

Características de la fuente receptora

Nombre de la fuente: Río Guaitara
Coordenadas (x,y) 956565,04;600680,76
Observación

Características fisicoquímicas de la fuente receptora

Parámetro	Símbolo	Unidades	Valor	Fuente
pH	pH_0	Unidades de pH	7,64	Muestreo calidad de agua
Temperatura del agua	T_0	°C	15,4	Muestreo calidad de agua
Oxígeno Disuelto	OD_0	mg/L	9,2	Muestreo calidad de agua
DBO_5	DBO_0	mg O2/L	5	Muestreo calidad de agua
DQO	DQO_0	mg O2/L	20	Muestreo calidad de agua
NTK	NTK_0	mg/L	3	Muestreo calidad de agua
Fósforo total	PT_0	mg/L	0,062	Muestreo calidad de agua
Sólidos Suspendidos Totales	SST_0	mg SS/L	88	Muestreo calidad de agua
NMP Coliformes Fecales	CF_0	NMP/100ml	452	Muestreo calidad de agua

Características hidráulicas de la corriente receptora

Parámetro	Símbolo	Unidades	Valor	Fuente
Caudal minimo	Q_{amb}	m^3/s	4,9355	HSEQ SAS
Profundidad media*	H_{med}	m	1,22	HSEQ SAS
Pendiente del lecho	S	%	2,80504909	HSEQ SAS
Velocidad mínima*	v_{min}	m/s		
Velocidad media*	v_{med}	m/s	0,71	HSEQ SAS
Velocidad máxima*	$v_{máx}$	m/s	0,92	HSEQ SAS
Fracción dispersiva	DF	Adim.	0,228	

Características del vertimiento de agua residual

Características fisicoquímicas del vertimiento

Parámetro	Símbolo	Unidades	Valor	Fuente
pH	pH_v	Unidades de pH	6,9	TEÓRICO
Temperatura del agua	T_v	°C	18,5	TEÓRICO
Oxígeno Disuelto	OD_v	mg/L	2,15	TEÓRICO
DBO_5	DBO_v	mg O2/L	500	TEÓRICO
DQO	DQO_v	mg O2/L	600	TEÓRICO
NTK	NTK_v	mg/L	45	TEÓRICO
Fósforo total	PT_v	mg/L	15	TEÓRICO
Sólidos Suspendidos Totales	SST_v	mg SS/L	20	TEÓRICO
NMP Coliformes Fecales	CF_v	NMP/100ml	80000	TEÓRICO

Caudal del vertimiento

Parámetro	Símbolo	Unidades	Valor	Fuente
Caudal del vertimiento	Q_v	m^3/s	0,00044	GEOCOL SAS

Datos que deben ser digitados

Datos que se calculan automáticamente

NITRÓGENO

Cálculo de la carga de entrada del tramo (W)

Caudal minimo (m^3/día)	**Qmin**	426427,2
Caudal del vertimiento (m3/día)	**Q_v**	38,016
Concentración en el cuerpo de agua (mg/m^3)	**NTK_0**	3000
Concentración en el vertimiento (mg/m^3)	**NTK_v**	45000
Carga de entrada (mg/día)	**W**	1,281E+09
Velocidad media (m/día)	**v_{med}**	61344
Concentración estándar (mg/m^3)	**C_{est}**	3000
Fracción dispersiva (Adim)	**DF**	0,228

Cálculo de la tasa de nitrificación (k_n)

Profundidad H_{med} 1,22 m

K_n 1,53

Los valores de K_n generalmente están en el rango de 0.1 a 0.5 d^{-1} para aguas profundas mientras que para aguas someras valores por encima de 1d^{-1} son encontrados frecuentemente.

Río	K_n (d^{-1})	Profundidad (m)	Reportado en
Mine Brook	8.00	0.2	Tuffey et al. (1974)
Oroua	6.70	0.25	Cooper (1986)
Waiohewa	5.90	0.3	Cooper (1986)
Speed	2.30	0.43	Gowda (1983)
Sweetwater	0.80	0.46	Cooper (1986)
Trace	2.20	0.46	Cooper (1986)
Trukee	2.40	0.51	Bansal (1976)
Grand	1.90	0.58	Bansal (1976)
Shenadoha	1.25	0.60	Deb y Bowers (1983)
Waiotapu	2.80	0.61	Cooper (1986)
Ootanaula	0.80	0.61	Cooper (1986)
Sitll	0.70	0.64	Curtis (1983)
Flint	1.53	0.66	Bansal (1976)
South Chickamauga	6.60	0.84	Cooper (1986)
Upper Mohawk	0.30	0.96	Bansal (1976)
Mud	0.50	1.00	Cooper (1986)
Big Blue	0.12	1.25	Bansal (1976)
Holston	0.23	1.30	Ruane y Krenekel (1977)
Chattahoockee	0.25	1.50	McCutcheon (1987)
Trinity	0.51	1.53	McCutcheon (1987)
Willamette	0.70	1.60	Cooper (1985)
Shenadoha	0.2	1.74	Deb y Bowers (1983)
Upper Mohawk	0.25	2.51	Bansal (1976)
Upper Mohawk	0.25	3.66	Bansal (1976)
Middle Mohawk	0.30	3.81	Bansal (1976)
Barge	0.25	3.9	Bansal (1976)
Anacostia	0.13	4.00	Sullivan y Brown (1988)
Lower Mohawk	0.30	4.25	Bansal (1976)
Seneca river	0.05	6.24	Canale et al (1995)
Ohio	0.25	8.15	Bansal (1976)

$$a_{NTK} = \left[(1 + DF * K_n t_{NTK}) * e^{(1-DF)*K_n t_{NTK}}\right] * Q$$

Cálculo del factor de asimilación (a)

a_{NTK} 426997,44 m^3/día

Comprobación del cálculo de a

	a_{NTK}	455043,33	m^3/día
Insertar semilla para t_{NTK}	**t_{NTK}**	0,0424645	día
	Celda objetivo	0,0656816	

Cálculo del tiempo medio de viaje para el nitrógeno (t_{NTK})

$$t_{NTK(i+1)} = t_{NTK(i)} - \frac{\left(1 + DF * k_n t_{NTK(i)}\right) * Q * e^{(1-DF)*K_n t_{NTK(i)}} - a_{NTK}}{k_n\left[1 + DF(1-DF) * k_n t_{NTK(i)}\right] * Q * e^{(1-DF)*K_n t_{NTK(i)}}}$$

Solución de la ecuación con el método de Newton-Raphson

$$X_{n+1} = X_n - \frac{f(X_n)}{f'(X_n)}$$

Tolerancia 0,0001

Iteración	X	(FX)	F'(X)	Menor a tolerancia
0		-532,224	652491,78	TODAVIA NO
1	0,0008157	0,3149211	653264,097	TODAVIA NO
2	0,0008152	1,101E-07	653263,64	SOLUCION
3	0,0008152	0	653263,64	SOLUCION
4	0,0008152	0	653263,64	SOLUCION
5	0,0008152	0	653263,64	SOLUCION
6	0,0008152	0	653263,64	SOLUCION
7	0,0008152	0	653263,64	SOLUCION
8	0,0008152	0	653263,64	SOLUCION
9	0,0008152	0	653263,64	SOLUCION
10	0,0008152	0	653263,64	SOLUCION
11	0,0008152	0	653263,64	SOLUCION
12	0,0008152	0	653263,64	SOLUCION
13	0,0008152	0	653263,64	SOLUCION
14	0,0008152	0	653263,64	SOLUCION
15	0,0008152	0	653263,64	SOLUCION
16	0,0008152	0	653263,64	SOLUCION
17	0,0008152	0	653263,64	SOLUCION
18	0,0008152	0	653263,64	SOLUCION
19	0,0008152	0	653263,64	SOLUCION
20	0,0008152	0	653263,64	SOLUCION
21	0,0008152	0	653263,64	SOLUCION
22	0,0008152	0	653263,64	SOLUCION
23	0,0008152	0	653263,64	SOLUCION
24	0,0008152	0	653263,64	SOLUCION
25	0,0008152	0	653263,64	SOLUCION
26	0,0008152	0	653263,64	SOLUCION
27	0,0008152	0	653263,64	SOLUCION
28	0,0008152	0	653263,64	SOLUCION
29	0,0008152	0	653263,64	SOLUCION
30	0,0008152	0	653263,64	SOLUCION

Tiempo medio de viaje definitivo t_{NTK} 0,04246453 día

Cálculo de la longitud aguas abajo donde se alcanza el factor de asimilación (L_{IV})

L_{IV} 2604,944 m

OXÍGENO DISUELTO Y DBO

Aproximación de Streeter - Phelps

Cálculo de la carga de entrada del tramo (W)

Caudal minimo (m^3/día)	Q_{min}	426427,2
Caudal del vertimiento (m^3/día)	Q_v	38,016
Concentración de oxigeno en el cuerpo de agua (mg/m^3)	OD_0	9200
Concentración de oxígeno en el vertimiento (mg/m^3)	OD_v	2150
Concentración de DBO en el cuerpo de agua (mg/m^3)	DBO_0	5000
Concentración de DBO en el vertimiento (mg/m^3)	DBO_v	500.000
Concentración de oxígeno en x=0 (mg/m^3)	OD_{x0}	9199
Concentración de DBO en x=0 (mg/m^3)	DBO_{x0}	5044
Velocidad media (m/día)	v_{med}	61344

Cálculo del déficit de oxígeno

Oxígeno de saturación (mg/m^3)	OD_S	9945,71
Déficit de oxígeno en x=0 (mg/m3)	DO_{x0}	746

Cálculo de la tasa de reaireación (k_a)

Para ríos de alta montaña

Caudal a la entrada del tramo (m^3/s)	Q	4,9355
Cambio en H (m)	ΔH	0,05610098
Constante (Adim)	c	0,177
Tasa de reaireación (d^{-1})	K_a	24,784

$$k_a = c\frac{\Delta H}{t_{med}}$$

c=0.36 para 0.028≤Q≤0.28 m³/s

c=0.177 para 0.708≤Q≤85 m³/s

Para ríos de planicie

Parámetro	O`Connor-Dobbins	Churchill	Owens-Gibbs
Profundidad (m)	0.30 – 9.14	0.31 – 3.35	0.12 – 0.73
Velocidad media (m/s)	0.15 – 0.49	0.55 – 1.52	0.03 – 0.55
Expresiones	$k_a = 3.93\frac{U^{0.5}}{H^{1.5}}$	$k_a = 5.026\frac{U}{H^{1.67}}$	$k_a = 5.32\frac{U^{0.67}}{H^{1.85}}$

Elija una de las ecuaciones para el cálculo de la tasa de reaireación en un río de planicie, teniendo en cuenta la profundidad y/o velocidad medio del cuerpo de agua

Profundidad de flujo, H (m)	1,22						
Velocidad de flujo, U (m/s)	0,71	K_a	2,45743466	K_a	2,00184285	K_a	2,16256892

El río analizado es de montaña o planicie? 1

Tasa de reaireación definitiva K_a 24,7843096 d^{-1}

Cálculo de la tasa de consumo de oxígeno por degradación de DBO (k_d)

Cálculo a partir de Ka

Cuerpo de agua	Rango de $f \equiv \kappa_d/\kappa_a$
Reservorio o lago pequeño	0.5 – 1.0
Curso lento, lago grande	1.0 – 2.0
Rio grande y lento	1.5 – 2.0
Rio grande con velocidad de flujo mediana	2.0 – 3.0
Curso rápido	3.0 – 5.0
Rápidas y caidas de agua	> 5.0

f	3
K_d	8,26143652

Cálculo a partir de Q

K_d 3,92679834

$$k_d = 1.796Q^{-0.49}$$

Para 0.3≤Q≤23 m³/s

Tasa por degradación de DBO definitiva K_d 8,26143652

ECUACIONES

$$DO = \frac{\kappa_d}{\kappa_a - \kappa_d} DBO_o\left(e^{-\kappa_d x/U} - e^{-\kappa_a x/U}\right) + DO_o e^{-\kappa_a x/U}$$

$$DBO = DBO_o e^{-\kappa_d x/U}$$

Cálculo del cambio en la concentración

x (m)	x/V_{med} (d)	DBO_5(mg/m^3)	DO	OD (mg/m^3)
0,5	0,00001	5043,79	746,52	9199,18
2	0,00003	5042,77	747,09	9198,62
4	0,00007	5041,41	747,84	9197,86
8	0,00013	5038,69	749,35	9196,36
10	0,00016	5037,34	750,10	9195,61
30	0,00049	5023,79	757,56	9188,15
100	0,00163	4976,65	782,91	9162,80
213	0,00347	4901,49	821,44	9124,27
300	0,00489	4844,39	849,17	9096,54
400	0,00652	4779,59	879,05	9066,65
500	0,00815	4715,65	906,90	9038,80
600	0,00978	4652,57	932,81	9012,89
700	0,01141	4590,33	956,87	8988,83
800	0,01304	4528,93	979,16	8966,54
2500	0,04075	3602,18	1154,37	8791,33
3000	0,04890	3367,61	1155,38	8790,33
3500	0,05706	3148,31	1142,39	8803,32
4000	0,06521	2943,29	1118,85	8826,85
4500	0,07336	2751,63	1087,55	8858,16
5000	0,08151	2572,44	1050,69	8895,02

GRÁFICAS DE RESULTADOS

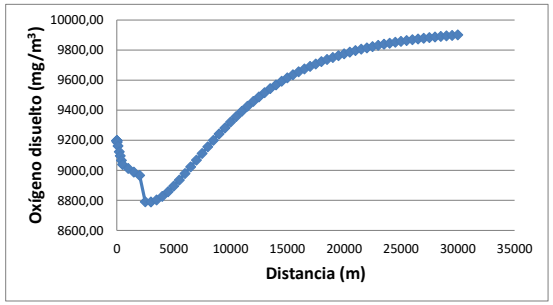

Para el oxígeno disuelto

L_{IV} 4000 m

7735

5500	0,08966	2404,92	1010,01	8935,70
6000	0,09781	2248,31	966,91	8978,80
6500	0,10596	2101,90	922,47	9023,24
7000	0,11411	1965,03	877,53	9068,18
7500	0,12226	1837,07	832,75	9112,95
8000	0,13041	1717,44	788,63	9157,08
8500	0,13856	1605,60	745,53	9200,18
9000	0,14671	1501,04	703,73	9241,98
9500	0,15486	1403,29	663,41	9282,29
10000	0,16302	1311,91	624,71	9320,99
10500	0,17117	1226,48	587,71	9357,99
11000	0,17932	1146,61	552,45	9393,26
11500	0,18747	1071,94	518,93	9426,78
12000	0,19562	1002,14	487,14	9458,56
12500	0,20377	936,88	457,06	9488,64
13000	0,21192	875,87	428,64	9517,07
13500	0,22007	818,83	401,82	9543,89
14000	0,22822	765,51	376,55	9569,16
14500	0,23637	715,66	352,76	9592,95
15000	0,24452	669,06	330,39	9615,32
15500	0,25267	625,49	309,36	9636,35
16000	0,26082	584,76	289,61	9656,09
16500	0,26897	546,68	271,08	9674,63
17000	0,27713	511,08	253,69	9692,01
17500	0,28528	477,80	237,39	9708,32
18000	0,29343	446,68	222,11	9723,60
18500	0,30158	417,60	207,79	9737,92
19000	0,30973	390,40	194,38	9751,33
19500	0,31788	364,98	181,82	9763,89
20000	0,32603	341,21	170,06	9775,65
20500	0,33418	318,99	159,05	9786,66
21000	0,34233	298,22	148,74	9796,96
21500	0,35048	278,80	139,10	9806,61
22000	0,35863	260,64	130,08	9815,63
22500	0,36678	243,67	121,64	9824,07
23000	0,37493	227,80	113,74	9831,97
23500	0,38309	212,97	106,35	9839,36
24000	0,39124	199,10	99,44	9846,27
24500	0,39939	186,13	92,98	9852,73
25000	0,40754	174,01	86,93	9858,77
25500	0,41569	162,68	81,28	9864,43
26000	0,42384	152,09	76,00	9869,71
26500	0,43199	142,18	71,05	9874,65
27000	0,44014	132,92	66,43	9879,28
27500	0,44829	124,27	62,11	9883,60
28000	0,45644	116,18	58,07	9887,64
28500	0,46459	108,61	54,29	9891,42
29000	0,47274	101,54	50,75	9894,95
29500	0,48089	94,93	47,45	9898,26
30000	0,48905	88,74	44,36	9901,34

Para la DBO_5

L_{IV} m

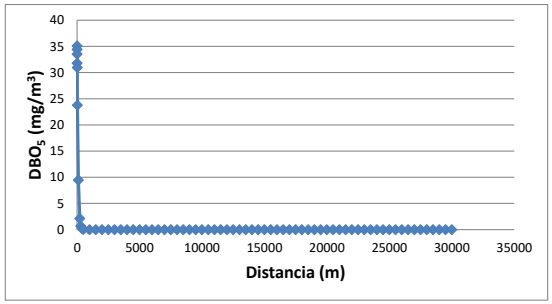

DEMANDA BIOQUÍMICA DE OXÍGENO (DBO)

Cálculo de la carga de entrada del tramo (W)

Caudal ambiental (m^3/día)	Q_{amb}	426427,2
Caudal del vertimiento (m^3/día)	Q_v	38,016
Concentración en el cuerpo de agua (mg/m^3)	DBO_0	5000
Concentración en el vertimiento (mg/m^3)	DBO_v	500000
Carga de entrada (mg/día)	W	2151144000
Velocidad media (m/día)	v_{med}	61344
Concentración estándar (mg/m^3)	C_{est}	5000
Fracción dispersiva (Adim)	DF	0,722

$$a_{DBO} = \left[\left(1 + DF * K_d t_{DBO}\right) * e^{(1-DF)*K_d t_{DBO}}\right] * Q$$

Cálculo de la tasa de consumo de oxígeno por degradación de DBO (k_d)

K_d 8,26143652 d^{-1}

Cálculo del factor de asimilación (a)

a_{DBO} 430228,8 m^3/día

Comprobación del cálculo de a

	a_{DBO}	438018,6833	m^3/día
Insertar semilla para t_{DBO}	t_{DBO}	0,003258173	día
	Celda objetivo	0,018106373	

Cálculo del tiempo medio de viaje para la DBO (t_{DBO})

$$t_{DBO(i+1)} = t_{DBO(i)} - \frac{\left(1 + DF * k_d t_{DBO(i)}\right) * Q * e^{(1-DF)*K_d t_{DBO(i)}} - a_{DBO}}{k_d\left[1 + DF(1-DF) * k_d t_{DBO(i)}\right] * Q * e^{(1-DF)*K_d t_{DBO(i)}}}$$

Solución de la ecuación con el método de Newton-Raphson

$$X_{n+1} = X_n - \frac{f(X_n)}{f'(X_n)}$$

Tolerancia 0,0001

Iteración	X	(FX)	F'(X)	Menor a tolerancia
0	0,014	46947,94239	3722803,427	TODAVIA NO
1	0,001389089	1143,939437	3542614,62	TODAVIA NO
2	0,001066181	0,729482208	3538097,211	TODAVIA NO
3	0,001065975	2,9715E-07	3538094,328	TODAVIA NO
4	0,001065975	0	3538094,328	SOLUCION
5	0,001065975	0	3538094,328	SOLUCION
6	0,001065975	0	3538094,328	SOLUCION
7	0,001065975	0	3538094,328	SOLUCION
8	0,001065975	0	3538094,328	SOLUCION
9	0,001065975	0	3538094,328	SOLUCION
10	0,001065975	0	3538094,328	SOLUCION
11	0,001065975	0	3538094,328	SOLUCION
12	0,001065975	0	3538094,328	SOLUCION
13	0,001065975	0	3538094,328	SOLUCION
14	0,001065975	0	3538094,328	SOLUCION
15	0,001065975	0	3538094,328	SOLUCION
16	0,001065975	0	3538094,328	SOLUCION
17	0,001065975	0	3538094,328	SOLUCION
18	0,001065975	0	3538094,328	SOLUCION
19	0,001065975	0	3538094,328	SOLUCION
20	0,001065975	0	3538094,328	SOLUCION
21	0,001065975	0	3538094,328	SOLUCION
22	0,001065975	0	3538094,328	SOLUCION
23	0,001065975	0	3538094,328	SOLUCION
24	0,001065975	0	3538094,328	SOLUCION
25	0,001065975	0	3538094,328	SOLUCION
26	0,001065975	0	3538094,328	SOLUCION
27	0,001065975	0	3538094,328	SOLUCION
28	0,001065975	0	3538094,328	SOLUCION
29	0,001065975	0	3538094,328	SOLUCION
30	0,001065975	0	3538094,328	SOLUCION

Tiempo medio de viaje definitivo t_{DBO} 0,00325817 día

Cálculo de la longitud aguas abajo donde se alcanza el factor de asimilación (L_{IV})

L_{IV} 199,8694 m

FÓSFORO TOTAL

Cálculo de la carga de entrada del tramo (W)

Caudal ambiental (m^3/día)	Q_{amb}	426427,2
Caudal del vertimiento (m^3/día)	Q_v	38,016
Concentración en el cuerpo de agua (mg/m^3)	PT_0	62
Concentración en el vertimiento (mg/m^3)	PT_v	15000
Carga de entrada (mg/día)	W	27008726
Velocidad media (m/día)	v_{med}	61344
Concentración estándar (mg/m^3)	C_{est}	62
Fracción dispersiva (Adim)	DF	0,2282609

Cálculo de la tasa de hidrólisis (k_p)

K_p	6	d^{-1}

Cálculo del factor de asimilación (a)

$$a_{PT} = \left[\left(1 + DF * K_p t_{PT}\right) * e^{(1-DF)*K_p t_{PT}}\right] * Q$$

a_{PT}	435624,6194	m^3/día

Comprobación del cálculo de a

	a_{PT}	530813,75	m^3/día
Insertar semilla para t_{PT}	t_{PT}	0,0366836	
	Celda objetivo	0,2185118	

Cálculo del tiempo medio de viaje para el fósforo total (t_{PT})

$$t_{PT(i+1)} = t_{PT(i)} - \frac{\left(1 + DF * k_p t_{PT(i)}\right) * Q * e^{(1-DF)*K_p t_{PT(i)}} - a_{PT}}{k_p\left[1 + DF(1-DF) * k_p t_{PT(i)}\right] * Q * e^{(1-DF)*K_p t_{PT(i)}}}$$

Solución de la ecuación con el método de Newton-Raphson

$$X_{n+1} = X_n - \frac{f(X_n)}{f'(X_n)}$$

Tolerancia 0,0001

Iteración	X	(FX)	F'(X)	Menor a tolerancia
0		-9159,403	2558791,296	TODAVIA NO
1	0,0035796	93,849425	2611399,561	TODAVIA NO
2	0,0035436	0,0095838	2610866,23	TODAVIA NO
3	0,0035436	0	2610866,175	SOLUCION
4	0,0035436	0	2610866,175	SOLUCION
5	0,0035436	0	2610866,175	SOLUCION
6	0,0035436	0	2610866,175	SOLUCION
7	0,0035436	0	2610866,175	SOLUCION
8	0,0035436	0	2610866,175	SOLUCION
9	0,0035436	0	2610866,175	SOLUCION
10	0,0035436	0	2610866,175	SOLUCION
11	0,0035436	0	2610866,175	SOLUCION
12	0,0035436	0	2610866,175	SOLUCION
13	0,0035436	0	2610866,175	SOLUCION
14	0,0035436	0	2610866,175	SOLUCION
15	0,0035436	0	2610866,175	SOLUCION
16	0,0035436	0	2610866,175	SOLUCION
17	0,0035436	0	2610866,175	SOLUCION
18	0,0035436	0	2610866,175	SOLUCION
19	0,0035436	0	2610866,175	SOLUCION
20	0,0035436	0	2610866,175	SOLUCION
21	0,0035436	0	2610866,175	SOLUCION
22	0,0035436	0	2610866,175	SOLUCION
23	0,0035436	0	2610866,175	SOLUCION
24	0,0035436	0	2610866,175	SOLUCION
25	0,0035436	0	2610866,175	SOLUCION
26	0,0035436	0	2610866,175	SOLUCION
27	0,0035436	0	2610866,175	SOLUCION
28	0,0035436	0	2610866,175	SOLUCION
29	0,0035436	0	2610866,175	SOLUCION
30	0,0035436	0	2610866,175	SOLUCION

Tiempo medio de viaje definitivo t_{PT} 0,03668362 día

Cálculo de la longitud aguas abajo donde se alcanza el factor de asimilación (L_{IV})

L_{IV}	2250,320	m

SÓLIDOS SUSPENDIDOS TOTALES

Cálculo de la carga de entrada del tramo (W)

Caudal ambiental (m^3/día)	Q_{amb}	426427,2
Caudal del vertimiento (m^3/día)	Q_v	38,016
Concentración en el cuerpo de agua (mg/m^3)	SST_0	88000
Concentración en el vertimiento (mg/m^3)	SST_v	20000
Carga de entrada (mg/día)	W	3,753E+10
Velocidad media (m/día)	v_{med}	61344
Concentración estándar (mg/m^3)	C_{est}	88000
Fracción dispersiva (Adim)	DF	0,228

Cálculo de la velocidad de sedimentación (v_{ss})

Tipo de partícula	Diámetro (µm)	Velocidad de sedimentación (m d^{-1})
Carbono orgánico particulado	1-10	0.2
	10-64	1.5
	> 64	2.3
Arcilla	2-4	0.3-1
Limo	10-20	3-30

v_{ss} 0,008 m/s

Cálculo de la tasa de sedimentación (k_s)

K_s 566,557377 d-1

$$a_{SST} = \left[(1 + DF * K_s t_{SST}) * e^{(1-DF)*K_s t_{SST}}\right] * Q$$

Cálculo del factor de asimilación (a)

a_{SST} 426435,84 m^3/día

Comprobación del cálculo de a

Insertar semilla para t_{SST}

a_{SST}	457080,05	m^3/día
t_{SST}	0,0001226	
Celda objetivo	0,0718612	

Cálculo del tiempo medio de viaje para los sólidos suspendidos totales (t_{SST})

Solución de la ecuación con el método de Newton-Raphson

$$t_{SST(i+1)} = t_{SST(i)} - \frac{\left(1 + DF * k_s t_{SST(i)}\right) * Q * e^{(1-DF)*K_s t_{SST(i)}} - a_{SST}}{k_s\left[1 + DF(1-DF) * k_s t_{SST(i)}\right] * Q * e^{(1-DF)*K_s t_{SST(i)}}}$$

$$X_{n+1} = X_n - \frac{f(X_n)}{f'(X_n)}$$

Tolerancia 0,0001

Iteración	X	(FX)	F'(X)	Menor a tolerancia
0		29,376	241617014,2	TODAVIA NO
1	-1,22E-07	0,000959	241601238,6	TODAVIA NO
2	-1,22E-07	0	241601238,1	SOLUCION
3	-1,22E-07	0	241601238,1	SOLUCION
4	-1,22E-07	0	241601238,1	SOLUCION
5	-1,22E-07	0	241601238,1	SOLUCION
6	-1,22E-07	0	241601238,1	SOLUCION
7	-1,22E-07	0	241601238,1	SOLUCION
8	-1,22E-07	0	241601238,1	SOLUCION
9	-1,22E-07	0	241601238,1	SOLUCION
10	-1,22E-07	0	241601238,1	SOLUCION
11	-1,22E-07	0	241601238,1	SOLUCION
12	-1,22E-07	0	241601238,1	SOLUCION
13	-1,22E-07	0	241601238,1	SOLUCION
14	-1,22E-07	0	241601238,1	SOLUCION
15	-1,22E-07	0	241601238,1	SOLUCION
16	-1,22E-07	0	241601238,1	SOLUCION
17	-1,22E-07	0	241601238,1	SOLUCION
18	-1,22E-07	0	241601238,1	SOLUCION
19	-1,22E-07	0	241601238,1	SOLUCION
20	-1,22E-07	0	241601238,1	SOLUCION
21	-1,22E-07	0	241601238,1	SOLUCION
22	-1,22E-07	0	241601238,1	SOLUCION
23	-1,22E-07	0	241601238,1	SOLUCION
24	-1,22E-07	0	241601238,1	SOLUCION
25	-1,22E-07	0	241601238,1	SOLUCION
26	-1,22E-07	0	241601238,1	SOLUCION
27	-1,22E-07	0	241601238,1	SOLUCION
28	-1,22E-07	0	241601238,1	SOLUCION
29	-1,22E-07	0	241601238,1	SOLUCION
30	-1,22E-07	0	241601238,1	SOLUCION

Tiempo medio de viaje definitivo t_{SST} 0,00012259 día

Cálculo de la longitud aguas abajo donde se alcanza el factor de asimilación (L_{IV})

L_{IV} 7,5 m

COLIFORMES FECALES

Cálculo de la carga de entrada del tramo (W)

Caudal ambiental (m^3/día)	Q_{amb}	426427,2
Caudal del vertimiento (m3/día)	Q_v	38,016
Concentración en el cuerpo de agua (mg/m^3)	CF_0	4.520.000
Concentración en el vertimiento (mg/m^3)	CF_v	800.000.000
Carga de entrada (mg/día)	W	1,95786E+12
Velocidad media (m/día)	v_{med}	61344
Concentración estándar (mg/m^3)	C_{est}	4.520.000
Fracción dispersiva (Adim)	DF	0,228

Tasa de decaimiento por muerte de patógenos (k_b)

$$k_b = 0.8 * 1.07^{T-20} + \frac{I_0}{0.55 * SST * H} * (1 - e^{-0.55*SST*H}) + F_p * \frac{v_{ss}}{H}$$

Donde:
T: Temperatura del agua (ºC)
I_0: Radiación solar (ly/hr)
SST: Concentración de sólidos suspendidos totales promedio en el tramo (mg/l)
H: Profundidad media del agua (m)
F_p: Fracción adsorbida de bacterias a las partículas sólidas. Valor típico: 0.7.
V_{ss}: Velocidad de sedimentación de las partículas (md^{-1})

T	15,4	ºC
I_0	35,93	ly/hr
SST_0	88	mg/l
H	1,22	m
v_{ss}	0,008	md^{-1}

k_b	1,20108181

$$a_{CF} = \left[(1 + DF * K_s t_{CF}) * e^{(1-DF)*K_s t_{CF}}\right] * Q$$

Cálculo del factor de asimilación (a)

a_{CF}	433155,696	m^3/día

Comprobación del cálculo de a

	a_{CF}	694506,1777	m^3/día
Insertar semilla para t_{CF}	t_{CF}	0,410943819	día
	Celda objetivo	0,603363836	

Cálculo del tiempo medio de viaje para los coliformes totales (t_{CF})

$$t_{CF(i+1)} = t_{CF(i)} - \frac{(1 + DF * k_b t_{CF(i)}) * Q * e^{(1-DF)*K_b t_{CF(i)}} - a_{CF}}{k_b\left[1 + DF(1 - DF) * k_b t_{CF(i)}\right] * Q * e^{(1-DF)*K_b t_{CF(i)}}}$$

Solución de la ecuación con el método de Newton-Raphson

$$X_{n+1} = X_n - \frac{f(X_n)}{f'(X_n)}$$

Tolerancia 0,0001

Iteración	X	(FX)	F'(X)	Menor a tolerancia
0		-6690,48	512219,614	TODAVIA NO
1	0,01306174	49,985352	519891,674	TODAVIA NO
2	0,012965595	0,0027343	519834,797	TODAVIA NO
3	0,012965589	0	519834,794	SOLUCION
4	0,012965589	0	519834,794	SOLUCION
5	0,012965589	0	519834,794	SOLUCION
6	0,012965589	0	519834,794	SOLUCION
7	0,012965589	0	519834,794	SOLUCION
8	0,012965589	0	519834,794	SOLUCION
9	0,012965589	0	519834,794	SOLUCION
10	0,012965589	0	519834,794	SOLUCION
11	0,012965589	0	519834,794	SOLUCION
12	0,012965589	0	519834,794	SOLUCION
13	0,012965589	0	519834,794	SOLUCION
14	0,012965589	0	519834,794	SOLUCION
15	0,012965589	0	519834,794	SOLUCION
16	0,012965589	0	519834,794	SOLUCION
17	0,012965589	0	519834,794	SOLUCION
18	0,012965589	0	519834,794	SOLUCION
19	0,012965589	0	519834,794	SOLUCION
20	0,012965589	0	519834,794	SOLUCION
21	0,012965589	0	519834,794	SOLUCION
22	0,012965589	0	519834,794	SOLUCION
23	0,012965589	0	519834,794	SOLUCION
24	0,012965589	0	519834,794	SOLUCION
25	0,012965589	0	519834,794	SOLUCION
26	0,012965589	0	519834,794	SOLUCION
27	0,012965589	0	519834,794	SOLUCION
28	0,012965589	0	519834,794	SOLUCION
29	0,012965589	0	519834,794	SOLUCION
30	0,012965589	0	519834,794	SOLUCION

Tiempo medio de viaje definitivo t_{CF} 0,411 día

Cálculo de la longitud aguas abajo donde se alcanza el factor de asimilación (L_{IV})

L_{IV} 25208,938 m

FUENTES DE INFORMACIÓN PARA CADA DETERMINANTE

En esta sección se presenta la fuente de información de los datos de entrada (recuadro rojo) para el cálculo de la longitud de asimilación de cada determinante.

Características hidráulicas de la corriente receptora

Parámetro	Símbolo	Fuente de información
Caudal mínimo	Q_{min}	QHSE SAS
Caudal medio	Q_{medio}	QHSE SAS
Caudal máximo	$Q_{máx}$	QHSE SAS
Profundidad del agua para caudal mínimo	H_{min}	QHSE SAS
Profundidad media del agua	H_{med}	QHSE SAS
Pendiente del lecho	S	QHSE SAS
Velocidad media	v_{med}	QHSE SAS
Velocidad máxima	$v_{máx}$	QHSE SAS

Nitrógeno

Parámetro	Símbolo	Fuente de información
Tasa de nitrificación	K_n	Cooper. 1986
Tolerancia	-	Criterio del profesional
Tiempo medio de viaje definitivo	t_{NTK}	Iteración

Oxígeno disuelto y DBO

Parámetro	Símbolo	Fuente de información
Cambio en H	ΔH	QHSE SAS
Constante (Adim.)	c	Modelo de Streeter y Phelps
Factor f para el cálculo de la tasa de consumo de oxígeno	f	Criterio de acuerdo a las características de la corriente receptora
Tiempo medio de viaje definitivo del oxígeno disuelto	t_{OD}	Iteración
Tiempo medio de viaje definitivo de la DBO	t_{DBO}	Iteración

Fósforo total

Parámetro	Símbolo	Fuente de información
Tasa de hidrólisis de fósforo	K_p	No aplica
Tolerancia	-	
Tiempo medio de viaje definitivo del fósforo total	t_{PT}	

Sólidos suspendido totales

Parámetro	Símbolo	Fuente de información
Tolerancia	-	Criterio del profesional
Tiempo medio de viaje definitivo de los SST	t_{SST}	Iteración
Velocidad de sedimentación	v_{ss}	ANLA. Metodología para la definición de la longitud de influencia de vertimientos sobre corrientes de agua superficial

Coliformes totales

Parámetro	Símbolo	Fuente de información
Radiación solar	I_0	No aplica
Tolerancia	-	
Tiempo medio de viaje definitivo de los coliformes totales	t_{CF}	

DATOS DE ENTRADA

Características de la fuente receptora

Nombre de la fuente: Río Sapuyes
Coordenadas (x,y) 954987,27;605047,87
Observación

Características fisicoquímicas de la fuente receptora

Parámetro	Símbolo	Unidades	Valor	Fuente
pH	pH_0	Unidades de pH	7,72	Muestreo calidad de agua
Temperatura del agua	T_0	°C	18	Muestreo calidad de agua
Oxígeno Disuelto	OD_0	mg/L	8,4	Muestreo calidad de agua
DBO_5	DBO_0	mg O2/L	5	Muestreo calidad de agua
DQO	DQO_0	mg O2/L	20	Muestreo calidad de agua
NTK	NTK_0	mg/L	3	Muestreo calidad de agua
Fósforo total	PT_0	mg/L	0,062	Muestreo calidad de agua
Sólidos Suspendidos Totales	SST_0	mg SS/L	21	Muestreo calidad de agua
NMP Coliformes Fecales	CF_0	NMP/100ml	308	Muestreo calidad de agua

Características hidráulicas de la corriente receptora

Parámetro	Símbolo	Unidades	Valor	Fuente
Caudal minimo	Q_{amb}	m^3/s	4,9355	HSEQ SAS
Profundidad media*	H_{med}	m	0,69	HSEQ SAS
Pendiente del lecho	S	%	6,58761528	HSEQ SAS
Velocidad mínima*	v_{min}	m/s		
Velocidad media*	v_{med}	m/s	0,75	HSEQ SAS
Velocidad máxima*	$v_{máx}$	m/s	0,98	HSEQ SAS
Fracción dispersiva	DF	Adim.	0,235	

Características del vertimiento de agua residual

Características fisicoquímicas del vertimiento

Parámetro	Símbolo	Unidades	Valor	Fuente
pH	pH_v	Unidades de pH	6,9	TEÓRICO
Temperatura del agua	T_v	°C	18,5	TEÓRICO
Oxígeno Disuelto	OD_v	mg/L	2,15	TEÓRICO
DBO_5	DBO_v	mg O2/L	500	TEÓRICO
DQO	DQO_v	mg O2/L	600	TEÓRICO
NTK	NTK_v	mg/L	45	TEÓRICO
Fósforo total	PT_v	mg/L	15	TEÓRICO
Sólidos Suspendidos Totales	SST_v	mg SS/L	20	TEÓRICO
NMP Coliformes Fecales	CF_v	NMP/100ml	80000	TEÓRICO

Caudal del vertimiento

Parámetro	Símbolo	Unidades	Valor	Fuente
Caudal del vertimiento	Q_v	m^3/s	0,00044	GEOCOL SAS

Datos que deben ser digitados

Datos que se calculan automáticamente

NITRÓGENO

Cálculo de la carga de entrada del tramo (W)

Caudal minimo (m^3/día)	**Qmin**	426427,2
Caudal del vertimiento (m3/día)	**Q_v**	38,016
Concentración en el cuerpo de agua (mg/m^3)	**NTK_0**	3000
Concentración en el vertimiento (mg/m^3)	**NTK_v**	45000
Carga de entrada (mg/día)	**W**	1,281E+09
Velocidad media (m/día)	**v_{med}**	64800
Concentración estándar (mg/m^3)	**C_{est}**	3000
Fracción dispersiva (Adim)	**DF**	0,235

Cálculo de la tasa de nitrificación (k_n)

Profundidad H_{med} 0,69 m

K_n 1,53

Los valores de K_n generalmente están en el rango de 0.1 a 0.5 d^{-1} para aguas profundas mientras que para aguas someras valores por encima de 1d^{-1} son encontrados frecuentemente.

Río	K_n (d^{-1})	Profundidad (m)	Reportado en
Mine Brook	8.00	0.2	Tuffey et al. (1974)
Oroua	6.70	0.25	Cooper (1986)
Waiohewa	5.90	0.3	Cooper (1986)
Speed	2.30	0.43	Gowda (1983)
Sweetwater	0.80	0.46	Cooper (1986)
Trace	2.20	0.46	Cooper (1986)
Trukee	2.40	0.51	Bansal (1976)
Grand	1.90	0.58	Bansal (1976)
Shenadoha	1.25	0.60	Deb y Bowers (1983)
Waiotapu	2.80	0.61	Cooper (1986)
Ootanaula	0.80	0.61	Cooper (1986)
Sitll	0.70	0.64	Curtis (1983)
Flint	1.53	0.66	Bansal (1976)
South Chickamauga	6.60	0.84	Cooper (1986)
Upper Mohawk	0.30	0.96	Bansal (1976)
Mud	0.50	1.00	Cooper (1986)
Big Blue	0.12	1.25	Bansal (1976)
Holston	0.23	1.30	Ruane y Krenekel (1977)
Chattahoockee	0.25	1.50	McCutcheon (1987)
Trinity	0.51	1.53	McCutcheon (1987)
Willamette	0.70	1.60	Cooper (1985)
Shenadoha	0.2	1.74	Deb y Bowers (1983)
Upper Mohawk	0.25	2.51	Bansal (1976)
Upper Mohawk	0.25	3.66	Bansal (1976)
Middle Mohawk	0.30	3.81	Bansal (1976)
Barge	0.25	3.9	Bansal (1976)
Anacostia	0.13	4.00	Sullivan y Brown (1988)
Lower Mohawk	0.30	4.25	Bansal (1976)
Seneca river	0.05	6.24	Canale et al (1995)
Ohio	0.25	8.15	Bansal (1976)

$$a_{NTK} = \left[(1 + DF * K_n t_{NTK}) * e^{(1-DF)*K_n t_{NTK}}\right] * Q$$

Cálculo del factor de asimilación (a)

a_{NTK} 426997,44 m^3/día

Comprobación del cálculo de a

	a_{NTK}	455040,51	m^3/día
Insertar semilla para t_{NTK}	**t_{NTK}**	0,0424645	día
	Celda objetivo	0,065675	

Cálculo del tiempo medio de viaje para el nitrógeno (t_{NTK})

$$t_{NTK(i+1)} = t_{NTK(i)} - \frac{\left(1 + DF * k_n t_{NTK(i)}\right) * Q * e^{(1-DF)*K_n t_{NTK(i)}} - a_{NTK}}{k_n\left[1 + DF(1-DF) * k_n t_{NTK(i)}\right] * Q * e^{(1-DF)*K_n t_{NTK(i)}}}$$

Solución de la ecuación con el método de Newton-Raphson

$$X_{n+1} = X_n - \frac{f(X_n)}{f'(X_n)}$$

Tolerancia 0,0001

Iteración	X	(FX)	F'(X)	Menor a tolerancia
0		-532,224	652491,78	TODAVIA NO
1	0,0008157	0,3139311	653261,668	TODAVIA NO
2	0,0008152	1,091E-07	653261,214	SOLUCION
3	0,0008152	0	653261,214	SOLUCION
4	0,0008152	0	653261,214	SOLUCION
5	0,0008152	0	653261,214	SOLUCION
6	0,0008152	0	653261,214	SOLUCION
7	0,0008152	0	653261,214	SOLUCION
8	0,0008152	0	653261,214	SOLUCION
9	0,0008152	0	653261,214	SOLUCION
10	0,0008152	0	653261,214	SOLUCION
11	0,0008152	0	653261,214	SOLUCION
12	0,0008152	0	653261,214	SOLUCION
13	0,0008152	0	653261,214	SOLUCION
14	0,0008152	0	653261,214	SOLUCION
15	0,0008152	0	653261,214	SOLUCION
16	0,0008152	0	653261,214	SOLUCION
17	0,0008152	0	653261,214	SOLUCION
18	0,0008152	0	653261,214	SOLUCION
19	0,0008152	0	653261,214	SOLUCION
20	0,0008152	0	653261,214	SOLUCION
21	0,0008152	0	653261,214	SOLUCION
22	0,0008152	0	653261,214	SOLUCION
23	0,0008152	0	653261,214	SOLUCION
24	0,0008152	0	653261,214	SOLUCION
25	0,0008152	0	653261,214	SOLUCION
26	0,0008152	0	653261,214	SOLUCION
27	0,0008152	0	653261,214	SOLUCION
28	0,0008152	0	653261,214	SOLUCION
29	0,0008152	0	653261,214	SOLUCION
30	0,0008152	0	653261,214	SOLUCION

Tiempo medio de viaje definitivo t_{NTK} 0,04246453 día

Cálculo de la longitud aguas abajo donde se alcanza el factor de asimilación (L_{IV})

L_{IV} 2751,702 m

OXÍGENO DISUELTO Y DBO

Aproximación de Streeter - Phelps

Cálculo de la carga de entrada del tramo (W)

Caudal minimo (m^3/día)	Q_{min}	426427,2
Caudal del vertimiento (m^3/día)	Q_v	38,016
Concentración de oxigeno en el cuerpo de agua (mg/m^3)	OD_0	8400
Concentración de oxígeno en el vertimiento (mg/m^3)	OD_v	2150
Concentración de DBO en el cuerpo de agua (mg/m^3)	DBO_0	5000
Concentración de DBO en el vertimiento (mg/m^3)	DBO_v	500.000
Concentración de oxígeno en x=0 (mg/m^3)	OD_{x0}	8399
Concentración de DBO en x=0 (mg/m^3)	DBO_{x0}	5044
Velocidad media (m/día)	v_{med}	64800

Cálculo del déficit de oxígeno

Oxígeno de saturación (mg/m^3)	OD_S	9403,55
Déficit de oxígeno en x=0 (mg/m3)	DO_{x0}	1004

Cálculo de la tasa de reaireación (k_a)

Para ríos de alta montaña

Caudal a la entrada del tramo (m^3/s)	Q	4,9355
Cambio en H (m)	ΔH	0,13175231
Constante (Adim)	c	0,177
Tasa de reaireación (d^{-1})	K_a	26,918

$$k_a = c\frac{\Delta H}{t_{med}}$$

c=0.36 para 0.028≤Q≤0.28 m³/s

c=0.177 para 0.708≤Q≤85 m³/s

Para ríos de planicie

Parámetro	O`Connor-Dobbins	Churchill	Owens-Gibbs
Profundidad (m)	0.30 – 9.14	0.31 – 3.35	0.12 – 0.73
Velocidad media (m/s)	0.15 – 0.49	0.55 – 1.52	0.03 – 0.55
Expresiones	$k_a = 3.93\frac{U^{0.5}}{H^{1.5}}$	$k_a = 5.026\frac{U}{H^{1.67}}$	$k_a = 5.32\frac{U^{0.67}}{H^{1.85}}$

Elija una de las ecuaciones para el cálculo de la tasa de reaireación en un río de planicie, teniendo en cuenta la profundidad y/o velocidad medio del cuerpo de agua

Profundidad de flujo, H (m)	0,69						
Velocidad de flujo, U (m/s)	0,75	K_a	5,93812788	K_a	5,47741734	K_a	6,43891629
El río analizado es de montaña o planicie?			1				

Tasa de reaireación definitiva K_a 26,918449 d^{-1}

Cálculo de la tasa de consumo de oxígeno por degradación de DBO (k_d)

Cálculo a partir de Ka

Cuerpo de agua	Rango de $f \equiv K_a/K_d$
Reservorio o lago pequeño	0.5 – 1.0
Curso lento, lago grande	1.0 – 2.0
Rio grande y lento	1.5 – 2.0
Rio grande con velocidad de flujo mediana	2.0 – 3.0
Curso rápido	3.0 – 5.0
Rápidas y caidas de agua	> 5.0

f	3
K_d	8,97281633

Cálculo a partir de Q

K_d 3,92679834

$$k_d = 1.796Q^{-0.49}$$

Para 0.3≤Q≤23 m³/s

Tasa por degradación de DBO definitiva K_d 8,97281633

ECUACIONES

$$DO = \frac{K_d}{K_a - K_d} DBO_o\left(e^{-K_d x/U} - e^{-K_a x/U}\right) + DO_o e^{-K_a x/U}$$

$$DBO = DBO_o e^{-K_d x/U}$$

Cálculo del cambio en la concentración

x (m)	x/V_{med} (d)	DBO_5(mg/m^3)	DO	OD (mg/m^3)
0,5	0,00001	5043,78	1004,24	8399,30
2	0,00003	5042,73	1004,67	8398,88
4	0,00006	5041,33	1005,23	8398,32
8	0,00012	5038,54	1006,35	8397,20
10	0,00015	5037,15	1006,91	8396,64
30	0,00046	5023,22	1012,45	8391,10
100	0,00154	4974,76	1031,19	8372,36
213	0,00329	4897,53	1059,35	8344,20
300	0,00463	4838,88	1079,34	8324,21
400	0,00617	4772,34	1100,60	8302,95
500	0,00772	4706,71	1120,09	8283,45
600	0,00926	4641,99	1137,91	8265,63
700	0,01080	4578,15	1154,13	8249,41
800	0,01235	4515,20	1168,84	8234,71
2500	0,03858	3568,16	1246,76	8156,79
3000	0,04630	3329,48	1228,19	8175,35
3500	0,05401	3106,76	1198,71	8204,84
4000	0,06173	2898,94	1161,32	8242,23
4500	0,06944	2705,03	1118,40	8285,14
5000	0,07716	2524,08	1071,84	8331,71

GRÁFICAS DE RESULTADOS

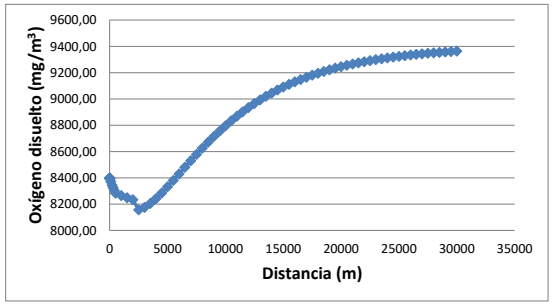

Para el oxígeno disuelto

L_{IV} 4000 m

7735

5500	0,08488	2355,24	1023,09	8380,45
6000	0,09259	2197,69	973,30	8430,25
6500	0,10031	2050,68	923,34	8480,20
7000	0,10802	1913,51	873,88	8529,66
7500	0,11574	1785,51	825,43	8578,12
8000	0,12346	1666,07	778,34	8625,21
8500	0,13117	1554,63	732,87	8670,67
9000	0,13889	1450,63	689,21	8714,34
9500	0,14660	1353,60	647,46	8756,08
10000	0,15432	1263,05	607,69	8795,85
10500	0,16204	1178,56	569,92	8833,63
11000	0,16975	1099,73	534,13	8869,41
11500	0,17747	1026,16	500,30	8903,25
12000	0,18519	957,52	468,38	8935,17
12500	0,19290	893,47	438,30	8965,25
13000	0,20062	833,70	410,00	8993,55
13500	0,20833	777,93	383,40	9020,15
14000	0,21605	725,90	358,42	9045,12
14500	0,22377	677,34	334,99	9068,55
15000	0,23148	632,03	313,03	9090,52
15500	0,23920	589,75	292,45	9111,10
16000	0,24691	550,30	273,18	9130,37
16500	0,25463	513,49	255,14	9148,40
17000	0,26235	479,14	238,27	9165,28
17500	0,27006	447,09	222,49	9181,06
18000	0,27778	417,19	207,73	9195,81
18500	0,28549	389,28	193,94	9209,60
19000	0,29321	363,24	181,05	9222,49
19500	0,30093	338,94	169,01	9234,54
20000	0,30864	316,27	157,76	9245,79
20500	0,31636	295,11	147,25	9256,29
21000	0,32407	275,37	137,44	9266,11
21500	0,33179	256,95	128,28	9275,27
22000	0,33951	239,76	119,72	9283,83
22500	0,34722	223,73	111,73	9291,82
23000	0,35494	208,76	104,27	9299,27
23500	0,36265	194,80	97,31	9306,24
24000	0,37037	181,76	90,81	9312,73
24500	0,37809	169,61	84,75	9318,80
25000	0,38580	158,26	79,08	9324,46
25500	0,39352	147,67	73,80	9329,75
26000	0,40123	137,80	68,87	9334,68
26500	0,40895	128,58	64,26	9339,28
27000	0,41667	119,98	59,97	9343,58
27500	0,42438	111,95	55,96	9347,59
28000	0,43210	104,46	52,22	9351,33
28500	0,43981	97,48	48,73	9354,82
29000	0,44753	90,96	45,47	9358,08
29500	0,45525	84,87	42,43	9361,12
30000	0,46296	79,19	39,59	9363,96

Para la DBO_5

L_{IV} m

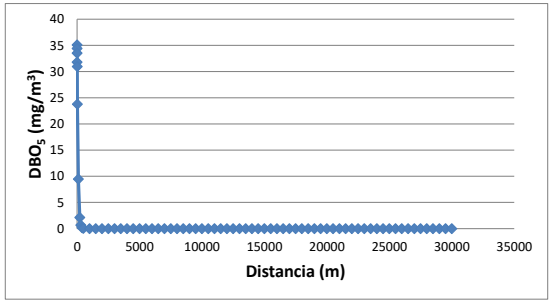

DEMANDA BIOQUÍMICA DE OXÍGENO (DBO)

Cálculo de la carga de entrada del tramo (W)

Caudal ambiental (m^3/día)	Q_{amb}	426427,2	
Caudal del vertimiento (m^3/día)	Q_v	38,016	
Concentración en el cuerpo de agua (mg/m^3)	DBO_0	5000	
Concentración en el vertimiento (mg/m^3)	DBO_v	500000	
Carga de entrada (mg/día)	W	2151144000	
Velocidad media (m/día)	v_{med}	64800	
Concentración estándar (mg/m^3)	C_{est}	5000	
Fracción dispersiva (Adim)	DF	0,722	

$$a_{DBO} = \left[\left(1 + DF * K_d t_{DBO}\right) * e^{(1-DF)*K_d t_{DBO}}\right] * Q$$

Cálculo de la tasa de consumo de oxígeno por degradación de DBO (k_d)

K_d	8,97281633	d^{-1}

Cálculo del factor de asimilación (a)

a_{DBO}	430228,8	m^3/día

Comprobación del cálculo de a

	a_{DBO}	439020,503	m^3/día
Insertar semilla para t_{DBO}	t_{DBO}	0,003258173	día
	Celda objetivo	0,020434948	

Cálculo del tiempo medio de viaje para la DBO (t_{DBO})

$$t_{DBO(i+1)} = t_{DBO(i)} - \frac{\left(1 + DF * k_d t_{DBO(i)}\right) * Q * e^{(1-DF)*K_d t_{DBO(i)}} - a_{DBO}}{k_d\left[1 + DF(1-DF) * k_d t_{DBO(i)}\right] * Q * e^{(1-DF)*K_d t_{DBO(i)}}}$$

Solución de la ecuación con el método de Newton-Raphson

$$X_{n+1} = X_n - \frac{f(X_n)}{f'(X_n)}$$

Tolerancia 0,0001

Iteración	X	(FX)	F'(X)	Menor a tolerancia
0	0,014	51446,46254	4062499,937	TODAVIA NO
1	0,001336255	1364,419938	3848609,933	TODAVIA NO
2	0,000981732	1,037408853	3842758,732	TODAVIA NO
3	0,000981462	6,01052E-07	3842754,28	TODAVIA NO
4	0,000981462	0	3842754,28	SOLUCION
5	0,000981462	0	3842754,28	SOLUCION
6	0,000981462	0	3842754,28	SOLUCION
7	0,000981462	0	3842754,28	SOLUCION
8	0,000981462	0	3842754,28	SOLUCION
9	0,000981462	0	3842754,28	SOLUCION
10	0,000981462	0	3842754,28	SOLUCION
11	0,000981462	0	3842754,28	SOLUCION
12	0,000981462	0	3842754,28	SOLUCION
13	0,000981462	0	3842754,28	SOLUCION
14	0,000981462	0	3842754,28	SOLUCION
15	0,000981462	0	3842754,28	SOLUCION
16	0,000981462	0	3842754,28	SOLUCION
17	0,000981462	0	3842754,28	SOLUCION
18	0,000981462	0	3842754,28	SOLUCION
19	0,000981462	0	3842754,28	SOLUCION
20	0,000981462	0	3842754,28	SOLUCION
21	0,000981462	0	3842754,28	SOLUCION
22	0,000981462	0	3842754,28	SOLUCION
23	0,000981462	0	3842754,28	SOLUCION
24	0,000981462	0	3842754,28	SOLUCION
25	0,000981462	0	3842754,28	SOLUCION
26	0,000981462	0	3842754,28	SOLUCION
27	0,000981462	0	3842754,28	SOLUCION
28	0,000981462	0	3842754,28	SOLUCION
29	0,000981462	0	3842754,28	SOLUCION
30	0,000981462	0	3842754,28	SOLUCION

Tiempo medio de viaje definitivo t_{DBO} 0,00325817 día

Cálculo de la longitud aguas abajo donde se alcanza el factor de asimilación (L_{IV})

L_{IV}	211,1296	m

FÓSFORO TOTAL

Cálculo de la carga de entrada del tramo (W)

Caudal ambiental (m^3/día)	Q_{amb}	426427,2
Caudal del vertimiento (m^3/día)	Q_v	38,016
Concentración en el cuerpo de agua (mg/m^3)	PT_0	62
Concentración en el vertimiento (mg/m^3)	PT_v	15000
Carga de entrada (mg/día)	W	27008726
Velocidad media (m/día)	v_{med}	64800
Concentración estándar (mg/m^3)	C_{est}	62
Fracción dispersiva (Adim)	DF	0,2346939

Cálculo de la tasa de hidrólisis (k_p)

K_p	6	d^{-1}

Cálculo del factor de asimilación (a)

$$a_{PT} = \left[\left(1 + DF * K_p t_{PT}\right) * e^{(1-DF)*K_p t_{PT}}\right] * Q$$

a_{PT}	435624,6194	m^3/día

Comprobación del cálculo de a

	a_{PT}	530777,31	m^3/día
Insertar semilla para t_{PT}	t_{PT}	0,0366836	
	Celda objetivo	0,2184282	

Cálculo del tiempo medio de viaje para el fósforo total (t_{PT})

$$t_{PT(i+1)} = t_{PT(i)} - \frac{\left(1 + DF * k_p t_{PT(i)}\right) * Q * e^{(1-DF)*K_p t_{PT(i)}} - a_{PT}}{k_p\left[1 + DF(1-DF) * k_p t_{PT(i)}\right] * Q * e^{(1-DF)*K_p t_{PT(i)}}}$$

Solución de la ecuación con el método de Newton-Raphson

$$X_{n+1} = X_n - \frac{f(X_n)}{f'(X_n)}$$

Tolerancia 0,0001

Iteración	X	(FX)	F'(X)	Menor a tolerancia
0		-9159,403	2558791,296	TODAVIA NO
1	0,0035796	93,551614	2611231,793	TODAVIA NO
2	0,0035438	0,0094935	2610701,84	TODAVIA NO
3	0,0035438	0	2610701,786	SOLUCION
4	0,0035438	0	2610701,786	SOLUCION
5	0,0035438	0	2610701,786	SOLUCION
6	0,0035438	0	2610701,786	SOLUCION
7	0,0035438	0	2610701,786	SOLUCION
8	0,0035438	0	2610701,786	SOLUCION
9	0,0035438	0	2610701,786	SOLUCION
10	0,0035438	0	2610701,786	SOLUCION
11	0,0035438	0	2610701,786	SOLUCION
12	0,0035438	0	2610701,786	SOLUCION
13	0,0035438	0	2610701,786	SOLUCION
14	0,0035438	0	2610701,786	SOLUCION
15	0,0035438	0	2610701,786	SOLUCION
16	0,0035438	0	2610701,786	SOLUCION
17	0,0035438	0	2610701,786	SOLUCION
18	0,0035438	0	2610701,786	SOLUCION
19	0,0035438	0	2610701,786	SOLUCION
20	0,0035438	0	2610701,786	SOLUCION
21	0,0035438	0	2610701,786	SOLUCION
22	0,0035438	0	2610701,786	SOLUCION
23	0,0035438	0	2610701,786	SOLUCION
24	0,0035438	0	2610701,786	SOLUCION
25	0,0035438	0	2610701,786	SOLUCION
26	0,0035438	0	2610701,786	SOLUCION
27	0,0035438	0	2610701,786	SOLUCION
28	0,0035438	0	2610701,786	SOLUCION
29	0,0035438	0	2610701,786	SOLUCION
30	0,0035438	0	2610701,786	SOLUCION

Tiempo medio de viaje definitivo t_{PT} 0,03668362 día

Cálculo de la longitud aguas abajo donde se alcanza el factor de asimilación (L_{IV})

L_{IV} 2377,098 m

SÓLIDOS SUSPENDIDOS TOTALES

Cálculo de la carga de entrada del tramo (W)

Caudal ambiental (m^3/día)	Q_{amb}	426427,2
Caudal del vertimiento (m^3/día)	Q_v	38,016
Concentración en el cuerpo de agua (mg/m^3)	SST_0	21000
Concentración en el vertimiento (mg/m^3)	SST_v	20000
Carga de entrada (mg/día)	W	8,956E+09
Velocidad media (m/día)	v_{med}	64800
Concentración estándar (mg/m^3)	C_{est}	21000
Fracción dispersiva (Adim)	DF	0,235

Cálculo de la velocidad de sedimentación (v_{ss})

Tipo de partícula	Diámetro (µm)	Velocidad de sedimentación (m d^{-1})
Carbono orgánico particulado	1-10	0.2
	10-64	1.5
	> 64	2.3
Arcilla	2-4	0.3-1
Limo	10-20	3-30

v_{ss} 0,008 m/s

Cálculo de la tasa de sedimentación (k_s)

K_s 1001,73913 d-1

$$a_{SST} = \left[(1 + DF * K_s t_{SST}) * e^{(1-DF)*K_s t_{SST}}\right] * Q$$

Cálculo del factor de asimilación (a)

a_{SST} 426463,4057 m^3/día

Comprobación del cálculo de a

	a_{SST}	481989,64	m^3/día
Insertar semilla para t_{SST}	t_{SST}	0,0001226	
	Celda objetivo	0,1302016	

Cálculo del tiempo medio de viaje para los sólidos suspendidos totales (t_{SST})

Solución de la ecuación con el método de Newton-Raphson

$$t_{SST(i+1)} = t_{SST(i)} - \frac{\left(1 + DF * k_s t_{SST(i)}\right) * Q * e^{(1-DF)*K_s t_{SST(i)}} - a_{SST}}{k_s\left[1 + DF(1 - DF) * k_s t_{SST(i)}\right] * Q * e^{(1-DF)*K_s t_{SST(i)}}}$$

$$X_{n+1} = X_n - \frac{f(X_n)}{f'(X_n)}$$

Tolerancia 0,0001

Iteración	X	(FX)	F'(X)	Menor a tolerancia
0		1,8102857	427206894,6	TODAVIA NO
1	-4,24E-09	3,631E-06	427205181,1	SOLUCION
2	-4,24E-09	0	427205181,1	SOLUCION
3	-4,24E-09	0	427205181,1	SOLUCION
4	-4,24E-09	0	427205181,1	SOLUCION
5	-4,24E-09	0	427205181,1	SOLUCION
6	-4,24E-09	0	427205181,1	SOLUCION
7	-4,24E-09	0	427205181,1	SOLUCION
8	-4,24E-09	0	427205181,1	SOLUCION
9	-4,24E-09	0	427205181,1	SOLUCION
10	-4,24E-09	0	427205181,1	SOLUCION
11	-4,24E-09	0	427205181,1	SOLUCION
12	-4,24E-09	0	427205181,1	SOLUCION
13	-4,24E-09	0	427205181,1	SOLUCION
14	-4,24E-09	0	427205181,1	SOLUCION
15	-4,24E-09	0	427205181,1	SOLUCION
16	-4,24E-09	0	427205181,1	SOLUCION
17	-4,24E-09	0	427205181,1	SOLUCION
18	-4,24E-09	0	427205181,1	SOLUCION
19	-4,24E-09	0	427205181,1	SOLUCION
20	-4,24E-09	0	427205181,1	SOLUCION
21	-4,24E-09	0	427205181,1	SOLUCION
22	-4,24E-09	0	427205181,1	SOLUCION
23	-4,24E-09	0	427205181,1	SOLUCION
24	-4,24E-09	0	427205181,1	SOLUCION
25	-4,24E-09	0	427205181,1	SOLUCION
26	-4,24E-09	0	427205181,1	SOLUCION
27	-4,24E-09	0	427205181,1	SOLUCION
28	-4,24E-09	0	427205181,1	SOLUCION
29	-4,24E-09	0	427205181,1	SOLUCION
30	-4,24E-09	0	427205181,1	SOLUCION

Tiempo medio de viaje definitivo t_{SST} 0,00012259 día

Cálculo de la longitud aguas abajo donde se alcanza el factor de asimilación (L_{IV})

L_{IV} 7,9 m

COLIFORMES FECALES

Cálculo de la carga de entrada del tramo (W)

Caudal ambiental (m^3/día)	Q_{amb}	426427,2
Caudal del vertimiento (m3/día)	Q_v	38,016
Concentración en el cuerpo de agua (mg/m^3)	CF_0	3.080.000
Concentración en el vertimiento (mg/m^3)	CF_v	800.000.000
Carga de entrada (mg/día)	W	1,34381E+12
Velocidad media (m/día)	v_{med}	64800
Concentración estándar (mg/m^3)	C_{est}	3.080.000
Fracción dispersiva (Adim)	DF	0,235

Tasa de decaimiento por muerte de patógenos (k_b)

$$k_b = 0.8 * 1.07^{T-20} + \frac{I_0}{0.55 * SST * H} * (1 - e^{-0.55*SST*H}) + F_p * \frac{v_{ss}}{H}$$

Donde:
T: Temperatura del agua (ºC)
I_0: Radiación solar (ly/hr)
SST: Concentración de sólidos suspendidos totales promedio en el tramo (mg/l)
H: Profundidad media del agua (m)
F_p: Fracción adsorbida de bacterias a las partículas sólidas. Valor típico: 0.7.
V_{ss}: Velocidad de sedimentación de las partículas (md^{-1})

T	18	ºC
I_0	35,93	ly/hr
SST_0	21	mg/l
H	0,69	m
v_{ss}	0,008	md^{-1}

k_b	5,21722436

$$a_{CF} = \left[(1 + DF * K_s t_{CF}) * e^{(1-DF)*K_s t_{CF}}\right] * Q$$

Cálculo del factor de asimilación (a)

a_{CF}	436301,486	m^3/día

Comprobación del cálculo de a

	a_{CF}	3307406,521	m^3/día
Insertar semilla para t_{CF}	t_{CF}	0,410943819	día
	Celda objetivo	6,580552964	

Cálculo del tiempo medio de viaje para los coliformes totales (t_{CF})

$$t_{CF(i+1)} = t_{CF(i)} - \frac{(1 + DF * k_b t_{CF(i)}) * Q * e^{(1-DF)*K_b t_{CF(i)}} - a_{CF}}{k_b\left[1 + DF(1 - DF) * k_b t_{CF(i)}\right] * Q * e^{(1-DF)*K_b t_{CF(i)}}}$$

Solución de la ecuación con el método de Newton-Raphson

$$X_{n+1} = X_n - \frac{f(X_n)}{f'(X_n)}$$

Tolerancia 0,0001

Iteración	X	(FX)	F'(X)	Menor a tolerancia
0		-9836,27	2224964,71	TODAVIA NO
1	0,004420865	107,94131	2273968,89	TODAVIA NO
2	0,004373397	0,0126189	2273437,24	TODAVIA NO
3	0,004373392	0	2273437,17	SOLUCION
4	0,004373392	0	2273437,17	SOLUCION
5	0,004373392	0	2273437,17	SOLUCION
6	0,004373392	0	2273437,17	SOLUCION
7	0,004373392	0	2273437,17	SOLUCION
8	0,004373392	0	2273437,17	SOLUCION
9	0,004373392	0	2273437,17	SOLUCION
10	0,004373392	0	2273437,17	SOLUCION
11	0,004373392	0	2273437,17	SOLUCION
12	0,004373392	0	2273437,17	SOLUCION
13	0,004373392	0	2273437,17	SOLUCION
14	0,004373392	0	2273437,17	SOLUCION
15	0,004373392	0	2273437,17	SOLUCION
16	0,004373392	0	2273437,17	SOLUCION
17	0,004373392	0	2273437,17	SOLUCION
18	0,004373392	0	2273437,17	SOLUCION
19	0,004373392	0	2273437,17	SOLUCION
20	0,004373392	0	2273437,17	SOLUCION
21	0,004373392	0	2273437,17	SOLUCION
22	0,004373392	0	2273437,17	SOLUCION
23	0,004373392	0	2273437,17	SOLUCION
24	0,004373392	0	2273437,17	SOLUCION
25	0,004373392	0	2273437,17	SOLUCION
26	0,004373392	0	2273437,17	SOLUCION
27	0,004373392	0	2273437,17	SOLUCION
28	0,004373392	0	2273437,17	SOLUCION
29	0,004373392	0	2273437,17	SOLUCION
30	0,004373392	0	2273437,17	SOLUCION

Tiempo medio de viaje definitivo t_{CF} 0,411 día

Cálculo de la longitud aguas abajo donde se alcanza el factor de asimilación (L_{IV})

L_{IV} 26629,159 m

FUENTES DE INFORMACIÓN PARA CADA DETERMINANTE

En esta sección se presenta la fuente de información de los datos de entrada (recuadro rojo) para el cálculo de la longitud de asimilación de cada determinante.

Características hidráulicas de la corriente receptora

Parámetro	Símbolo	Fuente de información
Caudal mínimo	Q_{min}	QHSE SAS
Caudal medio	Q_{medio}	QHSE SAS
Caudal máximo	$Q_{máx}$	QHSE SAS
Profundidad del agua para caudal mínimo	H_{min}	QHSE SAS
Profundidad media del agua	H_{med}	QHSE SAS
Pendiente del lecho	S	QHSE SAS
Velocidad media	v_{med}	QHSE SAS
Velocidad máxima	$v_{máx}$	QHSE SAS

Nitrógeno

Parámetro	Símbolo	Fuente de información
Tasa de nitrificación	K_n	Cooper. 1986
Tolerancia	-	Criterio del profesional
Tiempo medio de viaje definitivo	t_{NTK}	Iteración

Oxígeno disuelto y DBO

Parámetro	Símbolo	Fuente de información
Cambio en H	ΔH	QHSE SAS
Constante (Adim.)	c	Modelo de Streeter y Phelps
Factor f para el cálculo de la tasa de consumo de oxígeno	f	Criterio de acuerdo a las características de la corriente receptora
Tiempo medio de viaje definitivo del oxígeno disuelto	t_{OD}	Iteración
Tiempo medio de viaje definitivo de la DBO	t_{DBO}	Iteración

Fósforo total

Parámetro	Símbolo	Fuente de información
Tasa de hidrólisis de fósforo	K_p	No aplica
Tolerancia	-	
Tiempo medio de viaje definitivo del fósforo total	t_{PT}	

Sólidos suspendido totales

Parámetro	Símbolo	Fuente de información
Tolerancia	-	Criterio del profesional
Tiempo medio de viaje definitivo de los SST	t_{SST}	Iteración
Velocidad de sedimentación	v_{ss}	ANLA. Metodología para la definición de la longitud de influencia de vertimientos sobre corrientes de agua superficial

Coliformes totales

Parámetro	Símbolo	Fuente de información
Radiación solar	I_0	No aplica
Tolerancia	-	
Tiempo medio de viaje definitivo de los coliformes totales	t_{CF}	

ANEXO 3

RATAS, CONSTANTES Y FORMULACIONES CINÉTICAS EN EL MODELAMIENTO DE LA CALIDAD DEL AGUA SUPERFICIAL

United States
Environmental Protection
Agency

Environmental Research
Laboratory
Athens GA 30613

EPA/600/3-85/040
June 1985

Research and Development

EPA

Rates, Constants, and Kinetics Formulations in Surface Water Quality Modeling (Second Edition)

EPA/600/3-85/040
June 1985

RATES, CONSTANTS, AND KINETICS FORMULATIONS IN SURFACE WATER QUALITY MODELING (SECOND EDITION)

By

George L. Bowie, William B. Mills, Donald B. Porcella,
Carrie L. Campbell, James R. Pagenkopf, Gretchen L. Rupp,
Kay M. Johnson, Peter W.H. Chan, Steven A. Gherini

Tetra Tech, Incorporated
Lafayette, California 94549

and

Charles E. Chamberlin
Humboldt State University
Arcata, California 95521

Contract 68-03-3131

Project Officer

Thomas O. Barnwell, Jr.
Technology Development and Applications Branch
Environmental Research Laboratory
Athens, Georgia 30613

ENVIRONMENTAL RESEARCH LABORATORY
OFFICE OF RESEARCH AND DEVELOPMENT
U.S. ENVIRONMENTAL PROTECTION AGENCY
ATHENS, GEORGIA 30613

DISCLAIMER

The information in this document has been funded wholly or in part by the United States Environmental Protection Agency under Contract No. 68-03-3131 to Tetra Tech, Incorporated. It has been subject to the Agency's peer and administrative review, and it has been approved for publication as an EPA document. Mention of trade names or commercial products does not constitute endorsement or recommendation for use by the U.S. Environmental Protection Agency.

FOREWORD

As environmental controls become more costly to implement and the penalties of judgment errors become more severe, environmental quality management requires more efficient analytical tools based on greater knowledge of the environmental phenomena to be managed. As part of this Laboratory's research on the occurrence, movement, transformation, impact, and control of environmental contaminants, the Technology Development and Applications Branch develops management or engineering tools to help pollution control officials achieve water quality goals.

Basin planning requires a set of analysis procedures that can provide an assessment on the current state of the environment and a means of predicting the effectiveness of alternative pollution control strategies. This report contains a revised and updated compilation and discussion of rates, constants, and kinetics formulations that have been used to accomplish these tasks. It is directed toward all water quality planners who must interpret technical information from many sources and recommend the most prudent course of action that will minimize the cost of implementation of a pollutant control activity and maximize the environmental benefits to the community.

Rosemarie C. Russo
Director
Environmental Research Laboratory
Athens, Georgia

ABSTRACT

Recent studies are reviewed to provide a comprehensive volume on state-of-the-art formulations used in surface water quality modeling along with accepted values for rate constants and coefficients. Topics covered include: dispersion, heat budgets, dissolved oxygen saturation, reaeration, CBOD decay, NBOD decay, sediment oxygen demand, photosynthesis, pH and alkalinity, nutrients, algae, zooplankton, and coliform bacteria. Factors affecting the specific phenomena and methods of measurement are discussed in addition to data on rate constants.

This report was submitted in fulfillment of Contract No. 68-03-3131 by Tetra Tech, Incorporated, under the sponsorship of the U.S. Environmental Protection Agency. The report covers the period June 1983 to April 1985, and work was completed as of April 1985.

CONTENTS

Foreword iii
Abstract iv
Figures vii
Tables xi
Acknowledgments xvi

1. Introduction 1
   1.1 Background 1
   1.2 Purpose and Use of This Manual 2
   1.3 Scope and Arrangement of Manual 2
   1.4 General Observations on Model Formulations, Rate Constants, and Coefficients 3
   1.5 References. 4

2. Physical Processes 6
   2.1 Introduction 6
   2.2 Advective Transport 11
   2.3 Dispersive Transport 17
   2.4 Surface Heat Budget 61
   2.5 References 76

3. Dissolved Oxygen 90
   3.1 Dissolved Oxygen Saturation 90
   3.2 Reaeration 101
   3.3 Carbonaceous Deoxygenation 135
   3.4 Nitrogenous Biochemical Oxygen Demand 158
   3.5 Sediment Oxygen Demand (SOD) 173
   3.6 Photosynthesis and Respiration 188
   3.7 References 205

4. pH and Alkalinity 231
   4.1 Introduction 231
   4.2 Carbonate Alkalinity System 231
   4.3 Extended Alkalinity Approach 236
   4.4 Summary 241
   4.5 References 242

5. Nutrients 244
   5.1 Introduction 244
   5.2 Nutrient Cycles 245
   5.3 General Modeling Approach for All Nutrients 247
   5.4 Temperature Effects 253
   5.5 Carbon Transformations 255
   5.6 Nitrogen Transformations 257

5.7 Phosphorus Transformations 265
5.8 Silicon Transformations 265
5.9 Algal Uptake 268
5.10 Excretion 271
5.11 Sediment Release 272
5.12 Summary 273
5.13 References 274

6. Algae 279
6.1 Introduction 279
6.2 Modeling Approaches 281
6.3 Cell Composition 285
6.4 Growth 287
6.5 Respiration and Excretion 342
6.6 Settling 345
6.7 Nonpredatory Mortality 351
6.8 Grazing 357
6.9 Summary 363
6.10 References 365

7. Zooplankton 375
7.1 Introduction 375
7.2 Temperature Effects 376
7.3 Growth 378
7.4 Respiration and Mortality 400
7.5 Predatory Mortality 409
7.6 Summary 416
7.7 References 418

8. Coliform Bacteria 424
8.1 Introduction 424
8.2 Composition and Assay 426
8.3 Modeling Coliforms 428
8.4 Summary 449
8.5 References 450

FIGURES

Number		Page
2-1	One-dimensional geometric representation for river systems.	9
2-2	Two-dimensional geometric representation for lake systems.	10
2-3	Oscillation of velocity component about a mean value . .	18
2-4	Diffusion coefficients characteristic of various environments	20
2-5	Dependence of the horizontal diffusion coefficient on the scale of the phenomenon	31
2-6	Okubo's diffusion data and 4/3 power lines	32
2-7	Factors contributing to tidally averaged dispersion coefficients in the estuarine environment.	42
2-8	Dispersion coefficients in streams	54
2-9	Clear sky solar radiation according to Hamon, Weiss and Wilson (1954).	65
3-1	Predicted reaeration coefficients as a function of depth from thirteen predictive equations	111
3-2	Comparisons of predicted and observed reaeration coefficients for the formula of Dobbins (1965) (a) and Parkhurst-Pomeroy (1972) (b)	112
3-3	Formula of Bennett and Rathbun (1972) compared against observed reaeration coefficients	113
3-4	Calculated versus experimental reaeration coefficients for equations of (a) Tsivoglou and Wallace (1972), (b) Padden and Gloyna (1971), and (c) Parkhurst and Pomeroy (1972)	114

FIGURES (continued)

Number		Page
3-5	Reaeration coefficient versus energy dissipation (a) for flow rates between 10 and 280 cfs and (b) for flow rates less than 10 cfs.	115
3-6	Field data considered by three different investigations.	116
3-7	Reaeration coefficient (1/day) vs. depth and velocity using the suggested method of Covar (1976)	117
3-8	Ratio of reaeration coefficient under windy conditions to reaeration coefficient without wind, as a function of wind speed	123
3-9	Division of head loss structures by dam type	126
3-10	Sources and sinks of carbonaceous BOD in the aquatic environment.	137
3-11	Deoxygenation coefficient (k_d) as a function of depth. .	147
3-12	Example computation of k_R based on BOD measurements of stream water	156
3-13	Effect of reduced nitrogen concentration on nitrification rate as reported by Borchardt (1966) . .	162
3-14	Effect of temperature on nitrification as reported by Borchardt (1966).	166
3-15	pH dependence of nitrification	167
3-16	Nitrogenous biochemical oxygen demand versus travel time in Shenandoah River	171
3-17	Diurnal variation of (P-R) in Truckee River near Station 2B	198
3-18	Concept of Stokes total time derivative.	199
3-19	Algal productivity and chlorophyll relationships for streams.	202
4-1	$[\Sigma C_B - \Sigma C_A]$ plotted against reported alkalinity.	239
5-1	Nutrient interactions for carbon, nitrogen, and phosphorus	246

FIGURES (continued)

Number		Page
5-2	Nutrient interactions for silica	247
5-3	Nitrogen cycle	248
5-4	Phosphorus cycle	249
5-5	Effect of pH and temperature on unionized ammonia. . . .	264
6-1	Major types of temperature response curves for algal growth	294
6-2	Envelope curve of algal growth rate versus temperature for data compiled from many studies involving many different species.	298
6-3	Temperature-growth curves for major algal groups	304
6-4	Comparison of light response curves for algal growth . .	312
6-5	Michaelis-Menten saturation kinetics for algal growth limitation by a single nutrient.	324
7-1	Growth rate and grazing rate as a function of food supply for zooplankton with constant filtration rates and assimilation efficiencies.	380
7-2	Comparison of the Ivlev and Michaelis-Menten functions with the same half-saturation value	388
7-3	Comparison of reverse Michaelis-Menten formulation (a) and Canale *et al.*'s, (1975, 1976) formulation (b) for filtration rate as a function of food concentration. .	394
7-4	Frequency histograms for zooplankton assimilation efficiencies	403
7-5	Frequency histograms showing variations in zooplankton assimilation efficiencies with different food types. .	404
7-6	Frequency histograms of zooplankton respiration rates. .	415
7-7	Frequency histogram of nonpredatory mortality rates for zooplankton	416
8-1	Relationship between pathogen or virus decay rates and coliform decay rates based on figure presented by Chamberlin (1982).	425

FIGURES (continued)

Number		Page
8-2	Typical mortality curves for coliforms as a function of time.	440

TABLES

Number		Page
2-1	Major Reviews of Modeling State-of-the-Art	7
2-2	Values for Empirical Coefficients a_1 and a_2.	28
2-3	Tidally Averaged Dispersion Coefficients for Selected Estuaries.	45
2-4	Tidally Averaged Dispersion Coefficients	46
2-5	References Related to Longitudinal Dispersion.	49
2-6	Summary of Studies of Transverse Mixing in Streams . . .	57
2-7	Transverse Mixing Coefficients in Natural Streams and Channels	58
2-8	Summary of Field Data for Transverse Dispersion Coefficients	59
2-9	Summary of Nondimensional Diffusion Factors in Natural Streams.	60
2-10	Values for Short Wave Radiation Coefficients A and B . .	66
2-11	Values for Empirical Coefficients.	69
2-12	Evaporation Formula for Lakes and Reservoirs	71
3-1	Methods Used by Selected Models to Predict Dissolved Oxygen Saturation.	91
3-2	Solubility of Oxygen in Water Exposed to Water-Saturated Air at 1.000 Atmosphere Pressure	93
3-3	Values for the Bracketed Quantity Shown in Equation 3-11 to be Used with the Corresponding Temperatures and Pressures.	95
3-4	Comparison of Dissolved Oxygen Saturation Values from Ten Equations at 0.0 mg/l Salinity and 1 atm Pressure	97

TABLES (continued)

Number		Page
3-5	Comparison of Dissolved Oxygen Saturation Values from Selected Equations at a Chloride Concentration of 20,000 mg/l (36.1 ppt Salinity) and 1 atm Pressure . .	98
3-6	Reaeration Coefficients for Rivers and Streams	103
3-7	Summary of Studies which Reviewed Stream Reaeration Coefficients	108
3-8	Equations that Predict the Effects of Small Dams on Stream Reaeration.	125
3-9	Reported Values of Temperature Coefficient	127
3-10	Sources of Stram Reaeration Data	128
3-11	Reaeration Coefficients for Lakes.	130
3-12	Reaeration Coefficients for Estuaries.	132
3-13	Values of the Temperature Compensation Coefficient Used for Carbonaceous BOD Decay.	142
3-14	Coefficient of Bed Activity as a Function of Stream Slope.	143
3-15	Deoxygenation Rates for Selected U.S. Rivers	144
3-16	Expressions for Carbonaceous Oxygen Demand Used in Water Quality Models	150
3-17	Values of Kinetic Coefficients for Decay of Carbonaceous BOD.	152
3-18	Expressions for Nitrogenous Biochemical Oxidation Rates Used in a Variety of Water Quality Models . . .	160
3-19	Summary of Factors that Influence Nitrification.	164
3-20	Temperature Correction Factor, θ, for Nitrification. . .	165
3-21	Case Studies of Nitrification in Natural Waters.	169
3-22	Summary of Nitrification Rates	172

TABLES (continued)

Number		Page
3-23	Some Typical Values of the Temperature Coefficient for SOD Rate Coefficients Used in Water Quality Models . .	179
3-24	Model Formulations Commonly Used in SOD Computations . .	182
3-25	Average Values of Oxygen Uptake Rates of River Bottoms .	187
3-26	Measured Values of Sediment Oxygen Demand in Rivers and Streams.	189
3-27	Measured Values of Sediment Oxygen Demand in Lakes and Reservoirs	190
3-28	Measured Values of Sediment Oxygen Demand in Estuaries and Marine Systems	191
3-29	Oxygen Produced per Mass of Algae.	192
3-30	Oxygen Consumed per Mass of Algae.	193
3-31	Summary of Methods to Predict Photosynthetic Oxygen Production and Respiration without Simulating Algal Growth and Death	194
3-32	Photosynthetic Oxygen Production and Respiration Rates in Rivers.	204
4-1	Options and their Required Input Parameters for PHCALC .	240
5-1	Comparison of Nutrient Models.	254
5-2	Rate Coefficients for Carbon Transformations	256
5-3	Rate Coefficients for Nitrogen Transformations	259
5-4	Rate Coefficients for Denitrification.	262
5-5	Rate Coefficients for Phosphorus Transformations	266
5-6	Rate Coefficients for Silica Transformations	267
6-1	General Comparison of Algal Models	283
6-2	Nutrient Composition of Algal Cells - Percent of Dry Weight Biomass	286
6-3	Nutrient Composition of Algal Cells - Ratio to Carbon. .	288

TABLES (continued)

Number		Page
6-4	Nutrient Composition of Algal Cells - Ratio to Chlorophyll a.	289
6-5	Algal Maximum Growth Rates	291
6-6	Comparison of Temperature Adjustment Functions for Algal Growth	305
6-7	Comparison of Light Limitation Formulations.	319
6-8	Algal Saturating Light Intensities	320
6-9	Half-saturation Constants for Light Limitation	321
6-10	Half-Saturation Constants for Michaelis-Menten Growth Formulations.	327
6-11	Comparison of Algal Growth Formulations.	329
6-12	Half-Saturation Constants for Variable Stoichiometry Formulations	332
6-13	Minimum Cell Quotas	333
6-14	Maximum Internal Nutrient Concentrations	334
6-15	Maximum Nutrient Uptake Rates.	339
6-16	Half-Saturation Constants for Nutrient Uptake.	340
6-17	Model-Specific Nutrient Uptake Parameters.	341
6-18	Algal Respiration Rates.	346
6-19	Phytoplankton Settling Velocities.	352
6-20	Algal Nonpredatory Mortality Rates	358
7-1	General Comparison of Zooplankton Models	377
7-2	Zooplankton Maximum Consumption Rates.	382
7-3	Zooplankton Maximum Filtration Rates	383
7-4	Zooplankton Maximum Growth Rates	384

TABLES (continued)

Number		Page
7-5	Comparison of Temperature Adjustment Functions for Zooplankton Growth and Consumption	385
7-6	Michaelis-Menten Half-Saturation Constants for Zooplankton Consumption and Growth	390
7-7	Threshold Feeding Levels for Zooplankton	392
7-8	Comparison of Zooplankton Growth Formulations.	396
7-9	Zooplankton Assimilation Efficiencies.	401
7-10	Zooplankton Respiration Rates.	410
7-11	Zooplankton Mortality Rates.	413
8-1	Factors Affecting Coliform Disappearance Rates	435
8-2	Coliform Bacteria Freshwater Disappearance Rates Measured *In situ*	436
8-3	Values for Coliform-Specific Disappearance Rates Used in Several Modeling Studies.	437
8-4	Nutrient K_s Values for *Escherichia Coli*.	438
8-5	Values of Co, C', k, and k' from the Ohio River.	441
8-6	Summary of Decay Rates of Tc, Fc, and Fs	442
8-7	Comparison of k_ρ Estimates Based on Chamberlin and Mitchell (1978) with Additional Values	444
8-8	Parameter Estimates for Lantrip (1983) Multi-Factor Decay Models.	446
8-9	Experimental Hourly T-90 Values	449

ACKNOWLEDGMENTS

Special thanks are due to the participants in the Rates Manual Workshop held at Tetra Tech, Lafayette during November 29-30, 1984 to review the first draft of the report. These include Ray Whittemore (National Council of the Paper Industry for Air and Stream Improvement, Inc.), Steve McCutcheon (U.S. Geological Survey), Kent Thornton (Ford, Thornton, and Norton, Inc.), Vic Bierman (U.S. Environmental Protection Agency), Tom Barnwell (U.S. Environmental Protection Agency), Don Scavia (National Oceanic and Atmospheric Administration), Tom Gallagher (HydroQual, Inc.), Carl Chen (Systech, Inc.), Jerry Orlob (University of California, Davis), Lam Lau (National Water Research Institute, Ontario, Canada), Bill Walker (private consultant), and Peter Shanahan (Environmental Research and Technology, Inc.). Betsy Southerland (U.S. Environmental Protection Agency) was unable to attend but also participated in the review of the first draft. The above individuals provided many useful comments and references which were incorporated in the final report.

Numerous other individuals also provided reference materials during the preparation of this report. Although they are too numerous to mention here, their input is greatly appreciated.

We would also like to thank Trudy Rokas, Susan Madson, Gloria Sellers, Belinda Hamm, and Faye Connaway for typing and preparing the report, and Marilyn Davies for providing most of the graphics.

Finally, thanks are due most to Tom Barnwell and the U.S. Environmental Protection Agency, Environmental Research Laboratory, Athens, Georgia for both funding the project and providing technical input and guidance.

Chapter 1

INTRODUCTION

1.1 BACKGROUND

The use of mathematical models to simulate ecological and water quality interactions in surface waters has grown dramatically over the past two decades. Simulation techniques offer an integrated and relatively sound course for evaluating wasteload abatement alternatives. Predictions of system behavior based upon mathematical simulation techniques may be misleading, however, particularly if the physical mechanisms involved are not accurately represented in the model. Furthermore, even where the model does faithfully describe mechanisms in the prototype, poor results may be obtained where insufficient data are available to estimate rate constants and coefficients.

Much of the work done in the water quality modeling field has been oriented toward improvement of models--toward incorporating better numerical solution techniques, toward an expanded complement of water quality constituents simulated, and toward realistic representations of modeled physical, chemical, and biological phenomena. There is, however, a need for a document that summarizes the rate constants and coefficients (e.g., nitrification rates and reaeration rates) needed in the models. This document is intended to satisfy that need.

The first edition of this document was published seven years ago (Zison et al., 1978). Because an extensive body of literature on rate constants and modeling formulations has emerged since that time, the United States Environmental Protection Agency has sponsored an updating of the manual. In addition, a workshop was held to evaluate the manual, to review the

formulations and associated coefficients and rate values, and to provide further data for the final document. As a result of the literature review and workshop, a substantially new manual has been produced.

1.2 PURPOSE AND USE OF THIS MANUAL

This manual is intended for use by practitioners as a handbook--a convenient reference on modeling formulations, constants, and rates commonly used in surface water quality simulations. Guidance is provided in selecting appropriate formulations or values of rate constants for specific applications. The manual also provides a range of coefficient values that can be used to perform sensitivity analyses. Where appropriate, measurement techniques for rate constants are also discussed.

It was impossible, however, to encompass all formulations or to examine all recent reports containing rates data. It is hoped, therefore, that the user will recognize the desirability of seeking additional sources where questions remain about formulations or values. Data used from within this volume should be recognized as representing a sampling from a larger set of data. It should also be noted that there are often very real limitations involved in using literature values for rates rather than observed system values. It is hoped that this document will find its main use as a guide in the search for "the correct value" rather than as the sole source of that value.

1.3 SCOPE AND ARRANGEMENT OF MANUAL

In preparing this manual, an attempt was made to present a comprehensive set of formulations and associated constants. In contrast to the first edition (Zison et al.,1978), the manual has been divided into sections containing specific topics. Following this introduction, chapters are presented that discuss the following topics:

- Physical processes of dispersion and temperature
- Dissolved oxygen

- pH and alkalinity
- Nutrients
- Algae
- Zooplankton
- Coliforms

The parameters that are addressed in this manual are those that traditionally have been the focus of water quality management and the focus for control of conventional pollutants. These include temperature, dissolved oxygen, nutrients and eutrophication, and coliform bacteria. Higher organisms (fish, benthos) are not discussed, nor are the details of higher trophic levels in ecosystem models. Also, hydrodynamic processes, although important, are not dealt with in detail.

1.4 GENERAL OBSERVATIONS ON MODEL FORMULATIONS, RATE CONSTANTS, AND COEFFICIENTS

Each rate value or expression used in a model should not be chosen as an "afterthought", but should be considered as an integral part of the modeling process. A substantial portion of any modeling effort should go into selecting specific approaches and formulations based upon the objectives of modeling, the kinds and amounts of data available, and the strengths and weaknesses of the approach or formulation. Once formulations have been selected, a significant effort should be made to determine satisfactory values for parameters. Even where the parameter is to be chosen by calibration, it is clearly important to establish whether the calibrated value is within a reasonable range or not. Recent references on model calibration include Thomann (1983), National Council on Air and Stream Improvement (1982), and Beck (1983). Users should be aware that an acceptable model calibration does not imply that the model has predictive capability. The model may contain incorrect mechanisms, and agreement between model predictions and observations could have been obtained through an unrealistic choice of parameter values. Further, the future status of the prototype may be controlled by processes not even simulated in the model.

Values of many constants and coefficients are dependent upon the way they are used in modeling formulations. For example, while pollutant dispersion is an observable physical process, modeling this process is partly a mathematical construct. Therefore, constants that are used to represent the process (i.e., dispersion coefficients) cannot be chosen purely on the basis of physics since they also depend on the modeling approach. For example, to determine the dispersion coefficients in a model application to an estuary, both the time and length scales of the model must be considered. Whether the model is tidally averaged or simulates intra-tidal variations, and whether the model is 1-, 2-, or 3-dimensional, all influence the value of the appropriate dispersion coefficient for that model. Ford and Thornton (1979) discuss scale effects in ecological models, and conclude that inconsistent scales for the hydrodynamics, chemistry, and biology may produce erroneous model predictions.

Since coefficient values are never known with certainty, modelers are constantly faced with the question of how accurately rate constants should be known. The relationship between uncertainty in coefficient values and model predictions can be evaluated by performing sensitivity analyses. For models with few parameters, sensitivity analyses are generally straightforward. However, for complex models, sensitivity analyses are no longer straightforward since many dynamic interactions are involved. Sensitivity analyses are discussed in detail in Thornton and Lessem (1976), Thornton (1983), and Beck (1983).

1.5 REFERENCES

Beck, M.B. 1983. Sensitivity Analysis, Calibration, and Validation. In: Mathematical Modeling of Water Quality: Streams, Lakes, and Reservoirs. International Institute for Applied Systems Analysis. Editor: G.T. Orlob.

Ford, D.E. and K.S. Thornton. 1979. Time and Length Scales for the One-Dimensional Assumption and its Relation to Ecological Models. Water Resources Research. Vol. 15, No. 1, pp. 113-120.

National Council of the Paper Industry for Air and Stream Improvement, Inc. 1982. A Study of the Selection, Calibration and Verification of Mathematical Water Quality Models. NCASI Tech. Bull. 367, New York.

Thomann, R.V. 1982. Verification of Water Quality Models. Journal of Environmental Engineering Division, ASCE. Vol. 108, No. EE5, October, pp. 923-940.

Thornton, K.W. and A.S. Lessem. 1976. Sensitivity Analysis of the Water Quality for River-Reservoir Systems Model. U.S. Army Waterways Experiment Station. Misc. Paper Y-76-4.

Thornton, K.W. 1983. Sensitivity Analysis in Simulation Experimentation. Encyclopedia of Systems and Control. Pergamon Press.

Zison, S.W., W.B. Mills, D. Deimer, and C.W. Chen. 1978. Rates Constants and Kinetics Formulations in Surface Water Quality Modeling. Prepared by Tetra Tech, Inc., Lafayette, CA, for Environmental Research Laboratory, USEPA, Athens, GA. EPA-600/3-78-105. 335 pp.

Chapter 2

PHYSICAL PROCESSES

2.1 INTRODUCTION

The purpose of this chapter is to give the reader an overview of how the major physical processes are incorporated into water quality and ecosystem simulations. Since a detailed review is beyond the scope of this report, the reader is encouraged to review the articles listed in Table 2-1 which represent several of the more complete and recent reviews of the state-of-the-art in physical process modeling.

Physical processes often simulated in water quality models include flow and circulation patterns, mixing and dispersion, water temperature, and the density distribution (which is a function of temperature, salinity, and suspended solids concentrations) over the water column. It is stressed that quality predictions are very dependent upon the physical processes and how well these are represented in the water quality simulations. Despite this dependence, the modeler often is forced to make a trade-off between acceptable degree of detail in water quality vs. physical process simulation due to cost or other restrictions. It is desirable from the standpoint of both the engineer and ecosystem analyst, therefore, to select the simplest model which satisfies the temporal and spatial resolution required for water quality and/or ecosystem simulation. For example, the optimum time step for dynamic simulation of a fully-mixed impoundment would be 3-6 hours for capturing diurnal fluctuations, and daily or weekly for strongly stratified impoundments which normally exhibit slowly varying conditions. In terms of spatial resolution required, the analyst should take advantage of the possible simplifications of dominate physical characteristics (i.e., physical shape, stratified layers, mixing zones, etc.).

TABLE 2-1. MAJOR REVIEWS OF MODELING STATE-OF-THE-ART

French, R.H. 1983. Lake Modeling: State-of-the-Art. In: CRC Critical Reviews in Environmental Control, Vol. 13, Issue 4, pgs. 311-357.
Harleman, D.R.F. 1982. Hydrothermal Analysis of Lakes and Reservoirs. Journal of the Hydraulics Division, ASCE. Vol. 108, No. HY3, pp. 302-325.
Johnson, B. 1982. A Review of Multi-Dimensional Numerical Modeling of Reservoir Hydrodynamics. U.S. Army Corps of Engineers, Waterways Experiment Station.
Fischer, H.B., List, E.J., Koh, R.C.Y. Imberger, J., and Brooks, N.H. 1979. Mixing in Inland and Coastal Waters. Academic Press, New York.
Hinwood, J.B., and Wallis, I.G. 1975. Review of Models of Tidal Waters. Journal of the Hydraulics Division, ASCE, Vol. 101, No. HY11, Proc. Paper 11693, November, 1975.
Orlob, G.T., ed. 1984. Mathematical Modeling of Water Quality: Streams, Lakes, and Reservoirs. John Wiley and Sons, Wiley-Interscience, N.Y., N.Y.
Elhadi, N., A. Harrington, I. Hill, Y.L. Lau, B.G. Krishnappan. 1984. River Mixing: A State-of-the-Art Report. Canadian Journal of Civil Engineering. Vol. 11, No. 11, pp. 585-609.

2.1.1 Geometric Representation

2.1.1.1 Zero-Dimensional Models

Zero-dimensional models are used to estimate spatially averaged pollutant concentrations at minimum cost. These models predict a concentration field of the form $C = g(t)$, where t represents time. They cannot predict the fluid dynamics of a system, and the representation is usually such that an analytical solution is possible. As an example, the simplest representation of a lake is to consider it as a continuously stirred tank reactor (CSTR).

2.1.1.2 One-Dimensional Models

Most river models use a one-dimensional representation, where the system geometry is formulated conceptually as a linear network of segments or volume sections (see Figure 2-1). Variation of water quality parameters occur longitudinally (in the x-direction) as the water is transported out of one segment and into the next. The one-dimensional approach is also a popular method for simulation of small, deep lakes, where the vertical variation of temperature and other quality parameters is represented by a network of vertically stacked horizontal slices or volume segments.

2.1.1.3 Multi-Dimensional Models

Water quality models of lakes and estuaries are often two- or three-dimensional in order to represent the spatial heterogeneity of the water bodies. Depending on the system, two-dimensional representations include a vertical dimension with longitudinal segmentation for deep and narrow lakes, reservoirs, or estuaries (Figure 2-2).

Three-dimensional spatial representations have been used to model overall lake circulation patterns. Part of the reason for this need is the concern with the water quality of the near-shore zone as well as deep zones of lakes. In addition, the different water quality interactions in these zones can lead to changes in the overall lake quality that cannot be predicted without this spatial definition.

2.1.2 Temporal Variation

Ecological models are distinguished on a temporal basis as being either "dynamic" or "steady-state". A strict steady-state assumption implies that the variables in the system equations do not change with time. Forcing functions, or exogenous variables, that describe environmental conditions which are unaffected by internal conditions of the system, have constant values. Inflows and outflows are discharged to and drawn from the system at

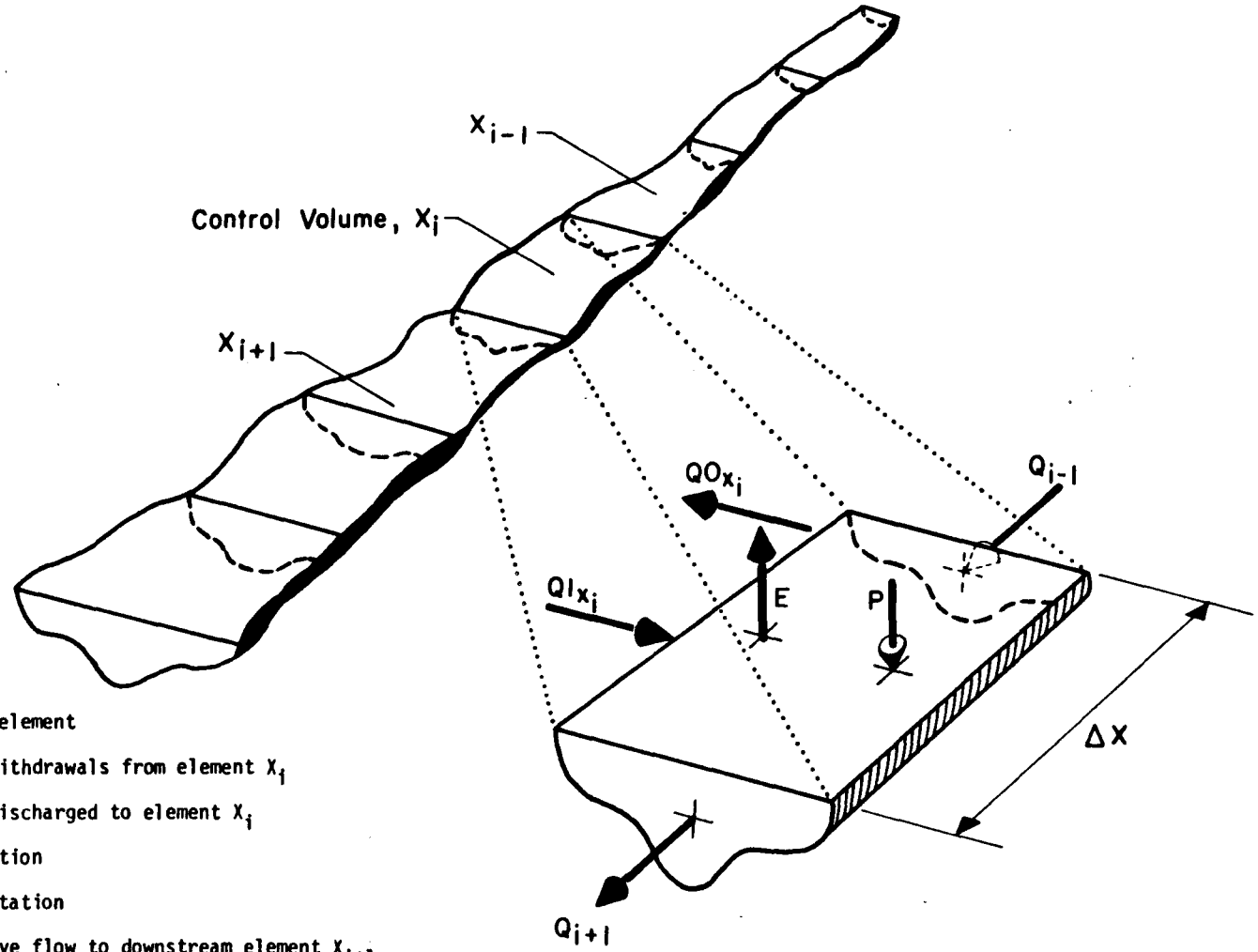

X_i = volume element

QO_{x_i} = water withdrawals from element X_i

QI_{x_i} = water discharged to element X_i

E = evaporation

P = precipitation

Q_{i+1} = advective flow to downstream element X_{i+1}

Q_{i-1} = advective flow from upstream element X_{i-1}

ΔX = longitudinal dimension of element

Figure 2-1. One-dimensional geometric representation for river systems (Chen and Wells, 1975).

a constant rate and any other hydrologic phenomena are also steady. Insolation, light intensity, photoperiods, extinction coefficients, and settling rates are a few examples of additional forcing functions which are held constant in a steady-state model. Constant forcing functions represent mean conditions observed in a system, and therefore the model cannot simulate cyclic phenomena.

A wide variety of planning problems can be analyzed by use of steady-state or quasi-steady (slowly varying) mathematical models which provide the necessary spatial detail for important water quality variables. Certain phenomena can achieve steady-state conditions within a short time interval and therefore can be modeled rather easily. Steady-state or quasi-steady representations are particularly useful because of their simplicity. Examples of phenomena which have been modeled on a steady-state basis are: 1) bacterial die-off, 2) dissolved oxygen concentrations (under certain conditions), and 3) nutrient distribution and recycle.

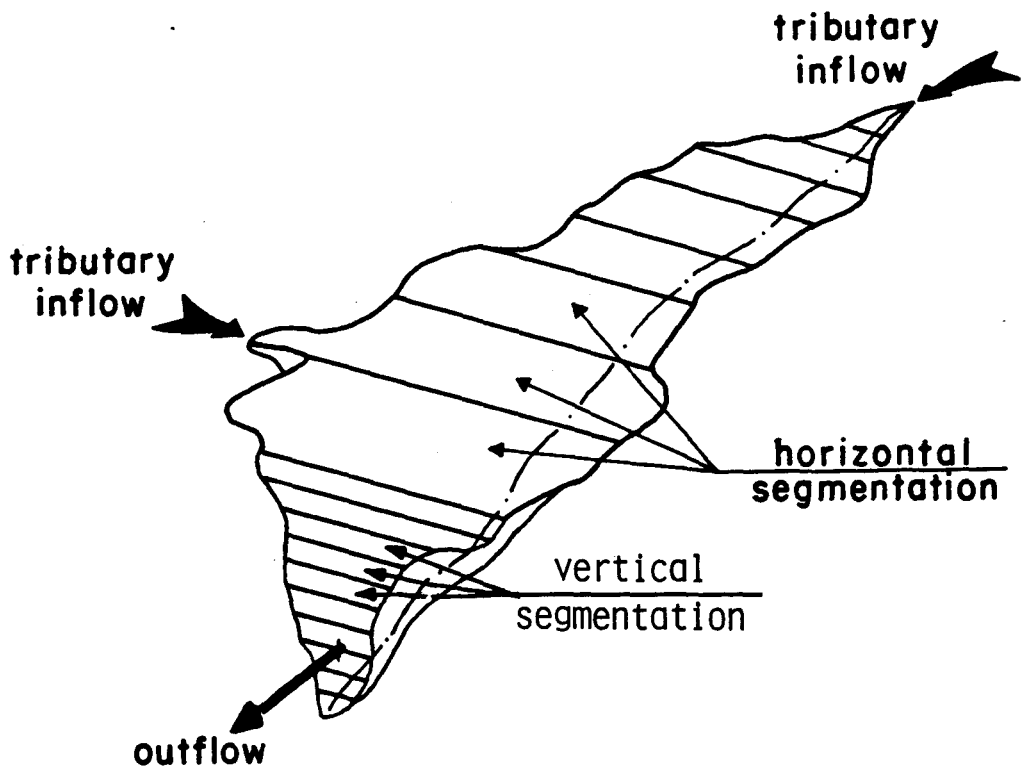

Figure 2-2. Two-dimensional geometric representation for lake systems (Baca and Arnett, 1976).

Many water quality or ecological models for rivers and lakes are concerned with the simulation of water quality variables that have substantial temporal variation and are linked to processes and variables that vary considerably. For example, the seasonal distribution of certain biological species and related abiotic substances may be of major importance. In these instances, dynamic models are required.

The process of selecting the correct time and length scales and then matching these with an appropriate model demands both an a priori understanding of the dominate physical, chemical and biological processes occurring within the system, as well as an understanding of a given model's theoretical basis and practical application limits. Proper guidance for model selection and application best comes from a thorough review of the relevant literature appropriate to the specific problem at hand. Ford and Thornton (1979), for example, present a detailed discussion of the time and length scales appropriate for the vertical one-dimensional modeling approach for reservoirs and lakes. The references presented in Table 2-1 as well as several others cited throughout this chapter discuss model compatibility requirements for various water body types and applications.

The remainder of this chapter focuses on advective transport, dispersive transport, and the surface heat budget.

2.2 ADVECTIVE TRANSPORT

The concentration of a substance at a particular site within a system is continually modified by the physical processes of advection and dispersion which transport fluid constituents from location to location. However, the total amount of a substance in a closed system remains constant unless it is modified by physical, chemical, or biological processes. Employing a Fickian type expression for turbulent mass flux, the three-dimensional advection-diffusion (mass balance) equation can be written as:

$$\frac{\partial c}{\partial t} + \frac{u\partial c}{\partial x} + \frac{v\partial c}{\partial y} + \frac{w\partial c}{\partial z} - \frac{\partial}{\partial x}\left(K_x \frac{\partial c}{\partial x}\right) - \frac{\partial}{\partial y}\left(K_y \frac{\partial c}{\partial y}\right) - \frac{\partial}{\partial z}\left(K_z \frac{\partial c}{\partial z}\right) = \Sigma S \qquad (2\text{-}1)$$

where c = mean concentration of constituent, mass/volume

u = mean velocity in x-direction, length/time

v = mean velocity in y-direction, length/time

w = mean velocity in z-direction, length/time

K_x, K_y, K_z = eddy diffusion coefficients, length^2/time

ΣS = sum of source/sink rates, mass/(volume-time)

t = time

Difficulties exist in trying to correctly quantify the terms in this equation. The unsteady velocity field (u,v,w) is usually evaluated separately from Equation (2-1) so that the pollutant concentration, c, can be prescribed. The complete evaluation of the velocity field involves the simultaneous solution of the momentum, continuity, hydrostatic, and state equations in three dimensions (see Leendertse and Liu, 1975; Hinwood and Wallis, 1975). Although sophisticated hydrodynamic models are available, the detail and expense of applying such models are often not justified in water quality computations, especially for long term or steady-state simulations where only average flow values are required. For example, the annual thermal cycle for a strongly stratified reservoir with a relatively low inflow to volume ratio has been successfully simulated with only a crude one-dimensional, steady-state application of mass and energy conservation principles. On the other hand, simulation of large, weakly stratified impoundments dominated by wind driven circulation may require the ultimate, full representation of the unsteady velocity field in three dimensions.

The purpose of this section is to briefly familiarize the reader with the various types of approaches used to evaluate the velocity field in water quality models. Most hydrodynamic models internally calculate hydrodynamics with relatively little user control except for specification of forcing conditions such as wind, tides, inflows, outflows and bottom friction. Thus, the following paragraphs present only a summary discussion of the approaches used, organized according to the dimensional treatment of the model.

2.2.1 Empirical Specification of Advection

This is the crudest approach, in that the advective terms of the advection-diffusion equation (Equation 2-1) are directly specified from field data. Empirical specification is quite common in water quality models for rivers, but is also often used in steady-state or slowly-varying estuary water quality models (e.g., O'Connor et al. (1973)). In these types of estuary models, specification of the dispersion coefficients is critical since dispersion must account for the mixing which in reality is caused by the oscillatory tidal action. Due to the highly empirical treatment of the physical processes in such models, the model "predictions" remain valid for only those conditions measured in the field. These models cannot predict water quality variations under other conditions, thus increasing the demand on field data requirements. Examples of models representative of the above approach include O'Connor et al. (1973) and Tetra Tech (1977).

2.2.2 Zero Dimensional Models for Lakes

A coarse representation of the water system as a continuously stirred tank reactor (CSTR) is often sufficient for problem applications to some lakes where detailed hydrodynamics are not required. Since in this zero-dimensional type of representation there is only a single element, no transport direction can be specified. The quantity of flow entering and leaving the system alone determines water volume changes within the element. Examples of zero-dimensional models include lake models by Anderson et al. (1976).

2.2.3 One-Dimensional Models for Lakes

For lake systems with long residence times and stratification in the vertical direction, vertical one-dimensional representations are common. Horizontal layers are imposed and advective transport is assumed to occur only in the vertical direction.

Generally the tributary inflows and outflows are assumed to enter and leave the lake at water levels of equal density. Since water is essentially incompressible the inflow is assumed to generate vertical advective flow (via the continuity equation) between all elements above the level of entry. The elements below this level, containing higher density water, are assumed to be unaffected. Examples of one-dimensional lake models include Lombardo (1972, 1973), Baca et al. (1974), Chen and Orlob (1975), Thomann et al. (1975), Imberger et al. (1977), HEC (1974), Markofsky and Harleman (1973), and CE-QUAL-R1 (1982).

For lake or reservoir systems exhibiting complex horizontal interflows, inflows, and outflows, semi-empirical formulations have been developed to distribute inflows and to determine the vertical location from which outflows arise, depending on stratification conditions. Examples include models by U.S. Army Corps of Engineers (1974), Baca et al. (1976), and Tetra Tech (1976).

2.2.4 One-Dimensional Models for Rivers

Most river models represent river systems conceptually as horizontal linear networks of segments or volume elements. The process of advection is assumed to transport a constituent horizontally by movement of the parcel of water containing the constituent. In general, there are two approaches to treat the advection in river models. One approach requires field calibration of the river flow properties by measuring flows and cross sectional geometry at each model segment over a range of flow magnitudes. A power series can then be developed for each cross section to interpolate or extrapolate for other flow events. Such an approach is especially appropriate for rivers exhibiting complex hydraulic properties (i.e., supercritical flows, cascades, etc.) and when steady state solutions are of interest. Examples of such models include Tetra Tech (1977).

A second, more rigorous approach for simulating river advection involves the simultaneous solution of the continuity and momentum equations for the portion of the river under study. This approach is considered more

"predictive" than the former since empirical flow data are required only for model calibration and verification. It is also more accurate and appropriate for use in transient water quality simulations. In either case, however, geometrical data on the cross-sectional shapes of the river are required. Examples of models representative of the latter approach include Brocard and Harleman (1976), and Peterson et al. (1973).

2.2.5 One-Dimensional and Pseudo-Two-Dimensional Models for Estuaries

A natural extension of the one-dimensional river model has been to estuary systems, either as a one-dimensional representation for narrow estuaries or as a system of multiple interconnecting one-dimensional channels for pseudo-representation of wider or multi-channeled estuaries. In either case, advection is determined through the simultaneous solution of the continuity and momentum equations together with appropriate tidal boundary conditions. These types of models are generally quite flexible in their ability to handle multiple inflows, transient boundary conditions, and complex geometrical configurations. Two primary approaches include the "link-node" network models by Water Resources Engineers (WRE) (1972), and the finite element model (Galerkin Method) by Harleman et al. (1977).

2.2.6 Two-Dimensional Vertically Averaged Models for Lakes and Estuaries

Vertically averaged, two-dimensional models have proven to be quite useful, especially in modeling the hydrodynamics and water quality of relatively shallow estuaries and wind-driven lakes. The crucial assumption of these models is the vertically well-mixed layer that allows for vertical integration of the continuity, momentum, and mass-transport equations. Such models are frequently employed to provide the horizontal advection for water quality models since they are relatively inexpensive to operate compared to the alternatives of large scale field measurement programs or fully three-dimensional model treatments. There exist well over fifty models which would fit into the two-dimensional, vertically averaged classification. Examples of models that have been widely used and publicized include Wang and Connor (1975), Leendertse (1970), Taylor and Pagenkopf (1980), and Simons (1976).

2.2.7 Two-Dimensional Laterally Averaged Models for Reservoirs and Estuaries

In recent years, laterally averaged models have become standard simulation techniques for reservoirs or estuaries which exhibit significant vertical and longitudinal variations in density and water quality conditions. The two-dimensional laterally averaged models require the assumption of uniform lateral mixing in the cross channel direction. Although this simplification eliminates one horizontal dimension, the solution of the motion equations in the remaining longitudinal and vertical dimensions requires a much more rigorous approach than for the two-dimensional vertically averaged models. In order to correctly simulate the vertical effects of density gradients on the hydrodynamics and mass transport, both the motion (continuity and momentum) and advective-diffusion equations must be solved simultaneously. In addition, such models must also treat the vertical eddy viscosity (momentum transfer due to velocity gradients) and eddy diffusivity (mass transfer due to concentration gradients) coefficients, which are directly related to the degree of internal mixing and the density structure over the water column. Mathematical treatment of vertical diffusion and vertical momentum transfer varies greatly between models, and will be discussed further in this document. Examples of laterally averaged reservoir models include Edinger and Buchak (1979) and Norton *et al*. (1973). Examples of laterally averaged models developed for estuaries include Blumberg (1977), Najarian *et al*. (1982) and Wang (1979).

2.2.8 Three-dimensional Models for Lakes and Estuaries

Fully three-dimensional and layered models have been the subject of considerable attention over the last decade. Although still a developing field, there are a number of models which have been applied to estuary, ocean, and lake systems with moderate success. As with laterally averaged two-dimensional models, the main technical difficulty in this approach is in the specification of the internal turbulent momentum transfer and mass diffusivities, which are ideally calibrated with field

observations, thus making availability of adequate prototype data an important consideration. An additional factor of great importance is the relatively large computation cost of running three-dimensional models, especially for long-term water quality simulations. In many cases, the effort and cost of running such models is difficult to justify from purely a water quality standpoint. However, as computational costs continue to decrease and sophistication of numerical techniques increases, such models will eventually play an important role in supplying the large scale hydrodynamic regimes in water quality simulations. Examples of the more prominent three-dimensional models include Blumberg and Mellor (1978), Leendertse and Liu (1975), Sheng and Butler (1982), Simons (1976) and King (1982).

2.3 DISPERSIVE TRANSPORT

2.3.1 Introduction

The purpose of this section is to show how dispersive transport terms are incorporated into the equations of motion and continuity by temporal and spatial averaging (a detailed discussion of this subject is also given by Fischer *et al.* (1979)). A consequence of temporal averaging of either instantaneous velocity or concentration is to produce a smoothed velocity or concentration response curve over time. Figure 2-3 illustrates both instantaneous velocity and time-smoothed curves. The velocities V and $\overline{V}$ are related by

$$V = \overline{V} + V' \tag{2-2}$$

where V = instantaneous velocity, length/time
$\overline{V}$ = time-smoothed velocity, length/time
V' = velocity deviation from the time-smoothed velocity, length/time

The velocity component V' is a random component of velocity which vanishes when averaged over the appropriate time interval (i.e., $\overline{V'} = 0$).

By averaging, the stochastic components are removed from the momentum and mass conservation equations. However, cross product terms appear in the equations, such as $\overline{V_x'V_x'}$ and $\overline{V_x'V_y'}$ in the case of the momentum equation, and $\overline{V_x'C'}$ and $\overline{V_y'C'}$ in the case of the mass conservation equation (where C' is the instantaneous concentration fluctuation, and V_x' and V_y' are the random velocity deviations in the x and y directions, respectively). In the case of the momentum equation these terms are called turbulent momentum fluxes, and in the case of the mass conservation equation they are called turbulent mass fluxes. It is through these terms that eddy viscosity and eddy diffusivity enter into the momentum and mass conservation equations.

To solve the time-smoothed equations, the time averaged cross product terms are expressed as functions of time averaged variables. Numerous empirical expressions have been developed to do this. The expressions most often applied are analogous to Newton's law of viscosity in the case of turbulent momentum transport and Fick's law of diffusion in the case of turbulent mass transfer. Expressed quantitatively these relationships are of the form:

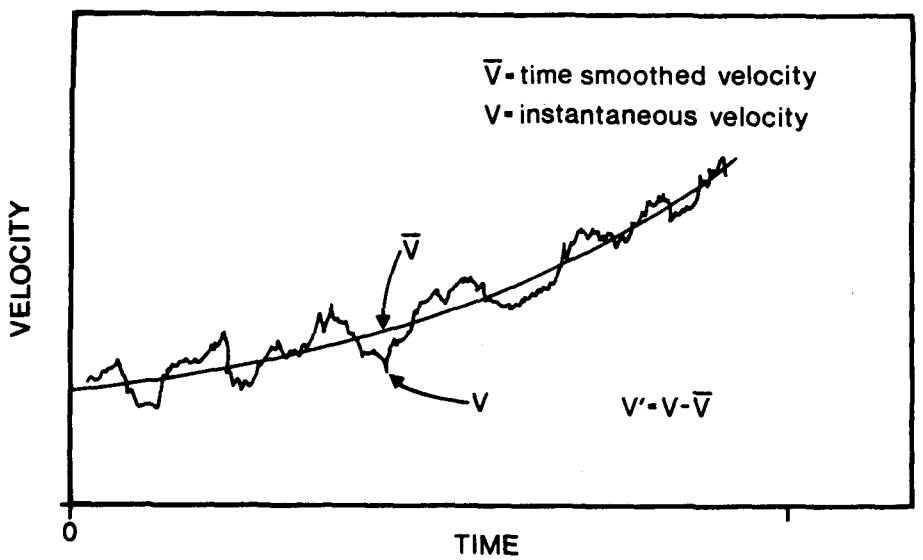

Figure 2-3. Oscillation of velocity component about a mean value (redrawn after Bird et al., 1960).

$$\overline{\rho V_x' V_y'} = E \frac{\partial \overline{V}_x}{\partial y} \tag{2-3}$$

$$\overline{V_y' C'} = K \frac{\partial \overline{C}}{\partial y} \tag{2-4}$$

where E = eddy viscosity, mass/(length-time)

K = eddy diffusivity, length^2/time

$\overline{V}_x$ = time smoothed velocity in the x direction, length/time

$\overline{C}$ = time smoothed concentration, mass/volume

ρ = mass density, mass/volume

In natural water bodies the turbulent viscosity and diffusivity given by Equations (2-3) and (2-4) swamp their counterparts on the molecular level. The relative magnitude between eddy diffusivities and molecular diffusion coefficients is depicted graphically in Figure 2-4.

In addition to temporal averaging, spatial averaging is often used to simplify three dimensional models to two or one dimensions. As an illustration consider the vertically averaged mass transport equation. Before averaging, the governing three dimensional mass transport equation is typically written as:

$$\frac{\partial c}{\partial t} + \frac{\partial (uc)}{\partial x} + \frac{\partial (vc)}{\partial y} + \frac{\partial (wc)}{\partial z} = \frac{\partial}{\partial x}(Q_x) - \frac{\partial}{\partial y}(Q_y) - \frac{\partial}{\partial z}(Q_z) \tag{2-5}$$

where c = the local (time smoothed) concentration, mass/volume

u,v,w = the local (time smoothed) water velocities, length/time

Q_x, Q_y, Q_z = the local diffusive fluxes, mass/(length^2-time)

Before spatial averaging, the local concentration and velocities can be expressed by a vertically averaged term and a deviation term:

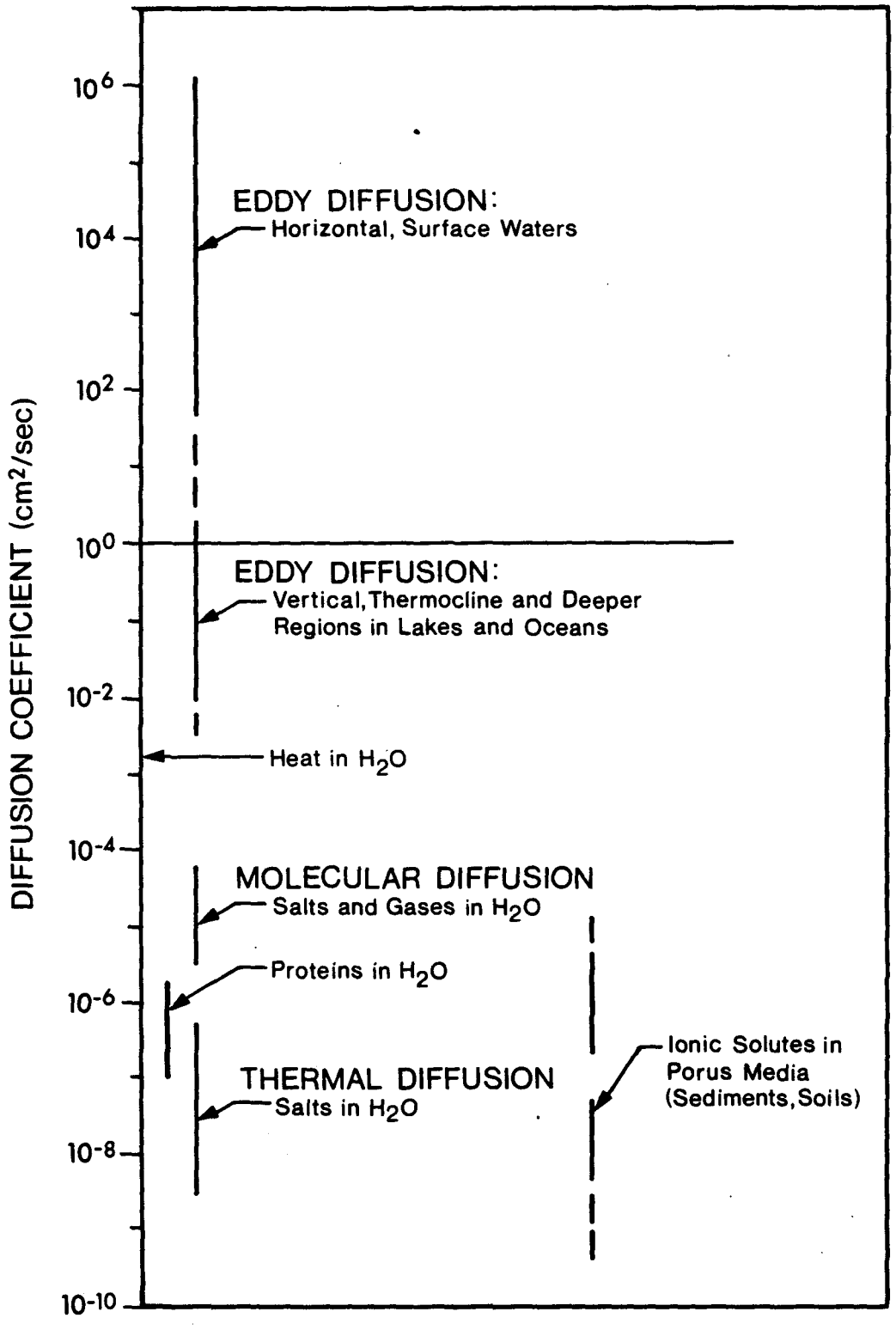

Figure 2-4. Diffusion coefficients characteristic of various environments (redrawn after Lerman, 1971).

$$c = c_h + c_h'$$
$$u = u_h + u_h'$$
$$v = v_h + v_h' \qquad (2\text{-}6)$$

where c, u, v = previously defined

c_h = vertically averaged concentration, mass/volume

$$= \frac{1}{h} \int_0^h c\,dz \qquad (2\text{-}7)$$

c_h' = deviation from c_h at any point in the water column, mass/volume

u_h, v_h = vertically averaged water velocities, length/time

$$= \int_0^h u\,dz, \quad \int_0^h v\,dz \qquad (2\text{-}8)$$

u_h', v_h' = deviation from u_h, v_h at any point in the water column, length/time

h = local water depth, length

Equation (2-5) can now be written in its vertically averaged form:

$$\frac{\partial c_h}{\partial t} + \frac{\partial (u_h c_h)}{\partial x} + \frac{\partial (v_h c_h)}{\partial y} = -\frac{\partial}{\partial x} \int_0^h (Q_x + u_h' c_h')\,dz - \frac{\partial}{\partial y} \int_0^h (Q_y + v_h' c_h')\,dz \qquad (2\text{-}9)$$

It is noted that when vertical integration is performed on the three-dimensional mass conservation equation, cross product terms appear in the resulting two-dimensional equation, just as they do when temporal averaging is done because vertical gradients generally exist in <u>both</u> the concentration and velocity fields. The horizontal turbulent diffusion fluxes Q_x, Q_y are usually expressed in terms of the gradients of the vertically averaged concentration and the turbulent diffusion coefficient, which in general form are written:

$$Q_x = -\varepsilon_{xx} \frac{\partial c_h}{\partial x} - \varepsilon_{xy} \frac{\partial c_h}{\partial y} \tag{2-10a}$$

$$Q_y = -\varepsilon_{yx} \frac{\partial c_h}{\partial x} - \varepsilon_{yy} \frac{\partial c_h}{\partial y} \tag{2-10b}$$

where ε_{xx}, ε_{xy}, ε_{yx}, ε_{yy} = turbulent eddy diffusion coefficients

By analogy, the horizontal transport terms, $u_h'c_h'$ and $v_h'c_h'$, associated with vertical velocity variations (i.e., differential advection), are expressed by means of the shear dispersion coefficients:

$$u_h'c_h' = -E_{xx}^d \frac{\partial c_h}{\partial x} - E_{xy}^d \frac{\partial c_h}{\partial y} \tag{2-11a}$$

$$v_h'c_h' = -E_{yx}^d \frac{\partial c_h}{\partial x} - E_{yy}^d \frac{\partial c_h}{\partial y} \tag{2-11b}$$

where $E_{xx}^d, E_{xy}^d, E_{yx}^d, E_{yy}^d$ = shear dispersion coefficients

By combining Equations (2-10) and (2-11), the final form of the vertically averaged mass transport equation can be written as:

$$\frac{\partial c_h}{\partial t} + \frac{\partial (u_h c_h)}{\partial x} + \frac{\partial (v_h c_h)}{\partial y} = \frac{\partial}{\partial x}\left(D_{xx} h \frac{\partial c_h}{\partial x} + D_{xy} h \frac{\partial c_h}{\partial y}\right)$$

$$\frac{\partial}{\partial y}\left(D_{xy} h \frac{\partial c_h}{\partial x} + D_{yy} h \frac{\partial c_h}{\partial y}\right) \tag{2-12}$$

where D_{xx}, D_{xy}, D_{yy} = dispersion coefficients which account for mass transport due to both concentration and velocity gradients over the vertical.

One-dimensional mass conservation equations result when a second spatial averaging is performed. The one-dimensional equations express changes along the main flow axis. As expected, the diffusion terms are again different from their two-dimensional counterparts. Consequently, the type and magnitude of the diffusion terms appearing in the simulation

equations depends not only on the water body characteristics, but the model used to simulate the water body.

2.3.2 Vertical Dispersive Transport

Vertical dispersive transport of momentum and mass becomes important in lakes or estuaries characterized by moderate to great depths. In a lake environment, vertical mixing is generally caused by wind action on the surface through which eddy turbulence is transmitted to the deeper layers by the action of shear stresses. In estuaries, typically the vertical mixing is induced by the internal turbulence driven by the tidal flows, in addition to surface wind effects. Similarly, the internal mixing in deep reservoirs is primarily caused by the flow-through action. In each environment, however, the amount of vertical mixing is controlled, to a large extent, by the degree of density stratification in the water body.

Treatment of vertical mixing processes in mathematical models is generally achieved through the specification of vertical eddy viscosity (E_v) and eddy diffusivity (K_v) terms, as previously discussed. As observed by McCutcheon (1983), however, there is little consensus on what values the vertical eddy coefficients should have and how eddy viscosity and eddy diffusivity are related. At present, the procedure for estimating these coefficients is generally limited to empirical techniques that range from specifying a constant E_v and K_v to relating to some measure of stability, i.e., the Richardson number Ri. In this approach, the ratio of the coefficients for stratified flow to the coefficients for unstratified flow is expressed as a function of stability f(s):

$$E_v/E_{vo} = f_1(s), \tag{2-13}$$

$$K_v/K_{vo} = f_2(s), \tag{2-14}$$

$$\text{and} \quad E_{vo} = Pr\ K_{vo} \tag{2-15}$$

where $E_{vo} = kzu_*(1 - z/h)$ for shear layers and Pr = the Prandtl or Schmidt number, which is generally close to unity for open-channel shear flow (Watanabe et al., 1984).

In addition

k = von Karman's constant (~0.4), dimensionless
z = distance above the bottom, length
u_* = shear velocity, length/time
h = depth of flow, length

A widely used formula which relates E_v/E_{vo} to stability involves the Munk and Anderson (1948) formulation (as reported by McCutcheon (1983)):

$$E_v/E_{vo} = (1 + 10\ Ri)^{-1/2} \tag{2-16}$$

and

$$K_v/K_{vo} = (1 + 3.33\ Ri)^{-3/2} \tag{2-17}$$

where $Ri = \frac{g}{\rho}\frac{\partial\rho}{\partial z}\Big/\left(\frac{\partial u}{\partial z}\right)^2$, dimensionless (2-18)

ρ = density, mass/volume
u = the mean horizontal velocity at a point z above the bottom, length/time
g = acceleration of gravity, length/time^2

As reported by McCutcheon (1983), in a recent review of available data for stratified water flows (Delft, 1979) Equations (2-16) and (2-17) were found to fit the data better than several other similar formulations. Models by Waldrop (1978), Harper and Waldrop (1981), Edinger and Buchak (1979), O'Connor and Lung (1981), Najarian et al. (1982), and Heinrich, Lick and Paul (1981) use this scheme. In some models, the coefficients and exponents in Equation (2-16) and (2-17) are not adjusted, and any discrepancies between field measurements and model predictions are attributed to the inexactness of the model. In other models, the coefficients and exponents are calibrated on a site specific basis.

For model simulations of mixing through and below the thermocline, the Munk and Anderson type formulas appear to be less adequate (McCutcheon, 1983). Odd and Rodger (1978) developed site specific eddy viscosity formulations for the Great Ouse Estuary in Britain:

$$E_v/E_{vo} = (1 + bRi)^{-n} \quad \text{for } Ri \leq 1 \tag{2-19}$$

and

$$E_v/E_{vo} = (1 + b)^{-n} \quad \text{for } Ri > 1 \tag{2-20}$$

where b and n are coefficients. The depth varying Ri is used if Ri increases continuously starting at the bed and extending over 75 percent or more of the depth. Where a significant peak in Ri occurs in the vertical gradient, that peak Ri is used for all depths in the equation above. McCormick and Scavia (1981) make a correction for K_v in Lake Ontario and Lake Washington studies that is similar to corrections of E_v by Odd and Rodger. Above the hypolimnion, they apply a modification of the Kent and Pritchard (1959) equation:

$$K_v = u_*/\beta R_o \tag{2-21}$$

where $R_o = -kz^2 \frac{g}{\rho} \frac{\partial \rho}{\partial z} / u_*^2$ (2-22)

β = constant

Below the thermocline a constant K_v was specified for Lake Ontario. In Lake Washington, Equation (2-21) and (2-22) were applied throughout the depth. In Lake Washington bottom shear was important for mixing as opposed to deeper Lake Ontario where surface wind shear dominated the mixing process.

Several other formulations for E_v and K_v have been developed which are not based on the Munk and Anderson equations. For example, Blumberg (1977), in his laterally averaged model of the Potomac River Estuary, employed an expression for K_v which uses a ratio of Ri to a critical Ri to relate K_v to stability, where:

$$K_v = K_1^2 z^2 \left(\frac{1-z}{h}\right)^2 \left|\frac{u}{z}\right| \left(1 - \frac{Ri}{Ri_c}\right)^{1/2} \qquad (2\text{-}23)$$

where K_1 is a turbulence constant which must be determined by calibration, and Ri_c is the critical Richardson number, which is the value of Ri at which mixing ceases due to strong stratification. Blumberg also related E_v to K_v through the following formulation:

$$E_v = K_v (1 + Ri) \qquad \text{for } 0 < Ri < Ri_c \qquad (2\text{-}24a)$$

$$E_v = K_v = 0 \qquad \text{for } Ri \geq Ri_c \qquad (2\text{-}24b)$$

Using the above formulations, Blumberg obtained reasonably good comparisons for salinity distributions in the Potomac River.

Simons (1973) based his formulation for K_v for Lake Ontario on the results of dye diffusion experiments performed by Kullenberg et al. (1973) where K_v is expressed as:

$$K_v = C \frac{W^2}{N^2} \left|\frac{\partial q}{\partial z}\right| \qquad (2\text{-}25)$$

where C = an empirical constant, $(2 \sim 8)10^{-8}$
W = wind speed, length/time
N^2 = Brunt-Väisälä frequency, $\frac{g}{\rho}\frac{\partial \rho}{\partial z}$, time^{-2}
$\frac{\partial q}{\partial z}$ = vertical shear of the current, time^{-1}

Simons also assumed that the vertical eddy viscosity coefficient was based on a similar relationship.

The above formulation is a result of experiments performed in fjords, coastal and open sea areas, as well as from Lake Ontario, and is generally valid for expressing the vertical mixing in the upper 20 m for persistent winds above 4-5 m/sec. The lower value of the numerical constant refers to the lake data and the higher value to the oceanic data.

For low and varying wind speeds Equation (2-25) will not be valid (Murthy and Okubo, 1975). In these cases the internal mixing is considered to be governed by local processes, i.e., the energy source is the kinetic energy fluctuations. Kullenberg (as reported by Murthy and Okubo (1975)) proposed the following relation for weak local winds:

$$K_v = 4.1\text{x}10^{-4}\ q'^2 (N^2)^{-1}\ \left|\frac{\partial q}{\partial z}\right| \tag{2-26}$$

where $q'^2 \equiv V_x'^2 + V_y'^2$

V_x', V_y' = velocity fluctuations in the x and y directions, respectively, length/time

Equation (2-26) is representative of the vertical mixing both above and below the thermocline under conditions of low wind speeds.

Tetra Tech (1975) has used the following empirical expressions for computation of the vertical eddy thermal diffusivity, K_v, in their three-dimensional hydrodynamic simulation of Lake Ontario.

$$K_v = 100\,\frac{|\tau_s|}{\rho_0}\left(\frac{3}{1+3.3Ri}\right)^{\frac{1}{2}} \tag{2-27}$$

where ρ_0 = density of fresh water at 4^oC, mass/volume
τ_s = surface wind stress, mass/(length-time^2).

Lake systems that are represented geometrically as a series of completely mixed horizontal slices consider advective and dispersive transport processes to occur in the vertical direction alone. Baca and Arnett (1976), in their one-dimensional hydrothermal lake model, proposed the following expression for determining the one-dimensional vertical dispersion coefficient:

$$K_v = a_1 + a_2\ V_w\ d^{-4.6z/d} \tag{2-28}$$

where K_v = vertical dispersion coefficient, m^2/sec

z = depth, m

V_w = wind speed, m/sec

d = depth of thermocline, m

a_1, a_2 = empirical constants, m^2/sec and m respectively

The following table of values (Table 2-2) for a_1 and a_2, as given by Baca and Arnett (1976), were obtained from previous model applications.

TABLE 2-2. VALUES FOR EMPIRICAL COEFFICIENTS a_1 and a_2

Lake	Description	Max. Depth (m)	a_1 (m^2/sec)	a_2 (m)
American Falls	well-mixed	18	1×10^{-5}	1×10^{-4}
Lake Washington	stratified	65	1×10^{-6}	1×10^{-5}
Lake Mendota	stratified	24	5×10^{-7}	5×10^{-5}
Lake Wingra	well-mixed	5	5×10^{-5}	2×10^{-4}
Long Lake	linearly stratified	54	5×10^{-6}	5×10^{-5}

The vertical eddy viscosity and eddy diffusivity concepts continue to be practical and are a popular means for simplifications of the momentum and mass conservation equations. As pointed out by Sheng and Butler (1982) and McCutcheon (1983), however, a wide variety exists among the various forms of the vertical turbulence stability functions determined empirically by various investigators, and suggest that the appropriate stability function is dependent on the type of numerical scheme used and the nature of the water body under study. The wide variation in formulations is, in part, due to the attempt to fit empirical functions determined under specific field conditions to a wider range of water body types and internal mixing phenomena. Due to the possibility of applying an empirical relationship

beyond its valid limits, site-specific testing of formulations for E_v and K_v will probably be required in most model applications.

The above discussion has concentrated on the eddy diffusion concept on which many models are based. However, an alternative to this approach is the mixed layer concept which has been successfully applied by numerous investigators to predict the vertical temperature regime of lakes and reservoirs. As summarized by Harleman (1982), the mixed layer or integral energy concept involves the following: the turbulent kinetic energy (TKE) generated by the surface wind stress is transported downward and acts to mix the upper water column layer. At the interface between the upper mixed layer and the lower quiescent layer, the remaining TKE, plus any that may be locally generated by interfacial shear (minus dissipation effects), is transferred into potential energy by entraining quiescent fluid from below the interface into the mixed layer. This entrainment, in addition to any vertical advective flows, determines the thickness of the mixed layer. TKE is also produced by convective currents which occur during periods of cooling, and can contribute to the mixing process. Also, the total vertical heat balance due to surface heat flux and internal absorption must be considered in evaluating the vertical density distribution and potential energy of the water column. A discussion of the mixed layer model approach can be found in Harleman (1982), French (1983) and Ford and Stefan (1980). Models based on this approach include those by Stefan and Ford (1980), Hurley-Octavio et al. (1977), Imberger et al. (1977) and CE-QUAL-R1 (1982).

2.3.3 Horizontal Eddy Diffusive Transport

Generally, horizontal eddy diffusivity is several orders of magnitude greater than the vertical eddy diffusivity (see Figure 2-4). The Journal of the Fisheries Research Board of Canada (Lam and Jacquet, 1976) reported a range of values for the horizontal diffusivity in lakes from 10^4 to 10^6 cm^2/sec. Unlike diffusive transport in open-channel type flows, diffusion in open water, such as in lakes and oceanic regimes, cannot be effectively related to the mean flow characteristics (Watanabe et al., 1984). Oceanic or lake turbulence represents a spectrum of different eddies resulting from

the breakdown of large-scale circulations in shore zones and by wind and wave induced circulations. Attempts to analyze this phenomenon have demonstrated that the horizontal diffusive transport, D_h depends on the length scale L of the phenomenon. The most widely used formula is the four-thirds power law:

$$D_h = A_D L^{4/3} \tag{2-29}$$

where A_D is the dissipation parameter (of the order .005, with D_h in cm^2/sec). The length scale L is loosely defined depending on the nature of the diffusion phenomenon. For a waste discharge in the ocean, for example, L is often estimated based on the diffuser length, which is typically the order of a kilometer. Another example is to estimate L based on the length of the tidal excursion in estuaries or coastal areas. When using Equation (2-29) to estimate the diffusion coefficient in two or three-dimensional numerical models, the length scale is often taken as the size of the horizontal grid spacing, since this approximates the minimum scale of eddies which can be reproduced in the model.

Useful summaries of lake and ocean diffusion data are given by Yudelson (1967), Okubo (1968) and Osmidov (1968). Okubo and Osmidov (1970) have graphed the empirical relationship between the horizontal eddy diffusivity and the length scale, as shown in Figure 2-5. According to Figure 2-5:

$$\begin{aligned} D_h &\approx 2 \times 10^{-3}\, L^{4/3} && \text{for } L < 10^5 \text{cm} \\ D_h &\approx 10^4 && \text{for } 10^5 < L < 5 \times 10^5 \text{ cm} \\ D_h &\approx 10^{-3}\, L^{4/3} && \text{for } L > 5 \times 10^5 \text{ cm} \end{aligned} \tag{2-30}$$

where D_h is in cm^2/sec and L in cm. Based on these empirical observations, it is seen that the dissipation parameter of the four-thirds law decreases at larger length scales.

A comprehensive collection of diffusion data in the ocean was presented by Okubo (1971), who proposed as best fit to all the data the relation:

$$D_h = 0.01L^{1.15} \qquad \text{for } 10^3 \leq L \leq 10^8 \text{ cm} \qquad (2\text{-}31)$$

which is graphed in Figure 2-6. According to Christodoulou et al. (1976), the four-thirds law seems theoretically and experimentally acceptable for expressing the horizontal eddy diffusivity in large lakes and in the ocean, providing the length scales of interest are not of the order of the size of the energy containing eddies. In addition, the four-thirds law is not fully acceptable near the shore, due to the shoreline and bottom interference.

Two examples of the use of Equation (2-29) in lake models are in Lam and Jacquet (1976) and Lick et al. (1976). Lam and Jacquet obtained the following formulation for the horizontal eddy diffusivity for lakes, based on experimental results:

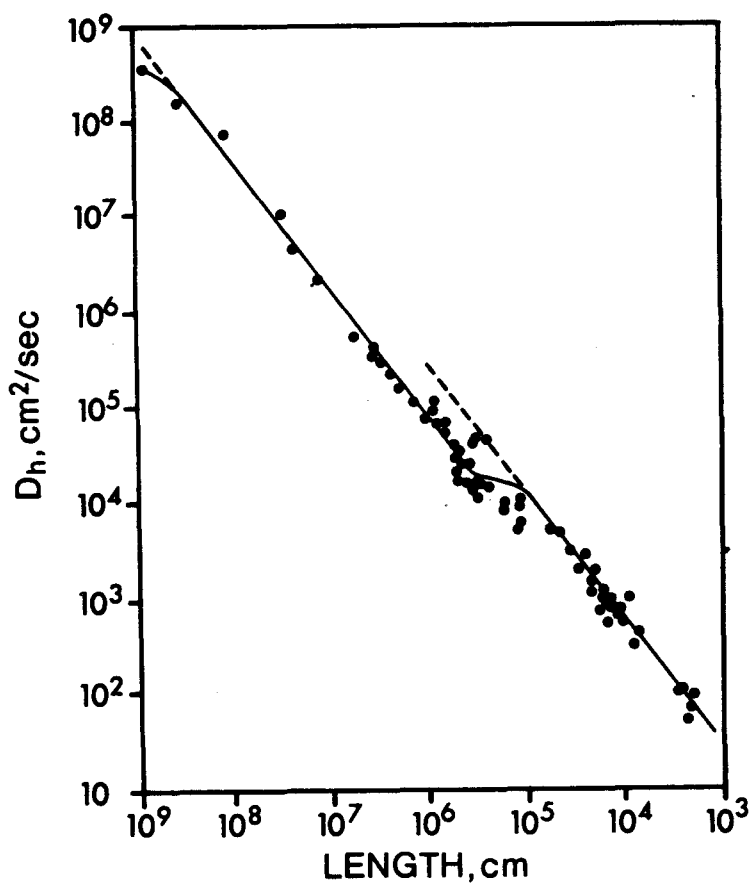

Figure 2-5. Dependence of the horizontal diffusion coefficient on the scale of the phenomenon (after Okubo and Osmidov (1970)).

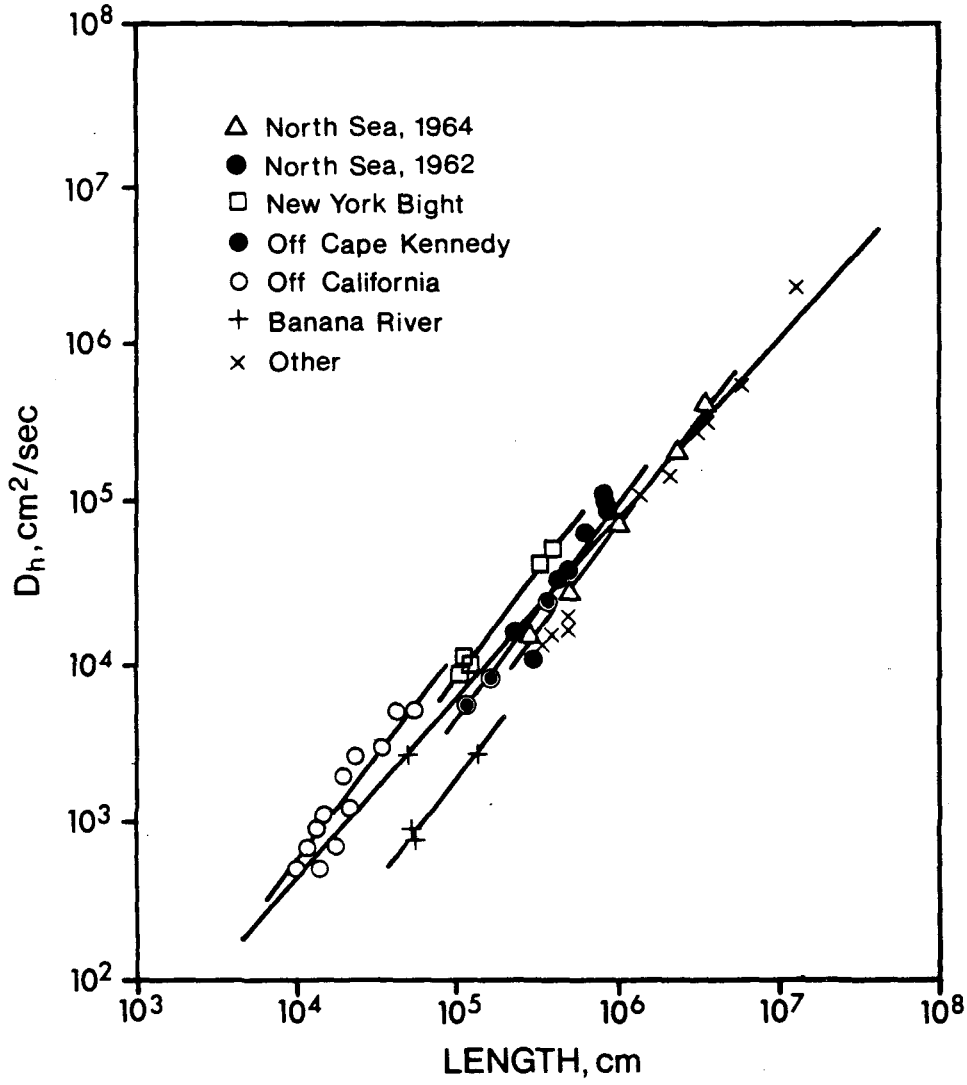

Figure 2-6. Okubo's diffusion data and 4/3 power lines (after Okubo (1971)).

$$D_h = .0056L^{1.3} \tag{2-32}$$

where D_h = horizontal eddy diffusivity, cm^2/sec
L = length scale of grid, cm

As reported by Lam and Jacquet, for a grid size larger than 20 km, the diffusivity is expected to be essentially constant (10^6 cm^2/sec).

Lick (1976) used a similar formulation after Osmidov (1968), Stommel (1949), Orlob (1959), Okubo (1971) and Csanady (1973):

$$D_h = a\ E^{1/3}\ L^{4/3} \tag{2-33}$$

where a = constant of proportionality, of the order 0.1

E = rate of energy dissipation per unit mass

Observations by Lick indicated values of 10^4 to 10^5 cm^2/sec for D_h for the overall circulation in the Great Lakes with smaller values indicated in the near-shore regions.

The above relationships can be used as a general guide to evaluate the horizontal diffusivities in a numerical model, where the grid size may be regarded as the approximate length scale of diffusion. However, as pointed out by Murthy and Okubo (1977): (1) the data upon which these empirical relations are obtained do not represent diffusion under severe weather conditions, and thus may include a bias towards relatively mild conditions; (2) the horizontal diffusivity can vary (depending primarily upon the environmental conditions) by an order of magnitude for the same length scale of diffusion; (3) the definition of the length scale of diffusion for the horizontal diffusivity is somewhat arbitrary; and (4) the horizontal diffusivity varies by an order of magnitude between the upper and lower layers of oceans and deep lakes. Thus, to develop reliable three-dimensional models the scale and stability dependence of eddy diffusivities and the large variability of the magnitude of the eddy diffusivity with depth and environmental factors (wind, waves, inflows, etc.) must somehow be incorporated into the models.

The formulations for horizontal eddy diffusivity discussed above are generally representative of empirical (physical) diffusion behavior and are most compatible with a three-dimensional approach. As previously discussed, horizontal dispersion is the "effective diffusion" that occurs in two-dimensional mass transport equations that have been integrated over the depth. Thus the horizontal dispersion must account for both horizontal eddy diffusivity due to horizontal turbulence and concentration gradients, as well as the effective spreading caused by velocity and concentration variations over the vertical. In addition, any simplifications in the

velocity field used in modeling must also be accounted for in the dispersion coefficients. The less detailed the flow field is modeled, the larger the dispersion coefficient needs to be to provide for the spreading that would occur under the actual circulation (Christodoulou and Pearce, 1975). Therefore, the dispersion coefficients are characteristic not only of the flow conditions to be simulated, but more significantly of the way the process is modeled. Hence these coefficients are model-dependent and difficult to quantify in any general, theoretical manner. For example, many two-dimensional models use a constant dispersion coefficient over the whole model domain as well as over time despite the fact that dispersion changes both spatially and temporally as the circulation features change. An example of a model that uses constant dispersion coefficients is Christodoulou et al. (1976).

One two-dimensional model which utilizes variable dispersion coefficients (velocity dependent) in time and space is the finite difference model by Taylor and Pagenkopf (1981). They utilize Elder's (1959) relationship for anisotropic flow where the dispersion of a substance is proportional to the friction velocity, u_*, and the water depth, h, as follows:

$$D_r = 5.9\, u_* h \tag{2-34}$$

$$D_n = 0.2\, u_* h \tag{2-35}$$

where D_r = dispersion coefficient along the flow axis, length^2/time

D_n = dispersion coefficient normal to the flow axis, length^2/time

u_* = $\sqrt{\frac{f}{8}}\,|\vec{U}|$, length/time

f = Darcy-Weisbach friction factor, dimensionless

$|\vec{U}|$ = absolute value of mean velocity along flow axis, length/time

The above relationship is incorporated into the two dimensional mass conservation equation resulting in an anisotropic mixing process which calculates a dispersion coefficient at each time step and node as a function

of the instantaneous flow conditions. The expressions used for the dispersion coefficients in the model are as follows:

$$D_{xx} = \sqrt{\frac{f}{8}(q_x^2 + q_y^2)}\,(5.9 - 5.7 \sin^2\theta) \qquad (2\text{-}36)$$

$$D_{xy} = 11.4\sqrt{\frac{f}{8}(q_x^2 + q_y^2)}\,\sin\theta\cos\theta \qquad (2\text{-}37)$$

$$D_{yy} = \sqrt{\frac{f}{8}(q_x^2 + q_y^2)}\,(5.9 - 5.7 \cos^2\theta) \qquad (2\text{-}38)$$

where D_{xx}, D_{xy}, D_{yy} = dispersion coefficients
θ = $\tan^{-1}(q_y/q_x)$
q_x = flow in x direction
q_y = flow in y direction

The above model has been successfully tested agai nst dye diffusion experiments in Flushing Bay, New York, and in Community Harbor, Sau di Arabia (Pagenkopf and Taylor (1985); Taylor and Pagenkopf (1981)).

A two-dimensional, finite element water quality model was developed by Chen et al. (1979), based on the earlier model by Christodoulou et al. (1976). They provided for flow-dependent anisotropic dispersion coefficients by using the following relationships:

$$D_x = \frac{\varepsilon_x^* q_x}{H^{1/6}} + \varepsilon_x^{**} \qquad (2\text{-}39)$$

$$D_y = \frac{\varepsilon_y^* q_y}{H^{1/6}} + \varepsilon_y^{**} \qquad (2\text{-}40)$$

where ε_x^* and ε_y^* are user-defined constants as are ε_x^{**} and ε_y^{**}, the latter being provided for additional dispersion effects such as wind and marine traffic.

Whether the two-dimensional model in question utilizes constant or flow-dependent dispersion coefficients, the dispersion mechanism is usually somewhat dependent on factors typically beyond user control, such as numerical instabilities and grid size averaging effects. It is therefore

stressed that any application of a two-dimensional water quality model be verified either through site-specific salinity or dye tracer data. Naturally, when performing field tracer experiments the time and length scales of the field phenomenon should be compatible with the time and length scales to be represented in the model. For example, a dye study lasting only a few hours is not valid for verification of a model using a daily computational time step. Similarly, a dye study confined to a small portion of a large lake or estuary will not allow for verification of the model over the entire system.

2.3.4 Longitudinal Dispersive Transport in Estuaries

As previously discussed, longitudinal dispersion is the "effective diffusion" that occurs in one-dimensional mass transport equations that have been integrated over the cross sectional area perpendicular to flow. This one-dimensional approach to modeling has often been applied to tidal and nontidal rivers, and to estuaries.

The magnitude of the one-dimensional dispersion coefficient in estuaries and tidal rivers is determined in part by the time scale over which the simulation is performed. The time scale specifies the interval over which quantities that generally change instantaneously, such as tidal current, are averaged. For shorter time scales the simulated hydrodynamics and therefore water quality relationships are resolved in greater detail and hence, in such models, smaller dispersion coefficients are needed than in those which, for example, average hydrodynamics over a tidal cycle.

The magnitude of the dispersion coefficient can also be expected to change as a function of location within an estuary. Since the one-dimensional dispersion coefficient is the result of spatial averaging over a cross section perpendicular to flow, the greater the deviation between actual velocity and the area-averaged velocity, and between actual constituent concentrations and area-averaged concentrations, the larger will be the dispersion coefficient. These deviations are usually largest near the mouths of estuaries due to density gradients set up by the

interface between fresh and saline water. Strong tidal currents may also result in large dispersion coefficients.

Because of the time scale and location dependency of the dispersion coefficient, it is convenient to divide the discussion of dispersion into time varying and tidally averaged time expressions, and then to subdivide these according to estuarine location, i.e, the salinity intrusion region and the freshwater tidal region. The salinity intrusion region is that portion of the estuary where a longitudinal salinity gradient exists. The location of the line of demarcation between the salinity intrusion region and the freshwater tidal region varies throughout the tidal cycle, and also depends on the volume of freshwater discharge. It should also be noted that the freshwater tidal region can contain saline water, if the water is of uniform density throughout the region (TRACOR, 1971). There is at present no analytical method for predicting dispersion in the salinity intrusion region of estuaries. However, because of the presence of a conservative constituent (salinity), empirical measurements are easily performed. In the freshwater tidal region, analytical expressions have been developed, while empirical measurements become more difficult due to the lack of a naturally occurring conservative tracer. Empirical measurements can alternatively be based, however, on dye release experiments.

2.3.4.1 Time Varying Longitudinal Dispersion

A model which is not averaged over the tidal cycle is more capable of representing the mixing phenomena since it represents the time varying advection in greater detail. However, the averaging effects of spatial velocity gradients (shear) and density gradients must still be accounted for. The specification of longitudinal dispersion coefficients is closely associated with the type of mathematical techniques used in a given model. Most of the model developments for one-dimensional representation of estuaries has occurred in the early 1970's, and the most prominent techniques are summarized below.

The "link-node" or network model developed originally by WRE (1972) and commonly known as the Dynamic Estuary Model (DEM) used the basic work of Feigner and Harris (1970) to describe the numerical dispersion in the constant density region of an estuary:

$$D_L = C_1 E^{1/3} L_e^{4/3} \tag{2-41}$$

where D_L = longitudinal dispersion coefficient, length^2/time
E = rate of energy dissipation per unit mass
L_e = mean size of eddies participating in the mixing process
C_1 = function of relative channel roughness

For computational purposes, Feigner used the following simplification:

$$D_L = 0.042 \, |u| \, R \tag{2-42}$$

where R = hydraulic radius, ft
$|u|$ = absolute value of velocity, ft/sec

There exists no corresponding formulation for the longitudinal dispersion coefficient in the salinity intrusion regions of estuaries. Rather, a careful calibration procedure is required using available salinity data to prescribe the appropriate dispersion coefficients. Obviously, this approach somewhat restricts the predictive nature of such models since a substantial amount of empirical data is necessary for proper model application.

Similar versions of the DEM exist in one form or another. Not all versions, however, include the option for specification of longitudinal dispersion. This stems from the fact that considerable numerical dispersion occurs in the DEM from the first order, explicit, finite difference treatment of the advective transport terms. Feigner and Harris (1970) gave some comparisons of different weightings of the first order differencing in terms of trade-offs between numerical mixing, accuracy, and stability. Work on this problem has been done by Bella and Grenney (1970) and a numerical

estimate of this dispersion can be given by the following equation:

$$D_{num} = \frac{V}{2}\left[(1-2\nu)\,\Delta x - V\Delta t\right] \tag{2-43}$$

where ν represents the weighting coefficient assigned to the concentrations of two adjacent nodes.

This equation shows that the numerical dispersion is a function of Δx, Δt, and the velocity, V, which is a function of location and time. This equation is useful for estimating the magnitude of numerical dispersion. It illustrates the lack of control that the modeler has over this phenomena in the DEM.

Daily and Harleman (1972) developed a network water quality model for estuaries which uses a finite element numerical technique. The hydraulics are coupled to the salinity through the density-gradient terms in the manner formulated by Thatcher and Harleman (1972). The high accuracy finite element Galerkin weighted residuals technique is relatively free of artificial numerical dispersion. The longitudinal dispersion formulation combines both the vertical shear effect and the vertical density-induced circulation effect through the following expression:

$$D(x,t) = K\left|\frac{\partial \bar{s}}{\partial \bar{x}}\right| + m\,D_T \tag{2-44}$$

where $D(x,t)$ = temporally and spatially varying dispersion coefficient, ft^2/sec.

$\bar{s}$ = s/s_o where $s(x,t)$ is the spatial and temporal distribution of salinity, ppm

s_o = ocean salinity, ppm

$\bar{x}$ = x/L

L = length of estuary, ft (to head of tide)

D_T = Taylor's dispersion coefficient in $ft^2/sec = 77\ u\ nR_h^{5/6}$

u = $u(x,t)$ tidal velocity, ft/sec

n = Manning's friction coefficient.

R_h = hydraulic radius, ft.

K = estuary dispersion parameter in $ft^2/sec = u_o L/1000$

u_o = maximum ocean velocity at the ocean entrance, ft/sec

m = a multiplying factor for bends and channel irregularities

One-dimensional, time varying modeling using this expression has been performed for several estuaries, a recent example being an application (Thatcher and Harleman, 1978) to the Delaware Estuary wherein the time-varying calculations were made for a period of an entire year in order to provide a model for testing different water management policies.

For real time simulations in the constant density region of estuaries and tidal rivers, the following expression has been proposed (TRACOR, 1971):

$$D_L = 100\ n\ U_{max}\ R_H^{5/6} \qquad (2\text{-}45)$$

where D_L = longitudinal dispersion coefficient in the constant density region, ft^2/sec

n = Manning's roughness coefficient, $ft^{1/6}$

U_{max} = maximum tidal velocity, ft/sec

R_H = hydraulic radius, ft.

The determination of real time dispersion coefficients in the salinity intrusion region requires field data on salinity distribution. Once the field data have been collected, the magnitudes of the dispersion coefficients can be found by fitting the solution of the salinity mass transport equation to the observed data. As reported in TRACOR (1971), this technique has been applied to the Rotterdam Waterway, an estuary of almost uniform depth and width. The longitudinal dispersion coefficient was found to be a function of x, the distance measured from the mouth (ft), as follows:

$$D_L = 13000 \left(1 - \frac{x}{L}\right)^3 \qquad (2\text{-}46)$$

where D_L = real time longitudinal dispersion coefficient in salinity intrusion region, ft^2/sec

L = length of entire tidal region of the estuary.

At the estuary mouth, D_L was found to be 13,000 ft^2/sec or 40 mi^2/day (1.2×10^7 cm^2/sec) by using the technique described above. Under the same conditions in a constant density region, Equation (2-38) predicts D_L = 175 ft^2/sec, or 0.5 mi^2/day (1.6×10^5 cm^2/sec). This illustrates the large difference that can be expected between the real time dispersion coefficient in the salinity intrusion region of an estuary and in the constant density region. For more detailed discussions of real time longitudinal dispersion in estuaries, see Holley et al. (1970) and Fischer et al. (1979).

2.3.4.2 Steady State Longitudinal Dispersion

For tidally averaged or net nontidal flow simulations, the dispersion coefficients must somehow include the effects of oscillatory tidal mixing which has been averaged out of the hydrodynamics representation. No known general analytical expressions exist for this coefficient. Hence, it is cautioned and emphasized that steady-state dispersion coefficients must be determined based on observed data, or based on empirical equations having parameters that are determined from observed data. This limitation exists for both the constant density and salinity intrusion regions of the estuary.

In their one-dimensional tidally averaged estuary model, Johanson et al. (1977) used an empirical expression, comprised of three principal components (tidal mixing, salinity gradient, and net freshwater advective flow) for the dispersion coefficient. The relative location in an estuary where each of these factors is significant, and their relative magnitudes, are shown in Figure 2-7.

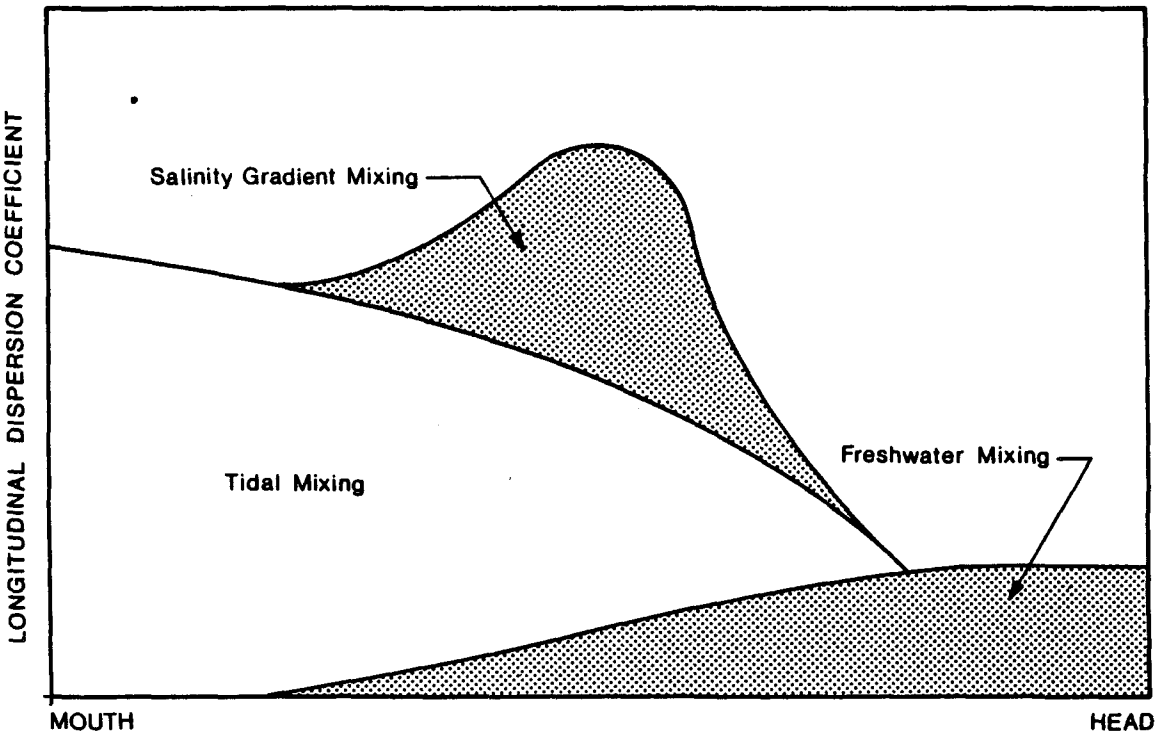

Figure 2-7. Factors contributing to tidally averaged dispersion coefficients in the estuarine environment (modified after Zison et al., 1977).

The expression used is:

$$D_L = C_1 \left(|\bar{u}| + \sigma_u \right) \left(\bar{y} + \sigma_y \right) + C_4 \left(\frac{\Delta S}{\Delta x} \right) \qquad (2\text{-}47)$$

where D_L = tidally averaged dispersion coefficient, ft^2/sec

C_1 = tidally-induced mixing coefficient (dimensionless)

$\bar{y}$ = tidally averaged depth, ft

$|\bar{u}|$ = tidally averaged absolute value of velocity, ft/sec

σ_u = standard deviation of velocity, ft/sec

σ_y = standard deviation of depth, ft

C_4 = density-induced mixing coefficient, $ft^3/sec/mg/l$-salinity

$\frac{\Delta S}{\Delta x}$ = salinity gradient, mg/l/ft

The first term on the right side of Equation (2-47) represents mixing brought about by the oscillatory flows associated with the ebbing and flooding of the tide. The second term represents additional mixing when longitudinal salinity gradients are present. It is noted that, in practice the above formulation requires careful calibration using field salinity data due to the high empirical dependency of this relationship.

One common method of experimentally determining the tidally averaged dispersion coefficient is by the "fraction of freshwater method," as explained by Officer (1976). The expression is:

$$D_L = \frac{Rs}{A(ds/dx)} = \frac{R(f-1)}{A(df/dx)} \qquad (2\text{-}48)$$

where D_L = tidally averaged dispersion coefficient, ft^2/sec

s = mean salinity at a particular location averaged over depth, mg/l

A = cross-sectional area normal to flow, ft^2

R = total river runoff flow rate, cfs

f = freshwater fraction = $\frac{\sigma - s}{\sigma}$, unitless

σ = normal ocean salinity of the coastal water into which the estuary empties, mg/l

x = distance along estuary axis, ft.

D_L can be calculated at any location within the estuary if the river flow, cross-sectional area, and salinity or freshwater fraction distributions are known.

The above method has certain pitfalls which are pointed out by Ward and Fischer (1971) in their analysis of such an application to the Delaware Estuary. They point out that the use of a dispersion coefficient relationship, i.e., a functional relationship of dispersion to distance, which is also directly related to the measured upstream freshwater inflow, neglects entirely the basic response of the waterbody to variations in freshwater inflow. Ward and Fischer show, for example, that it may take a period of months for the estuary to adjust to a short period change in

freshwater discharge and that any dispersion coefficient relationship based on a simple correlation analyses may be seriously in error.

Hydroscience (1971) has collected values of tidally averaged dispersion coefficients for numerous estuaries, and these values are shown in Table 2-3.

In his book, Officer (1976) reviews studies performed in a number of estuaries throughout the world. He discusses the dispersion coefficients which have been determined, and a summary of values for these estuaries is contained in Table 2-4. Many values were developed using the fraction of freshwater method just discussed. Additional values for the longitudinal dispersion coefficient have been summarized in Fischer et al. (1979).

2.3.4.3 The Lagrangian Method

The models discussed in previous sections of this chapter have all been based on the Eulerian concept of assigning velocities and concentrations to fixed points on a spatial grid. As previously discussed, the fixed grid approach tends to introduce a fictitious "numerical" dispersion into the mass transport solution since the length scale of the diffusion process is somewhat artificially imposed depending on the grid detail. To avoid such a problem, an alternative approach termed the Lagrangian method has been used by Fischer (1972), Wallis (1974), and Spaulding and Pavish (1984) for models of estuaries and tidal waters. Briefly, the Lagrangian method establishes marked volumes of water, distributed along the channel axis, which are moved along the channel at the mean flow velocity. Numerical diffusion is almost entirely eliminated, since there is no allocation of concentrations to specific grid points; rather, the "grid" is a set of moving points which represent the centers of the marked volumes. Longitudinal dispersion between marked volumes can be set according to appropriate empirical or theoretical diffusion behavior (Fischer et al., 1979). The Lagrangian method has been primarily applied to channelized estuaries such as the Suisun Marsh (Fischer, 1977) and Bolinas Lagoon (Fischer, 1972), and more recently has been extended by Spaulding and Pavish (1984) to simulate particulate transport in three dimensions.

TABLE 2-3. TIDALLY AVERAGED DISPERSION COEFFICIENTS FOR SELECTED ESTUARIES (from Hydroscience, 1971)

Estuary	Freshwater Inflow (cfs)	Low Flow Net Nontidal Velocity (fps) Head - Mouth	Dispersion Coefficient (mi^2/day)*	(ft^2/sec)
Delaware River	2,500	0.12-1.000	5	1610
Hudson River (NY)	5,000	0.037	20	6450
East River (NY)	0	0.0	10	3230
Cooper River (SC)	10,000	0.25	30	9680
Savannah River (GA, SC)	7,000	0.7-0.17	10-20	3230-6450
Lower Raritan River (NJ)	150	0.047-0.029	5	1610
South River (NJ)	23	0.01	5	1610
Houston Ship Channel (TX)	900	0.05	27	8710
Cape Fear River (NC)	1,000	0.48-0.03	2-10	645-3230
Potomac River (VA)	550	0.006-0.003	1-10	320-3230
Compton Creek (NJ)	10	0.10-0.013	1	320
Wappinger and Fishkill Creek (NY)	2	0.004-0.001	0.5-1	160-320

*1 mi^2/day = 322.67 ft^2/sec.

2.3.5 Dispersive Transport in Rivers

2.3.5.1 Introduction

Dispersive transport in rivers is typically, but not always, modeled using a one-dimensional equation such as:

$$\frac{\partial C}{\partial t} + \frac{U\partial C}{\partial x} = \frac{\partial}{\partial x}\left(D_L\frac{\partial C}{\partial x}\right) \qquad (2\text{-}49)$$

where C = concentration of solute, mass/$length^3$

U = cross-sectional averaged velocity, length/time

D_L = longitudinal dispersion coefficient, $length^2$/time

x = longitudinal coordinate, length

t = time

TABLE 2-4. TIDALLY AVERAGED DISPERSION COEFFICIENTS (FROM OFFICER, 1976)

Estuary	Dispersion Coefficient Range (ft2/sec)	Comments
San Francisco Bay, CA Southern Arm Northern Arm	 200-2,000 500-20,000	Measurements were made at slack water over a period of one to a few days. The fraction of freshwater method was used. Measurements were taken over three tidal cycles at 25 locations.
Hudson River, NY	4,800-16,000	The dispersion coefficient was derived by assuming D_L to be constant for the reach studied, and that it varied only with flow. A good relationship resulted between D_L and flow, substantiating the assumption.
Narrows of Mercey, UK	1,430-4,000	The fraction of freshwater method was used by taking mean values of salinity over a tidal cycle at different cross sections.
Potomac River, MD	65-650	The dispersion coefficient was found to be a function of distance below the Chain Bridge. Both salinity distribution studies (using the fraction of freshwater method) and dye release studies were used to determine D_L.
Severn Estuary, UK	75-750	Bowden recalculated D_L values originally determined by Stommel, who had used the fraction of freshwater method. Bowden included the freshwater inflows from tributaries, which produced the larger estimates of D_L.
Tay Estuary, UK	530-1,600	The fraction of freshwater method was used. At a given location, D_L was found to vary with freshwater inflow rate.
Thames Estuary, UK	3,640 (high flow) 600-1000 (low flow)	Calculations were performed using the fraction of freshwater method, between 10 and 30 miles below London Bridge.
Yaquina Estuary	650-9,200 (high flow) 140-1,060 (low flow)	The dispersion coefficients for high flow conditions were substantially higher than for low flow conditions, at the same locations. The fraction of freshwater method was used.

Because of the difficulty of accurately solving Equation (2-49) numerically, some researchers (e.g., Jobson, 1980a; Jobson and Rathbun, 1985) have chosen a Lagrangian approach, where the coordinate system is allowed to move with the local stream velocity. Using this approach, Equation (2-49) become:

$$\frac{\partial C}{\partial t} = \frac{\partial}{\partial \xi}\left(D_L \frac{\partial C}{\partial \xi}\right) \tag{2-50}$$

where $\xi = x - \int_0^t U d\tau$

The numerically troublesome advective term does not appear in Equation (2-50). In general, the equation can be solved more easily and with more accuracy than Equation (2-49).

A second method used to simulate dispersive transport in rivers is to consider lateral mixing in addition to longitudinal mixing. A typical form of the two-dimensional equation is:

$$\frac{\partial C}{\partial t} + u(y)\frac{\partial C}{\partial x} = \frac{\partial}{\partial x}\left(\varepsilon_x \frac{\partial C}{\partial x}\right) + \frac{\partial}{\partial y}\left(\varepsilon_y \frac{\partial C}{\partial y}\right) \tag{2-51}$$

where $u(y)$ = depth averaged velocity of water, which is a function of y, and is no longer the cross-sectional averaged velocity, length/time

ε_x = depth averaged longitudinal diffusion coefficient, length^2/time

ε_y = depth averaged lateral diffusion coefficient, length^2/time

y = lateral coordinate, length

Note that longitudinal dispersion coefficient, D_L, in Equation (2-49) is not the same as the longitudinal diffusion coefficient, ε_x, in Equation (2-51). Typically, $D_L \gg \varepsilon_x$.

2.3.5.2 Longitudinal Dispersion in Rivers

Fischer (1966, 1967a, 1967b, 1968) has performed much of the earlier research on longitudinal dispersion in natural channels. Prior to Fischer, Taylor (1954) studied dispersion in straight pipes and Elder (1959) studied dispersion in an infinitely wide open channel. More recently Fischer et al. (1979) and Elhadi et al. (1984) have provided a comprehensive review of dispersion processes.

Researchers have shown that Equation (2-49) is valid only after some initial mixing length, often called the Taylor length or convective period. While the convective period has been a topic of active research in the literature (e.g., Fischer, 1967a and b; McQuivey and Keefer, 1976a; Chatwin, 1980), this concept is not embodied in one-dimensional water quality models in general use.

Table 2-5 summarizes references on stream dispersion. The references include information from at least one of the following areas:

- methods to predict D_L, typically for model applications
- methods to measure D_L from field data
- data summaries of dispersion coefficients
- approaches used to simulate dispersion in a non-Fickian manner.

Bansal (1971), Elhadi and Davar (1976), Elhadi et al. (1984) also provide reviews of stream dispersion.

To date, the predictive capabilities of expressions for dispersion coefficients have not been thoroughly tested. However, it is known that the Taylor (1954) or Elder (1959) formulas do not accurately predict dispersion coefficients for natural streams. Glover (1964) found that dispersion coefficients in natural streams were likely to be 10 to 40 times higher than predicted by the Taylor or Elder equations. The lateral variation in stream velocity is the primary reason for the increased dispersion not accounted for by Taylor and Elder. Fischer (1967a) quantified the contribution of the

Reference	Comments
Taylor (1954)	$D_L = 10.1 R_p u_*$; pipe flow.
Elder (1959)	$D_L = 5.93 H u_*$; lateral velocity variation not considered.
Glover (1964)	$D_L = 500 R u_*$; natural streams.
Krenkel (1960)	$D_L = 6.4 H^{1.24} E^{0.3}$; two-dimensional channel.
	$(E = USg)$
Parker (1961)	$D_L = 14.3 R^{3/2} \sqrt{2_g S}$; open channel flow.
Fischer (1967a, 1967b)	$D_L = \frac{U^2}{2}\left(\frac{\sigma_{t2}^2-\sigma_{t1}^2}{t_2-t_1}\right)$; concentration variances are measured after an initial period. Long tails may introduce some error.
	$D_L = \frac{-1}{A}\int_0^b q'(y)dz \int_0^y \frac{1}{\varepsilon_y d(y)} dy \int_0^y q'(y)dy.$
	where $q'(y) = \int_0^{d(y)} (U(y,z)-\bar{u})dz$
	This formula considers the effects of lateral velocity changes.
	$D_L = \frac{1}{2}\frac{d\sigma_x^2}{dt}$
	$D_L = 0.3\overline{u'^2}\frac{l^2}{Ru_*}$; a simplification of the integral equation above
	Fischer also discusses another method for determining D_L called the routing procedure.
Elhadi and Davar (1976)	Reviewed many methods to predict D_L. Found $D_L/(Hu^*)$ is not a constant as reported by many researchers.
Fischer (1968)	Field measurements of D_L were made in the Green and Duwamish Rivers.
Bansal (1971)	$\log\left(\frac{KU_s D_L}{U^2 H}\right) = 6.45-0.762 \log\left(\frac{\rho UH}{\mu}\right)$
	$\log\left(\frac{KU_s}{U}\frac{D_L}{u_* H}\right) = 6.467-0.714 \log\left(\frac{\rho u_* H}{\mu}\right)$
Godfrey and Frederick (1970)	Dispersion tests were summarized in five natural streams; measured dispersion coefficients were from 4 to 35 times greater than predicted by Taylor's (1954) method.
Thackston (1966)	$D_L = 7.25 H u_* \left(\frac{U}{u_*}\right)$; 2-D channels.

(continued)

TABLE 2-5. (continued)

Reference	Comments
Thackston and Krenkel (1967)	The limitations of dispersion equations which do not consider lateral velocity variations are discussed. Site specific measurements of D_L are recommended.
Miller and Richardson (1974)	In laboratory experiments, D_L varied from 0.6 ft^2/sec to 66 ft^2/sec.
McQuivey and Keefer (1974)	Dispersion coefficient data were reviewed, including hydraulic data, for 17 rivers. $D_L = 0.66 \frac{U^3}{\bar{C}^3} Q_o/(2S_oW_o)$ $D_L = 0.058 \frac{Q_o}{S_oW_o}$
McQuivey and Keefer (1976b)	Dispersion tests performed in the Mississippi River are summarized.
Liu (1977)	$D_L = \frac{\beta Q^2}{u_* R^3}$ $\beta \simeq 0.18\left(\frac{\sqrt{gRS}}{U}\right)^{1.5}$ Summary of D_L values also reported.
Fischer (1975)	$D_L = \frac{0.011U^2W^2}{H_u}$ Liu (1977) shows this is a special case of his formula when $\beta = 0.011$.
Hays et al. (1966)	Several conceptual models of mass exchange with dead zones are presented and the Fickian Equation is modified to include mass transfer to and from dead zones.
Thackston and Schelle (1970)	Application of Hays et al. (1966) dead zone model to TVA stream data.
Day (1975)	Longitudinal dispersion of fluid particles in small mountain streams in New Zealand was investigated. It was shown that the dispersion coefficient increased with distance and never approached an asymptotic value.
Day and Wood (1976)	Longitudinal dispersion of fluid particles in the Missouri River and in a small mountain stream was investigated. The dispersing particles were shown to behave differently from the Taylor type model. A method to predict dispersion was developed.
Liu and Cheng (1980)	A non-Fickian model is presented to predict stream dispersion.

(continued)

TABLE 2-5. (continued)

Reference	Comments
Sabol and Nordin (1978)	A modified model of stream dispersion is presented that includes the effects of storage along the bed and banks.
Valentine and Wood (1977)	Effects of dead zones on stream dispersion are addressed
Valentine and Wood (1979)	Experimental results are provided to show how dead zones modify longitudinal dispersion.
Rutherford, Taylor, Davies (1980)	A hybrid method is discussed to predict dispersion in the Waikato River, New Zealand.
Beltaos (1980a)	Dispersion processes in streams are reviewed and it is shown that many experimental results do not comply with Fickian dispersion theory. A non-Fickian dispersion model is proposed.
Beltaos (1982)	Dispersion in steep mountain streams is examined.
Bajraktarevic - Dobran (1982)	Fischer's methods are successfully applied to predict dispersion in mountainous streams.
Beer and Young (1983)	Methods are developed to predict dispersion in rivers including the effects of dead zones, using a (j,n,m) model.
Jobson (1980a)	The Fickian Equation is solved with a Lagrangian scheme to avoid lumping numerical dispersion with actual physical dispersion. See Jobson (1980b).
Jobson (1985) and McBride and Rutherford (1984)	Determined that D_L and coefficients for nonconservative water quality constituents could be determined simultaneously during calibration. D_L determined by this method is in good agreement with literature values (Jobson) or match D_L values determined from dye studies (McBride and Rutherford).
Jobson and Rathbun (1985)	Numerical dispersion minimized with a Lagrangian routing procedure that provides more consistent estimates of D_L than the method of moments for pool and riffle streams. Applying this procedure to peak dye concentrations yielded D_L to within 10% of estimates based on the entire concentration-time curves.

(continued)

TABLE 2-5. (continued)

Footnotes:

A	= cross-sectional area
b	= channel width
$\bar{c}$	= wave velocity
$d(y)$	= depth of water at y
E	= rate of energy dissipation per unit mass of fluid
ε_y	= lateral turbulent mixing coefficient
H	= stream depth
K	= regional dispersion factor
l	= lateral distance from location of maximum velocity
σ_x^2	= variance of distance - concentration curves
$\sigma_{t2}^2, \sigma_{t1}^2$	= variance of time concentration curves
$\bar{t}_2, \bar{t}_1$	= mean times of passage
ρ	= mass density of water
Q_o	= discharge at steady base flow
$q'(y)$	= integral of velocity deviation on depth
R	= hydraulic radius
R_p	= pipe radius
S_o	= slope of energy gradient at steady base flow
U	= mean velocity of flow in reach
u'	= deviation of velocity from cross-sectional mean
U_s	= mean velocity of flow at sampling point
u_*	= shear velocity
μ	= coefficient of viscosity of water
W_o	= channel width at steady base flow

lateral velocity variation on stream dispersion.

A number of the formulas in Table 2-5 are of the type $D_L/(u_*H)$ = constant. However, several researchers, including Bansal (1971), Elhadi and Davar (1976), and Beltaos (1978a) have shown that the ratio $D_L/(u_*H)$ is not a constant. Figure 2-8 shows this ratio can vary by several orders of magnitude.

Two widely used methods of predicting the longitudinal dispersion coefficients were developed by Liu (1977) and Fischer (1975) and are shown in Table 2-5. Liu showed that Fischer's method is identical to his own when $\beta = 0.011$.

Although numerous researchers (e.g., Sabol and Nordin, 1978) have shown how to include the effects of dead zones on dispersive transport, this refinement does not yet appear to be in general use in water quality models today. In fact, some water quality models do not include dispersion at all (at least physical dispersion; numerical dispersion may be present, depending on the solution technique used).

Dispersion can be neglected in certain circumstances with very little effect on the predicted concentration distributions. Thomann (1973), Li (1972), and Ruthven (1971) have investigated the influence of dispersion. Ruthven gave a particularly simple expression for a pollutant which decays at a rate k. If

$$\frac{kD_L}{U^2} < \frac{1}{23} = .04$$

then the concentration profile will be affected by no more than 10 percent if dispersion is ignored. Consider, for example, a decaying pollutant with k = 0.5/day in a stream where U = 1 fps and D_L = 500 ft^2/sec. The ratio kD_L/U^2=.003, which indicates that dispersion can be ignored. This guideline assumes that the pollutant is being continuously released and conditions are at steady state. The basic presumption is that if the concentration gradient is small enough, the dispersive transport is also small, and

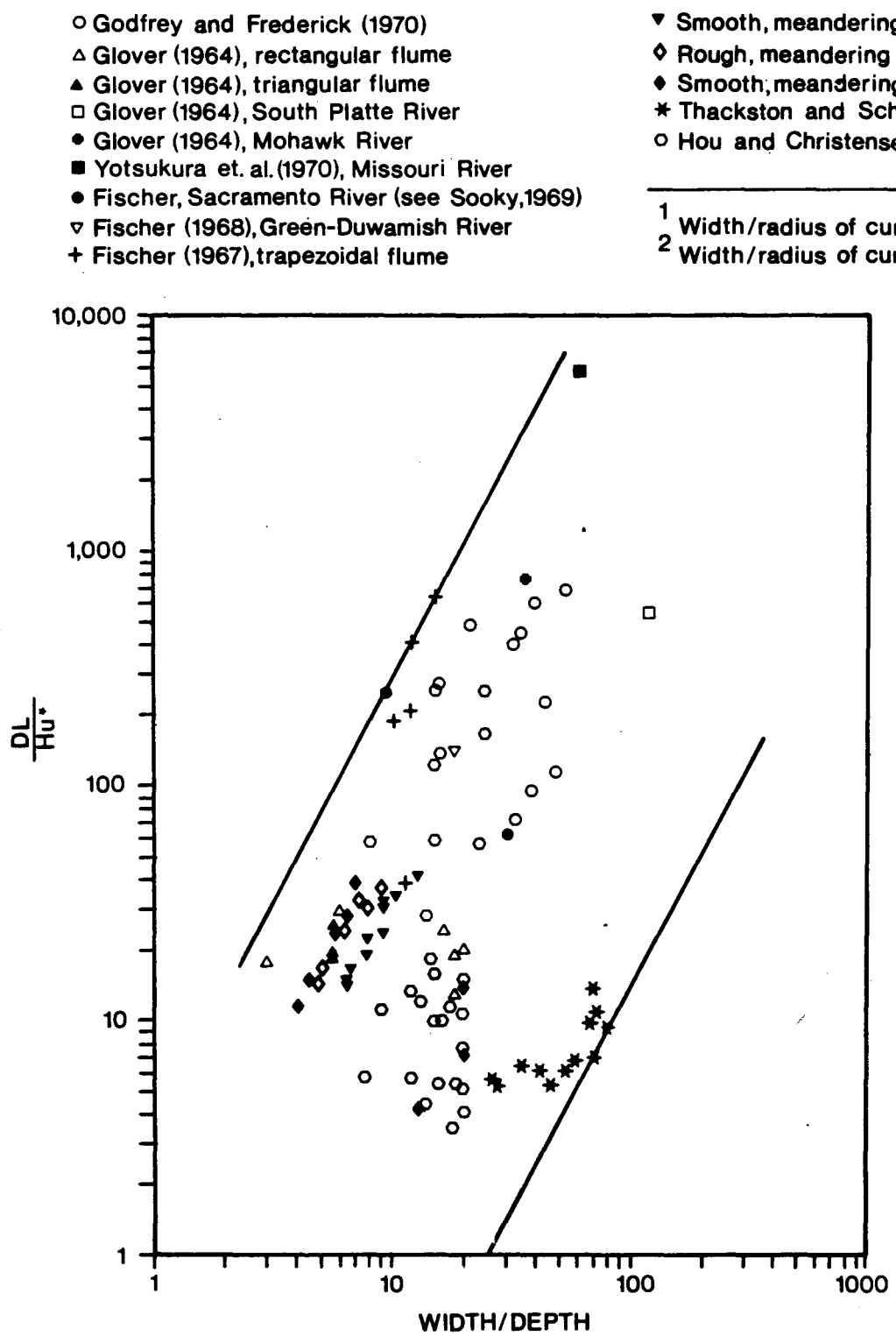

Figure 2-8. Dispersion coefficients in streams (Beltaos, 1978a).

perhaps negligible. On the other hand when pollutants are spilled, concentration gradients are large and dispersion is not negligible.

Thomann (1973) investigated the importance of longitudinal dispersion in rivers that received time variable waste loadings, and therefore produced concentration gradients in the rivers. His results showed that for small rivers, dispersion may be important when the waste loads vary with periods of 7 days or less. For large rivers, dispersion was found to be important whenever the waste load was time-variable.

2.3.5.3 Lateral Dispersion in Rivers

Although two-dimensional water quality models are less widely used in rivers than one-dimensional models, lateral mixing has been the topic of considerable research. Models that simulate lateral mixing are particularly useful in wide rivers where the one dimensional approach may not be applicable. Vertical mixing is rarely simulated in river modeling because the time required for vertical mixing is usually very rapid compared to the time required for lateral mixing. Thermal plumes are an exception.

An example of a model that simulates lateral mixing in rivers is the RIVMIX model of Krishnappan and Lau (1982). The model is particularly useful for delineating mixing zones or regulating the rate of pollutant discharge so that concentrations outside of the mixing zones are limited to allowable values.

When lateral and longitudinal mixing are both simulated, the x and y coordinates are generally assumed to continuously change to be oriented in the longitudinal and transverse directions. Although Equation (2-51) should rigorously contain metric factors (Fukuoka and Sayre, 1973) to account for these continuous changes, modelers typically assume the metric factors are unity.

Lateral mixing coefficients are usually presented in one of the following two forms:

$$\varepsilon_y = \alpha H u_*$$ (2-52)

or

$$D_y = \frac{\beta Q^2}{W}$$ (2-53)

where ε_y = lateral mixing coefficient, length^2/time
D_y = lateral diffusion factor, length^5/time^2
H = water depth, length
α,β = coefficients that vary from river to river
u_* = friction velocity, length/time
Q = stream flow, length^3/time
W = width of river, length

D_y and ε_y are related by the following formula:

$$D_y = H^2 U m_x \varepsilon_y$$ (2-54)

where m_x = average metric value in x- direction (≈ 1)

Equation (2-52) is generally the most widely used of the two formulas. Equation (2-53) is used when the two-dimensional convective-diffusion equation is expressed in terms of cumulative discharge (Yotsukura and Cobb, 1972).

Table 2-6 summarizes studies of transverse mixing in streams. Data from the literature are summarized in Tables 2-7 through 2-9. Table 2-9 contains values of β for use in Equation (2-53).

Elhadi et al. (1984) have recently provided a detailed review of lateral mixing in rivers. They concluded that lateral mixing coefficients can be predicted with accuracy only in relatively straight channels.

TABLE 2-6. SUMMARY OF STUDIES OF TRANSVERSE MIXING IN STREAMS

Reference	Comments
Okoye (1970)	This study presented a detailed analysis of laboratory experiments of lateral mixing.
Prych (1970)	This study detailed the effects of density differences on lateral mixing.
Yotsukura, Fischer, Sayre (1970)	A lateral dispersion coefficient of 1.3 ft^2/sec was determined for the Missouri River.
Yotsukura and Cobb (1972)	Studies of lateral mixing were performed on the South River, Atrisco Feeder Canal, Bernardo Conveyance Channel, and the Missouri River.
Holley (1975)	A two-dimensional model of contaminant transport in rivers was developed and applied to the Missouri and Clinch Rivers. ε_y was experimentally determined using $\varepsilon_y = \frac{U}{2}\frac{d\sigma_y^2}{dx}$
Holley and Abraham (1973)	Transverse dispersion measurements were made in the Waal and IJssel Rivers, Holland. The change of moments method was used.
Yotsukura and Sayre (1976)	Transverse cumulative discharge was used as an independent variable replacing transverse distance in the 2-D mass transport equation.
Shen (1978)	The approach of Yotsukura and Sayre (1976) was extended to include transient mixing.
Lau and Krishnappan (1981)	Field data for transverse mixing coefficients were summarized. A further extension of the approach of Yotsukura and Sayre was made. Values of $\varepsilon_y/(u_*H)$ were found to depend on depth/width ratios.
Somlyody (1982)	Tracer studies were performed in five streams to predict lateral mixing coefficients. A numerical model used in the study was an extension of the work of Yotsukura and Sayre (1976).
Gowda (1978)	Transverse mixing coefficients were measured in the Grand River.
Mescal and Warnock (1978)	A study of lateral mixing in the Ottawa River produced the expression $\varepsilon_y = 0.043HU$.
Benedict (1978)	This study reviewed various mixing expressions.
Henry and Foree (1979)	An approximate method of two-dimensional dispersion modeling was presented.
Beltaos (1980)	Transverse mixing characteristics of three rivers in Alberta, Canada were documented by tracer tests for open water and ice covered flow conditions.
Cotton and West (1980)	Rhodamine WT dye was used to determine the transverse diffusion coefficient on a straight reach of an open channel.
Holley and Nerat (1983)	Inclusion of secondary mixing as part of a lateral diffusion coefficient was concluded to have a limited physical basis.
Demetracopoulous and Stefan (1983)	Transverse mixing was studied in wide and shallow rivers using heated discharge as a tracer. A modified method of moments was developed to compute transverse mixing coefficients.
Webel and Schatzmann (1984)	An experimental study was conducted to investigate variations in transverse mixing coefficients in straight, rectangular channels. $\varepsilon_y/(u_*H)$ was found to be constant.

ε_y = lateral mixing coefficient

U = cross-sectional average velocity

σ_y^2 = variance of concentration in y-direction

u_* = shear velocity

H = depth

TABLE 2-7. TRANSVERSE MIXING COEFFICIENTS IN NATURAL STREAMS AND CHANNELS (FROM BELTAOS, 1978a)

Source	Channel and Description	W (m)	$\frac{W}{R}$	U (m/s)	f	$\varepsilon_y/(Hu_*)$	Comments
Glover 1964	Columbia River	305	100	1.35	.034	.74	Test results and analysis approximate
Yotsukura et al., 1970	Missouri River, two mild alternating bends	183	68.7	1.74	.014	.60	Flow distribution available at only two cross sections
Yotsukura and Cobb, 1972	South River, few mild bends	18.2	46.2	.21	.284	.30	Analysis by streamtube method
Sayre and Yeh, 1973	Missouri River, sinuous, severe bends	234	59.1	1.98	.015	3.30	Analysis by numerical and analytical methods. Periodical variation of ε_y detected; average value indicated here
Engmann and Kellerhais, 1974	Lesser Slave River, irregular, almost contorted meander, no bars; sinuosity = 2.0	43.0	17.0	.65	.045	.33	Effects of transverse advection lumped together with transverse dispersion. Reanalysis of ice covered data by streamtube method gave $\varepsilon_y/Ru_* = .16$
Meyer, 1977	Mobile River, mostly straight, one mild curve	430	87.2	.30	.028	7.20	Steady-state condition unlikely
Krishnappan & Lau, 1977	Meandering laboratory flume with "equilibrium bed". Planview sinusoidal. Meander wavelength=2 πW=1.88m	.30 .30 .30 .30 .30 .30 .30	10.5 15.9 7.6 10.2 9.0 11.6 10.0	.26 .27 .31 .30 .28 .23 .32	.162 .105 .163 .208 .271 .156 .101	- - - - - - -	Evaluation of ε_y by a numerical simulation method. Use of constant ε_y gave more consistent results than laterally variable values of ε_y.
Beltaos, 1978b	Athabasca River below Fort McMurray, straight with occasional islands, bars; sinousity=1.0	373	170	.95	.028	.75	Slug-injection tests; analysis by streamtube method applied to dosage (see also Beltaos 1975)
Beltaos, 1978b	Athabasca River below Athabasca, irregular meanders with occasional bars, islands; sinuosity=1.2	320	156	.86	.067	.41	
Beltaos, 1978b	Beaver River near Cold Lake, regular meanders, point bars and large dunes, sinuosity=1.3	42.7	44.6	.50	.062	1.0	Steady-state concentration tests. Analysis by stream-tube method.
Beltaos (unpublished)	North Saskatchewan River below Edmonton, nearly straight, few, very mild bends with occasional bars, islands; sinuosity=1.0	213	137	.58	.152	.25	By steady-state concentration and slug-injection tests. Analysis by streamtube and numerical methods respectively
Beltaos (unpublished)	Bow River at Calgary, sinuous with frequent islands; mid-channel bars diagonal bars, sinuosity=1.1	104	104	1.05	.143	.61	

A = amplitude of meanders
f = fraction factor
R = hydraulic radius
U = cross-sectionally averaged velocity
W = width
H = depth
ε_y = lateral mixing coefficient

TABLE 2-8. SUMMARY OF FIELD DATA FOR TRANSVERSE DISPERSION COEFFICIENTS (LAU AND KRISHNAPPEN, 1981)

Data Source	Width, in meters	W/H	Average velocity in meters per second	Shear Velocity in meters per second	Friction factor	Dispersion Coefficient, ε_y, in meters squared per second	ε_y/u_*W	ε_y/u_*H	Sinuosity S
Yotsukura and Cobb (1972) Missouri River near Blair	183.0	66.7	1.74	0.073	0.014	0.101	7.5×10^{-3}	0.50	1.1
Yotsukura and Cobb (1972) South River	18.3	46.2	0.18	0.040	0.220	0.0046	6.3×10^{-3}	0.29	1.0[a]
Yotsukura and Cobb (1972) Aristo Feeder Canal	18.3	27.3	0.67	0.062	0.069	0.0093	8.2×10^{-3}	0.22	1.0[a]
Yotsukura and Cobb (1972) Bernado Conveyance Channel	20.1	28.7	1.25	0.061	0.020	0.013	10.6×10^{-3}	0.30	1.0[a]
Beltaos (1978a), Athabasca below Fort McMurray	373.0	170.0	0.95	0.056	0.028	0.092	4.4×10^{-3}	0.75	1.0[a]
Beltaos (1978a), Athabasca River below Athabasca	320.0	156.0	0.86	0.079	0.067	0.066	2.6×10^{-3}	0.41	1.2
Beltaos (1978a), North Saskatchewan River below Edmonton	213.0	137.0	0.58	0.080	0.152	0.031	1.8×10^{-3}	0.25	1.0[a]
Beltaos (1978b), Bow River at Calgary	104.0	104.0	1.05	0.139	0.143	0.085	5.9×10^{-3}	0.61	1.1
Beltaos (1978b), Beaver River near Cold Lake	42.7	44.6	0.50	0.044	0.062	0.042	22.4×10^{-3}	1.00	1.3
Sayre and Yeh (1975) Missouri River below Cooper Generation Station	234.0	59.1	1.98	0.085	0.015	1.110	55.8×10^{-3}	3.30	2.1
Lau and Krishanppan (1977) Grand River below Kitchener	59.2	117.0	0.35	0.069	0.314	0.009	2.2×10^{-3}	0.26	1.1

TABLE 2-9. SUMMARY OF NONDIMENSIONAL DIFFUSION FACTORS IN NATURAL STREAMS (FROM GOWDA, 1984)

Source of data	Salient features	Discharge, in cubic meters per second	Mean width, in meters	Mean depth, in meters	Mean velocity in meters per second	Nondimensional diffusion factor, β
Hamdy and Kinkead (1979) St. Clair River	12.0 km straight stretch with an island	6,800.00	819.3	10.00	0.83	5.9×10^{-4}
Glover (1964) Columbia River near Richland	0.11 km stretch with a gradual S-curve	1,235.30	304.8	3.00	1.35	4.7×10^{-4}
Holley and Abraham (1973)Waal River	10.0 km straight stretch	1,027.75	266.1	4.70	0.82	5.3×10^{-4}
Yotsukura and Cobb (1972) Missouri River near Blair	10.0 km stretch with mild alternating curve	965.60	183.0	2.74	1.74	6.6×10^{-4}
Beltaos (1980b) Athabasca River below Fort McMurray	17.6 km stretch with occasional bars and islands	776.00	373.0	2.20	0.95	7.8×10^{-4}
Beltaos (1980b) Athabasca River below Athabasca	17.0 km stretch with irregular meanders, occasional bars and islands	566.00	320.0	2.05	0.86	8.4×10^{-4}
Holly and Abraham (1973) Ijssel River	8.6 km stretch with three alternating bends	269.75	69.5	4.00	0.97	23.0×10^{-4}
Beltaos (1980b) Beaver River near Cold Lake	1.5 km stretch with regular meanders, point bars and large dunes	20.5	42.7	0.96	0.50	41.0×10^{-4}
Yotsukura and Cobb (1972) Bernardo Conveyance Channel	2.0 km straight stretch	17.75	20.1	0.70	1.25	81.0×10^{-4}
Gowda (1980) Grand River below Waterloo	3.4 km stretch with two alternating curves	12.54	57.3	0.56	0.39	10.0×10^{-4}
Yotsukura and Cobb (1972) Atrisco Feeder Canal near Bernalillo	2.0 km straight stretch with a channel of nearly uniform cross-section	7.42	18.3	0.67	0.67	13.0×10^{-4}
Yotsukura and Cobb (1972) South River near the Town of Wayresboro	0.4 km stretch with a few very slight bends	1.53	18.2	0.38	0.21	25.0×10^{-4}
Gowda (1980) Boyne River below Alliston	0.2 km straight stretch	0.82	8.85	0.43	0.22	25.0×10^{-4}

Notes:

$$\beta = \frac{D_y W}{Q^2}$$

$$D_y = H^2 U m_x c_y$$

W = channel width
Q = flow rate
H = depth
U = velocity
m_x = average value of matrix (≈ 1) in x- direction

2.3.6 Summary

The previous sections have provided a brief review on the treatment of dispersive transport in water quality models. This has included a discussion of vertical dispersion in lakes and estuaries, and horizontal (lateral and longitudinal) dispersion in lakes, estuaries, and rivers. It is readily seen that a wide variety of numerical formulations for dispersion exist in the literature. Formulations for dispersion coefficients tend to be model-dependent and are all based to some extent on general lack of a complete understanding of the highly complex turbulence induced mixing processes which exist in natural water bodies. In all cases, due to this model and empirical dependence, it is desirable to include a careful calibration and/or verification exercise using on-site field data for any water quality modeling application.

2.4 SURFACE HEAT BUDGET

The total heat budget for a water body includes the effects of inflows (rivers, discharges), outflows, heat generated by chemical-biological reactions, heat exchange with the stream bed, and atmospheric heat exchange at the water surface. In all practicality, however, the dominant process controlling the heat budget is the atmospheric heat exchange, which is the focus of the following paragraphs. In addition, however, it is also important to include the proper boundary conditions for advective exchange (e.g., rivers, thermal discharges, or tidal flows) when the relative source temperature and rate of advective exchange is great enough to affect the temperature distribution of the water body.

The transfer of energy which occurs at the air-water interface is generally handled in one of two ways in river, lake, and estuary models. A simplified approach is to input temperature values directly and avoid a more complete formulation of the energy transfer phenomena. This approach is most often applied to those aquatic systems where the temperature can be readily measured. Alternatively, and quite conveniently, the various energy transfer phenomena which occur at the air-water interface can be considered in a heat budget formulation.

In a complete atmospheric heat budget formulation, the net external heat flux, H, is most often formulated as an algebraic sum of several component energy fluxes (e.g., Baca and Arnett, 1976; U.S. Army Corps of Engineers, 1974; Thomann et al., 1975; Edinger and Buchak, 1978; Ryan and Harleman, 1973; TVA, 1972). A typical expression is given as:

$$H = Q_s - Q_{sr} + Q_a - Q_{ar} - Q_{br} - Q_e \pm Q_c \qquad (2\text{-}55)$$

where H = net surface heat flux

$\downarrow Q_s$ = shortwave radiation incident to water surface, 30 to 300 kcal/m^2/hr

$\uparrow Q_{sr}$ = reflected short wave radiation, 5 to 25 kcal/m^2/hr

$\downarrow Q_a$ = incoming long wave radiation from the atmosphere, 225 to 360 Kcal/m^2/hr

$\uparrow Q_{ar}$ = reflected long wave radiation, 5 to 15 kcal/m^2/hr

$\uparrow Q_{br}$ = back radiation emitted by the body of water, 220 to 345 kcal/m^2/hr

$\uparrow Q_e$ = energy utilized by evaporation, 25 to 900 kcal/m^2/hr

$\updownarrow Q_c$ = energy convected to or from the body of water, -35 to 50 kcal/m^2/hr at the surface

NOTE: The magnitudes are typical for middle latitudes of the United States. The arrows indicate if energy is coming into the system ($\downarrow$), out of the system ($\uparrow$), or both ($\updownarrow$).

These flux components can be calculated within the models from semi-theoretical relations, empirical equations, and basic meteorological data. Depending on the algebraic formulation used for the net heat flux term and the particular empirical expressions chosen for each component, all or some of the following meteorological data may be required: atmospheric pressure, cloud cover, wind speed and direction, wet and dry bulb air temperatures, dew point temperature, short wave solar radiation, relative humidity, water temperature, latitude, and longitude.

Estimation of the various heat flux components has been the subject of many theoretical and experimental studies in the late 1960's and early

1970's. Most of the derived equations rely heavily on empirical coefficients. These formulations have been reviewed extensively by the Tennessee Valley Authority (1972), Ryan and Harleman (1973), Edinger et al. (1974), and Paily et al. (1974). A summary of the most commonly used formulations in water quality models is given in the following sections.

2.4.1 Measurement Units

The measurement units in surface heat transfer calculations do not follow any consistent units system. For heat flux, the English system units are BTU/ft^2/day. In the metric system, the units are either Kcal/m^2/hr or watt/m^2 (1 watt = 1 joule/sec). The Langley (abbreviated Ly), equal to 1 cal/cm^2, also persists in usage. The following conversions are useful in this section:

1 BTU/ft^2/day	= 0.131 watt/m^2	= 0.271 Ly/day	= 0.113 kcal/m^2/hr
1 watt/m^2	= 7.61 BTU/ft^2/day	= 2.07 Ly/day	= 0.86 kcal/m^2/hr
1 Ly/day	= 0.483 watt/m^2	= 3.69 BTU/ft^2/day	= 0.42 kcal/m^2/hr
1 kcal/m^2/hr	= 1.16 watt/m^2	= 2.40 Ly/day	= 8.85 BTU/ft^2/day
1 kilopascal	= 10 mb	= 7.69 mm Hg	= 0.303 in Hg
1 mb	= 0.1 kilopascal	= 0.769 mm Hg	= 0.03 in Hg
1 mm Hg	= 1.3 mb	= 0.13 kilopascal	= 0.039 in Hg
1 in Hg	= 33.0 mb	= 25.4 mm Hg	= 3.3 kilopascal

2.4.2 Net short wave Solar Radiation, Q_{sn}

Net short wave solar radiation is the difference between the incident and reflected solar radiations ($Q_s - Q_{sr}$). Techniques are available and described in the aforementioned references to estimate these fluxes as a function of meteorological data. However, in order to account for the reflection, scattering, and absorption incurred by the radiation through interaction with gases, water vapor, clouds, and dust particles, a great deal of empiricism is involved and the necessary data are relatively extensive if precision is desired.

One of the most common simplified formulations for net short wave solar radiation (Anderson, 1954; Ryan and Harleman, 1973) is expressed as:

$$Q_{sn} = Q_s - Q_{sr} \approx 0.94\ Q_{sc}\ (1-0.65C^2) \qquad (2\text{-}56)$$

where Q_{sc} = clear sky solar radiation, kcal/m^2/hr
C = fraction of sky covered by clouds

As reported by Shanahan (1984), Equation (2-56) is an approximation in that it assumes average reflectance at the water surface and employs clear sky solar radiation. In certain circumstances atmospheric attenuation mechanisms are much greater than normal, even under cloudless conditions. For such situations, the more complex formulae described by TVA (1972) are required.

A number of methods are available for estimating the clear sky solar radiation. TVA (1972) presents a formula for Q_{sc} as a function of the geographical location, time of year, and hour of the day. Thackston (1974) and Thompson (1975) report methods for calculating daily average values of solar radiation as a function of latitude, longitude, month, and sky cover. Hamon et al. (1954) have graphed the daily average insolation as a function of latitude, day of year and percent of possible hours of sunshine, and is given in Figure 2-9.

Lombardo (1972) represents the net short wave solar radiation, Q_{sn} (langleys/day), with the following expression:

$$Q_{sn} = (1-R)\ Q_s \qquad (2\text{-}57)$$

where Q_s = short wave radiation at the surface (langleys/day)
R = reflectivity of water = 0.03, or alternately:
R = $A\alpha^B$ (A,B given below in Table 2-10)
= sun's altitude in degrees

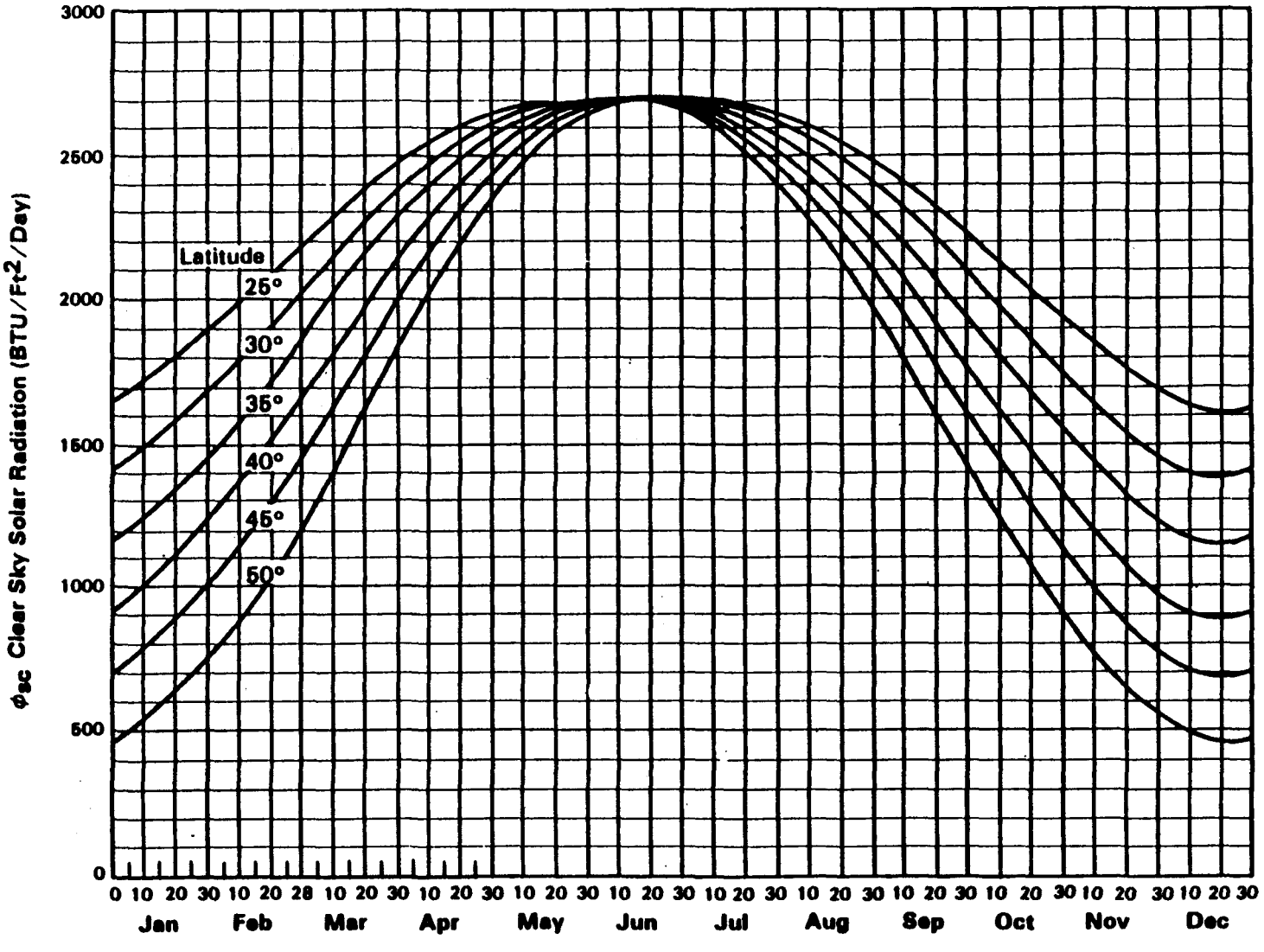

Figure 2-9. Clear sky solar radiation according to Hamon, Weiss and Wilson (1954)

TABLE 2-10. VALUES FOR SHORT WAVE RADIATION COEFFICIENTS A AND B (LOMBARDO, 1972)

Cloudiness	Clear	Scattered	Broken	Overcast
A	1.18	2.20	0.95	0.35
B	-0.77	-0.97	-0.75	-0.45

The WQRRS model by the U.S. Army Corps of Engineers (1974) considers the net short wave solar radiation rate (Q_s - Q_{sr}) as a function of sun angle, cloudiness, and the level of particulates in the atmosphere. Chen and Orlob, as reported by Lombardo (1973), determine the net short wave solar radiation by considering absorption and scattering in the atmosphere.

A final important note on calculation of the net short wave solar radiation regards the effects of shading from trees and banks primarily on stream systems or rivers with steep banks. Shading can significantly reduce the incoming solar radiation to the water surface, resulting in water temperatures much lower than those occurring in unobstructed areas. Jobson and Keefer (1979) present a method to account for the reduction of incoming solar radiation by prescribing geometric relations of vertical obstruction heights and stream widths for each subreach of their model of the Chattahoochee River.

2.4.3 Net Atmospheric Radiation, Q_{an}

The atmospheric radiation is characterized by much longer wavelengths than solar radiation since the major emitting elements are water vapor, carbon dioxide, and ozone. The approach generally adopted to compute this flux involves the empirical determination of an overall atmospheric emissivity and the use of the Stephan-Boltzman law (Ryan and Harleman, 1973). The formula by Swinbank (1963) has been adopted by many investigators for use in various water quality models (e.g., U.S. Army Corps of Engineers, 1974; Chen and Orlob, 1975; Brocard and Harleman, 1976). This

formula was believed to give reliable values of the atmospheric radiation within a probable error to ± 5 percent. Swinbank's formula is:

$$Q_{an} = Q_a - Q_{ar} = 1.16 \times 10^{-13} (1 + 0.17C^2) (Ta + 460)^6 \qquad (2\text{-}58)$$

where Q_{an} = net long wave atmospheric radiation, BTU/ft^2/day
C = cloud cover, fraction
T_a = dry bulb air temperature, ^oF

A recent investigation by Hatfield et al. (1983) has found that the formula by Brunt (1932) gives more accurate results over a range of latitudes of 26°13'N to 47°45'N and an elevation range of -30m to + 3,342m. Brunt's formula is:

$$Q_{an} = 2.05 \times 10^{-8} (1 + 0.17C^2)(T_a + 460)^4 (1 + 0.149\sqrt{e_2}) \qquad (2\text{-}59)$$

where Q_{an} = net long wave atmospheric radiation, BTU/ft^2/day
e_2 = the air vapor pressure 2 meters above the water surface, mm Hg
T_a = air temperature 2 meters above the water surface, ^oF

2.4.4 Long Wave Back Radiation, Q_{br}

The long wave back radiation from the water surface is usually the largest of all the fluxes in the heat budget (Ryan and Harleman, 1973). Since the emissivity of a water surface (0.97) is known with good precision, this flux can be determined with accuracy as a function of the water surface temperature:

$$Q_{br} = 0.97\, \sigma\, T_s^4 \qquad (2\text{-}60)$$

where Q_{br} = long wave back radiation, cal/m^2/sec
T_s = surface water temperature, ^oK
σ = Stefan-Boltzman constant $= 1.357 \times 10^{-8}$, cal/m^2/sec/$^oK^4$

The U.S. Army Corps of Engineers (1974) uses the following linearization of Equation (2-60) to express the back radiation emitted by the water body:

$$Q_{br} = 73.6 + 1.17\ T \qquad (2\text{-}61)$$

where T = water temperature, ^{o}C

In the range of 0° to $30^{o}C$, this linear function has a maximum error of less than 2.1 percent relative to Equation (2-60).

2.4.5 Evaporative Heat Flux, Q_e

Evaporative heat loss occurs as a result of the change of state of water from a liquid to vapor, requiring sacrifice of the latent heat of vaporization. The basic formulation used in all heat budget formulations (e.g., Ryan and Harleman, 1973; U.S. Army Corps of Engineers, 1974; Chen and Orlob, 1975; Lombardo, 1972) is:

$$Q_e = \rho L_w E \qquad (2\text{-}62)$$

where Q_e = heat loss due to evaporation, $kcal/m^2/sec$
ρ = fluid density, kg/m^3
L_w = latent heat of vaporization, kcal/kg
or $L_w = 597 - 0.57\ T_s$
E = evaporation rate, m/sec
T_s = surface water temperature, ^{o}C

The general expression for evaporation from a natural water surface is usually written as:

$$E = (a + bW)\ (e_s - e_a) \qquad (2\text{-}63)$$

where a,b = empirical coefficients

W = wind speed at some specified elevation above water surface, m/sec

e_s = saturation vapor pressure at the surface water temperature, mb

e_a = vapor pressure of the overlying atmosphere, mb

Various approaches have been used to evaluate the above expression. In a very simplified approach, the empirical coefficient, a, has often been taken to be zero, while b ranges from 1×10^{-9} to 5×10^{-9} (U.S. Army Corps of Engineers, 1974). The value of e_s is a nonlinear function of the surface water temperature. However e_s can be estimated in a piecewise linear fashion as follows:

$$e_s = \alpha_i + \beta_i T_s \tag{2-64}$$

where α_i, β_i = empirical coefficients with values as given in Table 2-11.

T_s = surface water temperature, ^oC

TABLE 2-11. VALUES FOR EMPIRICAL COEFFICIENTS

Temperature Range, ^oC	α_i	β_i
0-1	6.05	0.522
5-10	5.10	0.710
10-15	2.65	0.954
15-20	-2.04	1.265
20-25	-9.94	1.659
25-30	-22.29	2.151
30-35	-40.63	2.761
35-40	-66.90	3.511

A more convenient formula for the saturation vapor pressure, e_s, is presented by Thackston (1974) as follows:

$$e_s = \exp\left[17.62 - 9501/(T_s + 460)\right] \tag{2-65}$$

where e_s = saturation vapor pressure at the surface water temperature, in Hg

T_s = water temperature, ^oF

The standard error of prediction of Equation (2-55) is reported by Thackston (1974) to be 0.00335.

A large number of evaporation formula exist for a natural water surface, as demonstrated in Table 2-12 (Ryan and Harleman, 1973). Detailed comparisons of these formulae by the above authors showed that the discrepancies between these formulae were not significant. Both Ryan and Harleman (1973), and TVA (1968) recommend the use of the Lake Hefner evaporation formula developed by Marciano and Harbeck (1954), which has the best data base, and has been shown to perform satisfactorily for other water bodies. The Lake Hefner formula is written as:

$$Q_e = 17\ W_2\ (e_s - e_2) \qquad (2\text{-}66)$$

where Q_e = heat loss due to evaporation, BTU/ft^2/day

W_2 = wind speed at 2 meters above surface, mph

e_s = saturated vapor pressure at the surface water temperature, mm Hg

e_2 = vapor pressure at 2 meters above surface, mm Hg

It is important to note that the Lake Hefner formula was developed for lakes and may not be universally valid for streams or open channels due to physical blockage of the wind by trees, banks, etc.; and due to differences in the surface turbulence which affects the liquid film aspects of evaporation (McCutcheon, 1982). Jobson developed a modified evaporation formula which was used in temperature modeling of the San Diego Aqueduct (Jobson, 1980) and the Chattahoochee River (Jobson and Keefer, 1981). This formula is written as:

$$E = 3.01 + 1.13\ W\ (e_s - e_a) \qquad (2\text{-}67)$$

TABLE 2-12. EVAPORATION FORMULA FOR LAKES AND RESERVOIRS
(RYAN AND HARLEMAN, 1973)

Name	Formula in Original Form	Units*	Observation Levels	Time Increments	Water Body	Formula at sea-level Meas. Ht. Spec. Units BTU/ft2/day mph, mm Hg	Remarks
Lake Hefner	$E=6.25\cdot10^{-4}W_8(e_s-e_8)$	cm/3 hr knots mb	8m-wind 8m-e_a	3 hrs Day	Lake Hefner Oklahoma 2587 acres	$12.4W_8(e_s-e_8)$ $17.2W_2(e_s-e_2)$	Good agreement with Lake Mead, Lake Eucumbene, Russian Lakes.
Kohler	$E=.00304W_4(e_s-e_2)$	in./day miles/day in. Hg	4m-wind 2m-e_a	Day	Lake Hefner Oklahoma 2587 acres	$15.9W_4(e_s-e_2)$ $17.5W_2(e_s-e_2)$	Essentially the same as the Lake Hefner Formula.
Zaykov	$E=[.15+.108W_2](e_s-e_2)$	mm/day m/s mb	2m-wind 2m-e_a		Ponds and small reservoirs	$(43+14W_2)(e_s-e_2)$	Based on Russian experience. Recommended by Shulyakovskiy
Meyer	$E=10(1+.1W_8)(e_s-e_8)$	in./month mph in. Hg	25 ft-wind 25 ft-e_a	Monthly	Small lakes and reservoirs	$(73+7.3W_3)(e_s-e_8)$ $(80+10W_2)(e_s-e_2)$	e_a is obtained daily from mean morning and evening measurements of T_a, R_H. Increase constants by 10% if average of maximum and minimum used.
Morton	$E=(300+50W)(e_s-e_a)/p$	in./month mph in. Hg	8m-wind 2m-e_a	Monthly	Class A pan	$(73.5+12.2W_8)(e_s-e_2)$ $(73.5+14.7W_2(e_s-e_2)$	Data from meteorological stations. Measurement heights assumed.
Rohwer	$E=.771[1.465-.0186B]\times[.44+.118W](e_s-e_a)$ where B=atmos. press.	in./day mph in. Hg	0.5-1 ft-wind 1 inch-e_a	Daily	Pans 85 ft diameter tank 1300 acre Reservoir	$(67+10W_2)(e_s-e_2)$	Extensive pan measurements using several types of pans. Correlated with tank reservoir data.

*For each formula, the units are for evaporation rate, wind speed, and vapor pressure.

where E is in mm/day

W = wind speed at some specified elevation above the water surface, m/sec

e_a = vapor pressure at the same elevation as the wind, kilopascals

e_s = saturation vapor pressure at the water surface temperature, kilopascals

It is noted that the wind speed function of Equation (2-67) was reduced by 30 percent during calibration of the temperature model for the Chattahoochee River (McCutcheon, 1982). The original Equation (2-67) was developed for the San Diego Aqueduct which represented substantially different climactic and exposure conditions than for the Chattahoochee River. McCutcheon (1982) notes that the wind speed function is a catchall term that must compensate for a number of difficulties which include, in part:

- Numerical dispersion in some models.
- Inaccuracies in the measurement and/or calculation of wind speed, solar and long-wave radiation, air temperature, cloud cover, and relative humidity.
- Effects of wind direction, fetch, channel width, sinuosity, bank and tree height.
- Effects of depth, turbulence, and lateral velocity distribution.
- Stability of the air moving over the stream.

2.4.6 Convective Heat Flux, Q_c

Convective heat is transferred between air and water by conduction and transported away from (or toward) the air-water interface by convection

associated with the moving air mass. The convective heat flux is related to the evaporative heat flux, Q_e, through the Bowen ratio:

$$R = \frac{Qc}{Qe} = (6.19 \times 10^{-4})\ p \left| \frac{T_s - T_a}{e_s - e_a} \right| \qquad (2\text{-}68)$$

where R = Bowen Ratio

p = atmospheric pressure, mb

T_a = dry bulb air temperature, ^oC

T_s = surface water temperature, ^oC

e_s = saturation vapor pressure at the surface water temperature, mb

e_a = vapor pressure of the overlying atmosphere, mb

The above formulation is used in the surface heat transfer budget of several models (e.g., U.S. Army Corps of Engineers, 1974; Brocard and Harleman, 1976).

2.4.7 Equilibrium Temperature and Linearization

The preceding paragraphs present methods for estimating the magnitudes of the various components of heat transfer through the water surface. Several of these components are nonlinear functions of the surface water temperature, T_s. Thus, they are most appropriately used in transient water quality simulations where the need to predict temperature variations is on the time scale of minutes or hours. However, for long term water quality simulations or for steady state simulations, it is more economical to use a linearized approach to heat transfer. As developed by Edinger and Geyer (1965), and reported by Ryan and Harleman (1973), this approach involves two concepts, that of equilibrium temperature, T_E, and surface heat exchange, K, where H can now be written as:

$$H = K\ (T_s - T_E) \qquad (2\text{-}69)$$

The equilibrium temperature, T_E, is defined as that water surface temperature which, for a given set of meteorological conditions, causes the surface heat flux H, to equal zero. The surface heat exchange coefficient, K, is defined to give the incremental change of net heat exchange induced by an incremental change of water surface temperature. It varies with the surface temperature and thus should be recalculated as the water temperature changes.

2.4.7.1 Equilibrium temperature, T_E

The equilibrium temperature T_E is the temperature toward which every water body at the site will tend, and is useful because it is dependent solely upon meteorological variables at a given site. A water body at a surface temperature, T_w, less than T_E, will have a net heat input and thus will tend to increase its temperature. The opposite is true if $T_w > T_E$. Thus, the equilibrium temperature embodies all the external influences upon ambient temperatures.

Certain formulations for the equilibrium temperature have been developed which require an iterative or trial and error solution approach (Ryan and Harleman, 1973). An approximate formula for obtaining T_E has been developed by Brady et al. (1969) which has been shown to yield fairly accurate results:

$$T_E = \frac{Q_{sn}}{23 + f(W)\ (\beta + .255)} + T_d \qquad (2\text{-}70)$$

where Q_{sn} = net short wave solar radiation, BTU/ft^2/day

T_d = dew point temperature of air, ^oF

$f(w)$ = empirical wind speed relationship

= $17W_2$ (based on Lake Hefner data), BTU/ft^2/day/mm Hg

β = proportionality factor which is a function of temperature, mm Hg/^oF

W_2 = wind speed at 2 meters above surface, mph

The expression for β is written as:

$$\beta = .255 - .0085\ T^* + .000204\ T^{*2} \qquad (2\text{-}71)$$

where

$$T^* = \frac{1}{2}\ (T_w + T_d) \qquad (2\text{-}72)$$

2.4.7.2 Surface Heat Exchange Coefficient, K

The surface heat exchange coefficient, K, relates the net heat transfer rate to changes in water surface temperature. An expression for K developed by Brady et al. (1969), (and reported by Ryan and Harleman, 1973) is:

$$K = 23 + (\beta_w + .255)\ 17W_2 \qquad (2\text{-}73)$$

where W_2 = wind speed at 2 meters, mph

and β_w is evaluated at T_w based on Equation (2-62):

$$\beta_w = .255 - .0085\ T_w + .000204\ T_w^2 \qquad (2\text{-}74)$$

Charts giving K as a function of water surface temperature and wind speed are given by Ryan and Stolzenbach (1972), assuming an average relative humidity of 75 percent. Shanahan (1984) presents a calculation procedure to determine T_E and K from average meteorological data.

2.4.8 Heat Exchange with the Stream Bed

For most lakes, estuaries, and deep rivers, the thermal flux through the bottom is insignificant. However, as reported by Jobson (1980) and Jobson and Keefer (1979), the bed conduction term may be significant in determining the diurnal variation of temperatures in water bodies with depths of 10 ft (3m) or less. Jobson (1977) presents a procedure for accounting for bed conduction which does not require temperature measurements within the bed. Rather, the procedure estimates the heat

exchange based on the gross thermal properties of the bed, including the thermal diffusivity and heat storage capacity. The inclusion of this method improved dynamic temperature simulation on the San Diego Aqueduct and the Chattahoochee River.

2.4.9 Summary

The previous section has presented a brief summary of the most frequently used formulations for surface heat exchange in numerical water quality models. These formulations are widely used and have been shown to work quite well within the normal range of meteorological and surface water conditions, provided a reasonably complete data base is available on meteorological conditions at the site of interest. Meteorological data requirements include atmospheric pressure, cloud cover, and at a known surface elevation: wind speed and direction, relative humidity, and wet and dry bulb air temperatures. Shanahan (1984) presents a useful summary of meteorological data requirements for surface heat exchange computations.

2.5 REFERENCES

Anderson, D.R., J.A. Dracup, T.J. Fogarty, and R. Willis. 1976. Water Quality Modeling of Deep Reservoirs, J. Water Pollution Control Federation, Vol. 48, No. 1.

Anderson, E.R. 1954. Energy Budget Studies, Part of Water Loss Investigations - Lake Hefner Studies. USGS Prof. Paper 269.

Baca, R.G. and R.C. Arnett. 1976. A Limnological Model for Eutrophic Lakes and Impoundments, Battelle Inc., Pacific Northwest Laboratories, Richland, Washington.

Bajraktarevic-Dobran, H. 1982. Dispersion in Mountainous Natural Streams. Journal of the Environmental Engineering Division, ASCE. Vol. 108, No. EE3, pp. 502-514.

Bansal, M.K. 1971. Dispersion in Natural Streams. Journal of Hydraulics Division, ASCE. Vol. 97, No. HY 11, pp. 1867-1886.

Beer, T. and P.C. Young. 1983. Longitudinal Dispersion in Natural Streams. Journal of Environmental Engineering, ASCE. Vol. 109, No. 5, pp. 1049-1067.

Bella, D.A. and W.J. Grenney. 1970. Finite-Difference Convection Errors. Journal of the Sanitary Engineering Division, ASCE, Vol. 96, No. SA6, pp. 361-1375.

Beltaos, S. 1978a. Mixing Processes in Natural Streams. In: Transport Processes and River Modeling Workshop. Canada Center for Inland Water.

Beltaos, S. 1978b. Transverse Mixing in Natural Streams, Transportation and Surface Water Engineering Div., Alberta Research Council, Report No. SWE-78/01.

Beltaos, S. 1978c. An Interpretation of Longitudinal Dispersion Data in Rivers. Transportation and Surface Water Engineering Div., Alberta Research Council, Report No. SWE-78/03.

Beltaos, S. 1980a. Longitudinal Dispersion in Rivers. Journal of the Hydraulics Division, ASCE. Vol. 106, No. HY1, pp. 151-172.

Beltaos, S. 1980b. Transverse Mixing Tests in Natural Streams. Journal of the Hydraulics Division, ASCE. Vol. 106, No. HY10, pp. 1607-1625.

Beltaos, S. 1982. Dispersion in Tumbling Flow. Journal of the Hydraulics Division, ASCE. Vol. 108, No. HY4., pp. 591-612.

Benedict, B.A. 1978. Review of Toxic Spill Modeling, Department of Civil Engineering, Tulane University.

Bird, R.B., W.E. Stewart, and E.N. Lightfoot. 1960. Transport Phenomena. John Wiley and Sons, Inc.

Blumberg, A.F. 1977. Numerical Model of Estuarine Circulation, ASCE, Journal of the Hydraulics Division, Vol. 103, No. HY3, Proc. Paper 12815, pp. 295-310.

Blumberg, A.F. and G.L. Mellor. 1978. A Coastal Ocean Numerical Model. Submitted to the Proceedings of the Symposium on "Mathematical Modelling of Estuarine Physics," Springer-Verlag.

Brady, D.K., W.L. Graves, and J.C. Geyer. 1969. Surface Heat Exchange at Power Plant Cooling Lakes, Cooling Water Studies for Edison Electric Institute, Report No. 5, John Hopkins University, November 1969.

Brocard, D.N. and D.R.F. Harleman. 1976. One-Dimensional Temperature Predictions in Unsteady Flows. Journal of the Hydraulics Division, ASCE, No. HY3, Proc: Paper 11982, March, 1976.

Brunt, D. 1932. Notes on Radiation in the Atmosphere. Quarterly Journal of the Royal Meteorological Society, Vol. 58, pp. 389-418.

CE-QUAL-R1. 1982. A Numerical One-Dimensional Model of Reservoir Water Quality. User's Manual. U.S. Army Corps of Engineers, Waterways Experiment Station, Environmental and Water Quality Operational Studies, Instruction Report E-82-1.

Chatwin, P.C. 1980. Presentation of Longitudinal Dispersion Data. Journal of the Hydraulics Division, ASCE. Vol. 106, No. HY1, pp. 71-83.

Chen, C.W. and G.T. Orlob. 1972. Ecologic simulation for Aquatic Environments. WRE, Inc., Walnut Creek. Final Rep. to OWRR, December 1972, pp. 156.

Chen, C.W. and G.T. Orlob. 1975. Ecologic Simulation for Aquatic Environments, In: Systems Analysis and Simulation in Ecology, Vol. 3, B.C. Patten, ed., Academic Press, San Francisco, pp. 475-588.

Chen, C.W. and J. Wells. 1975. Boise River Water Quality-Ecological Model for Urban Planning Study, Tetra Tech technical report prepared by U.S. Army Engineering District, Walla Walla, Wash., Idaho Water Resources Board, and Idaho Dept. of Environmental and Community Services.

Chen, H.S., Lukens, R.J , and C.S. Fang. 1979. A Two-Dimensional Hydrodynamic and Biogeochemical Water Quality Model and Its Application to the Lower James River. Special Report No. 183 in Applied Marine Science and Ocean Engineering, Virginia Institute of Marine Science, Gloucester Pt., VA.

Christodoulou, G.C. and B.R. Pearce. 1975. Mathematical Modeling Relevant to the Glass Bead Study. R.M. Parsons Lab., MIT, Cambridge, Massachusetts.

Christodoulou, G.C., Connor, J.J. and B.R. Pearce. 1976. Mathematical Modeling of Dispersion in Stratified Waters. R.M. Parsons Laboratory, MIT, Technical Report No. 219.

Cooperative Instream Flow Service Group. 1981. Description and Application of the Stream Simulation and Assessment Model: Version IV (SSAMIV), Instream Flow Information Paper: No. 17.

Cotton, A.P. and J.R. West. 1980. Field Measurement of Transverse Diffusion in Undirectional Flow in a Wide, Straight Channel. Water Research. Vol. 14, pp. 1597-1604.

Csanady, G.T. 1973. Turbulent Diffusion in the Environment. D. Reidel Publ. Co.

Dailey, J.E. and D.R.F. Harleman. 1972. Numerical Model for the Prediction of Transient Water Quality in Estuary Networks. R.M. Parsons Laboratory, MIT, Technical Report No. 158.

Day, T.J. 1975. Longitudinal Dispersion in Natural Channels. Water Resources Research. Vol. 11, No. 6, pp. 909-918.

Day, T.J. and I.R. Wood. 1976. Similarity of the Mean Motion of Fluid Particles Disposing in a Natural Channel. Water Resources Research. Vol. 12, No. 4, pp. 655-666.

Delft Hydraulics Laboratory. 1979. Momentum and Mass Transfer in Stratified Flows. Report R880, 2nd Printing, Delft, the Netherlands.

Demetracopoulous, A.C. and H.G. Stefan. 1983. Transverse Mixing in Wide and Shallow River: Case Study. Journal of Environmental Engineering Division, ASCE. Vol. 109, No. 3, pp. 685-699.

Edinger, J.E. and E.M. Buchak. 1979. A Hydrodynamic Two-Dimensional Reservoir Model: Development and Test Application to Sutton Reservoir, Elk River, West Virginia, Prepared for U.S. Army Engineering Division, Ohio River, Cincinnati, Ohio, Contract No. DACW 27-76-C-0089.

Edinger, J.R. and J.C. Geyer. 1965. Cooling Water Studies for Edison Electric Institute, Project No. RP-49.

Edinger, J.E., D.K. Brady, and J.C. Geyer. 1974. Heat Exchange and Transport in the Environment. Report No. 14, Research Project RP-49. Electric Power Research Institute, Palo Alto, CA.

Elhadi, N. and K. Davar. 1976. Longitudinal Dispersion for Flow Over Rough Beds. Journal of the Hydraulics Division, ASCE. Vol. 102, No. HY4, pp. 483-498.

Elhadi, N., A. Harrington, I. Hill, Y.L. Lau, B.G. Krishnappan. 1984. River Mixing - A State-of-the-Art Report. Canadian Journal of Civil Engineering. Vol. 11, No. 11, pp. 585-609.

Elder, J.W. 1959. The Dispersion of Marked Fluid in Turbulent Shear Flow. Journal of Fluid Mechanics, Vol. 5, pp. 544-560.

Engmann, J.E.O. and R. Kellerhals. 1974. Transverse Mixing in an Ice-Covered River, Water Resources Res., Vol. 10, No. 4.

Feigner, K.D. and H.S. Harris. 1970. Documentation Report FWQA Dynamic Estuary Model, Federal Water Quality Administration, Washington, D.C., 248 p.

Fischer, H.B. 1966. Longitudinal Dispersion in Laboratory and Natural Streams. W.M. Keck Lab Report No. KH-12-12, California Institute of Technology.

Fischer, H.B. 1967a. The Mechanics of Dispersion in Natural Streams. Journal of the Hydraulics Division, ASCE, Vol. 93, No. HY6, pp. 187-216.

Fischer, H.B. 1967b. Dispersion Predictions in Natural Streams. Journal of the Sanitary Engineering Division, ASCE, Vol. 94, No. SA5, pp. 927-943.

Fischer, H.B. 1968. Methods for Predicting Dispersion Coefficients in Natural Streams, with Application to Lower Reaches of the Green and Dunwamish Rivers, Washington. U.S. Geological Survey Professional Paper 582-A.

Fischer, H.B. 1972. A Lagrangian Method for Predicting Pollutant Dispersion in Bolinas Lagoon, Marin County, California. U.S. Geological Survey Professional Paper 582-B.

Fischer, H.B. 1975. Discussion of: Simple Method for Predicting Dispersion in Streams. ASCE, Journal of Environmental Engineering Division. Vol. 101, No. EE3, pp. 453-455.

Fischer, H.B. 1977. A Numerical Model of the Suisun Marsh, California, Proceedings of the 17th Congress, International Association for Hydraulic Research, Baden-Baden, Germany 3, pp. 425-432.

Fischer, H.B., E.J. List, R.C.Y. Koh, J. Imberger, and N.H. Brooks. 1979. Mixing in Inland and Coastal Waters. Academic Press, New York. 483 p.

Ford, D.E. and K.W. Thornton. 1979. Time and Length Scales for the One-Dimensional Assumption and Its Relation to Ecological Models. Water Resources Res., Vol. 15, No. 1, pp. 113-120.

Ford, D.E. and H.G. Stefan. 1980. Thermal Predictions Using Integral Energy Model. Journal of the Hydraulics Division, ASCE. Vol. 106, No. HY1, pp. 39-55.

French, R.H. 1983. Lake Modeling: State of the Art. In: CRC Critical Reviews in Environmental Control, Vol. 13, Issue 4, pp. 311-357.

Fukuoka, S. and W.W. Sayre. 1973. Longitudinal Dispersion in Sinuous Channels. Journal of the Hydraulics Division, ASCE, Vol 99, No. HY1, pp. 195-217.

Glover, R.E. 1964. Dispersion of Dissolved or Suspended Materials in Flowing Streams, U.S. Geological Survey Professional Paper 433-13.

Godfrey, R.G. and B.J. Frederick. 1970. Streams Dispersion at Selected Sites. U.S. Geological Survey Professional Papers 433-K.

Gowda, T.P.H. 1978. Field Tests on Transverse Dispersion of Effluents in Streams. In: Transport Processes and River Modeling Workshop, Canada Center from Inland Waters.

Gowda, T.P.H. 1980. Stream Tube Model for Water Quality Prediction in Mixing Zones of Shallow Rivers, Water Resources Paper 14, Water Resources Branch, Ontario Ministry of the Environment, Toronto, Canada, July, 1980. 141 pp.

Gowda, T.P.H. 1984. Critical Point Method for Mixing Zones in Rivers. Journal Environmental Engineering Division, ASCE. Vol. 110, No. 1, pp. 244-262.

Hamdy, Y.S. and J.D. Kinkead. 1979. Waste Dispersion in the St. Clair River, St. Clair River Organics Study Technical Report, Water Resources Branch, Ontario Ministry of the Environment, Toronto, Canada, pp. 27.

Hamon, R.W., L.L Weiss, and W.T. Wilson. 1954. Insulation as an Empirical Function of Daily Sunshine Duration. Monthly Weather Review, Vol 82, No. 6.

Harleman, D.R.F., J.E. Dailey, M.L. Thatcher, T.O. Najarian, D.N. Brocard, and R.A. Ferrara. 1977. User's Manual for the M.I.T. Transient Water Quality Network Model--Including Nitrogen-Cycle Dynamics for Rivers and Estuaries, R.M. Parsons Laboratory, MIT, for U.S. Environmental Protection Agency, Corvallis, OR. EPA-600/3-77-110.

Harleman, D.R.F. 1982. Hydrothermal Analysis of Lakes and Reservoirs. Journal of the Hydraulics Division, ASCE. Vol. 108, No. HY3, pp. 302-325.

Harper, W.L. and W.R. Waldrop. 1981. A Two-Dimensional Laterally Averaged Hydrodynamic Model with Application to Cherokee Reservoir. Proceedings of the Symposium on Surface Water Impoundments, ASCE, pp. 508-517.

Hatfield, J.L., R.J Reginato, and S.B. Idso. 1983. Comparison of Long-Wave Radiation Calculation Methods Over the United States. Water Resources Research, Vol. 19, No. 1, pp. 285-288.

Hays, J.R., P.A.Krenkel, and K.B. Schnelle. 1966. Mass Transport Mechanisms in Open-Channel Flow, Tech. Report No. 8, Sanitary and Water Resources Engineering, Vanderbilt Univ. Nashville, TN.

Heinrich, J.C., W.J. Lick, and J.F. Paul. 1981. Temperatures and Currents in a Stratified Lake: A Two-Dimensional Analysis. Journal of Great Lakes Research, Vol. 7, No. 3, pp. 264-275.

Henry, J.F. and E.G. Foree. 1979. Dispersion Modeling in Time and Two Dimensions. Journal of the Enviornmental Engineering Division, ASCE, Vol. 105, No. EE6, pp. 1131-1147.

Hinwood, J.B. and I.G. Wallis. 1975. Review of Models of Tidal Waters, Journal of the Hydraulics Division, ASCE, Vol. 101, No. HY11, Proc. Paper 11693.

Holley, E.R., D.R.F. Harleman, and H.B. Fischer. 1970. Dispersion in Homogeneous Estuary Flow. Journal of the Hydraulics Division, ASCE, Vol. 96, No. HY8, pp. 1691-1709.

Holley, E.R. and G. Abraham. 1973. Field Tests and Transverse Mixing in Rivers. Journal of the Hydraulics Division, ASCE. Vol. 99, No. HY12, pp. 2313-2331.

Holly, F.M. 1975. Two-Dimensional Mass Dispersion in Rivers. Hydrology Paper 1978. Colorado State University.

Holly, F.M. and G. Neart. 1983. Field Calibration of Stream Tube Dispersion Model. Journal of Hydraulic Engineering, ASCE Vol. 109, No. 11, pp. 1455-1470.

Hurley-Octavio, K.A., G.H. Jirka, D.R.F. Harleman. 1977. Vertical Heat Transport Mechanisms in Lakes and Reservoirs. Ralph M. Parsons Laboratory, MIT, Technical Report No. 227.

Hydrologic Engineering Center. 1974. Water Quality for River Reservoir Systems. Generalized Computer Programs, 401-F2-L2100A. U.S. Army Corps of Engineers, Davis, CA.

Hydroscience, Inc. 1971. Simplified Mathematical Modeling of Water Quality, Environmental Protection Agency Water Programs.

Imberger, J., J. Patterson, B. Hebbert, and I. Loh. 1977. Simulation of the Dynamics of a Reservoir of Medium Size.

Jobson, H.E. 1977. Bed Conduction Computation for Thermal Models. Journal of the Hydraulics Division, ASCE, Vol. 103, No. HY10, pp. 1213-1217.

Jobson, H.E. and T.N. Keefer. 1979. Modeling Highly Transient Flow, Mass, and Heat Transport in the Chattahoochee River near Atlanta, Georgia. U.S. Geological Survey Professional Paper 1136.

Jobson, H.E. 1980. Thermal Modeling of Flow in the San Diego Aqueduct, California, and its Relation to Evaporation. U.S. Geological Survey Professional Paper 1122.

Jobson, H.E. 1980a. Temperature and Solute Transport Simulation in Streamflow using a Lagrangian Reference Frame, U.S. Geological Survey Water Resources Investigations 81-2, NSTL Station, MS.

Jobson, H.E. 1980b. Comment on 'A New Collocation Method for the Solution of the Convection-Dominated Transport Equation,' Water Res. Research, Vol. 16, No. 6, pp. 1135-1136.

Jobson, H.E. 1985. Simulating Unsteady Transport of Nitrogen, Biochemical Oxygen Demand, and Dissolved Oxygen in the Chattahoochee River Downstream of Atlanta, Georgia, USGS, WSP 2264.

Jobson, H.E. and R.E. Rathbun. 1985. Use of the Routing Procedure to Study Dye and Gas Transport in the West Fork Trinity River, Texas, USGS, WSP 2252.

Johanson, P., D. Smith, F. Haydock, and M. Lorenzen. 1977. Documentation Report for the Estuary Water quality Models, Tetra Tech Report TC-661, Lafayette, California.

Johnson. B. 1984. A Review of Multi-Dimensional Numerical Modeling of Reservoir Hydrodynamics. U.S. Army Corps of Engineers, Waterways Experiment Station.

Kent, R.E. and D.W. Pritchard. 1959. A Test of Mixing Length Theories in a Coastal Plain Estuary. Journal of Marine Research, Vol 13, No. 1, pp. 62-72.

King, I.P. 1982. A Finite Element Model for Three-Dimensional Flow. Resource Management Associates, Lafayette, CA. USCOE Contract No. DACW39-79-C-0079, Waterways Experiment Station, Vicksburg, MS.

Krenkel, P.A. 1960. Turbulent Diffusion and Kinetics of Oxygen Absorption. Dissertation presented to University of California, Berkeley.

Krishnappan, B.G. and Y.L. Lau. 1977. Transverse Mixing in Meandering Channels with Varying Bottom Topography, Journal of the Hydraulics Res., IAHR, Vol. 15, No. 4.

Krishnappan, B.G. and Y.L. Lau. 1982. User's Manual: Prediction of Transverse Mixing in Natural Streams - RIVMIX. National Water Research Institute. Canada Centre for Inland Waters.

Kullenberg, G.E.B. 1971. Results of Diffusion Experiments in the Upper Region of the Sea. Kobenhavns Universitet, Institut for Fysisk Oceanografi, Report No. 12, March 1971, Copenhagen, Denmark.

Kullenberg, G., C.R. Murthy, and H. Westerberg. 1973. An Experimental Study of Diffusion Characteristics in the Thermocline and Hypolimnion Regions of Lake Ontario. Internat. Assoc. Great lakes Research, Conf. Proc., 16, pp. 774-790.

Lam, D.C.L. and J.M. Jacquet. 1976. Computations of Physical Transport and Regeneration of Phosphorus in Lake Erie, Journal of the Fisheries Research Board of Canada, Vol. 33, No. 3, pp. 550-563.

Lau, Y.L. and B.G. Krishnappan. 1977. Transverse Dispersion in Rectangular Channels, Journal of the Hydraulics Division, ASCE, Vol. 103. No. HY10, Proc. Paper 13294, pp. 1173-1189.

Lau, Y.L. and B.G. Krishnappan. 1981. Modeling Transverse Mixing in Natural Streams. Journal of the Hydraulics Division, ASCE. Vol. 107, No. HY2, pp. 209-226.

Lerman, Abraham. 1971. Time to Chemical Steady-States in Lakes and Oceans, Advances in Chem. Series, Vol. 106 (Nonequilibrium Systems in Natural Water Chemistry).

Leendertse, J.J. 1970. A Water Quality Simulation Model for Well-Mixed Estuaries and Coastal Seas: Vol. I, Principles of Computation, Rand Corp., RM-6230-RC. Santa Barbara, CA.

Leenderste, J.J. and S.K. Liu. 1975. A 3-D Model for Estuaries and Coastal Seas: Vol. II, Aspects of Computation, Rand Corp., R-1764-OWRT. Santa Barbara, CA.

Lick, W., J. Paul and Y.P. Sheny. 1976. The Dispersion of Contaminants in the Nearshore Region. In: Mathematical Modeling of Biochemical Processes in Aquatic Ecosystems. R.P. Canale, Ed., Ann Arbor Science.

Liu, H. 1977. Predicting Dispersion Coefficient of Streams. Journal of the Environmental Engineering Division, ASCE. Vol. 103, No. EE1, pp. 59-69.

Liu, H. and A.H.D. Cheng. 1980. Modified Fickian Model for Predicting Dispersion. Journal of the Hydraulics Division, ASCE. Vol. 106, HY6, pp. 1021-1040.

Li, W. 1972. Effects of Dispersion on DO-sag in Uniform Flow. Journal of Sanitary Engineering Division, ASCE. Vol. 98, No. SA1, pp. 169-182.

Lombardo, P.S. 1972. Mathematical Model of Water Quality in Rivers and Impoundments, Technical Report, Hydrocomp, Inc.

Lombardo, P.S. 1973. Critical Review of Currently Available Water Quality Models, Hydrocomp, Inc., Technical Report, Contract No. 14-31-0001-3751.

Marciano and Harbeck. 1954. Mass Transfer Studies Water Loss Investigations: Lake Hefner. U.S. Geological Survey Prof. Paper 269.

Markofsky, M. and D.R.F. Harleman. 1973. Prediction of Water Quality in Stratified Reservoirs. Journal of the Hydraulics Division, ASCE, Vol. 99, No. HY5, Proc. Paper 9030, p. 729.

McBride, G.B. and J.C. Rutherford. 1984. Accurate Modeling of River Pollutant Transport, ASCE Journal of the Environmental Engineering Division, Vol. 110, No. 4, pp. 808-827.

McCormick, M.J. and D. Scavia. 1981. Calculation of Vertical Profiles of Lake-Averaged Temperature and Diffusivity in Lakes Ontario and Washington. Water Resources Research, Vol. 17, No. 2, pp. 305-310.

McCutcheon, S.C. 1982. Discussion with Harvey Jobson on Windspeed Coefficients for Stream Temperature Modeling. U.S. Geological Survey Memorandum, WRD, GCHC, NSTL Station, MS, March 29, 1982.

McCutcheon, S.C. 1983. Vertical Mixing in Models of Stratified Flow. Proceedings of the Conference on "Frontiers in Hydraulic Engineering," ASCE, pp. 15-20.

McQuivey, R.S. and T.N. Keefer. 1974. Simple Method for Predicting Dispersion in Streams. Journal of Environmental Engineering Division. Vol. 100, No. EE4, pp. 997-1011.

McQuivey, R.S. and T.N. Keefer. 1976a. Conservative Model of Longitudianl Dispersion. Journal of the Hydraulics Division, ASCE, Vol. 102, No. HY10, pp. 1409-1424.

McQuivey, R.S. and T.N. Keefer. 1976b. Dispersion-Mississippi River Below Baton Rouge, Louisiana. Journal of the Hydraulics Division, ASCE, Vol. 102, No. HY10, pp. 1426-1437.

Mescal, M.A. and R.G. Warnock. 1978. Field Study of Lateral Dispersion in the Ottawa River. In: Transport Processes and River Modeling Workshop, Canada Center for Inland Waters.

Meyer, W. 1977. Transverse Mixing in the Mobile River, Alabama. Journal of Research, U.S. Geological Survey, Vol. 5, No. 1.

Miller, A.C. and E.V. Richardson. 1974. Diffusional Dispersion in Open Channel Flow. Journal of the Hydraulics Division, ASCE. Vol. 100, No. HY1, pp. 159-171.

Munk, W.H. and E.R. Anderson. 1948. Notes on a Theory of the Thermocline. Journal of Marine Research, Vol 7, No. 3, pp. 276-295.

Murthy, C.R. and A. Okubo. 1977. Interpretation of Diffusion Characteristics of Oceans and Lakes Appropriate for Numerical Modeling. In: Symposium on Modeling of Transport Mechanisms in Oceans and Lakes, Marine Sciences Directorate, Dept. of Fisheries and the Environment, Manuscript Report Series No. 43, Ottawa, Canada.

Najarian, Thatcher & Associates, Inc. 1980. Review of Dynamic Estuarine Water Quality and Ecologic Models Applicable to the Chesapeake Bay Network, prepared for U.S. Environmental Protection Agency, Athens, Georgia.

Najarian, T.O., D.P. Wang, and P.S. Huang. 1982. Lagrangian Transport in Estuaries and Sea-Level Canals. Prepared for Maryland Power Plant Siting Program, Dept. of Natural Resources, Annapolis, Maryland, Report No. PPR P-6.

Norton, W.R., I.P. King, and G.T. Orlob. 1973. A Finite Element Model for Lower Granite Reservoir, Report to Walla Walla Dist. U.S. Corps of Engineers, by WRE, Inc.

Okoye, J.K. 1970. Characteristics of Transverse Mixing in Open-channel Flows, Report No. KH-R-23. California Institute of Technology.

O'Connor, D.J., R.V. Thomann, and D.M. Di Toro. 1973. Dynamic Water Quality Forecasting and Management. Manhatten College, Bronx, New York, for U.S. Environmental Protection Agency, Washington, D.C., EPA660/3-73-009, NTIS Doc. PB 225-048/8ST.

O'Connor, D.J. and W.S. Lung. 1981. Suspended Solids Analysis of Estuarine Systems. Journal of the Environmental Engineering Division, ASCE, Vol. 107, No. EE1, pp. 101-120.

Odd, N.V.M. and J.G. Rodger. 1978. Vertical Mixing in Stratified Tidal Flows. Journal of the Hydraulics Division, ASCE, Vol. 104, No. HY3, pp. 337-351.

Officer, C.B. 1976. Physical Oceanography of Estuaries (and Associated Coastal Waters), John Wiley and Sons, New York.

Okubo, A. 1968. A New Set of Oceanic Diffusion Diagrams. Chesapeake Bay Institute, Johns Hopkins University, Technical Report No. 38.

Okubo, A. and R.V. Ozmidov. 1970. Empirical Dependence of the Coefficient of Horizontal Turbulent Diffusion in the Ocean on the Scale of the Phenomenon in question, Izv. Acad. of Sciences USSR, Atmospheric and Oceanic Physics, Vol. 6, No. 5.

Okubo, A. 1971. Oceanic Diffusion Diagrams. Deep Sea Research, August 1971.

Orlob, G.T. 1959. Eddy Diffusion in Homogeneous Turbulence. Journal of Hydraulics Division, ASCE, Vol. 85, HY9.

Orlob, G.T., ed. 1984. Mathematical Modeling of Water Quality: Streams, Lakes, and Reservoirs. John Wiley and Sons, Wiley-Interscience, N.Y., pp. 274-336.

Ozmidov, R.V. 1968. Horizontal Turbulence and Turbulent Exchange in the Ocean (Moscow: Nauka).

Pagenkopf, J.R. and R.B. Taylor. 1985. An Implicit Mass Transport Model for Tidal Waters. In: Physics Based Environmental Modelling of Material Release and Waste Disposal. ASCE Special Publication (in publication).

Paily, P.O., E.O. Macagno, and J.F. Kennedy. 1974. Winter Regime Thermal Response of Heated Streams. Journal of the Hydraulics Division, ASCE, Vol. 100, No. HY4, pp. 531-551.

Parker, F.L. 1961. Eddy Diffusion in Reservoir and Pipelines. Journal of the Hydraulics Division, ASCE. Vol. 87, No. HY3, pp. 151-171.

Peterson, D.E., J.C. Sonnichsen, S.L. Engstrom, and P.M. Schrotke. 1973. Thermal Capacity of Our Nation's Waterways, Journal of the Power Division, ASCE.

Prych, E.A. 1970. Effects of Density Differences on Lateral Mixing in Open-Channel Flows, Report No. KH-12-21. California Institute of Technology.

Rutherford, J.C., M.E.U. Taylor, and J.D. Davies. 1980. Waikato River Pollutant Flushing Lakes. Journal of the Environmental Engineering Division, ASCE, Vol. 106, No. EE, pp. 1131-1150.

Ruthven, D.M. 1971. The Dispersion of a Decaying Effluent Discharged Continuously into a Uniformly Flowing Stream. Water Research, Vol. 5, pp. 343-352.

Ryan, P.J. and D.R.F. Harleman. 1973. An Analytical and Experimental Study of Transient Cooling Pond Behavior. R.M. Parsons Laboratory, MIT, Technical Report No. 161.

Ryan, P.J. and K.D. Stolzebach. 1972. Chapter 1: Environmental Heat Transfer, In: Engineering Aspects of Heat Disposal from Power Generation. R.M. Parsons Laboratory, MIT, Cambridge, Massachusetts.

Sabol, G.V. and C.F. Nordin. 1978. Dispersion in Rivers as Related to Storage Zones. Journal of the Hydraulics Division. ASCE, Vol. 104, No. HY5, pp. 695-707.

Sayre, W.W. and T.P. Yeh. 1973. Transverse Mixing Characteristics Missouri River Downstream from the Cooper Nuclear Station, IIHR Report 145, Iowa Institute of Hydraulics Research, University of Iowa, Iowa City, Iowa.

Shanahan, P. 1984. Water Temperature Modeling: A Practical Guide. Proceedings of the U.S. Environmental Protection Agency Stormwater and Water Quality Model Users Group Meeting, Detroit Michigan, April 1984.

Shen, H.T. 1978. Transient Mixing in River Channels. Journal of the Environmental Engineering Division, ASCE, Vol. 104, No. EE3, pp. 445-459.

Sheng, Y.P. and H.L. Butler. 1982. A Three-Dimensional Numerical Model of Coastal, Estuarine, and Lake Currents. ARO Report 82-3, Proceedings of the 1982 U.S. Army Numerical Analysis and Computer Conference.

Simons, T.J. 1973. Development of Three-Dimensional Numerical Models of the Great lakes. Scientific Series No. 12, Canada Centre for Inland Waters, Burlington, Ontario, Canada.

Simons, T.J. 1976. Verification of Numerical Models of Lake Ontario, III - Long-Term Heat Transports, Journal of the Phys. Oceanogr., Vol. 6, pp. 372-378.

Somlyody, L. 1982. An Approach to the Study of the Transverse Mixing in Streams, Journal of Hydraulic Research, Vol. 20(2), pp. 203-220

Sooky, A. 1969. Longitudinal Dispersion in Open Channels. Proc. ASCE, Journal Hyd. Div., Vol. 95, No. HY4.

Spaulding, M.L. and D. Pavish. 1984. A Three-Dimensional Numerical Model of Particulate Transport for Coastal Waters. Continental Shelf Research, Vol. 3, No. 1, pp. 55-67.

Stommel, H. 1949. Horizontal Diffusion Due to Oceanic Turbulence. Journal of Marine Research. 8:199-225.

Swinbank, W.C. 1963. Longwave Radiation from Clear Skies. Quarterly Journal of the Royal Meteorological Society, Vol. 89, pp. 339-348.

Taylor, G.I. 1954. The Dispersion of Matter in Turbulent Flow Through a Pipe Royal Soc. London Proc., Ser. A, Vol. 223, pp. 446-468.

Taylor, R.B. and J.R. Pagenkopf. 1981. TRANQUAL - Two-Dimensional Modeling of Transport Water Quality Processes. Proceedings, EPA Storm Water and Water quality Management Modeling Group Meeting, Niagara Falls, Canada.

Tennessee Valley Authority. 1972. Heat and Mass Transfer Between a Water Surface and the Atmosphere. TVA Water Resources Research Engineering Laboratory, Norris, TN Report 14, pp. 123.

Tetra Tech, Inc. 1975. A Comprehensive Water Quality Ecological Model for Lake Ontario (final report), Prepared for National Oceanic and Atmospheric Administration.

Tetra Tech, Inc. 1976. Documentation of Water quality Models for the Helms Pumped Storage Project, Prepared for Pacific Gas and Electric Company.

Tetra Tech, Inc. 1977. Documentation Manual for the Two River Water Quality Models, Prepared for Nassau-Suffolk Regional Planning Board, Hauppauge, New York.

Thackston, E.L. 1966. Longitudinal Mixing and Reaeration in Natural Streams. Dissertation Presented to Vanderbilt University, Nashville, TN.

Thackston, E.L. and P.A. Krenkel. 1967. Longitudinal Mixing in Natural Streams. Journal of Sanitary Engineering Division. Vol. 93, No. SA5, pp. 67-90.

Thackston, E.L. and K.B. Schnelle, Jr. 1969. Predicting Effects of Dead Zones on Stream Mixing. Proc. ASCE, Journal San. Eng. Div., Vol. 96, No. SA2.

Thackston, E.L. and K.B. Schelle. 1970. Predicting Efforts of Dead Zone on Stream Mixing, ASCE Journal of the Sanitary Engineering Division. Vol. 96, No. SA2, pp. 319-331.

Thackston, E.L. 1974. Effect of Geographical Variation on Performance of Recirculating Cooling Ponds. U.S. Environmental Protection Agency, Corvallis, OR., EPA-660/2-74-085.

Thatcher, M.L. and D.R.F. Harleman. 1972. A Mathematical Model for the Production of Unsteady Salinity Intrusion in Estuaries. R.M. Parsons Laboratory, MIT, Technical Report No. 144.

Thatcher, J.L. and D.R.F. Harleman. 1978. Development and Application of a Deterministic Time-Varying Salinity Intrusion Model for the Delaware Estuary (MIT-TSIM), Prepared for the Delaware River Basin Commission, West Trenton, New Jersey.

Thomann, R.V. 1973. Effects of Longitudinal Dispersion on Dynamic Water Quality Response of Streams and Rivers. Water Resources Research, Vol. 9, No. 2, pp. 355-366.

Thomann, R.V., D.M. Di Toro, R.P. Winfield, and D.J. O'Connor. 1975. Mathematical Modeling of Phytoplankton in Lake Ontario, Grosse Ile Laboratory, National Environmental Research Center, Grosse Ile, Michigan, EPA-660/3-75-005..

Thompson, E.S. 1975. Computation of Solar Radiation from Sky Cover. Water Resources Research, Vol. 12; No. 5, pp. 859-865, October 1975.

Tracor, Inc. 1971. Estuarine Modeling: An Assessment for Water Quality, Office of U.S. Environmental Protection Agency, Project 16070DZV.

U.S. Army Corps of Engineers (Hydrologic Engineering Center). 1974. Water Quality for River-Reservoir Systems (technical report).

Valentine, E.M. and I.R. Wood. 1977. Longitudinal Dispersion with Dead Zones, Journal of the Hydraulic Division, ASCE, Vol. 103, No. HY9.

Valentine, E.M. and I.R. Wood. 1979. Dispersion in Rough Rectangular Channels. Journal of the Hydraulics Division, ASCE, Vol. 105, No. HY12, pp. 1537-1553.

Waldrop, W.R. 1978. Hydrothermal Analyses Using Computer Modeling and Field Studies. Verification of Mathematical and Physical Models in Hydraulic Engineering, Proceedings of the 26th Annual Hydraulics Specialty Conference. ASCE, pp. 38-43.

Wang, J.D. 1979. Finite Element Model of 2-D Stratified Flow. Journal of the Hydraulics Division, ASCE, Vol. 105, No. HY12, Proc. Paper 15049, pp. 1473-1485.

Wang, J.D. and J.J. Connor. 1975. Mathematical Modeling of Near Coastal Circulation, Technical Report No. 200, R.M. Parsons Laboratory, MIT.

Wallis, I.G. 1974. Lagrangian Models of Waste Transport for Estuaries and Tidal Inlets. Geophysical Fluid Dynamics Laboratory, Monash University, Clayton, Victoria, Australia.

Ward, P.R.B. and H.B. Fischer. 1971. Some Limitations on Use of the One-Dimensional Dispersion Equation with Comments on Two Papers by R.W. Paulson. Water Resources Research, Vol. 7, No. 1.

Watanabe, M., D.R.F. Harleman, and O.F. Vasiliev. 1984. Two- and Three-Dimensional Mathematical Models for Lakes and Reservoirs. In: G.T. Orlob, ed. Mathematical Modeling of Water Quality: Streams, Lakes, and Reservoirs. John Wiley and Sons, Wiley-Interscience, N.Y., N.Y. pp. 274-336.

Water Resources Engineers, Inc. 1972. Ecologic Simulation for Aquatic Environments. Final Report to the Office of Water Resources Research, U.S. Department of the Interior, Washington, D.C.

Webel, G. and M. Schatzmann. 1984. Transverse Mixing in Open Channel Flow. Journal of Hydraulics Division, ASCE. Vol. 110, No. 4, pp. 423-435.

Yudelson, J.M. 1967. A Survey of Ocean Diffusion Studies and Data. W.M. Keck Laboratory, California Institute of Technology, TM 67-2.

Yotsukura, N. and W.W. Sayre. 1976. Transverse Mixing in Natural Channels. Water Resources Research. Vol. 12, No. 4, pp. 695-704.

Yotsukura, N., H.B. Fischer, and W.W. Sayre. 1970. Measurement of Mixing Characteristics of the Missouri River Between Sioux City, Iowa and Plattsmouth, Nebraska. U.S. Geological Survey Water-Supply Paper, 1899-G.

Yotsukura, N. and E.D. Cobb. 1972. Transverse Diffusion of Solutes in Natural Streams. Geological Survey Professional Paper 582-C.

Zison, S. W., W. B. Mills, D. Deimer, and C. W. Chen. 1978. Rates, Constants and Kinetics Formulations in Surface Water Quality Modeling. Prepared by Tetra Tech, Inc., Lafayette, CA for Environmental Research Laboratory, U.S. Environmental Protection Agency, Athens, GA. EPA-600/3-78-105. 335 pp.

Chapter 3

DISSOLVED OXYGEN

3.1 DISSOLVED OXYGEN SATURATION

3.1.1 Introduction

Dissolved oxygen saturation, commonly symbolized as C_s and expressed in mg/l, is a basic parameter used in a great many water quality models. Since dissolved oxygen predictions are often primary reasons for developing water quality models, accurate values for C_s are needed.

Table 3-1 illustrates the equations used to calculate saturation dissolved oxygen values in a number of water quality models. The most frequently used equation is the polynomial equation developed by Elmore and Hayes (1960) for distilled water (Equation (3-1) in Table 3-1). In this equation, neither pressure nor salinity effects are considered (pressure is assumed to be 1 atm and salinity is 0 ppt).

Effects of pressure on saturation values are expressed as a ratio of site pressure to sea level (Equation (3-5)) or as a function of elevation (Equation (3-6)). Effects of salinity (relevant to estuaries and oceanic systems) are considered in the last two model equations (Equations (3-7) and (3-8)). When used in fresh water applications, the sections of the equations in which the saline term appears reduce to zero and have no effect on the dissolved oxygen saturation. Every saturation equation, whether or not modified to include non-standard pressure or salinity, evaluates dissolved oxygen saturation as a function of temperature.

TABLE 3-1. METHODS USED BY SELECTED MODELS TO PREDICT DISSOLVED OXYGEN SATURATION

Equation Number	Model Name (or Description)	Model Reference	Equation or Method for Dissolved Oxygen Saturation C_s (mg/l)
3-1	Limnological Model for Eutrophic Lakes and Impoundments	Baca and Arnett, 1976	$C_s = 14.652 - (0.41022\ T) + (0.007991\ T^2) - (7.7774 \times 10^{-5}\ T^3)$ $T = {}^oC$
3-1	EXPLORE-1	Battelle, 1973	Same as above
3-1	Level III-Receive	Medina, 1979	Same as above
3-1	Water Quality Model for Large Lakes: Part 2: Lake Erie	Di Toro and Connolly, 1980	Same as above
3-2	WRECEV	Johnson and Duke, 1976	$C_s = 14.62 - 0.3898\ T + 0.006969\ T^2 - 5.897 \times 10^{-5}\ T^3$ $T = {}^oC$
3-3	QUAL-II	Roesner, et al., 1981	$C_s = 24.89 - 0.4259\ T + 0.003734\ T^2 - 1.328 \times 10^{-5}\ T^3$ $T = {}^oF$
3-4	CE-QUAL-R1	U.S. Army COE, 1982	$C_s = (14.6)e^{(-(0.027767 - 0.00027\ T + 0.000002\ T^2)\ T)}$ $T = {}^oC$
3-5	One Dimensional Steady State Stream Water Quality Model	Bauer, et al., 1979	$C_s = (14.652 - .41022\ T + 0.007910\ T^2 - 7.7774 \times 10^{-5}\ T^3)\ (BP/29.92)$ $T = {}^oC$ BP = Barometric pressure (in.Hg)
3-5	HSPF (Release 7.0)	Imhoff, et al., 1981	Same as above
3-6	DOSAG and DOSAG3	Duke and Masch, 1973	$(14.62 - (0.3898\ T) + (0.006969\ T^2) - (5.897 \times 10^{-5}\ T^3))$ $\left[1.0 - (6.97 \times 10^{-6}\ E)\right]^{5.167}$ $T = {}^oC$ E = Elevation, ft.
3-7	Pearl Harbor Version of Dynamic Estuary Model (DEM)	Genet et al., 1974	$C_s = 14.5532 - .38217\ T + .0054258\ T^2 - CL(1.665 \times 10^{-4} - 5.866 \times 10^{-6} T + 9.796 \times 10^{-8}\ T^2)$ $T = {}^oC$ CL = Chloride concentration (ppm)
3-8	RECEIV-II	Raytheon Co., 1974, and Weiss, 1970	$C_s = 1.4277 \exp[-173.492 + 24963.39/T + 143.3483 \ln(T/100.) - 0.218492\ T + S(-0.033096 + 0.00014259\ T - 0.00000017\ T^2)]$ $T_o = {}^oK = {}^oC + 273.15$ S = Salinity (ppt)

3.1.2 Dissolved Oxygen Saturation As Determined by the APHA

The APHA (1985) presents a tabulation of oxygen solubility in water as a function of both chlorinity and water temperature (see Table 3-2). This table is the work of Benson and Krause (1984) who collected the data and developed the equations for conditions in which the water was in contact with water saturated air at standard pressure (1.000 atm).

Since chlorinity is related to salinity, and salinity is more often measured than chlorinity, the relationship between the two quantities is of interest. The relationship, expressed here three ways, is:

$$\text{Salinity (ppt or } {}^{o}/_{oo}) = 0.03 + 0.001805 \text{ Chlorinity (mg/l)} \qquad (3\text{-}9a)$$

or

$$\text{Salinity (ppt or } {}^{o}/_{oo}) = 5.572 \times 10^{-4}(SC) + 2.02 \times 10^{-9}(SC)^2 \qquad (3\text{-}9b)$$

where SC = specific conductance in micromhos/cm

or

$$\text{Salinity} = 1.80655 \text{ (chlorinity as ppt)} \qquad (3\text{-}9c)$$

where chlorinity and salinity are as defined in the footnote to Table 3-2.

Equation (3-9b) is from USGS (1981) and Equation (3-9c) is from APHA (1985).

The APHA (1985) recommends that the concentration of oxygen in water (at different temperatures and salinity) at equilibrium with water saturated air be calculated using the equation below (Benson and Krause, 1984):

$$\begin{aligned} \ln C_s = & -139.34411 + (1.575701 \times 10^5/T) \\ & -(6.642308 \times 10^7/T^2) + (1.243800 \times 10^{10}/T^3) \\ & -(8.621949 \times 10^{11}/T^4) \\ & -Chl[(3.1929 \times 10^{-2}) - (1.9428 \times 10/T) \\ & \quad +(3.8673 \times 10^3/T^2)] \end{aligned} \qquad (3\text{-}10)$$

TABLE 3-2. SOLUBILITY OF OXYGEN IN WATER EXPOSED TO WATER-SATURATED AIR AT 1.000 ATMOSPHERIC PRESSURE (APHA, 1985)

Temp. in °C	Chlorinity, ppt 0.0	5.0	10.0	15.0	20.0	25.0	Difference per 0.1 ppt Chlorinity
	Dissolved Oxygen, mg/l						
0.0	14.621	13.728	12.888	12.097	11.355	10.657	0.016
1.0	14.216	13.356	12.545	11.783	11.066	10.392	0.015
2.0	13.829	13.000	12.218	11.483	10.790	10.139	0.015
3.0	13.460	12.660	11.906	11.195	10.526	9.897	0.014
4.0	13.107	12.335	11.607	10.920	10.273	9.664	0.014
5.0	12.770	12.024	11.320	10.656	10.031	9.441	0.013
6.0	12.447	11.727	11.046	10.404	9.799	9.228	0.013
7.0	12.139	11.442	10.783	10.162	9.576	9.023	0.012
8.0	11.843	11.169	10.531	9.930	9.362	8.826	0.012
9.0	11.559	10.907	10.290	9.707	9.156	8.636	0.012
10.0	11.288	10.656	10.058	9.493	8.959	8.454	0.011
11.0	11.027	10.415	9.835	9.287	8.769	8.279	0.011
12.0	10.777	10.183	9.621	9.089	8.586	8.111	0.011
13.0	10.537	9.961	9.416	8.899	8.411	7.949	0.010
14.0	10.306	9.747	9.218	8.716	8.242	7.792	0.010
15.0	10.084	9.541	9.027	8.540	8.079	7.642	0.010
16.0	9.870	9.344	8.844	8.370	7.922	7.496	0.009
17.0	9.665	9.153	8.667	8.207	7.770	7.356	0.009
18.0	9.467	8.969	8.497	8.049	7.624	7.221	0.009
19.0	9.276	8.792	8.333	7.896	7.483	7.090	0.009
20.0	9.092	8.621	8.174	7.749	7.346	6.964	0.009
21.0	8.915	8.456	8.021	7.607	7.214	6.842	0.008
22.0	8.743	8.297	7.873	7.470	7.087	6.723	0.008
23.0	8.578	8.143	7.730	7.337	6.963	6.609	0.008
24.0	8.418	7.994	7.591	7.208	6.844	6.498	0.008
25.0	8.263	7.850	7.457	7.083	6.728	6.390	0.007
26.0	8.113	7.711	7.327	6.962	6.615	6.285	0.007
27.0	7.968	7.575	7.201	6.845	6.506	6.184	0.007
28.0	7.827	7.444	7.079	6.731	6.400	6.085	0.007
29.0	7.691	7.317	6.961	6.621	6.297	5.990	0.007
30.0	7.559	7.194	6.845	6.513	6.197	5.896	0.007
31.0	7.430	7.073	6.733	6.409	6.100	5.806	0.006
32.0	7.305	6.957	6.624	6.307	6.005	5.717	0.006
33.0	7.183	6.843	6.518	6.208	5.912	5.631	0.006
34.0	7.065	6.732	6.415	6.111	5.822	5.546	0.006
35.0	6.950	6.624	6.314	6.017	5.734	5.464	0.006
36.0	6.837	6.519	6.215	5.925	5.648	5.384	0.006
37.0	6.727	6.416	6.119	5.835	5.564	5.305	0.006
38.0	6.620	6.316	6.025	5.747	5.481	5.228	0.006
39.0	6.515	6.217	5.932	5.660	5.400	5.152	0.005
40.0	6.412	6.121	5.842	5.576	5.321	5.078	0.005

DEFINITION OF SALINITY

Although salinity has been traditionally defined as the total solids in water after all carbonates have been converted to oxides, all bromide and iodide have been replaced by chloride, and all organic matter has been oxidized, the new scale used to define salinity is based on the electrical conductivity of seawater relative to a specified solution of KCl and H_2O (UNESCO, 1981). The scale is dimensionless and the traditional dimensions of parts per thousand (i.e., mg/g of solution) no longer applies.

DEFINITION OF CHLORINITY

Chlorinity is now defined in relation to salinity as follows:

Salinity = 1.80655 (Chlorinity)

Although chlorinity is not equivalent to chloride concentration, the factor for translating a chloride determination in seawater to include bromide, for example, is only 1.0045 based on the molecular weights and the relative amounts of the two ions. Therefore, for practical purposes, chloride (in mg/g of solution) is nearly equal to chlorinity in seawater. For wastewater, a knowledge of the ions responsible for the solution's electrical conductivity is necessary to correct for the ions impact on oxygen solubility and use of the tabular value or the equation is inappropriate unless the relative composition of the wastewater is similar to seawater.

where C_s = equilibrium oxygen concentration, mg/l, at 1.000 atm (standard pressure)

T = temperature (^oK) = ^oC+273.150 and ^oC is within 0.0 to 40.0^oC

Chl = chlorinity within 0.0 to 28.0, ppt

Table 3-2 replaces the older table of previous APHA Standard Methods editions. The USGS (1981) has replaced older tables based on calculations of Whipple and Whipple (1911) with tables generated from an equation by Weiss (1970) (Equation 3-8).

The APHA (1985) recommends that saturation dissolved oxygen concentration at non-standard pressure be calculated using the following equation:

$$C_s' = C_s P \left[\frac{(1-P_{wv}/P)\ (1-\theta P)}{(1-P_{wv})\ (1-\theta)} \right] \qquad (3\text{-}11)$$

where C_s' = equilibrium oxygen concentration at non-standard pressure, mg/l

C_s = equilibrium oxygen concentration at 1.000 atm, mg/l

P = pressure, atm, and is within 0.000 to 2.000 atm

P_{wv} = partial pressure of water vapor, atm, which may be computed

$\ln P_{wv} = 11.8571 - (3840.70/T_k) - (216961/T_k^2)$

T_k = temperature in ^oK

$\theta = 0.000975 - (1.426 \times 10^{-5} T_c) + (6.436 \times 10^{-8} T_c^2)$

T_c = temperature in ^oC

The expressions for P_{wv} and θ are also from APHA (1985).

For altitudes less than approximately 4000 feet the bracketed quantity is very nearly 1 and at these altitudes multiplying C_s by P(atm) alone results in a good approximation of C_s'. A more accurate calculation of C_s'

can be made by using Table 3-3. The quantity in brackets from Equation (3-11) is tabulated for temperatures between 0-40°C and for pressures from 1.1 to 0.5 atm (Benson and Krause, 1980). As an approximation of the influence of altitude, C_s decreases about 7 percent per 2,000 feet of elevation increase.

TABLE 3-3 VALUES FOR THE BRACKETED QUANTITY SHOWN IN EQUATION 3-11 TO BE USED WITH THE CORRESPONDING TEMPERATURES AND PRESSURES (BENSON AND KRAUSE, 1980)

	P atm						
T(°C)	1.1	1.0	0.9	0.8	0.7	0.6	0.5
0.0	1.0005	1.0000	0.9994	0.9987	0.9977	0.9963	0.9944
5.0	1.0007	1.0000	0.9991	0.9980	0.9966	0.9946	0.9918
10.0	1.0010	1.0000	0.9987	0.9971	0.9950	0.9922	0.9882
15.0	1.0015	1.0000	0.9982	0.9959	0.9929	(0.9889)	(0.9833)
20.0	1.0021	1.0000	0.9974	0.9942	(0.9901)	(0.9845)	[0.9767]
25.0	1.0029	1.0000	0.9965	0.9921	(0.9864)	(0.9787)	[0.9680]
30.0	1.0039	1.0000	0.9952	(0.9892)	(0.9814)	[0.9711]	[0.9566]
35.0	1.0053	1.0000	(0.9935)	(0.9854)	(0.9750)	[0.9610]	[0.9415]
40.0	1.0071	1.0000	(0.9913	(0.9805)	[0.9665]	[0.9479]	[0.9217]

Explanation of Interpolation Procedure:

Linear interpolation in P and T will introduce an error ≤0.02% in the upper and left sections of table. Interpolation using numbers in parentheses will lead to errors ≤0.05%. With the numbers in brackets, interpolation errors become larger. Either temperature or presssure may be interpolated first, as illustrated for T = 3.00°C and P = 0.67 atm by the two arrays shown below.

	Temperature Interpolated First				Pressure Interpolated First		
	0.7	0.67	0.6		0.7	0.67	0.6
0	0.9977		0.9963	0	0.9977	0.99728	0.9963
3	0.99704	0.9965 answer	0.99528	3		0.9965, answer	
5	0.9966		0.9946	5	0.9966	0.99600	0.9946

Earlier the APHA (1980) calculated the effects of barometric pressure on dissolved oxygen saturation as:

$$C_s' = C_s \left(\frac{P - P_{wv}}{1 - P_{wv}} \right)$$

This is equivalent to Equation (3-11) when $\theta = 0$.

3.1.3 Comparison of Methods

Table 3-4 compares the dissolved oxygen saturation values for Equations (3-1) through (3-8) and APHA (1971) against the values in Table 3-2 from the APHA (1985), Equation (3-10). The comparisons are performed at 0.0 mg/l salinity and sea level. When the values from the equations are compared with the APHA (1985) values within the temperature range 10-30°C* and the maximum differences examined, four "groups" of differences appear. Values from Equation (3-8) are in the group that shows the least difference from APHA (1985): 0.03 mg/l higher than the APHA (1985) predictions. Values from Equations (3-2), (3-4), (3-6) and APHA (1971) are in the second group with differences of .07 to .11 mg/l higher than APHA (1985). Values from Equations (3-1), (3-3) and (3-5) are in the third group with differences of .11 to .13 mg/l lower than APHA (1985). Equation (3-7) produced differences that comprise the fourth group with some values >0.4 mg/l higher than APHA (1985). Generally, the maximum differences with each equation occur at higher temperatures, when dissolved oxygen depletion may contribute to serious water quality problems.

In Table 3-5 Equations (3-7), (3-8), (3-13) and APHA (1971) (those including salinity factors) are evaluated at a chloride concentration of 20,000 mg/l at 1 atm pressure and compared to APHA (1985) values.

---

* Typically, the temperature range in which most freshwater water quality analyses take place.

TABLE 3-4. COMPARISON OF DISSOLVED OXYGEN SATURATION VALUES FROM TEN EQUATIONS AT 0.0 mg/l SALINITY AND 1 ATM PRESSURE

Temperature °C	Equation Number From Table 3-1 (3-1)	(3-2)	(3-3)	(3-4)	(3-5)	(3-6)	(3-7)	(3-8)	APHA (1971)	APHA(1985) 3-10
0.0	14.652	14.620	14.650	14.600	14.652	14.620	14.553	14.591	14.6	14.621
1.0	14.250	14.237	14.248	14.204	14.250	14.237	14.176	14.188	14.2	14.216
2.0	13.863	13.868	13.861	13.826	13.863	13.868	13.811	13.803	13.8	13.829
3.0	13.491	13.512	13.490	13.465	13.491	13.512	13.456	13.435	13.5	13.460
4.0	13.134	13.169	13.133	13.120	13.134	13.169	13.111	13.084	13.1	13.107
5.0	12.791	12.838	12.790	12.790	12.791	12.838	12.778	12.748	12.8	12.770
6.0	12.462	12.519	12.460	12.475	12.462	12.519	12.456	12.426	12.5	12.447
7.0	12.145	12.213	12.144	12.173	12.145	12.213	12.144	12.118	12.2	12.139
8.0	11.842	11.917	11.841	11.883	11.842	11.917	11.843	11.823	11.9	11.843
9.0	11.551	11.633	11.550	11.606	11.551	11.633	11.553	11.540	11.6	11.559
10.0	11.271	11.360	11.270	11.340	11.271	11.360	11.274	11.268	11.3	11.288
11.0	11.003	11.097	11.002	11.085	11.003	11.097	11.006	11.008	11.1	11.027
12.0	10.746	10.844	10.744	10.840	10.746	10.844	10.748	10.758	10.8	10.777
13.0	10.499	10.601	10.497	10.605	10.499	10.601	10.502	10.517	10.6	10.537
14.0	10.262	10.367	10.260	10.378	10.262	10.367	10.266	10.286	10.4	10.306
15.0	10.034	10.142	10.033	10.161	10.034	10.142	10.041	10.064	10.2	10.084
16.0	9.816	9.926	9.814	9.951	9.816	9.926	9.827	9.850	10.0	9.870
17.0	9.606	9.718	9.604	9.749	9.606	9.718	9.624	9.644	9.7	9.665
18.0	9.404	9.518	9.401	9.555	9.404	9.518	9.432	9.446	9.5	9.467
19.0	9.209	9.325	9.207	9.367	9.209	9.325	9.251	9.254	9.4	9.276
20.0	9.022	9.140	9.019	9.186	9.022	9.140	9.080	9.070	9.2	9.092
21.0	8.841	8.961	8.838	9.011	8.841	8.961	8.920	8.891	9.0	8.915
22.0	8.667	8.789	8.664	8.842	8.667	8.789	8.772	8.720	8.8	8.743
23.0	8.498	8.624	8.495	8.679	8.498	8.624	8.634	8.554	8.7	8.578
24.0	8.334	8.464	8.331	8.521	8.334	8.464	8.506	8.393	8.5	8.418
25.0	8.176	8.309	8.172	8.367	8.176	8.309	8.390	8.238	8.4	8.263
26.0	8.021	8.160	8.017	8.219	8.021	8.160	8.285	8.088	8.2	8.113
27.0	7.871	8.015	7.866	8.075	7.871	8.015	8.190	7.943	8.1	7.968
28.0	7.723	7.875	7.719	7.935	7.723	7.875	8.106	7.802	7.9	7.827
29.0	7.579	7.739	7.574	7.800	7.579	7.739	8.033	7.666	7.8	7.691
30.0	7.437	7.606	7.432	7.668	7.437	7.606	7.971	7.533	7.6	7.559
31.0	7.298	7.477	7.292	7.539	7.298	7.477	7.920	7.405	7.5	7.430
32.0	7.159	7.350	7.154	7.414	7.159	7.350	7.880	7.281	7.4	7.305
33.0	7.022	7.227	7.016	7.293	7.022	7.227	7.850	7.161	7.3	7.183
34.0	6.885	7.105	6.880	7.174	6.885	7.105	7.832	7.043	7.2	7.065
35.0	6.749	6.986	6.743	7.058	6.749	6.986	7.824	6.930	7.1	6.950
36.0	6.612	6.868	6.606	6.945	6.612	6.868	7.827	6.819	-	6.837
37.0	6.474	6.751	6.468	6.834	6.474	6.751	7.841	6.711	-	6.727
38.0	6.335	6.635	6.329	6.726	6.335	6.635	7.866	6.606	-	6.620
39.0	6.194	6.520	6.188	6.620	6.194	6.520	7.901	6.505	-	6.315
40.0	6.051	6.404	6.045	6.517	6.051	6.404	7.948	6.405	-	6.412

Equation (3-13) is based on the data of Green and Carritt (1967). From their data Hyer et al. (1971) developed an expression relating C_s to both temperature and salinity. C_s is given by:

$$C_s = 14.6244 - 0.367134T + 0.0044972T^2$$

$$- 0.0966S + 0.00205ST + 0.0002739S^2 \qquad (3\text{-}13)$$

TABLE 3-5. COMPARISON OF DISSOLVED OXYGEN SATURATION VALUES FROM SELECTED EQUATIONS AT A CHLORIDE CONCENTRATION OF 20,000 mg/l (36.1 ppt SALINITY) AND 1 ATM PRESSURE

Temperature °C	Equation Number from Table 3-1 (3-7)	(3-8)	(3-13)	APHA (1971)	APHA (1985) (3-10)
0.0	11.215	11.400	11.492	11.3	11.354
1.0	10.953	11.105	11.203	11.0	11.067
2.0	10.699	10.823	10.924	10.8	10.790
3.0	10.452	10.553	10.653	10.5	10.527
4.0	10.212	10.295	10.391	10.3	10.273
5.0	9.978	10.048	10.139	10.0	10.031
6.0	9.752	9.811	9.895	9.8	9.801
7.0	9.532	9.585	9.661	9.6	9.575
8.0	9.320	9.367	9.435	9.4	9.362
9.0	9.114	9.158	9.218	9.2	9.156
10.0	8.915	8.958	9.011	9.0	8.957
11.0	8.723	8.765	8.812	8.8	8.769
12.0	8.538	8.580	8.623	8.6	8.586
13.0	8.360	8.402	8.442	8.5	8.411
14.0	8.189	8.231	8.270	8.3	8.241
15.0	8.025	8.067	8.108	8.1	8.077
16.0	7.868	7.908	7.954	8.0	7.922
17.0	7.718	7.755	7.809	7.8	7.770
18.0	7.574	7.607	7.674	7.7	7.624
19.0	7.438	7.465	7.547	7.6	7.482
20.0	7.308	7.327	7.429	7.4	7.347
21.0	7.186	7.194	7.321	7.3	7.215
22.0	7.070	7.066	7.221	7.1	7.087
23.0	6.961	6.942	7.130	7.0	6.964
24.0	6.859	6.822	7.049	6.9	6.844
25.0	6.764	6.594	6.976	6.7	6.727
26.0	6.676	6.594	6.912	6.6	6.616
27.0	6.595	6.485	6.857	6.5	6.507
28.0	6.521	6.379	6.812	6.4	6.401
29.0	6.454	6.277	6.775	6.3	6.297
30.0	6.394	6.177	6.747	6.1	6.197
31.0	6.340	6.081	6.729	-	6.100
32.0	6.294	5.987	6.719	-	6.005
33.0	6.254	5.896	6.718	-	5.912
34.0	6.221	5.808	6.726	-	5.822
35.0	6.196	5.722	6.743	-	5.734
36.0	6.177	5.638	6.770	-	5.648
37.0	6.165	5.557	6.805	-	5.564
38.0	6.160	5.477	6.849	-	5.481
39.0	6.162	5.400	6.902	-	5.400
40.0	6.171	5.325	6.965	-	5.322

where T = temperature, ^{o}C

S = salinity, ppt.

The values were compared over a temperature range of 5-30°C. Equation (3-8), as before, agreed closely with APHA (1985) throughout the 5-30°C temperature range with a maximum difference of .022 mg/l less than APHA (1985). Equation (3-7) had differences of .08 less than and .04 mg/l greater than APHA (1985) from 5-25°C and near .2 mg/l higher than APHA (1985) at 30°C. The values from the APHA (1971) (reported to the nearest tenth mg/l) had a maximum difference range of 0 to .1 mg/l higher than APHA (1985) and the fourth equation, Equation (3-13), varied the most from APHA (1985) with differences in the range of approximately .03 to 0.5 mg/l higher.

3.1.4 Methods of Measurement

Elmore and Hayes (1960) have summarized the work of numerous researchers who have measured dissolved oxygen saturation. According to Elmore and Hayes, Fox in 1909 used a gasometric technique in which a known volume of pure oxygen was exposed to a known volume of water. After equilibrium had been established the volume of oxygen above the water was determined, and the solubility calculated assuming air contained 20.90 percent oxygen.

From Fox's expression, Whipple and Whipple (1911) converted their results from milliliters per liter to parts per million. These results were tabularized, circulated and used as standards by water agencies for years, and are only now being gradually replaced with tables developed from more elaborate equations.

Benson and Krause (1984) determined the solubility of oxygen in fresh and seawater over a temperature of 0-60°C using an equilibrator different from the Jacobsen Worthington-type equilibrator used in previous investigations. They felt the new apparatus minimized the uncertainties associated with methods involving thin films of liquids (Benson, et al.,

1979). The dissolved gas values were determined with use of a mercury manometric system. The resulting data and equations were compared to previous sets of values from Carpenter (1966), Green (1965), and Murray and Riley (1969). The APHA (1985) subsequently adopted the Benson and Krause concentrations as tabulated in Table 3-2. In earlier work involving fresh water only (Benson and Krause, 1980) the new concentration values were recommended by Mortimer (1981) for use in fresh water systems.

To date there is no "standard method" recommended by APHA to measure saturated dissolved oxygen. The laboratory methods noted in the preceeding paragraphs are sophisticated methods developed and/or modified for each research effort and are not conducive to simplier laboratory environments nor are they adaptable for field use.

Calibration of popular dissolved oxygen probes is carried out under saturation conditions by methods recommended by the instrument manufacturers in conjunction with a table such as Table 3-2. The values obtained may be verified with one of the several wet chemistry iodometric methods (or "Winkler" titrations) (APHA, 1985).

3.1.5 Summary

Notable differences exist among the results obtained by various methods used to determine saturated dissolved oxygen values under specified conditions of temperature, salinity and pressure. These discrepancies may be as high as 11 percent for high saline conditions (Table 3-5). Under conditions of zero salinity observed differences are generally less than 2 percent (Table 3-4). The accuracy of the Elmore and Hayes expression, one of the most frequently used formulas, rapidly deteriorates at water temperatures exceeding 25°C. The algorithm, Equation (3-8), used in the RECEIV-II model (Weiss, 1970 and USGS, 1981) matches the APHA (1985) data better than any formula reviewed, for both saline and freshwater conditions. The algorithm, Equation (3-10), presented in APHA (1985) and its corresponding table of saturation values, Table 3-2, are based on latest research and provide the most accurate values of C_s to date. Knowing the

possible sources of error using any other particular formulation for C_s permits the user to decide whether they are significant in a particular study.

3.2 REAERATION

3.2.1 Introduction

Reaeration is the process of oxygen exchange between the atmosphere and a water body in contact with the atmosphere. Typically, the net transfer of oxygen is from the atmosphere and into the water, since dissolved oxygen levels in most natural waters are below saturation. However, when photosynthesis produces supersaturated dissolved oxygen levels, the net transfer is back into the atmosphere.

The reaeration process is modeled as the product of a mass-transfer coefficient multiplied by the difference between dissolved oxygen saturation and the actual dissolved oxygen concentration, that is:

$$F_c = k_L(C_s - C) \tag{3-14}$$

where F_c = flux of dissolved oxygen across the water surface, mass/area/time

C = dissolved oxygen concentration, mass/volume

C_s = saturation dissolved oxygen concentration, mass/volume

k_L = surface transfer coefficient, length/time

For practically all river modeling applications and for vertically mixed estuaries a depth averaged flux (F_c'), is used:

$$F_c' = \frac{F_c}{H} = \frac{k_L}{H}(C_s - C) \tag{3-15}$$

where H = water depth, length

In Equation 3-15 the surface transfer rate and depth are typically combined into a single term, called the reaeration rate coefficient or reaeration coefficient, denoted in the literature by k_2 or k_a:

$$k_2 = \frac{k_L}{H} \tag{3-16}$$

3.2.2 Reaeration in Rivers

3.2.2.1 Overview

Rivers have been the focus of the majority of reaeration research in natural waters. Some of the equations that have been developed for rivers have been successfully applied to estuaries, and is indicative of the lack of estuarine reaeration research.

Table 3-6 summarizes reaeration coefficient expressions (k_2 values) for rivers. All formulas for reaeration in Table 3-6 are depth averaged values and are in units of 1/day. The table also shows the units required for the parameters in each formula, and when possible the range of conditions used in the development of the formulas. All values of k_2 are base e, and are referenced to 20°C, unless otherwise noted. Although base e values are used directly in most modeling formulations, in the earlier days of reaeration research, k_2 values were often expressed in base 10. The relationship between base e and base 10 reaeration coefficients is:

$$k_{2_{\text{base e}}} = \ln(10) k_{2_{\text{base 10}}} = 2.303\, k_{2_{\text{base 10}}} \tag{3-17}$$

Stream reaeration research began in earnest in the late 1950's, and continues today. The formulas that are shown in Table 3-6 are based on theory, empiricism, or a combination of the two. In the late 1960's the radioactive tracer method was introduced by Tsivoglou and Wallace (1972). The tracer method, or a modification of it, forms the basis for much of the research being conducted on reaeration today.

TABLE 3-6. REAERATION COEFFICIENTS FOR RIVERS AND STREAMS

Author(s)	k_2, base e(1/day at 20°C)	Units	Applicability
O'Connor and Dobbins (1958)	$\frac{12.9U^{0.5}}{H^{1.5}}$	U-fps H-feet	Moderately deep to deep channels; $1' \leq H \leq 30'$, $0.5 \leq U \leq 1.6$ fps; $0.05 \leq k_2 \leq 12.2$/day. O'Connor and Dobbins also developed a second formula for shallow streams but O'Connor (1958) showed the differences between the two formulas was insignificant, and recommended that the first formula be used.
Churchill *et al.* (1962)	$\frac{11.6U^{0.969}}{H^{1.673}}$	U-fps H-feet	Based on observed reaeration rates below dams from which oxygen deficient water was released. $2' \leq H \leq 11'$; $1.8 \leq U \leq 5$ fps. Churchill *et al.* also developed other formulas, but recommended this formula.
Owens *et al.* (1964)	$\frac{21.7U^{0.67}}{H^{1.85}}$	U-fps H-feet	Oxygen recovery monitored for six streams in England following deoxygenation with sodium sulfite. $0.1 \leq U \leq 5$ fps; $0.4' \leq H \leq 11'$.
Owens *et al.* (1964)	$\frac{23.3U^{0.73}}{H^{1.75}}$	U-fps H-feet	This is a second formula developed by Owens *et al.*, and applies for $0.1 \leq U \leq 1.8$ fps; $0.4' \leq H$ 11'.
Langbein and Durum (1967)	$\frac{7.6U}{H^{1.33}}$	U-fps H-feet	Based on synthesis of data from O'Connor-Dobbins (1958), Churchill *et al.* (1962), Krenkel and Orlob (1963), and Streeter *et al.* (1936).
Isaacs and Gaudy (1968)	$\frac{8.62U}{H^{1.5}}$	U-fps H-feet	Developed using regression analyses from data collected using a recirculating cylindrical tank. $0.6 \leq U \leq 1.6$ fps; $0.5' \leq H \leq 1.5'$.
Parkhurst and Pomeroy (1972)	$\frac{48.4(1+0.17F^2)(SU)^{3/8}}{H}$	U-m/s S-m/m H-meters	Developed from data collected in 12 sewers and in natural streams.
Negulescu and Rojanski (1969)	$10.9\left(\frac{U}{H}\right)^{0.85}$	U-fps H-feet	Developed from a recirculating flume with depths less than 0.5 feet.
Thackston and Krenkel (1969)	$\frac{24.9\left(1+F^{0.5}\right)u_*}{H}$	u_*-fps H-feet	Based on measurements made in a 2' wide flume with deoxygenated waters . $0.05' \leq H \leq 0.23'$.
Lau (1972b)	$2515\left(\frac{u_*}{u}\right)^3\frac{U}{H}$	u_*-fps U -fps H-feet	Based on reanalysis of the data of Thackston and Krenkel (1969), Krenkel (1960), and Churchill *et al.* (1962).

(continued)

TABLE 3-6. (continued)

Author(s)	k_2, base e(1/day at 20°C)	Units	Applicability
Krenkel and Orlob (1962)	$\frac{234(US)^{.408}}{H^{.66}}$	U-fps S-ft/ft H-feet	Based on 1' wide flume data. $0.08' \leq H \leq 0.2'$
Krenkel and Orlob (1962)	$\frac{8.4\ D_L^{1.321}}{H^{2.32}}$	D_L-ft^2/min H-feet	Experiments performed in a 1' wide flume by deoxygenating the water. Other similar formulas are also reported. The flume dispersion coefficient, D_L, was below the range expected in natural systems.
Padden and Gloyna (1971)	$\frac{6.9U^{0.703}}{H^{1.054}}$	U-fps H-feet	Regression analysis performed on data where $9.8 \leq k_2 \leq 28.8$/day.
Cadwallader and McDonnell (1969)	$\frac{336(US)^{0.5}}{H}$	U-fps S-ft/ft H-feet	Based on multivariate analysis of reaeration data.
Bansal (1973)	$\frac{4.67U^{0.6}}{H^{1.4}}$	U-fps H-feet	Based on reanalysis of reaeration data in numerous rivers.
Bennett and Rathbun (1972)	$\frac{106U^{0.413}S^{0.273}}{H^{1.408}}$ $\frac{20.2U^{0.607}}{H^{1.689}}$	U-fps S-ft/ft H-feet	These two equations are based on a reanalysis of historical data, with the second equation being al most as good a predictor as the first, but not having the slope term.
Dobbins (1964)	$\frac{117\left(1+F^2(US)^{0.375}\right)}{(0.9+F)^{1.5}H} \coth\left[\frac{4.10(US)^{0.125}}{(0.9+F)^{0.5}}\right]$	U-fps H-feet S-ft/ft	Theory combined with measurements in natural streams, and flume data of Krenkel and Orlob (1963).
Ice and Brown (1978)	$\frac{37W^{2/3}S^{1/2}U^{7/6}g^{1/2}}{Q^{2/3}}$	W-feet S-ft/ft U-fps Q-ft^3/sec	Based on data collected in several small Oregon streams.
McCutcheon and Jennings (1982)	$\frac{-\ln\left[1-2\left(\frac{\alpha I\ 24}{\pi(30.48H)^2}\right)^{1/2}\right]}{I}$ $I = \begin{cases} 0.0016 + 0.0005\ H & H \leq 2.26\ \text{ft} \\ 0.0097\ \ln(H) - 0.0052 & H > 2.26\ \text{ft} \end{cases}$	H-feet $\alpha = 1.42\ (1.1)^{T-20}$ T-°C	Based on the Velz method (1970) and replaces the iterative technique. The expressions for the mix internal I are based on an accumulation of applications of the Velz technique.

(continued)

TABLE 3-6. (continued)

Author(s)	k_2, base e(1/day at 20°C)	Units	Applicability
Long (1984)	$\frac{1.923U^{0.273}}{H^{0.894}}$	U-meters/sec H-meters	Known as the "Texas" equation. Based on data collected on streams in Texas.
Foree (1976)	$0.30+0.19S^{1/2}$ at 25°C	S-feet/mile	Radioactive tracer technique used on small streams in Kentucky. $0 \leq S \leq 42$ feet/mile.
Foree (1977)	• $0.888\ (0.63+0.4S^{1.15})q^{0.25}$ at 25°C for $0.05 \leq q \leq 1$ • $0.888\ (0.63+0.4\ S^{1.5})$ at 25°C for $q > 1$ • $0.42\ (0.63+0.4S^{1.15})$ at 25°C for $q < 0.05$	S-feet/mile q-cfs/mi^2	Reanalysis of Foree's (1976) data.
Tsivoglou and Wallace (1972)	$0.054\ \frac{\Delta h}{t}$ at 25°C	Δh-feet t-days	Based on summary of radioactive tracer applications to 5 rivers.
Tsivoglou and Neal (1976)	• $0.11\left(\frac{\Delta h}{t}\right)$ for $1 \leq Q \leq 10$ cfs • $0.054\left(\frac{\Delta h}{t}\right)$ for $25 < Q \leq 3000$ cfs	Δh-feet t-days	Based on data collected on 24 different streams using radioactive tracer method.
Grant (1976)	$0.09\left(\frac{\Delta h}{t}\right)$ at 25°C	Δh-feet t-days	Based on data from 10 small streams in Wisconsin using radioactive tracer techniques: $2.1 \leq k_2 \leq 55$/day $1.2 \leq S^2 \leq 70$ ft/mile $0.3 \leq Q \leq 37$ cfs
Grant (1978)	$0.06\left(\frac{\Delta h}{t}\right)$ at 25°C	Δh-feet t-days	Based on radioactive tracer data developed on Rock River, Wisconsin and Illinois: $0.01 \leq k_2 \leq 0.8$/day $0.25 \leq U^2 \leq 1.6$ fps $0.2 \leq S \leq 3.5$ ft/mile $260 \leq Q \leq 1030$ cfs

(continued)

TABLE 3-6. (continued)

Author(s)	k_2, base e(1/day at 20°C)	Units	Applicability
Shindala and Truax (1980)	• $0.08\left(\frac{\Delta h}{t}\right)$ at 25°C for $Q \leq 10$ cfs • $0.06\left(\frac{\Delta h}{t}\right)$ at 25°C for $10 < Q \leq 280$ cfs	Δh-feet t-days	Based on statistical analysis of reaeration coefficients for rivers in 7 states, where the radioactive tracer method was used to find the reaeration rates.
Eloubaidy and Plate (1972)	Wind effects analyzed. See text for discussion.		
Mattingly (1977)	Wind effects analyzed. See text for discussion.		
Gulliver and Stefan (1981)	Wind effects analyzed.		
Frexes *et al.* (1984)	Wind effects analyzed.		

Definitions of Symbols:

D_L = longitudinal dispersion coefficient

F = Froude number $= \frac{U}{(gh)^{0.5}}$

g = acceleration due to gravity

Δh = change in stream bed elevation between two points

q = stream discharge divided by drainage area

R = hydraulic radius

S = slope

t = travel time between two points where Δh measured

U = stream velocity

u_* = shear velocity = $\sqrt{gRS}$

W = width

3.2.2.2 Reviews of Stream Reaeration

Over the past decade, several researchers have reviewed reaeration formulas, and have tried to evaluate the performance of the formulas. One of the earlier reviews, Bennett and Rathbun (1972), is also an excellent source for reaeration theory. They describe the theories behind various conceptual models of reaeration (including film, renewal, penetration, film-penetration, and two-film theory models), semi-empirical models, and empirical models. They also discuss methods to determine the reaeration coefficient that include dissolved oxygen balances in natural streams, dissolved oxygen balances in recirculating flumes, the distributed equilibrium technique (where sodium sulfite is usually added to the water to deoxygenate it), and the radioactive tracer technique.

Table 3-7 summarizes the Bennett and Rathbun review in addition to other studies that have compared reaeration coefficients. The studies conclude that no single formula is best for all rivers. For one set of data one formula may be best, while for another set of data another formula may appear to be best.

Figure 3-1 compares 13 reaeration coefficient expressions for a range of depths (from Bennett and Rathbun, 1972). The figure illustrates the variability between predictions for a velocity of 1.0 fps and slope of 0.0001. The range of differences between predicted values spans one to two orders of magnitude. The formulas agree with each other best within the depth range of 1 to 10 feet, typical of many rivers.

Figure 3-2 compares calculated and observed reaeration coefficients for the formulas of Dobbins (1965) and Parkhurst and Pomeroy (1972). These formula were found by Wilson and MacLeod (1974) to best fit the observed data. Notice that the spread of data is slightly less than one order of magnitude.

The data of Wilson and Macleod also show that the depth - velocity model of Bennet and Rathbun (1972) does not fit the experimental data nearly

TABLE 3-7. SUMMARY OF STUDIES WHICH REVIEWED STREAM REAERATION COEFFICIENTS

Bennett and Rathbun (1972)

- Thirteen equations were evaluated.
- The standard error of the estimate was used as a measure of the difference between predicted values and data.
- The equation which provided the best fit to their original data set was Krenkel (1960).
- The equations which best fit the entire range of data were: O'Connor and Dobbins (1958), Dobbins (1965), Thackston and Krenkel (1969).
- Of the thirteen equations the Churchill et al. (1962) formula provided the best fit to natural stream data.
- The Bennett and Rathbun formula, developed from the data evaluated during their review, provided a smaller standard error for natural streams than the other 13 equations.
- There was a significant difference between predictions from equations derived from flume data and equations derived from natural stream data.
- The expected root-mean-square error from different measurement techniques is: 15 percent using the radioactive tracer technique; 65 percent using the dissolved oxygen mass balance, and 115 percent using the disturbed equilibrium method.

Lau (1972b)

- Both conceptual and empirical models were reviewed.
- Conclusions reported were similar to those of Bennett and Rathbun.
- It was found that no completely satisfactory method exists to predict reaeration.

Wilson and MacLeod (1974)

- Nearly 400 data points were used in the analysis.
- Sixteen equations were reviewed.
- The standard error of estimate and graphical results were both used in error analysis.
- It was concluded that equations which use only depth and velocity are not accurate over the entire range of data investigated.
- The methods of Dobbins (1965) and Parkhurst and Pomeroy (1972) gave the best fits to the data investigated.

Rathbun (1977)

- Nineteen equations were reviewed.
- Equation predictions were compared against radioactive tracer measurements on 5 rivers (Chattahoochee, Jackson, Flint, South, Patuxent).
- The best equations in terms of the smallest standard error estimates was Tsivoglou- Wallace (1972) (0.0528), Parkhurst-Pomeroy (1972) (0.0818), Padden-Gloyna (1971) (0.0712) and Owens et al. (1964), (0.0964).
- No one formula was best for all five rivers.

TABLE 3-7. (continued)

Rathbun and Grant (1978)

- Compared the radioactive and modified tracer techniques for Black Earth Creek and Madison Effluent Channel in Wisconsin.
- Differences in Black Earth Creek were -9% to 4% in one reach and 16% to 32% on another reach attributable to increased wind during the latter part of the test.
- Unsteady flow during the Madison Effluent Channel tests led to differences of as much as 25 to 58% in one case and -5% to 3% in another.

Shindala and Truax (1980)

- Reaeration measurements for streams in Mississippi, Wisconsin, Texas, Georgia, North Carolina, Kentucky, and New York were made using the radioactive tracer technique.
- The energy dissipation model resulted in the best correlation for reaeration coefficient prediction for small streams. The following escape coefficients (defined as the coefficients of $\frac{\Delta h}{t}$ in energy dissipation models for reaeration coefficients) were recommended:

  0.0802/ft ,for $Q < 10$ cfs
  0.0597/ft ,for $10 \leq Q \leq 280$ cfs

NCASI Bulletin (1982b)

- Six reaeration formulas were compared against measurements made using radioactive tracer techniques and hydrocarbon tracer techniques for a reach of the Ouachita River, Arkansas.
- The hydrocarbon tracer technique produced reaeration rates higher than both the radioactive tracer and empirical formulas.
- The O'Connor - Dobbins (1958) equation was chosen as the best empirical equation.

Kwasnik and Feng (1979)

- Thirteen reaeration formulas were reviewed and compared against values measured using the modified tracer technique for two streams in Massachusetts.
- The equations of Tsivoglou-Wallace (1972) and Bennett-Rathbun (1972) gave the closest predictions to the field values.
- The study indicates that results using the modified tracer technique are reproducible.

Grant and Skavroneck (1980)

- Four modified tracer methods and 20 predictive equations were compared against the radioactive tracer methods for 3 small streams in Wisconsin.
- Compared to the radioactive tracer method the errors in the modified tracer techniques were:

  11% for the propane-area method
  18% for the propane-peak method
  21% for the ethylene-peak method
  26% for the ethylene-area method

- Compared to the radioactive tracer method, the equations with the smallest errors were:

  18% for Tsivoglou-Neal (1976)
  21% for Negulescu-Rojanski (1969)
  23% for Padden-Gloyna (1971)
  29% for Thackston-Krenkel (1969)
  32% for Bansal (1973)

TABLE 3-7. (continued)

House and Skavroneck (1981)

- Reaeration coefficients were determined on two creeks in Wisconsin using the propane - area modified tracer technique and compared against 20 predictive formulas.
- The top five predictive formulas were:

  Tsivoglou - Neal (1976), 34% mean error
  Foree (1977), 35% mean error
  Cadwallader and McDonnell (1969), 45%, mean error
  Isaacs-Gaudy (1968), 45%, mean error
  Langbein-Durum (1967), 49%, mean error.

Zison et al. (1978)

- Thirteen reaeration formulas were reviewed, but none were compared against historical data.
- Covar's method (1976) was discussed which shows how stream reaeration can be simulated by using three formulas (O'Connor-Dobbins (1958), Churchill et al. (1962), and Owens et al. (1964)), each applicable in a different depth and velocity regime.

Yotsukura et al. (1983)

- Developed a steady injection method to avoid uncertainty in dispersion corrections.
- Determined reproducibility to be 4%.
- Found negligible effect of wind where stream banks are high.

Ohio Environmental Protection Agency (1983)

- Eighteen reaeration coefficient equations were compared against data collected in 28 Ohio streams.
- The streams were divided into four groups based on slope and velocity. The best predictive equations for each group are shown below:

Group	Slope (ft/mile)	Flow (cfs)	Preferred Equation
1	<3	All data	Negelescu-Royanski (1969) Krenkel-Orlob (1962)
2	3-10	≤30	Parkhurst-Pomeroy (1972)
3	3-10	>30	Thackston-Krenkel (1969)
4	>10	All data	Parkhurst-Pomeroy (1972) Tsivoglou-Neal (1976)

as well (see Figure 3-3). This was the formula which Bennett and Rathbun (1972) found produced the smallest error of the formulas they reviewed.

Figure 3-4 shows the three reaeration formulas found by Rathbun (1977) to best predict observed values for the Chattahoochee, Jackson, Flint,

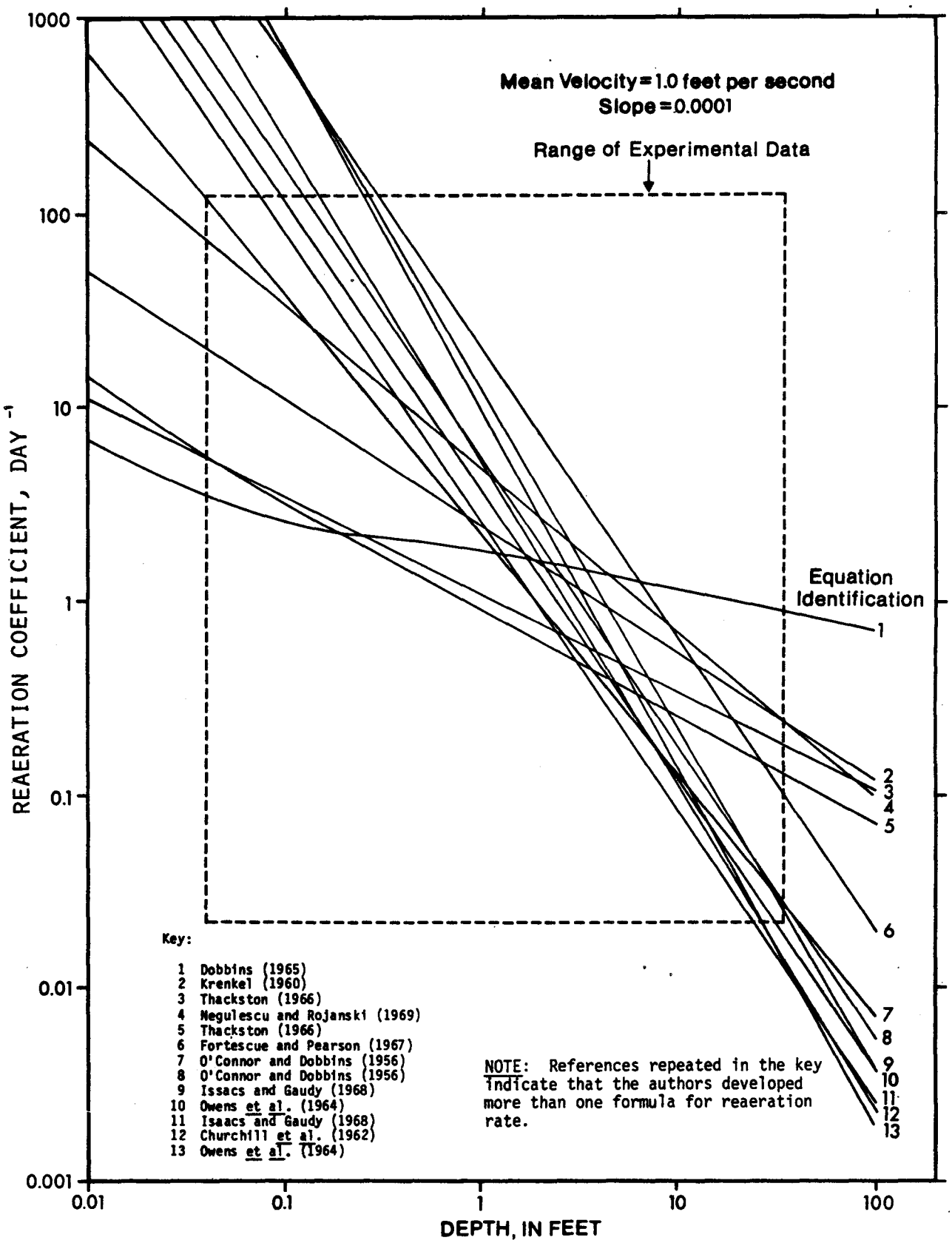

Figure 3-1. Predicted reaeration coefficients as a function of depth from thirteen predictive equations (from Bennett and Rathbun, 1972).

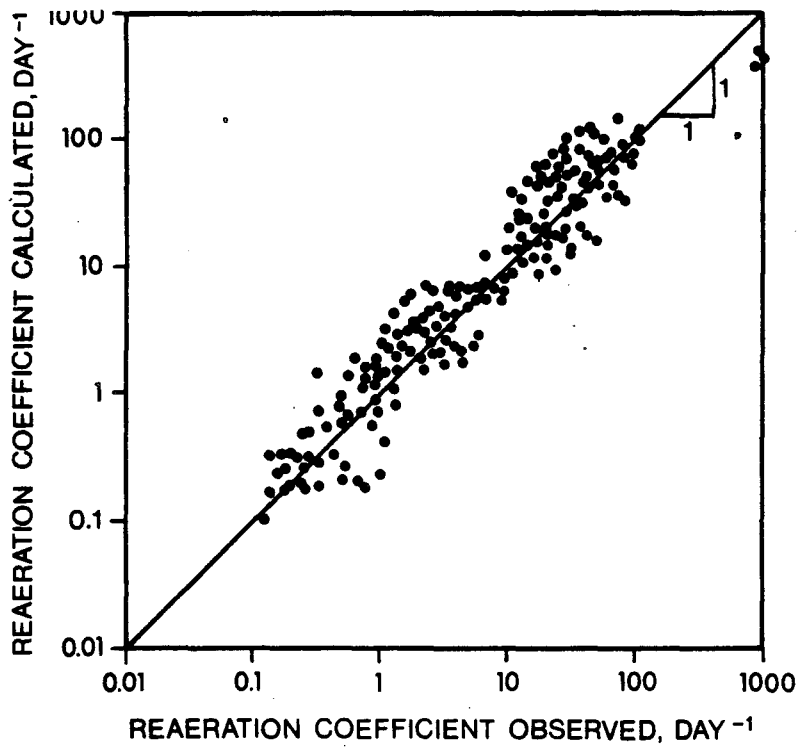

(a)

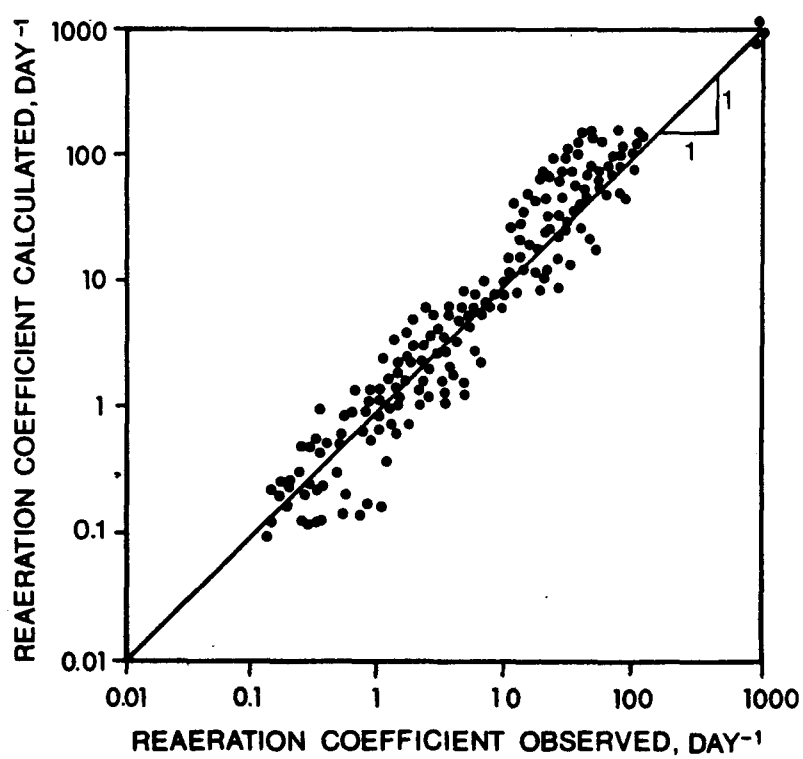

(b)

Figure 3-2. Comparisons of predicted and observed reaeration coefficients for the formula of Dobbins (1965) (a) and Parkhurst-Pomeroy (1972) (b).

South, and Patuxent Rivers. The range of reaeration coefficients analyzed here is considerably smaller than analyzed by Wilson and Macleod. The Tsivoglou - Wallace method is noticeably better than either the Padden-Gloyna or Parkhurst-Pomeroy methods. However, the Tsivoglou-Wallace method was originally developed using this data set, so it is not surprising that the fit is best.

Figure 3-5 shows the energy dissipation model of Shindala and Truax (1980) applied to streams with flow rates less than 280 cfs. They found that the best fit to the data was achieved when the flow rate was divided into two groups: less than 10 cfs and greater than 10 cfs.

Covar (1976), as discussed by Zison et al. (1978) found that the research of O'Connor-Dobbins (1958), Churchill et al. (1962), and Owens et al. (1964) could be used jointly to predict stream reaeration coefficients

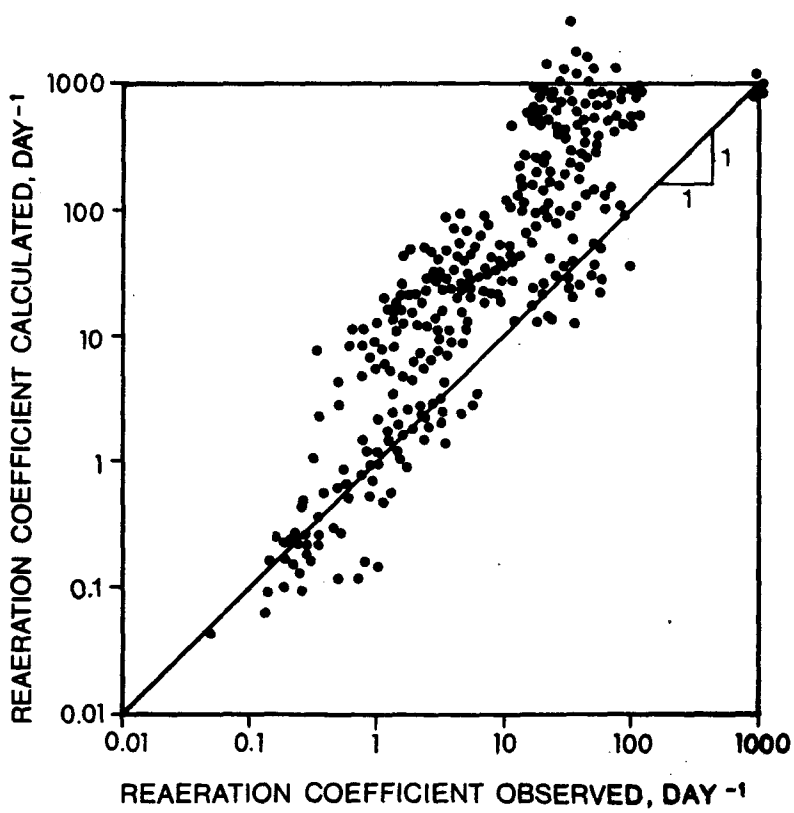

Figure 3-3. Formula of Bennett and Rathbun (1972) compared against observed reaeration coefficients.

for a range of depth and velocity combinations. Figure 3-6 shows the data points collected by each investigator and the regions Covar choose to divide the applicable formulas. Figure 3-7 shows the plots of reaeration prediction. Note that the predictions approximately match at the boundaries of each region.

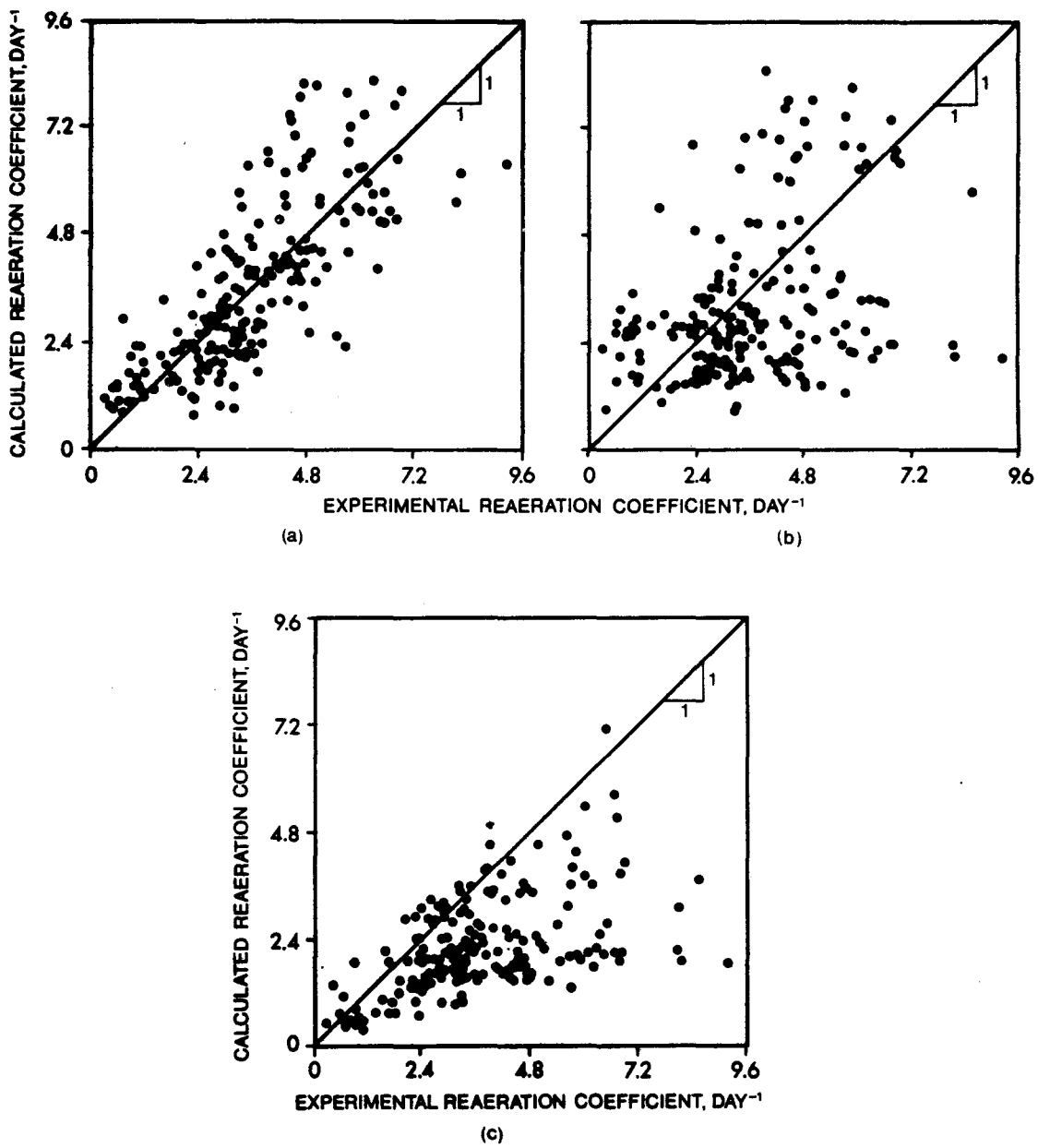

Figure 3-4. Calculated versus experimental reaeration coefficients for equations of (a) Tsivoglou and Wallace (1972), (b) Padden and Gloyna (1971), and (c) Parkhurst and Pomeroy (1972).

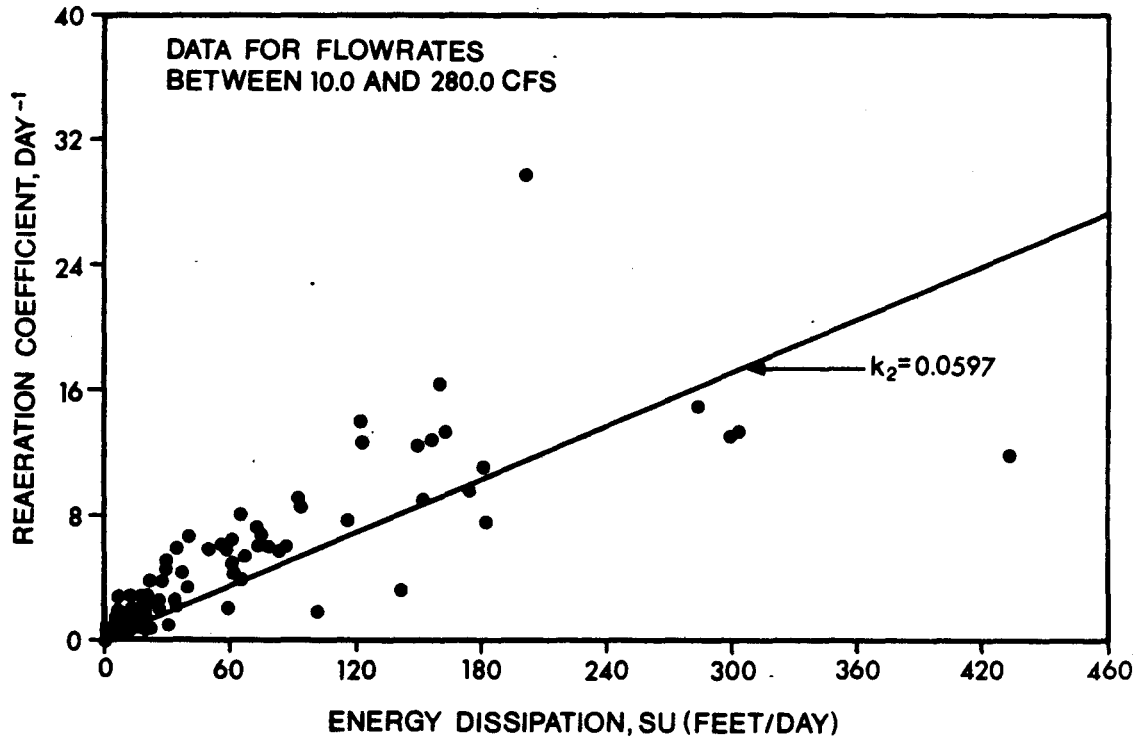

(a)

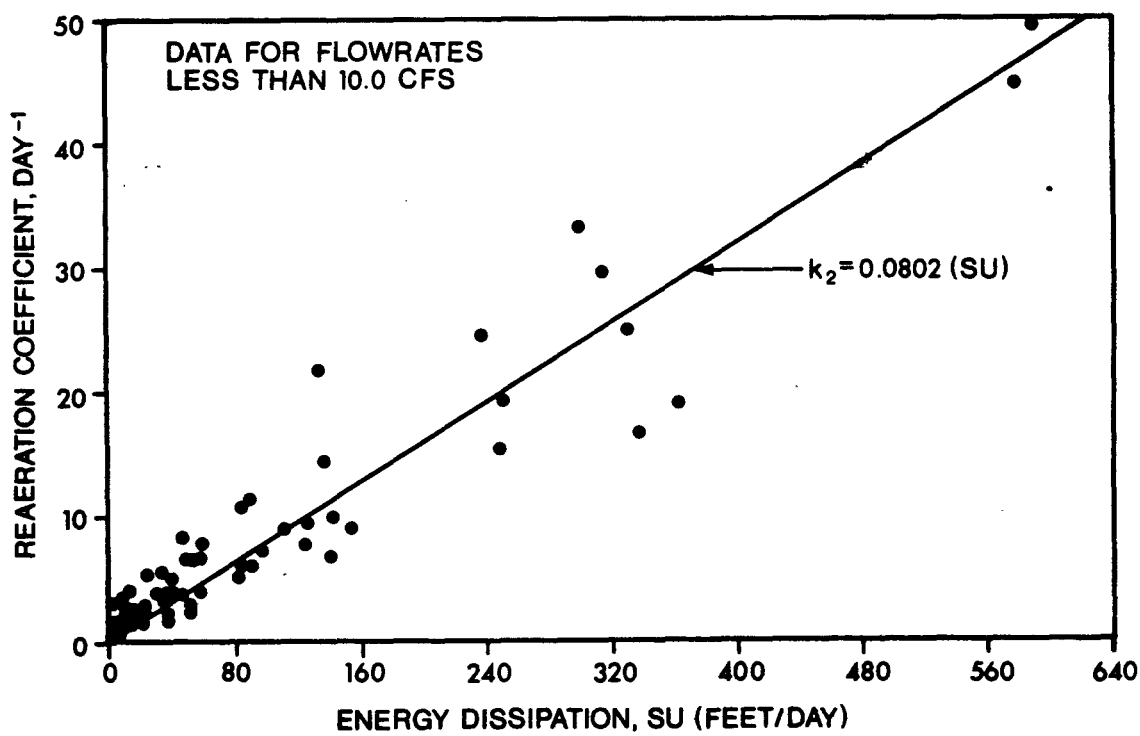

(b)

Figure 3-5. Reaeration coefficient versus energy dissipation (a) for flow rates between 10 and 280 cfs and (b) for flow rates less than 10 cfs. (Note: Curves for predicted reaeation coefficients are forced through the origin).

3.2.2.3 Measurement Techniques

Methods to determine reaeration rates based on instream data include the dissolved oxygen balance, deoxygenation by sodium sulfite, productivity measurements, and tracer techniques (both radioactive tracers and hydocarbon tracers). Today, use of tracers is the most widely accepted method. Productivity measurements are sometimes used, but because of their indirect approach could be subject to considerable error. Some of these methods are discussed in Kelly et al. (1975), Hornberger and Kelly (1975), and Waldon (1983). Only the tracer methods are discussed here.

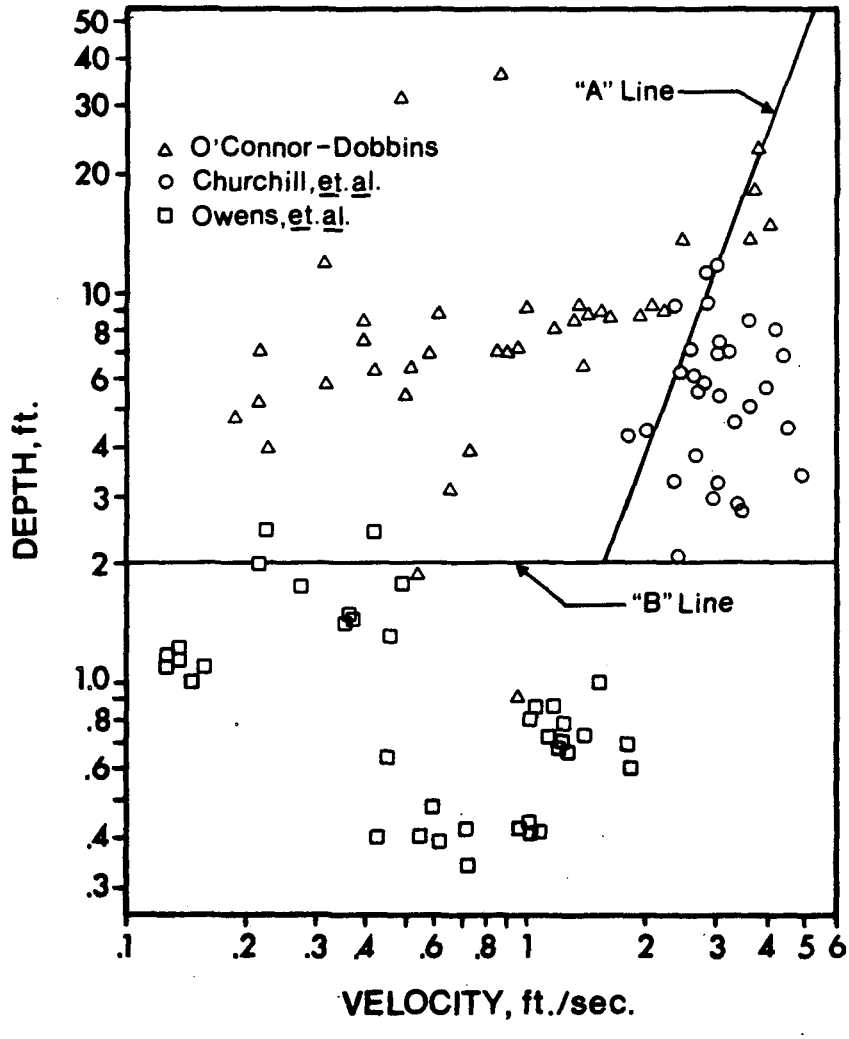

Figure 3-6. Field data considered by three different investigations.

The tracer method which appears to produce the most accurate results is the radioactive tracer technique developed and reported by Tsivoglou et al. (1965), Tsivoglou (1967), Tsivoglou et al. (1968), Tsivoglou and Wallace (1972), and Tsivoglou and Neal (1976). The method involves the instantaneous and simultaneous release of three tracers: krypton-85, tritium, and a fluorescent dye. The fluorescent dye indicates when to sample the invisible radioactive tracers and provides travel time information as well. The tritium acts as a surrogate for dispersion: the

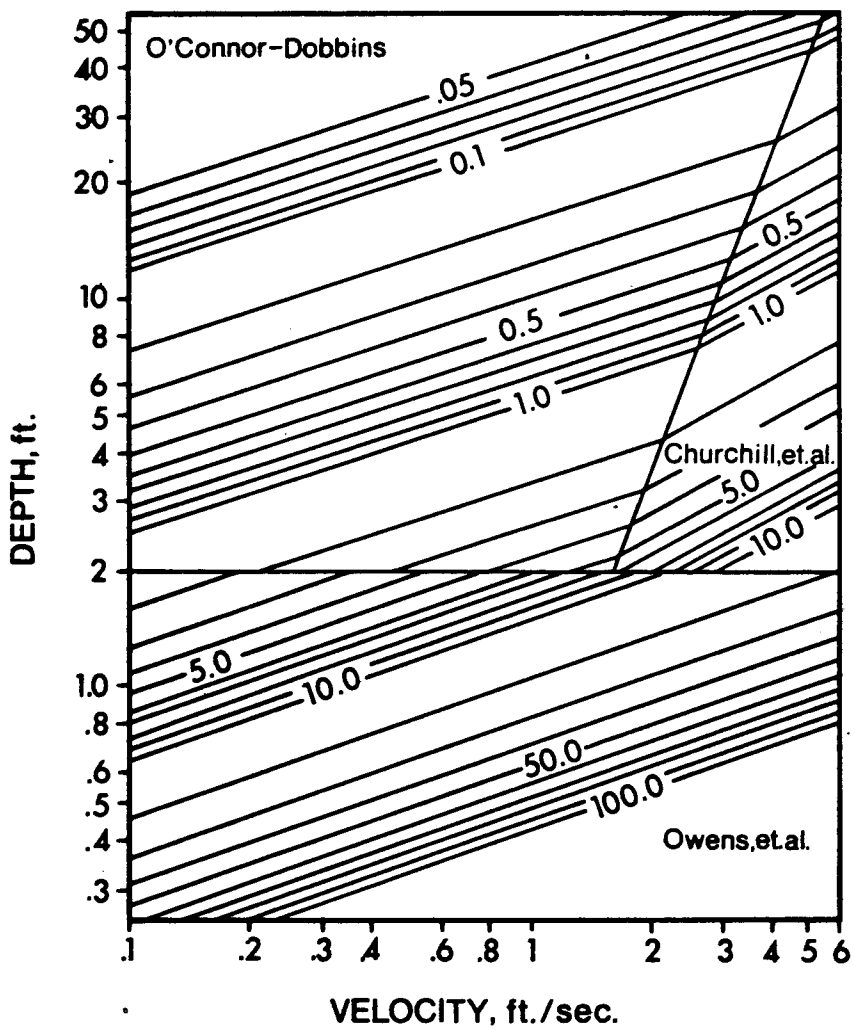

Figure 3-7. Reaeration coefficient (1/day) vs. depth and velocity using the suggested method of Covar (1976).

tritiated water disperses in the same manner as the natural water. The krypton-85 is lost to the atmosphere in a constant, known ratio compared with dissolved oxygen. The formula used is:

$$\frac{\left(\frac{C_{kr}}{C_{tr\ B}}\right)}{\left(\frac{C_{kr}}{C_{tr\ A}}\right)} = \exp\ (-k_{kr}t) \qquad (3\text{-}18)$$

where $\left(\frac{C_{kr}}{C_{tr}}\right)_{A,B}$ = concentration ratios of krypton and tritium at locations A and B when the dye peaks at each location

t = travel time between A and B

k_{kr} = atmospheric exchange rate of krypton

Since $\frac{k_{kr}}{k_2} = 0.83 \pm 0.04$, the dissolved oxygen reaeration rate, k_2, can be found directly from k_{kr}. The ratio 0.83 was found in the laboratory and has not been proven to be constant for all conditions.

Wilhelms (1980) has applied the radioactive tracer technique to flow through a hydraulic model. The results compared favorably with results from disturbed-equilibrium tests.

Because of the costs and potential hazards of using this method, other tracer techniques have been developed which do not use radioactive tracers. These methods have been discussed by Rathbun et al. (1975), Rathbun et al. (1978), Rathbun and Grant (1978), Kwasnik and Feng (1979), Bauer et al. (1979), Rathbun (1979), Jobson and Rathbun (undated), Grant and Skavroneck (1980), House and Skavroneck (1981), Rainwater and Holley (1984), Wilcock (1984a), and Wilcock (1984b). Not all researchers agree on the accuracy to the modified tracer techniques. Kwasnik and Feng (1979), Grant and Skavroneck (1980), House and Skavroneck (1981) all reported successful applications of the method. However, NCASI (1982b) reported that the hydrocarbon tracer technique produced results higher than both the radioactive tracer and empirical methods. The application was on a large

sluggish stream. Rainwater and Holley (1984) have investigated two assumptions of the hydrocarbon tracer technique (constant ratios between mass transfer coefficients and negligible absorptive losses) and found both assumptions to be valid for that particular study.

The modified tracer techniques use a hydrocarbon gas tracer and a fluorescent dye (e.g., rhodamine-WT) as the dispersion-dilution tracer. Sometimes two different tracer gases (e.g., ethylene and propane) can be used simultaneously to yield two estimates of reaeration rate. Two methods can be used: the peak concentration method and the total weight method.

Using the total-weight method the exchange rate of the tracer with the atmosphere, k_T is computed as follows:

$$k_T = \frac{1}{t_d - t_u} \log_e \left(\frac{A_u Q_u}{A_d Q_d} \right) \tag{3-19}$$

where A_u and A_d = areas under the gas concentration-versus-time curves at the upstream and downstream ends of the reach, respectively, and

Q_u and Q_d = stream discharge at each end of the reach.

The reaeration coefficient k_2 is computed as:

$$k_2 = \begin{cases} \dfrac{k_T}{.87} \text{ , ethylene} & \text{(3-20a)} \\[2ex] \dfrac{k_T}{.72} \text{ , propane} & \text{(3-20b)} \end{cases}$$

Recently Wilcox (1984a, b) has proposed methyl chloride as a gas tracer. At 20°C,

$$k_2 = \frac{k_T}{.707} \text{ , for methyl chloride} \tag{3-20c}$$

The methyl chloride transfer coefficient k_T was found to exhibit a temperature dependence.

The peak concentration method is similar in form to the radioactive tracer equation:

$$k_T = \frac{1}{t_d - t_u} \log_e \frac{\left(\frac{C_T}{C_D}\right)_u}{\left(\frac{C_T}{C_D}\right)_d} \frac{(A_D)_d}{(A_D)_u} \qquad (3\text{-}21)$$

where k_T = the base e desorption coefficient for the tracer gas;

$t_d - t_u$ = the time of travel between the peak concentrations;

C_T and C_D = the peak concentrations of the tracer gas and rhodamine-WT dye, respectively

$(A_D)_d$, $(A_D)_u$ = area under dye versus time curve downstream and uptream, respectively

More recently Yotsukura et al. (1983) have conducted tests to assess the feasibility of a steady-state propane gas tracer method as a means of estimating reaeration coefficients. The tests were conducted on Cowaselon Creek, New York. It was concluded that the steady state method, which also includes an instantaneous injection of dye tracer, is feasible and provides a reliable method of determining the reaeration coefficient.

3.2.2.4 Special Influences on Reaeration

In addition to hydraulic variables which typically appear in the expressions in Table 3-6, the reaeration coefficient can be influenced by certain special factors which include:

- surfactants
- suspended particles

- wind
- hydraulic structures, and
- water temperature

While surfactants, suspended solids, and wind can influence reaeration in rivers, in practice the effects of these factors are rarely if ever included in water quality models. Discussion of the influence of surfactants is given in Zison et al. (1978), Poon and Campbell (1967), and Tsivoglou and Wallace (1972). The influence of suspended solids is discussed by Holley (1975) and Alonso et al. (1975).

3.2.2.4.1 Wind Effects

While wind effects are typically not included in reaeration predictions in rivers, there is evidence that at high wind speeds, the reaeration rates can be significantly increased. These effects are occasionally alluded to in the literature when experimental measurements are abnormally high.

Eloubaidy and Plate (1972) performed experiments in the wind-wave facility at Colorado State University. They arrived at the following expression for the surface transfer coefficient, k_L, in feet per day:

$$k_L = \frac{CU_{*s}\, h\, U_{*c}}{\upsilon} \qquad (3\text{-}22)$$

where C = a constant of proportionality

υ = kinematic viscosity of water, m^2/sec

U_{*s} = surface shear velocity due to wind, m/sec = $0.0185\ V_w^{1.5}$

V_w = wind speed, m/sec

U_{*c} = water shear velocity defined as $\sqrt{ghS_c}$, m/sec

h = normal depth (i.e., depth with uniform flow), m

S_c = pressure-adjusted channel slope, unitless, $S_o + \frac{1dp}{\rho gdx}$

ρ = mass density of water, kg/m^3

g = gravitational constant, m/sec^2

S_o = slope of energy gradient (channel slope for uniform flow), unitless

$\frac{dP}{dx}$ = air pressure gradient in the longitudinal direction, kg/m^2-sec^2

From their experiments Eloubaidy and Plate found that C = .0027.

The variables comprising Equation 3-22 are readily obtainable, with the exception of the pressure gradient. The authors determined that an error on the order of 2 percent was obtained in k_2 (= k_L/h) by neglecting the pressure gradient.

A summary of the conditions under which Equation 3-22 was developed is:

channel slope:	.00043, .001
air velocity:	22, 30, 38 fps for each slope
discharge:	0.79, 0.83, 0.91 cfs at 0.001 slope
	0.58, 0.63, 0.75 cfs at 0.0043 slope
water depth:	0.385 feet

Note the extremely high wind velocities used in the experiments (greater than 22 fps). Hence the validity of the approach to lesser wind speeds typically encountered in the natural environment has not been demonstrated.

Mattingly (1977) also performed laboratory studies of the effects of wind on channel reaeration. He obtained this empirical expression:

$$\frac{k_2}{(k_2)_o} - 1 = 0.2395\ V_w^{1.643} \qquad (3\text{-}23)$$

where k_2 = reaeration coefficient under windy conditions, 1/day
$(k_2)_o$ = reaeration coefficient without wind, 1/day
V_w = wind velocity in meters per second in the free stream above the boundary layer near the water surface

A plot of the experimental data is shown in Figure 3-8. Note the importance of wind induced reaeration at moderate to high wind speeds. Further discussion of the effects of wind are found in Gulliver and Stefan (1981) and Frexes et al. (1984).

Because wind effects are typically neglected in river and stream reaeration modeling, this approach is equivalent to assuming a zero wind velocity. For many water quality modeling applications, such as wasteload allocation, this approach is reasonable.

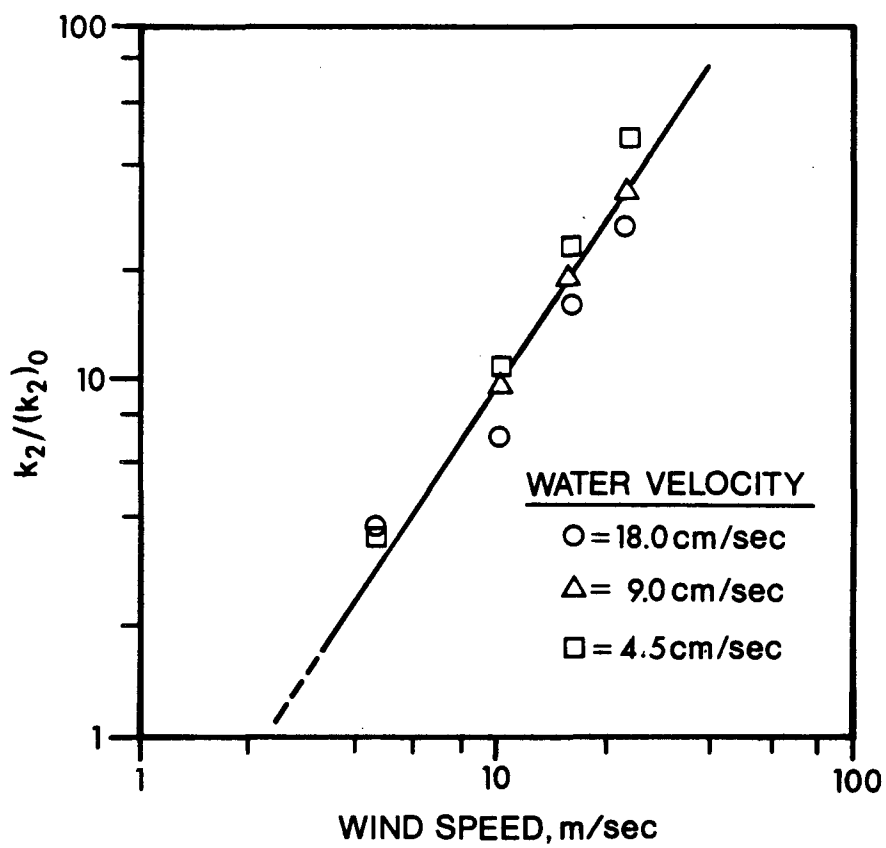

Figure 3-8. Ratio of reaeration coefficient under windy conditions to reaeration coefficient without wind, as a function of wind speed (based on laboratory studies).

3.2.2.4.2 Small Dams

On many rivers and streams small to moderate sized dams are present. Dams can influence reaeration by changing the dissolved oxygen deficit from 1 to 3 mg/l (typically) in a very short reach of the river. Table 3-8 summarizes various predictive equations that have been used to simulate the effects of small dams. Avery and Novak (1978) discuss limitations of these equations and aspects of oxygen transfer at hydraulic structures.

Butts and Evans (1983) have reviewed various approaches that predict the effects of small dams on channel reaeration and further collected field data on 54 small dams located in Illinois to determine their reaeration characteristics. They identified 9 classes of structures, and quantified the aeration coefficient b for use in the following formula:

$$r = \frac{C_s - C_u}{C_s - C_d} = 1 + 0.38abh\ (1 - 0.11h)\ (1 + 0.046T) \qquad (3\text{-}24)$$

where a = water quality factor (0.65 for grossly polluted streams; 1.8 for clean streams)

b = weir dam aeration coefficient

h = static head loss in meters

T = water temperature, ^{o}C

Figure 3-9 shows the general structural classification and the aeration coefficient, b, for each class.

The present review does not include influences of large dams, artificial reaeration, or other hydraulic structures. Cain and Wood (1981) discuss aeration over Aviemore Dam, 40 m (130 ft) in height, Banks et al. (1983) and NCASI (1969) discuss effects of artificial reaeration, and Wilhelms et al. (1981), Wilhelms (1980), and Wilhelms and Smith (1981) further discuss reaeration related to hydraulic structures.

TABLE 3-8. EQUATIONS THAT PREDICT THE EFFECTS OF SMALL DAMS ON STREAM REAERATION

Reference	Predictive Equation	Units	Source
Gameson (1957)	$r = 1+0.5abh$	h, in meters	field survey
Gameson *et al.* (1958)	$r = 1+0.11ab(1+0.046T)h$	h, in feet	model
Jarvis (1970)	$r_{15} = 1.05\ h^{0.434}$	h, in meters	model
Holler (1971)	$r_{20} = 1+0.91h$	h, in meters	model
Holler (1971)	$r_{20} = 1+0.21h$	h, in meters	prototype
Department of the Environment (1973)	$r = 1+0.69h(1-0.11h)(1+0.0464T)$	h, in meters	model
Department of the Environment (1973)	$r = 1+0.38abh(1-0.11h)(1+0.046T)$	h, in meters	model
Nakasome (1975)	$\log_e(r_{20}) = 0.0675h^{1.28}\ q^{0.62}\ d^{0.439}$	d, h, in meters q, in m^2/hr	model
Foree (1976)	$r = \exp(0.1bh)$	h, in feet	field survey

Symbols: $r_T = \frac{C_s-C_u}{C_s-C_d}$

C_s = dissolved oxygen saturation

C_u, C_d = concentration of dissolved oxygen upstream and downstream of dam, respectively

a = measure of water quality (0.65 for grossly polluted; 1.8 for clear)

b = function of weir type

h = water level difference

d = tailwater depth below weir

q = specific discharge.

T = water temperature, ^oC

3.2.2.4.3 Temperature Effects on Reaeration

The influence of temperature on reaeration is typically simulated using the following type of temperature dependence:

$$k_2(T)=k_2(20^oC)\theta^{T-20} \tag{3-25}$$

where T = water temperature, ^oC

θ = temperature adjustment factor

Table 3-9 summarizes values of θ from the literature. Typically values of 1.022 to 1.024 are used in most modeling applications.

Schneiter and Grenney (1983) developed a different approach to simulate temperature corrections over the ranges 4°C to 30°C. Their approach effectively allows θ to vary as a function of temperature. However, the approach is not widely used.

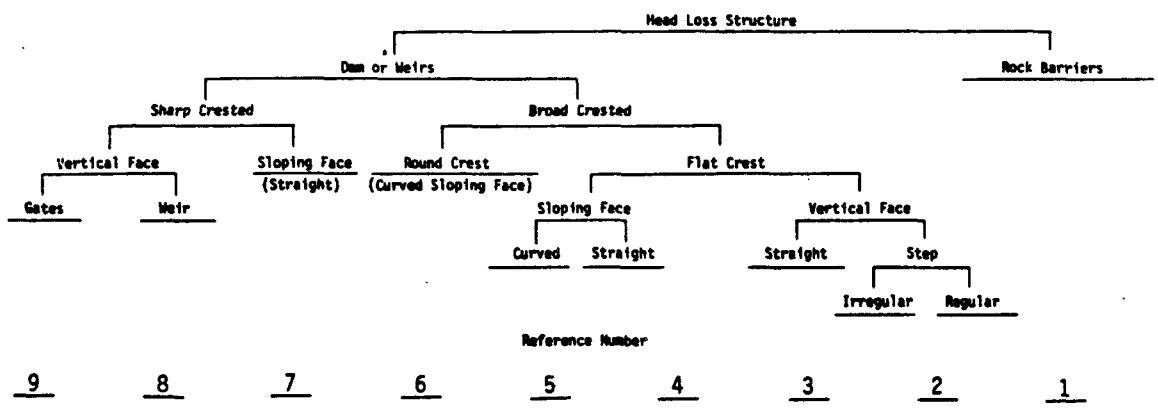

Reference Numbers	Dam Type (2)	b
1	Flat broad-crested regular step	0.70
2	Flat broad-crested irregular step	0.80
3	Flat broad-crested vertical face	0.80
4	Flat broad-crested straight slope face	0.90
5	Flat broad-crested curved face	0.75
6	Round broad-crested curved face	0.60
7	Sharp-crested straight slope face	1.05
8	Sharp-crested vertical face	0.80
9	Sluice gates with submerged discharge	0.05

Figure 3-9. Division of head loss structures by dam type.

TABLE 3-9. REPORTED VALUES OF TEMPERATURE COEFFICIENT

Temperature Coefficient, θ	Reference
1.047	Streeter, et al. (1926)
1.0241	Elmore and West (1961)
1.0226	Elmore and West (1961)
1.020	Downing and Truesdale (1955)
1.024	Downing and Truesdale (1955)
1.016	Dowining and Truesdale (1955)
1.016	Streeter (1926)
1.018	Truesdale and Van Dyke (1958)
1.015	Truesdale and Van Dyke (1958)
1.008	Truesdale and Van Dyke (1958)
1.024	Churchill et al (1962)
1.022	Tsivoglou (1967)
1.024	Committee on Sanitary Engineering Research (1960)

3.2.2.5 Sources of Data

Many sources of stream reaeration rates exist in the literature. Table 3-10 summarizes a number of the major sources. Many state agencies are also repositories of reaeration data.

3.2.3 Reaeration in Lakes

Simulation of reaeration in lakes is normally accomplished using the surface transfer coefficient k_L rather than the depth averaged k_2. Most often in lake simulations the surface transfer coefficient k_L is assumed to be a function of wind speed.

TABLE 3-10. SOURCES OF STREAM REAERATION DATA

Source	Contents
Owens et al., (1964)	Reaeration coefficients using disturbed equilibrium technique for six rivers in England (Ivel, Lark, Derwent, Black Beck, Saint Sunday's Beck, Yewdale Beck), and associated hydraulic data.
O'Connor and Dobbins (1958)	Reaeration data for Clarion River, Brandywine Creek, Illinois River, Ohio River, and Tennessee River.
Churchill et al. (1962)	Reaeration data using dissolved oxygen balance downstream from deep impoundments for Clinch River, Holston River, French Broad River, Watauga River, Hiwassee River.
Tsivoglou and Wallace (1972)	Hydraulic properties and radioactive tracer measured reaeration coefficients for Flint, South, Patuxent, Jackson, and Chattahoochee Rivers.
Bennett and Rathbun (1972)	Summaries of data from Churchill et al., (1962), Owens et al., (1964), Gameson et al. (1958), O'Connor and Dobbins (1958), Tsivoglou et al., (1967,1968), Negulescu and Rojanski (1969), Thackston (1966), Krenkel (1960).
Foree (1976)	Radioactive tracer measurements and reaeration hydraulic characteristics for small streams in Kentucky, and reaeration measurements for small dams in Kentucky.
Grant (1976)	Reaeration measurements and hydraulic characteristics for 10 small streams in Wisconsin.
Grant (1978)	Reaeration measurements and hydraulic characteristics for Rock River, Wisconsin.
Zison et al. (1978)	Summary of reaeration coefficients and hydraulic characteristics for rivers throughout the United States.
Kwasnik and Feng (1979)	Reaeration data using the modified tracer technique on selected streams in Massachusetts.
Grant and Skavroneck (1980)	Reaeration data from three small streams in Wisconsin.
House and Skavroneck (1981)	Reaeration data for two small streams in Wisconsin.
Shindala and Truax (1980)	Radioactive tracer measurements of reaeration rates and escape coefficients, plus hydraulic data, for rivers in Mississippi, Wisconsin, Texas, Georgia, North Carolina, Kentucky and New York.
Terry et al. (1984)	Hydrocarbon tracer measurements of k_2 and hydraulic data for Spring Creek, Osage Creek, and Illinois River, Arkansas. Bennett-Rathbun (1972) best fit all three streams. Eight equations were tested.
Bauer et al. (1979)	Hydrocarbon tracer measurements of k_2 and hydraulic data for the Yampa River, Colorado best matched the Tsivoglou Neal and Thackston and Krenkel energy dissipation type equations. Lau's equation was extremely error prone. Nineteen equations were tested.
Goddard (1980)	Hydrocarbon tracer measurements of k_2 and hydraulic data from the Arkansas River in Colorado were used to test 19 equations. The best fitting equations were those by Dobbins, Padden and Gloyna, Langbein and Durum, and Parkhurst and Pomeroy.

TABLE 3-10. (continued)

Source	Contents
Hren (1983)	Radioactive tracer measurements for the North Fork Licking River, Ohio.
Rathbun *et al*. (1975)	Hydrocarbon tracer measurements for West Hobolochitts Creek, Mississippi.
NCASI (1982c)	Radioactive tracer measurements for Ouachita River, Arkansas, and Dugdemona River, Louisiana.
Parkhurst and Pomeroy (1972)	Reaeration coefficients were determined by a deoxygenation method in 12 sewers in the Los Angeles County Sanitation District.
Ice and Brown (1978)	Reaeration coefficients were determined using sodium sulfite to deoxygenate the water in small streams in Oregon.
Ohio Environmental Protection Agency (1983)	Reaeration coefficients were determined for 28 different streams in Ohio using predominantly the modified tracer technique, and in one case the radioactive tracer technique.
Long (1984)	Reaeration coefficients, hydraulic data, and time of travel data collected on 18 streams in Texas.

Since many lakes are not vertically well-mixed, multiple layers are often used to simulate dissolved oxygen dynamics. Atmospheric reaeration occurs only through the surface layer, and then dissolved oxygen is dispersed and advected to layers lower in the water body.

Table 3-11 summarizes various methods that have been used to simulate reaeration in lakes. With the exception of the method of Di Toro and Connolly (1980), all formulas include a wind speed term. Di Toro and Connolly applied a constant surface transfer coefficient to Lake Erie. They found that the surface layer of the lake remained near saturation so that the value of k_L used was not important as long as it was sufficiently high to maintain saturated dissolved oxygen levels in the surface layer.

All the surface transfer coefficients shown in Table 3-11 should be viewed as empirical; the researchers have simply hypothesized that the suggested formulas are adequate to simulate reaeration. The coefficients (a and b) are of limited validity, and should be treated as calibration parameters. O'Connor (1983) has analyzed from a more theoretical point of view the effects of wind on the surface transfer coefficient.

TABLE 3-11 . REAERATION COEFFICIENTS FOR LAKES

Author(s)	Surface Transfer Rate, k_L (m/day)
Di Toro and Connolly (1980)	$k_L = 2.0$
Chen *et al.*, (1976)	$k_L = \frac{86400D}{(200-60\sqrt{V})10^{-6}}$ D = molecular diffusion coefficient of oxygen in water, m^2/sec V = wind speed, m/sec
Banks (1975)	$k_L = 0.362\ V^{1/2}$ for $0 \leq V \leq 5.5$ m/sec $k_L = 0.0277V^2$ for $V > 5.5$ m/sec
Baca and Arnett (1976)	$k_L = a + bV$ a = 0.005 - 0.01 m/day b = 10^{-6} - 10^{-5} m^{-1} V = wind speed, m/day
Smith (1978)	$k_L = a + bV^2$ a = 0.64 m/day b = 0.128 $sec^2m^{-1}day^{-1}$ V = wind speed, m/s
Liss (1973)	$k_L = 0.156\ V^{0.63}$ $V \leq 4.1$ m/sec $k_L = 0.0269V^{1.9}$ $V > 4.1$ m/sec V = wind speed, m/sec
Downing and Truesdale (1955)	$k_L = 0.0276V^{2.0}$ V = wind speed, m/sec
Kanwisher (1963)	$k_L = 0.0432V^2$ V = wind speed, m/sec
Broecker *et al.* (1978)	$k_L = 0.864V$ V = wind speed, m/sec
Yu *et al.* (1977)	$k_L = 0.319V$ V = wind speed, m/sec
Broecker and Peng (1974)	$k_L = 0.0449V^2$ V = wind speed, m/sec

TABLE 3-11. (Cont'd)

Author(s)	Surface Transfer Rate, k_L (m/day)
Weiler (1975)	$k_L = 0.398$ $V < 1.6$ m/sec $k_L = 0.155V^2$ $V \geq 1.6$ m/sec V = wind speed, m/sec

Notes:
1. Elevation of wind speed measurements is not always reported.
2. a and b are empirically determined.

Some limited research has addressed the influence of rainfall on reaeration (Banks et al., 1984; Banks and Herrera, 1977). Rainfall effects are more of theoretical interest rather of practical concern.

3.2.4 Reaeration in Estuaries

The present state of reaeration simulation in estuaries combines concepts used in river and lake approaches. Very little original research on estuarine reaeration has been completed to date.

Table 3-12 summarizes different formulations that have been used to predict reaeration in estuaries. The different approaches include both k_L (surface transfer) and k_2 (depth averaged) reaeration terms. In some models, k_2 can be specified (e.g., Genet et al., 1974 and MacDonald and Weismann, 1977). O'Connor et al. (1981) specified the surface transfer rate to be 1 m/day in their two-layered model of the New York Bight. One of the more widely used approaches is the O'Connor (1960) formula, which has subsequently been modified to include wind speed terms (Thomann and Fitzpatrick, 1982).

Few field studies have been performed for the purpose of directly measuring reaeration in estuaries. Baumgartner et al., (1970) used Krypton-85 to measure the range of reaeration in the Yaquina River Estuary. However, no predictive formulas were developed.

TABLE 3-12. REAERATION COEFFICIENTS FOR ESTUARIES

Reference	Reaeration Rate
O'Connor (1960)	$k_2 = \frac{(D_L U_o)^{1/2}}{H^{3/2}}$ (1/day) U_o = mean tidal velocity over a complete cycle, m/day D_L = molecular diffusivity of oxygen, m^2/day H = average depth, m
Genet *et al.*, (1974)	k_2 = user specified
O'Connor *et al.*, (1981)	k_L = 1 m/day
MacDonald and Weisman (1977)	k_2 = user specified
Harleman *et al.*, (1977)	$k_2^a = 10.86 \frac{V^{0.6} H W_T}{H^{1.4} A}$ (1/day) V = tidal velocity, ft/sec H = depth, ft W_T = top width, ft A = cross-sectional area, ft
Thomann and Fitzpatrick (1982)	$k_2 = \frac{13V^{0.5}}{H^{1.5}} + \frac{3.281}{H}(0.728W^{0.5} - 0.317W + 0.0372W^2)$ (1/day) V = depth averaged velocity, fps H = depth, ft W = wind speed, m/sec
Ozturk (1979)	$k_2 = \frac{4.56V^{4/3}}{H}$ (1/day) V = mean tidal velocity, m/sec H = mean depth, m

[a]The coefficient 10.86 is the recommended value, but can be changed as discussed by Harleman *et al.* (1977).

Tsivoglou (1980) has discussed the application of radioactive tracer techniques to small estuaries within the Chesapeake Bay. Special discussion was given to the Ware River Estuary.

3.2.5 Summary

The most common method of simulating reaeration in rivers is to use the depth averaged k_2 approach, while in lakes the surface transfer rate k_L is typically used. In estuaries either k_2 or k_L is used, depending on the importance of stratification. Very little research on reaeration has been done in either lakes or estuaries. In lakes, reaeration is typically specified to be a constant or to be a function of wind speed. Little information is available on how to select parameters in the wind speed functions. Site specific calibration of the parameters may be required.

In contrast to lakes and estuaries much research has been conducted on reaeration in rivers. Thirty-one formulas were shown earlier in Table 3-6. The formulas have been developed based on hydraulic parameters, most often depth and velocity. Consequently, the variables in reaeration expressions are generally not of concern in distinguishing among the utility of the formulas. One exception is formulas that contain longitudinal dispersion coefficients, which are difficult to quantify.

Considerable evidence shows that reaeration formulas are most applicable over the range of variables for which they were developed, and outside of that range, errors might be quite large. This suggests that reaeration rates developed from laboratory flume data may be quite limited for natural stream applications. Some research supports this supposition (Bennett and Rathbun, 1972).

Previous reviews of stream reaeration (see Table 3-7) have shown that no one formula is best under all conditions, and depending on the data set used, the range of the reaeration coefficients in the data set, and the error measurement selected, the "best" formula may change. Some of the reaeration rate expressions which have been judged "best" during past reviews are:

- The O'Connor and Dobbins (1958), Dobbins (1964), and Thackston and Krenkel (1969) formulas best fit the entire range of data reviewed by Bennett and Rathbun (1972).

- The Churchill et al. (1962) formula provided the best fit to natural stream data in the Bennett and Rathbun review.

- The methods of Dobbins (1964) and Parkhurst and Pomeroy (1972) gave the best fits to the data reviewed by Wilson and MacLeod (1974).

- The Tsivoglou-Wallace and Parkhurst-Pomeroy methods were best in the review by Rathbun (1977).

- The energy dissipation model produced the best correlation for small streams based on the study of Shindala and Truax (1980).

From previous reviews, one of the more popular and more accurate methods for reaeration rates prediction is the energy dissipation method of Tsivoglou. The method requires knowledge of the escape coefficient, which appears to depend on streamflow. Typical values of the escape coefficient are 0.08/ft for flow rates less than 10 cfs, and 0.06/ft for flow rates between 10 and 280 cfs.

The method of Covar (1976), which combines the O'Connor-Dobbins, Churchill et al., and Owens et al., formulas, has merit in that it attempts to limit the use of the three formulas to within the depth-velocity range for which they were developed. However, for relatively small and shallow streams, the method of Owens et al., tends to overestimate reaeration, so that the energy dissipation method, which appears to perform well in small streams, could be used to supplement the method.

The radioactive tracer method appears to be the best method for measuring stream reaeration coefficients. Even so, the coefficients that are predicted are valid only for the particular flow condition existing at the time of sampling. Thus to completely characterize the range of values of the reaeration coefficient would require numerous sampling events or use of an acceptable predictive equation.

Sampling methods which require indirect knowledge of parameters that are difficult to quantify should be avoided. The gas tracer method has been used with at least partial success, but applications do not yet appear widespread. When stream reaeration rates are being measured the wind should be light or calm; otherwise wind effects can produce atypical reaeration rates.

In deep, slowly moving backwater regions of rivers reaeration can either be simulated using a river formula or lake formula. The O'Connor-Dobbins method is probably the most appropriate stream formula to use, although for very slowly moving backwater regions the predicted reaeration coefficient can be between 0.01 to 0.05/day, which is below the range of k_2 values used in the development of the formula. If a lake reaeration formula is used, the reaeration rate coefficient can exceed the range predicted using the O'Connor-Dobbins formula. Under these conditions, wind and not depth and velocity can control the rate of reaeration.

3.3 CARBONACEOUS DEOXYGENATION

3.3.1 Introduction

Biochemical oxygen demand (BOD) is the utilization of dissolved oxygen by aquatic microbes to metabolize organic matter, oxidize reduced nitrogen, and oxidize reduced mineral species such as ferrous iron. The term BOD is also applied to the substrate itself. Concentrations of reduced minerals in waste streams are usually inconsequential, and so BOD is commonly divided into two fractions: that exerted by carbonaceous matter (CBOD) and that exerted by nitrogenous matter (NBOD). In domestic wastewaters, CBOD is typically exerted before NBOD, giving rise to the well-known two-stage BOD curve (although the processes can be simultaneous in natural systems and certain industrial effluents). Because wastewaters are potentially high in BOD, and because dissolved oxygen concentration is used as a principal determinant of the health of an aquatic system, BOD is a widely applied measure of aquatic pollution. This section discusses dissolved and

suspended CBOD; Section 3.4 deals with NBOD and Section 3.5 treats benthic oxygen demand or sediment oxygen demand (SOD). All are related processes.

Figure 3-10 shows the major sources and sinks of carbonaceous BOD in natural waters. Anthropogenic inputs include point sources and nonpoint sources such as urban runoff and feedlot runoff. Autochthonous sources derived from the aquatic biota (particularly algae) can be important in some systems. Also, re-entrainment of oxygen-demanding material from benthic deposits may occur. Removal of CBOD from the water column occurs through sedimentation, microbial degradation and the sorption to or uptake by the benthic flora. Some components of BOD may also volatilize from the water column. Carbonaceous material which has settled or been sorbed becomes part of the benthic oxygen demand.

It is important that the analyst distinguish in the modeling process between both the sources of BOD and the instream removal mechamisms. Waste load allocation decisions based upon models which consider CBOD as a "lumped" quantity may not accurately or fairly assess the water quality impact of the point sources.

Efforts to characterize CBOD kinetics have focused chiefly on water-column decay processes, and that is the major emphasis of this section. A general expression for BOD decay is:

$$\text{BOD} + \text{BACTERIA} + O_2 + \text{GROWTH FACTORS (NUTRIENTS)} \longrightarrow CO_2 + H_2O + \text{MORE BACTERIA} + \text{ENERGY}$$

3.3.2 Water Quality Modeling Needs

Nearly all water quality models characterize CBOD decay with first order kinetics represented by:

$$\frac{dL}{dt} = -k_d L \qquad (3\text{-}26)$$

where L = ultimate CBOD, mg/l

k_d = first order rate coefficient, 1/day, base e

t = time, days

This equation when coupled with stream dissolved oxygen kinetics becomes the classic Streeter-Phelps equation:

$$D = \frac{k_d L}{k_2 - k_d}\left[e^{-k_d t} - e^{k_2 t}\right] + D_o\, e^{-k_2 t} \qquad (3\text{-}27)$$

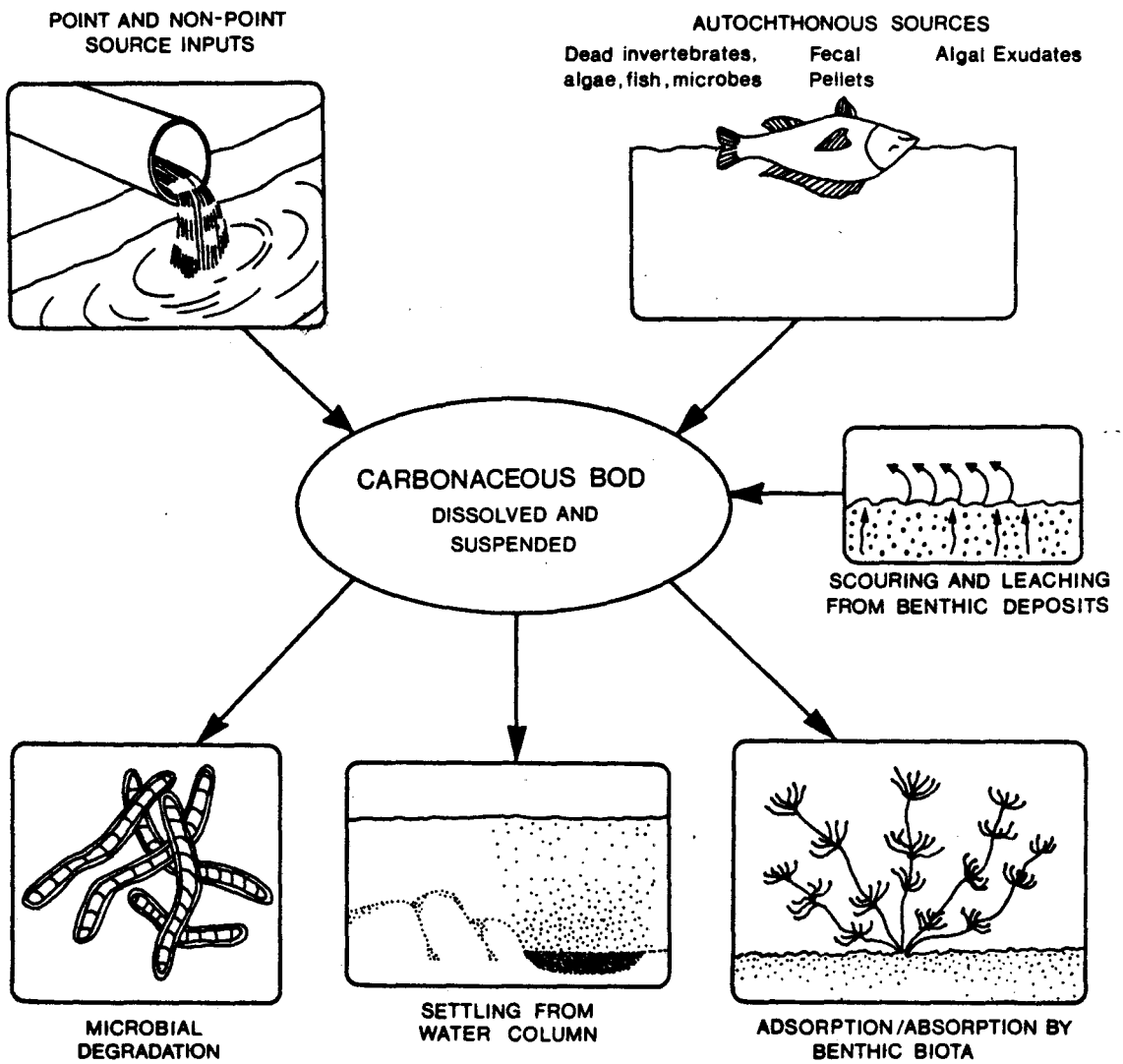

Figure 3-10. Sources and sinks of carbonaceous BOD in the aquatic environment.

where D = dissolved oxygen deficit, mg/l

k_2 = stream reaeration rate, 1/day, base e

D_o = initial stream deficit, mg/l

This equation in principle is similar in nearly all state-of-the-art water quality models.

In using this representation of BOD/DO for waste load allocation modeling, the analyst may require measurement or estimation of three independent factors which include:

(a) the magnitude of ultimate CBOD of the point sources and the resulting instream spatial distribution,

(b) the magnitude and spatial distribution of the instream CBOD removal rate, and

(c) the ratio of point source ultimate CBOD to 5-day CBOD (if compliance is to be based upon $CBOD_5$).

It is important to note that the water quality model is based upon ultimate CBOD and not $CBOD_5$. Some models internally convert from 5 day to ultimate using an assumed ratio. In the case of the QUAL-II model (NCASI, 1982a), this ratio is 1.46 and is not user specified. This assumption has significant implications to water quality modeling because recent experience has shown that this ratio is both wasteload and receiving water specific. Ultimate to 5 day ratios as high as 30 have been reported for some paper industry wastewaters (NCASI, 1982d). Since first order kinetics are assumed in most models, the ultimate to 5 day ratio is not independent of the decay rate, k_d. Consequently, analysts should be certain that the river water ultimate to 5 day BOD is not assigned independently of the rate, k_d.

3.3.3 Nomenclature

Since microbial degradation is not the only process contributing to the observed depletion of CBOD in a water body (see Figure 3-10), laboratory rates of carbonacous deoxygenation must be distinguished from those which

occur in the field. The following terms are used herein to maintain these distinctions:

k_1 = laboratory-derived CBOD decay rate,
k_d = CBOD decay rate in natural waters
k_s = CBOD settling rate
k_R = overall rate of CBOD removal from water column

By these definitions,

$$k_R = k_d + k_s \tag{3-28}$$

$$k_d \geqslant k_1, \text{ typically} \tag{3-29}$$

Note that uptake/sorption by the benthic biota is not explicitly dealt with. In practice, the effects of instream deoxygenation and benthic biological CBOD removal are difficult to distinguish. Thus reported k_d values may incorporate both processes. Unless otherwise specified, all rate coefficients discussed in this section are corrected to 20°C, are to the base e, and are in units of inverse days.

3.3.4 Factors Affecting CBOD Removal

A number of factors are known to influence the rate at which CBOD is removed from the water column. Chief among these are water temperature, hydraulic factors, stream geometry and the nature of the carbonaceous material. The influence of these factors has been described by both theoretical and empirical formulations.

Like all biochemical processes, CBOD decay occurs at a rate which increases with increasing temperature up to the point where protein denaturation begins. This temperature dependence is generally formulated for a limited range of temperature as:

$$k_T = k_{20}\,\theta^{(T-20)} \tag{3-30}$$

where k_T = rate constant at temperature T

k_{20} = rate constant at 20^oC

θ = an empirical coefficient.

This formulation is based on the Arrhenius equation which incorporates the energy of activation of the overall decay reaction. Arrhenius proposed the relationship:

$$\frac{d \ln k}{dT} = -\frac{E}{RT^2} \tag{3-31}$$

where T = absolute temperature, ^oK

R = universal gas constant

E = activation energy of the reaction

k = rate constant

Integrating Equation (3-31) results in

$$\ln \frac{k}{k_o} = \frac{-E\ (T-T_o)}{R\ T_o\ T} \tag{3-32}$$

where T_o = arbitarily chosen reference temperature, ^oK

k_o = rate constant at temperature T_o

Equation (3-32) can be rewritten as

$$k = k_o \exp\left(\frac{-E\ (T-T_o)}{R\ T_o\ T}\right) \tag{3-33}$$

Equations (3-30) and (3-33) are identical if θ is defined as

$$\theta = \exp\left(\frac{-E}{RT_oT}\right) \tag{3-34}$$

Note that whether $T-T_o$ is in units of ^oC or ^oK is of no concern. Thus θ, which is assumed to be independent of temperature in Equation (3-30), really has some slight temperature dependence.

Table 3-13 shows values of θ which have been used for CBOD decay. The value 1.047 is very widely used and corresponds to an energy of activation of 7900 calories per mole measured by Fair et al. (1968). There are limits to the applicability of this approach because the activation energy is not actually constant. Studies by Schroepfer et al. (1964) indicate that the value of 1.047 for θ is valid between 20°C and 30°C, but higher values are appropriate at lower temperatures. Fair et al. (1968) suggest θ values of 1.11 and 1.15 for 10°C and 5°C, respectively. Few water quality models incorporate a varying temperature dependence for CBOD degradation. Some impose temperature limits, generally 5-30°C, outside of which the reaction is considered not to occur. The model SSAM-IV (Grenney and Kraszewski, 1981) adjusts the BOD decay rate for temperature via the expression:

$$k_T = {}^{\tau}k_{20} \quad . \tag{3-35}$$

where $\tau = \dfrac{0.1393 \exp(0.174(T-2))}{0.9 + 0.1 \exp(0.174(T-2))}$

This is equivalent to varying the value of θ with temperature.

The 1.047 value originated from the work of Phelps and Theriault (Phelps, 1927, Theriault, 1927). The θ value of 1.047 was an average value obtained from three separate studies with a reported standard deviation of 0.005. Moore noted in 1941 that the correlation of the CBOD decay rate with temperature using the Arrenhius model was not strong, since correlation coefficients of 0.56 to 0.78 were obtained (Moore, 1941).

Water turbulence is hypothesized to influence the rate of BOD depletion in a receiving water in several ways. It influences k_s by controlling such processes as scour and sedimentation. Increased turbulence may enhance contact between BOD and the benthic biological community. It also influences the carbonacous deoxygenation rate, so that laboratory samples which are agitated during incubation yield higher k_1 values than quiescent samples (see Morrissette and Mavinic, 1978, for example). This confounds the use of k_1 values from static laboratory tests in place of field values

TABLE 3-13
VALUES OF THE TEMPERATURE COMPENSATION COEFFICIENT
USED FOR CARBONACEOUS BOD DECAY

θ, Temperature Correction Factor	Temperature Limits (^{o}C)	Reference
1.047		Chen(1970)
		Harleman et al. (1977)
		Medina (1979)
		Genet et al. (1974)
		Bauer et al. (1979)
		JRB (1983)
		Bedford et al. (1983)
		Thomahn and Fitzpatrick (1982)
		Velz (1984)
		Roesner et al. (1981)
1.05		Crim and Lovelace (1973)
		Rich (1973)
1.03-1.06	(0-5)-(30-35)	Smith (1978)
1.075		Imhoff et al. (1981)
1.024		Metropolitan Washington Area Council of Governments (1982)
1.02-1.06		Baca and Arnett (1976)
		Baca et al. (1973)
1.04		Di Toro and Connolly (1980)
1.05-1.15	5-30	Fair et al. (1968)

of k_d. To more closely duplicate natural conditions, some investigators used stirring during laboratory incubations (NCASI, 1982a). This particular experiment showed no effect of stirring on the reaction kinetics.

Adjustment factors based on stream characteristics have also been used in BOD calculations. Bosko (1966) expressed k_d in terms of k_1 for streams by the expression:

$$k_d = k_1 + n(V/D) \tag{3-36}$$

where V = stream velocity, length/time
D = stream depth, length
n = coefficient of bed activity, dimensionless

The coefficient of bed activity is a step function of stream gradient; values are given in Table 3-14. This expression has been used in a version of QUAL-II applied to rivers in New England (JRB, 1983; Van Benschoten and Walker, 1984; Walker, 1983), by Terry et al. (1984) on the Illinois River, Arkansas, and by Chen and Goh (1981).

TABLE 3-14. COEFFICIENT OF BED ACTIVITY AS A FUNCTION OF STREAM SLOPE (from BOSKO, 1966)

Stream Slope (ft/mi)	n
2.5	.1
5.0	.15
10.0	.25
25.0	.4
50.0	.6

Stream hydraulic factors may also account for differences between the deoxygenation rate k_d and the overall BOD removal rate k_R. Table 3-15 shows examples of such differences in six U.S. rivers. Higher values of k_R are attributable to settling of particulate BOD. Bhargava (1983) observed rapid settling of particulate BOD just downstream from sewage outfalls in two

Indian rivers, where k_R was several times greater than farther downstream. He modeled this effect by considering the BOD to be composed of two fractions, using the expression:

$$L_t = L_1(1 - \frac{V_s}{D}t) + L_2 \exp(-k_d t) \qquad (3\text{-}37)$$

where L_t = BOD remaining at downstream travel time t

L_1 = portion of original BOD removed by settling

L_2 = portion of original BOD subject to in-stream degradation

V_s = settling velocity of particulate BOD

D = average stream depth

TABLE 3-15. DEOXYGENATION RATES FOR SELECTED U.S. RIVERS (ECKENFELDER AND O'CONNOR, 1961)

River	Flow (cfs)	Temp. (^oC)	BOD_5 (mg/l)	k_d^* (day^{-1})	k_R^* (day^{-1})
Elk	5	12	52	3.0	3.0
Hudson	620	22	13	0.15	1.7
Wabash	2800	25	14	0.3	0.75
Willamette	3800	22	4	0.2	1.0
Clinton	33	--	--	.14-.13	2.5
Tittabawassee	--	--	--	0.05	0.5

*Note: These data are over 20 years old. It is likely that advances in waste treatment have altered the BOD kinetics in these waterways.

Some modelers distinguish between benthic and water-column CBOD removal, and assign rate coefficients to each type. For example, the sum of

settling and benthic biological CBOD uptake is widely portrayed as a first-order process (Baca and Arnett, 1976; Grenney and Kraszewski, 1981; Duke and Masch, 1973; Orlob, 1974):

$$\frac{\partial L}{\partial t} = -(k_d + k_3)L \tag{3-38}$$

where k_d = water-column deoxygenation rate
k_3 = total removal rate to the benthos by settling and sorption

The settling rate alone may be derived from the particle settling velocity and mean depth of the water column:

$$k_s = \frac{V_s}{D} \tag{3-39}$$

The effects of scour are often incorporated into the benthic removal coefficient k_3. This may be done implicitly, or by calculating k_3 as the sum of two first-order coefficients having opposite sign (Bauer et al., 1979). Scour of benthic BOD is also treated as a zero-order process (e.g., Baca et al., 1973):

$$\frac{\partial L}{\partial t} = -k_R L + L_a \tag{3-40}$$

where L_a = rate of BOD re-entrainment by scour, mg/(l-day).

The nature of the oxygen-demanding material also affects the rate of its removal from a receiving water. Particulate BOD, while it may be susceptable to settling, is more refractory than soluble BOD. Also two waters having the same ultimate BOD may show very different BOD depletion profiles. For in-stream BOD arising from a wastewater inflow, the degree of treatment of the wastewater is important. In general, the higher the degree of treatment, the greater the degree of waste stabilization, and the lower the deoxygenation rate will be. Fair et al. (1968) cite deoxygenation rates of 0.39, 0.35 and 0.12-0.23 per day for raw wastewater, primary and secondary effluent, respectively.

Martone (1976) observed a similar trend with paper industry wastewaters. Following biological treatment, rates as low as 0.02 per day, base e were observed. This low rate was attributed to the refractory humic material remaining in the wastewater. Similar low rates were also noted in receiving streams (NCASI, 1982a).

The U.S. Environmental Protection Agency (1983), using the data of Hydroscience (1971) and Wright-McDonnell (1979) has derived a relationship between stream depth and CBOD removal. This is shown in Figure 3-11. Note that the predicted decay rate corresponds to the sum of water column and benthic deoxygenation. Should SOD data be available, modelers are cautioned when using this figure to avoid double counting of SOD in the oxygen balance.

To this point, depletion of dissolved oxygen caused by CBOD decay has been implicitly considered to depend only on the concentration of substrate, i.e., CBOD. However, at low dissolved oxygen concentrations, oxygen may be limiting to the reaction. Provision for this "oxygen inhibition" is incorporated into many water quality models as discussed below.

Autochthonous sources may be a major influence on BOD dynamics. In lakes, carbon fixed by phytoplankton may become the predominant source of CBOD. Investigators have dealt with the input of autochthonous CBOD in several ways. Modeling Onondaga Lake in New York, Freedman et al. (1980) considered the biological contribution to water-column CBOD to be equivalent to the mass rate of phytoplankton production of organic material. Baca and Arnett (1976) considered the death rates of phytoplankton and zooplankton separately. These affected BOD according to the expression:

$$\frac{\partial L}{\partial t} = -k_d L + \alpha (F_p P + F_z Z) \qquad (3\text{-}41)$$

where α = stoichiometric coefficient, mgO_2/mgC

F_z = death rate of zooplankton from fish predation, 1/day

F_p = death rate of phytoplankton from zooplankton grazing, 1/day

P = phytoplankton concentration, mg-C/l

Z = zooplankton concentration, mg-C/l

A Potomac Estuary Model by Thomann and Fitzpatrick (1982) considers the "non-predatory" death rate of phytoplankton to augment water-column CBOD:

$$\frac{\partial L}{\partial t} = -k_d L + \alpha k_{1D} P_c / BOD_{u5} \qquad (3\text{-}42)$$

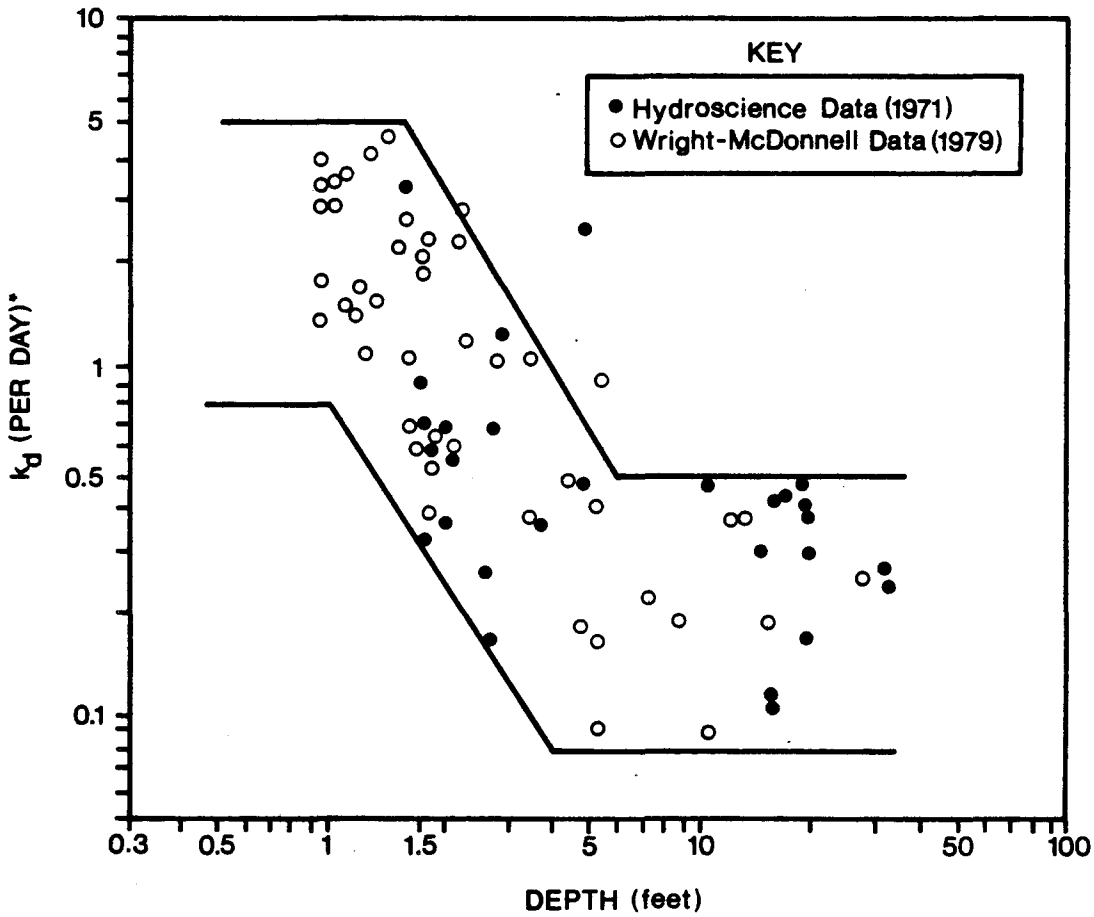

*NOTE: k_d includes a Benthic Deoxygenation Component

Figure 3-11. Deoxygenation coefficient (k_d) as a function of depth

where k_{1D} = death rate of phytoplankton other than from grazing, 1/days

P_c = phytoplankton carbon, mg/l

BOD_{u5} = ratio of ultimate to 5-day CBOD, taken as 1.85 for phytoplankton

3.3.5 Predictive Expressions for Deoxygenation

The carbonaceous deoxygenation rate is determined in two general ways. Most investigators base their measures of k_d on the results of field or laboratory experiments that monitor dissolved oxygen or ultimate CBOD. In stream modeling, this traditional approach has recently been augmented by efforts to quantify k_d as a function of hydraulic parameters.

It is important to note that these correlations relied upon published values of k_d (such as Figure 3-11). No distinction was made as to how k_d was obtained; and in these correlations, observed instream values have equal weight with measured laboratory values. Thus, considerable ambiguity exists in the published literature with regard to the meaning of k_d and the resulting correlation may be of limited value.

Bansal (1975) attempted to predict deoxygenation rates based on the Reynolds number and the Froude number. This approach was found to have limited applicability (Novotny and Krenkel, 1975). More commonly, k_d is found as a function of flow rate, hydraulic radius or average stream depth. Wright and McDonnell (1979) utilized data from 36 stream reaches in the U.S. to derive the expression:

$$k_d = (10.3)Q^{-0.49} \qquad (3\text{-}43)$$

where Q = flow rate, ft^3/sec

They found that above flow rates of about 800 ft^3/sec, k_d is not a function of flow rate. The lower limit of the applicability of this expression is approximately 10 ft^3/sec. Below this flow rate, deoxygenation

rates were noted to consistently fall in the range 2.5-3.5 per day, independent of streamflow. For this same range of flowrates (between 10 and 800 cfs), an expression based on channel wetted perimeter was also found successful in predicting k_d:

$$k_d = 39.6P^{-0.84} \tag{3-44}$$

where P = wetted perimeter, feet

The deoxygenation rate coefficient has also been expressed as an exponential function of stream depth (Hydroscience, 1971; Medina, 1979) and hydraulic radius (Grenney and Kraszewski, 1981).

Regardless of how carbonaceous deoxygenation rate coefficients are derived, they are widely applied in only two ways: first-order decay and simultaneous first-order decay. In the latter case, the CBOD is partitioned into more than one fraction; each fraction is degraded at a specific rate according to first-order kinetics. The first-order approximation for CBOD decay has been widely criticized, and multi-order or logarithmic models have been used by individual investigators (see Hunter, 1977 for a review).

Martone (1976), in a study of BOD kinetic models, observed that first order kinetics did not universally describe observed BOD data. In a few cases, a two-stage carbonaceous BOD model resulted in a better statistical fit (McKeown et al., 1981). The Wisconsin Department of Natural Resources included this alternative formulation in its QUAL-III model (Wisconsin DNR, 1979). However, no alternative formulation has been shown to be universally superior, and oxygen-sag computations are comparatively easily performed for first-order decay. Hence, this is the pre-eminent model in use today.

Table 3-16 shows the expressions used by water quality modelers to describe the consumption of oxygen as a function of water column CBOD decay. Note that nonoxidative processes such as settling, where CBOD is removed from or added to the water column, do not contribute to dissolved oxygen

TABLE 3-16. EXPRESSIONS FOR CARBONACEOUS OXYGEN DEMAND USED IN WATER QUALITY MODELS

Depletion Rate of Dissolved Oxygen by CBOD Decay, $\frac{\partial DO}{\partial t}$	Model and Reference
$-k_d L$	MIT-DNM (Harleman et al., 1977) Dynamic Estuary Model (DEM) (Genet et al., 1974) EXPLORE-I (Baca et al., 1973) USGS river model (Bauer et al., 1979) HSPF (Inhoff et al., 1981) DOSAG3 (Duke and Masch, 1973) DIURNAL (Deb and Bowers, 1983) QUAL-II (Roesner et al., 1981) O'Connor et al. (1981)*
$-k_d L \frac{O_2}{k_{O_2} + O_2}$	Lake Erie Model* (Di Toro and Connolly, 1980) Potomac Estuary Model (PEM) (Thomann and Fitzpatrick, 1982)
$-aD^b L$	Level III-Receiving (Medina, 1979)
$-aQ^b L$	Wright and McDonnell (1979) Rinaldi (1979)
$-aQ^b L \frac{O_2}{k_{O_2} + O_2}$	Bedford et al. (1983)
$-k_1 L_{sol} - k_2 L_{det}$	WQRRS (Smith, 1978) CE-QUAL-R1* (Corps of Engineers, 1982) Chen et al.* (1974)
$-k_d L$ (depth, $D > 2.44$m) $-\left(\frac{D}{2.44}\right)^{-0.434} k_d L$ ($D < 2.44$m)	RECEIV-II (Raytheon, 1974) WRECEV (Johnson and Duke, 1976)
$-C_1 (R_h \; C_2)_L$	SSAM-IV (Grenney and Kraszewski, 1981)
$-k_d \phi_c L$	Freedman et al. (1980)

*"L" represents a fraction of organic carbon, soluble and/or detrital, rather than CBOD.

Definition of symbols:

k_d	field CBOD oxidation rate
L	carbonaceous BOD concentration
O_2	concentration of dissolved oxygen
k_{O_2}	half-saturation constant for oxygen
a, b, C_1, C_2	empirically-determined coefficients
D	water depth
Q	stream flow rate
k_1, k_2	oxidation rates for two CBOD fractions
L_{sol}	soluble CBOD (or, dissolved organic carbon)
L_{det}	particulate CBOD (particulate organic carbon)
R_h	steam hydraulic radius
ϕc	nonlinear O_2 inhibition coefficient

depletion, and are not included in the expressions. In cases where k_d is calculated within the model using a hydraulic expression, that expression is included in the table. As shown, the rate expressions do not include temperature correction coefficients. Some of the models listed (starred references) do not treat CBOD per se, but organic carbon or carbonaceous detritus. The effect of low dissolved oxygen concentration is generally handled through a Michaelis-Menten formulation. A representative value of k_{O2}, the half-saturation coefficient for oxygen uptake, is 0.5 mg/l. Some models partition oxygen-demanding matter into soluble and particulate fractions, with different rate coefficients. In limnological models, the particulate or detrital fraction may be determined as a function of the death of phytoplankton and zooplankton, with no additional particulate CBOD present.

3.3.6 Values of Kinetic Coefficients

Table 3-17 is a compilation of deoxygenation rate coefficients and the methods by which they were determined. Unless otherwise specified, the coefficient is k_d. In some cases, investigators reported k_R values as such; in other cases, rates reported as deoxygenation were actually observations of total removal (k_R) and they are cited as such. Most of the data are from rivers, although some lake and estuary values have been reported. The range of values reported as in-stream deoxygenation rates is wide, spanning more than two orders of magnitude.

3.3.7 Measurement of Ultimate BOD Decay Rate

In laboratory studies using BOD bottles, BOD exertion is found as the difference between sample and control dissolved oxygen depletion. Respirometry studies and reaerated stirred-reactor studies involve essentially continuous monitoring of oxygen usage. The results of these laboratory experiments produce cumulative oxygen demand-vs-time relationships.

A number of methods have been used to derive k_1 from these curves. Among these are:

TABLE 3-17. VALUES OF KINETIC COEFFICIENTS FOR DECAY OF CARBONACEOUS BOD

Location	k_d (1/days @ 20°C, base e)	Method of Determining Coefficient	Reference
Potomac Estuary 1977 1978	0.14 ± 0.023 0.16 ± 0.05	field study	US EPA (1979a) US EPA (1979b)
Willamette River, OR	0.1-0.3		Baca et al. (1973)
Chattahoochee River, GA	0.16		Bauer et al. (1979)
Ganga River, India Yamuna River, India	3.5-5.6 (k_R) 1.4	field study	Bhargava (1983)
S. Fork, Shenandoah River	0.4(k_R)	field study	Deb and Bowers (1983)
Merrimack River, Mass	0.01-0.1	field study	Camp (1965)
Gray's Creek, Louisana	1.44 (k_R)	model calibration	Crane and Malone (1982)
Onondaga Lake, New York	0.10	model calibration	Freedman et al. (1980)
Yampa River, Colorado	0.40	model calibration	Grenney and Kraszewski (1981)
Skravad River, Denmark	0.15 0.90 (k_R)	field study	Hvitved-Jacobsen (1982)
Seneca Creek	0.008		Metropolitan Washington Council of Governments (1982)
Kansas (6 rivers) Michigan (3 rivers) Truckee River, Nevada Virginia (3 rivers) N. Branch, Potamac, WV South Carolina (3 rivers) New York (2 rivers) New Jersey (3 rivers) Houston Ship Channel, TX Cape Fear R. Estuary, NC	0.02-0.60 0.56-3.37 0.36-0.96 0.30-1.25 0.4 0.3-0.35 0.125-0.4 0.2-0.23 0.25 0.23	various methods	Reported by Bansal (1975)
Holston River, Tenn	0.4-1.5	model calibration	Novotny and Krenkel (1975)
New York Bight	0.05-0.25		O'Connor et al. (1981)
White River, Arkansas	0.004-0.66 (k_1)	laboratory study	Terry et al. (1983)
N. Fork Kings River, CA	0.2		Tetra Tech (1976)
Lake Washington, WA	0.2		Chen and Orlob (1975)
Ouachita River, Arkansas	0.15 0.17 (k_R) 0.02 (k_1)	calibration laboratory study	Hydroscience (1979) NCASI (1982a)
36 U.S. river reaches plus laboratory flume	0.08-4.24	field studies	Wright and McDonnell (1979)
San Francisco Bay Estuary	0.2		Chen (1970)
Boise River, ID	0.75		Chen and Wells (1975)
W. Fork, Trinity River, TX	0.06-0.30	laboratory study	Jennings et al. (1982)

TABLE 3-17. (Cont'd)

Location	k_d (1/days @ 20°C, base e)	Method of Determining Coefficient	Reference
Willamette River, OR	0.07-0.14	lab and field	McCutcheon (1983)
Arkansas River, CO	1.5	field study	
Lower Sacramento River, CA	0.41		Hydroscience (1972)
Delaware River Estuary	0.31		
Wappinger Creek Estuary, NY	0.31		
Potomac Estuary	0.16,0.21		Thomann and Fitzpatrick (1982)
Speed River, Ontario	1.0	field study	Gowda (1983)

1. The linear least-squares technique of Reed and Theriault
2. Thomas' graphical slope method
3. The moment method of Moore (1941)
4. Orford and Ingram's logarithmic method
5. Rhame's two-point method
6. Nemerow's general laboratory method (graphical)
7. The daily difference method of Tsivoglou (1958)
8. The rapid ratio method of Sheehy (1960)
9. Nonlinear regression method of NCASI (1982d).

The first six methods are discussed by Nemerow (1974). Gaudy et al. (1967) review and compare a number of calculation methods. Some of the techniques assume a particular kinetic model for the data, while others do not. The linear least-squares method can be used with a first or second-order BOD dependency, with somewhat different calculations. Orford and Ingram's method assumes that cumulative BOD exertion varies with the logarithm of elapsed time, and no limiting value is approached. The nonlinear regression technique has the advantage of flexibility in evaluating alternative BOD models.

Barnwell (1980) developed a nonlinear least-squares technique for fitting laboratory CBOD progressions. It is based upon the first-order decay model, and is suitable for implementation on programmable calculators or microcomputers. It allows computation of confidence contours for the estimates of k_1 and ultimate CBOD. The nonlinear regression technique also

provides estimates of the confidence contours. Further discussion of BOD measurement techniques are contained in Stover and McCartney (1984) and Stamer et al. (1983).

Estimates of the length of time necessary to evaluate the BOD parameters have been provided by Berthouex and Hunter (1971). They determined, using statistical arguments, that this length of time is a function of the anticipated decay rate, k_1. The time computed from $4/k_1$ is suggested as the maximum value. Barnwell (1980) and NCASI (1982d) have shown that the estimate of the confidence contours is directly related to the length of time the BOD experiment was conducted. As the length of time increases, the confidence contours get smaller.

In field estimation of deoxygenation rates, water samples from along the stream reach are collected, and their ultimate CBOD values are determined in the laboratory. Graphical methods are then used to find the CBOD decay rate. These techniques are based on a mass balance for BOD in the stream. Note that if unfiltered water samples are used, the rate calculated is k_R, not k_d. It may be that the two rates are essentially equivalent. An unvarying profile of suspended solids along the reach may indicate the validity of these measurements to estimate k_d. Alternatively, filtered samples may be incubated, and the contribution of particulate matter to BOD assumed to be insignificant.

The calculation methods described herein are based upon simplified forms of the BOD mass-balance equations. The user should assess carefully whether the necessary simplifying assumptions can reasonably be applied to the study system.

One simple and commonly used technique is for streams influenced by continuous point sources. The stream reach under study should have a relatively constant cross section, constant flow rate, and a single point-source BOD loading. The BOD concentration downstream from the source is given by:

$$L = L_o \exp\left(\frac{-k_R X}{V}\right) \qquad (3\text{-}45)$$

where X = distance downstream from source, length

L_o = BOD concentration immediately downstream from source, at X = 0, mass/volume

V = average stream velocity, length/time

A graph of the logarithm of BOD concentration versus distance downstream should show a straight-line relationship with a slope of $-k_R/V$ if decay is first order. Sometimes the slope may be more steep for the first few miles below a point source, where settling of BOD as well as decay is occurring (Deb and Bower, 1983). The slope may be found graphically or by linear regression. Figure 3-12 is an example of this type of computation. If the slope is determined by regression, the natural log of BOD should be regressed on distance. If the slope is found graphically from a semi-log plot, it must be multiplied by 2.3 (to convert from base-10 to base-e) for model applications.

The same approach is possible for tidally influenced rivers, as discussed in Zison et al. (1978). However, the tidally averaged dispersion coefficient is required as an additional piece of information and will add some degree of uncertainty to the predicted k_d value.

3.3.8 Summary and Recommendations

Although its shortcomings have been widely discussed, the first-order model is still the common method for simulating instream CBOD kinetics. Relative ease of computation, a long history of use and the absence of alternative formulations which are superior over a range of conditions are probably responsible for this precedent.

In estimating k_d, there is increasing use of various stream hydraulic parameters. Estimates based on flow rate seem to be most successful,

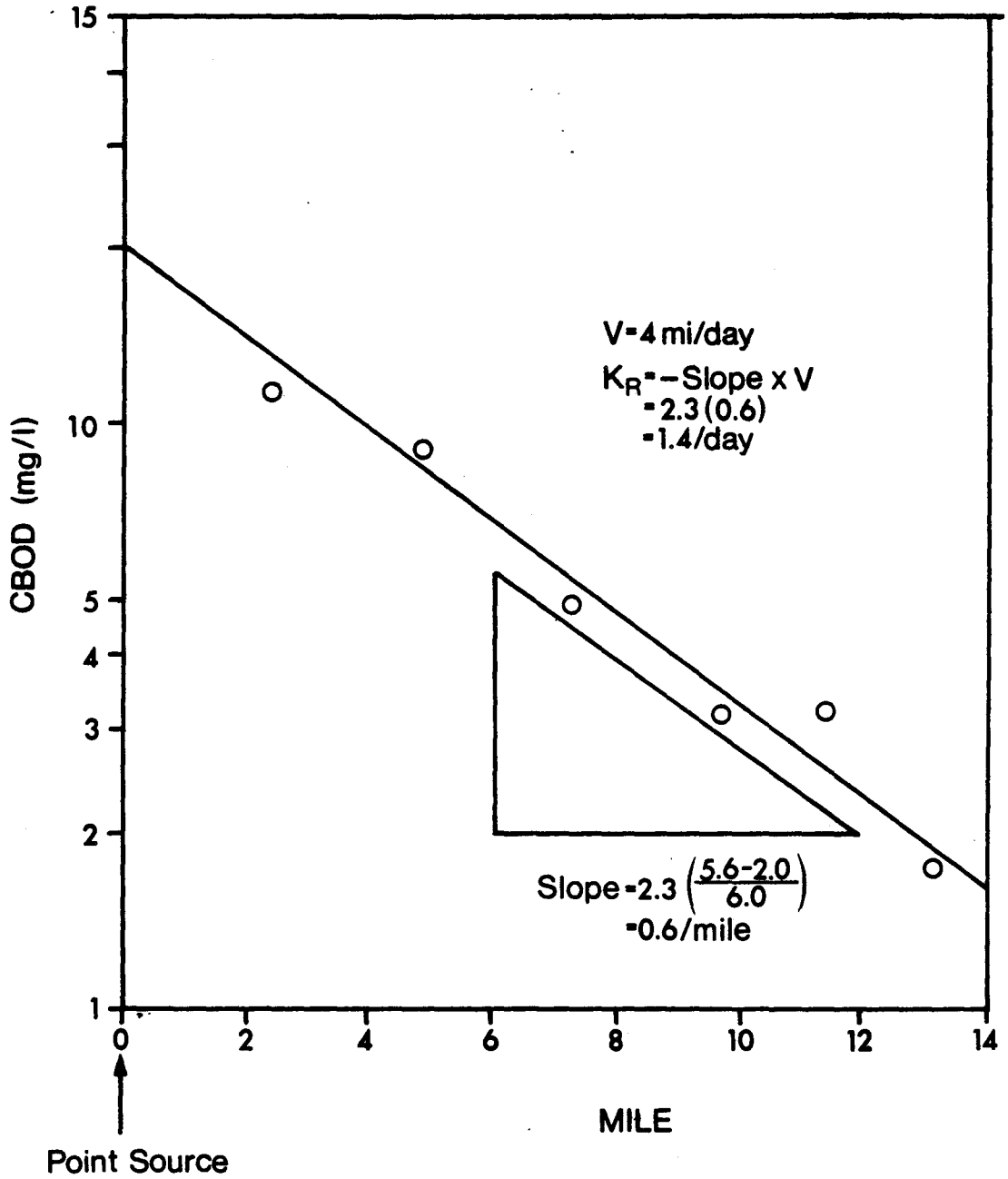

Figure 3-12. Example computation of k_R based on BOD measurements of stream water.

although stream geometric parameters such as hydraulic radius and depth are also used. The use of hydraulic characteristics for k_d prediction has limits, since deoxygenation is independent of flow rate at both high and low flow. These predictive equations should be used with caution.

To assess CBOD fluxes based on site-specific data, it is essential to have some familiarity with the water body under study. A reconnaissance survey can help elucidate the possible importance of CBOD sedimentation or resuspension, as well as the magnitude of aquatic biological processes. The survey is also an opportunity to assess what assumptions can reasonably be made about the system to simplify calculations.

For those river waters and effluents which contain significant concentrations of NBOD, the analyst must consider an appropriate procedure for the separation of NBOD from CBOD in the ultimate BOD test. Currently, two techniques are used which include: the use of nitrification inhibitors such as TCMP and others, and the monitoring of nitrogen series with time during the test to define the NBOD. There is currently no consensus as to which technique is best. Nitrification inhibitors have been observed to have an unpredictable inhibition effect on the CBOD kinetics as well (Martone, 1976). For large modeling projects, the monitoring of nitrogen species in the BOD bottle tests can create significant additional laboratory expense. Though likely to be more expensive, the latter technique provides more information regarding the CBOD and NBOD kinetics and is recommended by NCASI (1982b).

The investigator should exercise caution in using deoxygenation coefficients obtained for other water bodies. The wide range of values in Table 3-17 indicates substantial variation in rate estimation and reporting procedures. Unfortunately, many investigators automatically equate k_1 or k_R with k_d, and do not fully consider the different meanings of these rates. Some report k_d and k_R values without stating whether these apply to total BOD or CBOD, are temperature-corrected, are to base e or base 10, etc.

One way to handle these uncertainities is to conduct sensitivity analyses of model predictions. Such analyses are beyond the scope of many projects; however, results are available for many widely-used models either in the model documentation or in the final reports of large-scale projects. Examples of sensitivity analyses for deoxygenation rate coefficients are Crane and Malone (1982), Thomann and Fitzpatrick (1982) and NCASI (1982a).

In addition, it is possible to quantitatively evaluate the uncertainity associated with an estimated coefficient. Barnwell's (1980) and NCASI's (1982b) calculation techniques allow computation of confidence limits for an estimated k_1 value. Jaffe and Parker (1984) provide a procedure for estimating the uncertainty of k_d values as influenced by the field sampling scheme. Chadderton et al. (1982) evaluate the relative contributions to uncertainty of the parameters of the Streeter-Phelps equation.

3.4 NITROGENOUS BIOCHEMICAL OXYGEN DEMAND

3.4.1 Introduction

The transformation of reduced forms of nitrogen to more oxidized forms (nitrification) consumes oxygen. Although nitrification is also a nutrient transformation process, this section addresses the oxygen consumption aspects, since numerous models simulate nitrogenous biochemical oxygen demand (NBOD) without detailing nitrogen transformations.

Nitrification is a two-stage process. The first stage is the oxidation of ammonia to nitrite by Nitrosomononas bacteria:

$$NH_4^+ + 1.5\ O_2 \longrightarrow NO_2^- + H_2O + 2H^+ \qquad (3\text{-}46)$$

(14 gm) (48 gm)

Stoichiometrically 48/14 or 3.43 gm of oxygen are consumed for each gram of ammonia-nitrogen oxidized to nitrite-nitrogen. During the second stage of nitrification Nitrobacter bacteria oxidize nitrite to nitrate:

$$NO_2^- + 1/2\ O_2 \longrightarrow NO_3^- \qquad (3\text{-}47)$$

(14 gm) (16 gm)

Stoichiometrically 16/14 = 1.14 gm of oxygen are consumed per gram of nitrite-nitrogen oxidized. If the two reactions are combined, the complete oxidation of ammonia can be represented by:

$$NH_4^+ + 2\ O_2 \longrightarrow NO_3^- + H_2O + 2H^+ \qquad (3\text{-}48)$$

(14 gm) (64 gm)

As expected, 64/14 = 4.57 gm of oxygen are required for the complete oxidation of one gram of ammonia.

In the reactions above, the organic-nitrogen form does not appear, since organic-nitrogen is hydrolyzed to ammonia, and does not consume oxygen in the process. However, organic nitrogen will eventually contribute to the NBOD, as the following equation shows:

$$NBOD = 4.57\ (N_0 + N_1) + 1.14\ N_2 \quad . \qquad (3\text{-}49)$$

where N_0 = organic-nitrogen concentration, mass/volume
N_1 = ammonia-nitrogen concentration, mass/volume
N_2 = nitrite-nitrogen concentration, mass/volume

The stoichiometric coefficients of 3.43, 1.14, and 4.57 in the equations above are actually somewhat higher than the total oxygen requirements because of cell synthesis. Some researchers (e.g., Wezernak and Gannon, 1967 and Adams and Eckenfelder, 1977) have suggested that the three coefficients be reduced to 3.22, 1.11, and 4.33, respectively.

3.4.2 Modeling Approaches

Modelers use both the two-stage and one-stage approach to simulate NBOD decay, as shown by Table 3-18. First order kinetics is the predominant

method used to simulate the process. Oxygen limitation is used by some modelers (e.g., O'Connor et al., 1981; Thomann and Fitzpatrick, 1982; and Bedford et al., 1983).

Relatively few modelers explicitly simulate the effects of benthic nitrification (exceptions are Williams and Lewis, 1984 and Mills, 1976). The models of Williams and Lewis, and Mills were developed for relatively shallow streams where bottom effects could be important. Of these two, only Mills looks at the details of oxygen and nitrogen transfer from the water column into an attached nitrifying biofilm. Several studies (Kreutzberger and Francisco, 1977; Koltz, 1982) have confirmed that nitrifying bacteria can thrive in the beds of shallow streams, and that, in the streams they investigated, nitrification occurred primarily in the bed, and not in the water column. Denitrification has been shown to occur in stream sediments

TABLE 3-18. EXPRESSIONS FOR NITROGENOUS BIOCHEMICAL OXIDATION RATES USED IN A VARIETY OF WATER QUALITY MODELS

Expression for Nitrogenous Oxidation Rate, $\partial DO/\partial t$	Model and/or Reference
$-\alpha_1 k_{n_1} N_1 - \alpha_2 k_{n_2} N_2$	WQRRS (Smith, 1978)
	Bauer et al. (1979)
	QUAL-II (Roesner et al., 1981)
	SSAM IV (Grenney and Kraszewski, 1981)
	CE-QUAL-R1 (U.S. Army COE, 1982)
	RECEIV II (Raytheon, 1974)
	NCASI (1982d)
	Baca and Arnett (1976)
	MIT Transient Water Quality Model (Harleman et al., 1977)
	DOSAG3 (Duke and Masch, 1973)
	HSPF (Imhoff et al., 1981)
	Genet et al. (1974)
$-k_n L_n$	DIURNAL (Deb and Bowers, 1983)
	Gowda (1983)
	EXPLORE-1 (Baca et al., 1973)
	Bauer et al. (1979)
	Di Toro and Matystik, 1980

TABLE 3-18. (Cont'd)

Expression for Nitrogenous Oxidation Rate, $\partial DO/\partial t$	Model and/or Reference
$-\alpha_3 k_n \frac{O_2}{O_2 + K_{nit}} N_1$	O'Connor et al. (1981) Thomann and Fitzpatrick (1982)
$-\alpha_3 \alpha_4 Q^b \frac{O_2}{O_2 + K_{nit}} N_1$	Bedford et al. (1983)
Time Shifted First Order (time delayed)	NCASI (1982d)
Lagged First Order (nonoxidative step followed by an oxidative step)	NCASI (1982d)
Benthic Nitrification:	
$-\alpha_3 S_n$ (zero order kinetics)	Williams and Lewis (1984) Bauer et al. (1979)
$-J_c$ (Monod kinetics)	Mills (1976)

Definition of Symbols:

- k_{n_1} = ammonia to nitrite oxidation rate
- k_{n_2} = nitrite to nitrate oxidation rate
- k_n = NBOD decay rate
- α_1 = 3.43, typically
- α_2 = 1.14, typically
- α_3 = 4.57, typically
- α_4, b = unspecified
- N_1 = NH_4^+ -N
- N_2 = NO_2^- -N
- L_n = nitrogenous BOD
- O_2 = dissolved oxygen concentration
- K_{NIT} = half-saturation constant
- S_n = zero order benthic nitrification rate
- J_c = benthic oxygen flux rate by nitrifying organisms growing in an attached biofilm

as well (Wyer and Hill, 1984). Denitrification is discussed in more detail in Chapter 5.

The most straightforward method of including the effects of organic nitrogen on the potential depletion of dissolved oxygen is to simulate the conversion of organic nitrogen to ammonium nitrogen (a rate of 0.1/day is typically used). The increased ammonia concentration is then available to exert an oxygen demand. However, it is not clear that all the models in

Table 3-18 simulate the organic nitrogen to ammonia conversion. Some models appear to combine ammonia and organic nitrogen together into a single term.

While first order kinetics is the most popular approach for simulating nitrification in natural systems, Monod and zero-order kinetics are often used to simulate nitrification in wastewater treatment processes (Hall and Murphy, 1980; Charley et al., 1980; Rittmann and McCarty, 1978). Figure 3-13 shows how nitrification is simulated using Monod kinetics. At the high level of reduced nitrogen compounds found in wastewater, nitrification can proceed at its maximum rate, and thus is zero order (independent of substrate concentration). At lower reduced nitrogen concentrations, first order kinetics are applicable.

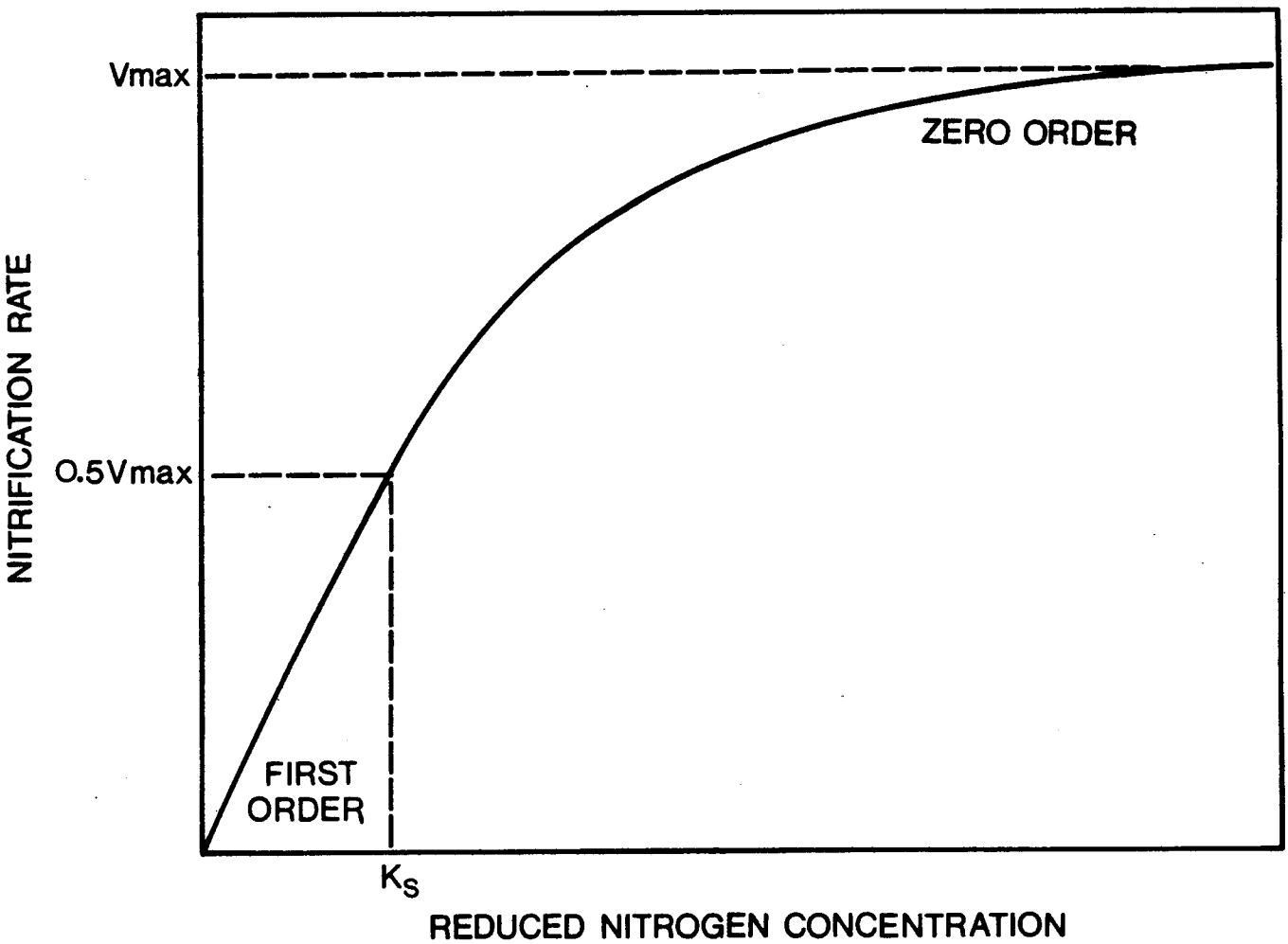

Figure 3-13. Effect of Reduced Nitrogen Concentration on Nitrification Rate as Reported by Borchardt (1966).

Several researchers (e.g., Wild et al., 1971; Kiff, 1972; Huang and Hopson, 1974) have established concentration ranges of ammonia nitrogen when zero order kinetics appear to be followed. The range is quite wide, from 1.6 mg/l to 673 mg/l. Concentrations of ammonia-nitrogen in natural waters can exceed the lower end of the scale reported, and indicate that zero order or Monod kinetics may be appropriate in these circumstances (e.g., see Wilber et al., 1979).

3.4.3 Factors That Affect Nitrification

Table 3-19 summaries studies that have investigated factors that influence the rate of nitrification. The factors include pH, temperature, ammonia and nitrite concentrations, dissolved oxygen, suspended solids, and organic and inorganic compounds. Sharma and Ahlert (1977) also provide a review of previous studies.

Many of the studies have been carried out in controlled environments, and not in natural waters. Also, the concentration of organic substances which have inhibitory effects on nitrification are often, but not always, well above 1 mg/l (Wood et al., (1981)), so that the compounds are not likely to be inhibitory in natural waters.

Modelers typically consider only the temperature effect on nitrification, although a few do model dissolved oxygen limitations (see Table 3-18). Other inhibitory or stimulatory effects are assumed to be included in the "reference" rate (typically at 20°C) measured or otherwise selected for the modeling applications.

Researchers have found that within the temperature range of 10°C to 30°C temperature effects can be simulated by the following expression:

$$k_n = k_{n20}\theta^{T-20} \qquad (3\text{-}50)$$

where k_{n20} = nitrification rate coefficient at 20°C
θ = temperature correction factor

TABLE 3-19. SUMMARY OF FACTORS THAT INFLUENCE NITRIFICATION

Reference	Factors Investigated	Comments
Sharma and Ahlert (1977)	Temperature, pH, Nitrogen Concentrations, Dissolved Oxygen, Organic Compounds	In reviews of previous studies found: 12 studies for dissolved oxygen, 15 studies for pH, 14 studies for the effect of ammonia levels on nitrification, 11 studies of effects of nitrate levels on nitrification, 34 studies on substances that are required or stimulate nitrification; 47 studies on substances that inhibit nitrification.
Stenstrom and Poduska (1980)	Dissolved Oxygen	In this literature review of the effects of dissolved oxygen concentrations on nitrification, the lowest concentration where nitrification occurred is approximately 0.3 mg/l. However, the dissolved oxygen level required for no oxygen inhibition varied to as high as 4.0 mg/l, while other researchers found only 0.5 mg/l is required.
Wild, Sawyer, and McMahon (1971)	pH, Temperature, Ammonia-nitrogen	Studies were conducted in a pilot nitrification unit receiving trickling filter effluent. Ammonia nitrogen did not inhibit nitrification at concentrations less than 60 mg/l. Optimum pH for nitrification was found to be 8.4. The rate of nitrification increased with temperature in the range 5°C to 30°C.
Kholdebarin and Oertli (1977a)	pH, Ammonia-nitrogen	For water samples collected from the Whitewater River, California, the optimum pH for nitrification of ammonia and nitrite was 8.5. Nitrite oxidation was stimulated by the addition of 3 mg/l ammonium.
Kholdebarin and Oertli (1977b)	Suspended Solids	In water from the Whitewater River in California, suspended solids were found to have a stimulatory effect on nitrification, presumably caused by the physical support provided by the solids.
Bridle, Climenhage, Stelzig (1979)	pH, Temperature, Ammonia-nitrogen, Copper	In batch reactors ammonia nitrification was not inhibited for TKN levels up to 340 mg/l. The optimum pH for nitrification was 8.5. The nitrification rate increased approximately 2.5 fold for each 10°C increase. Copper concentrations of 3000 mg/l produced no adverse effect; concentrations of 6000 mg/l were inhibitory.
Quinlan (1980)	Temperature	Temperature for optimal ammonia and nitrite oxidation was found to depend on nitrogen concentrations. At low nitrogen concentrations the optimum temperatures were 35.4°C for ammonia oxidation and 15.4°C for nitrite oxidation.
Wood, Hurley, Matthews (1981)	Organic Compounds	Laboratory studies were conducted using filtered liquor from return activated sludge. Approximately 20 compounds were tested in concentrations from 10 to 330 mg/l. Approximately half the compounds had no inhibitory effects.
Hockenbury and Grady (1977)	Organic Compounds	This study reviewed previous work on the influence of organic compounds on nitrification. Additionally, they found that many compounds did not inhibit nitrification at concentrations as high as 100 mg/l, while other compounds inhibited nitrification at concentrations less than 1 mg/l.

Values of the temperature correction factor are reported in Table 3-20. Temperature correction values are slightly higher for ammonia oxidation than for nitrite oxidation. The mean temperature correction values are 1.0850 for ammonia oxidation and 1.0586 for nitrite oxidation. Many models use temperature correction factors slightly lower than these values. Typically modelers use only one temperature correction coefficient, and do not distinguish between temperature corrections for ammonia and nitrite oxidation. Example of temperature correction factors used in selected models are:

- 1.05, EXPLORE-1 (Baca et al., 1973)
- 1.065, MIT Nitrogen model (Harleman et al., 1977)
- 1.08, New York Bight model (O'Connor et al., 1981)
- 1.047, QUAL-II (Roesner et al., 1981), USGS Steady State Model (Bauer et al., 1979)
- 1.045, Potomac Estuary Model (Thomann and Fitzpatrick, 1982)

TABLE 3-20

TEMPERATURE CORRECTION FACTOR, θ, FOR NITRIFICATION

Reference	Ammonia Oxidation	Nitrite Oxidation
Stratton (1966); Stratton and McCarty (1967)	1.0876	1.0576
Knowles et al. (1965)	1.0997	1.0608
Buswell et al. (1957)	1.0757	-
Wild et al. (1971)	1.0548	-
Bridle et al. (1979)	1.1030	-
Sharma and Ahlert (1977)	1.069	1.0470
Laudelout and Van Tichelen (1960)	-	1.0689
Mean	1.0850	1.0586

- 1.02-1.03, WQRRS (Smith, 1978)
- 1.08, Lake Erie model (Di Toro and Connolly, 1980)

While Equation (3-44) can provide adequate temperature correction up to approximately 30°C, beyond this temperature the nitrification rate is inhibited by the high temperature, so the relationship no longer holds. Figure 3-14 illustrates the effect of temperature on nitrification and shows that the rate rapidly decreases at temperatures beyond 30°C.

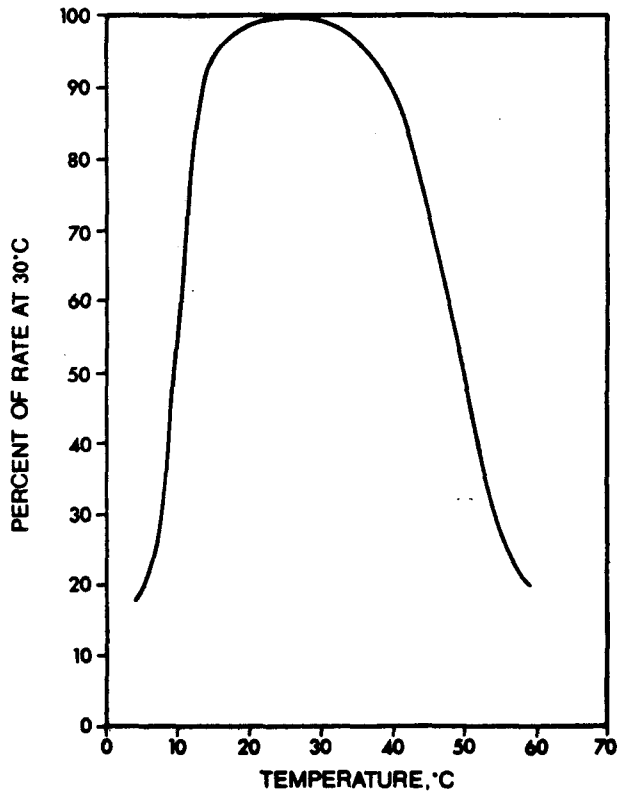

Figure 3-14. Effect of Temperature on Nitrification as Reported by Borchardt (1966).

The influence of pH on rates of nitrification is also quite important. If pH is outside of the range 7.0 to 9.8, significant reduction in nitrification rates can occur. Table 3-19 indicated that the optimal pH for nitrification is approximately 8.5 and at pH values below about 6.0, nitrification is not expected to occur. Figure 3-15 shows the effect of pH

on ammonia and nitrite oxidation. A more thorough review of pH effects is contained in Sharma and Ahlert (1977).

Effects of solid surfaces have frequently been documented as being important for nitrification (e.g., Kholdebarin and Oertli, 1977). The following section discusses this effect more fully through a number of case studies.

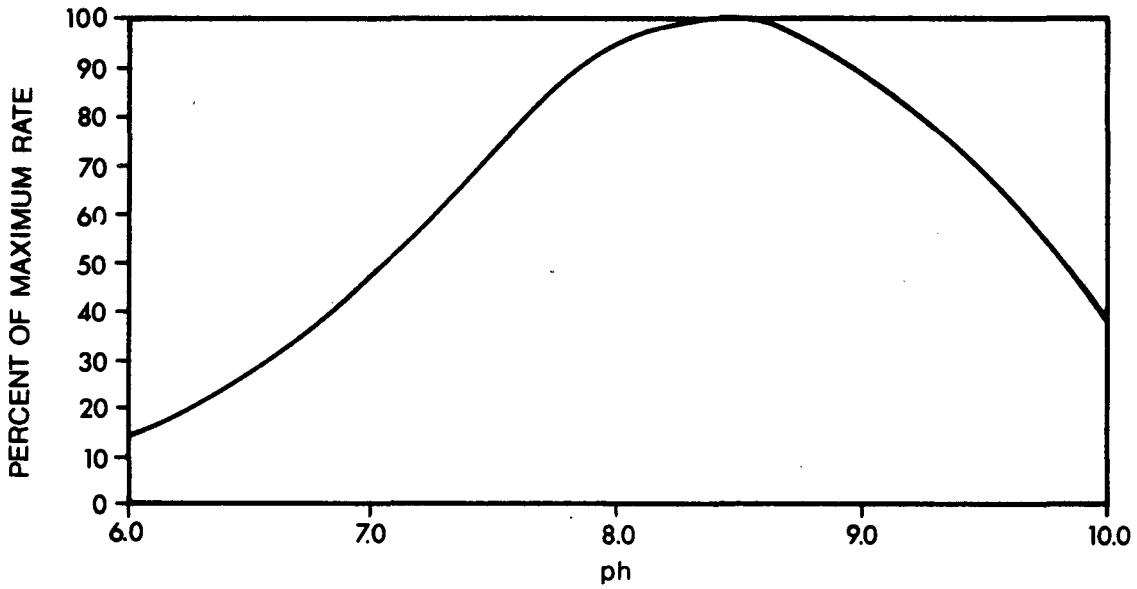

(a) AMMONIA OXIDATION (Wild et.al.,1971)

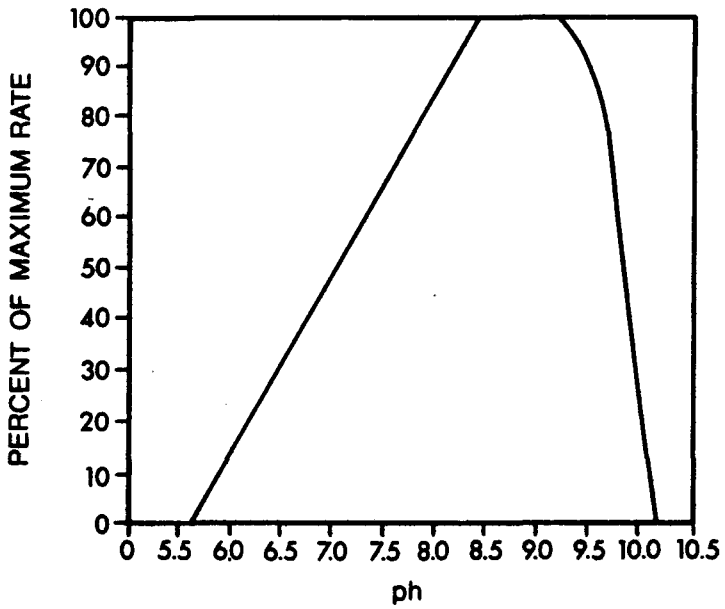

(b) NITRITE OXIDATION (Myerhof,1916)

Figure 3-15. pH Dependence of Nitrification.

3.4.4 Case Studies and Nitrification Rates

Table 3-21 summaries case studies of nitrification in natural waters. These studies are intended to show how various researchers have determined nitrification rates in natural waters, some of the complications that can occur in doing so, and what the rates are.

Except for Slayton and Trovato (1978, 1979) all the case studies are for streams or rivers. Note the high variability in nitrification rates from study to study. For rivers, documented first order nitrification rates varied from 0.0/day to 9.0/day. For the two Potomac estuary studies, the nitrification rates were fairly small and constant (0.1 to 0.14/day). The nitrification rate was often determined from plots of TKN or NBOD versus distance or travel time. Figure 3-16 shows an example. A number of the studies (e.g., Koltz (1982) and Ruane and Krenkel (1978)) emphasized that algal uptake of ammonia can be an important transformation and should be accounted for in the rate determination. The increase of nitrate nitrogen can be monitored, as well as the decrease in ammonia nitrogen for more conclusive evidence that nitrification is occurring. Bingham et al. (1984) show how the nitrification rate constant is changed in a QUAL-II application when algae is simulated compared to when algae is not simulated.

Several of the case studies have enumerated nitrifying bacteria present in the water column and in the sediments (e.g., Kreutzberger and Francisco (1977)). Far more nitrifying organisms are typically present in the sediments than in the water column. Case studies on the following rivers have reached the same conclusion:

- Kanawha River, West Virginia (U.S. EPA, 1975)
- Tame and Trent Rivers, England (Curtis et al., 1975)
- North Buffalo Creek, North Carolina (Williams and Lewis, 1984)
- Willamette River, Oregon (Rinella et al., 1981)
- Chattahoochee River, Georgia (Jobson, undated)

TABLE 3-21. CASE STUDIES OF NITRIFICATION IN NATURAL WATERS

Reference	Study Area	Purpose of Study	Reported Nitrification Rates	Methods of Determining Nitrification Rates	Comments
Wezernak and Gannon (1968) Stratton and McCarty (1969) Blain (1969)	Clinton River, Michigan, a shallow stream with velocities of 1-2 fps	To mathematically model nitrification in a stream (This was one of the earlier modeling attempts)	ammonia oxidation: 3.1-6.2/day nitrite oxidation: 4.3-6.6/day	Measurements of ammonia, nitrite, and nitrate at three locations within the stream	The nitrogen balance developed indicated that nitrification was primary mechanism responsible for observed nitrogen transformations.
Gowda (1983)	Speed River, Canada, a relatively shallow river with velocities from 0.3 to 1.5 fps	To determine the affects of nitrification on dissolved oxygen levels within the river	0.2-4.41/day	Plots of TKN versus travel time	NBOD predicted to be much more important on the dissolved oxygen deficit than CBOD.
Curtis (1983)	Still River, Connecticut	To determine the fate of ammonia in the river by simulating oxidative and non-oxidative transformations	0.0-0.4/day	Comparison of total ammonia decrease to nitrate increase	-
Deb and Bowers (1983)	South Fork of Shenandoah River	To simulate the dissolved oxygen of the river using the DIURNAL model	0.2-1.25/day	Plots of NBOD versus travel time	-
Deb, Klafter-Snyder, and Richards (1983)	Leatherwood, Creek, Arkansas	To simulate the dissolved oxygen dynamics of a small surface-active stream for wasteload allocation purposes	1.1-7.1/day	Plots of TKN versus travel time	-
Ruane and Krenkel (1978)	Holston River, Tennessee	To examine the various nitrogen transformations that occur in the river	0.15-0.3/day	Rate of ammonia reduction and rate of nitrate increase	The complexity of the nitrogen cycle in the Holston River is discussed including the effects of ammonia transformations other than caused by nitrification.
Koltz (1982)	Iowa and Cedar Rivers, Iowa	To determine the locations and rates of nitrification downstream from two wastewater treatment plants	0.5-9.0/day	Rate of ammonia reduction and rate of nitrate increase	Algal assimilation of ammonia appeared to be an important transformation process. Laboratory rates of nitrification varied from 0.02-0.35/day.

(continued)

TABLE 3-21. (continued)

Reference	Study Area	Purpose of Study	Reported Nitrification Rates	Methods of Determining Nitrification Rates	Comments
Kreutzberger and Francisco (1977)	Morgan Creek, Ruin Creek, and Little Lick Creek; three shallow streams in North Carolina	To determine the distributions of nitrifying organisms, and to examine the nitrogen transformation occurring in the streams	-	-	Counts of nitrifying organisms were enumerated in the water column and in the top 1 cm of sediments. The populations were much larger in the sediments, which indicated that nitrifica- was occurring predominantly in the sediments and not in water column.
Cirello et al. (1979)	Passaic River, New Jersey	To determine whether nitrification was a significant process in the Passaic River	-	-	There were high ammonia nitrogen concentrations in the river with relatively little nitrification occurring. The potential for nitrification appeared high, and was expected to be exerted if water quality within the river improved.
Finstein and Matulewich (1974)	Passaic River, New Jersey	To determine the distribution of nitrifying bacteria in the river	-	-	Nitrifying bacteria were found to be from 21 to 140,000 times more abundant volumetrically in sediments than in the water column.
Slayton and Trovato (1978, 1979)	Potomac Estuary	To determine factors important in the oxygen balance within the estuary	0.10-0.14/day	Thomas Graphical Method	-

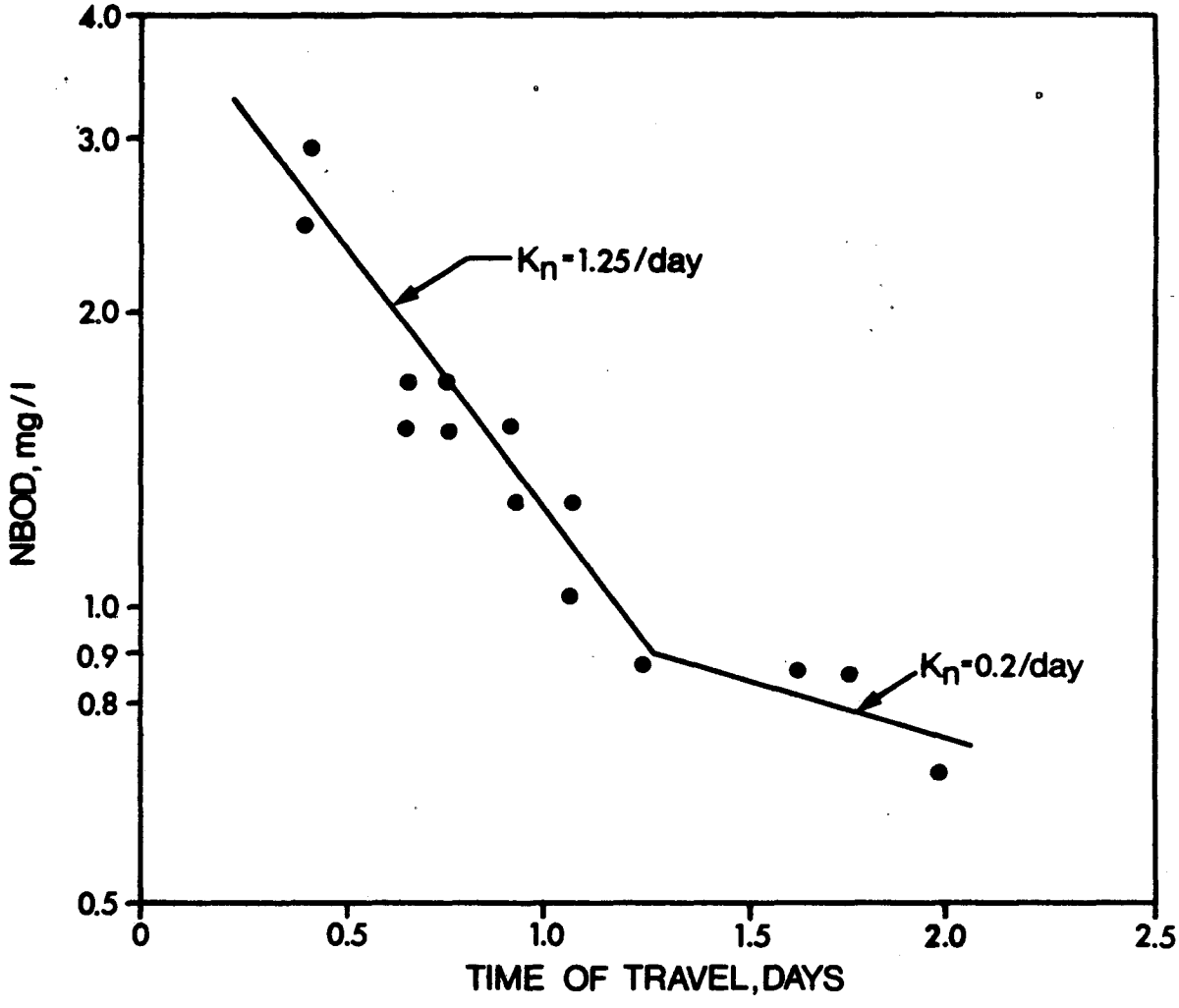

Figure 3-16. Nitrogenous biochemical oxygen demand versus travel time in Shenandoah River (Deb and Bowers, 1983).

Additional nitrification rates are shown in Table 3-22. Bansal (1976) has documented nitrification rates in numerous rivers throughout the United States, and developed a method to predict nitrification rate based on hydraulic data. His method has been criticized by Gujer (1977) and Brosman (1977) and is not reported.

Relatively few nitrification rates were found for lakes or estuaries. The few data in Table 3-22 for lakes and estuaries are generally in the range 0.1/day to 0.5/day.

TABLE 3-22. SUMMARY OF NITRIFICATION RATES

River	Maximum	Average	Minimum	Reference
Grand River, Michigan	3.9	2.6	1.9	Courchaine (1968)
Clinton River, Michigan	15.8 4.0	5.7 1.9	2.2 0.4	Wezernak and Gannon (1968)
Truckee River, Nevada	2.4	1.9	--	O'Connell and Thomas (1965)
South Chickamaugo Creek, Tennessee	1.9	--	1.1	Tennessee Valley Authority Ruane and Krenkel (1978)
Oostanaula Creek, Tennessee	0.8	--	0.1	Tennessee Valley Authority Ruane and Krenkel (1978)
Town Branch, Alabama	--	0.7	--	Tennessee Valley Authority Ruane and Krenkel (1978)
Chattahoochee River, Georgia	--	0.44	--	Stamer et al. (1979)
Willamette River, Oregon	0.7	--	0.4	Rinella et al. (1981)
Flint River, Michigan	2.5	1.4	0.1	Bansal (1976)
Upper Mohawk River, New York	0.3	0.25	0.25	Bansal (1976)
Lower Mohawk River, New York	0.3	0.3	0.3	Bansal (1976)
Bange Canal near Upper Mohawk River, New York	0.25	0.25	0.25	Bansal (1976)
Ohio River	0.25	0.25	0.25	Bansal (1976)
Big Blue River, Nebraska	0.25	0.11	0.03	Bansal (1976)
Delaware River Estuary	0.54	0.3	0.09	Bansal (1976)
Willamette River, Oregon	--	0.75* 1.05**	--	Alvarez-Montalvo, et al. undated
Ouachita River, Arkansas and Louisiana	--	0.1* 0.5**	--	NCASI (1982c)
Potomac Estuary	--	0.09-0.13	--	Thomann and Fitzpatrick, 1982
Lake Huron and Saginaw Bay	--	0.20	--	Di Toro and Matystik, 1980
New York Bight	--	0.025	--	O'Connor et al. 1981

Note: Nitrification rates are in units of 1/day.

* Ammonia Oxidation
** Nitrite Oxidation

3.4.5 Summary

Typically modelers simulate nitrification by first order kinetics, either the single stage or two stage approach. Most nitrification rate data have been collected in streams and rivers, where the rates can be quite variable due to bottom effects. Instream rates can differ significantly from laboratory or bottle rates. However, for large bodies of water (typically lakes or estuaries) the relative importance of the bottom is diminished, and nitrification rates tend to approach bottle rates. Available data suggest nitrification rates between 0.1 to 0.3/day are often appropriate for large lakes, large rivers, or estuaries.

In flowing waters, instream nitrification rates are often determined based on TKN versus travel time. Care should be taken that the assumptions of the approach are met, and that processes that transform nitrogen other than nitrification are assessed (i.e., the other components of the nitrogen cycle).

Because benthic nitrification can be important in small streams, it is important not to "doubly count" oxygen sinks in modeling applications. A component of the sediment oxygen demand would include benthic nitrification, so the two processes need to be accounted for in a mutually exclusive way for modeling applications.

Very few studies actually try to measure populations of nitrifiers in natural systems. This, however, is the most conclusive method to confirm that nitrification is occurring.

3.5 SEDIMENT OXYGEN DEMAND (SOD)

3.5.1 Concept of SOD

Oxygen demand by benthic sediments and organisms can represent a large fraction of oxygen consumption in surface waters. Benthal deposits at any given location in an aquatic system are the result of the transportation and

deposition of organic material. The material may be from a source outside the system such as leaf litter or wastewater particulate BOD (allochthonous material), or it may be generated inside the system as occurs with plant growth (autochthonous material). In either case, such organic matter can exert a high oxygen demand under some circumstances. In addition to oxygen demand caused by decay of organic matter, resident invertebrates can generate significant oxygen demand through respiration (Walker and Snodgrass, 1984). The importance of this process to water quality modeling is reflected in a recent symposium (Hatcher and Hicks, 1984). This same symposium also reviewed measurement techniques and a concensus favoring in situ measurement was reached.

It is generally agreed (e.g., Martin and Bella, 1971) that the organic matter oxygen demand is influenced by two different phenomena. The first is the rate at which oxygen diffuses into the bottom sediments and is then consumed. The second is essentially the rate at which reduced organic substances are conveyed into the water column, and are then oxidized. Traditional measurement techniques, whether they are performed in situ or in the laboratory, do not differentiate between the two processes but measure, either directly or indirectly, the gross oxygen uptake. Hence, in modeling dissolved oxygen, a single term in the dissolved oxygen mass balance formulation is normally used for both processes. If the two phenomena are modeled separately (e.g., see Di Toro, 1984), then additional modeling complexity is necessary.

The process is usually referred to as sediment oxygen demand (SOD) because of the typical mode of measurement: enclosing the sediments in a chamber and measuring the change in dissolved oxygen concentration at several time increments. This technique is used in the laboratory or in situ. The oxygen utilized per unit area and time (gO_2/m^2-day) is the SOD. The technique measures oxygen consumption by all of the processes enclosed in the chamber: chemical reactions, bacterially mediated redox reactions, and respiration by higher organisms (e.g., benthic worms, insects, and molluscs). Background water column respiration is then subtracted from this rate to compute the component due solely to the

sediment interface. SOD is usually assumed to encompass the flux of dissolved constituents such as DO to sediment and reduced chemicals to the water column. However, solid particle flux as BOD or sediment entrainment or settling is modeled separately.

The major factors affecting SOD are: temperature, oxygen concentration at the sediment water interface (available oxygen), makeup of the biological community, organic and physical characteristics of the sediment, current velocity over the sediments, and chemistry of the interstitial water. Each of these factors is a resultant of other interacting processes occurring elsewhere in the aquatic system. For example, temperature and available oxygen can be changed as a result of transport and biochemical processes in the water column or system boundaries. Temperature and oxygen are usually modeled explicitly, and can be used as input variables to the SOD process equations. Another important linkage is that the biological community will change with the water quality (e.g., oxygen and nutrient concentrations) and productivity of the system. The organic characteristics will change over the long term due to settling of organic matter (detritus, fecal matter, phytoplankton) and its subsequent degradation and/or burial by continued sedimentation. The biological community and the organic and physical characteristics of the bottom sediments are usually treated as a composite characteristic of the particular system. Recently, techniques have been developed for investigating these factors; however, the usual technique is to measure the SOD directly rather than the underlying factors that control the processes of SOD.

At least two major factors affecting SOD are usually neglected in SOD modeling. Current velocity is often neglected despite the fact that it has a major effect on the diffusive gradient of oxygen beginning just below the sediment-water interface. Most measurement techniques provide mixing by internal mixing or by recirculating or flow-through systems to minimize the effect of concentration gradients. However, the velocity of such systems may be insufficient (Whittemore, 1984a) or may be so vigorous as to cause scour and resuspension. Interstitial water chemistry affects substrates for biochemical and non-biochemical oxidation-reduction reactions and their

reaction rates. This factor is also usually neglected in SOD measurements and kinetic formulations.

3.5.2 Kinetics

The generalized equation for sediment oxygen demand is:

$$\frac{dC}{dt} = \frac{-SOD}{H} = f(\text{dissolved oxygen, temperature, organisms, substrate}) \qquad (3\text{-}51)$$

where H = water depth, m

SOD = sediment oxygen demand (as measured), gO_2/m^2-day

t = time

C = oxygen concentration in the overlying water, mg/l

3.5.2.1 Dissolved Oxygen

The benthic oxygen consumption has been hypothesized to depend on the dissolved oxygen concentration in the overlying waters (e.g., Edwards and Rolley, 1965; McDonnell and Hall, 1969):

$$SOD = a\ C^b \qquad (3\text{-}52)$$

where a,b = empirically determined constants

In the McDonnell and Hall (1969) study, b was found to be 0.30 and a to vary from 0.09 to 0.16, primarily as a function of the population density of benthic invertebrates.

Lam *et al*. (1984) use a Michaelis-Menten relationship to express the effects of oxygen on SOD:

$$\frac{dC}{dt} = -\frac{k_s A_s}{V} \frac{C}{K_{O_2} + C} \qquad (3\text{-}53)$$

where k_s = rate constant for SOD in Lake Erie, 0.1 g O_2/m^2-day
A_s = area of the sediment, m^2
V = volume of water layer, m^3
K_{O_2} = oxygen half saturation constant (1.4 mg/l)
C = oxygen concentration, mg/l

Walker and Snodgrass (1984) divided SOD in Hamilton Bay in Lake Ontario into two fractions: chemical-microbial (CSOD) and biological (BSOD). The chemical fraction was defined as a first-order function of oxygen:

$$CSOD = k_1(T)\ C \tag{3-54}$$

where $k_1(T)$ = temperature-adjusted rate constant for biochemical SOD, 1/day

The biological fraction was estimated to be 20-40 percent due to macroinvertebrates in Hamilton Bay sediments but still followed a Michaelis-Menten relationship:

$$BSOD = u(T)\ \frac{C}{K_{O_2} + C} \tag{3-55}$$

where $u(T)$ = temperature-adjusted rate constant for biological SOD (obtained by measurement: range = 0.58 to 5.52 g O_2/m^2-day), 1/day
K_{O_2} = oxygen half-saturation constant (1.4 mg/l)

It is interesting to note the similarity between the two estimates of K_{O_2} (Lam et al., 1984; Walker and Snodgrass, 1984).

The direct effects of dissolved oxygen on the rate constant are generally neglected except in a few models. For example, in the HSPF model (Johansen et al., 1981), dissolved oxygen concentration affects the rate of sediment oxygen utilization exponentially:

$$\frac{dC}{dt} = -\frac{k_T}{H}(1-e^{-1.22\ C}) \tag{3-56}$$

where k_T = the temperature adjusted rate constant, mg/m^2-day

3.5.2.2 Temperature

Temperature effects on SOD are most commonly modeled using the van't Hoff form of the Arrhenius relationship:

$$k_T = k_{Tr}\ \theta^{(T-Tr)} \tag{3-57}$$

where k_T = the rate at ambient temperature T

k_{Tr} = the rate at a reference temperature (usually Tr=20°C)

θ = the temperature coefficient for adjusting the rate (Table 3-23)

Although this form of the relationship is the most common and gives equivalent results to the Arrhenius equation, it is not preferred in standard nomenclature (Grau et al., 1982).

The exceptions to use of Equation (3-57) are RECEIV-II (Raytheon, 1974), HSPF (Johanson et al., 1981), and SSAM-IV (Grenney and Kraszewski, 1981). RECEIV-II apparently does not provide a temperature correction for the SOD rate coefficient although other rate coefficients in the model are adjusted according to Equation (3-57) with θ = 1.047 for CBOD. HSPF uses a linear function for adjusting the SOD for temperature:

$$k_T = 0.05\ T_w k_{20} \tag{3-58}$$

where k_T = the temperature adjusted coefficient

k_{20} = the rate constant at 20°C

T_w = water temperature, ^{o}C

TABLE 3-23. SOME TYPICAL VALUES OF THE TEMPERATURE COEFFICIENT FOR SOD RATE COEFFICIENTS USED IN WATER QUALITY MODELS

Model	θ	Q10(20°C)*	Reference
DOSAG-3	1.047	1.58	Duke & Masch (1973)
QUAL-II	1.047	1.58	Roesner et al. (1977)
Vermont QUALII	1.047	1.58	JRB (1983)
Lake Erie Model	1.08	2.16	Di Toro & Connolly (1980)
WASP	1.08	2.16	Thomann & Fitzpatrick (1982)
WASP	1.1	2.59	O'Connor et al. (1981)
LAKECO	1.02	1.22	Chen & Orlob (1972, 1975)
WQRRS	1.02-1.04	1.22-1.48	Smith (1978)
ESTECO	1.02-1.04	1.22-1.48	Brandes (1976)
DEM	1.04	1.48	Genet et al. (1974)
EAM	1.02	1.22	Bowie et al. (1980)
EAM	1.047	1.58	Tetra Tech (1980), Porcella et al. (1983)
USGS-Steady	1.065	1.88	Bauer et al. (1979)
AQUA-IV	1.02-1.09	1.22	Baca & Arnett (1976)
EXPLORE-I	1.05	1.63	Baca et al. (1973)
Laboratory/Field Studies	1.040-1.130	1.5-3.4	Zison et al. (1978); Whittemore (1984b)

* Q10(20°C) = ratio of k_2/k_1 at $k_2/k_1 = \theta^{10}$.

Grenney and Kraszewski (1981) used a modification of the Thornton and Lessem (1978) equation for SSAM-IV to provide, essentially, a continuously variable adjustment coefficient (θ) for the rate constants in biological processes. The equation adjusts over a temperature range of 5 to 30°C which is similar to using Equation (3-51) with a variable θ coefficient:

$$\tau_{11} = N \frac{K_1 e^{\gamma(T-T_1)}}{1-K_1(1-e^{\gamma(T-T_1)})} \tag{3-59}$$

where τ_{11} = a multiplier applied to the rate at the optimum temperature, dimensionless

N = an adjustment coefficient for rate processes, dimensionless

K_1 = reaction rate multiplier near lower threshold temperature, 1/day

γ = specific rate coefficient, 1/°C

T = environmental temperature, °C

T_1 = lower threshold temperature, °C

The coefficient τ_{11} is multiplied times the SOD (or benthic loading rate) directly in SSAM-IV.

Although many models use the same formulation (Equation (3-57)) of the temperature correction equation for the SOD rate constant, the value of the constant θ is in dispute. Whittemore (1984b) reviewed literature values as well as his laboratory values in an attempt to determine measurement uncertainty. For analysis of his data, Whittemore chose $\theta = 1.08$ with an estimate of uncertainty of ± 0.01. Then performing a sensitivity analysis for the range of $\theta = 1.07$-1.09 (1.08 ± 0.01), Whittemore showed that SOD would increase 12 percent when θ is increased by 0.01 for a temperature range of 12°C (20 to 32°C). He cautions that complete physical, chemical, and biological descriptions of SOD measurements are needed, both for <u>in situ</u> and studies measurements. Even in his own studies where a single method was used, the measured mean SOD using a stirred <u>in situ</u> respirometer had a standard deviation of 44 percent of the mean (Whittemore, 1984b).

Additional field experience and the use of divers to place the respirometers should measurably improve these results.

3.5.2.3 Biological Effects on SOD

The biological component is usually neglected when modeling SOD, because of the complexity of modeling benthic microorganisms and macroinvertebrates. The spatial and seasonal variability in SOD caused by sediment biological processes and communities results in variation in SOD that modelers appear to account for by varying the temperature coefficient. Some investigators have attempted to incorporate this variation directly in the model (Grenney and Kraszewski, 1981), or have suggested that the value of the temperature coefficient changes with season (e.g., Bradshaw et al., 1984) or with location downstream (e.g., Mancini et al.,1984). Other models (LAKECO, ESTECO, WQRRS, EAM) incorporate a benthic organisms compartment and may be able to evaluate the effects of benthos on SOD directly. However, no verification studies have been discovered that demonstrate this to be a useful technique.

3.5.2.4 Substrate Variability

The process describing the substrate utilized is where most models differ (Table 3-24). In the first water quality models that were widely used (DOSAG-3, QUAL-II), the decay of substrate is assumed to balance continued settling resulting in a steady-state sediment concentration of oxygen-demanding substrate. The resulting equation is:

$$\frac{dC}{dt} = -k_T/H, \qquad (3\text{-}60)$$

where k_T = temperature adjusted rate constant SOD, gO_2/m^2-day
H = mean water depth, m

As shown in Table 3-24, most models have followed this approach.

TABLE 3-24. MODEL FORMULATIONS COMMONLY USED IN SOD COMPUTATIONS

Formulation	Units	Description	Model (Reference)
k/A	k, mgO_2/m day A, m^2	SOD rate normalized by bottom area	DOSAG-3 (Duke & Masch, 1973) QUAL-II (Roesner et al. (1977)
k/H	k, mgO_2/m^2 day H, m	SOD rate normalized by mean depth	Vermont QUAL-II (JRB, 1983) USGS-Steady (Bauer et al. 1979) AQUA-IV (Baca & Arnett, 1976) WASP (O'Connor et al. 1981) RECEIV-II (Raytheon, 1974) DEM (Genet et al. 1974) HSPF (Johanson et al. 1981)
a k SED	a, mgO_2/mg Sed k, 1/day SED, mg Sed/m^3	Conversion factor Decay rate Sediment areal concentration	LAKECO* (Chen & Orlob, 1972, 1975) WQRRS* (Smith, 1978) EAM* (Bowie et al., 1980; Tetra Tech, 1980; Porcella et al., 1983) EXPLORE-I (Baca et al., 1973)

*NOTE: Additional SOD occurs due to respiration by the benthic organism compartment, which is modeled separately from sediment oxygen demand.

Substrate has been incorporated directly into ESTECO, LAKECO, WQRRS, EAM, and EXPLORE-I. Different settling rates of oxygen-demanding organic materials can lead to different amounts of sediment materials, and consequently different SOD rates calculated according to:

$$\frac{dC}{dt} = - a\ k\ SED \tag{3-61}$$

where a = stoichiometric conversion factor relating oxygen to organic sediment, mg O_2/mg sediment

k = sediment decay rate constant, 1/day

SED = sediment substrate that is subject to decay

In EXPLORE-I, only carbonaceous BOD is simulated as the substrate (SED), which in turn is affected by scour or settling from the water column. In the other models, all of the nutrient elements (C, N, P) are transformed according to a first-order reaction (k SED) but sediment oxygen demand is exerted only by carbon. Values of the conversion factor for sedimented organic carbon to O_2 lie in the range of 1.2 to 2.0 mgO_2/mg sediment. Nitrogen decays to ammonium and is released to the overlying waters where nitrification can take place (see Section 3.4). Other nutrients also enter the overlying waters as a result of similar transformations.

In some versions of the WASP model (Di Toro and Connolly, 1980; Thomann and Fitzpatrick, 1982), the oxygen-demanding materials in the sediment are divided into multiple compartments. First, the decay processes of sediment organic matter generate concentrations of CBOD and NBOD constituents in interstitial waters. Then both CBOD and NBOD are released to the water column where they subsequently decay in the appropriate compartments. In addition to CBOD release, oxygen utilization in the interstitial water is computed as oxygen equivalents, and diffusion into the interstitial water compartment is determined. If oxidation in excess of the amount available from diffusion occurs, these excess "oxygen equivalents" continue to represent a potential demand on the dissolved oxygen system. Finally, a deep oxygen demand has been hypothesized in an attempt to account for the measured oxygen demand. These concepts are described Di Toro and Connolly,

1980. More recently, Di Toro (1984) has provided an additional correction to SOD from denitrification of nitrate, although he suggests that this correction is usually negligible.

3.5.3 Measurement Techniques

Essentially three types of measurement techniques have been used to estimate SOD rates: model calibration to estimate SOD, in situ measurements using respiration chambers, and laboratory respiration chamber measurement using cores or dredged samples. However, all three methods have severe disadvantages and the uncertainty of calculating SOD rates is so great that the simple formulations in the model equations (Table 3-24) are very appealing to model users. Unfortunately, these simple formulations will not result in credible models with good predictive capability when single values are used for rates and coefficients.

It would be expected that considerable spatial and temporal variation would occur in SOD. Spatially, the bed sediments of streams, lakes , and estuaries vary in their physical and chemical characteristics, rates of deposition, and other factors. For example, a stream may have fine sediments in low velocity areas and coarse cobble or boulders in steep gradient-high velocity reaches. Depth and velocity can vary significantly in any one cross-section. Reservoirs have deposition zones near inlets and at dam structures. Estuaries like streams and lakes vary considerably in substrate type and water velocity but are influenced by the salinity gradient and an added factor of coagulation and rapid settling in zones where fresh and saline waters mix.

Another source of variation is temperature. Temperature varies seasonally but that is accounted for in use of the van't Hoff or similar relationships. However, temperature and season both cause a shift in benthic community composition. Macroinvertebrate populations, especially emergent insects, change dramatically with life stage. Also, it would be expected that considerable variation in microbial community characteristics would occur in response to temperature changes.

These spatial and seasonal characteristics suggest that a large number of SOD measurements would be required to estimate and obtain sufficient variation in rate coefficients. This has led to the development of in situ and laboratory methods for measuring SOD that will be site-specific and seasonal for SOD. SOD mapping strategies may be necessary. Ideally, in situ methods would provide the best approach, but considerable variation in results occurs because of problems associated with field sampling:

- Horizontal and longitudinal non-homogeneity of stream bottom materials. Areas of cobble, soft sediments, logs, and bedrock, increase the cost of measurement because more samples are needed. Soft, flocculent sediments are very difficult to evaluate with in situ methods. In some streams, an inaccurate characterization of reach-averaged SOD will be obtained.

- Difficulties in placement of respiration chamber. For example, obtaining a complete seal in cobbled and bouldered areas or where significant interaction with the ground water system occurs is essentially impossible.

- Mixing in the respiration chamber may not be modeled correctly nor simulate natural conditions and this is reflected in the wide variance in results from measurements. For example, the Institute of Paper Chemistry reported on a comparison of 5 in situ samplers of two basic types (recirculating and internally mixed) and found the results to be markedly different (Parker, 1977).

Laboratory measurements suffer from similar problems. They would appear to work reasonably well for aquatic systems of relatively uniform sediment characteristics, but heterogeneous sediments often lead to measurement variability.

Some practices improve laboratory measurement: correcting of results for varying sediment depth is usually unnecessary when depths exceed 5-10 cm; undisturbed core samples are preferred over dredge samples even though they are more costly to collect; storage of samples and acclimation of samples to laboratory temperatures is discouraged because of potential changes in benthos or substrate; divers may help to improve precision.

In regard to the effect of variability in oxygen-demanding materials, there appears to be no strong relationship between SOD and various measures of organic matter (NCASI, 1978), but this may have been due to inaccurate measurement techniques. Improper mixing (i.e, velocity too high or too low), inadequate oxygen supply, storage or improper pretreatment of samples in the laboratory, and inappropriate laboratory temperatures may lead to errors that prevent the derivation of SOD/substrate relationships. However, Gardiner et al. (1984), using a laboratory chamber, showed that SOD was related to chemical oxygen demand (COD) of the sediments in Green Bay, a large gulf in the northwest corner of Lake Michigan, according to the following equation:

$$SOD = 7.66\ COD/(156.5 + COD) \qquad (3\text{-}62)$$

As further evidence, the higher SOD values coincided with areas of summer dissolved oxygen depletion in Green Bay.

Given the many sources of measurement error, it is not surprising that Whittemore (1984b) was unable to correlate literature SOD values obtained in simultaneous field and laboratory measurements. He obtained a low r^2 value of 0.58. But even more significant, the in situ SOD values were consistently higher than laboratory derived values at low SOD concentrations and the reverse observed at high SOD concentrations. This systematic error indicates the need for better methods of estimating SOD as well as developing a better understanding of the component SOD mechanisms.

The model calibration approach to estimating SOD is essentially a determination of the SOD rate by calibration subject to the constraint of a

reasonable range of SOD values. Thomann (1972) used literature SOD rates and modeling experience to suggest SOD ranges for certain environments (Table 3-25). The model approach (e.g., Terry and Morris, 1984; Draper et al., 1984), by itself, contains considerable variance because there are uncertainties in the other processes (reaeration, nitrification, respiration, photosynthesis, flow) as well as the considerable spatial and temporal variation expected in most aquatic environments. Lam et al. (1984) suggest that variation in dissolved oxygen load to Lake Erie owing to

TABLE 3-25. AVERAGE VALUES OF OXYGEN UPTAKE RATES OF RIVER BOTTOMS (AFTER THOMANN, 1972)

	Uptake (g O_2/m^2-day) @ 20°C	
Bottom Type and Location	Range	Average
Sphaerotilus - (10 gm dry wt/m^2)	-	7
Municipal Sewage Sludge-Outfall Vicinity	2-10.0	4
Municipal Sewage Sludge-"Aged" Downstream of Outfall	1-2	1.5
Estuarine mud	1-2	1.5
Sandy bottom	0.2-1.0	0.5
Mineral soils	0.05-0.1	0.07

hydrologic fluctuations could easily mask the effects of SOD on water column oxygen.

3.5.4 Summary

There is a diversity of modeling and measurement techniques used for predicting oxygen consumption by sediments. This diversity reflects the need for better process descriptions and measurement techniques. Simple zero-order model formulations have been used, but first-order multi-component reactions with a separate benthic organism component may be needed to accurately model sediment oxygen demand (SOD).

Consequently, it is suggested that modelers use site-specific SOD rates. In situ methods such as described in Whittemore (1984a) and Markert et al. (1983) are more useful and credible than laboratory methods at this time.

As an aid to estimating SOD rates and establishing reasonable ranges for calibration, the SOD literature values in Tables 3-26, 3-27, and 3-28 are presented for rivers and streams, lakes and reservoirs, and estuaries and marine environments, respectively. These should be considered only as order of magnitude estimates.

3.6 PHOTOSYNTHESIS AND RESPIRATION

3.6.1 Introduction

Photosynthetic oxygen production (P) and respiration (R) can be important sources and sinks of dissolved oxygen in natural waters. Many models simulate these processes directly in terms of algal growth and respiration. For example, net algal growth is simulated with the QUAL-II model (Roesner et al., 1981) using:

$$\frac{\partial A}{\partial t} = (\mu - \rho - \sigma)A \qquad (3\text{-}63)$$

where A = algal concentration, mass/volume

μ = specific growth rate of algae, 1/time

ρ = algal respiration rate, 1/time

σ = algal settling rate, 1/time

The net algal oxygen production minus consumption is simulated by QUAL-II as:

$$\frac{\partial C}{\partial t} = (a_1\mu - a_2\rho)A \qquad (3\text{-}64)$$

where C = dissolved oxygen concentration, mass/volume

α_1 = oxygen production per unit of algal mass, mass oxygen/mass algae

α_2 = oxygen uptake per unit of algal mass, mass oxygen/mass algae

The stoichiometric coefficients α_1 and α_2 relate algal growth and death to oxygen production and consumption. Tables 3-29 and 3-30 summarize values of these coefficients used in different models.

TABLE 3-26. MEASURED VALUES OF SEDIMENT OXYGEN DEMAND IN RIVERS AND STREAMS

SOD, gO_2/m^2 day	Environment	Experimental Conditions	References
0.022-0.92	Upper Wisconsin River	60-hour laboratory core incubation, periodic mixing, 4°C, dark	Sullivan et al. (1978)
0.09±0.02 (@12°C) 0.15±0.04 (@20°C) 0.20±0.03 (@28°C) 0.29±0.07 (@36°C) 0.18±0.05 (@12°C) 0.55±0.22 (@20°C) 0.60±0.28 (@28°C) 0.87±0.23 (@36°C)	Eastern U.S. River Southeastern U.S. River	45 day incubation of 0.6 liters sediment in 3.85 liters BOD dilution water, light	NCASI (1981)
3.2-5.7 0.52-3.6	Fresh shredded tree bark Aged shredded tree bark	10-liter incubations in aged tap water, room temperature, light	NCASI (1971)
2-33 0.9-14.1	Four eastern U.S. rivers downstream of paper mill discharges	In-situ chamber respirometers, 22-27°C, light, stirred at varying rates; open-ended tunnel respirometer, in-situ, 22-27°C, dark	NCASI (1978)
<0.1-1.4 (@20°C)	Eastern U.S. river downstream of paper mill discharge	In-situ respirometer stirred at various rates 9-16°C, dark, θ = 1.08	NCASI (1979)
0.27-9.8	Northern Illinois rivers (N = 89 stations)	In-situ respirometry, dark, T = 5° - 31°C time = 1½ - 3 hours	Butts & Evans (1978)
0.10-5.30 (@20°C)	Six stations in eastern Michigan rivers	In-situ respirometry in stirred chambers, 15-27 hours dark, 19-25°C, θ = 1.08	Chiaro & Burke (1980)
1.1-12.8	New Jersey rivers (10 stations)	In-situ respirometer, dark, 30 minutes-8 hours, stirred. Temperature unknown	Hunter et al. (1973)
0.3-1.4	Swedish rivers	In-situ respirometer, light, stirred, 0-10°	Edberg & Hofsten (1973)
0.20-1.2	Swedish rivers	Laboratory incubations, stirred, dark, 5-10°C	Edberg & Hofsten (1973)
1.7-6.0	Spring Creek, PA	Laboratory incubators in dark, stirred, 20°C	McDonnell & Hall (1969)
1.5-9.8	74 samples from from 21 English rivers	Laboratory incubation of cores; 15°C	Rolley & Owens (1967)
4.6-44.	Streams	Oxygen mass balance	James (1974)

TABLE 3-27. MEASURED VALUES OF SEDIMENT OXYGEN DEMAND IN LAKES AND RESERVOIRS

SOD, gO_2/m^2 day	Environment	Experimental Conditions	References
1-7	Green Bay, Lake Michigan	Lab incubation in darkness, 20°C	Gardiner *et al.* (1984)
0-2.2	Fish culture ponds	*In situ* respirometry with 100-cm long plexiglass columns (dark pvc), over 47 days. Temperature unknown	Shapiro & Zur (1981)
0.4-2.6	Swedish lakes	*In situ* respirometer, light stirred, 5-18	Edberg & Hofsten (1973)
0.21-1.5	Swedish lakes	Laboratory incubations, stirred, dark, 10-13°C	Edberg & Hofsten (1973)
5.5 (31-32.5°C) 5.1 (22.5-25.6°C) 2.1 (13.2-16.1°C)	Horseshoe Lake, IL	*In situ* respirometry, dark, stirred about 1 hour	Butts & Evans (1979)
0.84-3.3	Lake Apopka, FL	Laboratory incubation of cores at room temperature, 2-3 hours, light. No stirring.	Belanger (1981)
0.4-3.6	Lake Apopka, FL	Laboratory flow-through system (closed, 100 l volume)	
0.40-0.45 0.27	Hyrum Reservoir, UT Lake Powell	3-phase microcosms, 25°C, dark	Medine *et al.* (1980)
0.12-0.22	Shagawa Lake	*In-situ* chambers ($1m^2$), at 7-12 m depths; 12-14°C (est.)	Sonzogni *et al.* (1977)
0.47-0.92	Swedish Lakes	Laboratory measurement with undisturbed cores; used *in situ* temperatures	Graneli (1977)
0.72-8.40	Lakes	Oxygen mass balance	James (1974)
0.6-3.6	Hamilton Harbor, Lake Ontario	*In situ* chambers, 11-16°C	Polak & Haffner (1978)
1.7-8.9	Lake Mohegan, NY	Measurement based on mass balance, continuous flow lab chamber, 22-32°C	Fillos (1977)
0.17-0.5	Swedish lakes	*In situ* & laboratory measurements, winter temperatures	Edberg (1977)
0.54-0.71	Swedish lakes	Laboratory incubation of undisturbed cores, 8°C	Andersen (1977)
0.3-1.0	Lake Hartwell, SC	Laboratory chambers, 18°C	Brewer *et al.* (1977)
0.076-0.48	Marion Lake, BC	Laboratory incubation of undisturbed cores, no mixing, 15°C	Hargrave (1969)
0.004-0.012	Lake Superior	Laboratory incubation of undisturbed cores, 4°C	Glass & Podolski (1975)

In addition to algal respiration, respiration from zooplankton and nekton can contribute to oxygen depletion, and would be included in Equation (3-64), along with additional equations to describe their growth and death. Models that simulate algae and zooplankton (such as those in Tables 3-29 and 3-30) are discussed in detail in Chapters 6 and 7 of this report. This section describes methods to predict P-R without simulating algal growth or respiration. The methods pertain largely to streams and rivers, and are useful in that they simplify the modeling approach.

It should be mentioned that some water quality models do not simulate photosynthesis and algal respiration. This approach is valid where P=0 and R=0. Other models simulate only daily average photosynthetic oxygen production ($\overline{P}$) and daily average respiration ($\overline{R}$). If, on a daily average basis, $\overline{P}-\overline{R}\approx 0$, these models would predict little effect of algal activity on dissolved oxygen. However, if $\overline{P}$ and $\overline{R}$ are both large numbers, then actual dissolved oxygen levels will be higher during the day and lower at night than predicted by the models.

3.6.2 Methods

Table 3-31 summarizes the methods reviewed to predict photosynthetic oxygen production and respiration without simulating algal growth. The methods consist of either single station methods or two-station methods. Odum (1956) appears to be one of the first researchers to use this approach.

TABLE 3-28. MEASURED VALUES OF SEDIMENT OXYGEN DEMAND IN ESTUARIES AND MARINE SYSTEMS

SOD, gO_2/m^2 day	Environment	Experimental Conditions	References
0.10±0.03 (@12°C) 0.20±0.05 (@20°C) 0.22±0.09 (@28°C) 0.37±0.15 (@36°C)	A North Carolinian estuary	45 day incubation of 0.6 liters sediment in 3.85 liters BOD dilution water, light	NCASI (1981)
2.32±0.16 1.88±0.018	Buzzards Bay near raw sewage outfall Buzzards Bay control	In-situ dark respirometers, stirred, 1-3 days. Temperature unknown	Smith et al. (1973)
0.14-0.68 (5°C) 0.20-0.76 (10°C) 0.30-1.52 (15°C)	Puget Sound sediment cores	Laboratory incubations	Pamatmat et al. (1973)
0.05-0.10	San Diego Trough (deep marine sediments)	In-situ respirometry for 5-13 hours, 4°C, light	Smith (1974)
1.25-3.9	Yaquina River estuary, Oregon	Dark laboratory incubators, stirred, 20°C	Martin & Bella (1971)
0.02-0.49	Eastern tropical Pacific	Shipboard incubations, 15°C stirred, dark	Pamatmat (1971)
0.9-3.0	The Baltic Sea	In-situ light respirometer, stirred, 10°C	Edberg & Hofsten (1973)
0.4-0.71	The Baltic Sea	Laboratory incubations, stirred, dark, 10°C	Edberg & Hofsten (1973)
0-10.7	Delaware Estuary (22 stations)	In-situ dark respirometry, 13-14°C	Albert (1983)
0.3-3.0	Fresh & brackish waters, Sweden	In-situ respirometry, 0-18°C Laboratory cores, 5-13°C	Edberg & Hofsten (1973)

TABLE 3-29. OXYGEN PRODUCED PER MASS OF ALGAE

Model	Value	Reference
DOSAG3	1.4 - 1.8 $\frac{\text{mg } O_2}{\text{mg algae (D.W.)}}$	Duke & Masch (1973)
QUAL-II	1.4 - 1.8 $\frac{\text{mg } O_2}{\text{mg algae (D.W.)}}$	Roesner *et al.* (1977)
WASP	2.67 mg O_2/mg C	Di Toro & Connolly (1980)
WASP	2.66 mg O_2/mg C	O'Connor *et al.* (1981)
	.133 mg O_2/mg Chl-*a*	O'Connor *et al.* (1981)
WASP	2.67 mg O_2/mg C	Thomann & Fitzpatrick (1982)
LAKE ECO	1.6 mg O_2/mg algae (D.W.)	Chen & Orlob (1975)
WQRRS	1.6 mg O_2/mg algae (D.W.)	Smith (1978)
AQUA-IV	1.6 - 2.66 mg O_2/mg C	Baca & Arnett (1976)
ESTECO	1.6 - 1.8 mg O_2/mg algae (D.W.)	Brandes (1976)
EAM	1.24 mg O_2/mg algae (D.W.)	Porcella *et al.* (1983)
EAM	1.6 mg O_2/mg algae (D.W.)	Bowie *et al.* (1980)
EAM	1.24mg O_2/mg algae (D.W.)	Tetra Tech (1980)
DEM	1.6 mg O_2/mg algae (D.W.)	Feigner & Harris (1970)
Vermont-QUAL-II	1.4 - 1.8 mg O_2/mg algae (D.W.)	JRB (1983)

Note:
D.W. = dry weight

Both numerical and analytical techniques have since been developed. The light-dark bottle technique and benthic chamber method are also included in the table.

As shown in Table 3-31, O'Connell and Thomas (1965) applied a total derivative approach for P-R calculation, and compared the results against a

second procedure using a submerged algal chamber. Respiration was corrected for oxygen consumption by bacterial oxidation. Figure 3-17 compares the two methods for a station on the Truckee River, and shows good agreement.

O'Connor and Di Toro (1970) use a half cycle sine wave or a Fourier series to find the time varying photosynthetic oxygen production rate. In

TABLE 3-30. OXYGEN CONSUMED PER MASS OF ALGAE

Model	Value	Reference
DOSAG 3	1.6 - 2.3 mg O_2/mg algae (D.W.)	Duke & Masch (1973)
QUAL-II	1.6 - 2.3 mg O_2/mg algae (D.W.)	Roesner *et al*. (1977)
WASP	1.87 mg O_2/mg C [1]	Di Toro & Connolly (1980)
WASP	2.0 mg O_2/mg C	Thomann & Fitzpatrick (1982)
WASP	2.0 mg O_2/mg C	O'Connor *et al*. (1981)
	.10 mg O_2/mg Chl-*a*	O'Connor *et al*. (1981)
LAKE ECO	1.6 mg O_2/mg algae (D.W.)	Chen & Orlob (1975)
WQRRS	1.6 - 2.0 mg O_2/mg algae (D.W.)	Smith (1978)
AQUA-IV	1.6 - 2.66 mg O_2/mg C	Baca & Arnett (1976)
ESTECO	1.6 - 1.8 mg O_2/mg algae (D.W.)	Brandes (1976)
EAM	.95 mg O_2/mg algae (D.W.)	Porcella *et al*. (1983)
EAM	1.6 mg O_2/mg algae (D.W.)	Bowie *et al*. (1980)
EAM	.95 mg O_2/mg algae (D.W.)	Tetra Tech (1980)
DEM	1.6 mg O_2/mg algae (D.W.)	Feigner & Harris (1970)
Vermont - QUAL-II	1.6 - 2.3 mg O_2/mg algae (D.W.)	JRB (1983)

[1] This is multiplied by an oxygen limitation factor, $\frac{O_2}{K + O_2}$, where K is a half-saturation constant equal to 0.1 mg/l.

Note:

D.W. = dry weight

TABLE 3-31. SUMMARY OF METHODS TO PREDICT PHOTOSYNTHETIC OXYGEN PRODUCTION AND RESPIRATION WITHOUT SIMULATING ALGAL GROWTH AND DEATH

Source	Equations	Symbols	Comments
Odum (1956)	see comments	see comments	1. Photosynthetic oxygen production was based on a graphical procedure. Either two stations or single station approaches could be used. A method was also presented to find the reaeration coefficient.
O'Connell and Thomas (1965)	$P - R = \frac{\partial C}{\partial t} + U\frac{\partial C}{\partial x} - k_2(C_s - C) + k_1 L + k_n N$	U = stream velocity k_2 = reaeration rate C = dissolved oxygen C_s = dissolved oxygen saturation k_1 = CBOD decay rate L = CBOD k_n = nitrification rate N = NBOD	1. P-R was found in two independent ways. In the first, all terms in the dissolved oxygen mass-balance were found independently and then P-R was found as the only remaining term in the oxygen balance. In the second method, an algal chamber was placed on the river bed. 2. The two methods gave comparable results. 3. The approach was used on the Truckee River, where attached algae were abundant.
O'Connor and Di Toro (1970)	<u>Half cycle sine wave</u>: $P = \begin{cases} P_m \sin\left\{\frac{\pi}{p}(t-t_s)\right\} & t_s \le t \le t_s + p \\ 0 \text{ when } & t_s + p \le t \le t_s + 1 \end{cases}$ <u>Fourier series extension</u>: $P = P_m\left\{\frac{2p}{\pi} + \sum_{n=1}^{\infty} b_n \cos\left[2\pi n(t-t_s - p/2)\right]\right\}$ where $b_n = \cos(n\pi p)\ \frac{4\pi/p}{(\pi/p)^2 - (2\pi n)^2}$	P = rate of photosynthetic oxygen production, mg/(l-day) $P_m(x)$ = maximum rate of photosynthetic oxygen production, mg/(l-day) t_s = time of day when source begins p = fraction of day when source is active	1. This approach is found in DIURNAL, a stream model developed by O'Connor and Di Toro. 2. The approach is potentially applicable to any vertically mixed water body. 3. The method of Erdmann (1979a) was used to evaluate P and R for a wasteload allocation application on the Shenondoah River (Deb and Bowers, 1983) and on Leatherwood Creek, Arkansas (Deb <u>et al</u>., 1983). 4. O'Connor and Di Toro (1970) applied the method to the Grand, Clinton, and Flint rivers in Michigan, the Truckee River in Nevada, and the Ivel River in Great Britain. They used a trial and error procedure to determine P_m, t_s, P and R to best fit observed diurnally varying dissolved oxygen data.

(continued)

TABLE 3-31. (continued)

Source	Equations	Symbols	Comments
Kelly, Hornberger, Cosby (1975)	$P - R = \frac{A_0}{2} + \sum_{n=1}^{\infty} A_n \cos(n\omega t)$	A_n = unknown coefficients $\omega = 2\pi/48$ The A_n are determined based on measurements of dissolved oxygen at either one of two locations in a stream. They are chosen to give a "best fit" between predicted and observed dissolved oxygen values.	1. A 48-hour cycle was used so that values at the beginning and end of a day are not constrained to be identical. 2. R is total respiration, including both algal respiration and bacterial decay. 3. The single station analysis can be used when the dissolved oxygen concentrations at the upstream and downstream stations are approximately the same.
Hornberger and Kelly (1972)	$P - R = \frac{\partial C}{\partial t} + U\frac{\partial C}{\partial x} - k_2(C_s - C)$	C = dissolved oxygen concentration U = stream velocity k_2 = reaeration rate C_s = dissolved oxygen saturation	1. Three methods were examined to predict P-R: a finite difference method, an analytical solution assuming P-R remains constant over the time interval, and a second analytical method assuming P-R varies linearly over a time step. 2. The analytical methods were preferred over the numerical approach from a conceptual point of view, and because time steps smaller than the residence time through the stream reach could be used.
Erdmann (1979a)	$P - R = k_2(C_s - C) - \frac{DC}{Dt}$ where: $\frac{DC}{Dt} = 1/2 \left\{ \frac{C_{21} - C_{11} + C_{22} - C_{12}}{t_2 - t_1} + \frac{C_{12} - C_{11} + C_{22} - C_{21}}{t_f} \right\}$	C_{nm} = concentration of dissolved oxygen at station m and time n t_2 = time of sample at downstream station t_1 = time of sample at upstream station t_r = travel time between two stations k_2 = reaeration rate C_s = dissolved oxygen saturation C = dissolved oxygen	1. Respiration is first computed at night when P = 0. Then P is computed during the day using known R. 2. The method was applied to Charles River, Massachusetts. 3. R is total oxygen consumption rate by both algae and bacteria.

(continued)

TABLE 3-31. (continued)

Source	Equations	Symbols	Comments
Erdmann (1979b)	$\bar{P} = (\Delta C_u + \Delta C_d)$ $\bar{R} = k_2 \left(\frac{D_u + D_d}{2}\right) + (\Delta C_u + \Delta C_d) - \left(\frac{C_d - C_u}{t_f}\right)$	$\bar{P}$ = daily average photosynthesis $\bar{R}$ = daily average respiration k_2 = reaeration rate t_f = travel time between two stations $\Delta C_u, \Delta C_d$ = diurnal range of dissolved oxygen at upstream stations D_u, D_d = daily average dissolved oxygen deficit at upstream and downstream stations C_u, C_d = daily average dissolved oxygen concentration at upstream and downstream stations	1. The method is a simplification of Erdmann (1979a) and is used to predict daily average values of P-R from data at two stations. 2. The method was applied to the Charles River, Massachusetts. 3. Some important assumptions include constant temperature and symmetrical diurnal curves.
Gulliver, Mattke, Stefan (1982)	$P - R = \frac{\partial C}{\partial t} + U \frac{\partial C}{\partial x} - \frac{\partial}{\partial x}\left(D_L \frac{\partial C}{\partial x}\right) - k_2(C_s - C)$	U = stream velocity k_2 = reaeration rate C = dissolved oxygen C_s = dissolved oxygen saturation D_L = longitudinal disperson coefficient	1. A finite difference computer model DORM was used to route dissolved oxygen changes between two stations and includes the effects of temperature variations and dissolved oxygen levels on respiration. 2. The model was applied to experimental stream reaches in the U.S. EPA's Monticello Ecological Research Station, Minnesota. 3. For the channels analyzed, it was found that affects of longitudinal dispersion were negligible. However the results were sensitive to reaeration, residence time between the two stations, and temperature dependent processes (saturation and respiration rates).

(continued)

TABLE 3-31. (continued)

Source	Equations	Symbols	Comments
U.S. EPA (1983)	light and dark bottle technique		1. Light and dark bottles are suspended at various depths in water and dissolved oxygen measurements are made at regular intervals to determine P-R. 2. This method suffers from numerous limitations which include: • only photosynthetic activity of algae in water column is measured • the estimate of R includes algal and bacterial respiration • the P-R is a point estimate, rather than representative of a reach.
U.S. EPA (1983)	benthic chamber		1. P-R of attached algae is measured using a clear benthic chamber and a covered (dark) chamber.

their applications, they used a trial and error procedure to determine P-R that best fit diurnally varying dissolved oxygen data. In the Deb and Bowers (1983) application of the same method, Erdmann's approach (1979a) was used to evaluate P-R. The method of Erdmann combines all terms which contribute to deoxygenation (algal respiration, CBOD decay and NBOD decay) into a single respiration term. To find algal respiration, CBOD and NBOD are subtracted from total community respiration.

Kelly et al., (1975), also shown in Table 3-31, use a Fourier series, but with a 48 hour period. The coefficients A_n are not true Fourier coefficients but are based on a best fit between predicted and observed dissolved oxygen values. Cohen and Church (1981) have more recently applied these methods to measure productivity of algae in cultures open to the atmosphere.

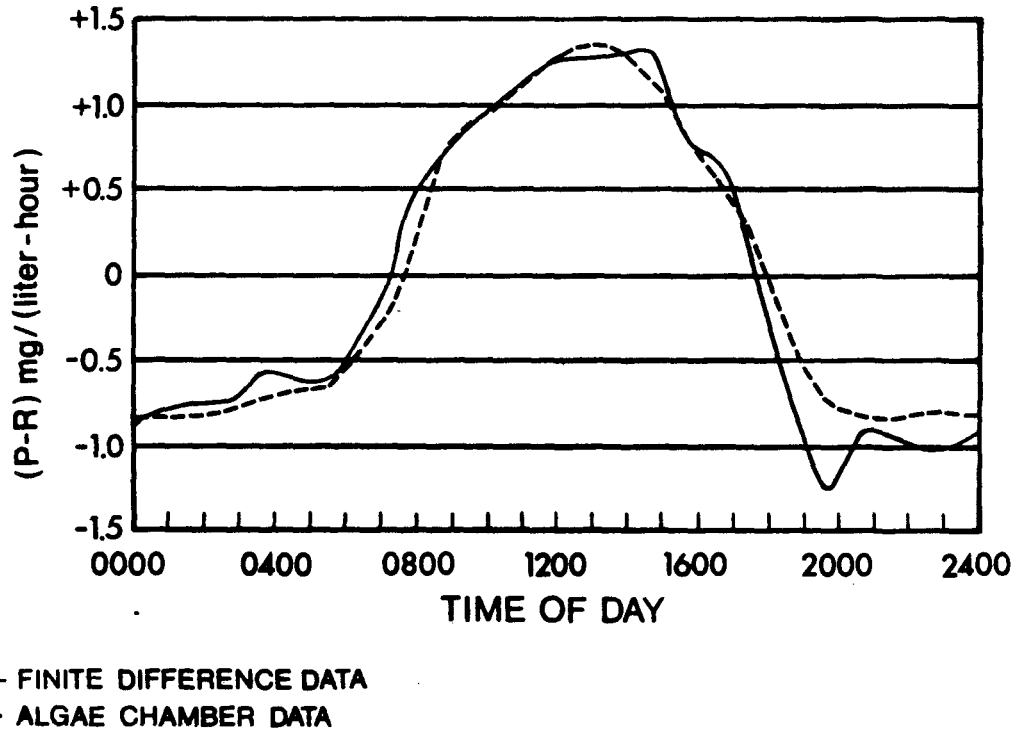

Figure 3-17. Diurnal variation of (P-R) in Truckee River near Station 2B (O'Connell and Thomas, 1965).

Erdmann (1979a, 1979b) has developed methods to predict time-varying P-R values and daily average values. In the time varying case the concept of the Stokes total time derivative is used (see Figure 3-18). The total derivative is the sum of the time derivative ($\partial C/\partial t$) and the advective derivative ($U\partial C/\partial x$). The time derivative is evaluated as the average of two times, and the advective derivative is the average between two stations.

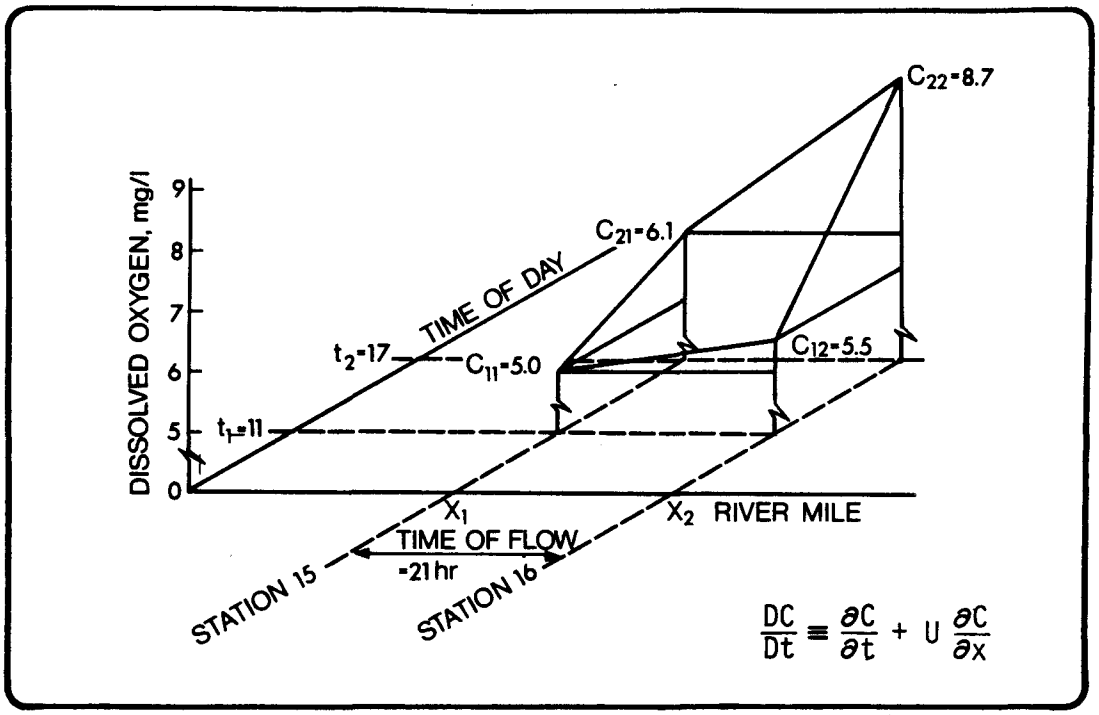

Figure 3-18. Concept of Stokes total time derivative. Here $DC/Dt = 0.43$ mg $O_2/l \cdot h$ (from Erdmann, 1979a).

Gulliver et al., (1982) provide a literature review of the various methods used to predict P-R in streams. They also developed a computerized model to determine P-R that includes dispersion. However, they found that effects of dispersion were negligible for their applications. Several applications of diurnal curve analyses not reported in Table 3-31 include the work of Schurr and Ruchts (1977) who used a single station method to predict monthly average P-R values, and the work of Simonsen and Harremoes (1978) who used a two station approach to predict P-R on a river in Denmark.

The final two methods shown in Table 3-31 are the light-dark bottle method and the benthic chamber method. These methods measure P-R of algae in the water column (light-dark bottles) and of attached algae (benthic chamber). The methods provide single point estimates that may not be representative of the water body as a whole.

Some models simulate daily average photosynthetic oxygen production rather than time-varing production. Erdmann (1979b) shows that, the daily average photosynthesis oxygen products rates, P, can be approximated by:

$$\overline{P} = \frac{2\Delta DO}{24} \text{ (mg/l/nr)} \tag{3-65}$$

where ΔDO = daily maximum dissolved oxygen concentration minus daily minimum dissolved oxygen concentration, mg/l

This approximation appears to be valid only for reaeration rates less than 0.2/day (Manhattan College, 1983).

A second method of estimating P is to integrate a sinusoidal curve that represents the instantaneous photosynthetic oxygen production rate. The result is:

$$\overline{P} = \frac{2\ P_m p}{\pi} \tag{3-66}$$

where P_m = maximum daily photosynthetic oxygen production rate, mg/l/day

p = fraction of day when algae are producing oxygen, decimal fraction

The U.S. EPA (1983) describes a third method to estimate daily average production based on light-dark bottle measurements:

$$\overline{P} = \frac{2P'\Delta T}{\cos(\pi t_1/f) - \cos(\pi t_2 f)} \tag{3-67}$$

where P' = observed average production rate between times t_2 and t_1

$\Delta T = (t_2 - t_1)/24$

f = number of hours in day when oxygen is being produced

Relationships between photosynthetic oxygen production and chlorophyll-a have been developed by a number of researchers. While a detailed review of these methods is outside of the scope of this section, several of the more commonly used formulations are summarized here. Megard et al. (1979) developed the following expression for daily average photosynthetic oxygen production:

$$\overline{P} = \frac{\ln\left(\frac{I_o}{I_z}\right) C_a P_m}{\varepsilon_c C_a + \varepsilon_w} \tag{3-68}$$

where I_o = light intensity at the water surface

I_z = light intensity at depth z

C_a = chlorophyll-a concentration

ε_c = specific attenuation of light by chlorophyll-a

ε_w = specific attenuation of light by all causes other than chlorophyll-a

P_m = maximum daily photosynthetic oxygen production rate, mg/l/day

Demetracopoulos and Stefan (1983) modified this expression to predict hourly photosynthetic oxygen production, and used the expression in a model of the Mississippi River.

In experiments on the Sacramento-San Joaquin Estuary, Bailey (1970) correlated the daily photosynthetic oxygen production rate to a number of factors. The resulting expression was:

$$P_{av} = 3.16\ C_a \frac{I^{0.677}}{k_e} + 0.16T - 0.56H \tag{3-69}$$

where P_{av} = average daily gross photosynthetic rate, mg/l-day

I = mean daily solar intensity, cal/sq.cm-day

k_e = light extinction coefficient, 1/meter

T = mean temperature, ^oC

H = mean water depth, m

C_a = mean chlorophyll, mg/l

Finally, simple relationships between chlorophyll-a and, P_m have been proposed (U.S. EPA, 1983). Figure 3-19 shows how Pm/Ca ratios are

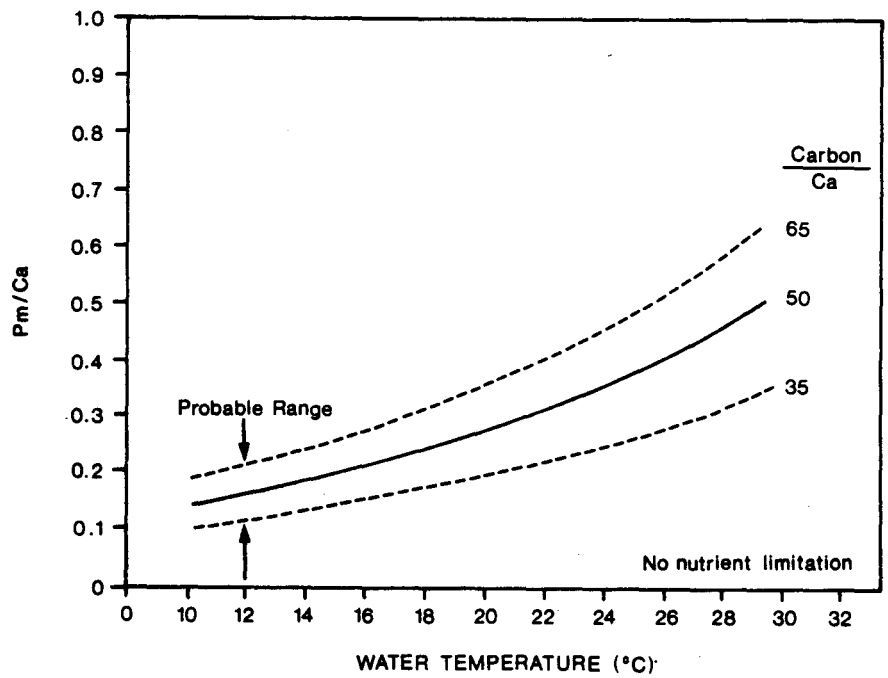

Figure 3-19. Algal productivity and chlorophyll relationships for streams (U.S. EPA, 1983).

influenced by water temperature and algal carbon/Ca ratios. For a typical water temperature (20^oC) and a typical carbon/Ca ratio (50), Pm/Ca = 0.25. However, this ratio is likely to vary between 0.1 to 0.6 for the range of conditions present in streams.

3.6.3 Data

Table 3-32 summarizes data reviewed on photosynthetic oxygen production and respiration. Respiration is sometimes reported as total community respiration and at other times as algal respiration. As shown by the data, photosynthetic oxygen production can be quite variable, both over distance and time. In the Havelse River, for example, average photosynthetic oxygen production rates varied from 0.2 to 25.9 g/(m^2-day). One of the primary reasons for the variability was because solar radiation intensity changed by more than an order of magnitude between measurement periods.

3.6.4 Summary

Most water quality models that simulate photosynthetic oxygen production and algal respiration simulate algal growth and respiration. Stoichiometric coefficients are used to convert growth and respiration to oxygen production and consumption. Tables 3-29 and 3-30 summarize these coefficients.

Some river water quality models use the approach that photosynthetic oxygen production and respiration can be modeled without the necessity of simulating algal activity. Rather, some type of curve, such as a sine curve or more generally a Fourier series, is used instead, where certain parameters must be delineated to characterize the curve.

Typically instream dissolved oxygen measurements at two stations are used to generate P-R data. Either finite difference or continuous solutions to dissolved oxygen mass balance equations are used. While light-dark bottles or benthic chambers can in principal be used to find the required information, these approaches are limited in a number of ways. The two station methods are better in that they provide an integrated estimate of algal activity.

However, two station methods should also be used cautiously. In a sense, the methods are curve fitting techniques: they are used to fit a

curve based on dissolved oxygen variation between two stations. Typically other rate constants such as reaeration rates, carbonaceous BOD decay, nitrogenous BOD decay are needed to fit the curves. Thus errors in these coefficients are propagated into P-R calculations. Also care should be taken if results are extrapolated to other situations (e.g., different temperatures, different solar intensities, and different nutrient loadings).

TABLE 3-32. PHOTOSYNTHETIC OXYGEN PRODUCTION AND RESPIRATION RATES IN RIVERS

Reference	River	T ^oC	P_m g/m^2-day	P_{av} g/m^2-day	R g/m^2-day
O'Connor and Di Toro (1970)	Grand, Michigan	28	12.7 - 37.6	4.4 - 13.0	9.3 - 12.7[a]
O'Connor and Di Toro (1970)	Clinton, Michigan	21	13.2 - 22.9	4.2 - 7.3	9.3[a]
O'Connor and Di Toro (1970)	Truckee, Nevada	28	12.9 - 26.	4.8 - 9.6	3.6 - 6.2[a]
O'Connor and Di Toro (1970)	Ivel, Great Britain	16	24.	9.0	4.6[a]
O'Connor and Di Toro (1970)	Flint, Michigan	28	4. - 40.	1.3 - 18.	4. - 20[a]
Thomas and O'Connell (1966)	North Carolina Streams	-	-	9.8	21.5[b]
Thomas and O'Connell (1977)	Laboratory Streams	-	-	3.4 - 4.0	2.4 - 2.9[b]
Erdmann (1979a,b)	Charles, Massachusetts	19-25	-	0.0 - 12.	0.0 - 36.[b]
Deb and Bowers (1983)	Shenandoah, Virginia	23	4.8 - 17.4	-	0.9 - 5.9[a]
Kelly et al. (1975)	Baker, Virginia	-	-	0.45	1.9[b]
Kelly et al. (1975)	Rappahannock, Virginia	-	-	6.1	7.3[b]
Kelly et al. (1975)	S. Fork Rivanna, Virginia	-	-	2.1	3.4[b]
Kelly et al. (1975)	Rivanna, Virginia	-	-	2.3	5.4[b]
Kelly et al. (1975)	South, Virginia	-	-	2.0	5.3[b]
Kelly et al. (1975)	Mechums, Virginia	-	-	1.3	2.6[b]
Simonsen and Harremoes (1978)	Havelse, Denmark	-	-	0.2 - 25.9[c]	4.8 - 22.9[b]
Gulliver et al. (1982)	Experimental Channels	9-24	5. - 45.	1.5 - 14.8	2.6 - 10.7[b]

[a]Algal respiration only

[b]Total community respiration

[c]Measurements were made over the period of one year, and solar radiation varied by more than a factor of 10.

In cases where diurnal water temperature changes are great, diurnal curve analyses should include temperature correction effects.

All of the approaches reviewed in Table 3-31 have apparently been successfully applied. However, no comprehensive comparison of the approaches against the same data set were found. In cases where a significant amount of data is available for analysis, a computerized approach such as Kelly et al. (1975) or Gulliver et al. (1982) appears to be better than trial and error procedures. The method that has been most rigorously tested is the DORM model of Gulliver et al. (1982). Also these methods can be used when the distance between stream stations is great, because the models do not assume that P-R remains constant over the travel time between the stations.

Under the appropriate conditions the simpler approach of Erdmann (1979a,b) can be used. One restriction on using approaches where P-R is assumed constant over the time increment is that the travel time between stations must be short (i.e., 1 to 3 hours) so that the constant P-R assumption is not violated.

3.7 REFERENCES

Adams, C.E. and W.W. Eckenfelder. 1977. Nitrification Design Approach for High Strength Ammonia Wastewaters, Journal of Water Pollution Control Federation, Vol. 49, No. 3, March, pp. 413-421. Albert, R.C. 1983. Report of Findings, Delaware Estuary Sediment Oxygen Demand Study. Delaware River Basin Commission. West Trenton, New Jersey.

Albert, R.C. 1983. Report of Findings, Delaware Estuary Sediment Oxygen Demand Study. Delaware River Basin Commission. West Trenton, New Jersey.

Alonso, C.V., J.R. McHenry, and J.C.S. Hong. 1975. The Influence of Suspended Sediment on the Reaeration of Uniform Streams, Water Research, Vol. 9, pp. 695-700.

Alvarez-Montalvo, A., R.A. Ferrara, and D.R.F. Harleman. Undated. Simulation of Water Quality in the Willamette River Using the M.I.T. Nitrogen Cycle Model.

Andersen, J.M. 1977. Importance of the Denitrification Process for the Rate of Degradation of Organic Matter in Lake Sediments. In: Interactions

Between Sediments and Fresh Waters. Proceedings of an International Symposium Held at Amsterdam, The Netherlands, Sept. 6-10, 1976, H.L. Golterman (Ed.), pp. 357-362, Dr. W. Junk, Publishers, The Hague.

APHA (American Public Health Association). 1971. Standard Methods for the Examination of Water and Wastewater, 14th Edition, APHA, Washington, D.C.

APHA (American Public Health Association). 1980. Standard Methods for the Examination of Water and Wastewater, 15th Edition, APHA, Washington, D.C.

APHA (American Public Health Association). 1985. Standard Methods for the Examination of Water and Wastewater, 16th Edition, APHA, Washington, D.C.

Avery, S.T., and P. Novak. 1978. Oxygen Transfer at Hydraulic Structures, ASCE, J. Hydraulics Division, Vol. 104, No. HY11, pp. 1521-1540.

Baca, R.G., W.W. Waddel, C.R. Cole, A. Brandstetter, and D.B. Caerlock. 1973. EXPLORE-I: A River-Basin Water Quality Model. Battelle Laboratories. Richland, WA.

Baca, R.G., and R.C. Arnett. 1976. A Limnological Model for Eutrophic Lakes and Impoundments, Battelle Inc., Pacific Northwest Laboratories, Richland, Washington.

Bacon, R.G., W.W. Waddel, C.R. Cole, A. Brandstetter, and D.B. Cearlock. 1973. EXPLORE-I: A River Basin Water Quality Model. Prepared by Battelle Pacific Northwest Laboratories, Richland, WA for U.S. EPA Office of Research and Monitoring. pp. 121.

Bailey, T.E. 1970. Estuarine Oxygen Resources-Photosynthesis and Reaeration, ASCE, Journal of Sanitary Engineering Division, Vol. 96, No. SA2, pp 279-296.

Banks, R.B. 1975. Some Features of Wind Action on Shallow Lakes, ASCE, J. Environmental Engineering Division, Vol. 101, No. EE5, pp. 813-827.

Banks, R.B., and F.F. Herrera. 1977. Effect of Wind and Rain on Surface Reaeration, ASCE, Journal Environmental Engineering Division, Vol. 103, No. EE3, pp. 489-504.

Banks, R.B., L. Raschid-Sally, and C. Polprasert. 1983. Mechanical Mixing and Surface Reaeration. ASCE, Journal of Environmental Engineering. Vol. 109, No. 1. pp. 232-241.

Banks, R.B., G.B. Wickramanayake, and B.N. Lohani. 1984. Effect of Rain on Surface Reaeration. ASCE Journal of Environmental Engineering. Vol. 110, No. 1. pp. 1-14.

Bansal, M.K. 1973. Atmospheric Reaeration in Natural Streams, Water Research, Vol. 7, pp. 769-782.

Bansal, M.K. 1976. Nitrification in Natural Streams, Journal of Water Pollution Control Federation, Vol. 48, No. 10, pp. 2380-2393.

Bansal, M.K. 1975. Deoxygenation in Natural Streams. Water Resources Bulletin 11:491-504.

Barcelona, M.J. 1983. Sediment Oxygen demand Fractionation, Kinetics and Reduced Chemical Substances. Water Res., 17:1081-1093.

Bard, Y. 1967. Nonlinear Parameter Estimation and Programming, IBM New York Sci. Center, Report 320-2902.

Barnwell, T.O. 1980. Least Squares Estimates of BOD Parameters. ASCE Journal of the Environmental Engineering Division. Vol. 106, No. EE6. pp. 1197-1202.

Barrett, M.J., A.L. Gameson, and C.G. Ogden. 1960. Aeration Study of Four Weir Systems, Water and Water Engineering, London.

Battelle, Inc., Pacific Northwest Laboratories. 1973. EXPLORE-I: A River Basin Water Quality Model, Richland, Washington.

Bauer, D.P., M.E. Jennings, and J.E. Miller, 1979. One-Dimensional Steady-State Stream Water-Quality Model. U.S. Geological Survey. WRI-79-45. NSTL Station, MS.

Bauer, D.P., R.E. Rathbun, H.W. Lowham. 1979. Travel Time, Unit-Concentration, Longitudinal Dispersion, and Reaeration Characteristics of Upstream Reaches of the Yampa and Little Snake Rivers, Colorado and Wyoming. USGS Water-Resources Investigations 78-122.

Baumgartner, D.J., M.H. Feldman, L.C. Bentsen, and T.L. Cooper. 1970. Field Studies in Yaquina River Estuary of Surface Gas Transfer Rates, Proceedings of a Symposium on Direct Tracer Measurement of the Reaeration Capacity of Streams and Estuaries, July 7-8.

Bedford, K.W., R.M. Sylees, and C. Libicki, 1983. Dynamic Advective Water Quality Model for Rivers. ASCE Jour. Env. Engr. 109:535-554.

Belanger, T.V. 1981. Benthic Oxygen Demand in Lake Apopka, FL. Water Res., 15:267-274.

Bennett, J.P., and R.E. Rathbun. 1972. Reaeration in Open-Channel Flow, U.S. Geological Survey Professional Paper 737.

Benson, B.B., D. Krause, Jr., and M.A. Peterson. 1979. The Solubility and Isotopic Fractionation of Gases in Aqueous Solution. I. Oxygen. Journ. of Solution Chem. Vol. 8(9) 655-690.

Benson, B.B. and D. Krause, Jr. 1980. The Concentration and Isotopic Fractionation of Gases Dissolved in Fresh Water in Equilibrium with the Atmosphere: I. Oxygen. Limnol. Oceanogr. 25(4):662-671.

Benson, B.B. and D. Krause, Jr. 1984. The Concentration and Isotopic Fractionation of Oxygen Dissolved in Fresh Water and Seawater in Equilibrium with the Atmosphere: I. Oxygen. Limnol. Oceanogr. 29(3)620-632.

Berthouex, M. and W. Hunter. 1971. Problems with Planning BOD Experiments, ASCE Vol. 97, No. SA3, pp. 333-334.

Bhargava, D.S. 1983. Most Rapid BOD Assimilation in Ganga and Yamura Rivers. ASCE Jour. Env. Eng. 109:174-188.

Bingham, D.R., C.H. Lin, and R.S. Hoag. 1984. Nitrogen Cycle and Algal Growth Modeling. Journal Water Pollution Control Foundation, Vol. 56, No. 10, pp. 1118-1122.

Blain, W.A. 1969. Discussion of Evaluation of Nitrification in Streams, Journal of the Sanitary Engineering Division, ASCE, SA5, pp. 956-958.

Borchardt, J.A. 1966. Nitrification in the Activated Sludge Process. In: The Activated Sludge Process, Division of Sanitary and Water Resources Eng., University of Michigan, Ann Arbor.

Bosko, K. 1966. Advances in Water Pollution Research. International Association on Water Pollution Research. Munich.

Bowie, G.L., C.W. Chen, and D.H. Dykstra. 1980. Lake Ontario Ecological Modeling, Phase III, Tetra Tech, Inc. Report TC-3942, for National Oceanic and Atmospheric Administration.

Bradshaw, H.D., M.M. Brinson, E.A. Matson, and G.J. Davis. 1984. Sediment Oxygen Demand and Production in Shallow Estuarine Tributaries in North Carolina. (See Hatcher and Hicks, 1984). In Press.

Brandes, R.J. 1976. An Aquatic Ecologic Model for Texas Bays and Estuaries. Contract No: 14-30027, Texas Water Development Board, Austin, TX.

Brewer, W.S., A.R. Abernathy, and M.J.B. Paynter. 1977. Oxygen Composition by Freshwater Sediments, Water Res., 11:471-473.

Brezonik, P.L. 1973. Nitrogen Sources and Cycling in Natural Waters, EPA-660/3-73-002.

Bridle, T.R., D.C. Climenhage, and A. Stelzig. 1979. Operation of a Full-Scale Nitrification-Denitrification Industrial Waste Treatment Plant. Journal Water Poll. Control Fed. Vol. 51, No. 1. pp. 127-139.

Broecker, H.C., J. Petermann, and W. Siems. 1978. The Influence of Wind on CO_2 Exchange in a Wind-Wave Tunnel, Journal of Marine Research, Vol. 36, No. 4, pp. 595-610.

Brosman, D.R. 1977. Discussion of Nitrification in Natural Streams, Journal of Water Pollution Control Federation, Vol. 49, No. 5, pp. 876-877.

Brotko, W.J., and R.L. Kabel. 1978. Transfer of Gases at Natural Air-Water Interfaces, J. of Physical Oceanography, Vol 8, pp. 543-556.

Brown, L.C., and C.R. Baillod. 1982. Modeling and Interpreting Oxygen Transfer Data, ASCE, Journal Environmental Engineering Division, Vol. 108, No. EE4, pp. 607-628.

Brown, L.C., and M.K. Stenstrom. 1980. Proposed Modifications of K2-Temperature Relation, ASCE, Journal Environmental Engineering Division, Vol. 106, No. EE6, pp. 1193-1197.

Buswell, A.M. et al. 1957. Laboratory Studies on the Kinetics of the Growth of Nitrosomonas with Relation to the Nitrification Phase of the BOD Test, Applied Microbiology, 2., 21-25.

Butts, T.A. and R.L. Evans. 1978. Sediment Oxygen Demand Studies of Selected Northeastern Illinois Streams. Illinois State Water Survey Circular 129. Urbana, IL.

Butts, T.A. and R.L. Evans. 1979. Sediment Oxygen Demand in Shallow Oxbow Lake. Illinois State Water Survey Circular 136. Urbana, IL.

Butts, T.A., and R.L. Evans. 1983. Small Stream Channel Dam Aeration Characteristics, Journal Environmental Engineering, Vol. 109, No. 3, pp. 555-573.

Cadwallader, T.E., and A.J. McDonnell. 1969. A Multivariate Analysis of Reaeration Data: Water Research, Pergamon Press, Oxford, England, V. 2, pp. 731-742.

Cain, P., and I.R. Wood. 1981. Measurements of Self-Aerated Flow on a Spillway, ASCE, Journal Hydraulics Division, Vol. 107, No. HY11, pp. 1425-1444.

Camp, T.R. 1965. Field Estimates of Oxygen Balance Parameters. ASCE Jour. San. Eng. Div. 91, S5A.

Carpenter, J.H. 1965. The Accuracy of the Winkler Method for Dissolved Oxygen Analysis, Limnology and Oceanography, 10:135-140.

Carpenter, J.H. 1966, Limnol. Oceanogr. 11:264-277.

Casey, T.J., and P.E. O'Connor. 1978. New Light on Mechanism of Air-Water Oxygen Exchange in Quiescent Systems, Water Research, Vol. 12, pp. 649-654.

Chadderton, R.A., A.C. Miller, and A.J. McDonnell. 1982. Uncertainty Analysis of Dissolved Oxygen Model. ASCE Jour. Env. Engr. Div. 108:1003-1013.

Chairo, P.S. and D.A. Burke. 1980. Sediment Oxygen Demand and Nutrient Release. Env. Eng. Div., Jour. ASCE. February 1980, pp. 177-195.

Charley, R.C., D.G. Hooper, and A.G. McLee. 1980. Nitrification Kinetics in Activated Sludge at Various Temperatures and Dissolved Oxygen Concentrations. Water Research. Vol. 14. pp. 1387-1396.

Chen, C.W. 1970. Concepts and Utilities of Ecological Model. ASCE Jour. San. Eng. Div. 96, SA5.

Chen, C.W. and G.T. Orlob. 1972. Ecologic Simulation for Aquatic Environments. WRE, Inc., Walnut Creek. Final Rep. to OWRR. PP. 156.

Chen, C.W., S.S. Lee, and M.W. Lorenzen. 1974. Final Report. Water Quality Study for the Proposed Lakeport Lake. Tetra Tech, Inc., Lafayette, CA.

Chen, C.W. and G.T. Orlob. 1975. Ecologic Simulation of Aquatic Environments. Systems Analysis and Simulation in Ecology, Vol. 3, B.C. Patten (ed.). Academic Press, New York, N.Y. pp. 476-588.

Chen, C.W. and S. Wells. 1975. Boise River Water Quality - Ecological Model for Urban Planning Study. Tetra Tech., Inc., Lafayette, CA.

Chen, C.W., D.J. Smith, and S. Lee. 1976. Documentation of Water Quality Models for the Helms Pumped Storage Project, Tetra Tech, Incorporated.

Churchill, M.A., H.L. Elmore, and R.A. Buckingham. 1962. The Prediction of Stream Reaeration Rates, ASCE, Journal Sanitary Engineering Division, Vol. No. 88, SA4, pp. 1-46.

Cirello, J., R.A. Rapaport, P.F. Strom, V.A. Matulewich, M.L. Morris, S. Goetz, and M.S. Finstein. 1979. The Question of Nitrification in the Passaic River, New Jersey: Analysis of Historical Data and Experimental Investigation. Water Research. Vol. 13, pp. 525-537.

Cohen, R.R. and M.R. Church. 1981. A Method for Studying Primary Productivity and Photosynthesis in Unenclosed Batch Culture and Field Samples. Arch. Hydrobiol., Vol. 91, No. 2, pp. 231-241.

Committee on Sanitary Engineering Research. 1960. Solubility of atmospheric oxygen in water; ASCE, Journal Sanitary Engineering Division, V. 86, no. SA-4, pp. 41-53.

Courchaine, R.J. 1968. Significance of Nitrification in Stream Analysis--Effects on the Oxygen Balance, Journal Water Pollution Control Fed., 40, 835.

Covar, A.P. 1976. Selecting the Proper Reaeration Coefficient for Use in Water Quality Models, Presented at the U.S. EPA Conference on Environmental Simulation and Modeling, April 19-22, Cincinnati, Ohio.

Crane, S.F. and R.F. Malone. 1982. Reliability Analysis of BOD Kinetics in a Small Southern Stream Governed by the Discharge of an Oxidation Pond. Louisana Water Resources Research Institute. Baton Rouge, LA, 123 pp.

Crim, R.L. and N.L. Lovelace. 1973. Auto-Qual Modeling System. U.S. Environmental Protection Agency. EPA-440/9-73-003.

Curtis, E.J.C., K. Durrant, and M.M.I. Harman. 1975. Nitrification in Rivers in the Trent Basin, Water Research, Vol. 9, pp. 255-268.

Curtis, M.D. 1983. Oxidative and Non-Oxidative Ammonia Modeling. In: A. Medine and M. Anderson, eds. Proceedings of the ASCE 1983 National Conference on Environmental Engineering, Boulder, Colorado. pp. 493-499.

Daniels, F. and R.A. Alberty. 1967. Physical Chemistry, 3rd Edition, John Wiley & Sons, New York.

Das, K.C. and J.J. Cibulka. 1976. A Case History of Water Quality Considerations in the James River at Richmond, Presented at the 49th Annual Water Pollution Control Federation Conference, Minneapolis, Minnesota, October 3-8.

Deb, A.K. and D. Bowers. 1983. Diurnal Water Quality Modeling - A Case Study. Journal Water Pollution Control Federation, Vol. 55, No. 12, pp. 1476-1488.

Deb, A.K., J. Klafter-Snyder, and W.G. Richards. 1983. Water Quality Modeling of Shallow Surface Active Streams - A Case Study. In: A. Medine and M. Anderson, eds. Proceedings of the 1983 National Conference on Environmental Engineering, Boulder Colorado. pp. 486-492.

Demetracopoulos, A.C. and H.G. Stefan. 1983. Model of Mississippi River Pool: Dissolved Oxygen. Journal of Environmental Engineering Division, ASCE, Vol. 109, No. 5, pp. 1020-1034.

Department of the Environment. 1973. Notes on Water Pollution. In: Aeration at Weirs. Department of the Environmental Water Research Laboratory, Elder Way, Stevenage, Herts, England, June, No.61.

Di Toro, D.M. and J.P. Connolly. 1980. Mathematical Models of Water Quality in Large Lakes. Part 2: Lake Erie. U.S. Environmental Protection Agency, Duluth, Minnesota. EPA-600/3-3-80-065.

Di Toro, D.M. and W.F. Matystik, Jr. 1980. Mathematical Models of Water Quality in Large Lakes. Part I: Lake Huron and Saginaw Bay Model Development, Verification, and Simulations. U.S. Environmental Protection Agency Ecological Research Series. EPA-600/3-80-056.

Di Toro, D.M. 1984. A Diagnetic Oxygen Equivalents Model of Sediment Oxygen Demand. (See Hatcher and Hicks, 1984). In Press.

Dierberg, F.E. and P.L. Brezonik. 1982. Nitrifying Population Densities and Inhibition of Ammonium Oxidation in Natural and Sewage - Enriched Cypress Swamps. Water Research. Vol 16, pp. 123-126.

Dobbins, W.E. 1964. BOD and Oxygen Relationships in Streams: Journal of the Sanitary Engineering Division, Proceedings of the American Society of Civil Engineers, V. 90, No. SA3, pp. 53-78.

Downing, A.L., and Truesdale, G.A. 1955. Some Factors Affecting the Rate of Solution of Oxygen in Water, Journal of Applied Chemistry, Vol. 5, pp. 570-581.

Draper, D.W., E.T. Smith, and A.C. Ron. 1984. A River Model Analysis of Oxygen Demand of Benthal Deposits. (See Hatcher and Hicks, 1984. In Press.

Driscoll, E.D, J.L. Mancini, and P.A. Mangarella. 1983. Technical Guidance Manual for Performing Waste Load Allocations, Book II Streams and Rivers, Prepared for Office of Water Regulations and Standards, Monitoring and Data Support Division, Monitoring Branch, U.S. EPA, Washington, D.C.

Duke, J.H., Jr. and F.D. Masch. 1973. Computer Program Documentation for the Stream Quality Model DOSAG3, Vol. I, Prepared for U.S. Environmental Protection Agency, Systems Development Branch, Washington, D.C.

Eckenfelder, W.W. and D.J. O'Connor. 1961. Biological Waste. Pergamon Press, New York.

Edberg, N. 1977. The Role of Sediments with Regard to Lake Oxygen Consumption. In: Interactions Between Sediments and Fresh Waters. Proceedings of an International Symposium Held at Amsterdam, The Netherlands, Sept. 6-10, 1976, H.L. Golterman (Ed.), p. 265, Dr. W. Junk, Publishers, The Hague.

Edberg, N. and B.V. Hofsten. 1973. Oxygen Uptake of Bottom Sediments Studied In situ and in the Laboratory. Water Res., 7:1285-1294.

Edwards, R.W. and H.L.J. Rolley. 1965. Oxygen Consumption of River Muds. J. of Ecol., 53:1.

Effler, S.W., P. Jaran, and C.F. Carter. 1983. Onondaga Lake and Dissolved Oxygen in Seneca River, ASCE, Journal Environmental Engineering Division, Vol. 109, No. 4, pp. 945-951.

Elmore, H.L. and T.W. Hayes. 1960. Solubility of Atmospheric Oxygen in Water. Twenty-Ninth Progress Report of the Committee on Sanitary Engineering Research, Journal Sanitary Engineering Division, ASCE. Vol. 86, SA4, pp 41-53.

Elmore, H.L., and W.F., West. 1961. Effects of Water Temperature on Stream Reaeration. Journal of Sanitary Engineering Division, ASCE, Vol. 87, No. SA6, 59.

Eloubaidy, A.F., and E.J. Plate. 1972. Wind Shear-Turbulence and Reaeration Coefficient, ASCE, Journal Hydraulics Division, Vol. 98, No. HY1, pp. 153-170.

Emerson, S. 1975. Gas Exchange Rates in Small Canadian Shield Lakes, Limnology and Oceanography, Vol. 20, No. 5, pp. 754-761.

Engel, M.S. and M. Alexander. 1958. Growth and Autotrophic Metabolism of Nitrosomonas Europaea, Journal Bacterio., 76, 127.

Erdmann, J.B. 1979a. Systematic Diurnal Curve Analysis. Journal Water Pollution Control Federation, Vol. 15, No. 1, pp. 78-86.

Erdmann, J.B. 1979b. Simplified Diurnal Curve Analysis. ASCE, Journal of Environmental Engineering Division, Vol. 105, No. EE6, pp. 1063-1074.

Fair, G.M., J.C. Geyer, and D.A. Okun. 1968. Water and Wastewater Engineering, John Wiley and Sons, New York.

Feigner, K.D. and H.S. Harris. 1970. Documentation Report FWQA Dynamic Estuary Model, Federal Water Quality Administration, Washington, D.C., 248 p.

Fillos, J. 1977. Effect of Sediments on the Quality of the Overlying Water. In: Interactions Between Sediments and Fresh Waters, Proceedings of an International Symposium Held at Amsterdam, The Netherlands, Sept. 6-10, 1976, H.L. Golterman (Ed.), pp. 266-271, Dr. W. Junk, Publishers, The Hague.

Finstein, M.S. and V.A. Matulewich. 1974. Distribution of Autrotrophic Nitrifying Bacteria in a Polluted Stream. Report A-030-N.J. Water Resources Research Institute, Rutgers University, New Brunswick, New Jersey.

Finstein, M.S., J. Cirello, P.F. Strom, Mil. Morris, R.A. Rapaport, and S. Goetz, April, 1977. Evaluation of Nitrification in the Water Column of the Passaic River, Water Resources Research Institute, Rutgers University, New Jersey.

Foree, E.G. 1976. Reaeration and Velocity Prediction for Small Streams, ASCE, Journal Environmental Engineering Division, Vol. 102, No. EE5, pp. 937-951.

Foree, E.G. 1977. Low-Flow Reaeration and Velocity Characteristics of Small Streams, (Update); Journal of Environmental Engineering Division, ASCE, EE5.

Fortescue, G.E. and J.R.A. Pearson. 1967. On Gas Absorption into a Turbulent Liquid. Chem. Eng. Sci. Vol. 22, pp. 1163-1176.

Freedman, P.L., R.P. Canale, and J.F. Pendergast. 1980. Modeling Storm Overflow Impacts on Eutrophic Lake. ASCE Jour. Env. Eng. 106:335-349.

Frexes, P., G.H. Jirka, W. Brutsaert. 1984. Examination of Recent Field Data on Stream Reaeration. ASCE, Journal of Environmental Engineeing Division. Vol. 110, No.6, pp. 1179-1183.

Gameson, A.L.H. 1957. Wiers and Aeration of Rivers. Journal of the Institution of Water Engineers. Vol. 6, No. 11, pp. 477-490.

Gameson, A.L., K.G. Van Dyke, and C.G. Oger. 1958. The Effect of Temperature on Aeration at Weirs, Water and Water Engineering, London.

Gardiner, R.D., M.T. Aver, and R.P. Canale. 1984. Sediment Oxygen Demand in Green Bay, Lake Michigan. In: Pirbazari and DeVinney (eds.), Environmental Engineering. Proceedings of the 1984 Specialty Conference. ASCE. NY, pp. 514-519.

Gaudy, A.F. 1967. Methods for Evaluating the First-Order Constants K and L for BOD Exertion. M-1 Center for Water Research in Engineering. Oklahoma State University.

Genet, L.A., D.J. Smith and M.B. Sonnen. 1974. Computer Program Documentation for the Dynamic Estuary Model, prepared for U.S. Environmental Protection Agency, Systems Development Branch, Washington, D.C.

Glass, G.E., and J.E. Podolski. 1975. Interstitial Water Components and Exchange Across the Water Sediment Interface of Western Lake Superior, Verh. Int. Verein. Limnol., 19:405-420.

Goddard, K.E. 1980. Calibration and Potential Uses of the Digital Water Quality Model for the Arkansas River in Pueblo, Colorado. USGS Water Resources Investigation Report 80-38, 87 p.

Gowda, T.P.H. 1983. Modeling Nitrification Effects on the Dissolved Oxygen Regime of the Speed River. Water Research 17:1917-1927.

Graneli, W. 1977. Sediment O Uptake in South Swedish Lakes. In: Interactions Between Sediments and Fresh Waters. Proceedings of an international symposium held at Amsterdam, The Netherlands, Sept. 6-10, 1976, H.L. Golterman (Ed.), p. 276, Dr. W. Junk, Publishers, The Hague.

Grant, R.S. 1976. Reaeration-Coefficient Measurements of 10 Small Streams in Wisconsin Using Radioactive Tracers... With a Section on the Energy-Dissipation Model, U.S. Geological Survey, Water Resources Investigations 76-96.

Grant, R.S. 1978. Reaeration Capacity of the Rock River between Lake Koshkonong, Wisconsin and Rockton, Illinois, U.S. Geological Survey, Water Resources Investigations 77-128.

Grant, R.S., and S. Skavroneck. 1980. Comparison of Tracer Methods and Predictive Equations for Determination Stream-Reaeration Coefficients on Three Small Streams in Wisconsin, U.S. Geological Survey, Water Resources Investigation 80-19.

Grau, P., P.M. Sutton, M. Henze, S. Elmaleh, C.P. Grady, W. Gujer, and J. Koller. 1982. Recommended notation for use in the Description of Biological Wastewater Treatment Processes. Water Research. 16:1501-1506.

Green, E.J. 1965. A Redetermination of the Solubility of Oxygen in Seawater and Some Thermodynamic Implications of the Solubility Relations. Ph.D. Thesis, Mass. Inst. of Technology.

Green, E.J. and D.E. Carritt. 1967. New Tables for Oxygen Saturation of Seawater, J. Marine Research, 25(2):140-147.

Grenney, W.J. and A.K. Kraszewski. 1981. Description and Application of the Stream Simulation and Assessment Model: Version IV (SSAM IV). (Instream flow information paper). 1981. Fish and Wildlife Service, Fort Collins, Colorado, Cooperative Instream Flow Service Group. pp. 213.

Gujer, W. 1977. Discussion of Nitrification in Natural Streams, Journal of Water Pollution Control Federation, Vol. 49, No. 5, pp. 873-875.

Gulliver, J.S. and H.G. Stefan. 1981. Air-Water Surface Exchange of Oxygen: Theory and Application to the USEPA Monticello Experimental Field Channels. St. Anthony Falls Hydraulic Laboratory External Memorandum No. 173, University of Minnesota, 108 pp.

Gulliver, J.S., T.W. Mattke, and H.G. Stefan. 1982. Numerical and Graphical Procedures for Estimation of Community Photosynthesis and Respiration in Experimental Streams. Prepared by University of Minnesota, St. Anthony Falls Hydraulic Laboratory, Minneapolis, Minnesota for U.S. Environmental Protection Agency. EPA-600/3-82-052. NTIS No. PB82-220765.

Gunnerson, C.G., and T.E. Bailey. 1963. Oxygen Relationships in the Sacramento River, ASCE, J. Sanitary Engineering Division, Vol. 89, No. SA4, pp. 95-124.

Hall, E.R. and K.L. Murphy. 1980. Estimation of Nitrifying Biomass and Kinetics in Wastewater. Water Research, Vol. 14. pp. 297-304.

Hargrave, B.T. 1969. Similarity of Oxygen Uptake by Benthic Communities, Limnol. Oceanogr. 14:801-805.

Harleman, D.R.F., J.E. Dailey, M.L. Thatcher, T.O. Najarian, D.N. Brocard, and R.A. Ferrara. 1977. User's manual for the M.I.T. Transient Water Quality Network Model--Including Nitrogen-Cycle Dynamics for Rivers and Estuaries. R.M. Parsons Laboratory for Water Resources and Hydrodynamics, Massachusetts Institute of Technology, Cambridge, Massachusetts, for U.S. Environmental Protection Agency, Corvallis, Oregon, EPA-600/3-77-010, January 1977.

Hatcher, K. and D. Hicks. 1984. Sediment Oxygen Demand: Processes, Modeling, and Measurement. WPCF, Washington, D.C. In Press.

Hickey, C.W. 1984. In situ Chamber Studies of River Oxygen Uptake by Benthic Microorganisms. (See Hatcher and Hicks, 1984. In Press.

Hockenbury, M.R. and C.P.L. Grady, Jr. 1977. Inhibition of Nitrification-Effects of Selected Organic Compounds. Journal Water Poll. Control Fed. May 1977. pp. 768-777.

Holler, A.G. 1971. The Mechanism Describing Oxygen Transfer from the Atmosphere to Discharge through Hydraulic Structures, Proceedings, XIV Congress, International Association for Hydraulics Research, Paper A45, pp. 373-382.

Holley, E.R. 1970. Effects of Oxygen Demand on Surface Reaeration, Research Report 46, Water Resources Center, University of Illinois, 80 p.

Holley, E.R. 1975. Oxygen Transfer at the Air-Water Interface, in Interfacial Transfer Processes in Water Resources, State University of New York at Buffalo. Report No. 75-1.

Hornberger, G.M. and M.G. Kelley. 1972. The Determination of Primary Production in a Stream Using an Exact Solution to the Oxygen Balance Equation. Water Resources Bulletin, 8, pp. 795-801.

Hornberger, G.M., and M.G. Kelly. 1975. Atmospheric Reaeration in a River Using Productivity Analysis, ASCE, J. Environmental Engineering Division, Vol. 101, No. EE5, pp. 729-739.

House, L.B., and S. Skavroneck. 1981. Comparison of the Propane-Area Tracer Method and Predictive Equations for Determination of Stream-Reaeration Coefficients on Two Small Streams in Wisconsin, U.S. Geological Survey, Water-Resources Investigations 80-105.

Hren, J. 1983. Measurement of the Reaeration Coefficients of the North Fork Licking River at Utica, Ohio by Radioactive Tracers. USGS Water-Resources Investigation Report 83-4192.

Huang, C. and N.E. Hopson. 1974. Nitrification Rate in Biological Processes. ASCE Journal of the Environmental Engineering Division. Vol. 100, No. EE2, pp. 409-421.

Hunter, J.V. 1977. Dissolved Oxygen and Biochemical Oxygen Demand. pp. 73-83. In: River-Quality Assessments. American Water Resources Association, Minneapolis, Minnesota.

Hunter, J.V., M.A. Harnett, and A.P. Cryan. 1973. A Study of the Factors Determining the Oxygen Uptake of Benthal Stream Deposits. Wate Resources Research Institute, Rutgers University, New Brunwsick, N.J. NTIS, PB-226-238. 28 pp.

Hvitved-Jacobsen, T. 1982. The Impact of Combined-Sewer Overflows on the Dissolved Oxygen Concentration of a River. Water Research 16:1099-1105.

Hydroscience, Inc. 1971. Simplified Mathematical Modeling of Water Quality. U.S. Environmental Protection Agency.

Hydroscience, Inc. 1972. Addendum to Simplified Mathematical Modeling of Water Quality. U.S. Environmental Protection Agency.

Hyer, P.V., C.S. Fang, E.P. Ruzecki, and W.J. Hargis. 1971. Hydrography and Hydrodynamics of Virginia Estuaries, Studies of the Distribution of Salinity and Dissolved Oxygen in the Upper York System, Virginia Institute of Marine Science.

Ice, G.G., and G.W. Brown. 1978. Reaeration in a Turbulent Stream System, Prepared for Office of Water Research and Technology, Washington, D.C.

Imhoff, J.C., J.L. Kittle, Jr., A.S. Donigian, Jr., and R.C. Johanson. 1981. User's Manual for Hydrological Simulation Program - Fortran (HSPF), Contract 68-03-2895, U.S. Environmental Protection Agency, Athens, Georgia. (Revision 7.0).

Isaacs, W.P., and A.F. Gaudy, Jr. 1968. Atmospheric Oxygenation in a Simulated Stream, ASCE, J. Sanitary Engineering Division, Vol. 94, No. SA2, pp. 319-344.

JRB Associates. 1983. User's Manual for Vermont QUAL-II model. SAI, Inc. McLean, Virginia.

Jaffe, P.R. and F.L. Parker. 1984. Uncertainty Analysis of First Order Decay Model. ASCE Jour. Env. Eng. Div. 110:131-140.

James, A. 1974. The Measurement of Benthal Respiration, Water Res., 8:955-959.

Jarvis, P.J. 1970. A Study in the Mechanics of Aeration at Weirs, thesis presented to the University of Newcastle upon Tyne, England, in 1970, in partial fulfillment of the requirements for the degree of Doctor of Philosophy.

Jennings, M.E., S.C. McCutcheon, and K.M. Flynn. 1982. Discussion: Least-Squares Estimates of BOD Parameters. ASCE Jour. Env. Eng. 108:215-217.

Jobson, H.E. (Undated). Simulating Unsteady Transport of Nitrogen, Biochemical Oxygen Demand, and Dissolved Oxygen in the Chattahoochee River Downstream from Atlanta, Georgia. USGS Water Supply Paper 2264.

Jobson, H.E. and R.E. Rathbun. (Undated). Use of the Routing Procedure to Study Dye and Gas Transport in the West Fork Trinity River, Texas. USGS Water Supply Paper 2252.

Johnson, A.E. and J.H. Duke, Jr. 1976. Computer Program Documentation for the Unsteady Flow and Water Quality Model WRECEV, Prepared for U.S. Environmental Protection Agency, Planning Assistance Branch, Washington, D.C.

Juliano, D.W. 1969. Reaeration Measurements in an Estuary, ASCE, Journal Sanitary Engineering Division, Vol. 95, No. SA6, pp. 1165-1178.

Kanwisher, J. 1963. On Exchange of Gases Between the Atmosphere and the Sea, Deep-Sea Research, Vol. 10, pp. 195-207.

Kelly, M.G., G.M. Hornberger, and B.J. Cosby. 1975. A Method for Monitoring Eutrophication in Rivers. Prepared by Department of Environmental Sciences, University of Virginia, Charlottesville, Virginia for Office of Water Research and Technology. NTIS, PB-252-058.

Kholdebarin, B. and J.J. Oertli. 1977a. Effect of pH and Ammonia on the Rate of Nitrification of Surface Water, Journal of the Water Pollution Control Federation, Vol. 49, No. 7, pp. 1688-1692.

Kholdebarin, B. and J.J. Oertli. 1977b. Effect of Suspended Particles and Their Sizes on Nitrification in Surface Waters, Journal of Water Pollution Control Federation, Vol. 49, No. 7, pp. 1693-1697.

Kiff, R.J. 1972. The Ecology of Nitrification/Denitrification Systems in Activated Sludge. Wat. Poll. Control 71, pp. 475-484.

Knowles, C., A.L. Downing, and M.J. Barrett. 1965. Determination of Kinetic Constants for Nitrifying Bacteria in Mixed Culture, with the Aid of an Electronic Computer, Journal of General Microbiology, 38, pp. 263-278.

Koltz, B.J. 1982. Nitrogen Transformations in the Iowa and Cedar Rivers. Master's Thesis. University of Iowa, Iowa City, Iowa. pp. 320.

Krenkel, P.A. 1960. Turbulent Diffusion and the Kinetics of Oxygen Absorption; Berkeley, California, University of California Department Sanitary Engineering Ph.D. dissert.

Krenkel, P.A., and G.T. Orlob. 1962. Turbulent Diffusion and The Reaeration Coefficient, ASCE, Journal Sanitary Engineering Division, Vol. 88, No. SA2, pp. 53-83.

Kreutzberger, W.A. and D.E. Francisco. 1977. An Investigation of the Distribution of Nitrifying Bacteria in Shallow Streams Upstream and Downstream from Wastewater Treatment Plants. Department of Environmental Sciences and Engineering, University of North Carolina. ESE Publication No. 483.

Kwasnik, J.M., and T.J. Feng. 1979. Development of a Modified Tracer Technique for Measuring the Stream Reaeration Rate, Water Resources Research Center, University of Massachusetts at Amherst, Publication No. 102.

Lam, D.C.L., W.M. Schertzer, and A.S. Fraser. 1984. Modelling the Effects of Sediment Oxygen Demand in Lake Erie Water Quality Conditions Under the Influence of Pollution Control and Weather Variations. (See Hatcher and Hicks, 1984). In Press.

Langbein, W.B., and W.H. Durum. 1967. The Aeration Capacity of Streams. U. S. Geological Survey Circular S42.

Lau, Y.L. 1972a. A Review of Conceptual Models and Prediction Equations for Reaeration in Open-Channel Flow, Inland Waters Branch, Department of the Environment, Ottawa, Canada, Technical bulletin No. 61.

Lau, Y.L. 1972b. Prediction Equation for Reaeration in Open-Channel Flow, ASCE, J. Sanitary Engineering Division, Vol. 98, No. SA6, pp. 1061-1068.

Lau, Y.L. 1975. An Experimental Investigation of Reaeration in Open-Channel Flow, Progress in Water Technology, Vol. 7, Nos. 3/4, pp. 519-530.

Laudelout, H. and L. Van Tichelen. 1960. Kinetics of the Nitrite Oxidation by Nitrobacter Winogradskyi. J. Bact. 79, pp. 39-42.

Liss, P.S., Processes of Gas Exchange Across an Air-Water Interface, Deep Sea Research, Vol. 20, 1973, pp. 221-238.

Long, E.G. 1984. Letter to Ray Whittemore of Tufts University from Texas Department of Water Resources.

Macdonald, G.J., and R.N. Weisman. 1977. Oxygen-Sag in a Tidal River, ASCE, J. Environmental Engineering Division, Vol. 103, No. EE3, pp. 473-488.

Mancini, J.L., P.H. Gruene, and F.B. Winslow. 1984. Sediment Interactions in Dissolved Oxygen Analysis: Two Case Studies. (See Hatcher and Hicks, 1984). In Press.

Manhattan College. 1983. Summer Institute on Water Pollution Control, Quality Models of Natural Water Systems.

Markert, B.E., M.G. Tesmer, and P.E. Parker. 1983. An In situ Sediment Oxygen Demand Sampler. Water Res., 17:603-605.

Martin, D.C. and D.H. Bella. 1971. Effect of Mixing on Oxygen Uptake Rate of Estuarine Bottom Deposits. JWPCF, 43:1865-1876.

Martone, C.H. 1976. Studies Related to the Determination of Biodegradability and Long Term BOD. M.S. Thesis. Tufts University, Medford, Massachusetts.

Matter-Muller, C., W. Gujer, and W. Giger. 1981. Transfer of Volatile Substances from Water to the Atmosphere, Water Research, Vol. 15, pp. 1271-1279.

Mattingly, G.E. 1977. Experimental Study of Wind Effects on Reaeration, ASCE, J. Hydraulics Division, Vol. 103, No. HY3, pp. 311.

Matulewich, V.A. and M.S. Finstein. 1975. Water Phase and Rock Surfaces as the Site of Nitrification, Abstr. Annual Meeting American Society of Microbiology, N. 30.

McCutcheon, S.C. 1983. Evaluation of Selected One-Dimensional Stream Water-Quality Models with Field Data. U.S. Army Engineer Waterways Experiment Station Technical Report E-83-11. Vicksburg, Mississippi.

McCutcheon, S.C. and M.E. Jennings. 1982. Discussion of: Stream Reaeration by Velz Method. ASCE, Journal of Environmental Engineering Division, Vol. 108, No. EE1., pp. 218-220.

McDonnell, A.S. and S.D. Hall. 1969. Effect of Environmental Factors on Benthal Oxygen Uptake. JWPCF, 41:R353-R363.

McKeown, J., L. Brown, and C. Martone. 1981. UBOD Estimation in Receiving Water Modeling. Water Science Tech., Vol. 13., pp. 363-370.

McQueen, D.J., and D.R.S. Lean. 1983. Hypolimnetic Aeration and Dissolved Gas Concentrations, Water Res., Vol. 17, No. 12, pp. 1781-1790.

Medina, M.A., Jr. 1979. Level II-Receiving Water Quality Modeling for Urban Stormwater Management. U.S. Environmental Protection Agency Municipal Env. Res. Laboratory. Cincinnati, Ohio. EPA-600/2-79-100.

Medine, A.J., D.P. Porcella, and V.D. Adams. 1980. Heavy Metal and Nutrient Effects on Sediment Oxygen Demand in Three-phase Aquatic Microcosms. J.P. Giesy, Jr. Published by U.S. Department of Energy, Symposium Series 52 (CONF-781101).

Megard, R.O., W.S. Combs, P.D. Smith, and A.S. Knoll. 1979. Attenuation of Light and Daily Integral Rates of Photosynthesis Attained by Planktonic Algae. Limnology and Oceanography. Vol. 24, No. 6, pp. 1038-1050.

Metropolitan Washington Council of Governments. 1982. Applicaton of HSPF to Seneca Creek Watershed, Washington, D.C.

Metzger, I. 1968. Effects of Temperature on Stream Aeration, ASCE, J. Sanitary Engineering Division, Vol. 94, No. SA6, pp. 1153-1159

Meyerhof, O. 1916. Arch. f. die ges Physiologie, 164, 416.

Meyerhof, O. 1917. Arch. f. die ges Physiologie, 166, 255.

Mills, W.B. 1976. A Computational Model for Predicting Biofilm Nitrification in Streams. Engineer's Thesis, Stanford University.

Moore, E.W. 1941. Long Time BOD at Low Temperature. Sewage Works Journal 13(3) pp. 561-577.

Morrissette, D.G. and D.S. Mavinic. 1978. BOD Test Variables. ASCE Jour. Env. Eng. Division 104:1213-1222.

Mortimer, C.H. 1981. The Oxygen Content of Air-Saturated Fresh Waters Over Ranges of Temperature and Atmospheric Pressure of Limnological Interest. Int. Assoc. of Theor. and Appl. Limnol. Communication No. 22, Stuttgart, Germany.

Murray, C.N. and J.P. Riley. 1969. The Solubility of Gases in Distilled Water and Seawater. 2. Oxygen. Deep-Sea Res. 16:311-320.

Nakasone, H. 1975. Derivation of Aeration Equation and Its Verification-Study on the Aeration at Falls and Spillways, Transactions, J.S.I.D.R.E. pp. 42-48.

National Council of the Paper Industry for Air and Stream Improvement, Inc. 1969. Artifical Reaeration of Receiving Waters. Technical Bulletin No. 229. NCASI, New York, NY. 44 pp.

National Council for Air and Stream Improvement, Inc. (NCASI) 1971. An Investigation of the Effects of Bark Leaching and Benthal Decomposition on Receiving Water Quality. NCASI Technical Bulletin No. 247. NY. 61 pp.

National Council for Air and Stream Improvement, Inc. (NCASI) 1978. Interfacial Velocity Effects on the Measurement of Sediment Oxygen Demand. NCASI Technical Bulletin No. 317. NY.

National Council for Air and Stream Improvement, Inc. (NCASI) 1979. Further Studies of Sediment Oxygen Demand Measurement and its Variability. NCASI Technical Bulletin No. 321. NY.

National Council for Air and Stream Improvement, Inc. (NCASI) 1981. The Effect of Temperature on Sediment Oxygen Demand as Related to Water Quality Modeling. NCASI Technical Bulletin No. 351. NY. 18 pp.

National Council of the Paper Industry for Air and Stream Improvement, Inc. 1982a. A Study of the Selection, Calibration and Verification of Mathematical Water Quality Models. NCASI Tech. Bull. 367, New York.

National Council of the Paper Industry for Air and Stream Improvement, Inc. 1982b. An Assessment of the Limitations of the Radiotracer Technique in Measuring Stream Reaeration Rates, Technical Bulletin No. 374.

National Council of the Paper Industry for Air and Stream Improvement, Inc. 1982c. A Comparison of Reaeration Estimation Techniques for the Ouachita River Basin, Technical bulletin No. 375.

National Council of the Paper Industry for Air and Stream Improvement, Inc. 1982d. A Review of Ultimate BOD Estimation and Its Kinetic Formulation for Pulp and Paper Mill Effluents. NCASI Tech. Bull. 382, New York.

Negulescu, M. and V. Rojanski. 1969. Recent Research to Determine Reaeration Coefficient, Water Research, Vol. 3, No. 3, 189.

Nelder, J.A. and R. Mead. 1965. A Simplex Method for Function Minimization, Computer Journal 7, pp. 308.

Nemerow, N.L. 1974. Scientific Stream Pollution Analysis. McGraw-Hill. Washington, D.C.

Novotny, V. and P.A. Krenkel. 1975. A Waste Assimilation Capacity Model for a Shallow, Turbulant Stream. Water Research 9:233-241.

O'Connell, R.L. and N.A. Thomas. 1965. Effect of Benthic Algae on Stream Dissolved Oxygen. Journal of Sanitary Engineering Division, ASCE, Vol. 91, No. SA3, pp. 1-16.

O'Connor, D.J. 1958. The Measurement and Calculation of Stream Reaeration Rates. Seminar on Oxygen Relationships in Streams. Robert A. Taft Sanitary Engineering Center Technical Report 58-2, pp. 35-45.

O'Connor, D.J., and W.E. Dobbins. 1958. Mechanism of Reaeration in Natural Streams, ASCE Transactions, pp. 641-684, Paper No. 2934.

O'Connor, D.J. 1960. Oxygen Balance of an Estuary, ASCE, J. Sanitary Engineering Division, Vol. 86, No. SA3, pp. 35-55.

O'Connor, D.J. and D.M. Di Toro. 1970. Photosynthesis and Oxygen Balance in Streams. ASCE, Journal of Sanitary Engineering Division, ASCE, Vol. 96, No. SA2, pp. 547-571.

O'Connor, D.J., J.L. Mancini, and J.R. Guerriero. 1981. Evaluation of Factors Influencing the Temporal Variation of Dissolved Oxygen in the New York Bight, Phase II, Manhattan College, Bronx, New York.

O'Connor, D.J. 1983. Wind Effects on Gas-Liquid Transfer Coefficients, J. Environmental Engineering, Vol. 109, No. 3, pp. 731-752.

Odum, H.T. 1956. Primary Production in Flowing Waters. Limnology and Oceanography, 1 pp. 102-117.

Ohio Environmental Protection Agency. 1983. Determining the Reaeration Coefficient for Ohio Streams. Draft.

Orlob, G.T. 1970. Mathematical Modeling of Estuarial Ecosystems. Proceedings, International Conference on Transport of Persistent Chemicals in Aquatic Ecosystems. Ottowa, Canada.

Orlob, G.T. 1974. Mathematical Modeling of Estuarial Ecosystems. Proceedings of the International Conference on Transport of Persistent Chemicals in Aquatic Ecosystems, Ottawa, Canada.

Owens, M., R.W. Edwards, and J.W. Gibbs. 1964. Some Reaeration Studies in Streams, Int. J. Air Wat. Poll., Vol. 8, pp. 469-486.

Ozturk, Y.F. 1979. Mathematical Modeling of Dissolved Oxygen in Mixed Estuaries, ASCE, J. Environmental Engineering Division, Vol. 105, No. EE5. pp. 883-904.

Padden, T.J., and E.F. Gloyna. 1971. Simulation of Stream Processes in a Model River: University of Texas, Austin, Report No. EHE-70-23, CRWR-72, 130 p.

Pamatmat, M.M. 1971. Oxygen Consumption by the Seabed. IV. Shipboard and Laboratory Experiments. Liminol. & Oceanogr., 16:536-550.

Pamatmat, M.M., R.S. Jones, R. Sanburn, and A. Bhagmat. 1973. Oxidation of Organic Matter in Sediments. U.S. Environmental Protection Agency, EPA-660/3-73-005, Washington, D.C.

Parker, P.E. 1977. Letter Report. February 23, 1977. Project 3300. The Institute of Paper Chemistry. Appleton, WI.

Parkhurst, J.E., and R.D. Pomeroy. 1972. Oxygen Absorption in Streams, ASCE, Journal Sanitary Engineering Division, Vol. 98, No. SA1.

Phelps, E.B. 1909. The Disinfection of Sewage and Sewage Filter Effluents. USGS Paper No. 229, pp. 74-88.

Polak, J., and G.D. Haffner. 1978. Oxygen Depletion of Hamilton Harbour, Water Res., 12:205-215.

Poon, C.P.C., and H. Campbell. 1967. Diffused Aeration in Polluted Water, Water and Sewage Works, Vol. 114, pp. 461-463.

Porcella, D.B., T.M. Grieb, G.L. Bowie, T.C. Ginn, and M.W. Lorenzen. 1983. Assessment Methodology for New Cooling Lakes, Vol. 1: Methodology to Assess Multiple Uses for New Cooling Lakes. Electric Power Research Institute, Report EPRI EA-2059.

Quinlan, A.V. 1980. The Thermal Sensitivity of Nitrification as a Function of the Concentration of Nitrogen Substrate. Water Research. Vol 14. pp. 1501-1507.

Rainwater, K.A., and E.R. Holley. 1984. Laboratory Studies on Hydrocarbon Tracer Gases, J. Environmental Engineering, Vol. 110, No. 1, pp. 27-41.

Rathbun, R.E., D.J. Shultz, D.W. Stephens. 1975. Preliminary Experiments with a Modified Tracer Technique for Measuring Stream Reaeration Coefficients. USGS Open File Report 75-256.

Rathbun, R.E. 1977. Reaeration Coefficients of Streams. State-of-the-Art, ASCE, J. Hydraulics Division, Vol. 103, No. HY4, pp. 409-424.

Rathbun, R.E. and R.S. Grant. 1978. Comparison of the Radioactive and Modified Techniques for Measurement of Stream Reaeration Coefficients. USGS Water Resources Investigations 78-68.

Rathbun, R.E., D.W. Stephens, D.J. Shultz, and D.Y. Tai. 1978. Laboratory Studies of Gas Tracers for Reaeration, ASCE, J. Environmental Engineering Division, Vol. 104, No. EE1, pp. 215-229.

Rathbun, R.E. 1979. Estimation the Gas and Dye Quantities for Modified Tracer Technique Measurements of Stream Reaeration Coefficients, U.S. Geological Survey, National Space Technology Laboratories Station, Mississippi.

Raytheon Company Oceanographic & Environmental Services. 1974. New England River Basins Modeling Project, Vol. III - Documentation Report, Part 1 - RECEIV-II Water quantity and Quality Model QUAL-II. EPA 600/9-81-015, U.S. Environmental Protection Agency, Athens. GE.

Rich, L.G. 1973. Environmental Systems Engineering. McGraw Hill Book Company.

Rinaldi, S., P. Romaro, and R. Sencini-Sesa. 1979. Parameter Estimation of Streeter-Phelps Models. ASCE Jour. Env. Engr. 105:75-88.

Rinella, F.A., S.W. McKenzie, and S.A. Wille. 1981. Dissolved Oxygen and Algal Conditions in Selected Locations of the Willamette River Basin, Oregon. USGS Open-File Report 81-529.

Rittmann, B.E. and P.L. McCarty. 1978. Variable - Order Model of Bacterial Film Kinetics. ASCE Journal of Environmental Engineering. Vol. 104, No. EE5. pp. 889-901.

Roesner, L.A., Giguere, P.A., and D.E. Evenson. 1981. User's Manual for Stream Quality Model (QUAL-II). U.S. Environmental Protection Agency Environmental Research Laboratory, Athens, Georgia. EPA-600/a-81-015.

Roesner, L.A., P.R. Giuere, and D.E. Evenson. 1977 (rev. 1981). Computer Program Documentation for the Stream Quality Model QUAL-II. EPA 600/9-81-014, U.S. Environmental Protection Agency, Athens, GE.

Rolley, H.S. and M. Owens. 1967. Oxygen Consumption Rates and Same Chemical Properties of River Muds. Water Res., 1:759-766.

Rood, O.E., and E.R. Holley. 1974. Critical Oxygen Deficit for a Bank Outfall, Journal of Environmental Engineering Division, ASCE, Vol. 100, EE3.

Ruane, R.J. and P.A. Krenkel. 1978. Nitrification and Other Factors Affecting Nitrogen in the Holston River. Jour. Water Poll. Control Fed. 50, 2016.

Rumer, R.R., Jr., E.R. Holley, O.H. Shemdin, R.P. Apmann, W. Brutsaert, and J.E. Edinger. 1975. Interfacial Transfer Processes in Water Resources, Water Resources and Environmental Engineering Research Report No. 75-1, Dept. of Civil Engineering, State Univ. of New York at Buffalo.

Sawyer, C.N. and P.L. McCarty. 1967. Chemistry for Sanitary Engineers, McGraw-Hill Book Company, New York, NY.

Schneiter, R.W., and W.J. Grenney. 1983. Temperature Corrections to Rate Coefficients, J. Environmental Engineering, Vol. 109, No. 3, pp. 661-667.

Schroepfer, G.J., M.L. Robins, and R.H. Susag. 1964. The Research Program on the Mississippi River in the Vicinity of Minneapolis and St. Paul. Advances in Water Pollution Research. Vol. I. Pergamon, London.

Schurr, J.M. and J. Ruckts. 1977. Dynamics of O_2 and CO_2 Exchange, Photosynthesis, and Respiration in Rivers From Time-Delayed Correlations With Ideal Sunlight. Limnology and Oceanography. Vol. 22, No. 2, pp. 208-225.

Shapiro, J. and O. Zor. 1981. A Simple In situ Method for Measuring Benthic Respiration. Water Res., 15:283-285.

Sharma, B. and R.C. Ahlert. 1977. Nitrification and Nitrogen Removal. Water Research Vol. 11. pp. 897-925.

Sheehy, J.P. 1960. Method for Solving First-Order Equations. JWPCF 32:646.

Shindala, A., and D.D. Truax. 1980. Reaeration Characteristics of Small Streams, Engineering and Industrial Research Station, Mississippi State University, Mississippi.

Simonsen, J.F. and P. Harremoes. 1978. Oxygen and pH Fluctuations in Rivers. Water Resources Research, 12, pp. 477-489.

Slayton, J.L. and E.R. Trovato. 1978. Simplified N.O.D. Determination. Annapolis field Office, Region III. USEPA. Available from NTIS. PB-297-995. pp. 32.

Slayton, J.L. and E.R. Trovato. 1979. Biochemical Studies of the Potomac Estuary-Summer, 1978. Annapolis Field Office, Region III, USEPA, Annapolis, Maryland. EPA 903/9-79-005. pp. 35.

Smith, D.J. 1978. WQRRS, Generalized Computer Program for River-Reservoir Systems. U.S. Army Corps of Engineers, Hydrologic Engineering Center (HEC), Davis, California. User's Manual 401-100, 100A, 210 pp.

Smith, K.L., G.T. Rowe, and S.A. Nichols. 1973. Benthic Community Respiration Near the Woods Hole Sewage Outfall. Estuarine & Coastal Mar. Sci., 1:65-70

Smith, K.L. 1974. Oxygen Demands of San Diego Trough Sediments: An In situ Study. Limnol. Oceanogr., 19:939-944.

Sonzogni, W.C., D.P. Larsen, K.W. Malueg, and M.D. Schuldt. 1977. Use of Submerged Chambers to Measure Sediment-Water Interactions, Water Res., 11:461-464.

Stamer, J.K., J.P. Bennett, and S.W. McKenzie. 1983. Determination of Ultimate Carbonaceous BOD and the Specific Rate Constant (k). USGS Open-File Report 82-645.

Stamer, J.K., R.N. Cherry, R.E. Faye, and R.L. Kleckner. 1979. Magnitudes, Nature, and Effects of Point and Nonpoint Discharges in the Chattahoochee River Basin, Atlanta to West Point Dam, Georgia. USGS Water Supply Paper 2059.

Stenstrom, M.K. and R.A. Poduska. 1980. The Effect of Dissolved Oxygen Concentration on Nitrification. Water Research. Vol 14. pp. 643-649.

Stover, E.L. and D.E. McCartney. 1984. BOD Results that are Believable. Water/Engineering and Management. pp. 37-62.

Stratton, F.E. 1966. Nitrification Effects on Oxygen Resources in Streams, Ph. D. Thesis, Stanford University.

Stratton, F.E. and P.L. McCarty. 1967. Prediction of Nitrification Effects on the Dissolved Oxygen Balance of Streams. Environmental Science and Technology. Vol. 1, No. 5, pp. 405-410.

Stratton, F.E. and P.L. McCarty. 1969. Discussion of Evaluation of Nitrification in Streams, Journal of the Sanitary Engineering Division, ASCE, SA5, pp. 952-955.

Streeter, H.W. 1926. The Rate of Atmospheric Reaeration of Sewage Polluted Streams, in Transactions of ASCE, Vol. 89, 1351.

Sullivan, J., R. Young, and S. Rogers. 1978. Methods and Results of Field Surveys Collected in 1977 and 1978 on the Upper Wisconsin River for the Development of a Water Quality Computer Model. Wisconsin Dept. Natural Resources, Rhinelander, WI.

Terry, J.E. and E.E. Morris. 1984. Benthic Oxygen Demand versus Streambed Oxygen Demand. (See Hatcher and Hicks, 1984). In Press.

Terry, J.E., E.E. Morris, J.C. Peterson, and M.E. Darling. 1984. Water Quality Assessment of the Illinois River Basin, Arkansas. USGS Water Resources Investigation Report 83-4092. 434 p.

Terry, J.E., E.E. Morris, and C.T. Bryant. 1983. Water-Quality Assessment of White River Between Lake Sequoyah and Beaver Reservoir, Washington County, Arkansas. U.S. Geological Survey, WRI 82-4063. Little Rock, Arkansas.

Tetra Tech., Inc. 1976. Documentation of Water Quality Models for the Helms Pumped Storage Project. Lafayette, CA.

Tetra Tech, Inc. 1980. Methodology for Evaluation of Multiple Power Plant Cooling System Effects, Volume IV. User's Guide to Model Operation. Electric Power Research Institute, Report EPRI EA-1111.

Thackston, E.L., 1966. Longitudinal Mixing and Reaeration in Natural Streams. Thesis Presented to Vanderbilt University.

Thackston, E.L., and P.A. Krenkel. 1969. Reaeration Prediction in Natural Streams, Journal of Sanitary Engineering Division, ASCE, Vol. 95, SA1, 65.

Theriault, E.J. 1927. The Oxygen Demand of Polluted Water. Public Health Bulletin No. 173.

Thomann, R.V. 1963. Mathematical Model for DO, Journal Sanitary Engineering Division, ASCE, Vol. 89, SA5, 1.

Thomann, R.V. et al., 1971. The Effect of Nitrification on the Dissolved Oxygen of Streams and Estuaries, Environ. Eng. and Sci. Program, Manhattan College, Bronx, New York.

Thomann, R.V. 1972. Systems Analysis and Water Quality Measurement. Environmental Research and Applications, Inc., NY.

Thomann, R.V. and J.J. Fitzpatrick. 1982. Calibration and Verification of a Mathematical Model of the Eutrophication of the Potomac Estuary, Prepared for Department of Environmental Services, Government of the District of Columbia.

Thomas, N.A. and R.L. O'Connell. 1966. A Method for Measuring Primary Production by Stream Benthos. Limnology and Oceanography, 11, pp. 386-392.

Thornton, K.W. and A.S. Lessem. 1978. A Temperature Algorithm and Modifying Biological Rates. Trans. Am. Fish. Soc., 107:284-287.

Truesdale, G.A., A.L. Downing, and G.F. Lowden. 1955. Journal of Applied Chemistry, Vol. 5, No. 53.

Truesdale, G.A., and K.G. Van Dyke. 1958. The Effect of Temperature on the Aeration of Flowing Waters, Water and Waste Treatment Journal, Vol. 7, 9.

Tsivoglou, E.C. 1958. Oxygen Relationships In Streams. Tech. Report W58-2. Robert A. Taft Sanitary Engineering Laboratory. Cincinnati, Ohio.

Tsivoglou, E.C., R.L. O'Connell, C.M. Walter, P.J. Godsil, and G.S. Logsdon. 1965. Tracer Measurements of Atmospheric Reaeration-I. Laboratory Studies, Journal Water Pollution Control Federation, Vol. 37, No. 10, pp. 1343-1362.

Tsivoglou, E.C. 1967. Tracer Measurement of Stream Reaeration, Federal Water Pollution Control Administration, Washington, D.C., PB-229 923.

Tsivoglou, E.C., J.B. Cohen, S.D. Shearer, and P.J. Godsil. 1968. Tracer Measurement of Stream Reaeration. II. Field Studies, Journal Water Pollution Control Federation, Vol. 40, No. 2, Part 1, pp. 285-305.

Tsivoglou, E.C., and J.R. Wallace. 1972. Characterization of Stream Reaeration Capacity, EPA-R3-72-012, Prepared for Office of Research and Monitoring, U.S. EPA, Washington, D.C.

Tsivoglou, E.C., and L.A. Neal. 1976. Tracer Measurement of Reaeration: 3. Predicting the Reaeration Capacity of Inland Streams, Journal Water Pollution Control Federation, Vol. 48, No.12, pp. 2669-2689.

Tsivoglou, E.C., 1980. Field Tracer Measurement of Reaeration in Tidal Systems, Prepared for U.S. EPA, Environmental Research Laboratory, Athens, Georgia.

U.S. Army Engineer Waterways Experiment Station. 1982. CE-QUAL-R1: A Numerical One-Dimensional Model of Reservoir Water Quality. U.S. Army Corps of Engineers Instruction Report E-821.

U.S. Environmental Protection Agency. 1976. Areawide Assessment Procedures Manual. Office of Research and Development, Cincinnati, Ohio, Report EPA-600/9-76-014.

U.S. Environmental Protection Agency. 1979a. Carbonaceous Nitrogenous Demand Studies of the Potomac Estuary. U.S. Environmental Protection Agency Annapolis Field Office. EPA 903/9-79-003.

U.S. Environmental Protection Agency. 1979b. Biochemical Studies of the Potomac Estuary - Summer, 1978. U.S. Environmental Protection Agency Annapolis Field Office. EPA 903/9-79-005.

U.S. Environmental Protection Agency. 1983. Technical Guidance Manual for Performing Waste Load Allocations. Book II: Streams and Rivers. Chapter 2: Nutrient/Eutrophication Impacts.

United States Environmental Protection Agency Training Manual. 1974. Chemical Analysis for Water Quality Treatment.

United States Environmental Protection Agency. 1975. Special Nitrifying, Bacteria Study: Kanawha River, West Virginia, United States Environmental, Protection Agency, Region III, Wheeling Field Office, Wheeling, West, Virginia.

UNESCO. 1981. Background Papers and Supporting Data on the Practical Salinity Scale 1978, Technical Paper Marine Science No. 37.

USGS (United States Geological Survey). 1981. Quality of Water Branch Technical Memorandum No. 81.11, May 8, 1981. 5 pp.

Van Benschoten, J. and W.W. Walker, Jr. 1984. Calibration and Application, of QUAL-II to the Lower Winooski River. Water Resources Bulletin. Vol. 20,, No. 1, pp. 109-117.

Velz, C.J. 1984. Applied Stream Sanitation. John Wiley and Sons.

Virginia, University of. 1975. A Method for Monitoring Eutrophication in, Rivers, Prepared for Office of Water Research and Technology, U.S. Dept. of, the Interior.

Waldon, M.G. 1983. Reaeration Rate Estimation Using the Lag in Dissolved, Oxygen Concentration, Prepared for U.S. Department of the Interior, Office, of Water Policy, Washington, D.C.

Walker, R.R. and W.J. Snodgrass. 1984. Modelling Sediment Oxygen Demand in, Hamilton Harbour. (See Hatcher and Hicks, 1984). In Press.

Walker, W.W. 1983. Some Recent Adaptations and Applications of QUAL-II in, the Northeast. In: Proceedings of the Stormwater and Water Quality Model, Users Group Meeting, January 27-28, 1983, T.O. Barnwell (editor)., U.S. Environmental Protection Agency, Environmental Research Laboratory, Athens, Georgia, EPA-600/9-83-015.

Ward, G.J., Jr. 1984. The Measurement of Benthal Oxygen Demand in the Houston Ship Channel, J. Water Pollution Control Federation, Vol. 56, No. 2, pp. 183-191.

Weiler, R.R. 1974. Carbon Dioxide Exchange Between Water and Atmosphere, Journal of Fisheries Research, Board Committee, Vol. 31, pp. 329-32.

Weiss, R.F. 1970. The Solubility of Nitrogen, Oxygen and Argon in Water and Sea Water. Deep-Sea Res. 17:721-735.

Wezernak, C.T. and J.J. Gannon. 1967. Oxygen-Nitrogen Relationships in Autotrophic Nitrification. Applied Microbiology, 15, pp. 1211-1215.

Wezernak, C.T. and J.J. Gannon. 1968. Evaluation of Nitrification in Streams. J. Sanit. Eng. Div. Am. Soc. Civ. Engrs. 94, pp. 883-895.

Whipple, G.C. and M.C. Whipple. 1911. Journal American Chemical Society, 33:362-365.

Whittemore, R.C. 1984a. The Significance of Interfacial Velocity Effects on the Exertion of SOD. (See Hatcher and Hicks, 1984). In Press.

Whittemore, R.C. 1984b. Implementation of In situ and Laboratory SOD Measurements in Water Quality Modeling. (See Hatcher and Hicks, 1984). In Press.

Wilber, W.G., J.G. Peters, M.A. Ayers, and C.G. Crawford. 1979. A One-Dimensional, Steady-State, Dissolved Oxygen Model and Waste Load Assimilation Study for Cedar Creek, Dekalb and Allen Counties, Indiana. USGS Open-File Report 79-1062.

Wilcock, R.J. 1984a. Methyl Chloride as a Gas-Tracer for Measuring Stream Reaeration Coefficients-I, Laboratory Studies, Water Research, Vol. 18, No. 1, pp. 47-52.

Wilcock, R.J. 1984b. Methyl Chloride as a Gas-Tracer for Measuring Stream Reaeration Coefficients-II, Stream Studies, Water Research, Vol. 18, No. 1, pp. 53-57.

Wild, H.E., C.N. Sawyer, and T.C. McMahon. 1971. Factors Affecting Nitrification Kinetics, Journal of Water Pollution Control Federation, Vol. 43, No. 9, pp. 1845-1854.

Wilhems, S.C. 1980. Tracer Measurement of Reaeration: Application to Hydraulic Models, U.S. Army Engineer Waterways Experiment Station, Hydraulics Laboratory, Vicksburg, Mississippi.

Wilhelms, S.C., L. Clark, J.R. Wallace, and D.R. Smith. 1981. Gas Transfer in Hydraulic Jumps. U.S. Army Waterways Experiment Sation. Report E-81-10.

Wilhelms, S.C., and D.R. Smith. 1981. Reaeration Through Gated-Conduit Outlet Works. U.S. Army Waterways Experiment Station. Report E-81-5.

Williams, R.E. and M.S. Lewis. 1984. Application of Zero Order Kinetics to Modeling Simultaneous Benthic Nitrification and Denitrification. In: M. Pirbazari and J.S. Devinny, eds. Proceedings of the 1984 ASCE National Conference on Environmental Engineering, Los Angeles, CA. pp. 502-507.

Wilson, G.T., and N. Macleod. 1974. A Critical Appraisal of Empirical Equations and Models for the Prediction of the Coefficient of Reaeration of Deoxygenated Water, Water Research, Vol. 8, pp. 341-366.

Winkler, L.W. 1891. Ber d. Deutschen Chem. Ges., Vol. 24, No. 89.

Wisconsin Department of Natural Resources. 1979. QUAL-III Water Quality Model Documentation (Revised Nov. 1979). Madison, Wisconsin.

Wood, L.B., B.J.E. Hurley and P.J. Matthews. 1981. Some Observations on the Biochemistry and Inhibition of Nitrification. Water Research. Vol. 15, pp. 543-551.

Wright, R.M. and A.J. McDonnell. 1979. In-Stream Deoxygenation Rate Prediction. ASCE Jour. Env. Eng. 105:323-335.

Wyer, M.D. and A.R. Hill. 1984. Nitrate Transformations in Southern Ontario Stream Sediments. Water Resources Bulletin. Vol. 20, No. 5, pp. 729-737.

Yotsukura, N., D.A. Stedfast, R.E. Draper, W.H. Brutsaert. 1983. An Assessment of Steady-State Propane-Gas Tracer Method for Reaeration, The Cowaselon Creek, New York. USGS Water Investigations Report 83-4183.

Yu, S.L., T.J. Tuffy, and D.S. Lee. 1977. Atmosphere Reaeration in a Lake, Office of Water Resources and Technology, U.S. Department of Interior.

Zison, S.W., W.B. Mills, D. Deimer, and C.W. Chen. 1978. Rates, Constants and Kinetics Formulations in Surface Water Quality Modeling. Prepared by Tetra Tech, Inc., Lafayette, CA for Environmental Research Laboratory, U.S. Environmental Protection Agency, Athens, GA. EPA-600/3-78-105. 335 pp.

Chapter 4

pH AND ALKALINITY

4.1 INTRODUCTION

The subjects of pH and alkalinity are becoming increasingly important as society begins to deal with acidic precipitation. New models developed to analyze effects of alternative controls on inputs of acidity to sensitive aquatic environments use alkalinity as a state variable, then predict pH from alkalinity (Gherini et al., 1984). Earlier models did not contain many of the processes that affect pH, and their predictive capability was adequate for some, but not all, environments (e.g. Henriksen, 1979). More elaborate models now exist which take into account a more complete picture of the constituents that comprise alkalinity in the dilute systems that are at risk from acidic precipitation (organic acids, other non-carbonate weak acids, etc.) and which compute other source-sinks of alkalinity and factors that affect pH (Chen et al., 1984).

4.2 CARBONATE ALKALINITY SYSTEM

The carbonate system is of great importance in lakes, rivers, and estuaries. Carbonate chemistry of natural waters has been described in detail elsewhere (Stumm and Morgan, 1970, 1981; Trussell and Thomas, 1971; Park, 1969; Butler, 1982; Chen and Orlob, 1972, 1975). The carbon dioxide (CO_2) - bicarbonate (HCO_3^-) - carbonate (CO_3^{2-}) equilibrium is the major buffer system in aquatic environments. This equilibrium directly affects the pH, which in turn can affect the biological and chemical constituents of the system. For example, it may become necessary to simulate pH and alkalinity in order to compute the toxicant, un-ionized ammonia (see Chapter 5), or to determine available concentrations of metals (e.g., Gherini et al., 1984).

Since algae use carbon dioxide as a carbon source during photosynthesis, this is a nutrient which can reduce the growth rate when alkalinity is low and other nutrients are high (Goldman, et al., 1972). Most models include a carbonate system representation which calculates the total inorganic carbon (TIC) as the sum of bicarbonate, carbonate, and carbon dioxide. Carbon dioxide is assumed to be produced by respiration and consumed by algal growth. The major source is atmospheric exchange.

The major chemical species considered to constitute alkalinity are dissolved carbon dioxide, bicarbonate, and carbonate ion, together with the hydrogen and hydroxyl ions. Mass balance equations assume that ionic equilibrium exists and calculate carbon inputs and outputs from a pool of total inorganic carbon (TIC). Conversions between different carbon forms are based on stoichiometric equivalents. The carbon dioxide form is involved in most of the important processes, including surface reaeration, respiration, excretion, algal uptake, and organic decay reactions. However, dissolved carbon dioxide combines with water to form carbonic acid, which, in turn, dissociates to bicarbonate ion, carbonate ion, and hydrogen ion. Since the dissociation reactions occur very rapidly in comparison to the other biological and chemical processes, dissolved carbon is modeled as the sum of $CO_2 + HCO_3^- + CO_3^{2-}$, and is referred to as total inorganic carbon (TIC).

Dissolved inorganic carbon is derived from several sources. These include surface reaeration; respiration by fish, zooplankton, benthic animals, and algae; soluble excretion by fish, zooplankton, and benthic animals; and the decay of organic matter in the form of detritus, sediment, and sewage BOD. Dissolved carbon is removed by assimilation during algal photosynthesis.

Conceptually, the mass balance equation defining these relationships for the EAM model (Tetra Tech, 1980) is expressed as follows:

$$
\begin{aligned}
(vol)\frac{d(TIC)}{dt} = (vol)\Big[& (det)(K_{det})(C_{det}) + (sed)(K_{sed})(C_{sed}) \\
& + \sum_{i=1}^{n_f}\sum_{j=1}^{n_L}(fish_{ij}\cdot Fr_{ij}\cdot C_{fish}) + (ben)(Br)(C_{ben}) \\
& + \sum_{i=1}^{n_z}(zoo_i\cdot Zr_i\cdot C_{zoo}) + \sum_{i=1}^{n_a}(alg_i\cdot Ar_i\cdot C_{alg}) \\
& + \sum_{i=1}^{n_f}\sum_{j=1}^{n_L}(fish_{ij}\cdot Fdex_i\cdot C_{fish}) \\
& + \sum_{i=1}^{n_z}(zoo_i\cdot Zdex_i\cdot C_{zoo}) + (ben)(Bdex)(C_{ben}) \\
& - \sum_{i=1}^{n_a}(alg_i\cdot Ag_i\cdot C_{alg}) \\
& + (BOD)(K_{BOD})(C_{BOD})\Big] \\
& + (R_{CO_2})(CO_{2_{sat}} - CO_2)(Area) \qquad (4\text{-}1)
\end{aligned}
$$

= detritus decay + sediment decay + fish respiration
+ benthic animal respiration + zooplankton respiration
+ algal respiration + fish excretion + zooplankton excretion
+ benthic animal excretion - algal assimilation
+ BOD decay + surface reaeration.

Although Equation (4-1) is a substantially complete picture of TIC dynamics in an aquatic system, most models do not contain the same degree of complexity. However, whether multi-compartmented or few compartments, the general aspects of the process are modeled similarly. Also, the inputs and outputs can be based on CO_2 with suitable stoichiometric conversions (e.g., Di Toro and Connolly, 1980) rather than TIC.

Surface reaeration of CO_2 from atmospheric sources is done in a way similar to oxygen (Section 3.2). However, only minimal effort to measure

CO_2 reaeration is necessary and literature values have been used (Emerson, 1975; Liss, 1973). Reaeration occurs only at the surface of the water body, and is a function of the carbon dioxide saturation level. The saturation concentration is a function of the water temperature as it affects the Henry's law constant (K_H) for computing CO_{2sat}:

$$CO_{2sat} = K_H \, pCO_2 \tag{4-2}$$

where pCO_2 is the partial pressure of CO_2 in the atmosphere (generally 0.00033 atmospheres is used) and

$$K_H = M_{CO_2} 10^{\left[\frac{2385.73}{T_K} - 14.0184 + 0.0152642\, T_K\right]} \tag{4-3}$$

where M_{CO_2} = 44,000 mg/mole, CO_2

T_K = temperature in K = 273.15 + ^oC

K_H = Henry's law constant, mg/(liter·atm)

After computing the total inorganic carbon according to the mass balance in Equation (4-1), the dissolved carbon dioxide concentration is calculated using relationships derived from the equilibrium constants of the dissociation reactions. The reactions involved are:

$$H_2CO_3 \rightleftharpoons HCO_3^- + H^+ \qquad K_1 \tag{4-4}$$

$$HCO_3^- \rightleftharpoons CO_3^= + H^+ \qquad K_2 \tag{4-5}$$

$$H_2O \rightleftharpoons H^+ + OH^- \qquad K_w \tag{4-6}$$

where the equilibrium constants are defined as

$$K_1 = \frac{\left[HCO_3^-\right]\left[H^+\right]}{\left[H_2CO_3\right]} \tag{4-7}$$

$$K_2 = \frac{\left[CO_3^{=}\right]\left[H^+\right]}{\left[HCO_3^-\right]} \tag{4-8}$$

$$K_w = \left[H^+\right]\left[OH^-\right] \tag{4-9}$$

The equilibrium constants K_1, K_2, and K_w vary with temperature according to the following relationships (Tetra Tech, 1979):

$$K_1 = 10^{\left[14.8435 - 0.032786\ T_K - (3404.71/T_K)\right]} \tag{4-10}$$

$$K_2 = 10^{\left[6.498 - 0.02379\ T_K - (2902.39/T_K)\right]} \tag{4-11}$$

$$K_w = 10^{\left[35.3944 - 0.00835\ T_K - (5242.4/T_K - 11.826\ \log(T_K)\right]} \tag{4-12}$$

In a carbonate system, the alkalinity (alk) is calculated according to the mass balance equation:

$$\text{alk} = \text{alkalinity} = \left[HCO_3^-\right] + 2\left[CO_3^{=}\right] + \left[OH^-\right] - \left[H^+\right] \tag{4-13}$$

Other processes can affect alkalinity in aquatic systems. Addition of acids and nitrification reduce alkalinity, and uptake of nitrate by algae increases alkalinity. Because of the magnitude of the ammonia concentration in waters receiving municipal effluents, nitrification can affect alkalinity substantially, generating 2 equivalents of acid (H^+) per equivalent of ammonia oxidized (see Section 3.4). Similarly in eutrophic waters, nitrate uptake can increase alkalinity by the production of approximately 1 equivalent of base (OH^-) per equivalent of nitrate taken up by plant cells. These corrections would be of consequence in low alkalinity waters (less than 200 μeq/l), and would be applied to Equation (4-13).

Once the total inorganic carbon and alkalinity have been determined using the mass balance equations (4-1, 4-13), the hydrogen ion concentration

can be calculated by trial and error solution of the following relationship:

$$alk = [TIC] \frac{1 + \frac{2K_2}{[H^+]}}{1 + \frac{[H^+]}{K_1} + \frac{K_2}{[H^+]}} + \frac{K_{w_s}}{[H^+]} - [H^+] \tag{4-14}$$

After $[H^+]$ is determined, it is substituted into the expression for CO_2, which can then be solved directly for the dissolved CO_2 concentration:

$$CO_2 = \frac{[TIC]}{1 + \frac{K_1}{[H^+]} + \frac{K_1 \cdot K_2}{[H^+]^2}} \tag{4-15}$$

Not all models compute inorganic carbon species or pH. Generally these computations have been made primarily in lake systems where they are of significance in acid precipitation or are used for additional model verification as in Di Toro and Connolly (1980). In all cases, the formulations are based on the above derivations, although the computation details may differ from model to model. Water quality models that contain the CO_2, alkalinity, pH formulations include those discussed in the following references:

Smith, 1978	WQRRS
Thomann et al., 1974	LAKE-3
Di Toro and Connolly, 1980	Lake Erie Model
Scavia, et al., 1976	Lake Ontario Model
Tetra Tech, 1980	EAM
WES, 1982	CE-QUAL-R1

4.3 EXTENDED ALKALINITY APPROACH

4.3.1 Definition of Extended Alkalinity

The mass balance equation (4-13) has ignored several H^+-ion acceptors, and is appropriate in many instances. In very low alkalinity waters,

however, the concentration of these neglected H^+-ion acceptors can be significantly large. The neglected H^+-ion acceptors include organic substances with carboxyl and phenolic hydroxyl groups, for example:

$$R\text{-}COO^- + H^+ \rightleftharpoons R\text{-}COOH \text{ (organic acids)} \tag{4-16}$$

and the monomeric aluminum species and their complexes, for example,

$$Al(OH)_2^+ + 2H^+ \rightleftharpoons Al^{3+} + 2H_2O \tag{4-17}$$

and

$$Al{\cdot}R + 3H^+ \rightleftharpoons Al^{3+} + H_3R. \tag{4-18}$$

An extended alkalinity relationship would include the alkalinity associated with water itself, the carbonate system, the monomeric aluminum system and its organic complexes, and dissolved organic acid anions. The dissolved organic carbon alkalinity can be represented by a triprotic (H_3R_1) and/or monoprotic (HR_1) model organic acid with fixed dissociation constants and a fixed number of acid-base functional groups per unit mass of carbon (eq/mgC). The components of the total alkalinity, as represented by the H^+-ion acceptors, are given below:

$$Alk = \underbrace{Alk_{H_2O}}_{\text{water}} + \underbrace{Alk_C}_{\text{carbonate system}} + \underbrace{Alk_{R_1} + Alk_{R_2}}_{\text{organic acids}} + \underbrace{Alk_{Al} + Alk_{Al\cdot O}}_{\text{aluminum system}} \tag{4-19}$$

where

$$Alk_{H_2O} = [OH^-] - [H^+] \tag{4-20}$$

$$Alk_C = [HCO_3^-] + 2[CO_3^{2-}] \tag{4-21}$$

$$Alk_{R_1} = [H_2R_1^-] + 2[HR_1^{2-}] + 3[R_1^{3-}] \tag{4-22}$$

$$Alk_{R_2} = [R_2^-] \tag{4-23}$$

$$Alk_{Al} = [Al(OH)^{2+}] + 2[Al(OH)_2^+] + 3[Al(OH)_3^o] + 4[Al(OH)_4^-] \tag{4-24}$$

$$Alk_{Al \cdot O} = 3[Al\ R_1] + [AlR_2^{2+}] + 2[Al(R_2)_2^+] + 3[Al(R_2)_3] \tag{4-25}$$

An alternative representation of solution-phase alkalinity, which is mathematically equivalent to the above is given as follows,

$$Alk = \Sigma_k\ Z_k N_k = \Sigma C_B - \Sigma C_A \tag{4-26}$$

where ΣC_B = the sum of the base cations

$$= 2\left[C_a^{2+}\right] + 2\left[Mg^{2+}\right] + \left[Na^+\right] + \left[K^+\right] + \left[NH_4^+\right] \tag{4-27}$$

ΣC_A = the sum of the strong acid anions

$$= 2\left[SO_4^{2-}\right] + \left[NO_3^-\right] + \left[Cl^-\right] \tag{4-28}$$

The derivation is based on the mass balance equation and the solution electroneutrality condition. Figure (4-1) shows the equivalence for lakes in the State of Washington.

4.3.2 Modeling Extended Alkalinity

The concept of extended alkalinity has been incorporated in a model called PHCALC. This model was developed primarily for the ILWAS model (Tetra Tech, 1983), and was later modified into an interactive FORTRAN program to compute any one of the following options: pH, alkalinity, total inorganic carbon (TIC) and "solution equilibration". The solution equilibration approach is similar to the approach for pH, except that alkalinity can be adjusted for gibbsite precipitation or dissolution. Table 4-1 shows the list of required parameters for any given option.

All the concentrations on the left-hand-side of Equations (4-20) through (4-25) can be expressed in terms of ionization fractions and

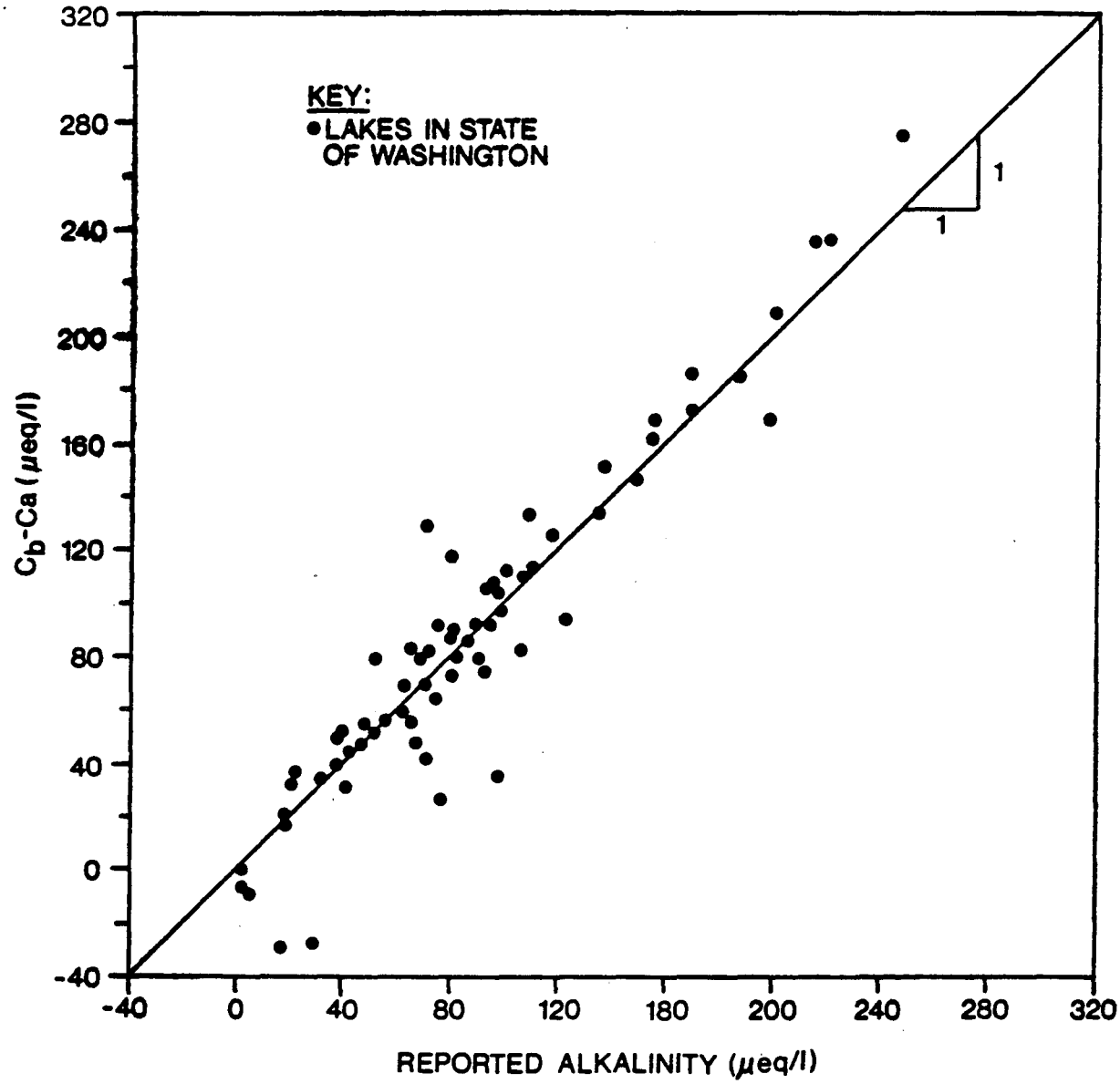

Figure 4-1. $[\Sigma C_B - \Sigma C_A]$ plotted against reported alkalinity (from Gherini et al., 1984).

temperature-dependent dissociation constants. Fluoride and sulfate concentrations are required for the determination of their complexations with aluminum.

4.3.3 Equilibrium Constants and Solubility Products

The equilibrium constants used in PHCALC are obtained by first expressing a thermodynamic temperature dependence for a related constant, K_i:

TABLE 4-1. OPTIONS AND THEIR REQUIRED INPUT PARAMETERS FOR PHCALC

Options*	Parameters Required to be Specified
pH	Alk, TIC or EQ_1, Al_T, OAC_1, OAC_2, F, SO_4^{2-}, T
Alk	pH, TIC or EQ_1, Al_T or EQ_2, OAC_1, OAC_2, F, SO_4^{2-}, T
TIC	pH, Alk, Al_T, or EQ_2, OAC_1, OAC_2, F, SO_4^{2-}, T
EQ	Alk, TIC or EQ_1, Al_T, EQ_2, OAC_1, OAC_2, F, SO_4^{2-}, T

Definition of Parameters:

Alk	alkalinity
TIC	total inorganic carbon
EQ	equilibration of a solution with $Al(OH)_3$
Al_T	total aluminum
OAC_1	total organic acid (1)
OAC_2	total organic acid (2)
F	fluoride concentration
SO_4^{2-}	sulfate concentration
T	temperature, ^oC
EQ_1	ratio of TIC to air-equilibrated TIC (specified for open system)
EQ_2	-log (Ksp) for $Al(OH)_3$ mineral or one of the following minerals for the equilibration with gibbsite

AG - amorphous gibbsite	(pK_{sp} = 31.19)
MG - microcrystalline gibbsite	(pK_{sp} = 32.64)
NG - natural gibbsite	(pK_{sp} = 33.22)
SG - synthetic gibbsite	(pK_{sp} = 33.88)

*Options are the parameters to be computed

$$\log_{10} K_i = a + \frac{b}{T} + cT + d\log_{10}T \qquad (4\text{-}29)$$

The constants a, b, c and d are given as follows:

	a	b	c	d	Reference
K_w	6.0875	-4470.99	-0.01706	0	Stumm & Morgan, 1981
K_1	545.56	-17052	0.12675	-215.21	Loewenthal & Marais, 1978
K_2	-6.498	2902.39	0.02379	0	Loewenthal & Marais, 1978
K_H	-14.0184	2385.73	0.0152642	0	Stumm & Morgan, 1981

K_w, K_1, and K_2 are dimensionless while K_H is in moles liter^{-1} atm^{-1}. K_H has to be multiplied by RT to convert to a dimensionless form. R is the universal gas constant and T is the absolute temperature in degrees Kelvin in the range of 273 K to 313 K.

The solubility products used in the equilibration with gibbsite were shown earlier in Table 4-1.

4.4 SUMMARY

Two approaches have been presented for the relationship of total inorganic carbon, alkalinity and pH. For waters with low dissolved organic carbon (with little color) and high alkalinity (alk $\geq$200μeq/l), the conventional alkalinity definition is recommended. For waters with high dissolved organic carbon and waters with alk <200 μeq/l where the alkalinities contributed by aluminum and organic acids are no longer negligible, the extended alkalinity approach is recommended. The equivalence between the expression Alk = $\Sigma C_B - \Sigma C_A$ and the extended alkalinity definition provides a convenient tool in alkalinity evaluation.

4.5 REFERENCES

Butler, J.N. 1982. Carbon Dioxide Equilibria and their Applications. Addison-Wesley Pub. London. 259 p.

Chen, C.W., and G.T. Orlob. 1972. Ecological Simulation for Aquatic Environments, Report to Office of Water Resources Research OWRR C-2044, Water Resources Engineers Inc., Walnut Creek, California.

Chen, C.W., and G.T. Orlob. 1975. Ecologic Simulation of Aquatic Environments. Systems Analysis and Simulation in Ecology, Vol. 3, B.C. Patten, (ed.). Academic Press, New York, N.Y. pp. 476-588.

Chen, C.W., S.A. Gherini, J.D. Dean, R.J.M. Hudson, and R.A. Goldstein. 1984. Development and Calibration of the Integrated Lake-Watershed Acidification Study Model. In Modeling of Total Acid Precipitation Impacts. J.L. Schnoor (Ed.), Butterworth, Boston, Mass.

Di Toro, D.M., and J.P. Connolly. 1980. Mathematical Models of Water Quality in Large Lakes Part 2: Lake Erie, EPA-600/3-80-065, U.S. Environmental Protection Agency, Duluth, Minnesota.

Emerson, S. 1975. Gas Exchange Rates in Small Canadian Shield Lakes. Limnol. Oceanogr. 20:754-761.

Gherini, S.A., C.W. Chen, L. Mok, R.A. Goldstein, R.J.M. Hudson, and G.F. Davis. 1984. The ILWAS Model: Formulation and Application. In the Integrated Lake-Watershed Acidification Study. 4: Summary of Major Results. EPRI EA-3221. p. 7-1 to 7-46.

Goldman, J.C., D.B. Porcella, E.J. Middlebrooke, and D.F. Toerien. 1972. Review Paper: The Effect of Carbon on Algal Growth: Its Relationship to Eutrophication. Water Res. 6:637-679.

Henriksen, A. 1979. A Simple approach For Identifying and Measuring Acidification in Freshwater. Nature, 278, 542.

Liss, P.S. 1973. Processes of Gas Exchange Across an Air-Water Interface. Deep-Sea Res. 20: 221-238.

Loewenthal, R.E., and G.V.R. Marais. 1978. Carbonate Chemistry of Aquatic Systems: Theory and Application. Volume 1. Ann Arbor Science, Michigan.

Parks, P.K. 1969. Oceanic CO_2 System: An Evaluation of Ten Methods of Investigation: 179-186.

Scavia, D., B.J. Eadie, and A. Robertson. 1976. An Ecological Model for Lake Ontario Model Formulation, Calibration, and Preliminary Evaluation. NOAA Technical Report ERL 371-GLERL 12. NOAA. Boulder Colorado. 63 p.

Smith, D.I. 1978. WQRRS, Generalized Computer Program for River-Reservoir Systems. User's Manual 401-100, 100A: U.S. Army Corps of Engineers, Hydrologic Engineering Center (HEC), Davis, California. 210 pp.

Snoeyink, V.L., and D. Jenkins. 1980. Water Chemistry. New York. John Wiley & Sons.

Stumm, W., and J.J. Morgan. 1970. Aquatic Chemistry. (New York: Wiley-Interscience).

Stumm, W., and J.J. Morgan. 1981. Aquatic Chemistry, 2nd Ed., Wiley, New York.

Tetra Tech, Inc. 1979. Methodology for Evaluation of Multiple Power Plant Cooling System Effects, Volume II: Technical Basis for Computations. Electric Power Research Institute, Report EPRI EA-1111.

Tetra Tech, Inc. 1980. Methodology for Evaluation of Multiple Power Plant Cooling System Effects, Volume V. Methodology Application to Prototype-Cayuga Lake. Electric Power Research Institute, Report EPRI EA-1111.

Tetra Tech, Inc. 1983. The Integrated Lake-Watershed Acidification Study, Volume 1: Model Principles and Application Procedures. Electric Power Research Institute. Report EPRI EA-3221.

Thomann, R.V., D.M. Di Toro, R.P. Winfield, and D.J. O'Connor. 1975. Mathematical Modeling of Phytoplankton in Lake Ontario. I. Model Development and Application. EPA-660/3-75-005. USEPA, Corvallis, Oregon, 97330. 177 p.

Trussell, R.R., and J.F. Thomas. 1971. A Discussion of the Chemical Character of Water Mixtures. J. American Water Works Assoc. 63(1), 49.

Chapter 5

NUTRIENTS

5.1 INTRODUCTION

Certain elements are referred to as nutrients because they are essential to the life processes of aquatic organisms. The major nutrients of concern are carbon, nitrogen, phosphorus, and silicon. Silicon is important only for diatoms, one of the major components of the algal community. Other micronutrients such as iron, manganese, sulphur, zinc, copper, cobalt, and molybdenum are also important. However, these latter nutrients are not considered in water quality models because they are required only in trace amounts and they are usually present in quantities adequate to meet the biochemical requirements of the organisms.

Nutrients are important in water quality modeling for several reasons. For example, nutrient dynamics are critical components of eutrophication models since nutrient availablility is usually the main factor controlling algal blooms. Algal growth is typically limited by either phosphorus or nitrogen, with the exception of diatoms which are often silicon limited. Some blue-green algae can fix nitrogen and are therefore not limited by nitrogen. Carbon is usually available in excess although in some cases it may also be limiting. Carbon is also important because of its role in the pH-carbonate system, as discussed in Chapter 4.

Nitrogen is important in water quality modeling for reasons other than its role as a nutrient. For example, the oxidation of ammonia to nitrate during the nitrification process consumes oxygen and may represent a significant portion of the total BOD. Also, high concentrations of unionized ammonia can be toxic to fish and other aquatic organisms.

5.2 NUTRIENT CYCLES

Nutrients are present in several different forms in aquatic systems:

- dissolved inorganic nutrients
- dissolved organic nutrients
- particulate organic (detrital) nutrients
- sediment nutrients
- biotic nutrients (algae, aquatic plants, zooplankton, fish, benthic organisms)

Only the dissolved inorganic forms are available for algal growth. These include dissolved CO_2, ammonia, nitrite, and nitrate nitrogen, orthophosphate, and dissolved silica.

Each nutrient undergoes continuous recycling between the major forms listed above. For example, dissolved inorganic nutrients are removed from the water column by algae and aquatic plants during photosynthesis. These nutrients are distributed to the other aquatic organisms through the food web. Dissolved inorganic nutrients are returned to the water through the soluble excretions of all organisms, the decomposition of organic detritus and sediments, and the hydrolysis of dissolved organic nutrients. In addition, dissolved CO_2 and N_2 gases exchange with the atmosphere. Suspended particulate nutrients are generated through the particulate excretions of aquatic animals and the death of planktonic organisms. Organic detritus and phytoplankton which settle to the bottom contribute to the sediment nutrients. Decomposition of suspended organic detritus and organic sediment releases both dissolved organic and dissolved inorganic nutrients to the water.

Many of the above interactions are shown in Figure 5-1 for carbon, nitrogen, and phosphorus and in Figure 5-2 for silicon. Figures 5-3 and 5-4 present more detailed descriptions of the nitrogen and phosphorus cycles.

In addition to the internal recycling of nutrients within the waterbody, nutrients are also introduced through wasteloads (both point and nonpoint sources), river or tributary inflows, runoff, and atmospheric precipitation.

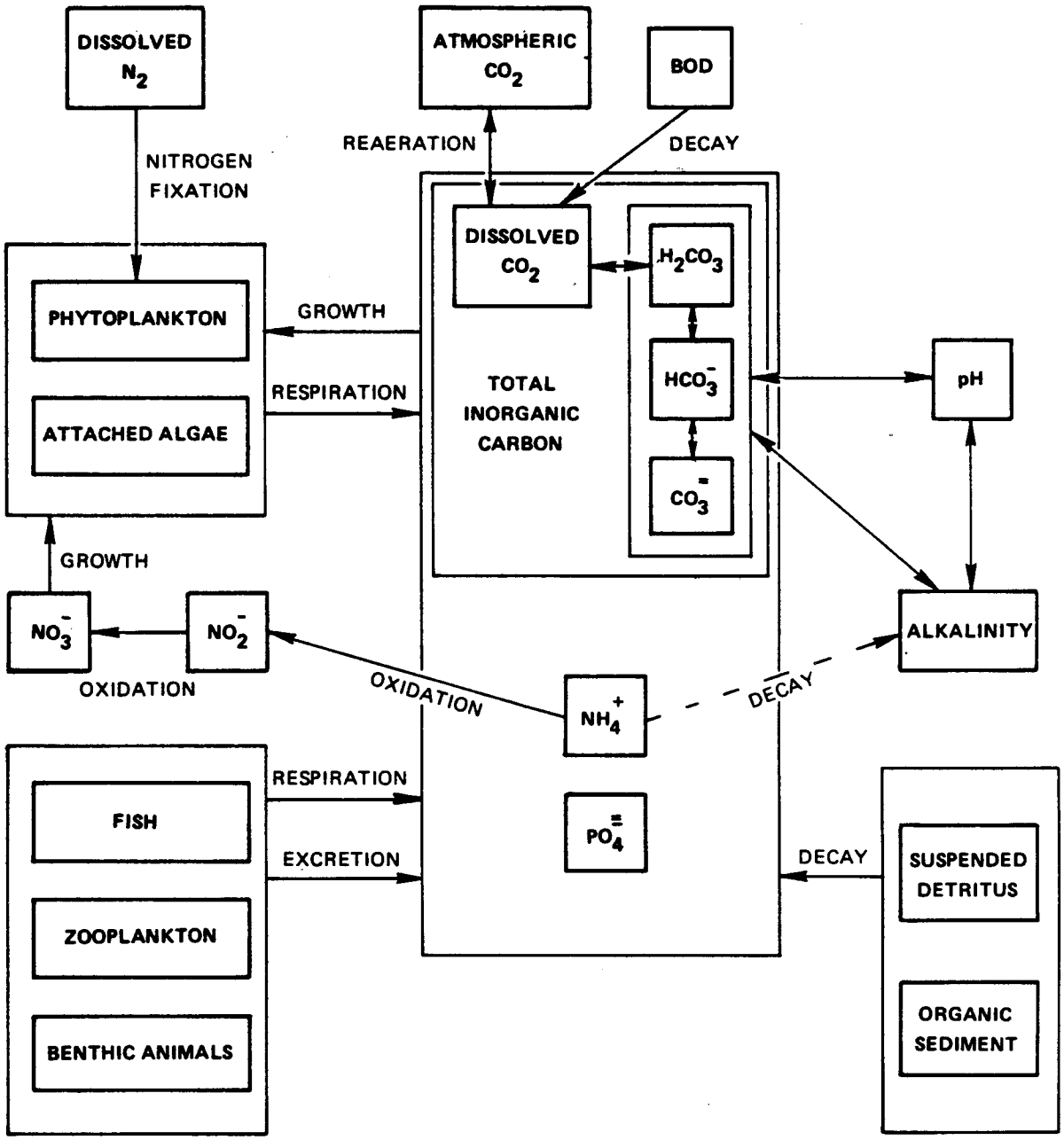

Figure 5-1. Nutrient interactions for carbon, nitrogen, and phosphorus (from Tetra Tech, 1979).

5.3 GENERAL MODELING APPROACH FOR ALL NUTRIENTS

Nutrient dynamics are governed by the following processes:

- dissolved inorganic nutrients
  - photosynthetic uptake
  - excretion
  - chemical transformations (e.g., oxidation of NH_3)
  - hydrolysis of dissolved organic nutrients
  - detritus decomposition
  - sediment decomposition and release
  - external loading

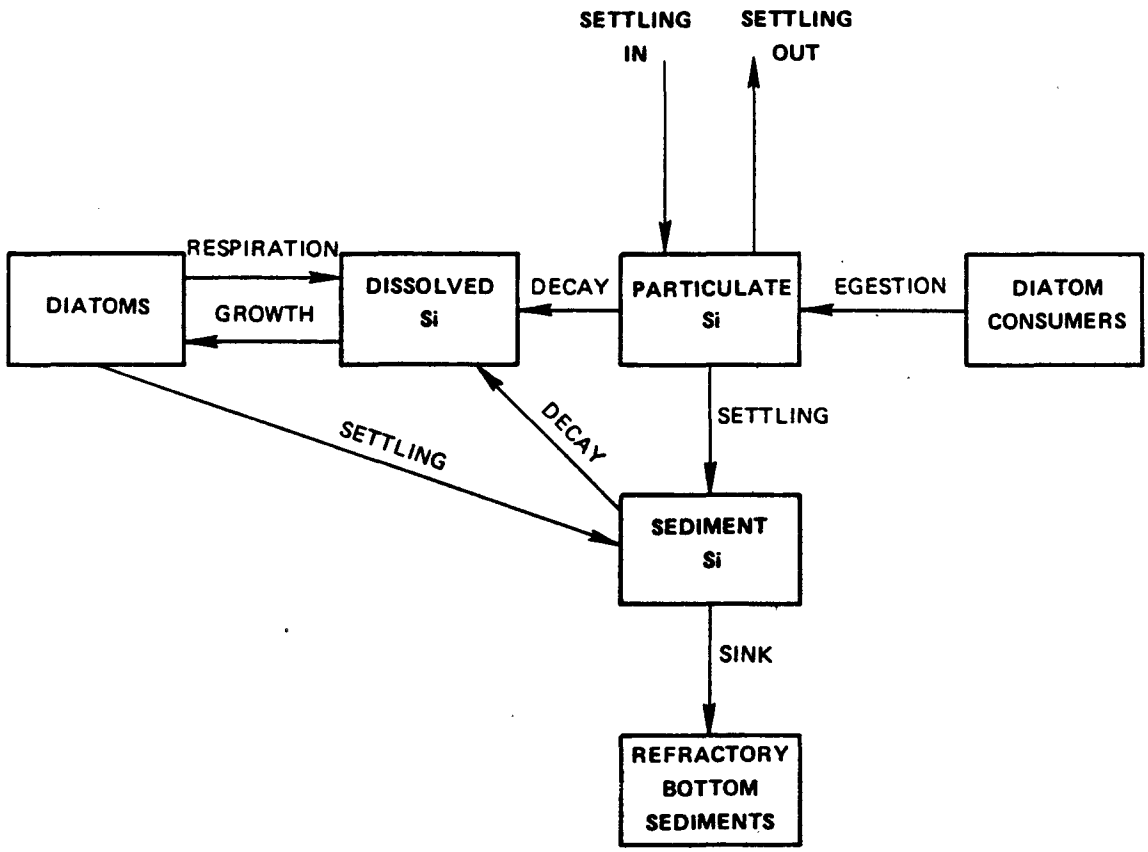

Figure 5-2. Nutrient interactions for silica (from Tetra Tech, 1979).

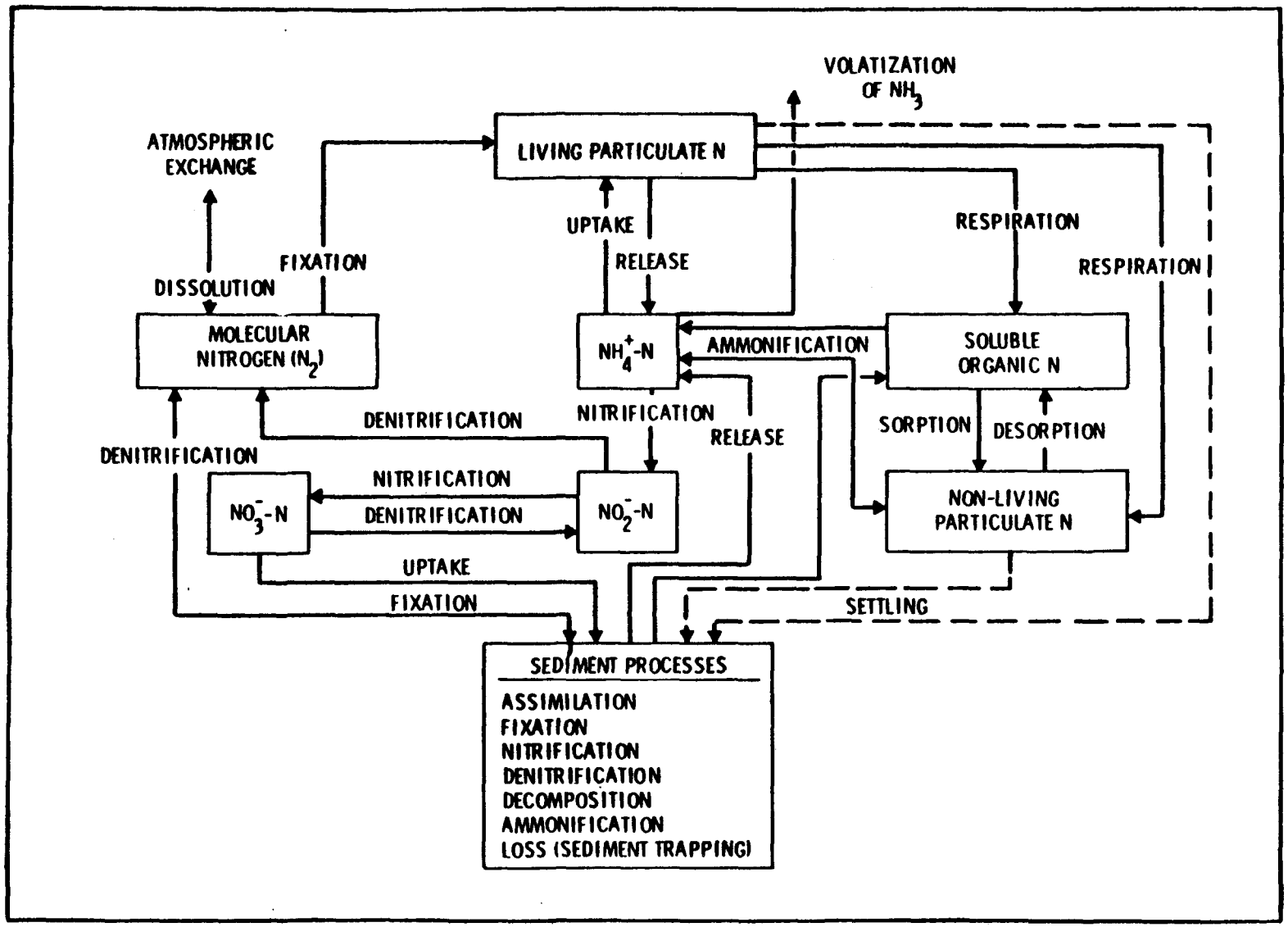

Figure 5-3. Nitrogen cycle (from Baca and Arnett, 1976).

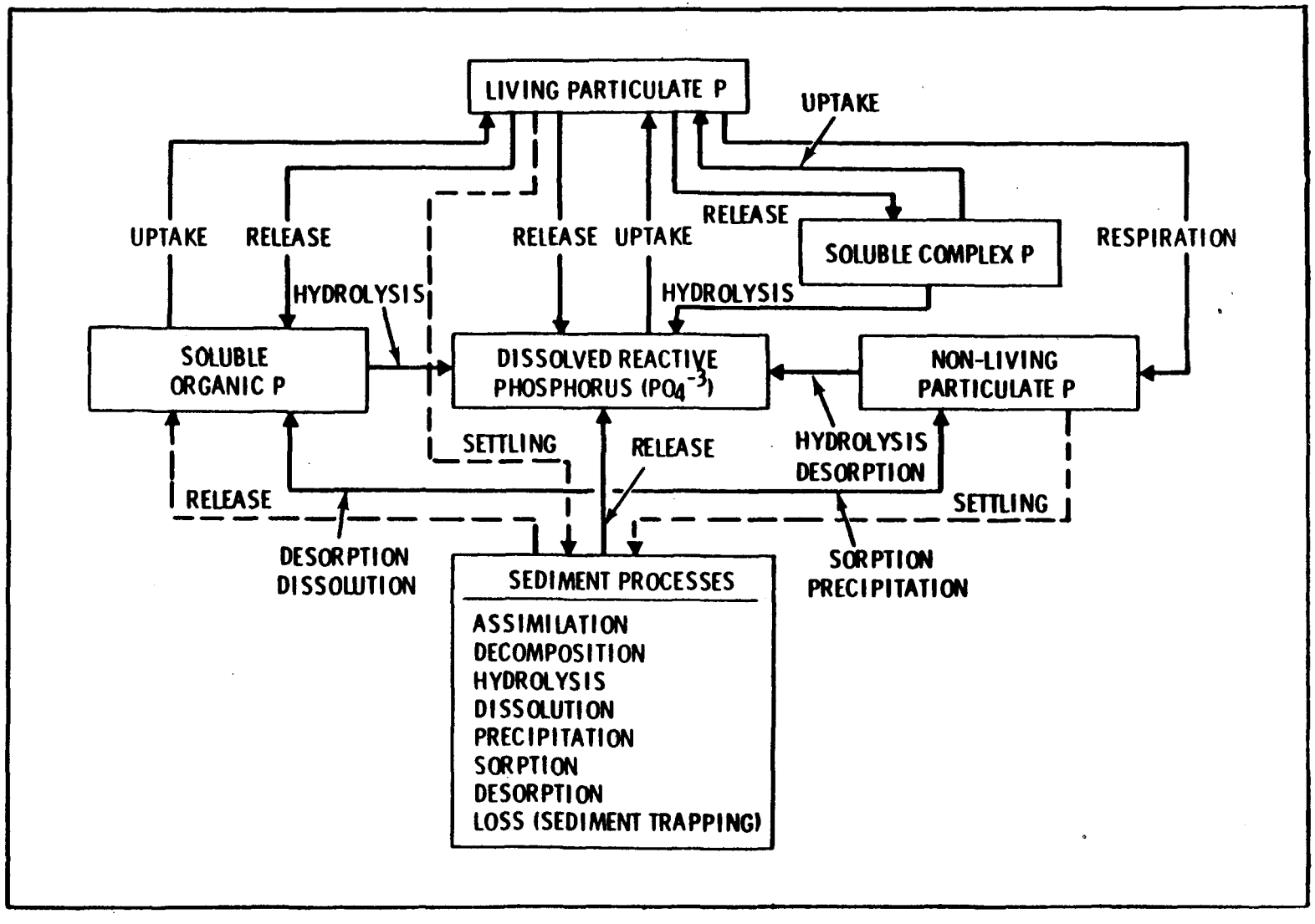

Figure 5-4. Phosphorus cycle (from Baca and Arnett, 1976).

- <u>dissolved organic nutrients</u>
  - excretion
  - hydrolysis
  - detritus decomposition
  - sediment decomposition and release
  - external loading

- <u>particulate organic nutrients</u>
  - particulate excretions
  - plankton mortality
  - decomposition
  - settling
  - zooplankton grazing
  - external loading

- <u>sediment nutrients</u>
  - detritus settling
  - algal settling
  - sediment decomposition and release

Only processes affecting the abiotic forms of nutrients are discussed in this chapter since the biotic components of water quality models are discussed in Chapters 6 (Algae) and 7 (Zooplankton).

Nutrients are modeled by using a system of coupled mass balance equations describing each nutrient compartment and each process listed above, plus the transport processes of advection and dispersion discussed in Chapter 2. The general equations for each nutrient, omitting the transport and external loading terms, can be expressed as follows:

<u>dissolved inorganic nutrients</u>:

$$\frac{dS}{dt} = - V_s + f_1 e_s + K_1 S' - K_2 S + K_{org} S_{org} + f_2 K_{det} S_{det} + f_3 K_{sed} S_{sed} \qquad (5\text{-}1)$$

dissolved organic nutrients:

$$\frac{dS_{org}}{dt} = (1 - f_1)\, e_s - K_{org}\, S_{org} + (1 - f_2)\, K_{det}\, S_{det} + (1 - f_3)\, K_{sed}\, S_{sed} \qquad (5\text{-}2)$$

particulate organic nutrients:

$$\frac{dS_{det}}{dt} = e_p + M_p - K_{det}\, S_{det} - K_s\, S_{det} - G_z \qquad (5\text{-}3)$$

sediment nutrients:

$$\frac{dS_{sed}}{dt} = K_s\, S_{det} + A_s - K_{sed}\, S_{sed} \qquad (5\text{-}4)$$

where S = dissolved inorganic nutrient concentration, mass/volume

S' = another inorganic form of the nutrient which decays to the form S (e.g., NH_3 NO_3), mass/volume

S_{org} = dissolved organic nutrient concentration, mass/volume

S_{det} = suspended particulate organic nutrient concentration, mass/volume

S_{sed} = organic sediment nutrient concentration, mass/volume

K_1 = transformation rate of S' into S, 1/time

K_2 = transformation rate of S into some other dissolved inorganic form of the nutrient, 1/time

K_{org} = hydrolysis rate of dissolved organic nutrient, 1/time

K_{det} = decomposition rate of particulate organic nutrient, 1/time

K_{sed} = decomposition rate of organic sediment nutrient, 1/time

K_s = settling rate for particulate organic nutrient, 1/time

V_s = photosynthetic uptake rate for nutrient S, mass/volume-time

e_s = soluble excretion rate of nutrient by all organisms, mass/volume-time

f_1 = fraction of soluble excretions which are inorganic

f_2 = fraction of detritus decomposition products which are immediately available for algal uptake

f_3 = fraction of sediment decomposition products which are immediately available for algal uptake

e_p = particulate excretion rate of nutrient by all animals, mass/volume-time

M_p = total rate of plankton mortality, mass/volume-time

G_z = detritus grazing rate by zooplankton, mass/volume-time

A_s = algal settling rate to sediment, mass/volume-time

Note that all of the transformations between the various abiotic nutrient compartments are described by first-order kinetics. This approach is used in almost all water quality models. Nutrient models differ primarily in the specific nutrients simulated (i.e., C, N, P, and Si) and in the number of compartments used to describe each nutrient cycle (i.e., dissolved inorganic forms such as NH_3, NO_2, and NO_3; dissolved organic components; particulate organic components; sediments; and biotic components such as algae and zooplankton).

For example, many models omit carbon since it does not limit algal growth in most situations. Silicon is generally modeled only when diatoms are simulated as a separate phytoplankton group.

The nutrient cycles are often simplified by combining or omitting some of the forms described above. For example, many models do not simulate sediment nutrients explictly with a mass balance equation such as Equation (5-4). Instead, user-specified sediment fluxes are specified in Equations (5-1) and (5-2). Dissolved organic nutrients are also left out of most models. In these cases, the decomposition products of the detritus and sediments as well as all soluble excretions go directly to the dissolved inorganic nutrient compartments. This in effect combines the suspended particulate and dissolved organic compartments into a single "unavailable" nutrient compartment which decays to produce available inorganic forms.

Nitrogen models also differ in the forms of inorganic nitrogen which are included, as well as in some of the processes modeled. For example, some models include only ammonia and nitrate, rather than the full oxidation sequence of ammonia to nitrite to nitrate. While most models include the nitrification reactions, only a few include denitrification. Also, only a few models include nitrogen-fixation by blue-green algae.

Sediments and particulate organic detritus are often modeled as single compartments, rather than having a separate compartment for each nutrient. In this case, the corresponding compartments for each nutrient are determined from the product of the total sediment and detritus concentrations and the stoichiometric ratios for each nutrient. The stoichiometric ratios are generally the same as those used for algae (see Section 6.3 of Chapter 6) so that mass is conserved during nutrient recycling.

Table 5-1 presents a comparison of the various nutrient forms included in several models. Transformation processes and the corresponding rate coefficients for each specific nutrient are discussed below, along with model formulations for nutrient uptake, excretion, and sediment release. Formulations for plankton mortality and zooplankton grazing are discussed in Chapters 6 and 7. Settling formulations for particulate organic detritus are essentially the same as the simplest formulations used for phytoplankton settling described in Chapter 6 (i.e., the settling rate equals the user-specified settling velocity divided by the depth of the model segment).

5.4 TEMPERATURE EFFECTS

Temperature influences the rates of all of the nutrient transformation processes discussed above. All of the first-order rate coefficients in Equations (5-1) through (5-4) are therefore temperature dependent. Almost all models use the exponential Arrhenius or van't Hoff relationship to describe these effects. A reference temperature of 20°C is usually assumed when specifying each rate coefficient, resulting in the following equation:

TABLE 5-1. COMPARISON OF NUTRIENT MODELS

Model (Author)	Nutrients Modeled				Nutrient Forms							Inorganic Nitrogen Forms				References
	C	N	P	Si	Dislvd. Inorg.	Dislvd. Organic	Partic. Organic	Sedi-ments	Algae	Zoo-plankton	Other Organisms	NH_3	NO_2	NO_3	Total Avail	
AQUA-IV		X	X		X	N	X	X	X	X		X	X	X		Baca & Arnett (1976)
CE-QUAL-R1	X	X	X		X		X	X	X	X	X	X	X	X		WES (EWQOS) (1982)
CLEAN	X	X	X		X	X	X	X	X	X	X				X	Bloomfield et al. (1973)
CLEANER	X	X	X		X	X	X	X	X	X	X				X	Scavia & Park (1976)
MS.CLEANER	X	X	X	X	X	X	X	X	X	X	X				X	Park et al. (1980)
DEM		X	X		X			X*	X			X	X	X		Feigner & Harris (1970)
DOSAG3		X	X		X			X*	X			X	X	X		Duke & Masch (1973)
EAM	X	X	X	X	X		X	X	X	X	X	X	X	X		Tetra Tech (1979, 1980)
ESTECO	X	X	X		X		X	X	X	X	X	X	X	X		Brandes & Masch (1977)
EXPLORE-1	X	X	X		X		X	P	X	X		X	X	X		Baca et al. (1973)
HSPF	X	X	X		X		X	X*	X	X		X	X	X		Johanson et al. (1980)
LAKECO	X	X	X		X		X	X	X	X	X	X	X	X		Chen & Orlob (1975)
MIT Network		X			X	N	X		X	X		X	X	X		Harleman et al. (1977)
QUAL-II		X	X		X			X*	X			X	X	X		Roesner et al. (1981)
RECEIV-II		X	X		X				X			X	X	X		Raytheon (1974)
SSAM IV		X	X		X				X			X		X		Grenney & Kraszewski (1981)
WASP	X	X	X	X	X	X	X	X	X	X		X		X		Di Toro et al. (1981)
WQRRS	X	X	X		X		X	X	X	X	X	X	X	X		Smith (1978)
Bierman		X	X	X	X		X		X	X					X	Bierman et al. (1980)
Canale		X	X	X	X	X	X		X	X		X		X		Canale et al. (1975, 1976)
Jorgensen		X	X		X		X	X	X	X	X				X	Jorgensen (1976)
Lehman	X	X	X		X				X						X	Lehman et al. (1975)
Nyholm		X	X		X		X	X	X						X	Nyholm (1978)
Scavia	X	X	X		X	N	X	X	X	X		X		X		Scavia et al. (1976)

*Specify flux.

$$K_T = K_{20}\,\theta^{(T-20)} \qquad 5\text{-}5)$$

where K_T = rate coefficient at temperature T, 1/time
T = temperature, ^oC
K_{20} = rate coefficient at 20^oC, 1/time
θ = temperature adjustment coefficient

This relationship is derived in Section 3.3 of Chapter 3.

A few models use different temperature adjustment formulations. For example, Canale (1976) uses a linear relationship and Grenney and Kraszweski (1981) use a logistic equation as a temperature adjustment function.

5.5 CARBON TRANSFORMATIONS

Table 5-2 presents rate coefficients for carbon decay processes along with the corresponding temperature adjustment factors. As shown in the table, these coefficients have a broad range, indicating a lack of detailed process characterization. Process characterization has been neglected in carbon models since the relationship of carbon dynamics to water quality modeling has not been considered essential. In fact, most water quality models do not include carbon since it is not usually a limiting nutrient. In the Lake Erie version of WASP (Di Toro and Connolly, 1980), the rate of decay of particulate organic carbon to CO_2 has been further reduced by using a saturation relationship (Di Toro and Connolly, 1980). However, the decay rates in all other models are computed according to the first-order kinetics discussed above.

Most of the temperature adjustment factors in Table 5-2 range from 1.02 to 1.047, corresponding to Q_{10} values ranging between 1.2 and 1.6. The exception is the Lake Erie WASP model (Di Toro and Connolly, 1980), which uses a temperature correction factor of 1.08 (Q_{10} = 2.16) for decay of settled algae and sediment organic matter. Also, the decay rate constants for these compartments are generally higher than those used in other models.

TABLE 5-2. RATE COEFFICIENTS FOR CARBON TRANSFORMATIONS

POC → CO_2		SOC → CO_2		SA → SOC		SA → CO_2		References
K	θ	K	θ	K	θ	K	θ	
0.1**	1.04	0.00025	1.08	0.02	1.08	0.02	1.08	Di Toro & Connolly (1980)
0.05	1.045							O'Connor *et al.* (1981)
0.001	1.02	0.001	1.02					Chen & Orlob (1972, 1975)
0.003	1.020	0.0015	1.047					Tetra Tech (1980)
0.02	1.020	0.001	1.020					Bowie *et al.* (1980)
0.1	1.047	0.0015	1.047					Porcella *et al.* (1983)
0.005-0.05***	1.02-1.04***	0.001-0.01***	1.02-1.04***					Smith (1978)
0.001-0.02***	1.040***	0.001-0.02***	1.040***					Brandes (1976)

*Abbreviations are defined as follows:

POC - Particulate Organic Carbon
CO_2 - Carbon Dioxide
SOC - Sediment Organic Carbon
SA - Settled Algae

**This rate is multiplied by an oxygen limitation factor, $\frac{O_2}{K_1+O_2}$, where K_1 is a half-saturation constant for oxygen.

***Model documentation values.

5.6 NITROGEN TRANSFORMATIONS

Nitrogen dynamics are modeled in a considerably more complex manner than carbon because of their substantial biogeochemical role, important oxidation-reduction reactions, and because other important water quality variables such as oxygen are affected by nitrogen. The processes that are simulated in water quality models include:

- Ammonification - release of ammonia due to decay processes (deamination, hydrolysis).

- Nitrification - oxidation of ammonia to nitrate (NO_3^-) directly (one-stage process) or to nitrite (NO_2^-) and then to nitrate (two-stage process). Nitrification is discussed in detail in Section 3.4 of Chapter 3 in reference to its effects on dissolved oxygen.

- Denitrification - reduction of nitrate to N_2 under anaerobic conditions. This process also produces N_2O (10 percent of total reduced), but since N_2O has not been shown to have an appreciable effect on water quality, N_2O production has not been modeled.

- Uptake - accumulation of inorganic nitrogen by plants during photosynthetic growth. Both ammonia and nitrate are accumulated, with preference for ammonia over oxidized forms, although not all models include this preference.

- Nitrogen fixation - reduction of N_2 to ammoniated compounds. Nitrogen fixation by blue-green algae is an important external input of nitrogen accumulation in waterbodies that materially affects nitrogen dynamics. However, uptake of inorganic ions takes precedence over nitrogen fixation.

In addition to the above processes, unionized ammonia can play a significant role as a toxicant depending on the ammonia concentration, pH, and temperature.

Table 5-3 presents rate coefficients for the major nitrogen decay and abiotic transformation processes along with the corresponding temperature ajdustment factors. The decay processes shown include breakdown of complex organic compounds (particulate organic nitrogen, PON) to simpler organics (dissolved organic nitrogen, DON) or to ammonia, the breakdown of sediment nitrogen to ammonia, and the oxidation of ammonia to nitrate. Rate constants for ammonia decay to nitrite and then to nitrate or from ammonia to nitrate directly are approximately commensurate as an overall rate process. The rate coefficients for some of the decay processes in some versions of WASP are further reduced by saturation kinetics (Di Toro and Connolly, 1980; Di Toro and Matystik, 1980; Thomann and Fitzpatrick, 1982; O'Connor et al., 1981). For example, the decay of particulate organic nitrogen to ammonia is reduced as chlorophyll a decreases, and the nitrification rate is reduced as dissolved oxygen decreases, according to saturation kinetics.

The temperature adjustment factors have a wide range of values, indicating some uncertainty in this coefficient. The Q_{10} values generally range from 1.2 to 2.4, but with one value as high as 3.7.

5.6.1 Denitrification and Nitrogen Fixation

Both of these processes affect the mass balance of nitrogen because nitrogen is transported to (denitrification) or from (nitrogen fixation) the atmosphere rather than recycling within the water. Although both processes have been shown to be important in certain aquatic environments, denitrification is not commonly included in models. HSPF (Johanson et al., 1980), CE-QUAL-R1 (WES, 1982), Jorgensen (1976), AQUA-IV (Baca and Arnett, 1976), and some versions of WASP (Di Toro and Connolly, 1980; Thomann and Fitzpatrick, 1982; O'Connor et al., 1981) include denitrification.

TABLE 5-3. RATE COEFFICIENTS FOR NITROGEN TRANSFORMATIONS

PON → DON		DON → NH_3		PON → NH_3		NH_3 → NO_2		NH_3 → NO_3		NO_2 → NO_3		SEDN → NH_3		References
K	θ	K	θ	K	θ	K	θ	K	θ	K	θ	K	θ	
								Calibration Values						
				0.035	(linear)			0.04	(linear)					Thomann et al. (1975)
				0.03**	1.08									Thomann et al. (1979)
				0.03***	1.08			0.12***	1.08			0.0025	1.08	Di Toro & Connolly (1980)
				0.03***	1.08			0.20	1.08					Di Toro & Matystik (1980)
				0.075	1.08			0.09-0.13***	1.08			0.0004	1.08	Thomann & Fitzpatrick (1982)
								0.025***	1.08					O'Connor et al. (1981)
				0.14	(linear)									Salas & Thomann (1978)
				0.001	1.02	0.003-0.03	1.02			0.09	1.02	0.001	1.02	Chen & Orlob (1972, 1975)
0.020	(linear)	0.020	(linear)					0.060	(linear)					Scavia et al. (1976)
0.020	(linear)	0.020	(linear)					0.1	(linear)					Scavia (1980)
0.02	1.020	0.02	1.020					0.1	1.020					Bowie et al. (1980)
0.02	(linear)	0.024	(linear)					0.16	(linear)					Canale et al. (1976)
				0.003	1.020	0.02	1.047			0.25	1.047	0.0015	1.047	Tetra Tech (1980)
				0.1	1.047	0.02	1.047			0.25	1.047	0.0015	1.047	Porcella et al. (1983)
				0.01**	NI							0.95-1.8***	1.14	Nyholm (1978)
				0.005**	1.08									Bierman et al. (1980)
				0.1**	1.02									Jorgensen (1976)
				0.2**	1.072									Jorgensen et al. (1978)

(continued)

TABLE 5-3. (continued)

PON → DON		DON → NH_3		PON → NH_3		NH_3 → NO_2		NH_3 → NO_3		NO_2 → NO_3		SEDN → NH_3		References
K	θ	K	θ	K	θ	K	θ	K	θ	K	θ	K	θ	
						Model Documentation Values								
				0.1-0.4	NI	0.1-0.5	NI			5.-10.	NI			Baca et al. (1973)
				0.02-0.04	1.02-1.09	0.1-0.5	1.02-1.09			3.-10.	1.02-1.09	0.01-0.1	1.02-1.09	Baca & Arnett (1976)
						0.1-0.5	1.047			0.5-2.0	1.047			Duke & Masch (1973)
						0.1-0.5	1.047			0.5-20	1.047			Roesner et al. (1978)
				0.005-0.05	1.02-1.04	0.05-0.2	1.02-1.03			0.2-0.5	1.02-1.03	0.001-0.01	1.02-1.04	Smith (1978)
				0.001-0.02	1.040	0.05-0.2	1.02			0.2-0.5	1.02	0.001-0.02	1.040	Brandes (1976)
								0.04-3.0	(logistic)					Greenney & Kraszewski (1981)
								0.001-1.3****	NI					Collins & Wlosinski (1983)

*Abbreviations are defined as follows:

NI - No Information
PON - Particulate Organic Nitrogen
DON - Dissolved Organic Nitrogen
SEDN - Sediment Organic Nitrogen

**Unavailable nitrogen decaying to algal-available nitrogen.

***Di Toro & Connolly (1980) and Di Toro & Matystik (1980) multiply the PON NH_3 rate by a chlorophyll limitation factor, $\frac{Chl\ a}{K_1+Chl\ a}$, where K_1 is half-saturation constant = 5.0 μg Chl a/l.

Di Toro & Connolly (1980) and Thomann & Fitzpatrick (1982) multiply the NH_3 NO_3 rate by an oxygen limitation factor, $\frac{O_2}{K_2+O_2}$, where K_2 is a half-saturation constant = 2.0 mgO_2/l.

O'Connor et al. (1981) multiply the NH_3 NO_3 rate by an oxygen limitation factor, $\frac{O_2}{K_3+O_2}$, where K_3 is a half-saturation constant = 0.5 mgO_2/l.

Nyholm (1978) uses a sediment release constant which is multiplied by the total sedimentation rate of algae and detritus.

****Literature value.

Denitrification rates and the corresponding temperature adjustment coefficients are listed in Table 5-4. The decay rates for the WASP model are further modified according to a saturation type relationship based on the dissolved oxygen concentration. The rate decreases rapidly as O_2 increases above 0.01 mg/l. This rate would be equivalent to that of Jorgensen (1976) when O_2 = 5 mg/l. This indicates disagreement in conceptualization of the process or in its quantitative response between the two models. Sediment nitrate denitrification helps decrease the gradient of the sediment oxygen demand (SOD) and may lead to a reduced requirement for SOD (see Chapter 3.5; also, Di Toro, 1984).

Nitrogen fixation by blue-green algae is modeled by assuming that growth is not limited by nitrogen and that nitrogen fixation makes up for all nitrogen requirements which cannot be satisfied by ammonia and nitrate. Some type of saturation relationship is typically used to partition the nitrogen requirements between nitrogen fixation and uptake of ammonia and nitrate. The major features of these relationships are as follows: 1) no fixation occurs when ammonia plus nitrate are above some critical threshold concentration; 2) for concentrations below the threshold, nitrogen fixation increases as ammonia and nitrate decrease; and 3) when ammonia and nitrate become very low, all of the nitrogen requirements are supplied by fixation. Nitrogen fixation is included in the EAM (Tetra Tech, 1979), Scavia et al. (1976), Canale et al. (1976), and Bierman et al. (1980) models.

5.6.2 Unionized Ammonia

Although nitrogen is an important nutrient required by microorganisms, plants, and animals, certain forms such as unionized ammonia (NH_3) can be toxic. Unionized ammonia is toxic to fish at fairly low concentrations. For example, water quality criteria ranging from 0.0015 to 0.12 mg N/l for the 30-day average concentration have been suggested (USEPA, 1984). This range exists because the biological response varies at different temperature and pH values.

Both analytical measurement techniques and most model formulations for ammonia are based on total ammonia:

TABLE 5-4. RATE COEFFICIENTS FOR DENITRIFICATION

Nitrate → Nitrogen Gas		References
K	θ	
0.1*	1.045	Di Toro & Connolly (1980)
0.1**	1.045	Di Toro & Connolly (1980)
0.09*	1.045	Thomann & Fitzpatrick (1982)
0.1*	1.045	O'Connor et al. (1981)
0.002	No Information	Jorgensen (1976)
0.02-0.03	No Information	Jorgensen et al. (1978)
0.-1.0***	1.02-1.09***	Baca & Arnett (1976)

*This rate is multiplied by an oxygen limitation factor, $\frac{K_1}{K_1+O_2}$, where K_1 is a half-saturation constant = $0.1 mgO_2/l$.

**The same rate applies to sediment NO_3 dentrification.

***Model documentation values.

$$X = \text{total ammonia} = NH_3 + NH_4^+ \tag{5-6}$$

The concentrations of NH_3 and NH_4^+ vary considerably over the range of pH and temperature found in natural waters, but each can be readily calculated assuming that equilibrium conditions exist (Stumm and Morgan, 1981). Unionized ammonia exists in equilibrium with ammonia ion and hydroxide ion (Emerson, et al., 1975):

$$NH_3(g) + nH_2O = NH_3{:}nH_2O = NH_4^+ + OH^- + (n-1)\ H_2O \tag{5-7}$$

The reaction occurs rapidly and is controlled largely by pH and temperature. Thus, unionized ammonia is calculated from the equilibrium expression:

$$K_i = \frac{(NH_4^+)(OH^-)}{(NH_3)(H_2O)} = \frac{(NH_4^+)K_w}{(NH_3)(H^+)} \tag{5-8}$$

Rearranging and taking the negative logarithm:

$$\log \frac{(NH_4^+)}{(NH_3)} = pK_w - pK_i - pH \tag{5-9}$$

The quantity pK_h is called the hydrolysis constant. Substituting and taking the inverse logarithms,

$$\left(\frac{X - NH_3}{NH_3}\right) = 10^{(pK_h - pH)} = R \tag{5-10}$$

and solving for NH_3,

$$NH_3 = \frac{X}{1 + R} \tag{5-11}$$

Thurston et al., (1974) determined the temperature correction for the hydrolysis constant as follows:

$$pK_h = 0.09018 + 2729.92/T \tag{5-12}$$

where T = absolute temperature, ^oK

Substituting this relationship into Equation 5-7, unionized ammonia in moles/liter becomes a function of measured ammonia, temperature, and pH. Most water quality models predict the concentration of measured ammonia (X) in units of weight/volume as a resultant of processes of nitrification, ammonification, respiration, and assimilation. For NH_3-N, there are 14,000 mg/mole and

$$NH_3\text{-N, mg/l} = \frac{14000(X)}{1 + R} \tag{5-13}$$

Although more cumbersome, a table of equilibrium values for unionized ammonia can be used in a model (e.g., USEPA, 1984). Figure 5-5 illustrates the relationship between pH, water temperature, and unionized ammonia.

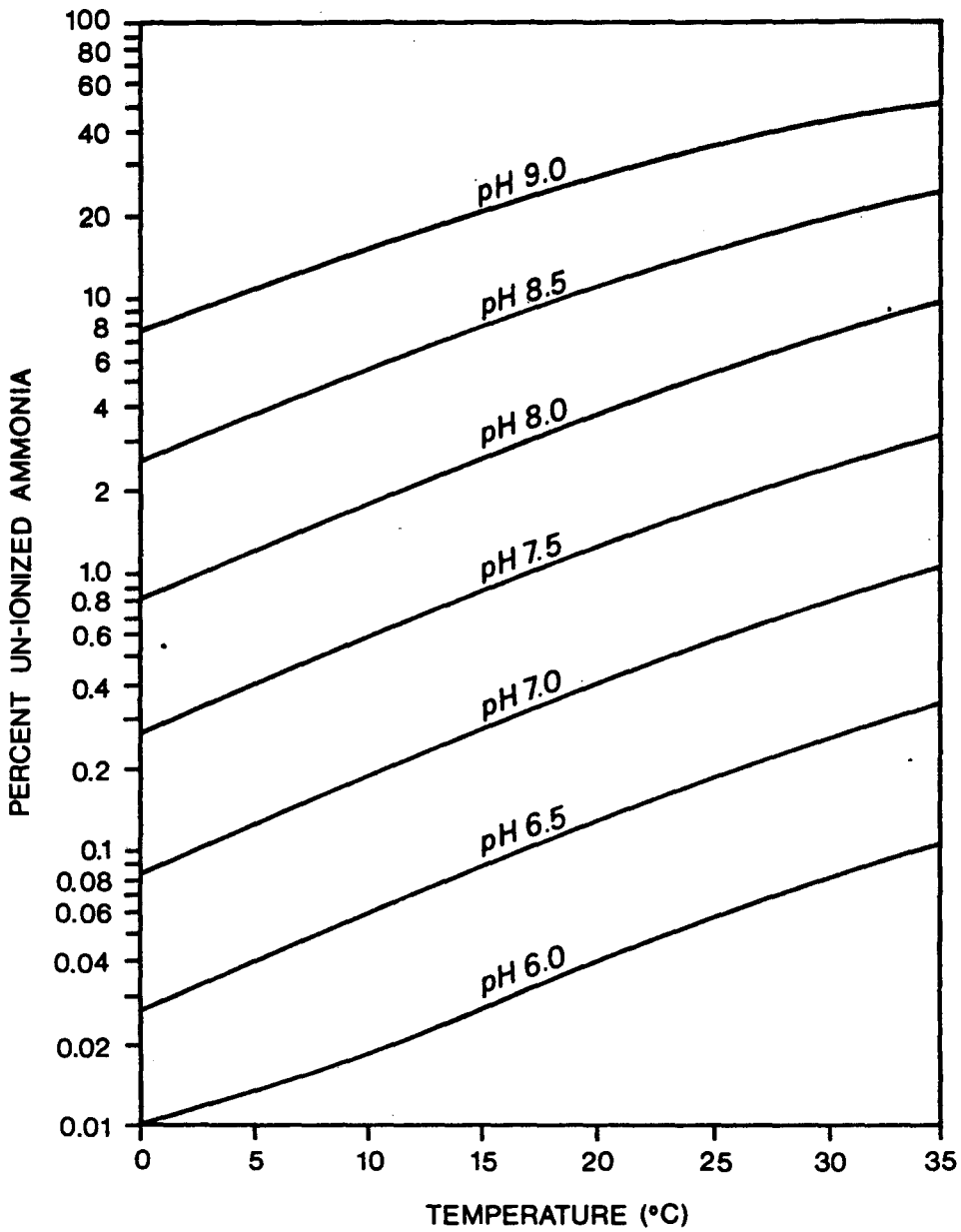

Figure 5-5. Effect of pH and temperature on unionized ammonia (from Willingham, 1976).

5.7 PHOSPHORUS TRANSFORMATIONS

Table 5-5 presents rate coefficients and temperature correction factors for the various phosphorus transformation processes included in water quality models. The transformations include the decay of particulate organic phosphorus (POP), sediment phosphorus (SEDP), and settled algae (SA) directly to PO_4-P or into intermediate forms (dissolved organic phosphorus, DOP) before decaying to PO_4-P. The decay rates have a broad range, indicating some uncertainty in quantifying these processes. Similarly, there is a broad range in temperature coefficients, with a Q_{10} range from 1.2 to 2.4, except for a Q_{10} value of 3.7 for Nyholm (1978). Several of the WASP models adjust the phosphorus decay rates using a saturation equation based on algal biomass (Di Toro and Connolly, 1980; Di Toro and Matystik, 1980; Salisbury et al., 1983; Thomann and Fitzpatrick, 1982). In the case where chlorophyll a is used to estimate algal biomass, the half-saturation constant is 5.0 g/l, and where carbon is used to estimate algal biomass, the value is 1.0 mgC/l.

5.8 SILICON TRANSFORMATIONS

Silicon can be limiting only for diatoms, so its biogeochemical cycle is simulated only when diatoms are modeled as a separate algal group. Diatoms are important because of their role in phytoplankton succession, their role in aquatic food chains, and their potential effects on water treatment plants. Table 5-6 presents decay rates and temperature adjustment coefficients for silicon. In contrast to the other nutrients, particulate and sediment silicon decay directly to dissolved inorganic silicon rather than passing through a dissolved organic phase. The range of the first-order decay rates for particulate silica decay is 0.003-0.1 (1/day). The temperature adjustment factor varies between 1.02 and 1.08, corresponding to a Q_{10} range of 1.2 to 2.2.

TABLE 5-5. RATE COEFFICIENTS FOR PHOSPHORUS TRANSFORMATIONS

POP → DOP		POP → PO_4		DOP → PO_4		SEDP → DOP		SEDP → PO_4		Sediment DOP → PO_4		Sediment SA → DOP		Sediment SA → PO_4		References
K	θ	K	θ	K	θ	K	θ	K	θ	K	θ	K	θ	K	θ	
		0.14	(linear)													Thomann et al. (1975)
		0.03	1.08													Thomann et al. (1979)
		0.03**	1.08													Di Toro & Connolly (1980) Di Toro & Matystik (1980) Salisbury et al. (1983)
0.22**	1.08			0.22**	1.08	0.0004	1.08	0.0004	1.08	0.0004	1.08	0.02	1.08	0.02	1.08	Thomann & Fitzpatrick (1982)
		0.14	(linear)													Salas & Thomann (1978)
		0.001	1.02					0.001	1.02							Chen & Orlob (1972, 1975)
		0.02	(linear)													Scavia et al. (1976) Scavia (1980)
0.2	(linear)			0.2	(linear)											Canale et al. (1976)
		0.003	1.020					0.0015	1.047							Tetra Tech (1980)
		0.02	1.020					0.001	1.020							Bowie et al. (1980)
		0.1	1.047					0.0015	1.047							Porcella et al. (1983)
		0.1	1.14					1.0-1.7	1.14**							Nyholm (1978)
		0.005	1.08													Bierman et al. (1980)
		0.1	1.02					0.0018	1.02							Jorgensen (1976)
		0.5-0.8	1.072													Jorgensen et al. (1978)
		0.1-0.7***	1.02-1.09***					0.1-0.7***	1.02-1.09***							Baca et al. (1973)
		0.1-0.7***	1.02-1.09***													Baca & Arnett (1976)
		0.005-0.05***	1.02-1.04***					0.001-0.01***	1.02-1.04***							Smith (1978)
		0.001-0.02***	1.040***													Brandes (1976)

Abbreviations are defined as follows:

POP - Particulate Organic Phosphorus
DOP - Dissolved Organic Phosphorus
PO_4 - Phosphate
SEDP - Sediment Organic Phosphorus
SA - Settled Algae

**Di Toro & Connolly (1980), Di Toro & Matystik (1980) and Salisbury et al. (1983) multiply this rate by a chlorophyll limitation factor, $\frac{\text{Chl a}}{K_1+\text{Chl a}}$, where K_1 is a half-saturation constant = 5.0 μg Chl a/l.

Thomann & Fitzpatrick (1982) multiply this rate by an algal carbon limitation factor, $\frac{\text{Algal-C}}{K_2+\text{Algal-C}}$, where K_2 is a half-saturation constant = 1.0mgC/l.

Nyholm (1978) utilizes a sediment release constant which is multiplied by total sedimentation of algae and detritus.

***Model documentation values.

TABLE 5-6. RATE COEFFICIENTS FOR SILICA TRANSFORMATIONS

Particulate Silica → Dissolved Silica		Sediment Silica → Dissolved Silica		References
K	θ	K	θ	
0.0175	1.08			Thomann *et al.* (1979)
0.1	1.08			Di Toro & Connolly (1980)
0.04	(linear)			Scavia (1980)
0.03	(linear)			Canale *et al.* (1976)
0.003	1.020	0.005	1.047	Tetra Tech (1980)
0.01	1.020	0.001	1.020	Bowie *et al.* (1980)
0.04	1.047	0.0015	1.047	Porcella *et al.* (1983)
0.005	1.08			Bierman *et al.* (1980)

5.9 ALGAL UPTAKE

Two major approaches are used to simulate nutrient uptake by algae in water quality models. The most common method is the fixed stoichiometry approach in which the nutrient composition of the algae is assumed to remain constant. Under this assumption, the nutrient uptake rates are equal to the algal gross growth rate times the corresponding nutrient fractions of the algal cells:

$$V_s = \alpha_s \mu A \tag{5-14}$$

where V_s = uptake rate for nutrient S, mass/volume-time
α_s = nutrient fraction of algal cells, mass nutrient/mass algae
μ = gross growth rate of algae, 1/time
A = algal concentration, mass/volume

This formulation is used in all fixed stoichiometry models. Typical values of the nutrient compositions of algae are given in Tables 6-2 to 6-4 of Chapter 6. Algal growth formulations and the corresponding model coefficients are discussed in Section 6.4 of Chapter 6.

The second approach to modeling nutrient uptake is the variable stoichiometry approach. In this method, the internal nutrient composition of the algal cells varies with time depending on the external nutrient concentrations in the water column and the relative rates of nutrient uptake and algal growth. The uptake rate depends on the difference between the internal nutrient concentration in the algal cells and the external concentration in the water. The internal concentration of each nutrient is assumed to range between a minimum stoichiometric requirement (called the minimum cell quota or subsistence quota) and some maximum internal concentration. In general, the uptake rate increases both as the external nutrient concentration increases and as the internal nutrient concentration decreases toward the minimum cell quota. However, the uptake rate decreases as the internal concentration approaches the maximum internal level, regardless of the external concentration in the water.

In contrast to fixed stoichiometry models, the uptake formulations used in variable stoichiometry models vary from model to model. Some models even use different formulations for different nutrients. Variable stoichiometry formulations for nutrient uptake are discussed in Section 6.4.4.3 of Chapter 6, since nutrient uptake is an integral part of the algal growth formulations in variable stoichiometry models. The major formulations are given in Equations (6-63) to (6-67).

5.9.1 Ammonia Preference Factors

Since algae use two forms of nitrogen, ammonia and nitrate, during uptake and growth, many models use ammonia preference factors in the uptake formulations to account for the fact that algae tend to preferentially uptake ammonia over nitrate. Ammonia preference factors are generally used in fixed stoichiometry models when both ammonia and nitrate are simulated. In this case, the uptake equations for ammonia and nitrate become:

$$V_{NH_3} = \beta_{NH_3} \alpha_N \mu A \tag{5-15}$$

and

$$V_{NO_3} = (1 - \beta_{NH_3}) \alpha_N \mu A \tag{5-16}$$

where V_{NH_3} = ammonia uptake rate, mass/volume-time

V_{NH_3} = nitrate uptake rate, mass/volume-time

β_{NH_3} = ammonia preference factor

α_N = nitrogen fraction of algal cells

Ammonia preference factors are generally not needed in variable stoichiometry models since separate formulations with different coefficients can be used to distinguish between ammonia and nitrate uptake rates.

The ammonia preference factor $_{NH_3}$ partitions the nitrogen uptake required for a given amount of algal growth between ammonia and nitrate. The preference factor can range from 0 to 1, with 1 corresponding to a

situation in which all the nitrogen requirements are obtained from ammonia uptake, and 0 corresponding to a situation in which all the nitrogen is obtained from nitrate. The value of the preference factor is generally a function of the ammonia and nitrate concentrations in the water.

The simplest form of the ammonia preference factor assumes there is no preference for either form of nitrogen and partitions the uptake according to the relative proportions of ammonia and nitrate in the water:

$$NH_3 = \frac{NH_3}{NH_3 + NO_3} \tag{5-17}$$

where NH_3 = ammonia concentration, mass/volume
NO_3 = nitrate concentration, mass/volume

This approach is used in EXPLORE-1 (Baca et al., 1973), LAKECO (Chen and Orlob, 1975), WQRRS (Smith, 1978), CE-QUAL-R1 (WES, 1982), EAM (Tetra Tech, 1979), ESTECO (Brandes, 1976), and earlier versions of WASP (Thomann et al., 1975).

Other models which assume there is a preference for ammonia uptake have used the following formulations for the preference factor:

$$\beta_{NH_3} = \frac{\gamma_1 \, NH_3}{\gamma_1 \, NH_3 + NO_3} \tag{5-18}$$

$$\beta_{NH_3} = \frac{NH_3}{\gamma_2 + NH_3} \tag{5-19}$$

$$\beta_{NH_3} = \frac{\gamma_3 \, NH_3}{\gamma_3 \, NH_3 + (1 - \gamma_3) \, NO_3} \tag{5-20}$$

$$\beta_{NH_3} = \left(\frac{NH_3}{NH_3 + \gamma_4}\right)\left(\frac{NO_3}{NO_3 + \gamma_4}\right) + \left(\frac{NH_3}{NH_3 + NO_3}\right)\left(\frac{\gamma_4}{\gamma_4 + NO_3}\right) \tag{5-21}$$

where γ_1, γ_2, γ_3, γ_4 = coefficients in ammonia preference factor formulations

Equation (5-18) is used in SSAM IV (Grenney and Kraszewski, 1981) and Scavia et al. (1976), Equation (5-19) in an early Lake Erie WASP model by Di Toro et al. (1975), Equation (5-20) in AQUA-IV (Baca and Arnett, 1976) and Canale et al. (1976), and Equation (5-21) in more recent versions of WASP by Thomann and Fitzpatrick (1982) and O'Connor et al. (1981).

5.10 EXCRETION

Nutrient excretion by algae and zooplankton is one of the major components of nutrient recycling. In almost all models, nutrient excretion is modeled as the product of the respiration mass flux and the nutrient stoichiometry of the organisms. The equations for algal excretion and zooplankton excretion are:

$$e_{sa} = \alpha_{sa} r_a A \tag{5-22}$$

and

$$e_{sz} = \alpha_{sz} r_z Z \tag{5-23}$$

where e_{sa} = algal excretion rate of nutrient S, mass/volume-time
e_{sz} = zooplankton excretion rate of nutrient S, mass/volume-time
α_{sa} = nutrient fraction of algal cells, mass nutrient/mass algae
α_{sz} = nutrient fraction of zooplankton, mass nutrient/mass zooplankton
r_a = algal respiration rate, 1/time
r_z = zooplankton respiration rate, 1/time
A = algal concentration, mass/volume
Z = zooplankton concentration, mass/volume

The excretion formulations for other organisms such as fish or benthic animals is the same as for zooplankton. Respiration rate formulations for algae and zooplankton are discussed in Section 6.5 (Chapter 6) and 7.4 (Chapter 7), respectively. The nutrient compositions of algae are presented in Tables 6-2 to 6-4 of Chapter 6. The nutrient compositions of zooplankton are typically assumed to be the same as for algae in fixed stoichiometry models so that nutrient mass is conserved as biomass cycles through the food web.

5.11 SEDIMENT RELEASE

Three major approaches have been used to simulate nutrient release from the sediments in water quality models. The simplest approach is to specify an areal flux from the bottom in the mass balance equations for dissolved nutrients. This technique is commonly used in river models and in models which do not dynamically simulate sediments as a separate constituent (e.g., QUAL-II (Roesner et al., 1981), DOSAG3 (Duke and Masch, 1973), and HSPF (Johanson et al., 1980)). Sediment release rates are highly site-specific, and are determined largely by model calibration of the dissolved nutrients.

The second approach is to model sediment nutrients as a dynamic pool using a mass balance equation such as Equation (5-4). In this method, nutrients are released according to a first-order decay rate:

$$R_s = \alpha_s K_{sed} \, Sed \tag{5-24}$$

where R_s = sediment release rate of nutrient S, mass/volume-time
α_s = stoichiometric ratio of nutrient per mass organic sediment
K_{sed} = organic sediment decay rate, 1/time
Sed = concentration of organic sediment, mass/volume

The organic sediment pool increases as algae and suspended organic detritus settle to the bottom, and decreases as the sediment decomposes. This approach is used in LAKECO (Chen and Orlob, 1975), Chen et al. (1975), WQRRS (Smith, 1978), CE-QUAL-R1 (WES, 1982), EAM (Tetra Tech, 1979), and ESTECO (Brandes, 1976). In some models, a fraction of the settled particulates is assumed to be refractory and unavailable for mineralization.

The third approach to modeling sediment release uses a more complex mechanistic approach in which: 1) organic sediments undergo the same decay sequences as particulate organics in the water column but with the decay products going to the interstitial water rather than the overlying water, and 2) the nutrients in the interstitial waters diffuse to the overlying water at a rate depending on the concentration gradient between the

interstitial water and overlying water. This approach is used in some versions of WASP (e.g., Di Toro and Connolly, 1980; Thomann and Fitzpatrick, 1982). A few models also include denitrification in the transformation reactions.

Nyholm (1978) simulates sediment release dynamically without actually modeling sediments by assuming the release rates equal the product of a temperature dependent coefficient times the sedimentation rates of algal and detrital nutrients to the bottom.

5.12 SUMMARY

Carbon, nitrogen, phosphorus, and silicon are the major growth limiting nutrients included in water quality models. Nitrogen is also important because of the effects of nitrification on dissolved oxygen dynamics and because of ammonia toxicity. All nutrients recycle continuously in the water column between particulate and sediment forms, dissolved organic forms, dissolved inorganic forms, and biotic forms. The important processes are decomposition of organic particulates and sediments, decay of dissolved organic to inorganic forms, chemical transformations such as nitrification, photosynthetic uptake of dissolved inorganic forms, and soluble and particulate excretion by aquatic organisms. Denitrification and nitrogen fixation are also important in some situations.

First-order kinetics are used in almost all models to describe the various decay processes and transformations. The exponential Arrhenius or van't Hoff relationship is used to adjust the rate coefficients for temperature effects. Some of the processes are modified by Michaelis-Menten type saturation kinetics in a few models. Uptake and excretion are based on algal growth rates and algal and zooplankton respiration rates combined with the nutrient stoichiometries of the organisms. More complex formulations are used for nutrient uptake in variable stoichiometry models. Sediment release rates are usually modeled either by specifying a nutrient flux or modeling sediments as a nutrient pool subject to first-order decay. A few models use more complex formulations which include decay reactions in the

interstitial waters and diffusion between the interstitial waters in the sediment and the overlying water column.

5.13 REFERENCES

Baca, R.G., W.W. Waddel, C.R. Cole, A. Brandstetter, and D.B. Clearlock. 1973. EXPLORE-I: A River Basin Water Quality Model. Battelle, Inc., Pacific Northwest Laboratories, Richland, Washington.

Baca, R.G. and R.C. Arnett. 1976. A Limnological Model for Eutrophic Lakes and Impoundments. Battelle, Inc., Pacific Northwest Laboratories, Richland, Washington.

Bierman, V.J., Jr. 1976. Mathematical Model of the Selective Enhancement of Blue-Green Algae by Nutrient Enrichment. In: Modeling Biochemical Processes in Aquatic Ecosystems. R.P. Canale (ed.). Ann Arbor Science Publishers, Ann Arbor, Michigan. pp. 1-31.

Bierman, V.J., Jr., D.M. Dolan, E.F. Stoermer, J.E. Gannon, and V.E. Smith. 1980. The Development and Calibration of a Multi-Class Phytoplankton Model for Saginaw Bay, Lake Huron. Great Lakes Environmental Planning Study. Contribution No. 33. Great Lakes Basin Commission, Ann Arbor, Michigan.

Bloomfield, J.A., R. A. Park, D. Scavia, and C.S. Zahorcak. 1973. Aquatic Modeling in the Eastern Deciduous Forest Biome. U.S. International Biological Program. In: Modeling the Eutrophication Process. E.J. Middlebrook, D.H. Falkenborg, and T.E. Maloney, (eds.). Utah State University, Logan, Utah. pp. 139-158.

Bowie, G.L., C.W. Chen, and D.H. Dykstra. 1980. Lake Ontario Ecological Modeling, Phase III, Tetra Tech, Inc., Lafayette, California. For National Oceanic and Atmospheric Administration, Great Lakes Environmental Research Laboratory, Ann Arbor, Michigan.

Brandes, R.J. 1976. An Aquatic Ecologic Model for Texas Bays and Estuaries. Water Resources Engineers, Inc., Austin, Texas. For the Texas Water Development Board, Austin, Texas.

Brandes, R.J. and F.D. Masch. 1977. ESTECO--Estuarine Aquatic Ecologic Model: Program Documentation and User's Manual. Water Resources Engineers, Inc., Austin, Texas. For the Texas Water Development Board, Austin, Texas.

Canale, R.P., L.M. Depalma, and A.H. Vogel. 1975. A Food Web Model for Lake Michigan. Part 2 - Model Formulation and Preliminary Verification. Tech. Report 43, Michigan Sea Grant Program, MICHU-SG-75-201.

Canale, R.P., L.M. Depalma, and A.H. Vogel. 1976. A Plankton-Based Food Web Model for Lake Michigan. In: Modeling Biochemical Processes in Aquatic Ecosystems. R.P. Canale (ed.). Ann Arbor Science Publishers, Ann Arbor, Michigan. pp. 33-74.

Chen, C.W. and G.T. Orlob. 1972. Ecologic Simulations of Aquatic Environments. Water Resources Engineers, Inc., Walnut Creek, California. For the Office of Water Resources Research.

Chen, C.W. and C.T. Orlob. 1975. Ecological Simulation for Aquatic Environments. In: Systems Analysis and Simulation in Ecology, Vol. 3. B.C. Patten (ed.). Academic Press, Inc., New York, New York. pp. 476-588.

Chen, C.W., M. Lorenzen, and D.J. Smith. 1975. A Comprehensive Water Quality-Ecological Model for Lake Ontario. Tetra Tech, Inc., Lafayette, California. For National Oceanic and Atmospheric Administration, Great Lakes Environmental Research Laboratory, Ann Arbor, Michigan.

Collins, C.D. and J.H. Wlosinski. 1983. Coefficients for Use in the U.S. Army Corps of Engineers Reservoir Model, CE-QUAL-R1. U.S. Army Corps of Engineers, Waterways Experiment Station, Vicksburg, Mississippi.

Di Toro, D.M., D.J. O'Connor, R.V. Thomann, and J.L. Mancini. 1975. Phytoplankton-Zooplankton Nutrient Interaction Model for Western Lake Erie. In: Systems Analysis and Simulation in Ecology, Vol. III. B.C. Patton (ed.). Academic Press, Inc., New York, New York. 423 pp.

Di Toro, D.M. and J.P. Connolly. 1980. Mathematical Models of Water Quality in Large Lakes. Part II: Lake Erie. U.S. Environmental Protection Agency, Ecological Research Series. EPA-600/3-3-80-065.

Di Toro, D.M. and W.F. Matystik, Jr. 1980. Mathematical Models of Water Quality in Large Lakes. Part I: Lake Huron and Saginaw Bay. U.S. Environmental Protection Agency, Ecological Research Series. EPA-600/3-80-056.

Duke, J.H., Jr. and F.D. Masch. 1973. Computer Program Documentation for the Stream Quality Model DOSAG3, Vol. I. Water Resources Engineers, Inc., Austin, Texas. For U.S. Environmental Protection Agency, Systems Development Branch, Washington, D.C.

Emerson, K., R.C. Russo, R.E. Lund, and R.V. Thurston. 1975. Aqueous Ammonia Equilibrium Calculations: Effect of pH and Temperature. J. Fish. Res. Board Can., 32(12):2379-2383.

Feigner, K.D. and H. Harris. 1970. FWQA Dynamic Estuary Model, Documentation Report. U.S.D.I., F.W.Q.A., Washington, D.C.

Grenney, W.J. and A.K. Kraszewski. 1981. Description and Application of the Stream Simulation and Assessment Model: Version IV (SSAM IV). Instream Flow Information Paper. U.S. Fish and Wildlife Service, Fort Collins, Colorado, Cooperative Instream Flow Service Group.

Harleman, D.R.F., J.E. Dailey, M.L. Thatcher, T.O. Najarian, D.N. Brocard, and R.A. Ferrara. 1977. User's Manual for the M.I.T. Transient Water Quality Network Model--Including Nitrogen-Cycle Dynamics for Rivers and Estuaries. R.M. Parsons Laboratory for Water Resources and Hydrodynamics,

Massachusetts Institute of Technology, Cambridge, Massachusetts. For U.S. Environmental Protection Agency, Corvallis, Oregon. EPA-600/3-77-010.

Johanson, R.C., J.C. Imhoff, and H.H. Davis. 1980. User's Manual for Hydrological Simulation Program - Fortran (HSPF). Hydrocomp, Inc., Mountain View, California. For U.S. Environmental Protection Agency, Athens, Georgia. EPA-600/9-80-015.

Jorgensen, S.E. 1976. A Eutrophication Model for a Lake. Ecol. Modeling, 2:147-165.

Jorgensen, S.E., H. Mejer, and M. Friis. 1978. Examination of a Lake Model. Ecol. Modeling, 4:253-278.

Lehman, J.T., D.B. Botkin, and G.E. Likens. 1975. The Assumptions and Rationales of a Computer Model of Phytoplankton Population Dynamics. Limnol. and Oceanogr., 20(3):343-364.

Nyholm, N. 1978. A Simulation Model for Phytoplankton Growth and Nutrient Cycling in Eutrophic, Shallow Lakes. Ecol. Modeling, 4:279-310.

O'Connor, D.J., J.L. Mancini, and J.R. Guerriero. 1981. Evaluation of Factors Influencing the Temporal Variation of Dissolved Oxygen in the New York Bight, Phase II. Manhattan College, Bronx, New York.

Park, R.A., C.D. Collins, C.I. Connolly, J.R. Albanese, and B.B. MacLeod. 1980. Documentation of the Aquatic Ecosystem Model MS.CLEANER. Rensselaer Polytechnic Institute, Center for Ecological Modeling, Troy, New York. For U.S. Environmental Protection Agency, Environmental Research Laboratory, Office of Research and Development, Athens, Georgia.

Porcella, D.B., T.M. Grieb, G.L. Bowie, T.C. Ginn, and M.W. Lorenzen. 1983. Assessment Methodology for New Cooling Lakes, Vol. 1: Methodology to Assess Multiple Uses for New Cooling Lakes. Tetra Tech, Inc., Lafayette, California. For Electric Power Research Institute. Report EPRI EA-2059.

Raytheon Company, Oceanographic & Environmental Services. 1974. New England River Basins Modeling Project, Vol. III - Documentation Report, Part 1 - RECEIV-II Water Quantity and Quality Model. For Office of Water Programs, U.S. Environmental Protection Agency, Washington, D.C.

Roesner, L.A., P.R. Giguere, and D.E. Evenson. 1981. Computer Program Documentation for the Stream Quality Model QUAL-II. U.S. Environmental Protection Agency, Athens, Georgia. EPA 600/9-81-014.

Salas, H.J. and R.V. Thomann. 1978. A Steady-State Phytoplankton Model of Chesapeake Bay. Journal WPCF, 50(12):2752-2770.

Salisbury, D.K., J.V. DePinto, and T.C. Young. 1983. Impact of Algal-Available Phosphorus on Lake Erie Water Quality: Mathematical Modeling. For U.S. Environmental Protection Agency, Environmental Research Laboratory, Duluth, Minnesota.

Scavia, D., B.J. Eadie, and A. Robertson. 1976. An Ecological Model for Lake Ontario - Model Formulation, Calibration, and Preliminary Evaluation. Natl. Ocean. and Atmos. Admin., Boulder, Colorado. NOAA Tech. Rept. ERL 371-GLERL 12.

Scavia, D. and R.A. Park. 1976. Documentation of Selected Constructs and Parameter Values in the Aquatic Model CLEANER. Ecol. Modeling, 2:33-58.

Scavia, D. 1980. An Ecological Model of Lake Ontario. Ecol. Modeling, 8:49-78.

Smith, D.I. 1978. Water Quality for River-Reservoir Systems. Resource Management Associates, Inc., Lafayette, California. For U.S. Army Corps of Engineers, Hydrologic Engineering Center (HEC), Davis, California. pp 210.

Stumm, W. and J.J. Morgan. 1970 (First Edition). 1981 (Second Edition). Wiley-Interscience. New York, New York. 583 pp., 780 pp.

Tetra Tech, Inc. 1979. Methodology for Evaluation of Multiple Power Plant Cooling System Effects, Volume II. Technical Basis for Computations. Tetra Tech, Inc., Lafayette, California. For Electric Power Research Institute. Report EPRI EA-1111.

Tetra Tech, Inc. 1980. Methodology for Evaluation of Multiple Power Plant Cooling System Effects, Volume V. Methodology Application to Prototype - Cayuga Lake. Tetra Tech, Inc., Lafayette, California. For Electric Power Research Institute. Report EPRI EA-1111.

Thomann, R.V., D.M. Di Toro, R.P. Winfield, and D.J. O'Connor. 1975. Mathematical Modeling of Phytoplankton in Lake Ontario, Part 1. Model Development and Verification. Manhattan College, Bronx, New York. For U.S. Environmental Protection Agency, Corvallis, Oregon. EPA-600/3-75-005.

Thomann, R.V., J. Segna, and R. Winfield. 1979. Verification Analysis of Lake Ontario and Rochester Embayment Three-Dimensional Eutrophication Models. Manhattan College, Bronx, New York. For U.S. Environmental Protection Agency, Office of Research and Development.

Thomann, R.V. and J.J. Fitzpatrick. 1982. Calibration and Verification of a Mathematical Model of the Eutrophication of the Potomac Estuary. Government of the District of Columbia, Washington, D.C.

Thurston, R.V., R.C. Russo, and K. Emerson. 1974. Aqueous Ammonia Equilibrium Calculations. Fisheries Bioassay Laboratory, Montana State Univ., Boseman, Montana. Technical Report No. 74-1.

U.S. Environmental Protection Agency. 1984. Water Quality Criteria for the Protection of Aquatic Life and Its Uses - Ammonia. USEPA, Criteria and Standards. Washington, D.C.

WES (Waterways Experiment Station). 1982. CE-QUAL-R1: A Numerical One-Dimensional Model of Reservoir Water Quality, Users Manual. Environmental

and Water Quality Operational Studies (EWQOS), U.S. Army Corps of Engineers, Waterways Experiment Station, Vicksburg, Mississippi.

Willingham, W.T. 1976. Ammonia Toxicity. EPA 908/3-76-001.

Chapter 6

ALGAE

6.1 INTRODUCTION

Algae are important components of water quality models for several reasons. For example:

- Algal dynamics and nutrient dynamics are closely linked together since nutrient uptake during algal growth is the main process which removes dissolved nutrients from the water, and algal respiration and decay are major components of nutrient recycling.

- Algal processes can cause diurnal variations in dissolved oxygen due to photosynthetic oxygen production during the daylight combined with oxygen consumption due to algal respiration during the night. Seasonal oxygen dynamics may also be closely tied to algal dynamics, particularly in highly productive stratified systems, since the respiration and decomposition of algae which settles below the photic zone is often a major source of oxygen depletion.

- Algae can affect pH through the uptake of dissolved CO_2 during photosynthesis and the recycling of CO_2 during respiration.

- Algae are the dominant component of the primary producers in many systems, particularly in lakes and estuaries. Since

they form the base of the food chain, they play a major role in the dynamics of all successive trophic levels.

- Suspended algae are often a major component of turbidity.

- Algal blooms can restrict recreational uses of water, sometimes resulting in fish kills under severe conditions.

- Algae can cause taste and odor problems in water supplies, and filter clogging problems at water treatment facilities.

Two general approaches have been used to simulate algae in water quality models: 1) aggregating all algae into a single constituent (for example, total algae or chlorophyll a), or 2) aggregating the algae into a few dominant functional groups (for example, green algae, diatoms, blue-greens, dinoflagellates, etc.).

The first approach is commonly used in river models since the major focus is on short term simulations (days to weeks) where the primary interest is the effects of algae on general water quality parameters such as dissolved oxygen, nutrients, and turbidity. Typical examples include QUAL-II (Roesner et al., 1981; NCASI, 1982, 1983), DOSAG3 (Duke and Masch, 1973), and RECEIV-II (Raytheon, 1974). In contrast, lake and reservior models tend to use the second approach since the focus is on long term simulations (months to years) of eutrophication problems where seasonal variations in different types of algae are important (Bierman, 1976; Bierman et al., 1973, 1980; Canale et al., 1975, 1976; Chen et al., 1975; Tetra Tech, 1979, 1980; Park et al., 1974, 1975, 1979, 1980; Scavia et al., 1976; Scavia, 1980; Lehman et al., 1975). Species-specific differences in nutrient requirements, nutrient uptake rates, growth rates, and temperature preference ranges result in a seasonal succession of dominance by different phytoplankton groups. It is often important to distinguish these differences in order to realistically model both nutrient dynamics and phytoplankton dynamics, and to predict the occurrence of specific problems such as blue-green algal blooms. Multi-group models typically use the same

general model formulations for all groups, but provide different coefficient values to characterize the differences between groups.

6.2 MODELING APPROACHES

Phytoplankton dynamics are governed by the following processes: growth, respiration and excretion, settling, grazing losses, and nonpredatory mortality (or decomposition). A general equation which includes all of these processes and forms the basis for almost all phytoplankton models can be expressed as:

$$\frac{dA}{dt} = (\mu - r - e_x - s - m)\, A - G \qquad (6\text{-}1)$$

where A = phytoplankton biomass or concentration (dry weight biomass, chlorophyll a, or equivalent mass of carbon, nitrogen, or phosphorus), mass or mass/volume

μ = gross growth rate, 1/time

r = respiration rate, 1/time

e_x = excretion rate, 1/time

s = settling rate, 1/time

m = nonpredatory mortality (or decomposition) rate, 1/time

G = loss rate due to grazing, mass/time or mass/volume-time

This equation is appropriate when phytoplankton are modeled in terms of either biomass or nutrient equivalents (carbon, nitrogen, phosphorous, etc.). However, if phytoplankton are expressed in terms of cell numbers, the growth rate is replaced with the cell division rate, and the respiration and excretion terms are omitted since they pertain to changes in biomass rather than cell numbers. The resulting equation is:

$$\frac{dA_n}{dt} = (\mu_n - s - m)\, A_n - G_n \qquad (6\text{-}2)$$

where A_n = phytoplankton cell numbers, numbers or numbers/volume

μ_n = cell division rate, 1/time

G_n = loss rate due to grazing, numbers/time or numbers/volume-time

The cell division rate in Equation (6-2) is assumed to be a continuous process although in reality cell division is a discrete event which is often expressed in terms of the number of divisions per day, n_d. The continuous division rate μ_n is related to the discrete rate n_d by $\mu_n = n_d \ln 2$.

Most models express phytoplankton in terms of biomass (or nutrient or chlorophyll a equivalents) rather than cell numbers. This facilitates the modeling of both nutrient cycles and food web dynamics since it allows a more direct linkage between the phytoplankton equations and the mass balance equations for both nutrients and higher trophic levels such as zooplankton and fish. Phytoplankton cell numbers are used in a few models whose focus is restricted to phytoplankton dynamics (e.g., Lehman et al., 1975; Cloern, 1978).

The major differences between different phytoplankton models are: 1) the number of phytoplankton groups modeled, 2) the specific formulations used for each process, and 3) the manner in which the various processes and corresponding terms in Equations (6-1) or (6-2) are combined. Some of the basic features of different phytoplankton models are compared in Table 6-1. The specific process formulations are discussed in later sections.

Many models combine several of the processes in Equation (6-1) into a single term, thereby simplifying the equation. For example, respiration and excretion are usually combined into a single respiration term. Respiration is often combined with growth so that the growth rate μ represents the net growth rate, rather than the gross growth rate as in Equation (6-1). This is consistent with net growth rates typically reported in the literature from laboratory cultures. Some models combine respiration with the other loss terms to give a net loss rate which includes respiration and mortality. Other models combine grazing and nonpredatory mortality into a single mortality term, particularly when algal grazers are not modeled explicitly.

TABLE 6-1. GENERAL COMPARISON OF ALGAL MODELS

Model (Author)	Number of Groups			Processes Computed Separately in Model					Algal Units					Reference
	Phyto-plankton	Attached Algae	Zoo-plankton	Growth	Respir-ation	Settling	Nonpredatory Mortality	Predatory Mortality	Dry Wt. Biomass	Chl *a*	Carbon	Other Nutrient	Cell Numbers	
AQUA-IV	1		1	X	X	X	X	X			X			Baca & Arnett (1976)
CE-QUAL-R1	2		1	X	X	X		X	X					WES (EWQOS) (1982)
CLEAN	2	1	3	X	X	X	X	X	X					Bloomfield *et al*. (1973)
CLEANER	3	1	3	X	X	X	X	X	X					Scavia & Park (1976)
MS.CLEANER	4	1	5	X	X	X	X	X	X					Park *et al*. (1980)
DEM	1			X	X	X				X				Feigner & Harris (1970)
DOSAG3	1			X	X	X				X				Duke & Masch (1973)
EAM	4	1	3	X	X	X		X	X					Tetra Tech (1979, 1980)
ESTECO	2		1	X	X	X		X	X					Brandes & Masch (1977)
EXPLORE-1	1		1	X	X			X			X			Baca *et al*. (1973)
HSPF	1	1	1	X	X	X	X	X	X					Johanson *et al*. (1980)
LAKECO	2		1	X	X	X		X	X					Chen & Orlob (1975)
MIT Network	1		1	X	X		X	X				N		Harleman *et al*. (1977)
QUAL-II	1			X	X	X				X				Roesner *et al*. (1981)
RECEIV-II	1			X	X		X			X				Raytheon (1974)
SSAM IV	1	1		X			X		X					Grenney & Kraszewski (1981)
WASP	2		2	X	X	X	X	X		X	X			Di Toro *et al*. (1981)
WQRRS	2	2	1	X	X	X		X	X					Smith (1978)
Bierman	5		2	X	X	X	X	X	X					Bierman *et al*. (1980)
Canale	4		9	X	X	X		X			X			Canale *et al*. (1975, 1976)
Jorgensen	1		1	X	X	X	X	X	X					Jorgensen (1976)
Lehman	5			X	X	X	X						X	Lehman *et al*. (1975)
Nyholm	1			X		X	X		X					Nyholm (1978)
Scavia	5		6	X	X	X	X	X			X			Scavia *et al*. (1976)

Because of these variations, it is very important to understand the assumptions of a particular model when selecting coefficients. Care must be taken both when extracting values from one model and applying them to another, or when using experimental measurements reported in the literature. For the latter case, the experimental conditions should be checked to make sure they are consistent with the assumptions of the model. If they are different, the appropriate adjustments should be made.

Attached algae (periphyton) and aquatic macrophytes have the same growth requirements as phytoplankton (light and nutrients) and are subject to the same basic processes of growth, respiration and excretion, grazing,and nonpredatory mortality. Therefore, they are usually modeled using the same general approach and process formulations as phytoplankton, although the specific values of the model coefficients will vary. The major differences are: 1) periphyton and macrophytes are associated with the bottom substrate and are expressed in terms of areal densities rather than volumetric densities or concentrations; 2) periphyton and macrophytes do not have settling losses, but instead they have additional losses due to sloughing or scouring from the bottom substrate; 3) periphyton and macrophytes are not subject to hydrodynamic transport; and 4) macrophytes use nutrients from the sediments and interstitial waters rather than nutrients in the water column. The general model equation for attached algae and macrophytes can be expressed as:

$$\frac{dA_b}{dt} = (\mu - r - e_x - s_1 - m)\, A_b - G_b \qquad (6\text{-}3)$$

where A_b = periphyton or macrophyte biomass (dry weight biomass, chlorophyll a, or equivalent mass of carbon, nitrogen, or phosphorus), mass or mass/area

S_1 = sloughing or scouring rate, 1/time

G_b = loss rate due to grazing, mass/time or mass/area-time

Benthic algae or macrophytes are included in only a few models such as CLEAN (Park et al., 1974), CLEANER (Park et al., 1975), MS.CLEANER

(Park et al., 1980), EAM (Tetra Tech, 1979, 1980), WQRRS (Smith, 1978), HSPF (Johanson et al., 1980), SSAM IV (Grenney and Kraszewski, 1981), and in Canale and Auer (1982) and Scavia et al. (1975).

6.3 CELL COMPOSITION

The majority of models express algae and other biological constituents as either dry weight biomass (Chen and Orlob, 1972; Chen et al., 1975; Park et al., 1974, 1975, 1979, 1980; Tetra Tech, 1979, 1980; Brandes and Masch, 1977; Smith, 1978; Johanson et al., 1980; Grenney and Kraszewski, 1981; Bierman et al., 1973, 1980; Jorgensen, 1976; Jorgensen et al., 1978; Nyholm, 1977, 1978) or carbon (Baca and Arnett, 1976; Baca et al., 1973, 1974; Canale et al., 1975, 1976; Scavia et al., 1976; Scavia, 1980). Nitrogen or phosphorus have also been used in a few models which focus on a single nutrient cycle and assume that particular nutrient always limits algal growth (Najarian and Harleman, 1975; Harleman et al., 1977). Some models express phytoplankton as chlorophyll a since both field measurements and water quality standards are often reported in these units (Roesner et al., 1981; Duke and Masch, 1973; Raytheon, 1974; Di Toro et al., 1971, 1977; Di Toro and Matystik, 1980; Di Toro and Connolly, 1980; O'Connor et al., 1975; Thomann et al., 1975, 1979).

Dry weight biomass is related to the major nutrients (carbon, nitrogen, and phosphorus) and chlorophyll a through stoichiometric ratios which give the ratios of each nutrient to the total biomass. Typical algal nutrient compositions are summarized in Tables 6-2 to 6-4. Algae expressed as carbon, nitrogen, phosphorus, or chlorophyll a can be converted to dry weight biomass or any of the other units by using the stoichiometric ratios presented in the tables.

Most conventional water quality models assume the nutrient compositions of the cells and the resulting stoichiometric ratios are constant. In reality, cell stoichiometry varies with species, cell size, physiological condition, and recent environmental conditions (external nutrient concentrations, light, and temperature), although it is often assumed

TABLE 6-2. NUTRIENT COMPOSITION OF ALGAL CELLS - PERCENT OF DRY WEIGHT BIOMASS

Algal Type	Percent of Dry Weight Biomass					References
	C	N	P	Si	Chl *a*	
Total Phytoplankton	40.-50.	8.-9.	1.5			Tetra Tech (1976) Chen & Wells (1975, 1976)
	40.	7.2	1.0			Tetra Tech (1980) Bowie *et al*. (1980) Porcella *et al*. (1983)
					2.	Bierman (1976)
	60.					Nyholm (1978)
		6.1	0.88			Jorgensen (1976)
	40.-50.*	7.-9.*	1.-1.2*			Smith (1978)
		8.-9.*	1.2-1.5*		5.-10.*	Roesner *et al*. (1980) Duke & Masch (1973)
	50.*	9.*	1.2*			Brandes (1976)
	42.9-70.2**	0.6-16.**	0.16-5.**			Baca & Arnett (1976)
		1.5-9.3**	0.08-1.17**			Jorgensen (1979)
Diatoms	40.	7.2	1.0	20.-24.		Tetra Tech (1980) Bowie *et al*. (1980) Porcella *et al*. (1983)
				50.		Bierman *et al*. (1976)
	19.-50.**	2.7-5.9**	0.4-2.0**			Di Toro *et al*. (1971)
	20.-53**					Bierman *et al*. (1980)
Green Algae	40.	7.2	1.0			Tetra Tech (1980) Bowie *et al*. (1980) Porcella *et al*. (1983)
	35.-48.**	6.6-9.1**	2.4-3.3**			Di Toro *et al*. (1971)
	15.-74.**					Bierman *et al*. (1980)
Blue-green Algae	40.	7.2	1.0			Tetra Tech (1980) Bowie *et al*. (1980) Porcella *et al*. (1983)
	28.-45.**	4.5-5.8**	0.8-1.4**			Di Toro *et al*. (1971)
	38.-39.**					Bierman *et al*. (1980)
					1.-3.**	Baca & Arnett (1976)
					0.25**	Jorgensen (1979)

TABLE 6-2. (continued)

Algal Type	Percent of Dry Weight Biomass					References
	C	N	P	Si	Chl-a	
Dinoflagellates					275.	O'Connor et al. (1981)
	37.-47**	3.3-5.0**	0.6-1.1**			Di Toro et al. (1971)
	10.-43.**					Bierman et al. (1980)
Flagellates	40.	7.2	1.0			Tetra Tech (1980) Bowie et al. (1980) Porcella et al. (1983)
	29.-67.**					Bierman et al. (1980)
Chrysophytes	35.-45.**	7.8-9.0**	1.2-3.0			Jorgensen (1979)
Benthic Algae	40.	7.2	1.0			Tetra Tech (1980) Bowie et al. (1980) Porcella et al. (1983)
	40.-50.*	7.-9.*	1.-1.2*			Smith (1978)

*Model documentation values.
**Literature values.

constant for modeling purposes. Several of the more recent algal models, however, have included variable cell stoichiometry in their formulations to simulate processes such as luxury uptake and storage of nutrients (Bierman et al., 1973, 1980; Bierman, 1976; Lehman et al., 1975; Jorgensen, 1976; Jorgensen et al., 1978; Nyholm, 1977, 1978; Park et al., 1979, 1980; Canale and Auer, 1982). These models are discussed later with reference to phytoplankton growth and nutrient uptake formulations.

6.4 GROWTH

Algal growth is a function of temperature, light, and nutrients. The major growth limiting nutrients are assumed to be phosphorus, nitrogen, and carbon, with the addition of silicon for diatoms. Other essential micronutrients such as iron, manganese, sulfur, zinc, copper, cobalt,

molybdenum, and vitamin B_{12} may also limit growth under conditions of restricted availability (particularly in oligotrophic systems). However, these effects are generally not included in models since micronutrients are usually not simulated. The algal growth rate formulations used in almost all models can be expressed in general functional form as:

$$\mu = \mu_{max}(T_{ref})\ f(T)\ f(L,P,N,C,Si) \qquad (6\text{-}4)$$

where μ = algal growth rate, 1/time

$\mu_{max}(T_{ref})$ = maximum growth rate at a particular reference temperature T_{ref} under optimal conditions of saturated light intensity and excess nutrients, 1/time

$f(T)$ = temperature function for growth

T = temperature, ^{o}C

$f(L,P,N,C,Si)$ = growth limiting function for light and nutrients

L = light intensity

P = available inorganic phosphorus concentration, mass/volume

TABLE 6-3. NUTRIENT COMPOSITION OF ALGAL CELLS - RATIO TO CARBON

Algal Type	$\frac{N}{C}$	$\frac{P}{C}$	$\frac{Si}{C}$	References
Total Phytoplankton	0.17 - 0.25	0.025		Thomann & Fitzpatrick (1982) Di Toro *et al.* (1971)
	0.18	0.024		Scavia et al. (1976) Scavia (1980)
	0.2			Canale *et al.* (1976)
	0.05 - 0.17**	0.024 - 0.24**		Baca & Arnett (1976)
	0.05 - 0.43**	0.025 - 0.05**		Jorgensen (1979)
Diatoms	0.18	0.024	0.6	Scavia (1980)
	0.067 - 0.21**	0.003 - 0.14**	0.06-0.77**	Jorgensen (1979)

**Literature Values.

TABLE 6-4. NUTRIENT COMPOSITION OF ALGAL CELLS - RATIO TO CHLOROPHYLL a

Algal Type	C / Chl a	N / Chl a	P / Chl a	Si / Chl a	References
Total Phytoplankton	50.-100.	7.-15.	0.5-1.0		Thomann et al. (1975, 1979) O'Connor et al. (1981) Di Toro & Matystik (1980) Di Toro & Connolly (1980) Salas & Thomann (1978)
			0.5		Salisbury et al. (1983)
		7.2	0.63		Larsen et al. (1973)
	25.-112.**	7.-29.**	1.0**		Jorgensen (1979)
	10.-100.**	2.7-9.1**			O'Connor et al. (1981)
Diatoms	100.	10.-15.	0.5-1.0	40.-50.	Di Toro & Connolly (1980) Di Toro & Matystik (1980) Thomann et al. (1979)
			0.5		Salisbury et al. (1983)
	50.-200.*				Baca & Arnett (1976)
	18.-500**	2.2-74.6**	0.27-19.2**	2.4-50.7**	Di Toro et al. (1971)
Green Algae	25.-100.*				Baca & Arnett (1976)
Blue-green Algae	14.-67.*				Baca & Arnett (1976)
Dinoflagellates	275.	19.3			O'Connor et al. (1981)

*Model documentation values.

**Literature values.

N = available inorganic nitrogen concentration, mass/volume

C = available inorganic carbon concentration, mass/volume

Si = available inorganic silicon concentration, mass/volume

Note that the growth limiting function f(L,P,N,C,Si) is simplified in many models by excluding some of the nutrients. For example, silicon is

included only in models which simulate diatoms as a separate algal group (Bierman et al., 1973, 1980; Bierman, 1976; Canale et al., 1975, 1976; Scavia et al., 1976; Scavia, 1980; Chen et al., 1975; Tetra Tech, 1979, 1980; Lehman et al, 1975; Park et al., 1979, 1980; Di Toro and Connolly, 1980). Carbon is frequently omitted since it is often available in excess relative to phosphorus and nitrogen (Bierman et al., 1980; Scavia et al., 1976; Nyholm, 1978; Canale et al., 1975, 1976; Baca and Arnett, 1976; Di Toro and Matystik, 1980). Some models include only one nutrient, phosphorus or nitrogen, and assume that nutrient is limiting at all times for the particular system under consideration (Najarian and Harleman, 1975; Canale and Auer, 1982).

It should also be noted that the nutrient concentrations in the growth limiting function f(L,P,N,C,Si) correspond to the "external" nutrient concentrations in the water for some models, and to the "internal" nutrient concentrations in the algal cells for other models. These distinctions will be discussed in more detail below.

6.4.1 Temperature Effects On Maximum Growth Rates

The quantity $\mu_{max}(T_{ref})$ f(T) in Equation (6-4) represents the effects of temperature variations on maximum algal growth rates under conditions of optimum light and nutrients. The maximum growth rate μ_{max} must be specified at a reference temperature T_{ref} which is consistent with the particular temperature function f(T) used in the model. The reference temperature may correspond to 20°C, optimum temperature conditions, or some other temperature, depending on the form of the temperature function. Therefore, maximum growth rate coefficients obtained from one model may have to be adjusted before using the coefficients in another model which has a different temperature adjustment function. Maximum growth rates for algae are tabulated in Table 6-5, along with the corresponding reference temperatures.

Although numerous temperature adjustment functions have been used to model algae, most of them fall into one of three major categories

TABLE 6-5. ALGAL MAXIMUM GROWTH RATES

Algal Type	Maximum Growth Rate (1/day)	Reference Temperature (°C)	References
Total Phytoplankton	1.3 - 2.5	20°C	O'Connor et al. (1975, 1981) Thomann et al. (1974, 1975, 1979) Thomann & Fitzpatrick (1982) Di Toro & Connolly (1980) Di Toro & Matystik (1980) Di Toro et al. (1971, 1977) Salas & Thomann (1978) Salisbury et al. (1983)
	1. - 2.5	20°C	Chen (1970) Chen & Orlob (1975) Chen & Wells (1975, 1976) Tetra Tech (1976)
	1. - 2.	20°C	Battelle (1974)
	1.5	20°C	Grenney & Kraszewski (1981)
	1. - 2.7	T_{opt}	Scavia & Park (1976) Youngberg (1977)
	1.5	20°C	Nyholm (1978)
	1.8 - 2.53	T_{opt}	Jorgensen (1976) Jorgensen et al. (1978)
	2.4	T_{opt}	Larsen et al. (1973)
	0.2 - 8.*	20°C	Baca & Arnett (1976)
	1. - 3.*	T_{opt}	Smith (1978)
	1. - 3.*	20°C	Roesner et al. (1980) Duke & Masch (1973)
	0.2 - 8.*	20°C	Grenney & Kraszewski (1981)
	1.5 - 2.*	20°C	Brandes (1976)
	0.58 - 3.**	20°C	Jorgensen (1979)
Diatoms	2.1	20°C	Di Toro & Connolly (1980) Thomann et al. (1979) Salisbury et al. (1983)
	2.0 - 2.5	T_{opt}	Tetra Tech (1980) Bowie et al. (1980) Porcella et al. (1983)
	2.0 - 2.1	20°C	Canale et al. (1976)
	2.1	25°C	Bierman (1976)
	1.6	10° - 14°C	Bierman et al. (1980)
	1.8 - 2.5	T_{opt}	Scavia et al. (1976) Scavia (1980)
	3.0	T_{opt}	Lehman et al. (1975)

TABLE 6-5. (continued)

Algal Type	Maximum Growth Rate (1/day)	Reference Temperature (^oC)	References
	1.75**	27^oC**	Di Toro *et al*. (1971)
	0.55 - 3.4**	20^oC**	Collins & Wlosinski (1983)
	1.1 - 5.0**	20^oC**	Jorgensen (1979)
Green Algae	1.9	25^oC	Bierman (1976)
	1.4	20^oC	Bierman *et al*. (1980)
	2.0 - 2.5	T_{opt}	Tetra Tech (1980) Bowie *et al*. (1980) Porcella *et al*. (1983)
	1.9	20^oC	Canale *et al*. (1976)
	1.8 - 2.5	T_{opt}	Scavia *et al*. (1976) Scavia (1980)
	1.6	25^oC	DePinto *et al*. (1976)
	3.0	T_{opt}	Lehman *et al*. (1975)
	1.5 - 3.9**	25^oC**	Di Toro *et al*. (1971)
	0.7 - 2.1**	20^oC	Collins & Wlosinski (1983)
	0.9 - 4.1**	25^oC**	
	9.0 - 9.2**	39^oC**	
	1.4 - 2.4**	20^oC**	Jorgensen (1979)
	1.5 - 3.9**	25^oC**	
	1.3 - 4.3**	35^oC**	
	5.65**	40^oC**	
Blue-green Algae	0.8	25^oC	Bierman (1976)
	0.7 - 1.0	20° - 25^oC	Bierman *et al*. (1980)
	1.6	20^oC	Canale *et al*. (1976)
	1.4 - 1.9	T_{opt}	Youngberg (1977)
	1.1 - 2.0	T_{opt}	Scavia & Park (1976) Scavia (1980)
	1.1	25^oC	DePinto *et al*. (1976)
	2.5	T_{opt}	Lehman *et al*. (1975)
	1.6 - 2.5	T_{opt}	Tetra Tech (1980) Bowie *et al*. (1980) Porcella *et al*. (1983)
	0.41 - 0.86**	20^oC**	Jorgensen (1979)
	0.2 - 4.9**	25^oC**	Collins & Wlosinski (1983)
	2.0 - 3.9**	35^oC**	
	0.5 - 11.**	40^oC**	

TABLE 6-5. (continued)

Algal Type	Maximum Growth Rate (1/day)	Reference Temperature (^oC)	References
Dinoflagellates	0.2 - 0.28	20^oC	O'Connor et al. (1981)
	2.16**	20^oC	Di Toro et al. (1971)
	0.2 - 2.1**	20^oC	Collins & Wlosinski (1983)
Flagellates	1.6	T_{opt}	Tetra Tech (1980) Porcella et al. (1983)
	1.2	20^oC	Bierman et al. (1980)
	1.5	T_{opt}	Lehman et al. (1975)
Chrysophytes	1.5	T_{opt}	Lehman et al. (1975)
	0.4 - 2.9**	25^oC**	Collins & Wlosinski (1983)
Coccolithophores	1.75 - 2.16**	25^oC**	Jorgensen (1979)
Benthic Algae	0.5 - 1.5	T_{opt}	Tetra Tech (1980) Porcella et al. (1983)
	1.08	T_{opt}	Auer and Canale (1982)
	1.5	20^oC	Grenney & Kraszewski (1981)
	0.2 - 0.8*	20^oC	Grenney & Kraszewski (1981)
	0.5 - 1.5*	T_{opt}	Smith (1978)

*Model documentation values.
**Literature values.

(Figure 6-1): 1) linear increases in growth rate with temperature, 2) exponential increases in growth rate with temperature, and 3) temperature optimum curves in which the growth rate increases with temperature up to the optimum temperature and then decreases with higher temperatures.

The simplest type of temperature adjustment function assumes a linear temperature response curve above some minimum temperature T_{min}. This relationship can be expressed in general form as:

$$f(T) = \frac{T - T_{min}}{T_{ref} - T_{min}} \qquad (6\text{-}5)$$

$$= \left(\frac{1}{T_{ref} - T_{min}}\right) T - \left(\frac{T_{min}}{T_{ref} - T_{min}}\right)$$

$$= \gamma\, T + \beta$$

where T_{min} = lower temperature limit at which the growth rate is zero, ^{o}C

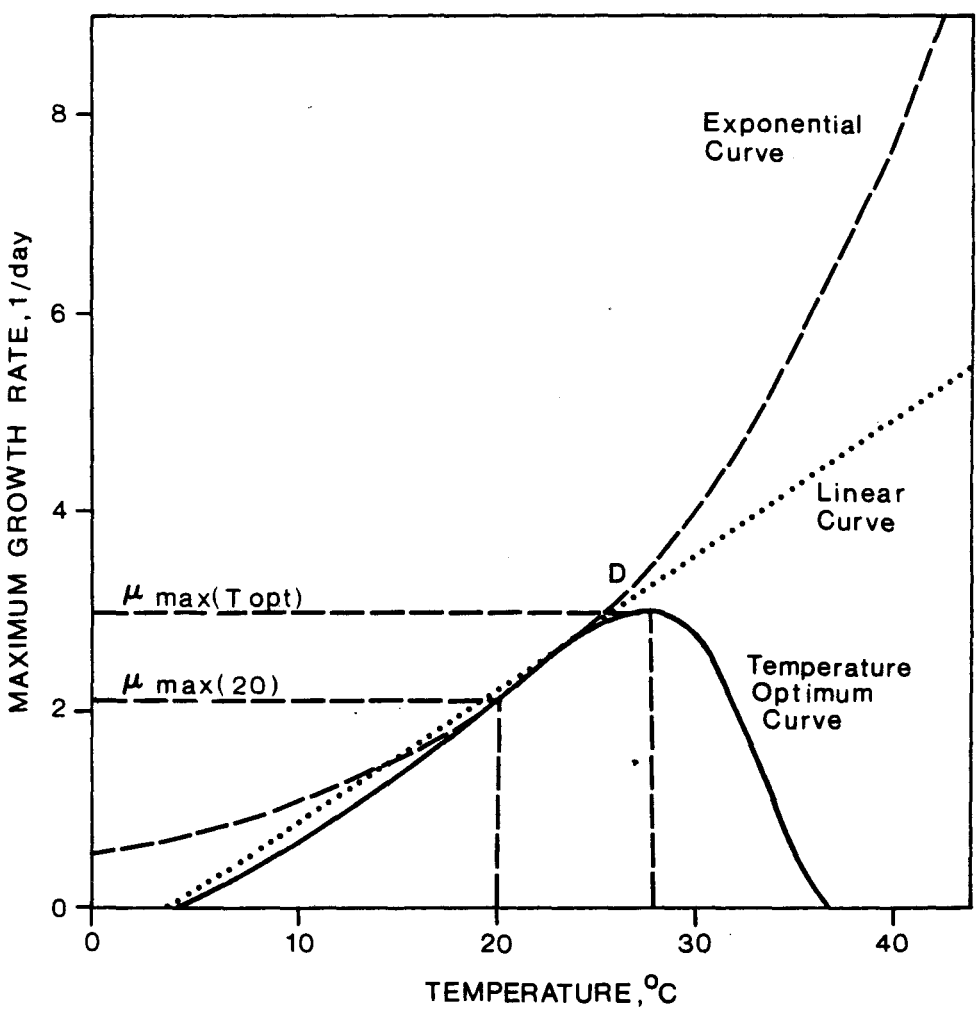

Figure 6-1. Major types of temperature response curves for algal growth.

T_{ref} = reference temperature corresponding to the value of the maximum growth rate $\mu_{max}(T_{ref})$, ^{o}C

$\gamma = \frac{1}{(T_{ref} - T_{min})}$ = slope of growth vs. temperature curve

$\beta = \frac{T_{min}}{T_{ref} - T_{min}}$ = y-intercept of growth vs. temperature curve

This equation is typically used in simplified form by choosing a lower temperature limit T_{min} equal to zero so that Equation (6-5) becomes:

$$f(T) = \frac{T}{T_{ref}} \tag{6-6}$$

Reference temperatures of either $20^{o}C$ or $1^{o}C$ are usually used which results in:

$$f(T) = \frac{T}{20} \tag{6-7}$$

or

$$f(T) = T \tag{6-8}$$

This approach is used in EXPLORE-I (Baca et al., 1973) and RECEIV-II (Raytheon, 1974) and by Di Toro et al. (1971) in an early version of WASP.

Some models use piecewise linear functions for algal growth with different slopes over different temperature ranges (Bierman et al., 1980; Canale et al., 1975, 1976). HSPF (Johanson et al., 1980) uses Equation (6-5) over the temperature range between T_{min} and the optimum temperature for maximum growth T_{opt}, followed by a constant temperature function above T_{opt}:

$$f(T) = \left(\frac{1}{T_{opt} - T_{min}}\right) T - \left(\frac{T_{min}}{T_{opt} - T_{min}}\right) \quad \text{for } T \leq T_{opt} \tag{6-9a}$$

$$f(T) = 1 \quad \text{for } T > T_{opt} \tag{6-9b}$$

with $$\mu_{max}(T_{ref}) = \mu_{max}(T_{opt}) \tag{6-9c}$$

where T_{opt} = optimum temperature at which the growth rate is maximum, ^{o}C

This assumes growth increases linearly with temperature until the maximum growth rate is attained, and then remains at the maximum rate as temperature increases further.

The most commonly used exponential temperature adjustment functions are based on the Arrhenius or van't Hoff equation:

$$Q_{10} = \left(\frac{K_2}{K_1}\right)^{\left(\frac{10}{T_2-T_1}\right)} \tag{6-10}$$

where K_1 = reaction rate at temperature T_1
K_2 = reaction rate at temperature T_2
Q_{10} = ratio of reaction rates at $10^{o}C$ temperature increments

This equation can be rearranged into a more useful form as:

$$K_2 = K_1\ Q_{10}^{\left(\frac{T_2-T_1}{10}\right)} \tag{6-11}$$

or

$$K(T) = K(T_{ref})\ Q_{10}^{\left(\frac{T-T_{ref}}{10}\right)} \tag{6-12}$$

$$= K(T_{ref})\ f(T)$$

where f(T) is the temperature adjustment function:

$$f(T) = Q_{10}^{\left(\frac{T-T_{ref}}{10}\right)} \tag{6-13}$$

The temperature adjustment function (Equation (6-13)) is generally expressed in a more simplified form as:

$$f(T) = Q_{10}^{(1/10)(T-T_{ref})} \tag{6-14}$$

$$= \theta^{(T-T_{ref})}$$

where $\theta = Q_{10}^{(1/10)}$ = temperature adjustment coefficient

The temperature adjustment coefficient θ typically has a value between 1.01 and 1.2, with a value of 1.072 corresponding to a doubling of the growth rate for every $10^{o}C$ increase in temperature. Eppley (1972) found that θ equals 1.066 for an exponential envelope curve of growth rate versus temperature data compiled from a large number of studies involving many different species (Figure 6-2).

Most models which use exponential temperature functions assume a reference temperature of $20^{o}C$ which gives the familiar equation (Chen and Orlob, 1975; Baca and Arnett, 1976; Roesner et al., 1981; Brandes and Masch, 1977; Duke and Masch, 1973; Thomann et al., 1979; Thomann and Fitzpatrick, 1982; Di Toro and Matystik, 1980; Di Toro and Connolly, 1980; O'Connor et al., 1981):

$$f(T) = \theta^{(T-20^{o}C)} \tag{6-15a}$$

with

$$\mu_{max}(T_{ref}) = \mu_{max}(20^{o}C) \tag{6-15b}$$

However, Thomann et al. (1975) and Eppley (1972) use a reference temperature of $0^{o}C$ which results in:

$$f(T) = \theta^{T} \tag{6-16a}$$

with

$$\mu_{max}(T_{ref}) = \mu_{max}(0^{o}C) \tag{6-16b}$$

The above equations assume that the temperature adjustment coefficient θ has the same value regardless of the reference temperature. However, a few models have applied Equation (6-14) in a piecewise manner assuming that the value of θ varies over different temperature intervals.

Many formulations have been used to generate temperature optimum curves for algal growth. The reference temperature is generally set at the optimum temperature for maximum growth, and the temperature adjustment function is normalized so it has a maximum value of 1.0 at the optimum temperature and smaller values elsewhere. Most curves begin with a zero value at the lower temperature tolerance limit, increase to a maximum value of 1.0 at the optimum temperature, and then decrease back to a value of zero at the upper temperature tolerance limit. These types of curves are typically based on growth vs. temperature data for a single species. These data generally show no growth at very low temperatures followed by an exponential increase in

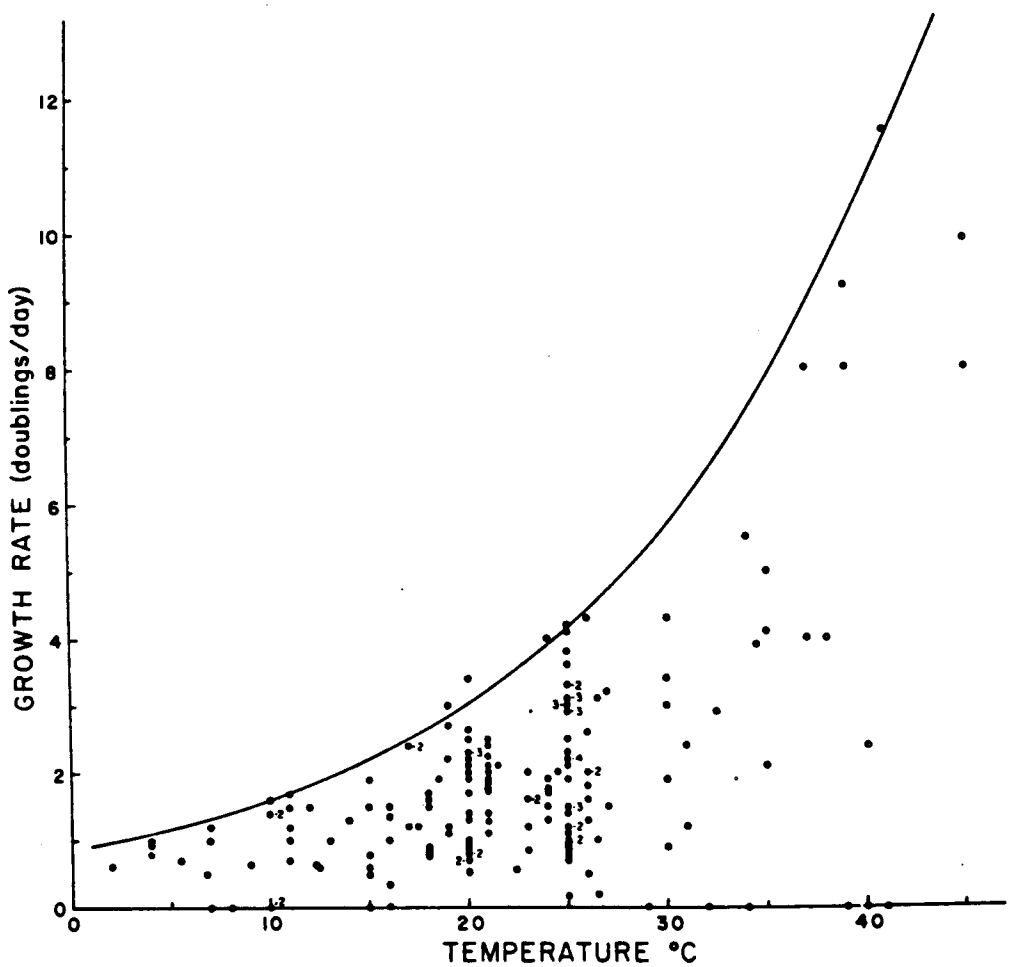

Figure 6-2. Envelope curve of algal growth rate versus temperature for data compiled from many studies involving many different species (adapted from Eppley, 1972; Goldman, 1981).

growth with temperature over a large part of the temperature range. However, the growth rate eventually levels off to some maximum value at the optimum temperature, and then begins to decline at very high temperatures until growth finally ceases at some upper temperature limit.

Lehman et al. (1975) use a skewed normal distribution as a temperature optimum curve for phytoplankton growth. The equation is:

$$f(T) = \exp\left[-2.3\left(\frac{T - T_{opt}}{T_x - T_{opt}}\right)^2\right] \tag{6-17a}$$

with

$$\mu_{max}(T_{ref}) = \mu_{max}(T_{opt}) \tag{6-17b}$$

where T_{opt} = optimum temperature at which the growth rate is maximum, ^oC

T_x = T_{min} for $T \leq T_{opt}$
= T_{max} for $T > T_{opt}$

T_{min} = lower temperature limit at which the growth rate is zero, ^oC

T_{max} = upper temperature tolerance limit at which growth ceases, ^oC

Jorgensen (1976) and Jorgensen et al. (1978) use a modified form of Equation (6-17a) which is expressed as:

$$f(T) = \exp\left(-2.3\left|\frac{T - T_{opt}}{T_{opt} - T_{min}}\right|\right) \tag{6-18}$$

Several models including CLEAN (Bloomfield et al., 1973), CLEANER (Scavia and Park, 1976), MS.CLEANER (Park et al, 1979, 1980), and Scavia et al. (1976) use a temperature optimum function originally developed by Shugart et al. (1974). This formulation can be expressed as:

$$f(T) = V^x e^{x(1-V)} \tag{6-19a}$$

$$V = \frac{T_{max} - T}{T_{max} - T_{opt}} \tag{6-19b}$$

$$x = \left[\frac{W\,(1 + \sqrt{1 + 40/W})}{20} \right]^2 \tag{6-19c}$$

$$W = (\ln Q_{10})\,(T_{max} - T_{opt}) \tag{6-19d}$$

with

$$\mu_{max}(T_{ref}) = \mu_{max}(T_{opt}) \tag{6-19e}$$

where Q_{10} is defined as in Equations (6-10) through (6-14).

The temperature function in Equations (6-19a) through (6-19e) has been modified in the ecosystem model MS.CLEANER by adding a temperature adaption formulation which essentially shifts the whole curve by varying the values of T_{opt} and T_{max} to account for acclimation to different temperatures (Park et al., 1980). This formulation was originally developed by O'Neill (1972), and can be expressed as:

$$T_{shift} = T_{smax}\left[1 - e^{-K_{ac}|T_{avg} - T_{opt}|}\right] \tag{6-20}$$

where T_{shift} = magnitude of acclimation (translation of T_{opt} and T_{max}), ^oC

T_{smax} = maximum magnitude of acclimation, ^oC

K_{ac} = acclimation rate coefficient

T_{avg} = average temperature for previous 2 weeks, ^oC

Lassiter and Kearns (1973) and Lassiter (1975) developed a temperature optimum equation of the form:

$$f(T) = \left(e^{K_a(T-T_{opt})}\right)\left(\frac{T_{max} - T}{T_{max} - T_{opt}}\right)^{K_a(T_{max}-T_{opt})} \tag{6-21a}$$

with

$$\mu_{max}(T_{ref}) = \mu_{max}(T_{opt}) \tag{6-21b}$$

where K_a = a scaling constant used in the original equation from which Equation (6-21a) was derived,

$$\frac{df(T)}{dt} = K_a \left(\frac{T_{max} - T}{T_{max} - T_{opt}} \right) \tag{6-21c}$$

These equations result in a temperature optimum curve which is always skewed to the right.

Thornton and Lessem (1978) developed a temperature optimum curve by combining two logistic equations, one describing the rising limb of the curve below the optimum temperature and one describing the falling limb of the curve above the optimum temperature. The second curve is rotated about the y-axis and shifted to the right along the x-axis until the approximate peaks of both curves coincide. The left side of the temperature curve is expressed as:

$$K_A(T) = \frac{K_1 \, e^{\gamma_1 (T - T_{min})}}{1 + K_1 \left[e^{\gamma_1 (T - T_{min})} - 1 \right]} \tag{6-22a}$$

$$\gamma_1 = \frac{1}{(T_{opt(1)} - T_{min})} \ln \left[\frac{K_2 \, (1 - K_1)}{K_1 \, (1 - K_2)} \right] \tag{6-22b}$$

and the right side is expressed as:

$$K_B(T) = \frac{K_4 \, e^{\gamma_2 (T_{max} - T)}}{1 + K_4 \left[e^{\gamma_2 (T_{max} - T)} - 1 \right]} \tag{6-23a}$$

$$\gamma_2 = \frac{1}{(T_{max} - T_{opt(2)})} \ln \left[\frac{K_3 \, (1 - K_4)}{K_4 \, (1 - K_3)} \right] \tag{6-23b}$$

where $T_{opt(1)}$ = lower limit of optimum temperature range, ^oC
$T_{opt(2)}$ = upper limit of optimum temperature range, ^oC
γ_1 = rate coefficient for left side of curve
γ_2 = rate coefficient for right side of curve
K_1 = rate multiplier near the lower temperature limit T_{min}
K_4 = rate multiplier near the upper temperature limit T_{max}
K_2 = 0.98
K_3 = 0.98

The temperature curve is defined as the product of Equations (6-22a) and (6-23a):

$$f(T) = K_A(T)\ K_B(T) \tag{6-24a}$$

with

$$\mu_{max}(T_{ref}) = \mu_{max}(T_{opt}) \tag{6-24b}$$

By using different values of the logistic equation parameters for each side, an assymmetric growth curve can be generated. The values of K_2 and K_3 are set equal to 0.98 rather than 1.0 so that the peak of the combined logistic equation is close to 1.0 (since the logistic equation would otherwise only approach 1.0 assymptotically). Two values of the optimum temperature, $T_{opt(1)}$ and $T_{opt(2)}$, are used to allow an optimum temperature range, rather than a single optimum temperature value. This formulation is used in CE-QUAL-R1 (WES, 1982), WQRRS (Smith, 1978), and EAM (Tetra Tech, 1979, 1980). The left side of the curve (the basic logistic equation, Equation (6-22a)) is also used as a temperature adjustment curve in SSAM IV (Grenney and Kraszewski, 1981).

The MIT one-dimensional network model (Najarian and Harleman, 1975; Harleman et al., 1977) uses a temperature optimum curve which is defined as:

$$f(T) = \left(\frac{T}{T_{opt}}\right)^n \exp\left[1 - \left(\frac{T}{T_{opt}}\right)^n\right] \qquad \text{for } T < T_{opt} \tag{6-25a}$$

and $$f(T) = 1 - \left(\frac{T - T_{opt}}{T_{max} - T_{opt}}\right)^m \qquad \text{for } T > T_{opt} \qquad (6\text{-}25b)$$

with $$\mu_{max}(T_{ref}) = \mu_{max}(T_{opt}) \qquad (6\text{-}25c)$$

The values of the exponents n and m are 2.5 and 2.0, respectively (Najarian and Harleman, 1975).

Some type of temperature optimum curve is generally more appropriate than a linear or exponential formulation when considering a single algal species or functional group, since growth usually slows down and eventually ceases above some upper temperature limit for any given species. This approach is used in most models which simulate several algal groups (e.g., Chen et al., 1975; Tetra Tech, 1979, 1980; Park et al., 1979, 1980; Canale et al., 1975, 1976; Scavia et al., 1976; Lehman et al., 1975; Smith, 1978; WES, 1982), since seasonal variation in temperature is one of the major factors causing seasonal succession in the dominance of different groups (diatoms, greens, blue-greens, etc.). However, since many species are lumped into a few functional groups, the temperature optimum curves and maximum growth rates should be defined so that they encompass the temperature-growth curves of all dominant species in the defined groups. Canale and Vogel (1974) developed a set of temperature-growth curves for diatoms, green algae, blue-green algae, and flagellates based on a literature review of growth data for many species (Figure 6-3).

Since the temperature function includes both the effects of increasing temperature on the growth rates of many individual species as well as shifts in the species composition toward dominance by warmer water species, some modelers have preferred to use exponential or linear formulations over the whole temperature range, particularly when only one or two groups are simulated (Chen and Orlob, 1975; Thomann et al., 1979; Di Toro and Matystik, 1980; Di Toro and Connolly, 1980; Nyholm, 1978). This assumes that as temperature increases, the species composition changes so that species with optimum temperatures near the ambient temperature (and with

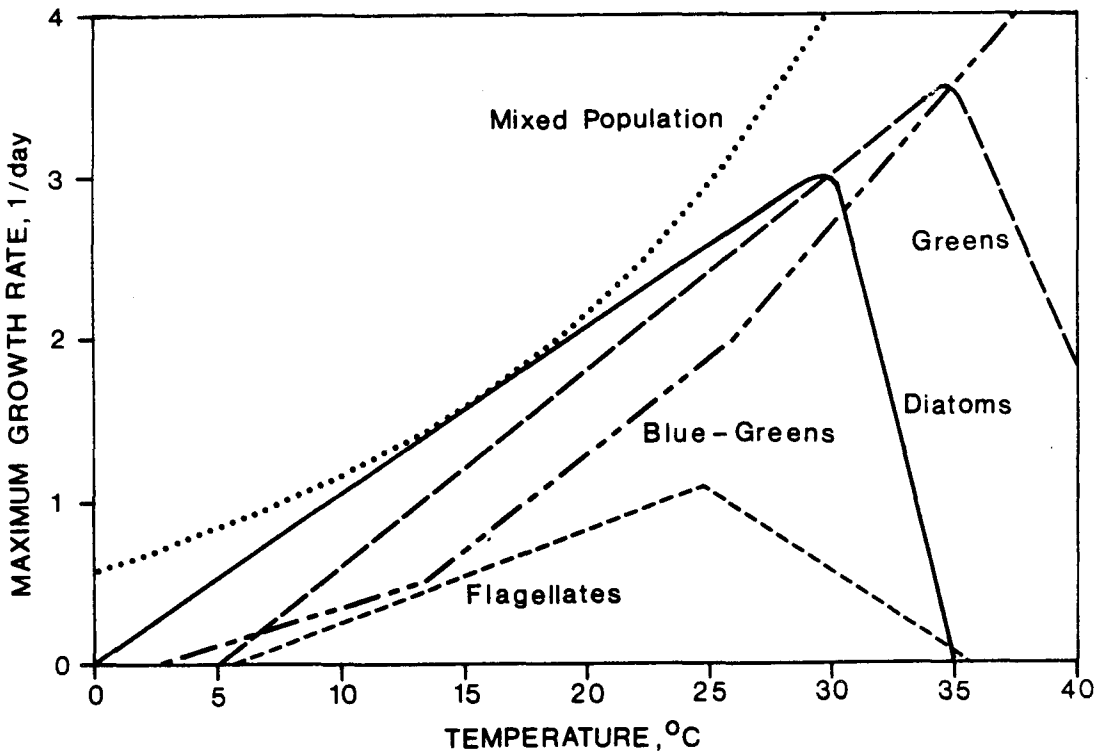

Figure 6-3. Temperature-growth curves for major algal groups (from Canale and Vogel, 1974).

higher maximum growth rates) tend to dominate the phytoplankton assemblage. Eppley (1972) showed that an exponential relationship describes the envelope curve of growth rate versus temperature data from a large number of studies with many different species (Figure 6-2). However, this approach may overestimate the net growth of the assemblage if the growth rates are based on the maximum growth rate of the species assumed to be dominant at any given instant, since much of the biomass will include species which predominated earlier under different temperature conditions (Swartzman and Bentley, 1979). Exponential or linear functions which increase indefinitely with temperature can also be justified in situations where the maximum water temperatures are always below the optimum temperatures for the species present. For example, Canale and Vogel (1974) assumed a linear relationship below the temperature optimum for each algal group in Figure 6-3.

The temperature formulations used in different models are compared in Table 6-6.

TABLE 6-6. COMPARISON OF TEMPERATURE ADJUSTMENT FUNCTIONS FOR ALGAL GROWTH

Model (Author)	Temperature Formulation (Equation No.)				Reference Temperature	Reference
	Linear	Exponential	Optimum Curve	Other Curve		
AQUA-IV		6-14			20°C	Baca & Arnett (1976)
CE-QUAL-R1			6-24		T_{opt}	WES (EWQOS) (1982)
CLEAN			6-19		T_{opt}	Bloomfield et al. (1973)
CLEANER			6-19		T_{opt}	Scavia & Park (1976)
MS.CLEANER			6-19		T_{opt}	Park et al. (1980)
DEM		6-14			20°C	Feigner & Harris (1970)
DOSAG3		6-14			20°C	Duke & Masch (1973)
EAM			6-24		T_{opt}	Tetra Tech (1979, 1980)
ESTECO		6-14			20°C	Brandes & Masch (1977)
EXPLORE-1	6-6				1°C	Baca et al. (1973)
HSPF				piecewise linear saturation		Johanson et al. (1980)
LAKECO		6-14			20°C	Chen & Orlob (1975)
MIT Network			6-25		T_{opt}	Harleman et al. (1977)
QUAL-II		6-14			20°C	Roesner et al. (1981)
RECEIV-II	6-6				1°C	Raytheon (1974)
SSAM IV				logistic equation	20°C	Grenney & Kraszewski (1981)
WASP		6-14			20°C	Di Toro et al. (1981)
WQRRS			6-24		T_{opt}	Smith (1978)
Bierman	piecewise linear			piecewise linear saturation		Bierman et al. (1980)
Canale	piecewise linear				1°C	Canale et al. (1975, 1976)
Jorgensen			6-18		T_{opt}	Jorgensen (1976)
Lehman			6-17		T_{opt}	Lehman et al. (1975)
Nyholm		6-14			20°C	Nyholm (1978)
Scavia			6-19		T_{opt}	Scavia et al. (1976)

6.4.2 Algal Growth Limitation

In addition to temperature effects, algal growth rates are limited by both light and nutrient availability. As mentioned above, only macronutrients (phosphorous, nitrogen, carbon, and silicon) are generally included in models. Growth limitation was expressed previously as the factor f(L,P,N,C,Si) in the algal growth equation:

$$\mu = \mu_{max}(T_{ref})\ f(T)\ f(L,P,N,C,Si) \qquad (6\text{-}4)$$

Separate growth limiting factors are typically computed for light and each potentially limiting nutrient. The number of nutrients considered will vary between models depending on the particular system under consideration. Each growth limitation factor can range from a value of 0 to 1. A value of 1 means the factor does not limit growth (i.e., light is at optimum intensity, nutrients are available in excess, etc.) and a value of 0 means the factor is so severely limiting that growth is stopped entirely.

Four major approaches have been used to combine the limiting factors for light and each limiting nutrient:

1) a multiplicative formulation in which all factors are multiplied together:

$$f(L,P,N,C,Si) = f(L)\ f(P)\ f(N)\ f(C)\ f(Si) \qquad (6\text{-}26)$$

where f(L) = light limitation factor
f(P) = nutrient limitation factor for phosphorous
f(N) = nutrient limitation factor for nitrogen
f(C) = nutrient limitation factor for carbon
f(Si) = nutrient limitation factor for silicon (for diatoms)

2) a minimum formulation in which the most severely limiting factor alone is assumed to limit growth:

$$f(L,P,N,C,Si) = \min\left[f(L),f(P),f(N),f(C),f(Si)\right] \qquad (6\text{-}27)$$

where $\min\left[x_1,x_2,x_3,\ldots\right]$ = minimum of each factor x_i

3) a harmonic mean formulation which combines the reciprocal of each limiting factor in the following manner:

$$f(L,P,N,C,Si) = \frac{n}{\frac{1}{f(L)} + \frac{1}{f(P)} + \frac{1}{f(N)} + \frac{1}{f(C)} + \frac{1}{f(Si)}} \qquad (6\text{-}28)$$

where n = number of limiting factors (5 in this case)

4) an arithmetic mean formulation which uses the average of each limiting factor:

$$f(L,P,N,C,Si) = \frac{f(L) + f(P) + f(N) + f(C) + f(Si)}{n} \qquad (6\text{-}29)$$

The multiplicative formulation has been used in many models (Chen and Orlob, 1972, 1975; Di Toro _et al_., 1971, 1977; Di Toro and Matystik, 1980; Di Toro and Connolly, 1980; Thomann _et al_., 1975, 1979; O'Connor _et al_., 1975; Jorgensen, 1976; Jorgensen _et al_., 1978; Canale _et al_., 1975, 1976; Lehman _et al_., 1975; Roesner _et al_., 1981; Baca _et al_., 1973; Duke and Masch, 1973; Brandes and Masch, 1977). This approach assumes that several nutrients in short supply will more severely limit growth than a single nutrient in short supply. The major criticism of this approach is that the computed growth rates may be excessively low when several nutrients are limiting. Also, the severity of the reduction increases with the number of limiting nutrients considered in the model, making comparison between models difficult. Many models assume that light limitation is multiplicative, but use one of the other approaches for nutrient limitation (e.g., Bierman _et al_., 1980; Bierman, 1976; Baca and Arnett, 1976; Nyholm, 1978; Raytheon, 1974).

The minimum formulation is based on "Liebig's law of the minimum" which states that the factor in shortest supply will control the growth of algae.

This approach has been popular in many recent algal models (Bierman et al., 1980; Park et al., 1979, 1980; Scavia, 1980; Smith 1978; Tetra Tech, 1979, 1980; WES, 1982; Johanson et al., 1980; Grenney and Kraszewski, 1981; Chen et al., 1975; Baca and Arnett, 1976). The minimum formulation is often used only for nutrient limitation, with a multiplicative formulation for the light limitation factor.

The harmonic mean formulation is based on an electronic analogy of several resistors in series. The rationale for this formulation is that it includes some interaction between multiple limiting nutrients, but it is not as severely limiting as the multiplicative formulation. This approach has been used in only a few models, for example, the original CLEAN (Bloomfield et al., 1973) and CLEANER (Scavia and Park, 1976) models and Nyholm (1978). The current version of MS.CLEANER (Park et al., 1980) has abandoned this formulation in favor of the minimum formulation. In fact, the harmonic mean formulation and minimum formulation produce similar growth response curves under a wide range of conditions (Swartzman and Bentley, 1979).

The rationale for the arithmetic mean formulation is the same as for the harmonic mean formulation (i.e., it considers the effects of multiple nutrient limitation, but is not as severely limiting as the multiplicative formulation). However, this formulation (e.g., Patten, 1975; Patten et al., 1975) is rarely used since it does not restrict growth enough. For example, the arithmetic mean formulation allows growth even if a critical nutrient such as phosphorus is totally absent, as long as other nutrients are available.

These and other formulations for combining multiple growth limitation factors are reviewed in De Groot (1983).

6.4.3 Light Limitation

Light limitation formulations consist of two components: 1) a relationship describing the attenuation of light with depth and the effect

of algae on light attenuation, and 2) a relationship defining the effect of the resulting light levels on algal growth and photosynthesis.

The attenuation of light with depth is defined in essentially all models by the Beer-Lambert law:

$$I(z) = I_0 \, e^{-\gamma z} \tag{6-30}$$

where $I(z)$ = light intensity at depth z below the surface
z = depth, length
I_0 = light intensity at the surface
γ = light extinction coefficient, 1/length

The light intensity at the surface I_0 is a function of location, time of year, time of day, meterological conditions, and shading from topographic features or riparian vegetation. The surface light intensity used in the algal growth formulations corresponds only to the visible range, which is typically about 50 percent of the total surface solar radiation used in the heat budget computations. Almost all radiation outside of the visible range is absorbed within the first meter below the surface (Orlob, 1977). In addition, some models (for example, MS. CLEANER) assume that only a portion of the visible radiation (about 50%) is available for photosynthesis (Park et al., 1980; Strickland, 1958).

Light attenuation in models differs primarily in the way the light extinction coefficient γ is formulated. The simplest approach is to assume a constant value of γ. This approach is reasonable for short term simulations or over periods when turbidity does not change significantly. However, in long term simulations, γ should be computed dynamically to account for seasonal variations in turbidity due to algal shading or variations in suspended solids loads.

The light extinction coefficient is most commonly defined as the linear sum of several extinction coefficients representing each component of light absorption. The components include all suspended particulates

(phytoplankton, zooplankton, organic and inorganic particulates) as well as dissolved organic matter. The general equation is:

$$\gamma = \gamma_0 + \sum_{i=1}^{n} \gamma_i \tag{6-31}$$

$$= \gamma_0 + \sum_{i=1}^{n} a_i C_i \tag{6-32}$$

where γ_0 = base light extinction coefficient for water without particulates or dissolved organic matter, 1/length

γ_i = light extinction coefficient corresponding to each component of light absorption i, 1/length

n = total number of absorption components considered in the formulation

C_i = concentration of absorption component i, mass/volume

a_i = coefficient for absorption component i relating the concentration C_i to the light extinction coefficient γ_i

Many models include the effects of all components except phytoplankton in the base extinction coefficient γ_0 (by assigning a higher value), and then compute the temporal variations in γ as a function of the algal densities only. This assumes phytoplankton blooms are the major cause of turbidity changes. Equation (6-32) then becomes:

$$\gamma = \gamma_0 + a_1 A \tag{6-33}$$

where γ_0 = light extinction coefficient for all absorption components but phytoplankton, 1/length

a_1 = coefficient relating the phytoplankton concentration A to the corresponding light extinction coefficient for phytoplankton (also called the self-shading factor), 1/(length-mass/volume)

A = phytoplankton concentration, mass/volume

This provides a way of incorporating self-shading effects in the light limitation portion of the algal growth formulation. Some models which use this approach use a nonlinear formulation to describe the relationship between the phytoplankton concentration and the light extinction coefficient. The general expression is:

$$\gamma = \gamma_0 + a_1 A + a_2 A^{b_2} \tag{6-34}$$

where a_1, a_2 = coefficients of the equation relating phytoplankton concentrations to the light extinction coefficient

b_2 = exponent of the equation relating phytoplankton concentrations to the light extinction coefficient

The second component of the light limitation formulation represents the light limitation factor f(L) in Equations (6-26) through (6-29). f(L) defines the relationship between ambient light levels and algal growth rates or rates of photosynthesis. Essentially all formulations fall into one of two major categories (Figure 6-4): 1) saturation type relationships in which the growth rate increases linearly with light at low intensities, but gradually levels off at high intensities to reach a maximum value at the optimum (or saturating) light intensity, or 2) photoinhibition relationships which are similar to the above curves below the optimum light intensity, but which predict decreases in growth rates above the optimum intensity due to photoinhibition effects.

Saturation type responses are typically described by either a Michaelis-Menten (1913) type relationship (Chen and Orlob, 1975; Jorgensen, 1976; Duke and Masch, 1973; Tetra Tech, 1979; Roesner et al., 1981; Johanson et al., 1980; Smith, 1978; WES, 1982):

$$f(L) = \frac{I}{K_L + I} \tag{6-35}$$

where f(L) = light limitation function for algal growth

I = light intensity

K_L = half-saturation constant defining the light level at which growth is one-half the maximum rate

or a Smith (1936) formulation (Park et al., 1980):

$$f(L) = \frac{\alpha_1 I}{\sqrt{1 + (\alpha_1 I)^2}} \tag{6-36}$$

where α_1 = constant in the Smith formulation ($1/\alpha_1$ is the slope of the linear portion of the photosynthesis vs. light curve), 1/light

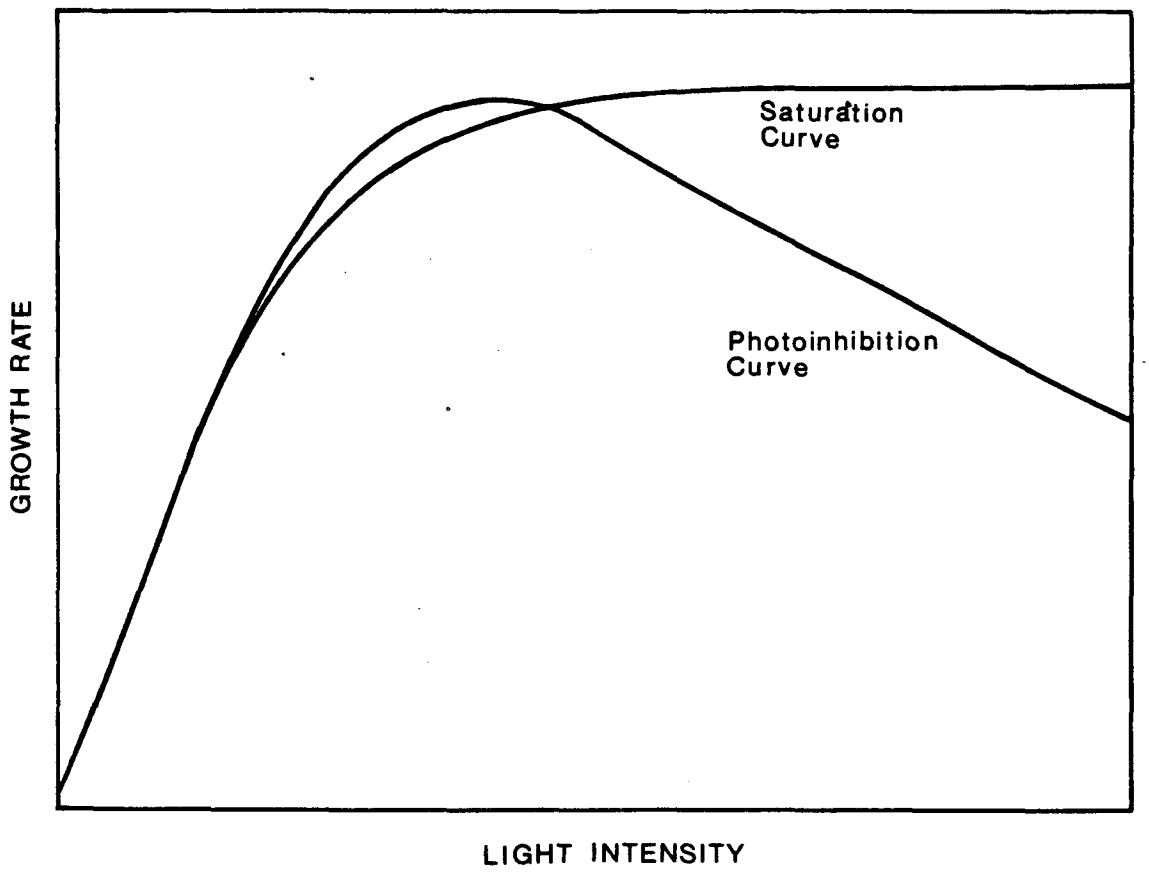

Figure 6-4. Comparison of light response curves for algal growth.

Vollenweider (1965) modified the Smith formulation to give a more general relationship of which the Smith equation is a special case. The Vollenweider form includes photoinhibition effects, and is expressed as:

$$f(L) = \left(\frac{\alpha_1 I}{\sqrt{1 + (\alpha_1 I)^2}}\right)\left(\frac{1}{\sqrt{(1 + (\alpha_2 I)^2)^n}}\right) \qquad (6\text{-}37)$$

where α_2 = photoinhibition factor, 1/light
n = exponent

Baca and Arnett (1976) use this formulation in AQUA-IV with the exponent n equal to 1.

The most commonly used photoinhibition relationship is the Steele (1965) formulation:

$$f(L) = \frac{I}{I_s} e^{\left(1 - \frac{I}{I_s}\right)} \qquad (6\text{-}38)$$

where I_s = optimum (saturating) light intensity

This formulation is used in many models including Di Toro _et al_. (1971, 1977), Di Toro and Matystik (1980), Di Toro and Connolly (1980), Thomann _et al_. (1975, 1979), Thomann and Fitzpatrick (1982), O'Connor _et al_. (1981), Bloomfield _et al_. (1973), Park _et al_. (1974, 1975, 1979, 1980), Scavia _et al_. (1976), Najarian and Harleman (1975), Bierman _et al_. (1980), Canale _et al_. (1975, 1976), Lehman _et al_. (1975), and Baca _et al_. (1973).

Park _et al_. (1980) use the Steele formulation above the saturating light intensity I_s and the Smith formulation below I_s. They feel that the Steele formulation is not accurate below the inhibition threshold since the predicted photosynthesis response is partially dependent on the response above the threshold (Park _et al_., 1979). Under non-inhibiting light

conditions, this may result in a light limitation factor which is too low (Groden, 1977).

Walker (1975) found that the Steele formulation underpredicts photosynthesis rates at high light intensities (above saturation) for some algae, so he modified it by adding an additional parameter n:

$$f(L) = \left(\frac{I}{I_s}\right)^n e^{\left[1 - \left(\frac{I}{I_s}\right)^n\right]} \tag{6-39}$$

where n = parameter for modified Steele formulation

This parameter adjusts the rate of decline of the photosynthesis vs. light curve for light intensities above and below the optimum. The original Steele formulation assumes n=1, while Walker used n values of 0.67, 0.80, and 1.0 for three different algal groups.

A few models include light adaptation algorithms in their light limitation formulations to account for the fact that algae adapted to low light levels have a more rapid response to changing light conditions (steeper slope of photosynthesis vs. light curve) than algae adapted to high light levels. Algae adapt to changing light conditions by varying the chlorophyll content of their cells, with algae adapted to lower light intensities having more chlorophyll.

Nyholm (1978) simulates this effect by varying the value of the saturating light intensity at different times of the year to shift the peak of the light limitation function f(L). The I_s values are maximum during summer and minimum during winter. This shifts the slope of the light response curve so it is steepest during the winter when the algae are adapted to low light levels.

Groden (1977) developed a more complicated formulation for the MS.CLEANER model which dynamically computes the slope of the photosynthesis

vs. light curve as a function of light intensity, and then uses this information to compute the saturating light intensity as a function of both light and temperature. The equation for the slope of the photosynthesis vs. light curve in the light inhibited range is:

$$\alpha = K_1 \ln(I) - K_2 \tag{6-40}$$

where α = slope of photosynthesis vs. light curve

K_1, K_2 = constants

This is based on the assumptions that 1) the slope α is a linear function of the chlorophyll content of the cells and 2) chlorophyll decreases exponentially with light intensity until it reaches some minimum value (Groden, 1977). The values of K_1 and K_2 used in MS.CLEANER are 0.1088 and 0.0704, respectively (Groden, 1977; Park et al., 1980). The equation for the saturating light intensity is:

$$I_s = \frac{\mu_{max}(T_{ref})\ f(T)\ e}{\alpha} \tag{6-41}$$

$$= \frac{\mu_{max}(T_{ref})\ f(T)\ e}{K_1 \ln(I) - K_2}$$

Smith (1980) developed a formulation for computing the saturating light intensity as a function of the maximum photosynthetic quantum yield, maximum growth rate, temperature, light extinction coefficient per unit chlorophyll, and the carbon to chlorophyll ratio of the algae. The equation is:

$$I_s = \frac{\mu_{max}(T_{ref})\ f(T)\ C_r\ e}{\phi_{max}\ a_c} \tag{6-42}$$

where C_r = carbon to chlorophyll ratio

ϕ_{max} = maximum photosynthetic quantum yield, moles carbon fixed/mole photons absorbed

a_c = coefficient for light extintion per unit chlorophyll, 1/(length-mass chlorophyll/volume)

The effects of light adaptation are included in the carbon to chlorophyll ratio C_r. This ratio typically ranges from 20 to 100, with 20 corresponding to low-light, high-temperature conditions, and 100 corresponding to high-light, low-temperature conditions (Smith, 1980; Eppley, 1972). Based on observations that the maximum photosynthesis rate typically occurs at the depth where the light intensity is about 30 percent of the surface value ($I_s = 0.3\ I_o$), Smith (1980) suggested the following relationship for estimating C_r as a function of the ambient light levels:

$$C_r = \frac{0.3\ \bar{I}_o\ \phi_{max}\ a_c}{\mu_{max}(T_{ref})\ f(T)\ e} \qquad (6\text{-}43)$$

$$= \frac{0.11\ \bar{I}_o\ \phi_{max}\ a_c}{\mu_{max}(T_{ref})\ f(T)}$$

where $\bar{I}_o$ = daily average light intensity at the surface

These formulations are used by Thomann and Fitzpatrick (1982) in the Potomac Estuary version of WASP. One advantage of this approach is that I_s and C_r are defined in terms of parameters which are well documented in the literature (ϕ_{max}, μ_{max}, a_c), and which have a fairly narrow range of values over a wide range of environmental conditions.

All of the above relationships for the light limitation factor f(L) have been used to fit experimental measurements of the effects of light on photosynthesis under laboratory conditions. However, in water quality models, these expressions are generally integrated over the depth of each model segment or layer since light varies with depth due to attenuation. The light attenuation formulations (Equations (6-30) through (6-34)) are substituted for the light intensity I in the light limitation formulations (Equations (6-35) through (6-39)), and the light limitation functions are integrated and depth averaged.

Since light also varies continuously with time, most models integrate the light limitation function f(L) over 24 hours to get a daily average value for a given time of the year and set of meteorological conditions. This is generally approximated by multiplying the light limitation function by the photoperiod (expressed as the fraction of the day in which the sun is out) and by using the average light intensity during the daylight hours as I_o in the formulation. This approach is used in steady-state models and dynamic models which use daily time steps. The alternative approach when short time steps (minutes to hours) are used is to compute the light limitation and algal growth formulations dynamically throughout the day using instantaneous values of I_o. The latter method simulates the diurnal variations in algal photosynthesis.

The depth and time integrated Michaelis-Menten formulation for light limitation (Equation (6-35)) is expressed as:

$$f(L) = \frac{f_p}{\gamma d} \ln\left(\frac{K_L + I_o}{K_L + I_o e^{-\gamma d}}\right) \tag{6-44}$$

where f_p = photoperiod (expressed as a fraction of the day)
d = water depth, length
I_o = average light intensity at the surface during the daylight hours

when averaged over the whole water depth or as:

$$f(L) = \frac{f_p}{\gamma (z_2 - z_1)} \ln\left(\frac{K_L + I_o e^{-\gamma z_1}}{K_L + I_o e^{-\gamma z_2}}\right) \tag{6-45}$$

where z_1 = depth at top of layer, length
z_2 = depth at bottom of layer, length

when averaged over a single layer (for example, in a vertically segmented lake model).

The analogous expressions for the Smith formulation (Equation (6-36)) are:

$$f(L) = \frac{f_p}{\gamma\, d} \ln \left[\frac{\alpha_1 I_o + \sqrt{1 + (\alpha_1 I_o)^2}}{\alpha_1 I_o e^{-\gamma d} + \sqrt{1 + (\alpha_1 I_o e^{-\gamma d})^2}} \right] \tag{6-46}$$

and

$$f(L) = \frac{f_p}{\gamma\, (z_2 - z_1)} \ln \left[\frac{\alpha_1 I_o e^{-\gamma z_1} + \sqrt{1 + (\alpha_1 I_o e^{-\gamma z_1})^2}}{\alpha_1 I_o e^{-\gamma z_2} + \sqrt{1 + (\alpha_1 I_o e^{-\gamma z_2})^2}} \right] \tag{6-47}$$

For the Steele formulation (Equation (6-38)), the depth and time integrated expressions are:

$$f(L) = \frac{2.718\, f_p}{\gamma\, d} \left(e^{-\frac{I_o}{I_s} e^{-\gamma d}} - e^{-\frac{I_o}{I_s}} \right) \tag{6-48}$$

and

$$f(L) = \frac{2.718\, f_p}{\gamma\, (z_2 - z_1)} \left(e^{-\frac{I_o}{I_s} e^{-\gamma z_2}} - e^{-\frac{I_o}{I_s} e^{-\gamma z_1}} \right) \tag{6-49}$$

Light limitation factors are compared for several models in Table 6-7. Saturating light intensities and half-saturation constants for light limitation are presented in Tables 6-8 and 6-9.

6.4.4 Nutrient Limitation

Two major approaches have been used to compute nutrient limitation factors in algal models. The first approach is based on Monod (1949) or Michaelis-Menten (1913) kinetics and assumes that the growth rates are determined by the external concentrations of available nutrients. External here refers to the nutrient concentrations in the water column as opposed to the internal concentrations in the algal cells. This approach assumes the nutrient composition of the algal cells remains constant, and is generally referred to as fixed stoichiometry models.

TABLE 6-7. COMPARISON OF LIGHT LIMITATION FORMULATIONS

Model (Author)	Light Limitation Formulation					Reference
	Steele	Smith	Michaelis-Menten	Vollenweider	Other	
AQUA-IV				X		Baca & Arnett (1976)
CE-QUAL-R1			X			WES (EWQOS) (1982)
CLEAN	X					Bloomfield et al. (1973)
CLEANER	X					Scavia & Park (1976)
MS.CLEANER	X*	X*				Park et al. (1980)
DEM			X			Feigner & Harris (1970)
DOSAG3			X			Duke & Masch (1973)
EAM			X			Tetra Tech (1979, 1980)
ESTECO			X			Brandes & Masch (1977)
EXPLORE-1	X					Baca et al. (1973)
HSPF			X			Johanson et al. (1980)
LAKECO			X			Chen & Orlob (1975)
MIT Network	X					Harleman et al. (1977)
QUAL-II			X			Roesner et al. (1981)
RECEIV-II	X					Raytheon (1974)
SSAM IV					none	Grenney & Kraszewski (1981)
WASP	X					Di Toro et al. (1981)
WQRRS			X			Smith (1978)
Bierman	X					Bierman et al. (1980)
Canale	X					Canale et al. (1975, 1976)
Jorgensen			X			Jorgensen (1976)
Lehman	X					Lehman et al. (1975)
Nyholm					piecewise linear saturation	Nyholm (1978)
Scavia	X					Scavia et al. (1976)

*Smith formulation used below light saturation, Steele formulation used above light saturation.

TABLE 6-8. ALGAL SATURATING LIGHT INTENSITIES

Algal Type	Saturating Light Intensity (langleys/day)	References
Total Phytoplankton	300 - 350	Thomann et al. (1975, 1979) Salas & Thomann (1978) Di Toro et al. (1971) Di Toro & Connolly (1980) Di Toro & Matystik (1980) O'Connor et al. (1975)
	250 - 350	Scavia et al. (1976) Scavia & Park (1976) Scavia (1980)
	200 - 300	Youngberg (1977)
	216	Desormeau (1978)
	288	Larsen et al. (1973)
Diatoms	225	Thomann et al. (1979) Di Toro & Connolly (1980)
	300	Scavia et al. (1976) Scavia (1980)
	88 - 100	Bierman (1976) Bierman et al. (1980)
	225	Canale et al. (1976)
	144	Lehman et al. (1975)
Green Algae	88 - 100	Bierman (1976) Bierman et al. (1980)
	160	Canale et al. (1976)
	65	Lehman et al. (1975)
Blue-green Algae	44 - 50	Bierman (1976) Bierman et al. (1980)
	43	Lehman et al. (1975)
	600	Canale et al. (1976)
	300 - 350	Youngberg (1977)
	250	Scavia (1980)
Flagellates	288	Lehman et al. (1975)
	100	Bierman et al. (1980)
Chrysophytes	86	Lehman et al. (1975)

TABLE 6-9. HALF-SATURATION CONSTANTS FOR LIGHT LIMITATION

Algal Type	Half-Saturation Constant ($Kcal/m^2/sec$)	References
Total Phytoplankton	0.002 - 0.006	Chen (1970) Chen & Orlob (1975) Chen & Wells (1975, 1976) U.S. Army Corps of Engineers (1974) Tetra Tech (1976)
	0.0046	Jorgensen (1976) Jorgensen *et al.* (1978)
	0.002 - 0.006*	Smith (1978)
	0.005*	Roesner *et al.* (1980) Duke & Masch (1973)
	0.003 - 0.005*	Brandes (1976)
	0.004 - 0.006**	Jorgensen (1979)
	0.0044**	Collins & Wlosinski (1983)
Diatoms	0.003	Tetra Tech (1980) Bowie *et al.* (1980) Porcella *et al.* (1983)
	0.002*	Tetra Tech (1979)
	0.00005 - 0.0012**	Jorgensen (1979)
	0.00005 - 0.0026**	Collins & Wlosinski (1983)
Green Algae	0.002 - 0.004	Tetra Tech (1980) Bowie *et al.* (1980) Porcella *et al.* (1983)
	0.002*	Tetra Tech (1979)
	0.0003 - 0.0011**	Jorgensen (1979)
	0.0003 - 0.0106**	Collins & Wlosinski (1983)
Blue-green Algae	0.002 - 0.004	Tetra Tech (1980) Bowie *et al.*(1980) Porcella *et al.* (1983)
	0.002*	Tetra Tech (1979)
Dinoflagellates	0.002*	Tetra Tech (1979)
	0.0043 - 0.0053**	Collins & Wlosinski (1983)

(continued)

TABLE 6-9. (continued)

Algal Type	Half-Saturation Constant ($Kcal/m^2/sec$)	References
Flagellates	0.002 - 0.004	Tetra Tech (1980) Porcella et al. (1983)
	0.0044**	Collins & Wlosinski (1983)
Chrysophytes	0.002*	Tetra Tech (1979)
	0.0014 - 0.0017**	Collins & Wlosinski (1983)
Coccolithophores	0.0003 - 0.0016**	Collins & Wlosinski (1983)
Benthic Algae	0.01 - 0.005	Tetra Tech (1980) Bowie et al. (1980) Porcella et al (1983)
	0.002 - 0.006*	Smith (1978)

*Model documentation values.

**Literature values.

The second approach assumes that algal growth is a two-step process, the first step being nutrient uptake and the second step being cell growth or division. Cell growth depends on the internal concentrations of nutrients within the cells, rather than external concentrations in the water. The uptake rates are dependent on both the external and internal concentrations. Since uptake and growth are modeled separately, the nutrient composition of the cell may change with time, resulting in variable stoichiometry or internal pool models. These models simulate processes such as luxury uptake of nutrients which allows growth even when external nutrients are depleted.

6.4.4.1 Nutrient Limitation in Fixed Stoichiometry Models

The majority of water quality models are of the fixed stoichiometry type. These models are generally based on conventional Monod or Michaelis-Menten kinetics. The algal growth equation for a single limiting nutrient under conditions of optimum temperature and light can be expressed as:

$$\mu = \mu_{max}\left(\frac{s}{K_s + s}\right) \tag{6-50}$$

$$= \mu_{max}\ f(s)$$

where s = concentration of the limiting nutrient in the water, mass/volume

K_s = half-saturation constant for the limiting nutrient, mass/volume

The quantity $f(s) = (\frac{s}{K_s + s})$ is the growth limitation factor for the nutrient s. The half-saturation constant refers to the concentration of the nutrient at which the growth rate is one half of its maximum value. The above equation results in a hyperbolic growth curve (Figure 6-5) in which growth increases approximately linearly with nutrients at very low nutrient concentrations, but gradually levels off to a maximum growth rate at high nutrient levels (growth saturation). At this point, the nutrient is no longer limiting, so further increases in the external nutrient supply do not affect growth.

Fixed stoichiometry models typically compute a separate growth limitation factor f(s) for each nutrient modeled, and then combine the factors using any one of the four methods discussed above in Equations (6-26) to (6-29) (i.e., multiplicative formulation, minimum formulation, harmonic mean formulation, or arithmetic mean formulation). The specific nutrient limitation factors are:

$$f(P) = \frac{PO_4}{K_P + PO_4} \tag{6-51}$$

$$f(N) = \frac{(NH_3 + NO_3)}{K_N + (NH_3 + NO_3)} \tag{6-52}$$

$$f(C) = \frac{CO_2}{K_C + CO_2} \tag{6-53}$$

$$f(Si) = \frac{Si}{K_{Si} + Si} \tag{6-54}$$

where PO_4 = available dissolved inorganic phosphorus concentration (orthophosphate), mass/volume

(NH_3+NO_3) = available dissolved inorganic nitrogen concentration (ammonia plus nitrate), mass/volume

CO_2 = available dissolved inorganic carbon concentration (carbon dioxide), mass/volume

Si = available dissolved silicon concentration, mass/volume

K_P = half-saturation constant for phosphorus, mass/volume

K_N = half-saturation constant for nitrogen, mass/volume

K_C = half-saturation constant for carbon, mass/volume

K_{Si} = half-saturation constant for silicon, mass/volume

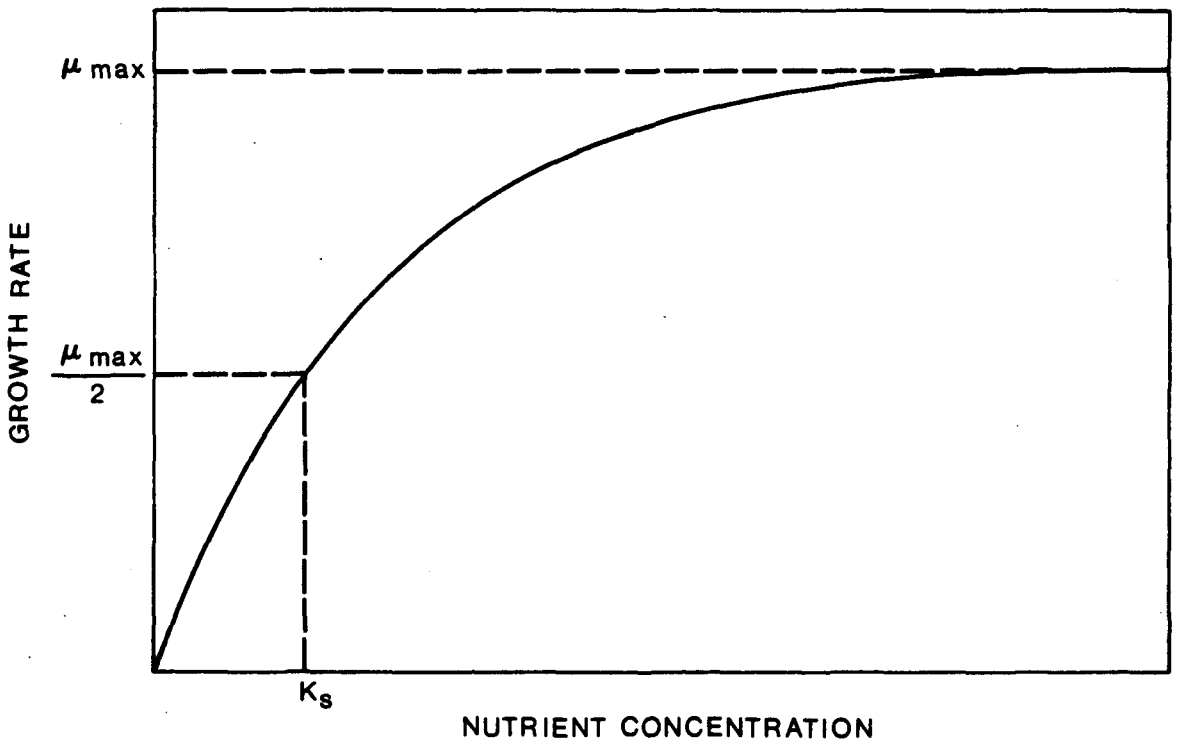

Figure 6-5. Michaelis-Menten saturation kinetics for algal growth limitation by a single nutrient.

The number of growth limiting factors included in a given model depends on both the particular algal species present and the chemistry of the water body under consideration. For example, silicon limitation is only appropriate for diatoms. Nitrogen limitation can generally be omitted for nitrogen-fixing blue-green algae (although nitrogen kinetics for blue-greens must still be included to correctly describe the nitrogen cycle). Carbon limitation is frequently excluded from algal models since carbon is often assumed to be available in excess and is therefore not modeled as a state variable. Lake models often assume phosphorus is the only limiting nutrient, while estuary models often assume nitrogen is limiting at all times.

The way in which nitrogen limitation is computed also varies from model to model. For example, some models simulate available nitrogen as a single constituent (Bierman et al., 1980; Jorgensen et al., 1978; Nyholm, 1978; Thomann et al., 1979), while other models simulate ammonia, nitrite, and nitrate separately and assume both ammonia and nitrate are available for algal growth (Chen and Orlob, 1975; Baca and Arnett, 1976; Baca et al., 1973; Smith, 1978; Najarian and Harleman, 1975; Duke and Masch, 1973). QUAL-II simulates the various forms of nitrogen, but assumes algal growth is only limited by nitrate (Roesner et al., 1981). Some models include factors to account for ammonia preference by algae in their nutrient uptake formulations (Scavia et al., 1976; Canale et al., 1976; Grenney and Kraszewski, 1981; Thomann and Fitzpatrick, 1982; O'Connor et al., 1981; JRB, 1983). Ammonia preference factors are discussed in Chapter 5.

Values of the Michaelis-Menten half-saturation constants for each limiting nutrient are available from many sources, including both the modeling literature and the experimental literature. However, care must be taken when using this information since the values reported will depend on the particular model formulations used for the modeling literature, and on the experimental conditions for the scientific literature. For example, if a multiplicative formulation is used to compute algal growth (Equation(6-26)), the half-saturation constants should be smaller than the corresponding constants where a minimum formulation is used (Equation

(6-27)). In general, the more limiting nutrients that are considered with a multiplicative formulation, the smaller the value of each half-saturation constant. This is necessary in order to get the same growth response with both formulations when more than one nutrient is limiting simultaneously. This is true of both the modeling literature and the experimental literature. When the harmonic mean formulation is used (Equation (6-28)), the half-saturation constants should generally be somewhere between the values of the minimum and multiplicative formulations. Half-saturation constants for each limiting nutrient are tabulated in Table 6-10.

Table 6-11 compares the algal growth formulations used in several models, including the growth limiting factors used, the specific formulations for nutrient limitation, and the methods for combining multiple limiting factors.

6.4.4.2 Nutrient Limitation In Variable Stoichiometry Models

Variable stoichiometry models assume that the growth limiting factor for nutrients, f(P,N,C,Si) in Equation (6-4), is a function of the internal levels of the nutrients in the algal cells rather than the external concentrations in the water column. The internal concentrations are generally defined as:

$$q = \frac{\text{internal mass of nutrient in cells}}{\text{dry weight biomass of cells}} \qquad (6\text{-}55)$$

where q = internal nutrient concentration, mass nutrient/biomass algae

Internal nutrient levels depend on the relative magnitudes of the nutrient uptake rates and the algal growth rates. The uptake rates are functions of both the internal and external nutrient concentrations, while the growth rates depend primarily on the internal concentrations.

Variable stoichiometry models differ in 1) the specific process formulations used to simulate uptake and growth, 2) the number of nutrients considered, and 3) the ways in which multiple limiting factors are combined.

TABLE 6-10. HALF-SATURATION CONSTANTS FOR MICHAELIS-MENTEN GROWTH FORMULATIONS

Algal Type	Half-Saturation Constant				References
	Nitrogen (mg/l)	Phosphorus (mg/l)	Carbon (mg/l)	Silicon (mg/l)	
Total Phytoplankton	0.025	0.0005 - 0.03			O'Connor et al. (1975, 1985) Thomann et al. (1974, 1975, 1979) Thomann & Fitzpatrick (1982) Di Toro & Matystik (1980) Di Toro & Connolly (1980) Di Toro et al. (1971, 1977) Salas & Thomann (1978) Salisbury et al. (1983)
	0.01 - 0.4	0.004 - 0.08	0.03 - 0.8		Chen (1970) Chen & Orlob (1975) Chen & Wells (1975, 1976) U.S. Army Corps of Engineers (1974) Tetra Tech (1976)
	0.2	0.02 - 0.03	0.5		Jorgensen (1976) Jorgensen et al. (1978)
	0.025	0.006 - 0.025			Battelle (1974)
	0.06 - 0.08	0.02			Grenney & Kraszewski (1981)
	0.015	0.0025			Canale et al. (1976)
	0.014	0.001			Larsen et al. (1973)
	0.025 - 0.3*	0.006 - 0.03*			Baca & Arnett (1976)
	0.04 - 0.10*	0.02 - 0.05*	0.02 - 0.04*		Smith (1978)
	0.2 - 0.4*	0.03 - 0.05*			Roesner et al. (1980) Duke & Masch (1973)
	0.015 - 0.3*	0.0025 - 0.08*			Grenney & Kraszewski (1981)
	0.10 - 0.4*	0.03 - 0.05*	0.15*		Brandes (1976)
	0.0014 - 0.018	0.006**			Di Toro et al. (1971)
	0.025 - 0.2**	0.002 - 0.08**			Jorgensen (1979)
	0.0015 - 0.15**				O'Connor et al. (1981)
		0.02 - 0.075**			Collins & Wlosinski (1983)
Diatoms	0.015 - 0.03	0.002	0.03	0.08	Tetra Tech (1980) Bowie et al. (1980) Porcella et al. (1983)
	0.025	0.001 - 0.002		0.030 - 0.1	Thomann et al. (1979) Di Toro & Connolly (1980) Salisbury et al. (1983)
	0.025 - 0.030	0.004 - 0.009		0.03	Scavia et al. (1976) Scavia (1980)
	0.015	0.0025		0.03	Canale et al. (1976)
				0.1	Bierman (1976)
	0.015*	0.03*	0.03*	0.08*	Tetra Tech (1979)
	0.0063 - 0.12**	0.01 - 0.025**			Di Toro et al. (1971)
		0.025**			Jorgensen (1979)
	0.003 - 0.923**	0.001 - 0.163**			Collins & Wlosinski (1983)

TABLE 6-10. (continued)

Algal Type	Half-Saturation Constant Nitrogen (mg/l)	Phosphorus (mg/l)	Carbon (mg/l)	Silicon (mg/l)	References
Green Algae	0.03 - 0.035	0.004	0.03		Tetra Tech (1980) Bowie et al. (1980) Porcella et al. (1983)
	0.15	0.01			Di Toro et al. (1971)
	0.001 - 0.035	0.005 - 0.024			Scavia et al. (1976) Scavia & Park (1976) Scavia (1980)
	0.15	0.0025			Canale et al. (1976)
	0.03*	0.03*	0.03*		Tetra Tech (1979)
	0.005 - 0.15**	0.01**			Jorgensen (1979)
	0.006 - 1.236**	0.002 - 0.475**	0.068 - 1.5**		Collins & Wlosinski (1983)
Blue-green Algae	0.	0.010 - 0.02	0.03		Tetra Tech (1980) Bowie et al. (1980) Porcella et al. (1983)
	0.001	0.01 - 0.015			Scavia & Park (1976) Scavia (1980)
		0.01			Di Toro et al. (1971)
	0.015	0.0025			Canale et al. (1976)
	0.*	0.06*	0.03*		Tetra Tech (1979)
	0.062 - 4.34**	0.006**	0.031 - 0.088**		Collins & Wlosinski (1983)
Dinoflagellates	0.005				O'Connor et al. (1981)
	0.08*	0.06*	0.03*		Tetra Tech (1979)
	0.007 - 0.13**				Di Toro et al. (1971)
	0.019 - 0.589**				Collins & Wlosinski (1983)
Flagellates	0.08	0.012	0.03		Tetra Tech (1980) Porcella et al. (1983)
	0.0084 - 0.13**				Jorgensen (1979)
	0.001 - 0.052**				Collins & Wlosinski (1983)
Chrysophytes	0.015	0.02*	0.03*		Tetra Tech (1979)
	0.006**	0.047 - 0.076**			Collins & Wlosinski (1983)
Coccolithophores	0.006 - 0.019**				Collins & Wlosinski (1983)
Benthic Algae	0.05 - 0.1	0.004 - 0.008	0.03 - 0.1		Tetra Tech (1980) Bowie et al. (1980) Porcella et al. (1983)
	0.06 - 0.08	0.02			Grenney & Kraszewski (1981)
	0.04 - 0.10*	0.02 - 0.05*	0.02 - 0.04*		Smith (1978)
	0.015 - 0.3*	0.0025 - 0.08*			Grenney & Kraszewski (1981)

*Model documentation values.

**Literature values.

TABLE 6-11. COMPARISON OF ALGAL GROWTH FORMULATIONS

Model (Author)	Growth Limiting Factors						Stoichiometry		Nutrient Limitation Formulation		Method for Combining Factors			Reference
	Light	PO_4	NO_3	NH_3	CO_2	Si	Fixed	Variable	Michaelis-Menten	Other	Multiplicative	Minimum	Harmonic Mean	
AQUA-IV	X	X	X	X			X		X		light	nutrients		Baca & Arnett (1976)
CE-QUAL-R1	X	X	X	X	X		X		X			X		WES (EWQOS) (1982)
CLEAN	X	X	X	X	X		X		X				X	Bloomfield et al. (1973)
CLEANER	X	X	X	X	X		X		X				X	Scavia & Park (1976)
MS.CLEANER	X	X	X	X	X	X	C & Si	N & P	X*	6-51*		X		Park et al. (1980)
DEM	X	X	X				X		X		X			Feigner & Harris (1970)
DOSAG3	X	X	X				X		X		X			Duke & Masch (1973)
EAM	X	X	X	X	X	X	X		X			X		Tetra Tech (1979, 1980)
ESTECO	X	X	X	X	X		X		X		X			Brandes & Masch (1977)
EXPLORE-1	X	X	X	X			X		X		X			Baca et al. (1973)
HSPF	X	X	X	X	X		X		X			X		Johanson et al. (1980)
LAKECO	X	X	X	X	X		X		X		X			Chen & Orlob (1975)
MIT Network	X		X	X			X		X		light			Harleman et al. (1977)
QUAL-II	X	X	X				X		X		X			Roesner et al. (1981)
RECEIV-II	X	X	X	X			X		X		light	nutrients		Raytheon (1974)
SSAM IV		X	X	X			X		X			X		Grenney & Kraszewski (1981)
WASP	X	X	X	X		X	X		X		X			Di Toro et al. (1981)
WQRRS	X	X	X	X	X		X		X			X		Smith (1978)
Bierman	X	X	X	X		X	Si	N & P	X**	6-52**	light	nutrients		Bierman et al. (1980)
Canale	X	X	X	X		X	X		X		X			Canale et al. (1975, 1976)
Jorgensen	X	X	X	X	X			X		6-53	X			Jorgensen (1976)
Lehman	X	X	X	X	X	X		X		6-53	X			Lehman et al. (1975)
Nyholm	X	X	X	X				X		6-54, 55	light		nutrients	Nyholm (1978)
Scavia	X	X	X	X		X	X		X			X		Scavia et al. (1976)

*Fixed stoichiometry Michaelis-Menten formulation used for carbon and silicon, with variable stoichiometry formulations for nitrogen and phosphorus.
**Fixed stoichiometry Michaelis-Menten formulation used for silicon, with variable stoichiometry formulations for nitrogen and phosphorus.

Several different formulations have been used to compute nutrient limitation factors in variable stoichiometry models. As with fixed stoichiometry models, the limitation factors may range from 0 to 1. Most models assume a minimum internal stoichiometric nutrient requirement at which growth is zero. This minimum level is often called the minimum cell quota or subsistence quota. Algal growth (and the nutrient limitation factors) are assumed to increase with increasing internal nutrient levels above the minimum cell quota until the maximum growth rate is attained. Some type of hyperbolic function is typically used to express this saturation type relationship.

The following expressions have been used to determine growth limitation factors in variable stoichiometry models:

$$f(q) = \frac{q}{K_1 + q} \tag{6-56}$$

$$f(q) = \frac{(q - q_{min})}{K_2 + (q - q_{min})} \tag{6-57}$$

$$f(q) = \left(1 - \frac{q_{min}}{q}\right) = \left(\frac{q - q_{min}}{q}\right) \tag{6-58}$$

$$f(q) = \frac{q - q_{min}}{q_{max} - q_{min}} \tag{6-59}$$

$$f(q) = \left[\frac{(q - q_{min})}{K_3 + (q - q_{min})}\right]\left[\frac{K_3 + (q_{max} - q_{min})}{(q_{max} - q_{min})}\right] \tag{6-60}$$

where $f(q)$ = nutrient limitation factor

q = internal nutrient concentration, mass nutrient/biomass algae

q_{min} = minimum internal stoichiometric requirement (cell quota), mass nutrient/biomass algae

q_{max} = maximum internal nutrient concentration, mass nutrient/biomass algae

K_1, K_2, K_3 = half-saturation constants for growth limitation

Equation (6-56) is equivalent in form to the Michaelis-Menten relationship except that the internal rather than the external nutrient concentration is the independent variable. This equation is used in MS.CLEANER for both nitrogen and phosphorus limitation (Park et al., 1980). Equation (6-57) also has the same form as the Michaelis-Menten relationship, but the independent variable is the internal nutrient concentration in excess of the minimum cell quota. This equation is used by Bierman (1976) and Bierman et al. (1973, 1980) for nitrogen and phosphorus. Equation (6-58) was originally developed by Droop (1968), and it is used in several models including Lehman et al. (1975), Jorgensen (1976), Jorgensen et al. (1978, 1981), and Canale and Auer (1982) for all nutrients simulated in these models. Equation (6-58) can be derived from Equation (6-57) by assuming $K_2 = q_{min}$, as was demonstrated by Rhee (1973, 1978) for phosphorus and nitrogen (Bierman, 1981). Equations (6-59) and (6-60) are used by Nyholm (1978) for nitrogen and phosphorus, respectively. Note that Equation (6-59) is a linear rather than hyperbolic relationship. Also, Equation (6-60) is similar to Equation (6-57) since the second factor in Equation (6-60) is a constant once q_{min}, q_{max}, and K_3 are defined.

Since variable stoichiometry formulations have not been widely used, data for the model parameters are limited. Values for the various half-saturation constants are presented in Table 6-12. Note that the half-saturation constants (K_1,K_2, and K_3) have different values since the corresponding equations are different. Minimum cell quotas and maximum internal nutrient concentrations are tabulated in Tables 6-13 and 6-14.

The ways in which variable stoichiometry formulations are used varies between different models. Some models use variable stoichiometry formulations only for phosphorus and nitrogen, combining them with conventional Michaelis-Menten kinetics for carbon and silica (Park et al., 1980; Bierman et al., 1980), while other models use variable stoichiometry formulations for all nutrients modeled (Lehman et al., 1975; Jorgensen, 1976). In a few cases, different internal nutrient formulations are used for different nutrients in the same model (Nyholm, 1978). In some models,

TABLE 6-12. HALF-SATURATION CONSTANTS FOR VARIABLE STOICHIOMETRY FORMULATIONS

Nutrient	Half-Saturation Constant Type	Half-Saturation Constant Value	Algal Type	Reference
Phosphorus	K_1	0.005 g/m^3	Total Phytoplankton	Desormeau (1978)
	K_2	0.724×10^{-7} μmole/cell 0.0005 mg/mg (D.W.)	Diatoms	Bierman et al. (1980)
		0.312×10^{-8} μmole/cell 0.0005 mg/mg (D.W.)	Green Algae	
		0.148×10^{-7} μmole/cell 0.0005 mg/mg (D.W.)	Flagellates	
		0.488×10^{-8} μmole/cell 0.0007 mg/mg (D.W.)	Blue-greens (N-fixing)	
		0.566×10^{-8} μmole/cell 0.0007 mg/mg (D.W.)	Blue-greens (non N-fixing)	
	K_3	0.003 mg/mg (D.W.)	Total Phytoplankton	Nyholm (1978)
Nitrogen	K_1	0.05 g/m^3	Total Phytoplankton	Desormeau (1978)
	K_2	0.801×10^{-5} μmole/cell 0.025 mg/mg (D.W.)	Diatoms	Bierman et al. (1980)
		0.345×10^{-6} μmole/cell 0.025 mg/mg (D.W.)	Green Algae	
		0.163×10^{-5} μmole/cell 0.025 mg/mg (D.W.)	Flagellates	
		0.377×10^{-6} μmole/cell 0.025 mg/mg (D.W.)	Blue-greens (N-fixing)	
		0.438×10^{-6} μmole/cell 0.025 mg/mg (D.W.)	Blue-greens (non N-fixing)	
	K_2	0.14×10^{-7} μmole/cell	Diatoms	Bierman (1976)
		0.14×10^{-7} μmole/cell	Green Algae	
		0.23×10^{-7} μmole/cell	Blue-greens (N-fixing)	
		0.14×10^{-7} μmole/cell	Blue-greens (non N-fixing)	

carbon and silica are not included as potentially limiting nutrients (Nyholm, 1978).

The combined effects of multiple limiting nutrients in variable stoichiometry models are dealt with in the same basic ways as in fixed stoichiometry models (i.e., multiplicative formulation (Equation (6-26)), minimum formulation (Equation (6-27)), or harmonic mean formulation (Equation (6-28)). However, when a minimum (or threshold) formulation is used, the limiting nutrient is often determined by comparing the internal

TABLE 6-13. MINIMUM CELL QUOTAS

Algal Type	Minimum Cell Concentration				Units	References
	Nitrogen	Phosphorus	Carbon	Silicon		
Total Phytoplankton	0.015-0.02	0.001-0.003	0.15-0.18		mg/mg (D.W.)	Jorgensen (1976, 1983)
	0.015	0.001	0.15-0.4		mg/mg (D.W.)	Jorgensen et al. (1978, 1981)
	0.04	0.00146			mg/mg (D.W.)	Nyholm (1978)
			0.3-0.7**		mg/mg (D.W.)	Jorgensen (1981)
Diatoms	0.520×10^{-7}	0.20×10^{-8}			µmoles/cell	Bierman (1976)
	0.801×10^{-5} 0.025	0.724×10^{-7} 0.0005			µmoles/cell mg/mg (D.W.)	Bierman et al. (1980)
	$6. \times 10^{-7}$**	$0.9\text{-}30. \times 10^{-9}$**		$0.2\text{-}40. \times 10^{-7}$**	µmoles/cell	Lehman et al. (1975)
		0.45-0.6**			$\mu g/mm^3$ cell volume	Jorgensen (1979)
Green Algae	0.520×10^{-7}	0.20×10^{-8}			µmoles/cell	Bierman (1976)
	0.345×10^{-6} 0.025	0.312×10^{-8} 0.0005			µmoles/cell mg/mg (D.W.)	Bierman et al. (1980)
		$1.7\text{-}4.5 \times 10^{-9}$**			µmoles/cell	Lehman et al. (1975)
		>0.5**			$\mu g/mm^3$ cell volume	Jorgensen (1979)
Blue-green Algae	$0.520\text{-}0.853 \times 10^{-7}$	$0.583\text{-}1.34 \times 10^{-9}$			µmoles/cell	Bierman (1976)
	$0.377\text{-}0.438 \times 10^{-6}$ 0.025	$0.488\text{-}0.566 \times 10^{-8}$ 0.0007			µmoles/cell mg/mg (D.W.)	Bierman et al. (1980)
	1.1×10^{-7}**	2.5×10^{-9}**			µmoles/cell	Lehman et al. (1975)
		>0.5**			$\mu g/mm^3$ cell volume	Jorgensen (1979)
Dinoflagellates	3.9×10^{-7}**	$11. \times 10^{-9}$**			µmoles/cell	Lehman et al. (1975)
Flagellates	0.163×10^{-5} 0.025	0.148×10^{-7} 0.0005			µmoles/cell mg/mg (D.W.)	Bierman et al. (1980)
Chrysophytes	$0.18\text{-}0.3 \times 10^{-7}$**	0.5×10^{-9}**			µmoles/cell	Lehman et al. (1975)
Benthic Algae		0.0005			mg/mg (D.W.)	Auer and Canale (1982)

**Literature values.

TABLE 6-14. MAXIMUM INTERNAL NUTRIENT CONCENTRATIONS

Algal Type	Maximum Cell Concentration				Units	References
	Nitrogen	Phosphorus	Carbon	Silicon		
Total Phytoplankton	0.08-0.12	0.013-0.03	0.6		mg/mg (D.W.)	Jorgensen (1976, 1983) Jorgensen *et al*. (1978, 1981)
	0.1	0.02			mg/mg (D.W.)	Nyholm (1978)
	0.08-0.12**	0.013-0.035**			mg/mg (D.W.)	Jorgensen *et al*. (1981)

**Literature values.

phosphorus to internal nitrogen ratio with a threshold ratio, rather than computing the growth limitation factor for each nutrient and using the smallest value.

Table 6-11 compares the growth formulations used in several variable stoichiometry and fixed stoichiometry models. The comparisons show which limiting factors are included, which formulations are used to compute nutrient limitation, and how multiple limiting factors are combined.

6.4.4.3 Nutrient Uptake In Variable Stoichiometry Models

In fixed stoichiometry models, the nutrient composition of the algal cells is assumed to remain constant, so nutrient uptake is directly related to the algal growth rate by the stoichiometric ratio of nutrient mass to cell biomass. The nutrient uptake rate can then be expressed as:

$$v = \mu q_c \tag{6-61}$$

where v = nutrient uptake rate, mass nutrient/mass algae-time
μ = algal growth rate, 1/time
q_c = constant internal nutrient concentration, mass nutrient/biomass algae

The growth rates are assumed to be functions of the external nutrient supplies (plus temperature and light) as computed by Michaelis-Menten type relationships (Equation (6-50)).

In contrast, nutrient uptake rates in variable stoichiometry models are functions of both internal nutrient levels in the cells and external nutrient concentrations in the water. The general relationship is typically of the form:

$$v = v_{max}(T_{ref})\ f(T)\ f(q,s)\ f(L) \tag{6-62}$$

where $v_{max}(T_{ref})$ = maximum nutrient uptake rate at reference

temperature T_{ref}, mass nutrient/mass algae-time

f(T) = temperature function for uptake

f(q,s) = nutrient uptake limitation function

q = internal nutrient concentration, nutrient mass/cell biomass

s = external nutrient concentration, mass/water volume

f(L) = light limitation function for uptake

The temperature and light functions for uptake are essentially the same as those used for algal growth.

Variable stoichiometry models are distinguished primarily by the specific formulations used for the uptake limitation function f(q,s). These functions define the feedback between uptake rates and both internal and external nutrient levels. Some formulations attempt a more mechanistic approach, while others tend to be empirically based. In general, the uptake rates increase with the external nutrient supplies but at the same time decrease as the internal nutrient levels approach their saturation values. Uptake rates approach zero when either external nutrients are depleted or when internal nutrients reach their maximum saturated levels. However, neither of these conditions can persist since nutrients are continually recycled and since phytoplankton growth increases the algal biomass relative to the internal nutrient mass which in effect reduces the internal nutrient concentrations under conditions of restricted uptake.

The following formulations have been used to express internal and external nutrient effects on uptake rates in variable stoichiometry models:

$$f(q,s) = (q_{max} - q)\left(\frac{s}{K_{u1} + s}\right) \tag{6-63}$$

$$f(q,s) = \left(\frac{q_{max} - q}{q_{max} - q_{min}}\right)\left(\frac{s}{K_{u2} + s}\right) \tag{6-64}$$

$$f(q,s) = \frac{1}{\left(1 + \frac{K_{u3}}{s}\right)\left(1 + \frac{C_i}{K_i}\right)}$$

$$= \left(\frac{K_i}{K_i + C_i}\right)\left(\frac{s}{K_{u3} + s}\right)$$

$$= \left(\frac{K_i}{K_i + q\ f_i}\right)\left(\frac{s}{K_{u3} + s}\right) \qquad (6\text{-}65)$$

$$f(q,s) = \left(\frac{K_i}{K_i + (q - q_{min})}\right)\left(\frac{s}{K_{u3} + s}\right) \qquad (6\text{-}66)$$

$$f(q,s) = \left(\frac{1}{1 + K_a\ q_d}\right) - \left(\frac{1}{1 + K_a\ s}\right) \qquad (6\text{-}67a)$$

with

$$q_d = q_{dmin}\ e^{\left(\frac{q}{q_{min}} - 1\right)} \qquad (6\text{-}67b)$$

where q_{max} = maximum internal nutrient concentration, mass nutrient/biomass algae

q_{min} = minimum internal stoichiometric requirement (cell quota), mass nutrient/biomass algae

q_d = internal available nutrient concentration, mass nutrient/volume

q_{dmin} = minimum internal available nutrient concentration, mass nutrient/volume

C_i = internal concentration of uptake inhibitor, mass nutrient/biomass algae

f_i = fraction of total internal nutrient concentration which acts as an inhibitor to nutrient uptake (this corresponds to the acid-soluble polyphosphate fraction of total internal phosphorus, or the cellular free amino acid fraction of total internal nitrogen)

K_{u1}, K_{u2}, K_{u3} = half-saturation constants for nutrient uptake, mass nutrient/volume water

K_i = half-saturation constant for inhibition of nutrient uptake, mass nutrient/biomass algae

K_a = affinity coefficient, volume/mass nutrient

Equation (6-63) is used by Koonce and Hasler (1972), Equation (6-64) by Lehman et al. (1975) and Jorgensen (1976), Equation (6-65) by Rhee (1973) and Park et al. (1980), Equation (6-66) by Di Toro (1980), Auer and Canale (1982), and Canale and Auer (1982), and Equations (6-67a) and (6-67b) by Bierman et al. (1973, 1980).

Maximum nutrient uptake rates and half-saturation constants for uptake are presented in Tables 6-15 and 6-16. Minimum cell quotas and maximum internal nutrient concentrations were presented previously in Tables 6-13 and 6-14. Some of the more model specific parameters are presented in Table 6-17.

Although variable stoichiometry models more realistically represent nutrient uptake and cell growth than fixed stoichiometry models, they do it at the expense of additional model complexity and computational costs. Algal growth computations in variable stoichiometry models require shorter time steps since the time scale for nutrient uptake is on the order of hours while the time scale for algal growth is on the order of days. Also, spatial variability in external and internal nutrient concentrations complicates transport since algae with different internal stoichiometries will be transported into the same model segment, requiring some type of averaging procedure at each time step.

Another criticism of variable stoichiometry models is that more model coefficients are required than in fixed stoichiometry models. Several coefficients are required for both the uptake and growth formulations. Since these coefficients must describe the response of species assemblages rather than the single species evaluated in laboratory experiments, they must be determined largely by model calibration. This introduces additional uncertainty in the model results. Also, the data base for variable stoichiometry coefficients is much smaller than for conventional Michaelis-Menten parameters.

TABLE 6-15. MAXIMUM NUTRIENT UPTAKE RATES

Algal Type	Maximum Uptake Rate				Units	References
	Nitrogen	Phosphorus	Carbon	Silicon		
Total Phytoplankton	0.15	0.0014	0.55		1/day	Jorgensen (1983)
	0.012-0.03	0.0014-0.008	0.40-1.21		1/day	Jorgensen *et al.* (1978, 1981)
	0.14	0.1			1/day	Desormeau (1978)
	0.01-0.035**	0.003-0.01**	0.2-0.7**		1/day	Jorgensen *et al.* (1978)
	0.01-0.035**	0.003-0.01**	0.2-1.4**		1/day	Jorgensen (1981)
	0.0024**	0.02-2.95**			μmoles/hr	Jorgensen (1979)
Diatoms	0.015	0.024			1/day	Bierman (1976)
	0.125	0.500			1/day	Bierman *et al.* (1980)
	0.72-4.32**				1/day	Jorgensen (1979)
	$0.3\text{-}120.\times10^{-8}$**	$0.7\text{-}8.\times10^{-9}$**		$2.6\text{-}950.\times10^{-9}$**	μmoles/cell-hr	Lehman *et al.* (1975)
	$1.52\text{-}8.33\times10^{-6}$**			$0.073\text{-}26.6\times10^{-6}$**	μmoles/cell-hr	Jorgensen (1979)
Green Algae	0.060	0.133			1/day	Bierman (1976)
	0.125	0.500			1/day	Bierman *et al.* (1980)
	$2.2\text{-}10.6\times10^{-8}$**	$1.2\text{-}4.\times10^{-8}$**			μmoles/cell-hr	Lehman *et al.* (1975)
	$2.14\text{-}5.56\times10^{-6}$**				μmoles/cell-hr	Jorgensen (1979)
Blue-green Algae	0.040	0.042-0.059			1/day	Bierman (1976)
	0.125	0.500			1/day	Bierman *et al.* (1980)
	0.042×10^{-6}**				μmoles/cell-hr	Jorgensen (1979)
Flagellates	0.125	0.500			1/day	Bierman *et al.* (1980)
Chrysophytes	$1.4\text{-}3.8\times10^{-8}$**	2.4×10^{-7}**			μmoles/cell-hr	Lehman *et al.* (1975)
		$2.01\text{-}13.9\times10^{-9}$**			μmoles/cell-hr	Jorgensen (1979)
Coccolithophores	$4.\text{-}9.\times10^{-10}$**				μmoles/cell-hr	Lehman *et al.* (1975)
Benthic Algae		0.045			1/day	Auer and Canale (1982)

**Literature values.

TABLE 6-16. HALF-SATURATION CONSTANTS FOR NUTRIENT UPTAKE

Phytoplankton Group	Half-Saturation Constant				References
	Nitrogen (mg/l)	Phosphorus (mg/l)	Carbon (mg/l)	Silicon (mg/l)	
Total Phytoplankton	0.2	0.02-0.03	0.5		Jorgensen (1976, 1983)
	0.2	0.02	0.5-0.6		Jorgensen et al. (1978)
	0.05	0.07			Desormeau (1978)
	0.0014-0.007**	0.0028-0.053**			Jorgensen (1979)
Diatoms	0.030*	0.060*			Bierman et al. (1980)
	0.0028-0.105**	0.18-0.053		0.022-0.098**	Lehman et al. (1975)
	0.0014-0.130**				Eppley et al. (1969)
	0.0042-0.105**	0.0002-0.053**		0.0053-0.098**	Jorgensen (1979)
Green Algae	0.030*	0.020*			Bierman et al. (1980)
	0.0024-0.02**	0.019-0.155**			Lehman et al. (1975)
	0.0014-0.02**				Eppley et al. (1969)
	0.0024-0.02**	0.0009-1.500**			Jorgensen (1979)
Blue-green Algae	0.030*	0.015-0.060*			Bierman et al. (1980)
	0.980**				Lehman et al. (1975)
	0.0067-0.980**				Jorgensen (1979)
Dinoflagellates	0.0015-0.133**				Lehman et al. (1975)
	0.0015-0.144**				Eppley et al. (1969)
	0.0014-0.133*				Jorgensen (1979)
Flagellates	0.030*	0.060*			Bierman et al. (1980)
	0.007-0.077**				Jorgensen (1979)
Chrysophytes	0.0014-0.0084**	0.016-0.496**			Lehman et al. (1975)
	0.0014-0.0084**				Eppley et al. (1969)
	0.0014-0.0084**	0.009-0.496**			Jorgensen (1979)
Coccolithophores	0.0014**				Lehman et al. (1975)
	0.0014-0.0028**				Eppley et al. (1969)
	0.0014-0.0043**				Jorgensen (1979)
Bacillariophyceae	0.0063-0.120**				Jorgensen (1979)
Benthic Algae		0.125			Auer and Canale (1982)

*Apparent half-saturation values under nutrient-starved conditions.
**Literature values.

TABLE 6-17. MODEL-SPECIFIC NUTRIENT UPTAKE PARAMETERS

Nutrient	Model Parameter Type	Model Parameter Value	Algal Type	Reference
Phosphorus	K_i	0.0001 g/m^3	Total Phytoplankton	Desormeau (1978)
	K_i	0.0007 mg/mg (D.W.)	Benthic Algae	Auer and Canale (1982)
	f_i	0.01%	Total Phytoplankton	Desormeau (1978)
	K_a	0.518×10^6 l/mol	Diatoms	Bierman et al. (1980)
		0.167×10^7 l/mol	Green Algae	
		$0.518\text{-}2.0 \times 10^6$ l/mol	Blue-green Algae	
		0.518×10^6 l/mol	Flagellates	
	K_a	0.50×10^6 l/mol	Diatoms	Bierman (1976)
		0.50×10^6 l/mol	Green Algae	
		$0.90\text{-}1.0 \times 10^6$ l/mol	Blue-green Algae	
	q_{dmin}	0.5 µg/l	Diatoms	Bierman et al. (1980)
		0.5 µg/l	Green Algae	
		0.5 µg/l	Blue-green Algae	
		0.5 µg/l	Flagellates	
	q_{dmin}	0.215×10^{-7} mol/l cell vol.	Diatoms	Bierman (1976)
		0.215×10^{-7} mol/l cell vol.	Green Algae	
		0.107×10^{-7} mol/l cell vol.	Blue-green Algae	
Nitrogen	K_i	0.0005 g/m^3	Total Phytoplankton	Desormeau (1978)
	f_i	0.05%	Total Phytoplankton	Desormeau (1978)
	K_a	0.100×10^7 l/mol	Diatoms	Bierman et al. (1980)
		0.100×10^7 l/mol	Green Algae	
		0.100×10^7 l/mol	Blue-green Algae	
		0.100×10^7 l/mol	Flagellates	
	K_a	0.10×10^7 l/mol	Diatoms	Bierman (1976)
		0.10×10^7 l/mol	Green Algae	
		0.10×10^7 l/mol	Blue-green Algae	
	q_{dmin}	3. µg/l	Diatoms	Bierman et al. (1980)
		3. µg/l	Green Algae	
		3. µg/l	Blue-green Algae	
		3. µg/l	Flagellates	
	q_{dmin}	0.267×10^{-6} mol/l cell vol.	Diatoms	Bierman (1976)
		0.267×10^{-6} mol/l cell vol.	Green Algal	
		0.267×10^{-6} mol/l cell vol.	Blue-green Algae	

Di Toro (1980) and Di Toro and Connolly (1980) have shown that since the time scale for nutrient uptake is a fraction of the time scale for algal growth and is usually much smaller than the time scale for changes in external nutrient concentrations, many of the complexities of variable stoichiometry models can be avoided by assuming cellular equilibrium with

external nutrient concentrations at each time step. This allows algal growth to be computed using conventional Michaelis-Menten kinetics, but at the same time allows the internal stoichiometry of the algae to vary. Since the cells are assumed to equilibrate immediately with the external nutrient concentrations during transport, both the computational difficulties associated with the rapid uptake dynamics and the problem of algae with different internal stoichiometries being transported into the same model segment are eliminated. Variable stoichiometry formulations are more important to accurately simulating nutrient recycling than to computing algal growth, so this scheme may be a reasonable compromise between the variable stoichiometry formulations discussed above and conventional fixed stoichiometry formulations.

6.5 RESPIRATION AND EXCRETION

Respiration and excretion are generally combined and modeled as a single term which includes all metabolic losses and excretory processes. These losses represent the difference between gross growth and net growth. Since net growth (rather than gross growth) is typically reported in the literature, some models lump respiration, excretion, and gross growth into a single net growth term, rather than simulating each process separately. However, it is generally more appropriate to compute growth and respiration separately since growth rates are sensitive to nutrient supplies while respiration rates depend primarily on temperature. Also, respiration and excretion are important components of nutrient recycling, so these processes are usually computed separately for use in the nutrient dynamic equations.

Most models express respiration (plus excretion) as either a constant loss term or as a function of temperature. The general expression is:

$$r = r(T_{ref})\ f_r(T) \tag{6-68}$$

where r = rate of respiration plus excretion, 1/time

$r(T_{ref})$ = respiration rate at a particular reference temperature T_{ref}, 1/time

$f_r(T)$ = temperature function for respiration

The temperature functions for respiration use the same formulations discussed above for growth (Equations (6-5) through (6-25)). Most models use the same temperature function and coefficients for both processes. The major approaches are 1) linear increases in respiration with temperature, 2) exponential increases in respiration with temperature, and 3) temperature optimum curves in which respiration increases with temperature up to the optimum temperature and then decreases with higher temperatures. The most commonly used exponential formulation is the Arrhenius relationship with a reference temperature of 20°C (Equation (6-15a)). Some models, for example CE-QUAL-R1 (WES, 1982), use the left hand side of a temperature optimum curve or a logistic equation (Equation (6-22a)) to define temperature effects on respiration. This approach assumes respiration increases exponentially at low temperatures, but eventually levels off to some maximum value at higher temperatures.

A few models use formulations which relate the respiration rate to the physiological condition of the algal cells. For example, Scavia (1980) represents respiration as the sum of two components, 1) a low maintenance rate representing periods of minimal growth, and 2) a rate which is directly proportional to the photosynthesis rate (as defined by the growth limitation factor):

$$r(T_{ref}) = r_{min}(T_{ref}) + k_r(T_{ref})\ f(L,P,N,C,Si) \qquad (6\text{-}69)$$

where $r_{min}(T_{ref})$ = base respiration rate under conditions of minimal growth (poor physiological condition) at reference temperature T_{ref}, 1/time

$K_r(T_{ref})$ = maximum incremental increase in respiration under conditions of maximum growth (optimum physiological condition) at reference temperature T_{ref}, 1/time

Both rates are multiplied by a temperature adjustment function.

The MS.CLEANER model uses a similar formulation which expresses respiration as the sum of endogenous respiration and photorespiration

(Groden, 1977; Park et al., 1980). The endogenous respiration is defined as:

$$r_e = .0175\ e^{.069T} \tag{6-70}$$

where r_e = endogenous respiration rate, 1/time
T = temperature, ^oC

Photorespiration is defined as a constant fraction of the temperature adjusted maximum photosynthesis rate in early versions of MS.CLEANER (Groden, 1977):

$$r_p = K_{p1}\ \mu_{max}(T_{ref})\ f(T) \tag{6-71}$$

where r_p = photorespiration rate, 1/time
K_{p1} = fraction of maximum photosynthesis rate which is oxidized by photorespiration (typically 5 to 15%)

and as a fraction of the actual photosynthesis rate (including temperature, light, and nutrient limitation effects) in later versions (Park et al., 1980):

$$r_p = K_{p2}\ \mu \tag{6-72}$$

$$= K_{p2}\ \mu_{max}(T_{ref})\ f(T)\ f(L,P,N,C,Si)$$

where K_{p2} = fraction of actual photosynthesis rate which is oxidized by photorespiration

MS.CLEANER also considers excretion as a separate loss term, in contrast to most models which lump respiration and excretion together. Excretion is formulated similar to photorespiration. However, since the excretion of photosynthate and photorespiratory compounds relative to carbon assimilation (photosynthesis) is highest at both low light levels and inhibitory high light levels, the excretion rate is expressed as (Desormeau, 1978; Collins, 1980):

$$e_x = K_e \left(1 - f(L)\right) \mu \qquad (6\text{-}73)$$

where e_x = excretion rate, 1/time

K_e = fraction of photosynthesis excreted

$f(L)$ = light limitation factor

μ = growth (photosynthesis) rate, including effects of temperature, light, and nutrient limitation, 1/time

Lehman et al. (1975), Jorgensen (1976), and Jorgensen et al. (1978, 1981) use variable stoichiometry formulations which relate the respiration rate to the internal carbon levels of the cells. The ratio of the internal carbon level to the maximum internal carbon level is used to define the physiological state of the cells. The respiration rate increases with the internal carbon level according to the equation:

$$r(T_{ref}) = r_{max}(T_{ref}) \left(\frac{C_{int}}{C_{max}}\right)^{2/3} \qquad (6\text{-}74)$$

where $r_{max}(T_{ref})$ = maximum respiration rate at reference temperature T_{ref}, 1/time

C_{int} = internal carbon level, mass carbon/biomass algae

C_{max} = maximum internal carbon level, mass carbon/biomass algae

Algal respiration rates are tabulated in Table 6-18.

6.6 SETTLING

Phytoplankton settling rates depend on the density, size, shape, and physiological state of the phytoplankton cells, the viscosity and density of the water, and the turbulence and velocities of the flow field. The settling velocities for spherical particles in still water can be computed from Stoke's law. Stoke's law can be modified to account for non-spherical phytoplankton cells by using an "equivalent radius" and "shape factor" in the formulation (Scavia, 1980):

TABLE 6-18. ALGAL RESPIRATION RATES

Algal Type	Respiration Rate (1/day)	Reference Temperature (^{o}C)	References
Total Phytoplankton	0.05 - 0.15	$20^{o}C$	Di Toro et al. (1971, 1977) O'Connor et al. (1975, 1981) Thomann et al. (1974, 1975, 1979) Di Toro & Matystik (1980) Di Toro & Connolly (1980) Thomann & Fitzpatrick (1982) Salisbury et al. (1983)
	0.05 - 0.10	$20^{o}C$	Chen & Orlob (1975) Chen & Wells (1975, 1976) Tetra Tech (1976)
	0.08	$20^{o}C$	Canale et al. (1976)
	0.10	$20^{o}C$	Lombardo (1972)
	0.088 - 0.6	T_{opt}	Jorgensen (1976) Jorgensen et al. (1978)
	0.051	$20^{o}C$	Brandes (1976)
	0.05	$20^{o}C$	Grenney & Kraszewski (1981)
	0.005 - 0.12*	$20^{o}C$	Baca & Arnett (1976)
	0.05 - 0.2*	$20^{o}C$	Smith (1978)
	0.05 - 0.5*	$20^{o}C$	Roesner et al. (1980) Duke & Masch (1973)
	0.02 - 0.8*	$20^{o}C$	Grenney & Kraszewski (1981)
	0.05 - 0.10**	$20^{o}C$	Collins & Wlosinski (1983)
	0.05 - 0.20**	$20^{o}C$	Jorgensen (1979)
Diatoms	0.04 - 0.08	$20^{o}C$	Thomann et al. (1979) Di Toro & Connolly (1980) Salisbury et al. (1983) Di Toro et al. (1971)
	0.07 - 0.08	$20^{o}C$	Porcella et al. (1983) Tetra Tech (1980)
	0.03 - 0.05	$20^{o}C$	Bierman (1976) Bierman et al. (1980)
	0.05 - 0.25	T_{opt}	Scavia et al. (1976) Scavia (1980) Bowie et al. (1980)
	0.05 - 0.59**	$20^{o}C$	Collins & Wlosinski (1983)

(continued)

TABLE 6-18. (continued)

Algal Type	Respiration Rate (1/day)	Reference Temperature (^{o}C)	References
Green Algae	0.05 - 0.07	$20^{o}C$	Tetra Tech (1980) Porcella et al. (1983)
	0.05 - 0.25	T_{opt}	Scavia et al. (1976) Scavia (1980) Bowie et al. (1980)
	0.03 - 0.05	$20^{o}C$	Bierman (1976) Bierman et al. (1980)
	0.01 - 0.46**	$20^{o}C$	Collins & Wlosinski (1983)
Blue-green Algae	0.05 - 0.065	$20^{o}C$	Tetra Tech (1980) Porcella et al. (1983)
	0.05 - 0.25	T_{opt}	Scavia et al. (1976) Scavia (1980) Bowie et al. (1980)
	0.03 - 0.05	$20^{o}C$	Bierman (1976) Bierman et al. (1980)
	0.10 - 0.92**	$20^{o}C$	Collins & Wlosinski (1983)
Dinoflagellates	0.047	$20^{o}C$	O'Connor et al. (1981)
Flagellates	0.05	$20^{o}C$	Bierman et al. (1980)
	0.05 - 0.06	$20^{o}C$	Tetra Tech (1980) Porcella et al. (1983)
Chrysophytes	0.15 - 0.32**	$20^{o}C$	Collins & Wlosinski (1983)
Benthic Algae	0.02 - 0.1	$20^{o}C$	Tetra Tech (1980) Bowie et al. (1980) Porcella et al. (1983)
	0.44	T_{opt}	Auer and Canale (1982)
	0.1	$20^{o}C$	Grenney & Kraszewski (1981)
	0.02 - 0.8*	$20^{o}C$	Grenney & Kraszewski (1981)
	0.05 - 0.2*	$20^{o}C$	Smith (1978)

*Model documentation values.
**Literature values.

$$V_s = \frac{2}{9} \frac{g R^2 (\rho_p - \rho_w)}{\nu F_s} \tag{6-75}$$

where V_s = settling velocity, length/time

g = acceleration of gravity, length/time^2

R = equivalent radius (based on a sphere of equivalent volume), length

ρ_p = density of the cell, mass/length^3

ρ_w = water density, mass/length^3

ν = kinematic viscosity

F_s = shape factor

The shape factor has a value ≥ 1.0 and accounts for all factors which reduce the settling velocities below that of an equivalent spherical particle, for example increased drag due to diatom spicules, flat or elongated cells, clusters or colonies of cells, etc. In a model of Lake Ontario, Scavia (1980) used a shape correction factor of 1.3 for small diatoms, 2.0 for large diatoms, and 1.0 for all other algal groups.

In practice, very few models use Stoke's law as a model formulation (Scavia et al., 1976; Scavia, 1980; Park et al., 1980). Most models lump many species into a few algal groups, so representative values of the cell radius, shape factor, and cell density are difficult to define, making this level of detail unnecessary. Since the shape factor is really a calibration parameter, it is more direct to simply use the settling velocity as a calibration parameter. Also, Stoke's law does not account for turbulence and flow velocities which tend to keep algae in suspension or resuspend settled algae. Additional factors which further complicate settling include the production of gas vacuoles or gelatinous sheaths which make some species buoyant, and the fact that settling velocities may vary with the nutritional state or physiological condition of the cells.

Settling rates are also partly dependent on the structure of the model. For example, one-dimensional layered lake models typically use settling velocities which are an order of magnitude lower than measured values or

values used in two-or three-dimensional models which simulate hydrodynamic processes (Scavia and Bennett, 1980). This is probably because one-dimensional models do not adequately represent vertical transport process such as upwelling or entrainment of phytoplankton in large-scale circulations which effectively reduce the net settling rates (Scavia and Bennett, 1980).

Because of the above factors, most models specify phytoplankton settling velocities directly as model coefficients. The settling rate in Equations (6-1) or (6-2) is generally expressed as:

$$s = \frac{V_s}{d} \tag{6-76}$$

where s = settling rate, 1/time
V_s = settling velocity, length/time
d = water depth, length

In layered models, algae settling in from the above layer, as well as algae settling out of the layer, must be included in the formulation. This also requires consideration of the bottom topography, since a fraction of the algae will settle onto the bottom area associated with each layer.

Equation (6-76) is refined in some models by including a temperature function which accounts for changes in settling velocities due to temperature effects on the density and viscosity of water. The settling rate is then expressed as:

$$s = \frac{V_s(T_{ref})}{d} f_s(T) \tag{6-77}$$

where $V_s(T_{ref})$ = settling velocity at reference temperature T_{ref}, length/time
$f_s(T)$ = temperature adjustment function for the settling velocity

Typical examples of temperature adjustment functions include (Tetra Tech, 1980):

$$f_s(T) = \frac{157.5}{0.069T^2 - 5.3T + 177.6} \tag{6-78}$$

where T = temperature in ^oC.

or (Scavia and Park, 1976):

$$f_s(T) = 1 + a_s T \tag{6-79}$$

where a_s = slope of settling velocity vs. temperature curve

Scavia et al. (1976) have also expanded the settling rate formulation to account for variations in settling velocities due to the physiological condition of the phytoplankton cells. The basic assumption is that the cells are healthiest and the settling rates smallest when neither light nor nutrients are limiting growth. The settling rates are therefore expressed as a function of the growth limitation factor f(L,P,N,C,Si). Potential formulations include (Scavia et al., 1976; Scavia, 1980):

$$s = \frac{V_{smax}(T_{ref})}{d} f_s(T) \left(\frac{K_{set_1}}{f(L,P,N,C,Si) + K_{set_1}} \right) \tag{6-80}$$

or

$$s = \frac{V_{smax}(T_{ref})}{d} f_s(T) \left[1 - K_{set_2} f(L,P,N,C,Si) \right] \tag{6-81}$$

where $V_{smax}(T_{ref})$ = maximum settling velocity at reference temperature T_{ref} under poor physiological condition, length/time

K_{set_1}, K_{set_2} = constants of the settling formulations

A few models require specification of the settling rate s rather than the settling velocity V_s as a model calibration coefficient. When used in

this way, the settling rate may take on a wide range of values since it depends as much on the water depth as the settling velocities of the algae.

Phytoplankton settling velocities are presented in Table 6-19. Additional data are available in a review by Smayda (1970).

6.7 NONPREDATORY MORTALITY

Nonpredatory mortality accounts for all algal losses which are not explicitly accounted for by the grazing term or other loss processes in the model (for example, settling and respiration if they are not computed explicitly). Nonpredatory mortality includes processes such as senescence, bacterial decomposition of cells (parasitism), and stress-induced mortality due to severe nutrient deficiencies, extreme environmental conditions, or toxic substances. The nonpredatory mortality rate in Equations (6-1), (6-2), or (6-3) is generally specified as a constant model coefficient. This is in contrast to the predatory mortality or grazing rate which is computed dynamically to reflect changes in the predator densities.

In some models, a temperature adjustment function is used with nonpredatory mortality which results in:

$$m = m(T_{ref})\ f_m(T) \tag{6-82}$$

where m = nonpredatory mortality rate, 1/time

$m(T_{ref})$ = nonpredatory mortality rate at reference temperature T_{ref}, 1/time

$f_m(T)$ = temperature function for mortality

The temperature functions for mortality generally use the same formulations used for growth and respiration (Equations (6-5) through (6-25)). However, if a temperature optimum curve is used for growth, the temperature function for mortality will often use only the left hand portion of the curve to produce a temperature response curve in which mortality increases with temperature until some maximum mortality rate is reached.

TABLE 6-19. PHYTOPLANKTON SETTLING VELOCITIES

Algal Type	Settling Velocity (m/day)	References
Total Phytoplankton	0.05 - 0.5	Chen & Orlob (1975) Tetra Tech (1976) Chen (1970) Chen & Wells (1975, 1976)
	0.05 - 0.2	O'Connor *et al.* (1975, 1981) Thomann *et al.* (1974, 1975, 1979) Di Toro & Matystik (1980) Di Toro & Connolly (1980) Thomann & Fitzpatrick (1982)
	0.02 - 0.05	Canale *et al.* (1976)
	0.4	Lombardo (1972)
	0.03 - 0.05	Scavia (1980)
	0.05	Bierman *et al.* (1980)
	0.2 - 0.25	Youngberg (1977)
	0.04 - 0.6	Jorgensen (1976) Jorgensen *et al.* (1978, 1981)
	0.01 - 4.0*	Baca & Arnett (1976)
	0. - 2.0*	Chen & Orlob (1975) Smith (1978)
	0.15 - 2.0*	Duke & Masch (1973) Roesner *et al.* (1977)
	0. - 0.2*	Brandes (1976)
	0. - 30.**	Jorgensen (1979)
Diatoms	0.05 - 0.4	Bierman (1976) Bierman *et al.* (1980)
	0.1 - 0.2	Thomann *et al.* (1979) Di Toro & Connolly (1980)
	0.1 - 0.25	Tetra Tech (1980) Porcella *et al.* (1983)
	0.03 - 0.05	Canale *et al.* (1976)
	0.3 - 0.5	Smayda & Boleyn (1965)
	2.5	Lehman *et al.* (1975)
	0.02 - 14.7**	Collins & Wlosinski (1983)
	0.08 - 17.1**	Jorgensen (1979)

(continued)

TABLE 6-19. (continued)

Algal Type	Settling Velocity (m/day)	References
Green Algae	0.05 - 0.19	Jorgensen *et al.* (1978)
	0.05 - 0.4	Bierman (1976) Bierman *et al.* (1980)
	0.02	Canale *et al.* (1976)
	0.8	Lehman *et al.* (1975)
	0.1 - 0.25	Tetra Tech (1980) Porcella *et al.* (1983)
	0.3	DePinto *et al.* (1976)
	0.08 - 0.18**	Collins & Wlosinski (1983)
	0.27 - 0.89**	Jorgensen (1979)
Blue-green Algae	0.05 - 0.15	Bierman (1976) Bierman *et al.* (1980)
	0.	Canale *et al.* (1976)
	0.2	Lehman *et al.* (1975)
	0.1	DePinto *et al.* (1976)
	0.08 - 0.2	Tetra Tech (1980) Porcella *et al.* (1983)
	0.10 - 0.11**	Collins & Wlosinski (1983)
Flagellates	0.5	Lehman *et al.* (1975)
	0.05	Bierman *et al.* (1980)
	0.09 - 0.2	Tetra Tech (1980) Porcella *et al.* (1983)
	0.07 - 0.39**	Collins & Wlosinski (1983)
Dinoflagellates	8.0	O'Connor *et al.* (1981)
	2.8 - 6.0**	Collins & Wlosinski (1983)
Chrysophytes	0.5	Lehman *et al.* (1975)
Coccolithophores	0.25 - 13.6	Collins & Wlosinski (1983)
	0.3 - 1.5**	Jorgensen (1979)

*Model documentation values.

**Literature values.

A few models use more sophisticated formulations for nonpredatory mortality which try to relate the mortality rate to the physiological condition of the algal cells or to the size of the decomposer population (De Pinto, 1979). For example, Scavia et al. (1976) use the value of the growth limitation factor f(L,P,N,C,Si) as a measure of cell health and express the mortality rate as:

$$m(T_{ref}) = m_{max}(T_{ref}) \left[1 - f(L,P,N,C,Si)\right] \qquad (6\text{-}83)$$

where $m_{max}(T_{ref})$ = maximum nonpredatory mortality under poor physiological conditions at reference temperature T_{ref}, 1/time

This assumes minimal mortality and algal decomposition when growth conditions are optimal, and maximum mortality when conditions are severely limiting.

Lehman et al. (1975) use a similar approach, but also include the duration of growth limiting conditions in the formulation. They define the mortality rate as:

$$m(T_{ref}) = m_{max}(T_{ref}) \left(1 - e^{-K_{so}T_{so}}\right) \qquad (6\text{-}84)$$

where T_{so} = number of days of suboptimal conditions (defined as μ/μ_{max} .05), time

K_{so} = coefficient defined as ln2 divided by the number of days at suboptimal conditions until m increases to ½ m_{max}

MS.CLEANER expresses nonpredatory mortality as a function of both the internal nutrient concentrations and temperature such that the mortality rate increases exponentially under conditions of either nutrient starvation or critically high temperatures. The equation is (Desormeau, 1978; Park et al., 1980):

$$m = K_m \, e^{K_n(N_{crit} - f(P,N,C,Si))} \, e^{(T-T_{crit})} \qquad (6\text{-}85)$$

where K_m = nonpredatory mortality rate coefficient, 1/time

K_n = exponent for nutrient starvation

$f(P,N,C,Si)$ = variable stoichiometry nutrient limitation factor for algal growth

N_{crit} = critical value of $f(P,N,C,Si)$ for starvation mortality

T_{crit} = critical temperature for nonpredatory mortality

This assumes that when the internal nutrient levels drop below the subsistence quota, increased senescence, bacterial colonization, and cell lysis occur.

Bierman et al. (1980) use a nonpredatory mortality function which indirectly includes the size of the decomposer bacteria population in the formulation. Although the bacteria are not modeled explicitly, they are assumed to increase in proportion to the total algal concentration (the sum of all algal groups in the model). Therefore, increases in the bacteria associated with the bloom of one algal group will result in higher mortality rates for all other groups since a higher decomposer population is established. The equation is:

$$m(T_{ref}) = K_m(T_{ref}) \sum_{i=1}^{n} A_i \qquad (6\text{-}86)$$

where $K_m(T_{ref})$ = nonpredatory mortality rate coefficient at reference temperature T_{ref}, 1/time-algae

A_i = concentration of algal group i, mass/volume

n = total number of algal groups

Nyholm (1978) uses a Michaelis-Menten type saturation function of the algal concentrations in his formulation for algal mortality:

$$m(T_{ref}) = m_{max}(T_{ref}) \left(\frac{A}{K_{m1} + A}\right) \qquad (6\text{-}87)$$

where $m_{max}(T_{ref})$ = maximum nonpredatory mortality rate at reference temperature T_{ref}, 1/time

A = algal concentration, mass/volume

K_{m1} = half-saturation constant for algal nonpredatory mortality, mass/volume

At high algal concentrations, this is equivalent to the basic first order formulation (Equation (6-82)), while at very low algal levels, the mortality rate is essentially a second order relationship analogous to Equation (6-86). However, even though the mortality rate is second order at low algal densities, the Michaelis-Menten term reduces the net rate at low densities below the maximum first-order rate at high algal densities.

The Michaelis-Menten formulation is also used by Di Toro and Matystik (1980), Di Toro and Connolly (1980), and Thomann and Fitzpatrick (1982) in their formulation for the decomposition of organic matter (dead algal cells), although a basic first-order formulation is used for algal nonpredatory mortality. These models use the Michaelis-Menten formulation to account for the effects of the bacterial population on decomposition rates, assuming that decomposers (and the resulting decomposition rates) increase in proportion to the algal densities at low concentrations, but that other factors limit decomposition rates at high algal densities (Di Toro and Matystik, 1980; Di Toro and Connolly, 1980). These mechanisms could also be assumed for nonpredatory mortality.

Rodgers and Salisbury (1981) use a modified Michaelis-Menten formulation for nonpredatory mortality which includes the effects of both bacterial activity and the physiological condition of the algal cells on algal decomposition:

$$m(T_{ref}) = m_{max}(T_{ref}) \left(\frac{A/\mu}{K_{m2} + A/\mu} \right) \qquad (6\text{-}88)$$

where μ = algal growth rate, 1/time

K_{m2} = half-saturation constant for algal nonpredatory mortality, mass-time/volume

The mortality rate is directly proportional to the algal biomass (an indicator of bacterial activity) and inversely proportional to the algal growth rate (an indicator of the physiological condition of the cells), both through a saturation type relationship which limits the maximum rate.

Some models include formulations to account for stress-induced mortality due to factors such as extreme temperatures or toxic substances. Stress related mortality is typically modeled by expanding the nonpredatory mortality term to include additional terms for these effects, for example:

$$m = m(T_{ref})\ f_m(T) + m_T(T_{ref})\ f_T(T) + m_x\ f_x(X) \qquad (6\text{-}89)$$

where $m_T(T_{ref})$ = thermal mortality rate at reference temperature T_{ref}, 1/time

$f_T(T)$ = thermal mortality response curve

m_x = toxic mortality rate, 1/time

$f_x(X)$ = dose-response curve for toxic mortality

X = concentration of toxicant, mass/volume

Toxic effects can also be included in the growth and respiration formulations.

Algal nonpredatory mortality rates are presented in Table 6-20.

6.8 GRAZING

Algal grazing losses can be modeled in several ways, depending on 1) whether predator populations are simulated in the model, and 2) whether alternate food items are available for the predators.

When predators are not explicitly modeled, predator-prey dynamics cannot be simulated, so grazing effects are typically handled by either assuming a constant grazing loss which is specified by the user as a model input parameter:

TABLE 6-20. ALGAL NONPREDATORY MORTALITY RATES

Algal Type	Nonpredatory Mortality Rate (1/day)	References
Total Phytoplankton	0.02	Thomann & Fitzpatrick (1982)
	0.003 - 0.17	Baca & Arnett (1976)
	0.03	Scavia *et al*. (1976)
	0.005 - 0.10	Salas & Thomann (1978)
	0.01 - 0.1	Jórgensen (1976) Jorgensen *et al*. (1978)
Diatoms	0.03	Scavia *et al*. (1976)
Benthic Algae	0.- 0.8	Tetra Tech (1980) Bowie *et al*. (1980) Porcella *et al*. (1983)

$$G = \text{constant} \tag{6-90}$$

where G = loss rate due to grazing, mass algae/time

or by assuming a loss rate which is directly proportional to the algal densities (e.g., RECEIV-II (Raytheon, 1974)):

$$G = e_z A \tag{6-91}$$

or

$$G = e_z(T_{ref})\ f_g(T)\ A \tag{6-92}$$

where e_z = grazing rate coefficient, 1/time

A = algal biomass or density, mass or mass/volume

$e_z(T_{ref})$ = grazing rate coefficient at reference temperature T_{ref}, 1/time

$f_g(T)$ = temperature function for grazing

The second formulation is equivalent to that often used for non-predatory mortality (Equation (6-82)), so both nonpredatory mortality and grazing losses are typically combined into a single total mortality term when predator populations are not directly simulated:

$$m_{tot} = \left(m(T_{ref}) + e_z(T_{ref})\right) f_m(T)$$

$$= m_{tot}(T_{ref})\ f_m(T) \qquad (6\text{-}93)$$

where m_{tot} = total mortality rate, 1/time

$m_{tot}(T_{ref})$ = total mortality rate at reference temperature T_{ref}, 1/time

$f_m(T)$ = temperature function for mortality

The temperature functions used for grazing are the same as those discussed previously for algal growth, respiration, and mortality (Equations (6-5) to (6-25)).

Many general water quality models include a single zooplankton group to provide a more realistic grazing formulation for algae (Baca et al., 1973; Johanson et al., 1980; Najarian and Harleman, 1975). The zooplankton are often added only to obtain better simulations of algal dynamics, rather than to evaluate the zooplankton dynamics of the system. The coupled algae and zooplankton equations provide the major features of predator-prey interactions since the algal grazing rate is defined as a function of the zooplankton density which in turn varies dynamically with the food supply (algal concentration). The algal grazing rate in these models is typically expressed either in terms of a zooplankton filtration rate:

$$G = C_f\ A\ Z \qquad (6\text{-}94)$$

or

$$G = C_f(T_{ref})\ f_g(T)\ A\ Z \qquad (6\text{-}95)$$

where C_f = zooplankton filtration rate, water volume/mass zooplankton-time

Z = zooplankton biomass or concentration, mass or mass/volume

$C_f(T_{ref})$ = filtration rate at reference temperature T_{ref}, water volume/mass zooplankton-time

or in terms of a zooplankton ingestion rate:

$$G = C_g Z \tag{6-96}$$

or

$$G = C_g(T_{ref})\ f_g(T)\ Z \tag{6-97}$$

where C_g = zooplankton ingestion rate, mass algae/mass zooplankton-time

$C_g(T_{ref})$ = ingestion rate at reference temperature T_{ref}, mass algae/mass zooplankton-time

Ingestion rates are often back-calculated from computed zooplankton growth rates based on the equation (Chen and Orlob, 1975; Smith, 1978; Tetra Tech, 1979; WES, 1982):

$$C_g = \frac{g_z}{E} \tag{6-98}$$

where g_z = zooplankton growth rate, 1/time

E = zooplankton assimilation efficiency

In this approach, zooplankton growth rates are first computed as a function of food supply and temperature, and then the amount of algae which would have to be consumed to produce the growth is computed from Equation (6-98). The alternative approach is to specify or compute the ingestion rates directly, and then calculate the zooplankton growth rates based on the amount of food consumed and the assimilation efficiencies. Specific formulations for zooplankton filtration rates, ingestion rates, growth rates, and assimilation efficiencies are discussed in detail in Chapter 7.

Models which simulate only a single algal and zooplankton group tend to oversimplify predator-prey dynamics since a single constituent represents all primary producers and another single constituent represents all consumers. This ignores the complexities of the food web, as well as differences in foraging strategies, grazing rates, and food preferences between different types of predator organisms. This approach may be adequate in short term simulations where one group of phytoplankton and zooplankton are dominant. However, in long term simulations, more than one group of algae and zooplankton should be used to adequately simulate predator-prey interactions and population dynamics.

Algal grazing rates in multi-group models are functions of alternative food sources and food preferences, as well as predator densities, algal densities, and temperature. The basic grazing formulations are essentially the same as those mentioned above for a single zooplankton group, except that 1) grazing losses must be considered for each potential predator which grazes the algae, and 2) total grazing rates calculated for a given predator must be partitioned among the various food items which it consumes. Some models also consider differences in the ingestion or assimilation efficiencies between different food items (Scavia et al., 1976; Park et al., 1980), and differences in the feeding behavior of different zooplankton groups (e.g., non-selective filterers, selective filterers, carnivorous raptors, omnivores, etc.) (Canale et al., 1975, 1976; Park et al., 1980).

Grazing losses for non-selective feeders can be partitioned between different algal groups by distributing them in proportion to the algal concentrations:

$$G_{ij} = C_j \frac{A_i}{\sum_{k=1}^{n} F_k} Z_j \qquad (6\text{-}99)$$

where G_{ij} = loss rate of algal group i due to grazing by zooplankton group j, mass algae/time

C_j = total ingestion rate of zooplankton group j on all food items, mass food/mass zooplankton-time

A_i = biomass or concentration of algal group i, mass or mass/volume

F_k = biomass or concentration of potential food item k consumed by zooplankton group j, mass or mass/volume

n = number of potential food items

Z_j = biomass or concentration of zooplankton group j, mass or mass/volume

When grazing is expressed in terms of a filtration rate this partitioning is done automatically since the grazing losses are simply the algal concentrations times the volumetric filtration rates.

The above expression can be modified to account for selective feeding behavior by using food preference factors. These are weighting factors which reflect the probability that a given food will be consumed relative to the others when all foods are present in equal concentrations. The preference factors account for feeding differences due to factors like food particle size and shape, desirability and quality of food, and zooplankton feeding behavior. The grazing losses for each algal group subject to selective feeding can be expressed as:

$$G_{ij} = C_j \frac{P_{ij} A_i}{\sum_{k=1}^{n} P_{kj} F_k} Z_j \qquad (6\text{-}100)$$

where P_{ij} = preference factor for zooplankton j grazing on algal group i

P_{kj} = preference factor for zooplankton j grazing on food item k

The total ingestion rates C_j for each predator are the same as discussed above for a single zooplankton group (Equations (6-94) through (6-98)).

When several predators are modeled, the total grazing loss for a given algal group is the sum of the grazing losses from each predator:

$$G_i = \sum_{j=1}^{n_p} G_{ij} \qquad (6\text{-}101)$$

where G_i = loss rate for algal group i due to grazing by all predators, mass algae/time

n_p = total number of predators grazing on algal group i

Any of the previous formulations can be used to define the incremental grazing rates G_{ij} associated with each predator.

Zooplankton grazing rates are tabulated in Chapter 7, along with more detailed descriptions of the grazing formulations for zooplankton.

6.9 SUMMARY

Phytoplankton and attached algae are generally modeled as a biomass pool using the same mass balance approach used for nutrients and other constituents. The simpler models lump all algae into a single group, while more complex models distinguish between different functional groups such as green algae, diatoms, and blue-green algae. Single-group models are commonly used in rivers, while multi-group models are more common in lakes where long-term simulations of the seasonal succession of different types of phytoplankton are important.

Algal dynamics depend on growth, respiration, excretion, settling, nonpredatory mortality, and predation. Although some of these processes can be measured in the field or laboratory, most of the coefficients defining the process rates are usually determined by model calibration. This is necessary since the rates will vary with environmental conditions such as temperature, light, nutrient concentrations, and predator densities as well as with the species composition of the algae, all of which change continually with time. Literature values from laboratory experiments are useful for establishing reasonable ranges for the coefficients. However,

specific experimental results are difficult to apply directly since experiments typically use a single species rather than the species assemblages represented in models, and since experimental conditions may not represent conditions in the field. Model constructs must be relied upon to describe the effects of changing environmental and ecological conditions on the process rates.

Most processes in algal models are assumed to be temperature dependent. Three major approaches have been used to describe these effects: linear temperature response curves, exponential curves, and temperature optimum curves. The exponential Arrhenius relationship is commonly used when only one algal group is simulated, while temperature optimum curves are more common in multi-group models.

The most important and complex formulations in algal models are the growth formulations. Growth is a function of temperature, light, and nutrients. Light limitation is typically defined by either a saturation type relationship or a photoinhibition relationship in which growth decreases at light intensities above the optimum. Most models use Michaelis-Menten kinetics to describe nutrient limitation effects and assume the nutrient composition of the algal cells remains constant. More sophisticated models allow the internal stoichiometry of the algae to vary with changes in the external nutrient concentrations. These models simulate nutrient uptake and algal growth as two separate steps. Nutrient uptake is first computed as a function of both the internal nutrient levels in the cells and the external concentrations in the water. Algal growth is then computed based on the internal nutrient concentrations in the cells. Various formulations have been used to describe uptake and growth kinetics in variable stoichiometry models. These formulations are more complex and involve more model coefficients than fixed stoichiometry models.

Most models use simple temperature-dependent first-order relationships to describe respiration, settling, and nonpredatory mortality. A few models include the effects of the physiological condition of the algae on these processes by making them a function of the growth rate, growth limitation factor, or internal nutrient level (in variable stoichiometry models). Some

models also include the effects of the decomposer bacteria population on nonpredatory mortality. These latter effects are modeled indirectly by assuming the decomposers increase in proportion to the algal densities and using algal concentrations as an indicator of the bacterial population, rather than by simulating the decomposers directly. Both second-order mortality formulations and Michaelis-Menten type saturation relationships have been used to describe these effects.

Algal grazing is usually modeled as a first-order loss when zooplankton are not simulated. When zooplankton are modeled, algal grazing is a function of the algal densities, zooplankton densities, and the zooplankton filtration rates or consumption rates. In multi-group models which include several algal and zooplankton groups, selective feeding behavior can be simulated by including food preference factors in the grazing formulations.

6.10 REFERENCES

Auer, M.T. and R.P. Canale. 1982. Ecological Studies and Mathematical Modeling of Cladophora in Lake Huron: 2. Phosphorus Uptake Kinetics. J. Great Lakes Res., 8(1):84-92.

Auer, M.T. and R.P. Canale. 1982. Ecological Studies and Mathematical Modeling of Cladophora in Lake Huron: 3. The Dependence of Growth Rates on Internal Phosphorus Pool Size. J. Great Lakes Res., 8(1):93-99.

Baca, R.G., W.W. Waddel, C.R. Cole, A. Brandstetter, and D.B. Clearlock. 1973. EXPLORE-I: A River Basin Water Quality Model. Battelle, Inc., Pacific Northwest Laboratories, Richland, Washington.

Baca, R.G., M.W. Lorenzen, R.D. Mudd, and L.V. Kimmel. 1974. A Generalized Water Quality Model for Eutrophic Lakes and Reservoirs. Battelle, Inc. Pacific Northwest Laboratories, Richland, Washington.

Baca, R.G. and R.C. Arnett. 1976. A Limnological Model for Eutrophic Lakes and Impoundments. Battelle, Inc., Pacific Northwest Laboratories, Richland, Washington.

Battelle, Inc. 1973. EXPLORE-I: A River Basin Water Quality Model. Battelle, Inc., Pacific Northwest Laboratories, Richland, Washington.

Battelle, Inc. 1974. Development of a Mathematical Water Quality Model for Grays Harbor and the Chehalis River, Washington: Documentation Report. Battelle, Inc., Pacific Northwest Laboratories, Richland, Washington.

Bierman, V.J., Jr. 1976. Mathematical Model of the Selective Enhancement of Blue-Green Algae by Nutrient Enrichment. In: Modeling Biochemical Processes in Aquatic Ecosystems. R.P. Canale (ed.). Ann Arbor Science Publishers, Ann Arbor, Michigan. pp. 1-31.

Bierman, V.J., Jr. 1981. Phytoplankton-Nutrient Kinetics Mechanisms in Mathematical Simulation Models, with Special Attention to Reservoirs and Impoundments. In: Phytoplankton-Environmental Interactions in Reservoirs, Vol. I. M.W. Lorenzen (ed.). Papers presented at Workshop, April 10-12, 1979, Monterey, California.

Bierman, V.J., Jr., F. H. Verhoff, T.L. Poulson, and M.W. Tenney. 1973. Multi-nutrient Dynamic Models of Algal Growth and Species Competition in Freshwater Lakes. In: Modeling the Eutrophication Process. E.J. Middlebrook, D.H. Falkenborg, and E.G. Maloney (eds.). Utah State University, Logan, Utah, September 5-7, 1973. pp. 89-109.

Bierman, V.J., Jr., D.M. Dolan, E.F. Stoermer, J.E. Gannon, and V.E. Smith. 1980. The Development and Calibration of a Multi-Class Phytoplankton Model for Saginaw Bay, Lake Huron. Great Lakes Environmental Planning Study. Contribution No. 33. Great Lakes Basin Commission, Ann Arbor, Michigan.

Bloomfield, J.A., R. A. Park, D. Scavia, and C.S. Zahorcak. 1973. Aquatic Modeling in the Eastern Deciduous Forest Biome. U.S. International Biological Program. In: Modeling the Eutrophication Process. E.J. Middlebrook, D.H. Falkenborg, and T.E. Maloney, (eds.). Utah State University, Logan, Utah. pp. 139-158.

Bowie, G.L., C.W. Chen, and D.H. Dykstra. 1980. Lake Ontario Ecological Modeling, Phase III. Tetra Tech, Inc., Lafayette, California. For National Oceanic and Atmospheric Administration, Great Lakes Environmental Research Laboratory, Ann Arbor, Michigan.

Brandes, R.J. 1976. An Aquatic Ecologic Model for Texas Bays and Estuaries. Water Resources Engineers, Inc., Austin, Texas. For the Texas Water Development Board, Austin, Texas.

Brandes, R.J. and F.D. Masch. 1977. ESTECO--Estuarine Aquatic Ecologic Model: Program Documentation and User's Manual. Water Resources Engineers, Inc., Austin, Texas. For the Texas Water Development Board, Austin, Texas.

Canale, R.P. and A.H. Vogel. 1974. Effects of Temperature on Phytoplankton Growth. ASCE, Journal of the Environmental Engineering Division, Vol. 100, No. EE1, p. 231.

Canale, R.P., L.M. Depalma, and A.H. Vogel. 1975. A Food Web Model for Lake Michigan. Part 2 - Model Formulation and Preliminary Verification. Tech. Report 43, Michigan Sea Grant Program, MICHU-SG-75-201.

Canale, R.P., L.M. Depalma, and A.H. Vogel. 1976. A Plankton-Based Food Web Model for Lake Michigan. In: Modeling Biochemical Processes in Aquatic Ecosystems. R.P. Canale (ed.). Ann Arbor Science Publishers, Ann Arbor, Michigan. pp. 33-74.

Canale, R.P. and M.T. Auer. 1982. Ecological Studies and Mathematical Modeling of Cladophora in Lake Huron. J. Great Lakes Res., 8(1):112-125.

Chen, C.W. 1970. Concepts and Utilities of Ecological Model. ASCE Journal of the Sanitary Engineering Division, Vol. 96, No. SA5.

Chen, C.W. and G.T. Orlob. 1972. Ecologic Simulation for Aquatic Environments. Water Resources Engineers, Inc., Walnut Creek, California. For the Office of Water Resources Research.

Chen, C.W. and G.T. Orlob. 1975. Ecologic Simulation for Aquatic Environments. Systems Analysis and Simulation in Ecology, Vol. 3. B.C. Patten, (ed.). Academic Press, New York, New York. pp. 476-588.

Chen, C.W., M. Lorenzen, and D.J. Smith. 1975. A Comprehensive Water Quality-Ecological Model for Lake Ontario. Tetra Tech Inc., Lafayette, California. For National Oceanic and Atmospheric Administration, Great Lakes Environmental Research Laboratory, Ann Arbor, Michigan.

Chen, C.W. and J.T. Wells, Jr. 1975. Boise River Water Quality-Ecological Model for Urban Planning Study. Tetra Tech, Inc., Lafayette, California. For U.S. Army Engineering District, Walla Walla, Wash., Idaho Water Resources Board, and Idaho Dept. of Environmental and Community Services.

Chen, C.W. and J.T. Wells, Jr. 1976. Boise River Modeling. In: Modeling Biochemical Processes in Aquatic Ecosystems. R.P. Canale (ed.). Ann Arbor Science Publishers, Ann Arbor, Michigan. pp. 171-204.

Cloern, J.E. 1978. Simulation Model of Cryptomonas ovata Population Dynamics in Southern Kootenay Lake, British Columbia. Ecol. Modeling, 4:133-149.

Collins, C.D. 1980. Formulation and Validation of a Mathematical Model of Phytoplankton Growth. Ecology, 61:639-649.

Collins, C.D. and J.H. Wlosinski. 1983. Coefficients for Use in the U.S. Army Corps of Engineers Reservoir Model, CE-QUAL-R1. U.S. Army Corps of Engineers, Waterways Experiment Station, Vicksburg, Mississippi.

De Groot, W.T. 1983. Modelling the Multiple Nutrient Limitation of Algal Growth. Ecol. Modeling, 18:99-119.

DePinto, J.V., V.J. Bierman, Jr., and F.H. Verhoff. 1976. Seasonal Phytoplankton Succession as a Function of Phosphorus and Nitrogen Levels. In: Modeling Biochemical Processes in Aquatic Ecosystems. R.P. Canale (ed). Ann Arbor Science Publishers, Ann Arbor, Michigan. pp. 141-169.

DePinto, J.V. 1979. Water column Death and Decomposition of Phytoplankton: An Experimental and Modeling Review. In: Perspectives in Lake Ecosystem Modeling. D. Scavia and A. Robertson (eds.). Ann Arbor Science Publishers, Ann Arbor, Michigan. pp. 25-52.

Desormeau, C.J. 1978. Mathematical Modeling of Phytoplankton Kinetics with Application to Two Alpine Lakes. Report #4, Center for Ecological Modeling, Rensselaer Polytechnic Institute, Troy, New York.

Di Toro, D.M. 1980. Applicability of Cellular Equilibrium and Monod Theory to Phytoplankton Growth Kinetics. Ecol. Modeling, 8:201-218.

Di Toro, D.M., D.J. O'Connor, and R.V. Thomann. 1971. A Dynamic Model of the Phytoplankton Population in the Sacramento-San Joaquin Delta. In: Nonequilibrium Systems in Natural Water Chemistry, Adv. Chem. Ser. 106. American Chemical Society, Washington, D.C. pp. 131-180.

Di Toro, D.M., R.V. Thomann, D.J. O'Connor, and J.L. Mancini. 1977. Estuarine Phytoplankton Biomass Models - Verification Analyses and Preliminary Applications. In: The Sea, Marine Modeling, Vol. 6. E.D. Goldberg, I.N. McCave, J.J. O'Brien, and J.H. Steele (eds.). Wiley-Interscience Publications, New York, New York.

Di Toro, D.M. and J.F. Connolly. 1980. Mathematical Models of Water Quality in Large Lakes. Part II: Lake Erie. U.S. Environmental Protection Agency, Ecological Research Series. EPA-600/3-80-065.

Di Toro, D.M. and W.F. Matystik, Jr. 1980. Mathematical Models of Water Quality in Large Lakes. Part I: Lake Huron and Saginaw Bay. U.S. Environmental Protection Agency, Ecological Research Series. EPA-600/3-80-056.

Di Toro, D.M., J.J. Fitzpatrick, and R.V. Thomann. 1981. Water Quality Analysis Simulation Program (WASP) and Model Verification Program (MVP) - Documentation. Hydroscience, Inc., Westwood, New Jersey. For U.S. Environmental Protection Agency, Duluth, Minnesota.

Duke, J.H., Jr. and F.D. Masch. 1973. Computer Program Documentation for the Stream Quality Model DOSAG3, Vol. I. Water Resources Engineers, Inc., Austin, Texas. For U.S. Environmental Protection Agency, Systems Development Branch, Washington, D.C.

Droop, M.R. 1968. Vitamin B12 and Marine Ecology. IV. The Kinetics of Uptake, Growth and Inhibition in Monochrysis lutheri. J. Mar. Biol. Assoc. U.K., 48:689-733.

Eppley, R.W., J.N. Rogers, and J.J. McCarthy. 1969. Half-Saturation Constants for Uptake of Nitrate and Ammonium by Marine Phytoplankton. Limnol. Oceanogr., 14:912-920.

Eppley, R.W. 1972. Temperature and Phytoplankton Growth in the Sea. Fish. Bull., 70:1063-1085.

Feigner, K.D. and H. Harris. 1970. FWQA Dynamic Estuary Model, Documentation Report. U.S.D.I., F.W.Q.A., Washington, D.C.

Goldman, J.C. 1981. Influence of Temperature on Phytoplankton Growth and Nutrient Uptake. In: Phytoplankton-Environmental Interactions in Reservoirs, Vol. I. M.W. Lorenzen, (ed.). Papers presented at Workshop, April 10-12, 1979, Monterey, California.

Groden, T.W. 1977. Modeling Temperature and Light Adaptation of Phytoplankton. Report No. 2. Center for Ecological Modeling, Rensselaer Polytechnic Institute, Troy, New York.

Grenney, W.J. and A.K. Kraszewski. 1981. Description and Application of the Stream Simulation and Assessment Model: Version IV (SSAM IV). Instream Flow Information Paper. U.S. Fish and Wildlife Service, Fort Collins, Colorado, Cooperative Instream Flow Service Group.

Harleman, D.R.F., J.E. Dailey, M.L. Thatcher, T.O. Najarian, D.N. Brocard, and R.A. Ferrara. 1977. User's Manual for the M.I.T. Transient Water Quality Network Model--Including Nitrogen-Cycle Dynamics for Rivers and Estuaries. R.M. Parsons Laboratory for Water Resources and Hydrodynamics, Massachusetts Institute of Technology, Cambridge, Massachusetts. For U.S. Environmental Protection Agency, Corvallis, Oregon. EPA-600/3-77-010.

Johanson, R.C., J.C. Imhoff, and H.H. Davis. 1980. User's Manual for Hydrological Simulation Program - Fortran (HSPF). Hydrocomp, Inc., Mountain View, California. For U.S. Environmental Protection Agency, Athens, Georgia. EPA-600/9-80-015.

Jorgensen, S.E. 1976. A Eutrophication Model for a Lake. Ecol. Modeling, 2:147-165.

Jorgensen, S.E. (ed.). 1979. Handbook of Environmental Data and Ecological Parameters. International Society for Ecological Modeling.

Jorgensen, S.E., H. Mejer, and M. Friis. 1978. Examination of a Lake Model. Ecol. Modeling, 4:253-278.

Jorgensen, S.E. 1983. Eutrophication Models of Lakes. In: Application of Ecological Modeling in Environmental Management, Part A. S.E. Jorgensen (ed.). Elsevier Scientific Publishing Company.

JRB Associates, Inc. 1983. User's Manual for Vermont QUAL-II Model. JRB Associates, Inc., McLean, Virginia. For U.S. Environmental Protection Agency, Washington, D.C.

Koonce, J.F. and A.D. Hasler. 1972. Phytoplankton Succession and a Dynamic Model of Algal Growth and Nutrient Uptake. Laboratory of Limnology, University of Wisconsin, Madison, Wisconsin. Eastern Deciduous Forest Biome Memo Report No. 72-114.

Larsen, D.P., H.T. Mercier, and K.W. Malueg. 1973. Modeling Algal Growth Dynamics in Shagawa Lake, Minnesota, with comments Concerning Projected Restoration of the Lake. In: Modeling the Eutrophication Process. E.J. Middlebrooks, D.H. Falkenborg, and T.E. Maloney (eds.). Utah State University, Logan, Utah, September 5-7, 1973. pp. 15-31.

Lassiter, R. and D.K. Kearns. 1973. Phytoplankton Population Changes and Nutrient Fluctuations in a Simple Aquatic Ecosystem Model. In: Modeling the Eutrophication Process. E.J. Middlebrook, D.H. Falkenborg, and T.E. Maloney (eds.). Utah State University, Logan, Utah, September 5-7, 1973.

Lassiter, R.P. 1975. Modeling Dynamics of Biological and Chemical Components of Aquatic Ecosystems. Southeast Environmental Research Laboratory, U.S. Environmental Protection Agency, Athens, Georgia.

Lehman, J.T., D.B. Botkin, and G.E. Likens. 1975. The Assumptions and Rationales of a Computer Model of Phytoplankton Population Dynamics. Limnol. and Oceanogr., 20(3):343-364.

Lombardo, P.S. 1972. Mathematical Model of Water Quality in Rivers and Impoundments. Hydrocomp, Inc., Palo Alto, California.

Michaelis, L. and M.L. Menten. 1913. Biochemische Zeitschrift, 49:333.

Monod, J. 1949. The Growth of Bacterial Culture. Annual Review of Microbiology, 3:371-394.

Najarian, T.O. and D.R.F. Harleman. 1975. A Nitrogen Cycle Water Quality Model for Estuaries. R.M. Parsons Laboratory for Water Resources and Hydrodynamics, Massachusetts Institute of Technology, Cambridge, Massachusetts. Tech. Report No. 204.

National Council of the Paper Industry for Air and Stream Improvement, Inc. (NCASI). 1982. The Mathematical Water Quality Model QUAL-II and Guidance for its Use - Revised Version, Technical Bulletin No. 391.

National Council of the Paper Industry for Air and Stream Improvement, Inc. (NCASI). 1984. Modifications to the QUAL-II (SEMCOG) Water Quality Model and User Manual, Technical Bulletin, No. 437.

Nyholm, N. 1977. Kinetics of Phosphate Limited Algal Growth. Biotech. and Bioeng., 14:467-492.

Nyholm, N. 1978. A Simulation Model for Phytoplankton Growth and Nutrient Cycling in Eutrophic, Shallow Lakes. Ecol. Modeling, 4:279-310.

Nyholm, N. 1978. A Mathematical Model for Growth of Phytoplankton. Mitt. Internat. Verein. Limnol., 21:193-206.

O'Connor, D.J., D.M. Di Toro, and R.V. Thomann. 1975. Phytoplankton Models and Eutrophication Problems. In: Ecological Modeling in a Resource Management Framework. C.S. Russell (ed.). Resources for the Future, Inc., Washington, D.C.

O'Connor, D.J., J.L. Mancini, and J.R. Guerriero. 1981. Evaluation of Factors Influencing the Temporal Variation of Dissolved Oxygen in the New York Bight, PHASE II. Manhattan College, Bronx, New York.

O'Neill, R.V., R.A. Goldstein, H.H. Shugart, and J.B. Mankin. 1972. Terrestrial Ecosystem Energy Model. Eastern Deciduous Forest Biome Memo Report 72-19.

Orlob, G.T. 1977. Mathematical Modeling of Surface Water Impoundments, Volume 1. Resource Management Associates, Inc., Lafayette, California. For Office of Water Research and Technology, U.S. Department of the Interior.

Park, R.A. 1978. A Model for Simulating Lake Ecosystems. Report #3, Center for Ecological Modeling, Rensselaer Polytechnic Institute, Troy, New York.

Park, R.A., D. Scavia, and N.L. Clesceri. 1975. CLEANER, The Lake George Model. In: Ecological Modeling in a Resource Management Framework. C.S. Russell (ed.). Resources for the Future, Inc., Washington, D.C. pp. 49-82.

Park, R.A., R.V. O'Neill, J.A. Bloomfield, H.H. Shugart, Jr., R.S. Booth, R.A. Goldstein, J.B. Mankin, J.F. Koonce, D. Scavia, M.S. Adams, L.S. Clesceri, E.M. Colon, E.H. Dettmann, J.A. Hoopes, D.D. Huff, S. Katz, J.F. Kitchell, R.C. Kohberger, E.J. LaRow, D.C. McNaught, J.L. Peterson, J.E. Titus, P.R. Weiler, J.W. Wilkinson, and C.S. Zahorcak. 1974. A Generalized Model for Simulating Lake Ecosystems. Simulation, 23(2): 33-50.

Park, R.A., C.D. Collins, D.K. Leung, C.W. Boylen, J. Albanese, P. deCaprariis, and H. Forstner. 1979. The Aquatic Ecosystem Model MS.CLEANER. Proc. of First International Conf. on State of the Art of Ecol. Model., Denmark.

Park, R.A., T.W. Groden, and C.J. Desormeau. 1979. Modifications to the Model CLEANER Requiring Further Research. In: Perspectives on Lake Ecosystem Modeling. D. Scavia and A. Robertson (eds.). Ann Arbor Science Publishers, Ann Arbor, Michigan. pp. 87-108.

Park, R.A., C.D. Collins, C.I. Connolly, J.R. Albanese, and B.B. MacLeod. 1980. Documentation of the Aquatic Ecosystem Model MS.CLEANER. Rensselaer Polytechnic Institute, Center for Ecological Modeling, Troy, New York. For U.S. Environmental Protection Agency, Environmental Research Laboratory, Office of Research and Development, Athens, Georgia.

Patten, B.C. 1975. A Reservoir Cove Ecosystem Model. Trans. Am. Fish Soc., 3:596-619.

Patten, B.C. et al. 1975. Total Ecosystem Model for a Cove in Lake Texoma. In: Systems Analysis and Simulation in Ecology. Patten, B.C. (ed.). Academic Press, New York, New York. pp. 206-415.

Porcella, D.B., T.M. Grieb, G.L. Bowie, T.C. Ginn, and M.W. Lorenzen. 1983. Assessment Methodology for New Cooling Lakes, Vol. 1: Methodology to Assess Multiple Uses for New Cooling Lakes. Tetra Tech, Inc., Lafayette, California. For Electric Power Research Institute. Report EPRI EA-2059.

Raytheon Company, Oceanographic & Environmental Services. 1974. New England River Basins Modeling Project, Vol. III - Documentation Report, Part 1 - RECEIV-II Water Quantity and Quality Model. For Office of Water Programs, U.S. Environmental Protection Agency, Washington, D.C.

Rhee, G.Y. 1973. A Continuous Culture Study of Phosphate Uptake, Growth Rate and Polyphosphate in Scenedesmus sp. J. Phycol., 9:495-506.

Rhee, G.Y. 1978. Effects of N:P Atomic Ratios and Nitrate Limitation on Algal Growth, Cell Composition and Nitrate Uptake. Limnol. Oceanogr., 23:10-25.

Rodgers, P. and D. Salisbury. 1981. Water Quality Modeling of Lake Michigan and Consideration of the Anomalous Ice Cover of 1976-1977. J. Great Lakes Res., 7(4):467-480.

Roesner, L.A., P.R. Giguere, and D.E. Evenson. 1981. Computer Program Documentation for the Stream Quality Model QUAL-II. U.S. Environmental Protection Agency, Athens, Georgia. EPA 600/9-81-014.

Roesner, L.A., P.R. Giguere, and D.E. Evenson. 1981. User's Manual for the Stream Water Quality Model QUAL-II. U.S. Environmental Protection Agency, Athens, Georgia. EPA-600/9-81-015.

Salas, H.J. and R.V. Thomann. 1978. A Steady-State Phytoplankton Model of Chesapeake Bay. Journal WPCF, 50(12):2752-2770.

Salisbury, D.K., J.V. DePinto, and T.C. Young. 1983. Impact of Algal-Available Phosphorus on Lake Erie Water Quality: Mathematical Modeling. For U.S. Environmental Protection Agency, Environmental Research Laboratory, Duluth, Minnesota.

Scavia, D. 1979. Examination of Phosphorus Cycling and Control of Phytoplankton Dynamics in Lake Ontario with an Ecological Model. J. Fish. Res. Board Can., 36:1336-1346.

Scavia, D. 1980. An Ecological Model of Lake Ontario. Ecol. Modeling, 8:49-78.

Scavia, D., C.W. Boylen, R.B. Sheldon, and R.A. Park. 1975. The Formulation of a Generalized Model for Simulating Aquatic Macrophyte Production. Rensselaer Polytechnic Institute, Troy, New York. Eastern Deciduous Forest Biome Memo Report 75-4.

Scavia, D., B.J. Eadie, and A. Robertson. 1976. An Ecological Model for Lake Ontario - Model Formulation, Calibration, and Preliminary Evaluation. National Oceanic and Atmospheric Administration, Boulder, Colorado. NOAA Tech. Rept. ERL 371-GLERL 12.

Scavia, D. and R.A. Park. 1976. Documentation of Selected Constructs and Parameter Values in the Aquatic Model CLEANER. Ecol. Modeling, 2:33-58.

Scavia, D. and J.R. Bennett. 1980. Spring Transition Period in Lake Ontario - A Numerical Study of the Causes of the Large Biological and Chemical Gradients. Can. J. Fish. Aquat. Sci., 37:823-833.

Shugart, H.H., R.A. Goldstein, R.V. O'Neill, and J.B. Mankin. 1974. TEEM: A Terrestrial Ecosystem Energy Model for Forests. Oecol. Plant., 9(3):231-264.

Smayda, T.I. 1970. The Suspension and Sinking of Phytoplankton in the Sea. Oceanogr. Mar. Biol. Ann. Rev., 8:353-414.

Smayda, T.I. and B.J. Boleyn. 1965. Experimental Observations on the Floatation of Marine Diatoms. Part I: Thalassiosira naria, T. rotula and Nitzschia seriata. Limnol. and Oceanogr., 10:499-510.

Smith, D.J. 1978. Water Quality for River-Reservoir Systems. Resource Management Associates, Inc., Lafayette, California. For U.S. Army Corps of Engineers, Hydrologic Engineering Center (HEC), Davis, California.

Smith, E.L. 1936. Photosynthesis in Relation to Light and Carbon Dioxide. Nat. Acad. Sci. Proc., 22:504-511.

Smith, R.A. 1980. The Theoretical Basis for Estimating Phytoplankton Production and Specific Growth Rate from Chlorophyll, Light and Temperature Data. Ecol. Modeling, 10:243-264.

Steele, J.H. 1965. Notes on Some Theoretical Problems in Production Ecology. In: Primary Production in Aquatic Environments. C.R. Goldman (ed.). University of California Press, Berkeley, California. pp. 393-398.

Strickland, J.D.H. 1958. Solar Radiation Penetrating the Ocean - A Review of Requirements, Data and Methods of Measurement, with Particular Reference to Photosynthetic Productivity. J. Fish. Res. Bd. Canada, 14:453-493.

Swartzman, G.L. and R. Bentley. 1979. A Review and Comparison of Plankton Simulation Models. J. Inter. Soc. Ecol. Mod., 1:30-81.

Tetra Tech, Inc. 1976. Documentation of Water Quality Models for the Helms Pumped Storage Project. Tetra Tech, Inc., Lafayette, California. For Pacific Gas and Electric Company.

Tetra Tech, Inc. 1979. Methodology for Evaluation of Multiple Power Plant Cooling System Effects, Volume II. Technical Basis for Computations. Tetra Tech, Inc., Lafayette, California. For Electric Power Research Institute. Report EPRI EA-1111.

Tetra Tech, Inc. 1980. Methodology for Evaluation of Multiple Power Plant Cooling System Effects, Volume V. Methodology Application to Prototype - Cayuga Lake. Tetra Tech, Inc., Lafayette, California. For Electric Power Research Institute. Report EPRI EA-1111.

Thomann, R.V., D.M. Di Toro, and D.J. O'Connor. 1974. Preliminary Model of Potomac Estuary Phytoplankton. ASCE, J. Environ. Engr. Div., Vol. 100, No. EE1:699-715.

Thomann, R.V., D.M. Di Toro, R.P. Winfield, and D.J. O'Connor. 1975. Mathematical Modeling of Phytoplankton in Lake Ontario, Part 1. Model Development and Verification. Manhattan College, Bronx, New York. For U.S. Environmental Protection Agency, Corvallis, Oregon. EPA-600/3-75-005.

Thomann, R.V., J. Segna, and R. Winfield. 1979. Verification Analysis of Lake Ontario and Rochester Embayment Three-Dimensional Eutrophication Models. Manhattan College, Bronx, New York. For U.S. Environmental Protection Agency, Office of Research and Development, Duluth, Minnesota.

Thomann, R.V., and J.J. Fitzpatrick. 1982. Calibration and Verification of a Mathematical Model of the Eutrophication of the Potomac Estuary. For Department of Environmental Services, Government of the District of Columbia, Washington, D.C.

Thornton, K.W. and A. S. Lessem. 1978. A Temperature Algorithm for Modifying Biological Rates. Trans. Am. Fish. Soc., 107(2):284-287.

U.S. Army Corps of Engineers. 1974. Water Quality for River-Reservoir Systems. U.S. Army Corps of Engineers, Hydrologic Engineering Center (HEC), Davis, California.

Vollenweider, R.A. 1965. Calculation Models of Photosynthesis-Depth Curves and Some Implications Regarding Day Rate Estimating in Primary Production Measurements. In: Primary Productivity in Aquatic Environments. C.R. Goldman (ed.). University of California Press, Berkeley, California. pp. 425-457.

Walker, W.W. 1975. Description of the Charles River Basin Model. Chapter 6 of the Final Report on the Storrow Lagoon Demonstration Plant. Process Research, Inc., Cambridge, Massachusetts. For Commonwealth of Massachusetts, Metropolitan District Commission.

WES (Waterways Experiment Station). 1982. CE-QUAL-R1: A Numerical One-Dimensional Model of Reservoir Water Quality, Users Manual. Environmental and Water Quality Operational Studies (EWQOS), U.S. Army Corps of Engineers, Waterways Experiment Station, Vicksburg, Mississippi.

Youngberg, B.A. 1977. Application of the Aquatic Model CLEANER to Stratified Resevoir System. Report #1. Center for Ecological Modeling, Rensselaer Polytechnic Institute, Troy, New York.

Chapter 7

ZOOPLANKTON

7.1 INTRODUCTION

Zooplankton are included in water quality models primarily because of their effects on algae and nutrients. Algal dynamics and zooplankton dynamics are closely tied through predator-prey interactions. Nutrient dynamics are also influenced by zooplankton since zooplankton excretion is an important component of nutrient recycling, and because of the effects zooplankton have on algal dynamics. These interrelationships are particularly important for long-term simulations in lakes and estuaries since both zooplankton and algal densities may change by orders of magnitude over periods of several months.

As with phytoplankton, zooplankton have been modeled both as a single constituent representing total zooplankton and as several functional groups. The functional groups may represent different feeding types (e.g., herbivores, carnivores, omnivores, non-selective filter feeders, selective filter feeders, etc.) or different taxonomic groups (cladocerans, copepods, rotifers, etc.). While many models use only one group, multiple-group models more realistically represent trophic interactions since, for example, herbivorous zooplankton can be distinguished from carnivorous species. However, multi-group models require more coefficients and model parameters, as well as more detailed information for model calibration.

Zooplankton dynamics are governed by the same general processes as phytoplankton: growth, respiration and excretion, predation, and nonpredatory mortality. The major difference is that zooplankton are not subject to settling losses since they are motile and migrate vertically in the water column, typically in a diurnal pattern. As a result, zooplankton

are usually simulated using the same types of equations and formulations as used for phytoplankton. The general zooplankton equation which forms the basis of almost all models is:

$$\frac{dZ}{dt} = (g_z - r_z - m_z)\ Z - G_z \tag{7-1}$$

where Z = zooplankton biomass or equivalent nutrient mass, mass or mass/volume

g_z = gross growth rate, 1/time

r_z = respiration and excretion rate, 1/time

m_z = nonpredatory mortality rate, 1/time

G_z = loss rate due to predation, mass/time or mass/volume-time

The above equation treats zooplankton populations as a biomass pool. Zooplankton population models have also been developed which partition the population into a series of age classes, including all important developmental stages from eggs to adults. Growth, respiration, mortality, and reproduction are computed separately for each life stage. Both changes in numbers and changes in the average weights of each age class are typically included in the model structure. While this approach may give a more realistic representation of zooplankton population dynamics, it is generally too detailed to be used in general water quality modeling. As a result, most models use the biomass pool approach, both because it is simpler and because it is consistent with the phytoplankton and nutrient formulations typically used.

As with phytoplankton models, the major differences between zooplankton models are the number of zooplankton groups, the formulations used for each process, and the way in which various processes are combined. Some of these features are compared in Table 7-1 for several zooplankton models. Process formulations are discussed in the following sections.

7.2 TEMPERATURE EFFECTS

Most models include temperature response relationships for essentially all processes affecting zooplankton. Growth, consumption, respiration, and

TABLE 7-1. GENERAL COMPARISON OF ZOOPLANKTON MODELS

Model (Author)	Number of Groups			Zooplankton Processes Computed Separately in Model				Zooplankton Units			Reference
	Zoo-plankton	Phyto-plankton	Fish	Growth	Respiration	Nonpredatory Mortality	Predatory Mortality	Dry Wt. Biomass	Carbon	Other Nutrient	
AQUA-IV	1	1		X	X	X			X		Baca & Arnett (1976)
CE-QUAL-R1	1	2	3	X	X	X	X	X			WES (EWQOS) (1982)
CLEAN	3	2	3	X	X	X	X	X			Bloomfield et al. (1973)
CLEANER	3	3	3	X	X	X	X	X			Scavia & Park (1976)
MS.CLEANER	5	4	8	X	X	X	X	X			Park et al. (1980)
EAM	3	4	20	X	X	X	X	X			Tetra Tech (1979, 1980)
ESTECO	1	2	3	X	X	X	X	X			Brandes & Masch (1977)
EXPLORE-1	1	1		X	X	X			X		Baca et al. (1973)
HSPF	1	1		X	X	X		X			Johanson et al. (1980)
LAKECO	1	2	3	X	X	X	X	X			Chen & Orlob (1975)
MIT Network	1	1		X	X	X				N	Harleman et al. (1977)
WASP	2	2		X	X	X	X		X		Di Toro et al. (1981)
WQRRS	1	2	3	X	X	X	X	X			Smith (1978)
Bierman	2	5		X	X	X		X			Bierman et al. (1980)
Canale	9	4		X	X	X	X		X		Canale et al. (1975, 1976)
Jorgensen	1	1	1	X	X	X	X	X			Jorgensen (1976)
Scavia	6	5		X	X	X	X		X		Scavia et al. (1976)

nonpredatory mortality are generally direct functions of temperature, and predation is indirectly related through temperature effects on the consumption rates of zooplankton predators. In most models, the temperature response formulations used for zooplankton are identical to those used for phytoplankton, and the same temperature function is generally used for all processes affecting a given zooplankton group. The major differences in the response functions between different organisms are the particular coefficient values used to define the shapes and slopes of the response curves, the optimum temperatures, and the upper and lower lethal limits. A few models use different formulations for each process. For example, CE-QUAL-R1 (WES, 1982) uses an optimum curve for growth, a logistic equation for respiration, and a reverse logistic equation for nonpredatory mortality.

The various formulations used to define temperature effects are described in detail in the algal growth section of the report (Section 6.3.1), and they will not be repeated here. In general, all formulations can be classified as either linear response curves, exponential response curves, or temperature optimum curves which exhibit maximum process rates at the optimum temperature and decreasing rates as the temperature moves away from the optimum.

7.3 GROWTH

Zooplankton growth formulations represent increases in the biomass of the population due to both reproduction and the growth of individuals. The growth rate depends on the amount of food which is ingested and assimilated, and is therefore a function of food densities, ingestion rates, and assimilation efficiencies. Part of the assimilated food goes into individual growth and metabolic losses, and part goes into reproduction.

Both ingestion rates and assimilation efficiencies vary according to many factors, including (Leidy and Ploskey, 1980):

- Zooplankton factors such as species, age, size, feeding type, sex, reproductive state, and physiological or nutritional state

- Food related factors such as food concentration, type, particle size, quality, and desirability of the food

- Temperature

Ingestion rates also vary on a diurnal basis, with maximum feeding rates typically occurring at night. Peak nighttime grazing rates have been shown to range from 2 to 27 times the minimum daytime rates (Leidy and Ploskey, 1980).

Almost all zooplankton growth formulations are based on the following fundamental relationship:

$$g_z = C_g E \tag{7-2}$$

where g_z = zooplankton growth rate, 1/time
C_g = ingestion or grazing rate, mass food/mass zooplankton-time
E = assimilation efficiency, fraction

Since most zooplankton are filter feeders, the ingestion rate is often expressed in terms of a volumetric filtration rate multiplied times the total available food concentration. In this case, the above equation becomes:

$$g_z = C_f F_T E \tag{7-3}$$

where C_f = zooplankton filtration rate, water volume/mass zooplankton-time
F_T = total available food concentration, mass/volume

For raptorial feeders, the previous equation (Equation (7-2)) is generally used.

The simplest growth formulations assume constant filtration rates and assimilation efficiencies (Figure 7-1). For this situation, the growth rate

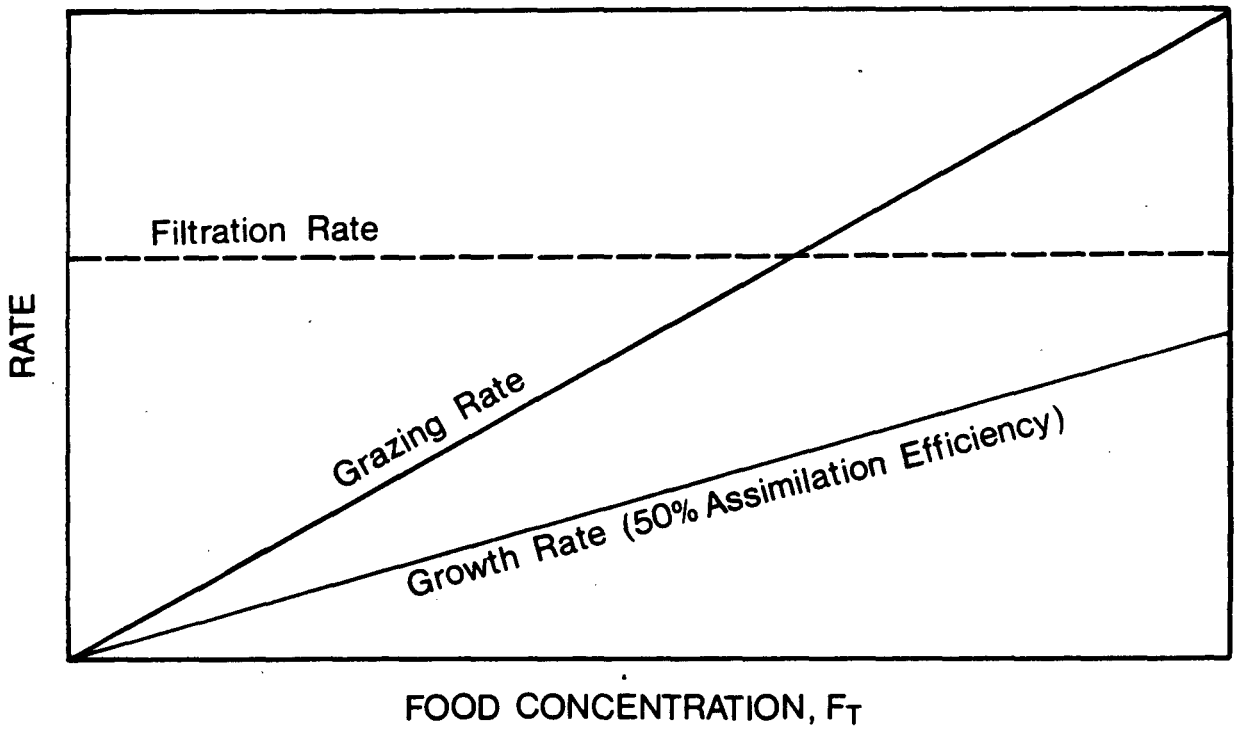

Figure 7-1. Growth rate and grazing rate as a function of food supply for zooplankton with constant filtration rates and assimilation efficiencies (adapted from Leidy and Ploskey, 1980).

is directly proportional to the food supply. More sophisticated models include more complex formulations for the ingestion (or filtration) rates and the assimilation efficiencies to account for variability due to factors like food densities, food types, different feeding methods, and temperature effects on feeding and growth (Canale et al., 1975, 1976; Scavia et al., 1976; Scavia, 1980; Scavia and Park, 1976; Park et al., 1975, 1979, 1980). The effects of food density and temperature on zooplankton growth rates can be expressed in general functional form as:

$$g_z = C_{gmax}(T_{ref})\ E_{max}(T_{ref})\ f(T)\ f_g(F_1,F_2,\ldots F_n) \qquad (7\text{-}4)$$

or

$$g_z = C_{fmax}(T_{ref})\ E_{max}(T_{ref})\ f(T)\ F_T\ f_f(F_1,F_2,\ldots F_n) \qquad (7\text{-}5)$$

where $C_{gmax}(T_{ref})$ = maximum ingestion rate at reference temperature T_{ref} under conditions of saturated feeding

(excess food supply), mass food/mass zooplankton-time

$C_{fmax}(T_{ref})$ = maximum filtration rate at reference temperature T_{ref}, water volume/mass zooplankton-time

$E_{max}(T_{ref})$ = maximum assimilation efficiency at reference temperature T_{ref}, fraction

$f(T)$ = temperature function for ingestion or filtration and assimilation

$f_g(F_1,F_2,...F_n)$ = growth limitation factor for ingestion formulation (Equation (7-2)) accounting for food density effects on ingestion rates and/or assimilation rates (where $F_1,F_2,...F_n$ are the concentrations of the potential food items)

$f_f(F_1,F_2,...F_n)$ = growth limitation factor for filtration formulation (Equation (7-3)) accounting for food density effects on filtration rates and/or assimilation rates

In some models, the maximum ingestion rate and the maximum assimilation efficiency are combined into a single parameter representing the maximum growth (or assimilation) rate (Chen and Orlob, 1972, 1975; Chen et al., 1975; Jorgensen, 1976; Jorgensen et al., 1978, 1981, 1983; Najarian and Harleman, 1975; Smith, 1978; WES, 1982; Tetra Tech, 1979). In this case, Equation (7-4) becomes:

$$g_z = g_{max}(T_{ref})\ f(T)\ f_g(F_1,F_2,...F_n) \qquad (7\text{-}6)$$

where $g_{max}(T_{ref})$ = maximum zooplankton growth rate at reference temperature T_{ref}, 1/time

Maximum consumption rates, filtration rates, and growth rates are presented in Tables 7-2, 7-3, and 7-4, respectively.

TABLE 7-2. ZOOPLANKTON MAXIMUM CONSUMPTION RATES

Zooplankton Group	Maximum Consumption Rate (1/day)	References
Total Zooplankton	0.8	Scavia & Park (1976)
	0.35 - 0.50	Bierman (1976)
	0.24 - 1.2**	Collins & Wlosinski (1983)
Omnivores	1.4	Scavia (1980) Bowie *et al.* (1980)
	0.43	Canale *et al.* (1976)
Carnivores	1.6	Scavia *et al.* (1976)
	0.7	Canale *et al.* (1976)
Fast Ingesters	0.7	Bierman *et al.* (1980)
Slow Ingesters	0.1	Bierman *et al.* (1980)
Cladocerans	1.6 - 1.9	Scavia *et al.* (1976) Scavia (1980) Bowie *et al.* (1980)
	0.045 - 13.8**	Leidy & Ploskey (1980)
	0.045 - 2.3**	Collins & Wlosinski (1983)
Copeods	1.7 - 1.8	Scavia *et al.* (1976) Scavia (1980) Bowie *et al.* (1980)
	0.10 - 0.47**	Collins & Wlosinski (1983)
Rotifers	1.8 - 2.2	Scavia *et al.* (1976) Scavia (1980) Bowie *et al.* (1980)
	3.44**	Leidy & Ploskey (1980)
	3.44**	Collins & Wlosinski (1983)
Mysids	1.0 - 1.2	Scavia *et al.* (1976) Scavia (1980) Bowie *et al.* (1980)

**Literature values.

TABLE 7-3. ZOOPLANKTON MAXIMUM FILTRATION RATES

Zooplankton Group	Maximum Filtration Rate	Units	References
Total Zooplankton	0.13 - 1.2	l/mgC-day	Di Toro et al. (1971) O'Connor et al. (1975, 1981)
	0.05 - 0.2*	l/mgC-day	Baca & Arnett (1976)
	0.8 - 1.10**	l/mg(D.W.)-day	Di Toro et al. (1971)
Herbivores	0.7 - 1.4	l/mgC-day	Thomann et al. (1975, 1979) Di Toro & Connolly (1980) Di Toro & Matystik (1980) Salisbury et al. (1983)
Carnivores	1.0 - 3.9	l/mgC-day	Thomann et al. (1975, 1979) Di Toro & Connolly (1980) Di Toro & Matystik (1980) Salisbury et al. (1983)
Cladocerans	3.5 - 4.0	l/mg(D.W.)-day	Canale et al. (1976)
	0.2 - 1.6**	l/mg(D.W.)-day	Di Toro et al. (1971)
	0.192 - 0.682**	l/mg(D.W.)-day	Lombardo (1972)
	0.2 - 1.6**	l/mg(D.W.)-day	Jorgensen (1979)
	0.009 - 177**	ml/animal-day	Leidy & Ploskey (1980)
	0.18 - 9.4**	ml/animal-day	Wetzel (1975)
	0.18 - 9.4**	ml/animal-day	Jorgensen (1979)
Copepods	1.0 - 6.5	l/mg(D.W.)-day	Canale et al. (1976)
	0.05 - 2.2**	l/mg(D.W.)-day	Di Toro et al. (1971)
	0.161 - 2.21**	l/mg(D.W.)-day	Lombardo (1972)
	0.05 - 2.2**	l/mg(D.W.)-day	Jorgensen (1979)
	0.02 - 4.1**	ml/animal-day	Wetzel (1975)
	0.02 - 5.28**	ml/animal-day	Jorgensen (1979)
	0.006 - 35.**	ml/animal-day	Leidy & Ploskey (1980)
Rotifers	0.6 - 1.5**	l/mg(D.W.)-day	Di Toro et al. (1971)
	0.6 - 1.5**	ml/animal-day	Jorgensen (1979)
	0.007 - 0.576**	ml/animal-day	Leidy & Ploskey (1980)

*Model documentation values.

**Literature values.

The temperature function f(T) in the above equations uses the same types of formulations discussed previously for phytoplankton. Experimental results suggest optimum type response curves for short term changes in temperature, but more of a linear response curve when acclimation has time to occur (Leidy and Ploskey, 1980). Work by Geller (1975) indicates acclimation times may range from 4 to 6 weeks, which is short enough for zooplankton to acclimate to the typical seasonal variations in temperature, but not to rapid changes (for example, thermal plume effects). However, since feeding is expected to slow down or cease as the temperature approaches the upper lethal limit, an optimum type response curve is appropriate if it is skewed so that the optimum occurs near the upper lethal limit. Table 7-5 presents a comparison of the temperature adjustment functions used in several zooplankton models.

TABLE 7-4. ZOOPLANKTON MAXIMUM GROWTH RATES

Zooplankton Group	Maximum Growth Rate (1/day)	References
Total Zooplankton	0.15 - 0.25	Chen (1970) Chen & Orlob (1975) Chen & Wells (1975, 1976)
	0.175 - 0.2	Jorgensen (1976) Jorgensen *et al*. (1978)
	0.1 - 0.3*	U.S. Army Corps of Engineers (1974) Brandes (1976) Smith (1978)
	0.15 - 0.30**	Jorgensen (1979)
Cladocerans	0.35 - 0.5	Tetra Tech (1980) Porcella *et al*. (1983)
	0.27 - 0.74**	Jorgensen (1979)
Copepods	0.5	Tetra Tech (1980)
Rotifers	0.44 - 0.45	Porcella *et al*. (1983)
	0.24 - 0.76**	Jorgensen (1979)
Mysids	0.14	Tetra Tech (1980)

*Model documentation values.

**Literature values.

TABLE 7-5. COMPARISON OF TEMPERATURE ADJUSTMENT FUNCTIONS FOR ZOOPLANKTON GROWTH AND CONSUMPTION

Model (Author)	Temperature Formulation (Equation No.)				Reference Temperature	Reference
	Linear	Exponential	Optimum Curve	Other Curve		
AQUA-IV				none		Baca & Arnett (1976)
CE-QUAL-R1			6-24		T_{opt}	WES (EWQOS) (1982)
CLEAN			6-19		T_{opt}	Bloomfield et al. (1973)
CLEANER			6-19		T_{opt}	Scavia & Park (1976)
MS.CLEANER			6-19		T_{opt}	Park et al. (1983)
EAM			6-24		T_{opt}	Tetra Tech (1979, 1980)
ESTECO		6-14			$20^{o}C$	Brandes & Masch (1977)
EXPLORE-1	X				$1^{o}C$	Baca et al. (1973)
HSPF		6-14			$20^{o}C$	Johanson et al. (1980)
LAKECO		6-14			$20^{o}C$	Chen & Orlob (1975)
MIT Network			6-25		T_{opt}	Harleman et al. (1977)
WASP	X				$1^{o}C$	Di Toro et al. (1981)
WQRRS			6-24		T_{opt}	Smith (1978)
Bierman		X			$20^{o}C$	Bierman et al. (1980)
Canale	piecewise linear				$1^{o}C$	Canale et al. (1975, 1976)
Jorgensen			6-18		T_{opt}	Jorgensen (1976)
Scavia			6-19		T_{opt}	Scavia et al. (1976)

7.3.1 Growth Limitation

The growth limitation functions used in the above equations, $f_g(F_1,F_2,\ldots F_n)$ and $f_f(F_1,F_2,\ldots F_n)$, are somewhat different since the latter function is multiplied times the total available food concentration F_T to give the net grazing rate. Therefore:

$$f_g(F_1,F_2,\ldots F_n) \approx f_f(F_1,F_2,\ldots F_n)\ F_T \qquad (7\text{-}7)$$

Both functions typically represent some type of saturation response to feeding, assimilation, and growth. Experimental observations show that at low food concentrations, zooplankton ingestion rates increase with increases in the food supply. For filter feeders which are filtering water at a constant rate, the grazing rate is directly proportional to the food concentration (Figure 7-1). Grazing rates for predatory zooplankton also increase with the food supply at low food concentrations since less energy and time are required to find and capture prey items as the prey density increases. However, as food becomes more abundant, the grazing rates eventually become saturated and level off at some maximum value after which the grazing rate becomes independent of the food supply. Filter feeders can regulate their ingestion rates at high food levels by reducing their filtering rates as the food concentration increases. At low concentrations, the feeding rate is limited by the ability of the zooplankton to filter water, while at high concentrations, it is limited by the ability to ingest and digest the food (Leidy and Ploskey, 1980). Similarly, the feeding rates for carnivorous zooplankton are limited at low prey densities by the ability of the zooplankton to find and capture prey items, while at high prey densities, they are limited by the ability to process, ingest, and digest the prey. Also, at very high ingestion rates, zooplankton growth may be limited by assimilation rates since ingested food remains in the gut for less time, resulting in only partial digestion and reduced assimilation efficiencies.

While the saturation type feeding response has been demonstrated in numerous studies, work by Mayzaud and Poulet (1978) indicates that zooplankton may be able to acclimate to changing food concentrations by adjusting their digestive enzyme levels, allowing them to filter at maximum rates over a much wider range than suggested by the saturation response curves of short term experiments (Leidy and Ploskey, 1980). This results in a linear response curve with ingestion rates directly proportional to the food supply. However, some upper limit on feeding and growth must exist based on theoretical arguments, so a saturation response curve is probably appropriate, even though the saturating food levels may be much higher than

typically experienced in the field except perhaps during phytoplankton blooms.

Two major approaches are used to simulate saturation responses in zooplankton models, the Michaelis-Menten (1913) formulation and the Ivlev (1966) formulation. The Michaelis-Menten formulation is a hyperbolic function analagous to that used in phytoplankton growth calculations, and is probably the most common approach used in water quality models (Chen and Orlob, 1972, 1975; Di Toro and Connolly, 1980; Di Toro and Matystik, 1980; Bloomfield et al., 1973; Park et al., 1974, 1975, 1979, 1980; Scavia et al., 1976; Scavia, 1980; Canale et al., 1975, 1976; Bierman, 1976; Bierman et al., 1980; Baca et al., 1973, 1974; Baca and Arnett, 1976; Najarian and Harleman, 1975). The basic equation is:

$$f_g(F_1,F_2,\ldots F_n) = \frac{F_T}{K_z + F_T} \tag{7-8}$$

where F_T = total available food supply, mass/volume

K_z = half-saturation constant for zooplankton feeding and growth, mass/volume

The Ivlev formulation is an exponential function which is more popular in biologically oriented models (Kremer and Nixon, 1978). The general equation is:

$$f_g(F_1,F_2,\ldots F_n) = 1 - e^{-K\,F_T} \tag{7-9}$$

where K = proportionality constant for Ivlev formulation

Figure 7-2 shows a comparison of the Michaelis-Menten and Ivlev functions where both functions have the same half-saturation value (i.e., $K = -\ln(\frac{1}{2})/K_z$). Both response functions range from minimum values of 0 at very low food concentrations to maximum values of 1 at food saturation. However, for food concentrations below the half-saturation constant (K_z), the Ivlev function is slightly lower than the Michaelis-Menten function.

For food concentrations above K_z, the Ivlev function is higher and approaches saturation sooner than the Michaelis-Menten function. Note that both functions are used with the total ingestion form of the growth equation (Equation (7-4)) rather than with the filtration form (Equation (7-5)), since the growth limitation function in the filtration form must always be multiplied times the total food supply to get the net response.

Both the Michaelis-Menten and Ivlev formulations can be modified to allow for threshold food concentrations below which zooplankton do not feed. This provides a refuge for prey organisms when they are present in very low concentrations. The resulting equations are:

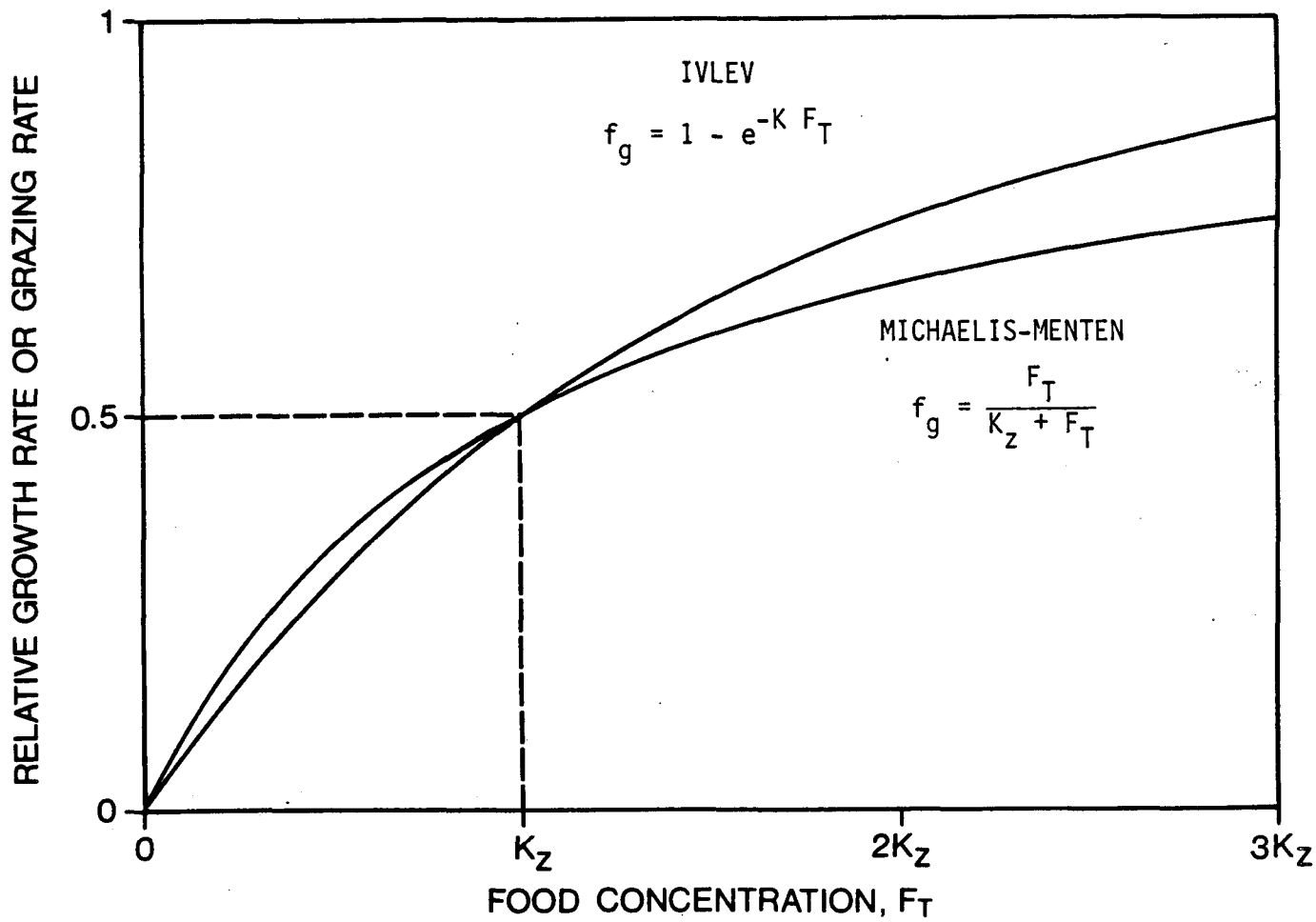

Figure 7-2. Comparison of the Ivlev and Michaelis-Menten functions with the same half-saturation value (i.e., $K = -\ln(\frac{1}{2})/K_z$) (adapted from Swartzman and Bentley, 1977, and Leidy and Ploskey, 1980).

$$f_g(F_1,F_2,\ldots F_n) = \frac{F_T - F_o}{K_z + (F_T - F_o)} \tag{7-10}$$

$$f_g(F_1,F_2,\ldots F_n) = \frac{F_T - F_o}{K_z + F_T} \tag{7-11}$$

and

$$f_g(F_1,F_2,\ldots F_n) = 1 - e^{-K(F_T-F_o)} \tag{7-12}$$

where F_o = threshold food concentration below which feeding does not occur, mass/volume

Zooplankton half-saturation constants and threshold feeding levels are presented in Tables 7-6 and 7-7.

A few models, for example CLEAN, CLEANER, and MS.CLEANER (Bloomfield et al., 1973; Park et al., 1974, 1975, 1979, 1980; Scavia and Park, 1976), use a modified Michaelis-Menten formulation in which the half-saturation constant varies as a function of zooplankton densities to account for competition and feeding interference effects. The equation is:

$$K_z = K_{z1} + K_{z2}\, Z \tag{7-13}$$

where K_{z1} = feeding area coefficient, mass/volume
K_{z2} = competition or interference coefficient

Other saturation response functions besides the Michaelis-Menten and Ivlev formulations have been used in some models. For example, rectilinear saturation curves have been constructed by assuming feeding increases linearly with food concentration until a critical food density is reached, and then levels off at a maximum rate for all concentrations above the critical density. This is expressed as:

$$f_g(F_1,F_2,\ldots F_n) = \frac{F_T}{F_{sat}} \qquad \text{for } F_T < F_{sat} \tag{7-14}$$

$$= 1 \qquad \text{for } F_T \geq F_{sat}$$

TABLE 7-6. MICHAELIS-MENTEN HALF-SATURATION CONSTANTS FOR ZOOPLANKTON CONSUMPTION AND GROWTH

Zooplankton Group	Half-Saturation Constant***	Units	References
Total Zooplankton	0.010 - 0.060	mg(Chl a)/l	Di Toro et al. (1971) O'Connor et al. (1975, 1981)
	0.5 (growth)	mg/l	Chen (1970) Chen & Orlob (1975) Chen & Wells (1975, 1976)
	0.5 - 2.0	mg/l	Jorgensen (1976) Jorgensen et al. (1978)
	1.0	mg/l	Bierman et al. (1980)
	0.2 - 0.6* (growth)	mg/l	U.S. Army Corps of Engineers (1974) Brandes (1976) Smith (1978)
	0.06 - 0.6*	mg/l	Baca & Arnett (1976)
Herbivores	0.010 - 0.015	mg(Chl a)/l	Thomann et al. (1975, 1979) Di Toro & Connolly (1980) Di Toro & Matystik (1980) Salisbury et al. (1983)
Carnivores	0.010	mg(Chl a)/l	Thomann et al. (1975)
	0.02	mgC/l	Scavia et al. (1976)
	0.2	mgC/l	Canale et al (1976)
Omnivores	0.2	mgC/l	Canale et al. (1976)
	0.15	mgC/l	Scavia (1980)
	0.375	mg/l	Bowie et al. (1980)
Cladocerans	0.16 - 0.2	mgC/l	Scavia et al. (1976) Scavia (1980)
	0.5	mg/l	Bowie et al. (1980)
	0.8 (growth)	mg/l	Tetra Tech (1980)
	1.8 (growth)	mg/l	Porcella et al. (1983)
Copepods	0.16 - 0.4	mgC/l	Scavia et al. (1976) Scavia (1980)
	1.0	mg/l	Bowie et al. (1980)
	1.2 (growth)	mg/l	Tetra Tech (1980)
Rotifers	0.2 - 0.6	mgC/l	Scavia et al. (1976) Scavia (1980)

TABLE 7-6. (continued)

Zooplankton Group	Half-Saturation Constant***	Units	References
	0.5	mg/l	Bowie et al. (1980)
	2.0 (growth)	mg/l	Porcella et al. (1983)
Mysids	0.10 - 0.20	mgC/l	Scavia et al. (1976) Scavia (1980)
	0.5	mg/l	Bowie et al. (1980)
	2.0 (growth)	mg/l	Tetra Tech (1980)

*Model documentation values.

***Half-saturation constants are for consumption unless specified for growth.

where F_{sat} = food concentration when feeding saturation occurs, mass/volume

or

$$f_g(F_1,F_2,\ldots F_n) = \frac{F_T - F_o}{F_{sat} - F_o} \qquad \text{for } F_T < F_{sat} \qquad (7\text{-}15)$$

$$= 1 \qquad \text{for } F_T \geq F_{sat}$$

when a threshold feeding concentration F_o is used.

The growth limitation functions used with the filtration form of the growth equation (Equation (7-5)) are different than the saturation response functions discussed above since they must be multiplied by the available food concentration to get the total response. In contrast to the previous functions, these functions generally decrease with increases in the food supply to account for factors like reduced filtering rates, adjustments in particle size selectivity, and reduced assimilation efficiencies which occur at high food concentrations. These types of functions generally have maximum values of 1 at low food densities and decrease assymptotically toward some minimum value as the food density increases.

Di Toro and Matystik (1980) and Di Toro and Connolly (1980) use a reverse Michaelis-Menten formulation to simulate reductions in filtration rates as food concentration increases:

$$f_f(F_1,F_2,\ldots F_n) = 1 - \frac{F_T}{F_T + K_f} \qquad (7\text{-}16)$$

$$= \frac{K_f}{F_T + K_f}$$

where K_f = food concentration at which the filtration rate is 1/2 of its maximum value, mass/volume

TABLE 7-7. THRESHOLD FEEDING LEVELS FOR ZOOPLANKTON

Zooplankton Group	Threshold Feeding Level	References
Total Zooplankton	0.028 mg/l	Scavia & Park (1976)
	0.01 mg/l	Youngberg (1977)
	0.20 mg/l	Bierman et al. (1980)
Carnivores	0.01 mgC/l	Scavia et al. (1976)
Omnivores	0.001 mgC/l	Scavia (1980)
	0.025 mg/l	Bowie et al. (1980)
Cladocerans	0.02 - 0.05 mgC/l	Scavia et al. (1976) Scavia (1980)
	0.05 mg/l	Bowie et al. (1980)
Copepods	0.02 - 0.05 mgC/l	Scavia et al. (1976) Scavia (1980)
	0.05 mg/l	Bowie et al. (1980)
Rotifers	0.02 - 0.05 mgC/l	Scavia et al. (1976) Scavia (1980)
	0.05 mg/l	Bowie et al. (1980)
Mysids	0.02 - 0.05 mgC/l	Scavia et al. (1976) Scavia (1980)
	0.05 mg/l	Bowie et al. (1980)

This function approaches 0 assymptotically at high food densities, resulting in a saturation response for total consumption (Figure 7-3a).

Canale et al. (1975, 1976) use a slightly different formulation to account for reductions in filtering rates and changes in particle size selectivity at high food levels:

$$f_f(F_1,F_2,\ldots F_n) = \frac{K_1 F_T + K_2}{F_T + K_2} \qquad (7\text{-}17)$$

where K_1 = multiplier for minimum filtering rate (minimum value of f_f)
K_2 = food concentration at which the filtering rate is half way between its minimum and maximum value,
$f_f = 1/2\ (K_1 + 1)$, mass/volume

This function approaches K_1 assymptotically at high food levels rather than 0. As a result, the total consumption rate continues to increase in proportion to the food supply at high food concentrations since the volumetric filtration rate remains at a constant minimum level (Figure 7-3b). However, a saturation type response can be generated by setting the minimum multiplier K_1 equal to 0, in which case this formulation is identical to Equation (7-16).

A reverse Michaelis-Menten formulation has also been used to simulate reductions in the assimilation efficiencies of filter feeders at high food concentrations (Di Toro et al., 1971, 1977; Di Toro and Matystik, 1980; Di Toro and Connolly, 1980; Thomann et al., 1975, 1979; Canale et al., 1975, 1976). The equation is:

$$f_f(F_1,F_2,\ldots F_n) = \frac{K_a}{F_T + K_a} \qquad (7\text{-}18)$$

where K_a = food concentration at which the assimilation efficiency is 1/2 of its maximum value, mass/volume

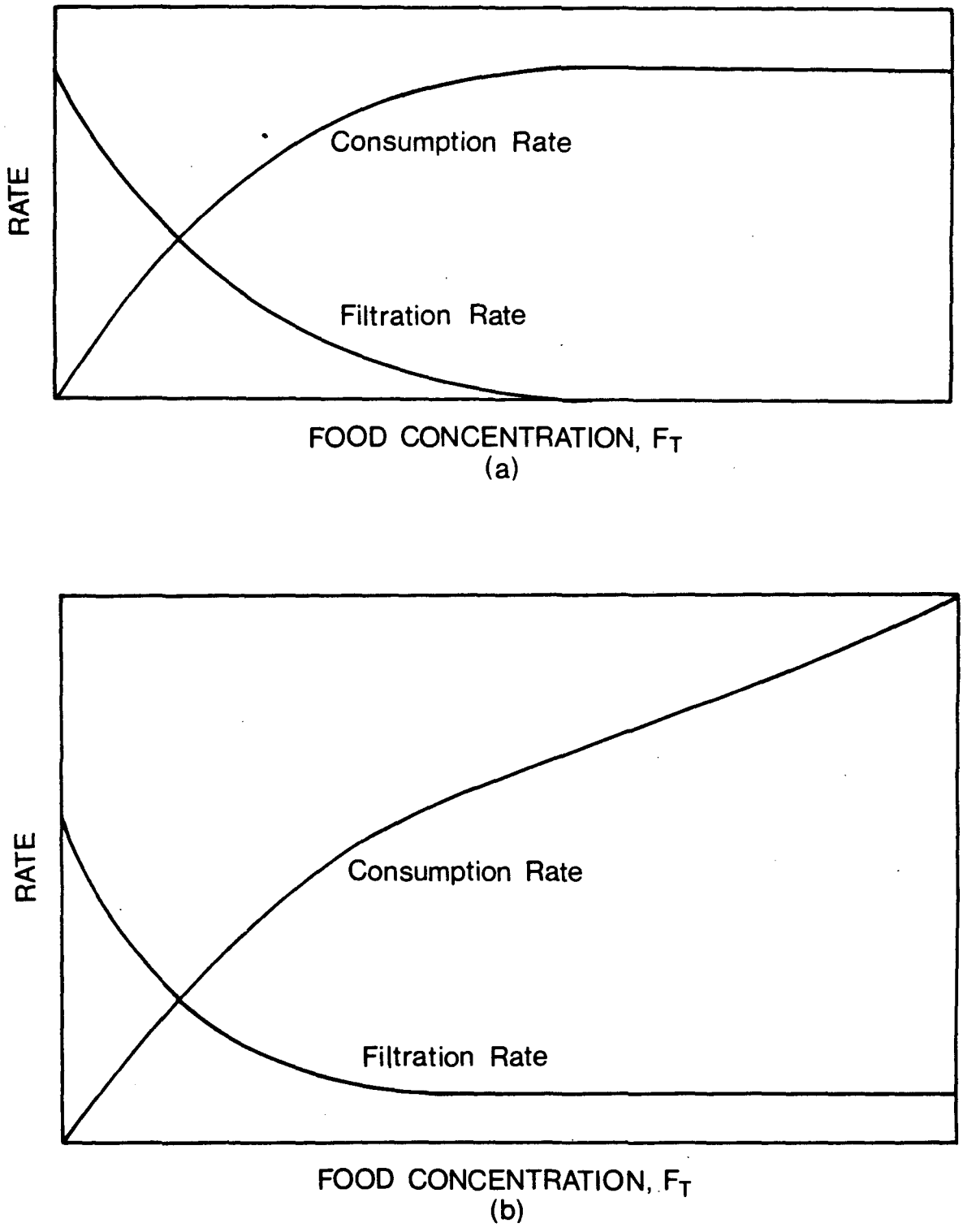

Figure 7-3. Comparison of reverse Michaelis-Menten formulation (a) and Canale et al.'s (1975, 1976) formulation (b) for filtration rate as a function of food concentration.

If a constant volumetric filtration rate is used (Di Toro et al., 1971, 1977; Canale et al., 1975, 1976), this results in a Michaelis-Menten type relationship for total consumption in which the maximum assimilation rate (growth rate) equals the product of the constant filtration rate, maximum assimilation efficiency, and the food concentration at half-maximum assimilation efficiency K_a (ignoring temperature effects):

$$g_z = C_{fmax} E_{max} F_T \left(\frac{K_a}{F_T + K_a} \right)$$

$$= C_{fmax} E_{max} K_a \left(\frac{F_T}{K_a + F_T} \right) \qquad (7\text{-}19)$$

However, Di Toro and Matystik (1980) and Di Toro and Connolly (1980) also use this formulation with a reverse Michaelis-Menten formulation for the filtration rate, which results in a more complicated expression for total consumption involving the product of a Michaelis-Menten term and a reverse Michaelis-Menten term:

$$g_z = C_{fmax} E_{max} K_a \left(\frac{F_T}{K_a + F_T} \right) \left(\frac{K_f}{K_f + F_T} \right) \qquad (7\text{-}20)$$

Zooplankton growth and consumption formulations are compared for several models in Table 7-8.

7.3.2 Food Supply

The total available food concentration F_T used in all of the above growth formulations can be defined in several ways. The simplest approach is to assume all potential food items can be consumed with equal efficiency and define F_T as the sum of the available food concentrations:

$$F_T = \sum_{k=1}^{n} F_K \qquad (7\text{-}21)$$

TABLE 7-8. COMPARISON OF ZOOPLANKTON GROWTH FORMULATIONS

	Food Sources				Basic Approach			Growth Limitation Formulation					Assimilation Efficiency		
Model (Author)	Phyto-plankton	Detritus	Zoo-plankton	Preference Factors Used	Growth Computed Directly	Total Ingestion Computed	Filtration Rate Computed	Michaelis-Menten	Ivlev	Variable Assimilation Efficiency	Variable Filtration Rate	Threshold Feeding Included	Constant	Varies with Food Type	Varies with Food Conc.
AQUA-IV	1					X		X					X		
CE-QUAL-RI	2	1		X		X		X					X		
CLEAN	2	1	3	X		X		X				X		X	
CLEANER	3	1	3	X		X		X				X		X	
MS.CLEANER	4	2	5	X		raptorial feeders	filter feeders	raptors & saturation filterers		X*		X		X	
EAM	4	1	3	X				X					X		
ESTECO	2	1		X	X			X					X		
EXPLORE-1	1					X		X					X		
HSPF	1						X			X					X
LAKECO	2	1		X				X					X		
MIT Network	1				X			X					X		
WASP	2		1				X			X	X				X
WQRRS	2	1		X	X			X					X		
Bierman	5			X		X		X				X	X		
Canale	4		9	X		carnivores	filter feeders	carnivores		nonselective filterers	selective filterers		carnivores & selec-tive filterers		nonselective filterers
Jorgensen	1				X			X				X	X		
Scavia	5	1	6	X		X		X				X		X	

*Maximum assimilation rate used for constant rate filters, with excess consumption egested as pseudofeces.

where F_k = concentration of potential food item k, mass/volume
n = total number of potential food items

A more realistic approach recognizes that food items vary in the efficiency and frequency at which they are utilized by zooplankton, even if all food items are present in equal concentrations. This is due to factors such as food particle size and shape, desirability and quality of different types of food, ease of capture, and zooplankton feeding behavior. For example, many filter feeders are able to selectively filter different food items with different efficiencies, varying their selectivity according to the abundance and desirability of the various food items present. Food particle shape and size are important distinguishing features since, for example, filamentous algae are often actively rejected or avoided while individual cells of the same species in suspension may be consumed (Leidy and Ploskey, 1980). However, the quality and desirability of the food are also important, since senescent cells are less likely to be consumed than healthy cells of the same species. For raptorial feeders, particle size and shape are not quite as critical since they are able to tear large prey items into smaller pieces before consuming them. Prey desirability and ease of capture then become more important.

The above factors are accounted for in models by assigning feeding preference factors to each potential food item. Preference factors can have values ranging from 1 to 0, with 1 corresponding to a food item which is desirable and easily captured and consumed (or filtered), and 0 corresponding to a food item which is never consumed. Food preference factors have been called selectivity coefficients, electivities, ingestion efficiencies, and several other names in different models, but they all basically represent the same thing--weighting factors which reflect the probability that a given food item will be consumed relative to the others when all foods are present in equal concentrations. They account for the fact that some food items may be less available for consumption than indicated by their concentrations alone. When food preference factors are specified, the total available food concentration F_T is defined as:

$$F_T = \sum_{k=1}^{n} P_k F_k \qquad (7\text{-}22)$$

where P_k = food preference factor for food item k
F_k = concentration of food item K, mass/volume
n = total number of potential food items

Vanderploeg and Scavia (1979) show how preference factors can be derived from the different forms of data reported in zooplankton feeding experiments. In field situations, preference factors may change as the composition of the food supply changes. However, this level of sophistication is generally not included in current ecological models.

7.3.3 Assimilation Efficiencies

In addition to differences in food preferences or ingestion efficiencies for different food types, food items may also differ in their assimilation efficiency by zooplankton. The assimilation efficiencies for different food types varies with the energy content, digestibility, and quality of the food (Leidy and Ploskey, 1980). For example, the assimilation efficiencies for algae are typically higher than for detritus and bacteria, although the assimilation efficiencies for blue-green algae are also generally low. Algae with gelatinous sheaths or resistant cell walls and masses of colonial cells may pass through a zooplankton gut intact and in viable condition (Wetzel, 1975), indicating minimal assimilation efficiencies for these food items. The animal foods of raptorial feeders are assimilated more efficiently than plant foods. Also, since the energy content and digestibility of algae and detritus vary much more widely than animal foods, the assimilation efficiencies for herbivores and detritivores typically cover a much wider range than for carnivorous zooplankton (Leidy and Ploskey, 1980).

Variations in the assimilation efficiencies of different food items can be modeled in several ways. One approach is to incorporate these effects in the food preference factors, for example, by assigning a low value to the preference factor for blue-green algae relative to the other algal groups.

This in effect lowers the amount of blue-green algae available for zooplankton assimilation and growth. Another approach is to define different maximum assimilation efficiencies for different food items, to compute net assimilation separately for each food item, and then to sum the individual assimilation terms to get the total zooplankton growth rate (Scavia et al., 1976; Scavia, 1980). This can be expressed for the total consumption formulation (Equation (7-4)) as (ignoring temperature effects):

$$g_z = C_{gmax} \sum_{k=1}^{n} \left[E_{max_k} \; f_{g_k}(F_1, F_2, \ldots F_n) \right] \tag{7-23}$$

where C_{gmax} = maximum total consumption rate, mass food/mass zooplankton-time

E_{max_k} = maximum assimilation efficiency for food item k

$f_{g_k}(F_1, F_2, \ldots F_n)$ = growth limitation factor for food item k

n = total number of potential food items

and for the filtration formulation (Equation (7-5)) as:

$$g_z = C_{fmax} \; f_f(F_1, F_2, \ldots F_n) \sum_{k=1}^{n} \left[E_{max_k} \; P_k \; F_k \right] \tag{7-24}$$

where C_{fmax} = maximum volumetric filtration, volume/mass zooplankton-time

$f_f(F_1, F_2, \ldots F_n)$ = growth limitation function for filtration formulation

P_k = food preference factor for food item k

F_k = concentration of food item k, mass/volume

Note that growth limitation factors must be computed separately for each food item in the total consumption formulation since the quantities which are summed must reflect both the assimilation efficiencies and the amounts of food consumed for each different food item.

For the Michaelis-Menten formulation, the individual growth limitation factor may be defined as:

$$f_{g_k}(F_1,F_2,\ldots F_n) = \frac{P_k\ F_k}{K_z + \sum_{k=1}^{n} P_k\ F_k} \tag{7-25}$$

This is equivalent to the total Michaelis-Menten factor when summed over all food items:

$$\sum_{k=1}^{n} f_{g_k}(F_1,F_2,\ldots F_n) = \sum_{k=1}^{n} \frac{P_k\ F_k}{K_z + \sum_{k=1}^{n} P_k F_k} = \frac{\sum_{k=1}^{n} P_k F_k}{K_z + \sum_{k=1}^{n} P_k F_k} \tag{7-26}$$

Analogous expressions for the Ivlev formulation are more difficult to formulate, since the individual terms are not consistent with the total growth limitation function, even under conditions of equal assimilation efficiencies.

As discussed previously, assimilation efficiencies may decrease with increases in ingestion rate at high food concentrations since the retention time in the gut decreases resulting in incomplete digestion and reduced assimilation. Model formulations to describe these effects have already been discussed in the growth limitation section (Equation (7-18)).

Zooplankton average assimilation efficiencies are presented in Table 7-9. Figures 7-4 and 7-5 present frequency histograms of assimilation efficiency data compiled by Leidy and Plosky (1980).

7.4 RESPIRATION AND MORTALITY

Zooplankton respiration and mortality are modeled using the same general formulations as phytoplankton. Almost all models represent both respiration and nonpredatory mortality rates as either constant coefficients or simple functions of temperature. The basic equations are:

TABLE 7-9. ZOOPLANKTON ASSIMILATION EFFICIENCIES

Zooplankton Group	Assimilation Efficiency	References
Total Zooplankton	0.60 - 0.75	Di Toro et al. (1971) O'Connor et al. (1975, 1981)
	0.63	Jorgensen (1976) Jorgensen et al. (1978)
	0.7	Tetra Tech (1976) Chen & Wells (1975, 1976)
	0.6	Bierman et al. (1980)
	0.5 - 0.8*	Brandes (1976) Smith (1978)
	0.5 - 0.7*	Baca & Arnett (1976)
Herbivores	0.6 (max.)	Thomann et al. (1975, 1979) Di Toro & Connolly (1980) Di Toro & Matystik (1980) Salisbury et al. (1983)
Carnivores	0.6 (max.)	Thomann et al. (1975, 1979) Di Toro & Connolly (1980) Di Toro & Matystik (1980) Salisbury et al. (1983)
	0.5	Scavia et al. (1976)
	0.4 (Cladocerans)	Canale et al. (1976)
Omnivores	0.5 (0.2 for detritus, blue-green algae)	Scavia (1980) Bowie et al. (1980)
	0.4	Canale et al. (1976)
Cladocerans	0.5 (0.2 for detritus, blue-green algae)	Scavia et al. (1976) Scavia (1980) Bowie et al. (1980)
	0.5	Tetra Tech (1980) Porcella et al. (1983)
	0.8 (max.)	Canale et al. (1976)
Copepods	0.5 (0.2 for detritus, blue-green algae)	Scavia et al. (1976) Scavia (1980) Bowie et al. (1980)
	0.7	Canale et al. (1976)

TABLE 7-9. (continued)

Zooplankton Group	Assimilation Efficiency	References
Rotifers	0.5 (0.2 for detritus, blue-green algae)	Scavia et al. (1976) Scavia (1980) Bowie et al. (1980)
	0.5	Tetra Tech (1980) Porcella et al. (1983)
Mysids	0.5 (0.2 for detritus, blue-green algae)	Scavia et al. (1976) Scavia (1980) Bowie et al. (1980)
	0.5	Tetra Tech (1980)

*Model documentation values.

$$r_z = r_z(T_{ref})\ f_r(T) \tag{7-27}$$

and

$$m_z = m_z(T_{ref})\ f_m(T) \tag{7-28}$$

where r_z = zooplankton respiration rate, 1/time
$r_z(T_{ref})$ = respiration rate at reference temperature T_{ref}, 1/time
$f_r(T)$ = temperature function for respiration
m_z = zooplankton nonpredatory mortality rate, 1/time
$m_z(T_{ref})$ = nonpredatory mortality at reference temperature T_{ref}, 1/time
$f_m(T)$ = temperature function for nonpredatory mortality

Since the respiration and nonpredatory mortality rate equations have the same basic form and typically use the same temperature functions, many models combine both processes into a single loss term:

$$r_z + m_z = d_z(T_{ref})\ f_r(T) \tag{7-29}$$

where $d_z(T_{ref})$ = total loss rate due to both respiration and nonpredatory mortality at reference temperature T_{ref}, 1/time

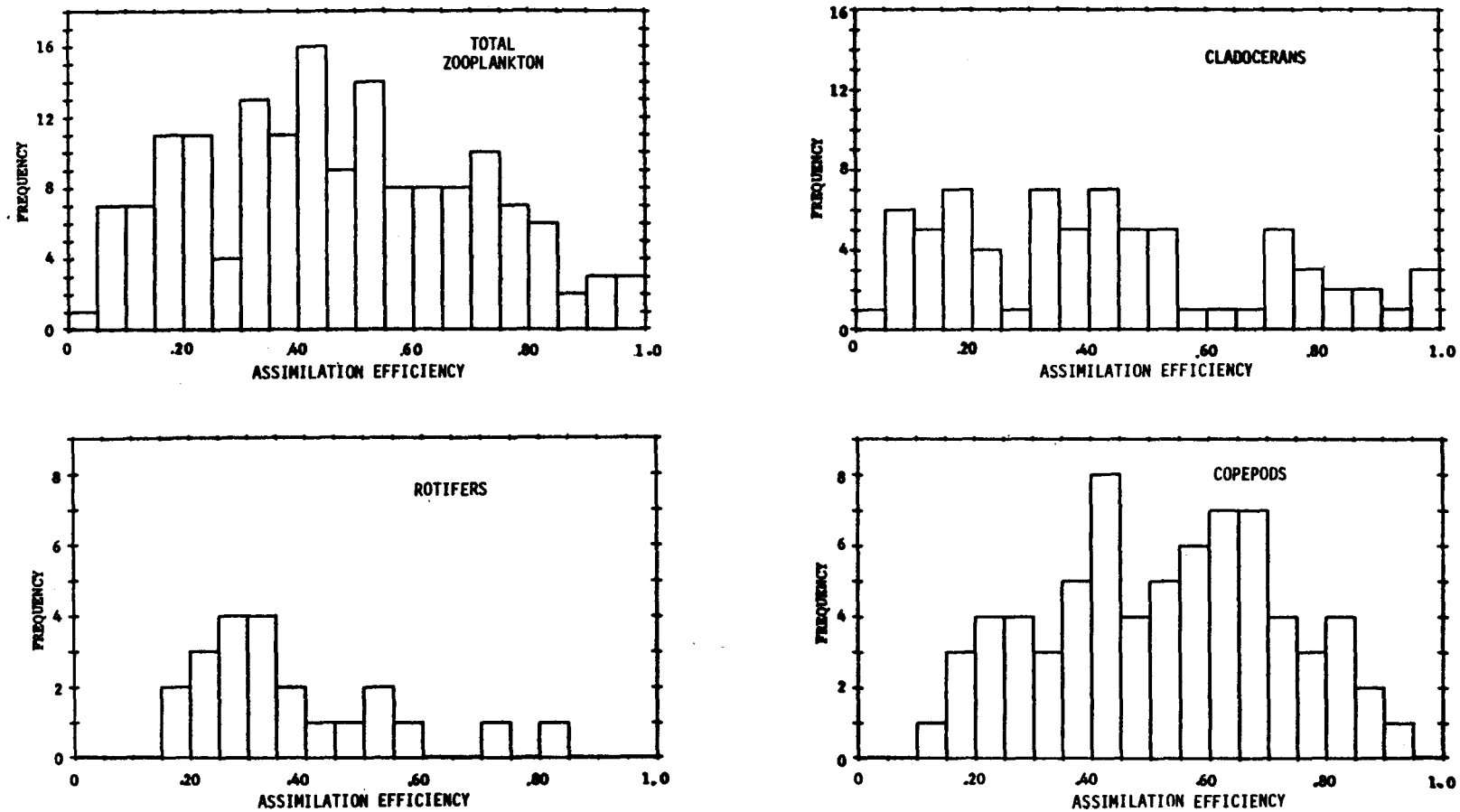

Figure 7-4. Frequency histograms for zooplankton assimilation efficiencies (from Leidy and Ploskey, 1980).

In a few models, the respiration rate is partitioned into two components, 1) the standard respiration rate representing the combined basal metabolism and digestion energetics and 2) the active respiration rate which represents the additional respiration associated with zooplankton activity. These two components can be distinguished by using different temperature response functions for each component. For example, standard respiration is

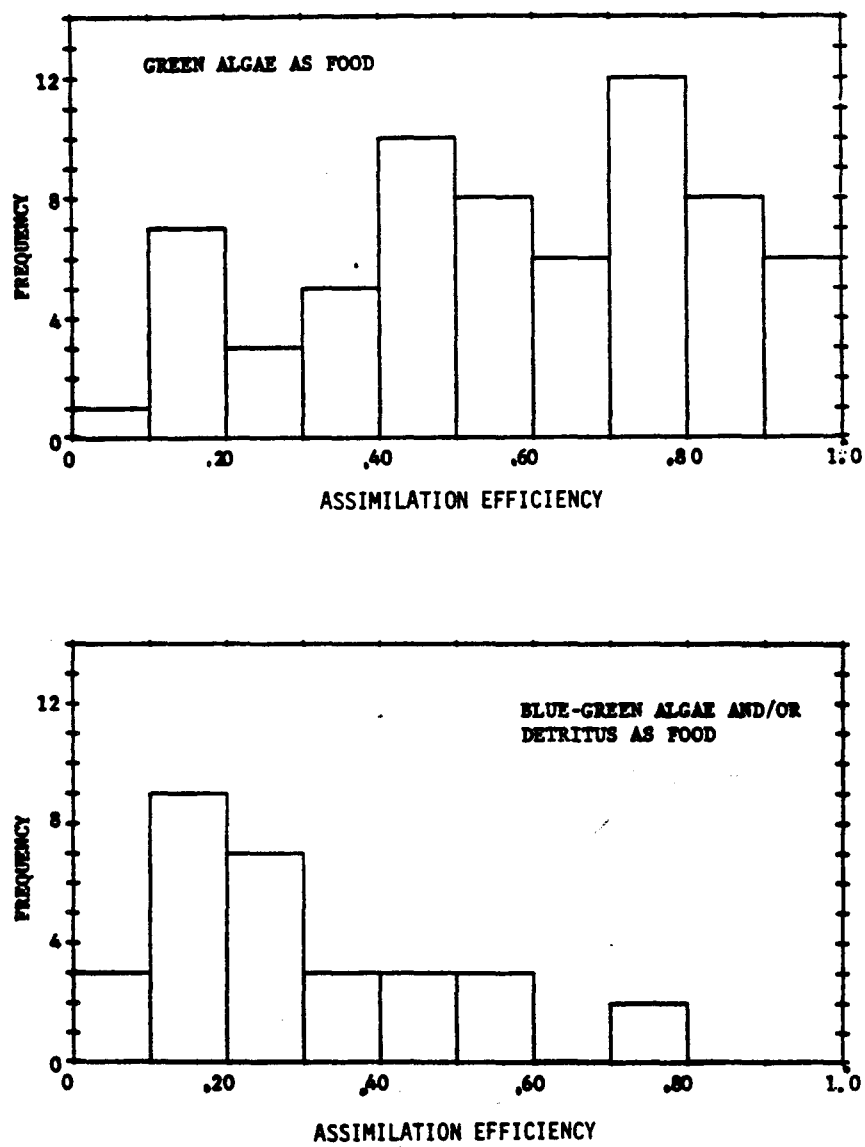

Figure 7-5. Frequency histograms showing variations in zooplankton assimilation efficiencies with different food types (from Leidy and Ploskey, 1980)

typically associated with an exponential temperature curve which increases until the upper lethal limit is approached, while the active respiration rate may be associated with a temperature optimum curve:

$$r = r_{std}(T_{ref})\ f_s(T) + r_{act}(T_{ref})\ f_a(T) \qquad (7\text{-}30)$$

where $r_{std}(T_{ref})$ = standard respiration rate at reference temperature T_{ref}, 1/day

$f_s(T)$ = temperature function for standard respiration

$r_{act}(T_{ref})$ = active respiration rate at reference temperature T_{ref}, 1/day

$f_a(T)$ = temperature function for active respiration

Another approach is to assume that the activity level (and active respiration) is proportional to the feeding level by using a Michaelis-Menten or Ivlev function:

$$r = r_{std}(T_{ref})\ f_s(T) + r_{act}(T_{ref})\ f_a(T)\ f(F_1, F_2, \ldots F_n) \qquad (7\text{-}31)$$

where $f(F_1, F_2, \ldots F_n)$ = growth limitation factor as a function of food supply

This approach is used by Scavia et al. (1976) and Scavia (1980) where the first term represents the minimum endogenous respiration rate under starvation conditions and the second term represents the increase in respiration associated with feeding.

A similar formulation is used in CLEANER (Scavia and Park, 1976) and MS.CLEANER (Park et al., 1979, 1980) where the active respiration rate is expressed as a fraction of the total consumption rate:

$$r = \left[r_{min}(T_{ref}) + K_r\ C_g\right] f(T) \qquad (7\text{-}32)$$

where $r_{min}(T_{ref})$ = minimum endogenous respiration under starvation conditions at reference temperature T_{ref}, 1/time

K_r = fraction of ingested food which is respired

C_g = ingestion rate, 1/time

The CLEANER and MS.CLEANER models also include additional factors to account for crowding effects and population age effects on both respiration and nonpredatory mortality rates. The crowding factor is expressed as:

$$f_{crd} = 1 + \frac{K_c Z}{Z_{cap}} \tag{7-33}$$

where f_{crd} = crowding factor

K_c = crowding coefficient

Z_{cap} = zooplankton carrying capacity, mass or mass/volume

This factor increases the respiration and mortality rates as zooplankton density increases. The age factor accounts for the effects of the population age structure on the net respiration and mortality rates since these rates generally vary with age. The basic assumption is that the population consists primarily of immature individuals at low zooplankton densities and of adults at high population densities (Scavia and Park, 1976). The age factor represents the difference between adult and juvenile rates. The age factor for respiration is expressed as:

$$f_{rage} = 1 + K_{rx}\left(\frac{Z_{cap} - Z}{Z_{cap}}\right) \tag{7-34}$$

where f_{rage} = age factor for respiration

K_{rx} = fractional increase in respiration rate between young zooplankton and adults

and the age factor for mortality is expressed as:

$$f_{mage} = 1 - K_{mx}\left(\frac{Z_{cap} - Z}{Z_{cap}}\right) \tag{7-35}$$

where f_{mage} = age factor for nonpredatory mortality

K_{mx} = fractional decrease in mortality rate between young zooplankton and adults

Both the crowding and age structure factors are multiplied with the respiration and nonpredatory mortality rates defined in Equations (7-32) and (7-28) to incorporate these effects into the rates.

Some versions of CLEANER (Youngberg, 1977) also include an oxygen reduction factor in the respiration equation to account for decreases in respiration at low dissolved oxygen levels. The equation is:

$$f_{ox} = \frac{O_2 - O_{min}}{K_{ox} + (O_2 - O_{min})} \tag{7-36}$$

where f_{ox} = oxygen reduction factor
O_2 = ambient oxygen concentration, mg/l
O_{min} = minimum oxygen requirement, mg/l
K_{ox} = half-saturation constant for oxygen limitation (set at 0.9 mg/l)

Bierman et al. (1980) use a second order formulation for zooplankton mortality when the zooplankton density exceeds a critical level. This accounts for density dependent effects on both natural mortality and predatory mortality (which is not directly simulated in this model) at high densities. The equation is:

$$m = \left[m_1(T_{ref}) + K_m(T_{ref})\ Z \right] f(T) \tag{7-37}$$

where $m_1(T_{ref})$ = mortality rate below the critical zooplankton density at reference temperature T_{ref}, 1/time
$K_m(T_{ref})$ = density dependent mortality coefficient for increased mortality above the critical zooplankton density at reference temperature T_{ref}, 1/mass zooplankton-time

The nonpredatory mortality rate can also be partitioned into several components which account for specific types of mortality such as natural senescence, thermally-induced mortality, toxic mortality, and stress-induced mortality due to low dissolved oxygen, pH extremes, starvation, etc. The general equation is:

$$m_z = m_z(T_{ref})\ f_m(T) + m_T(T_{ref})\ f_T(T) + m_x(T_{ref})\ f_1(T)\ f_x(X)$$

$$+ m_s(T_{ref})\ f_2(T)\ f(O_2, pH, \ldots) + m_f(T_{ref})\ f_3(T) + f_f(F_T) \quad (7\text{-}38)$$

where $m_z(T_{ref})$ = mortality rate due to senescence at reference temperature T_{ref}, 1/time

$f_m(T)$ = temperature function for senescent mortality

$m_T(T_{ref})$ = thermal mortality rate at reference temperature T_{ref}, 1/time

$f_T(T)$ = thermal mortality response curve

$m_x(T_{ref})$ = toxic mortality rate at reference temperature T_{ref}, 1/time

$f_1(T)$ = temperature function for toxic mortality

$f_x(X)$ = dose-response curve for toxic mortality

X = concentration of toxicant, mass/volume

$m_s(T_{ref})$ = stress-induced mortality rate for low dissolved oxygen, pH extremes, etc., at reference temperature T_{ref}, 1/time

$f_2(T)$ = temperature function for stress-induced mortality

$f(O_2, pH\ldots)$ = stress-induced mortality function for low dissolved oxygen, pH extremes, etc.

$m_f(T_{ref})$ = starvation-induced mortality rate at reference temperature T_{ref}, 1/time

$f_3(T)$ = temperature function for starvation mortality

$f_f(F_T)$ = starvation mortality function

Various formulations could be used to define these effects, although most current models deal only with natural mortality and sometimes thermal effects.

Zooplankton respiration rates and mortality rates are presented in Tables 7-10 and 7-11. Figures 7-6 and 7-7 present frequency histograms of respiration rates and nonpredatory mortality rates from data compiled by Leidy and Ploskey (1980).

7.5 PREDATORY MORTALITY

Zooplankton predatory mortality is modeled using the same formulations described previously for phytoplankton. However, since zooplankton are often the highest trophic level included in water quality models, predator-prey dynamics between zooplankton and higher trophic levels cannot usually be simulated. Therefore, predation by fish and carnivorous zooplankton is modeled by either assuming a constant predation loss which is specified as a model input parameter:

$$G_z = \text{constant} \tag{7-39}$$

where G_z = total predatory mortality rate by all zooplankton consumers, mass zooplankton/time

or by assuming a loss rate which is directly proportional to the zooplankton densities:

$$G_z = e_z Z \tag{7-40}$$

or

$$G_z = e_z(T_{ref}) f_e(T) Z \tag{7-41}$$

where e_z = predatory mortality rate coefficient, 1/time

Z = zooplankton biomass or concentration, mass or mass/volume

$e_z(T_{ref})$ = predatory mortality rate coefficient at reference temperature T_{ref}, 1/time

$f_e(T)$ = temperature function for predatory mortality

Since these formulations are essentially the same as those used for nonpredatory mortality, nonpredatory mortality and predation losses are

TABLE 7-10. ZOOPLANKTON RESPIRATION RATES

Zooplankton Group	Respiration Rate	Units	Temperature	References
Total Zooplankton	0.01	1/day	20°C	Chen (1970) Chen & Orlob (1975) Chen & Wells (1975, 1976)
	0.02 - 0.035	1/day	20°C	Jorgensen (1976) Jorgensen *et al*. (1978)
	0.36	1/day	20°C	Lombardo (1972)
	0.02 - 0.16	1/day	20°C	O'Connor *et al*. (1975)
	0.005 - 0.02	1/day	20°C	Tetra Tech (1976)
	0.001 - 0.11*	1/day	20°C	U.S. Army Corps of Engineers (1974) Brandes (1976) Smith (1978)
	0.005 - 0.3*	1/day	20°C	Baca & Arnett (1976)
Herbivores	0.02 - 0.03	1/day	20°C	Thomann et al. (1975, 1979) Di Toro & Connolly (1980) Di Toro & Matystik (1980) Salisbury *et al*. (1983)
Carnivores	0.007 - 0.02	1/day	20°C	Thomann *et al*. (1975, 1979) Di Toro & Connolly (1980) Di Toro & Matystik (1980) Salisbury *et al*. (1983)
	0.30	1/day	T_{opt}	Scavia *et al*. (1976)
	0.04 - 0.06	1/day	20°C	Canale *et al*. (1976)
Omnivores	0.08 - 0.33	1/day	T_{opt}	Scavia (1980) Bowie *et al*. (1980)
	0.04 - 0.06	1/day	20°C	Canale *et al*. (1976)
Cladocerans	0.1 - 0.36	1/day	T_{opt}	Scavia *et al*. (1976) Scavia (1980) Bowie *et al*. (1980)
	0.017 - 0.10	1/day	20°C	Tetra Tech (1980) Porcella *et al*. (1983)
	0.04 - 0.06	1/day	20°C	Canale *et al*. (1976)
	0.157 - 0.413**	1/day	20°C	Lombardo (1972)
	0.090 - 0.216**	1/day	20°C	Leidy & Ploskey (1980)
	0.006 - 0.772**	1/day	T_{opt}	Collins & Wlosinski (1983)
	8.5 - 14.2**	$\frac{ml\ O_2}{mg(D.W.)\text{-}day}$	18°C	Di Toro *et al*. (1971)

TABLE 7-10. (continued)

Zooplankton Group	Respiration Rate	Units	Temperature	References
	5.4 - 14.2**	$\frac{ml\ O_2}{mg(D.W.)\text{-}day}$	20°C	Lombardo (1972)
	14.2**	$\frac{ml\ O_2}{mg(D.W.)\text{-}day}$	20°C	Jorgensen (1979)
Copepods	0.1 - 0.35	1/day	T_{opt}	Scavia et al. (1976) Scavia (1980) Bowie et al. (1980)
	0.04 - 0.06	1/day	20°C	Canale et al. (1976)
	0.017	1/day	20°C	Tetra Tech (1980)
	0.085 - 0.550**	1/day	20°C	Lombardo (1972)
	0.064 - 0.738**	1/day	20°C	Leidy & Ploskey (1980)
	0.043 - 0.695**	1/day	T_{opt}	Collins & Wlosinski (1983)
	3.0 - 12.2**	$\frac{ml\ O_2}{mg(D.W.)\text{-}day}$	20°C	Di Toro et al. (1971)
	2.93 - 18.9**	$\frac{ml\ O_2}{mg(D.W.)\text{-}day}$	20°C	Lombardo (1972)
	3.0 - 13.5**	$\frac{ml\ O_2}{mg(D.W.)\text{-}day}$	20°C	Jorgensen (1979)
Rotifers	0.12 - 0.40	1/day	T_{opt}	Scavia et al. (1976) Scavia (1980) Bowie et al. (1980)
	0.15	1/day	20°C	Porcella et al. (1983)
	0.163 - 0.677**	1/day	20°C	Leidy & Ploskey (1980)
Mysids	0.05 - 0.28	1/day	T_{opt}	Scavia et al. (1976) Scavia (1980) Bowie et al. (1980)
	0.022	1/day	20°C	Tetra Tech (1980)

*Model documentation values.
**Literature values.

often combined into a single total mortality term when higher trophic levels are not directly simulated:

$$m_{tot} = \left[m_z(T_{ref}) + e_z(T_{ref}) \right] f_m(T) \qquad (7\text{-}42)$$

$$= m_{tot}(T_{ref})\ f_m(T)$$

where m_{tot} = total mortality rate, 1/time

$m_{tot}(T_{ref})$ = total mortality rate at reference temperature T_{ref}, 1/time

In ecologically oriented models where long term seasonal changes in population dynamics are important, zooplankton are often separated into several functional groups based on general feeding types (filter feeders, carnivorous raptors, omnivores, etc.) or on major taxonomic groups (cladocerans, copepods, rotifers) (Canale et al., 1975, 1976; Scavia et al., 1976; Scavia, 1980; Park et al., 1974, 1975, 1979, 1980; Chen et al., 1975; Tetra Tech, 1979). Although several species must be lumped into each functional group, this approach recognizes the importance of complexities in the food web, different foraging strategies, and predator population dynamics in evaluating both zooplankton and phytoplankton dynamics. Several planktivorous fish groups are also sometimes provided for the same reasons. (Chen et al., 1975; Tetra Tech, 1979; Park et al., 1979, 1980).

In these situations, zooplankton predation rates are computed as the sum of the consumption rates by all potential predators, including carnivorous or omnivorous zooplankton and planktivorous fish. The general relationship for predatory mortality can be expressed as:

$$G_{z_i} = \sum_{j=1}^{n_p} \left[C_j \, X_j \, \frac{P_{ij} \, Z_i}{\sum_{k=1}^{n_j} P_{kj} \, F_{kj}} \right] \qquad (7\text{-}43)$$

where G_{z_i} = total predatory mortality rate for zooplankton group i, mass zooplankton/time

n_p = total number of zooplankton consumers

C_j = total consumption rate by predator group j, 1/time

X_j = biomass or concentration of predator group j, mass or mass/volume

P_{ij} = food preference factor for predator group j feeding on zooplankton group i

TABLE 7-11. ZOOPLANKTON MORTALITY RATES

Zooplankton Group	Mortality Rate (1/day)	Mortality Type	References
Total Zooplankton	0.075	total	Di Toro *et al*. (1971)
	0.125	nonpredatory	Jorgensen (1976)
	0.025 - 0.033	nonpredatory	Jorgensen *et al*. (1978)
	0.005	nonpredatory	Chen and Wells (1975, 1976)
	0.02	nonpredatory	Tetra Tech (1980)
	0.015	total	O'Connor *et al*. (1981)
	0.005*	nonpredatory	U.S. Army Corps of Engineers (1974)
	0.001 - 0.005*	nonpredatory	Brandes (1976)
	0.005 - 0.02*	nonpredatory	Smith (1978)
	0.003 - 0.075**	total	Jorgensen (1979)
Carnivores	0.01	nonpredatory	Scavia *et al*. (1976)
	0.01	fish grazing	Scavia *et al*. (1976)
Omnivores	0.005	fish grazing	Scavia (1980)
Fast Ingesters	0.05	nonpredatory	Bierman *et al*. (1980)
Slow Ingesters	0.01	nonpredatory	Bierman *et al*. (1980)
Cladocerans	0.01	nonpredatory	Scavia *et al*. (1976)
	0.04 - 0.05	fish grazing	Scavia *et al*. (1976)
	0.001 - 0.005	fish grazing	Scavia (1980)
	0.01	nonpredatory	Tetra Tech (1980)
	0.1	nonpredatory	Porcella *et al*. (1983)
	0.0007 - 0.027**	nonpredatory	Leidy & Ploskey (1980)
	0.001 - 0.027**	nonpredatory	Collins & Wlosinski (1983)
Copepods	0.01	nonpredatory	Scavia *et al*. (1976)
	0.05	fish grazing	Scavia *et al*. (1976)
	0.002	fish grazing	Scavia (1980)
	0.003 - 0.005	nonpredatory	Canale *et al*. (1976)
	0.01	nonpredatory	Tetra Tech (1980)

TABLE 7-11. (continued)

Zooplankton Group	Mortality Rate (1/day)	Mortality Type	References
	0.0005 - 0.153**	nonpredatory	Leidy & Ploskey (1980)
	0.003 - 0.155**	nonpredatory	Collins & Wlosinski (1983)
Rotifers	0.01	nonpredatory	Scavia et al. (1976)
	0.12	nonpredatory	Porcella et al. (1983)
Mysids	0.01	nonpredatory	Scavia et al. (1976)
	0.1	fish grazing	Scavia et al. (1976)
	0.08	fish grazing	Scavia (1980)
	0.01	nonpredatory	Tetra Tech (1980)

*Model documentation values.

**Literature values.

Z_i = biomass or concentration of zooplankton group i, mass or mass/volume

n_j = total number of potential food items for predator group j

P_{kj} = food preference factor for predator group j feeding on food item k

F_{kj} = biomass or concentration of potential food item k consumed by predator group j, mass or mass/volume

The quantity $(P_{ij} Z_i / \sum_{k=1}^{n_j} P_{kj} F_{kj})$ in Equation (7-43) represents the fraction of the total food consumption by predator group j which is provided by zooplankton group i. The quantity $C_j X_j$ represents the total rate of food ingestion by predator group j. Ingestion rate formulations for carnivorous zooplankton were discussed in the previous section. Consumption rates for planktivorous fish are generally modeled in the same way. As discussed in the algae chapter, consumption rates are sometimes back-calculated from computed growth rates and known assimilation efficiencies using the equation:

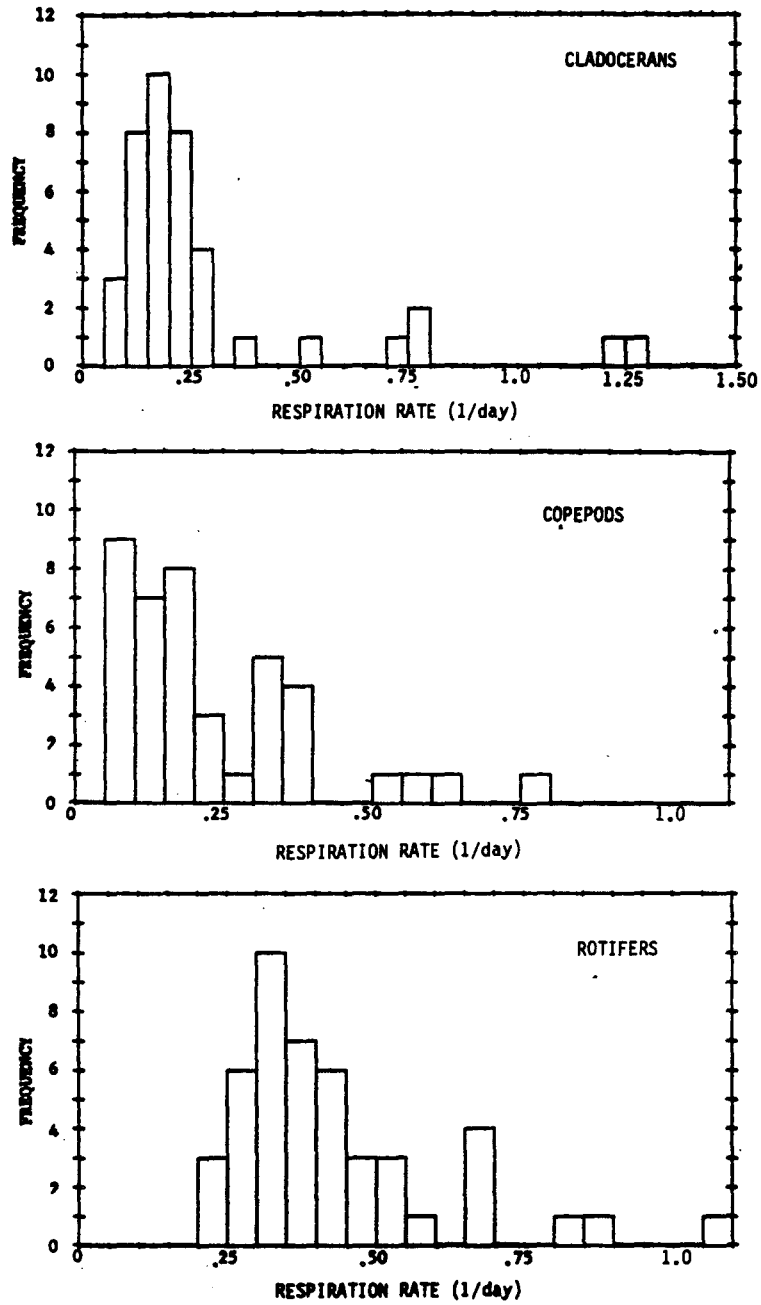

FIGURE 7-6. Frequency histograms of zooplankton respiration rates (from Leidy and Ploskey, 1980).

$$C_j = \frac{g_j}{E_j} \tag{7-44}$$

where C_j = total consumption rate for predator group j, 1/time
g_j = growth rate for predator group j, 1/time
E_j = assimilation efficiency for predator group j

When different assimilation efficiencies are used for different food items, consumption rates are generally calculated directly for each food item and combined with the food specific assimilation efficiencies to determine net growth (as discussed in Section 7.3.3).

7.6 SUMMARY

Zooplankton are typically modeled as a biomass pool using the same mass balance approach used for nutrients, phytoplankton, and other constituents.

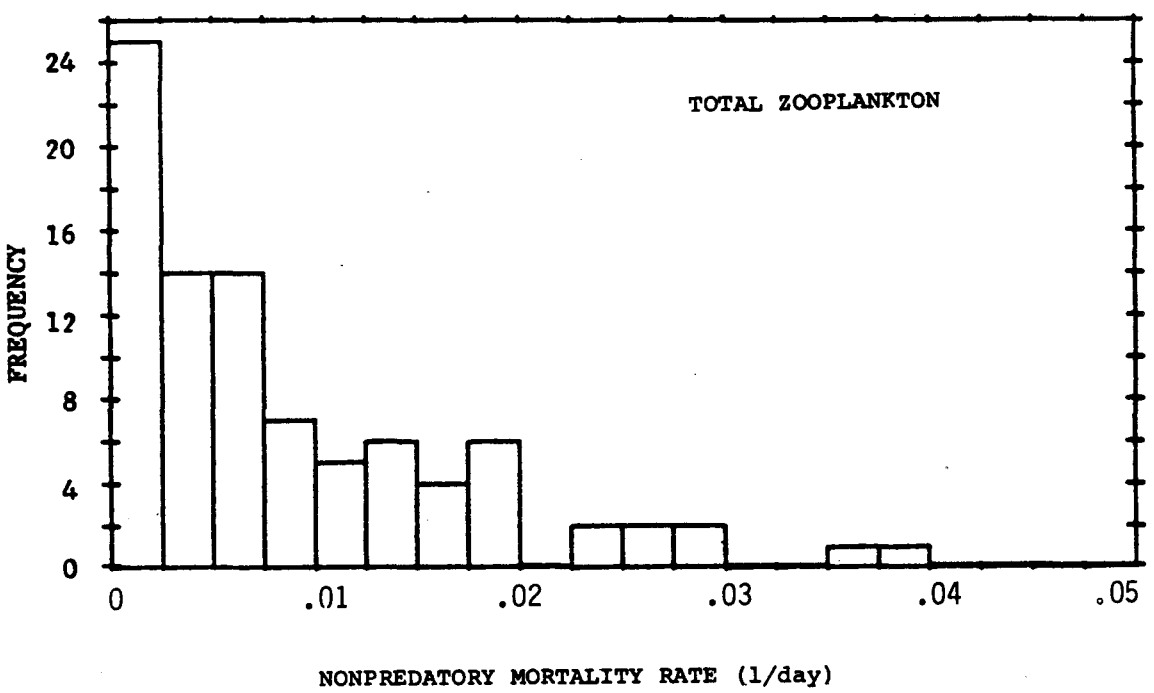

Figure 7-7. Frequency histogram of nonpredatory mortality rates for zooplankton (from Leidy and Ploskey, 1980).

The simplest models lump all zooplankton into a single group, while more complex models distinguish between different feeding types or different taxonomic groups.

Zooplankton dynamics depend on growth, reproduction, respiration, excretion, predation, and nonpredatory mortality. However, these processes are not generally measured in the field for a specific model application since: 1) many of them are difficult or impossible to measure directly; 2) the rates depend on environmental conditions (e.g., temperature), ecological conditions (e.g., food supply and predator densities), and the species composition of the zooplankton, all of which change continually with time; and 3) the fluxes depend largely on the zooplankton densities, which may vary by orders of magnitude over a seasonal cycle.

As a result, many of the model coefficients must be determined by model calibration rather than by measurement. Model constructs must be relied upon to describe the effects of different factors on these processes. Literature values from laboratory experiments are useful for establishing reasonable ranges of the process rates and coefficients. However, specific experimental results are difficult to apply directly since experiments typically use a single species rather than the species assemblages represented in models, and since experimental conditions may not represent conditions in the field.

Most models include formulations to describe the effects of temperature on all process rates. Food density effects on growth and consumption are typically modeled using saturation kinetics similar to those used for phytoplankton. Respiration and mortality rates are most commonly modeled as first-order losses, although a few models use more complicated formulations which include the effects of other factors, for example, crowding effects. Since few models include higher trophic levels such as fish, predatory mortality is typically treated in a simplistic manner.

7.7 REFERENCES

Baca, R.G., W.W. Waddel, C.R. Cole, A. Brandstetter, and D.B. Clearlock. 1973. EXPLORE-I: A River Basin Water Quality Model. Battelle, Inc., Pacific Northwest Laboratories, Richland, Washington.

Baca, R.G., M.W. Lorenzen, R.D. Mudd, and L.V. Kimmel. 1974. A Generalized Water Quality Model for Eutrophic Lakes and Reservoirs. Battelle, Inc., Pacific Northwest Laboratories, Richland, Washington.

Baca, R.G. and R.C. Arnett. 1976. A Limnological Model for Eutrophic Lakes and Impoundments. Battelle, Inc., Pacific Northwest Laboratories, Richland, Washington.

Bierman, V.J., Jr. 1976. Mathematical Model of the Selective Enhancement of Blue-Green Algae by Nutrient Enrichment. In: Modeling Biochemical Processes in Aquatic Ecosystems. R.P. Canale (ed.). Ann Arbor Science Publishers, Ann Arbor, Michigan. pp. 1-31.

Bierman, V.J., Jr., D.M. Dolan, E.F. Stoermer, J.E. Gannon, and V.E. Smith. 1980. The Development and Calibration of a Multi-Class Phytoplankton Model for Saginaw Bay, Lake Huron. Great Lakes Environmental Planning Study. Contribution No. 33. Great Lakes Basin Commission, Ann Arbor, Michigan.

Bloomfield, J.A., R. A. Park, D. Scavia, and C.S. Zahorcak. 1973. Aquatic Modeling in the Eastern Deciduous Forest Biome. U.S. International Biological Program. In: Modeling the Eutrophication Process. E.J. Middlebrook, D.H. Falkenborg, and T.E. Maloney, (eds.). Utah State University, Logan. pp. 139-158

Bowie, G.L., C.W. Chen, and D.H. Dykstra. 1980. Lake Ontario Ecological Modeling, Phase III. Tetra Tech, Inc., Lafayette, California. For National Oceanic and Atmospheric Administration, Great Lakes Environmental Research Laboratory, Ann Arbor, Michigan.

Brandes, R.J. 1976. An Aquatic Ecologic Model for Texas Bays and Estuaries. Water Resources Engineers, Inc., Austin, Texas. For the Texas Water Development Board, Austin, Texas.

Brandes, R.J. and F.D. Masch. 1977. ESTECO--Estuarine Aquatic Ecologic Model: Program Documentation and User's Manual. Water Resources Engineers, Inc., Austin, Texas. For the Texas Water Development Board, Austin, Texas.

Canale, R.P., L.M. Depalma, and A.H. Vogel. 1975. A Food Web Model for Lake Michigan. Part 2 - Model Formulation and Preliminary Verification. Tech. Report 43, Michigan Sea Grant Program, MICHU-SG-75-201.

Canale, R.P., L.M. Depalma, and A.H. Vogel. 1976. A Plankton-Based Food Web Model for Lake Michigan. In: Modeling Biochemical Processes in Aquatic Ecosystems. R.P. Canale (ed.). Ann Arbor Science Publishers, Ann Arbor, Michigan. pp. 33-74.

Chen, C.W. 1970. Concepts and Utilities of Ecological Model. ASCE Journal of the Sanitary Engineering Division, Vol. 96, No. SA5.

Chen, C.W. and G.T. Orlob. 1972. Ecologic Simulation for Aquatic Environments. Water Resources Engineers, Inc., Walnut Creek, California. For the Office of Water Resources Research.

Chen, C.W. and G.T. Orlob. 1975. Ecologic Simulation for Aquatic Environments. Systems Analysis and Simulation in Ecology, Vol. 3. B.C. Patten, (ed.). Academic Press, New York, N.Y. pp. 476-588.

Chen, C.W., M. Lorenzen, and D.J. Smith. 1975. A Comprehensive Water Quality-Ecological Model for Lake Ontario. Tetra Tech, Inc., Lafayette, California. For National Oceanic and Atmospheric Administration, Great Lakes Environmental Research Laboratory, Ann Arbor, Michigan.

Chen, C.W. and J.T. Wells, Jr.. 1975. Boise River Water Quality-Ecological Model for Urban Planning Study. Tetra Tech, Inc. For U.S. Army Engineering District, Walla Walla, Wash., Idaho Water Resources Board, and Idaho Dept. of Environmental and Community Services.

Chen, C.W. and J.T. Wells, Jr. 1976. Boise River Modeling. In: Modeling Biochemical Processes in Aquatic Ecosystems. R.P. Canale (ed.). Ann Arbor Science Publishers, Ann Arbor, Michigan. pp. 171-204.

Collins, C.D. and J.H. Wlosinski. 1983. Coefficients for Use in the U.S. Army Corps of Engineers Reservoir Model, CE-QUAL-R1. U.S. Army Corps of Engineers, Waterways Experiment Station, Vicksburg, Mississippi.

Di Toro, D.M., D.J. O'Connor, and R.V. Thomann. 1971. A Dynamic Model of the Phytoplankton Population in the Sacramento-San Joaquin Delta. In:Nonequilibrium Systems in Natural Water Chemistry, Adv. Chem. Ser. 106. American Chemical Society, Washington, D.C. pp. 131-180

Di Toro, D.M., R.V. Thomann, D.J. O'Connor, and J.L. Mancini. 1977. Estuarine Phytoplankton Biomass Models - Verification Analyses and Preliminary Applications. In: The Sea, Vol. 6, Marine Modeling. E.D. Goldberg, I.N. McCave, J.J. O'Brien, and J.H. Steele (eds.). Wiley-Interscience Publications, New York, N.Y.

Di Toro, D.M. and J.F. Connolly. 1980. Mathematical Models of Water Quality in Large Lakes. Part II: Lake Erie. U.S. Environmental Protection Agency, Ecological Research Series. EPA-600/3-80-065.

Di Toro, D.M. and W.F. Matystik, Jr. 1980. Mathematical Models of Water Quality in Large Lakes. Part I: Lake Huron and Saginaw Bay Model Development, Verification, and Simulations. U.S. Environmental Protection Agency, Ecological Research Series. EPA-600/3-80-056.

Di Toro, D.M., J.J. Fitzpatrick, and R.V. Thomann. 1981. Water Quality Analysis Simulation Program (WASP) and Model Verification Program (MVP) - Documentation. Hydroscience, Inc., Westwood, New Jersey. For U.S. Environmental Protection Agency, Duluth, Minnesota.

Geller, W. 1975. Die Nahrungs aufnahme von Daphnia pulex in Abhangigkeit von der Futterhonzentration, der Temperatur, der Korpergroesse und dem Hungerzustand der Tiere. (The food uptake of Daphnia pulex as a function of food concentration, temperature, animals' body length, and starvation). Archivfuer Hydrobiologie Supplementband. 48:47-107. (Fisheries and Marine Service of Canada Translation Series No. 4017, 1977, 96 pp.)

Harleman, D.R.F., J.E. Dailey, M.L. Thatcher, T.O. Najarian, D.N. Brocard, and R.A. Ferrara. 1977. User's Manual for the M.I.T. Transient Water Quality Network Model--Including Nitrogen-Cycle Dynamics for Rivers and Estuaries. R.M. Parsons Laboratory for Water Resources and Hydrodynamics, Massachusetts Institute of Technology, Cambridge, Massachusetts. For U.S. Environmental Protection Agency, Corvallis, Oregon. EPA-600/3-77-010.

Ivlev, V.S. 1966. The Biological Productivity of Waters. J. Fish. Res. Bd. Can., 23:1727-1759.

Johanson, R.C., J.C. Imhoff, and H.H. Davis. 1980. User's Manual for Hydrological Simulation Program - Fortran (HSPF). Hydrocomp, Inc., Mountain View, California. For U.S. Environmental Protection Agency, Athens, Georgia. EPA-600/9-80-015.

Jorgensen, S.E. 1976. A Eutrophication Model for a Lake. Ecol. Modeling 2:147-165.

Jorgensen, S.E. (ed.) 1979. Handbook of Environmental Data and Ecological Parameters. International Society for Ecological Modeling.

Jorgensen, S.E., H. Mejer, and M. Friis. 1978. Examination of a Lake Model. Ecol. Modeling, 4:253-278.

Jorgensen, S.E., L.A. Jorgensen, L. Kamp-Nielsen, and H.F. Mejer. 1981. Parameter Estimation in Eutrophication Modeling. Ecol. Modeling, 13:111-129.

Jorgensen, S.E. 1983. Eutrophication Models of Lakes. In: Application of Ecological Modeling in Environmental Management, Part A. S.E. Jorgensen (ed.). Elsevier Scientific Publishing Company. Chapter 7.

Kremer, J.N. and S.W. Nixon. 1978. A Coastal Marine Ecosystem, Simulation and Analysis. Springer-Verlag. 217 pp.

Leidy, G.R. and G.R. Ploskey, 1980. Simulation Modeling of Zooplankton and Benthos in Reservoirs: Documentation and Development of Model Constructs. U.S. Fish and Wildlife Service, Fayetteville, Arkansas. For U.S. Army Corps of Engineers, Waterways Experiment Station (WES), Vicksburg, Mississippi.

Lombardo, P.S. 1972. Mathematical Model of Water Quality in Rivers and Impoundments. Hydrocomp, Inc., Mountain View, California.

Mayzaud, P. and S.A. Poulet. 1978. The Importance of the Time Factor in the Response of Zooplankton to Varying Concentrations of Naturally Occurring Particulate Matter. Limnol and Oceanogr., 23:1144-1154.

Michaelis, L. and M.L. Menten. 1913. Biochemische Zeitschrift., 49:333.

Najarian, T.O. and D.R.F. Harleman. 1975. A Nitrogen Cycle Water Quality Model for Estuaries. R.M. Parsons Laboratory for Water Resources and Hydrodynamics, Massachusetts Institute of Technology, Cambridge, Massachusetts. Tech. Report No. 204.

O'Connor, D.J., D.M. Di Toro, and R.V. Thomann. 1975. Phytoplankton Models and Eutrophication Problems. In: Ecological Modeling in a Resource Management Framework. C.S. Russell (ed.). Proceedings of Symposium Sponsored by NOAA and Resources for the Future.

O'Connor, D.J., J.L. Mancini, and J.R. Guerriero. 1981. Evaluation of Factors Influencing the Temporal Variation of Dissolved Oxygen in the New York Bight, PHASE II. Manhattan College, Bronx, New York.

Park, R.A., R.V. O'Neill, J.A. Bloomfield, H.H. Shugart, Jr., R.S. Booth, R.A. Goldstein, J.B. Mankin, J.F. Koonce, D. Scavia, M.S. Adams, L.S. Clesceri, E.M. Colon, E.H. Dettmann, J.A. Hoopes, D.D. Huff, S. Katz, J.F. Kitchell, R.C. Kohberger, E.J. LaRow, D.C. McNaught, J.L. Peterson, J.E. Titus, P.R. Weiler, J.W. Wilkinson, and C.S. Zahorcak. 1974. A Generalized Model for Simulating Lake Ecosystems. Simulation, 23(2):33-50.

Park, R.A., D. Scavia, and N.L. Clesceri. 1975. CLEANER, The Lake George Model. In: Ecological Modeling in a Resource Management Framework. C.S. Russell (ed.). Resources for the Future, Inc., Washington, D.C. pp. 49-82.

Park, R.A., C.D. Collins, D.K. Leung, C.W. Boylen, J. Albanese, P. deCaprariis, and H. Forstner. 1979. The Aquatic Ecosystem Model MS.CLEANER. Proc. of First International Conf. on State of the Art of Ecol. Modeling, Denmark.

Park, R.A., C.D. Collins, C.I. Connolly, J.R. Albanese, and B.B. MacLeod. 1980. Documentation of the Aquatic Ecosystem Model MS.CLEANER. Rensselaer Polytechnic Institute, Center for Ecological Modeling, Troy, New York. For U.S. Environmental Protection Agency, Environmental Research Laboratory, Office of Research and Development, Athens, Georgia.

Porcella, D.B., T.M. Grieb, G.L. Bowie, T.C. Ginn, and M.W. Lorenzen. 1983. Assessment Methodology for New Cooling Lakes, Vol. 1: Methodology to Assess Multiple Uses for New Cooling Lakes. Tetra Tech, Inc., Lafayette, California. For Electric Power Research Institute, Report EPRI EA-2059.

Salisbury, D.K., J.V. DePinto, and T.C. Young. 1983. Impact of Algal-Available Phosphorus on Lake Erie Water Quality: Mathematical Modeling. For U.S. Environmental Protection Agency, Environmental Research Laboratory, Duluth, Minnesota.

Scavia, D. 1980. An Ecological Model of Lake Ontario. Ecol. Modeling, 8:49-78.

Scavia, D., B.J. Eadie, and A. Robertson. 1976. An Ecological Model for Lake Ontario-Model Formulation, Calibration, and Preliminary Evaluation. NOAA Tech. Rept. ERL 371-GLERL 12. Natl. Ocean. and Atmos. Admin., Boulder, Colorado.

Scavia, D. and R.A. Park. 1976. Documentation of Selected Constructs and Parameter Values in the Aquatic Model CLEANER. Ecol. Modeling, 2:33-58.

Smith, D.J. 1978. Water Quality for River-Reservoir Systems. Resource Management Associates, Inc., Lafayette, California. For U.S. Army Corps of Engineers, Hydrologic Engineering Center (HEC), Davis, California.

Swartzman, G.L. and R. Bentley. 1977. A Comparison of Plankton Models with Emphasis on Application to Assessing Non-Radiological Nuclear Plant Impacts on Plankton in Natural Ecosystems. Center for Quantitative Science, College of Fisheries, University of Washington, Seattle, Washington.

Tetra Tech, Inc. 1979. Methodology for Evaluation of Multiple Power Plant Cooling System Effects, Volume II. Technical Basis for Computations. Electric Power Research Institute, Report EPRI EA-1111.

Tetra Tech, Inc. 1980. Methodology for Evaluation of Multiple Power Plant Cooling System Effects, Volume V. Methodology Application to Prototype-Cayuga Lake. Electric Power Research Institute, Report EPRI EA-1111.

Thomann, R.V., D.M. Di Toro, R.P. Winfield, and D.J. O'Connor. 1975. Mathematical Modeling of Phytoplankton in Lake Ontario, Part 1. Model Development and Verification. Manhattan College, Bronx, New York. For U.S. Environmental Protection Agency, Corvallis, Oregon. EPA-600/3-75-005.

Thomann, R.V., J. Segna, and R. Winfield. 1979. Verification Analysis of Lake Ontario and Rochester Embayment Three-Dimensional Eutrophication Models. Manhattan College, Bronx, New York. For U.S. Environmental Protection Agency, Office of Research and Development, Duluth, Minnesota.

U.S. Army Corps of Engineers. 1974. Water Quality for River-Reservoir Systems. U.S. Army Corps of Engineers, Hydrologic Engineering Center (HEC), Davis, California.

Vanderploeg, H.A. and D. Scavia. 1979. Calculation and Use of Selectivity Coefficients of Feeding: Zooplankton Grazing. Ecol. Modeling, 7:135-149.

WES (Waterways Experiment Station). 1982. CE-QUAL-R1: A Numerical One-Dimensional Model of Reservoir Water Quality, Users Manual. Environmental and Water Qualtiy Operational Studies (EWQOS), U.S. Army Corps of Engineers, Waterways Experiment Station, Vicksburg, Mississippi.

Wetzel, R.G. 1975. Limnology. W. B. Saunders Co., Philadelphia, Pennsylvania. 743 pp.

Youngberg, B.A. 1977. Application of the Aquatic Model CLEANER to Stratified Reservoir System. Center for Ecological Modeling, Report #1, Rensselaer Polytechnic Institute, Troy, New York.

CHAPTER 8

COLIFORM BACTERIA

8.1 INTRODUCTION

Coliform concentrations in natural waters have been used as an indicator of potential pathogen contamination since at least the 1890's (Whipple, 1917). Until recently, coliforms have been considered to be less sensitive to environmental stresses than enteric pathogens. Accordingly, coliforms were believed to be more persistent in natural waters and, therefore, a "safe" or conservative index of potential pathogen levels.

However, recent evidence about enteric viruses, opportunistic pathogens, and pathogenic Escherichia coli have raised doubts that coliforms are the "ideal indicator" (Sobsey and Olson, 1983). First, enteric viruses appear to generally have both lower decay rates than coliforms and also a lower ID-50 (i.e., the dose required to infect 50 percent of the persons exposed) than most bacterial enteric pathogens. Second, opportunistic pathogens (e.g., Pseudomonas aeruginosa, Aeromonas hydrophila, and Legionella pneumophila) often have major non-fecal sources and are able to grow in natural waters. These pathogens generally have a high ID-50, threatening primarily immunologically compromised persons such as hospital patients who are being given immunological suppressants. Finally, some strains of E. coli produce an enteric toxin that results in gastroenteritis.

In the context of drinking water, Olivieri (1983) has recommended that different indicators be used when different aspects of pathogen behavior are of interest, e.g., indicator of feces, treatment efficiency, or post-treatment contamination. Chamberlin (1982) has compared coliform (combining Total Coliform, Fecal Coliform, and E. coli) decay rates with pathogen and

virus decay rates measured simultaneously and has found that the respective decay rates were highly correlated (r^2 = 0.73) and that within-species variability was as great as pathogen-to-coliform variation (see Figure 8-1). At low decay rates, coliform decay rates were approximately equal to pathogen decay rates while at the highest decay rates, pathogen decay was slower.

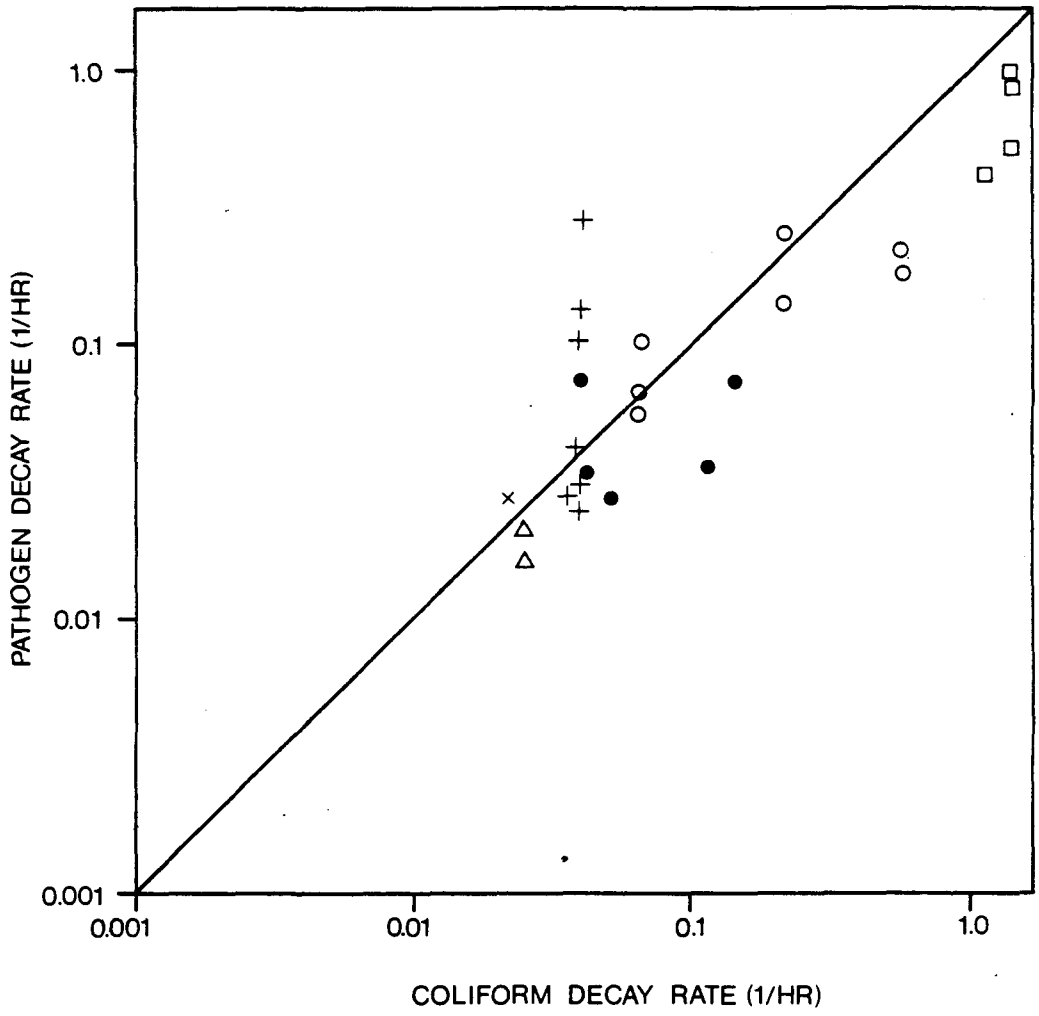

Figure 8-1. Relationship between pathogen or virus decay rates and coliform decay rates based on figure presented by Chamberlin (1982). Decay rates were estimated by Chamberlin based on data from Baross et al. (1975) (△), Morita (1980) (X), McFeters et al. (1974) (+), McCambridge and McMeekin (1981) (○), Lantrip (1983) (●), and Kapuscinski and Mitchell (1981) (□). The line shown represents coliform decay rates equal to pathogen decay rates.

In addition, epidemiological studies have revealed that enterococci levels are more closely associated with enteric disease than are coliforms (Cabelli et al. 1982). This work has in part motivated a proposed revision of the contact recreation bacterial water quality criteria: switching from fecal coliforms to E. coli and/or enterococci (U.S. Environmental Protection Agency, 1984).

Taken as a whole, these issues may serve to motivate modelers to include additional indicators as state variables and to use coliforms as an indicator rather than as the indicator.

8.2 COMPOSITION AND ASSAY

The coliform group consists of both fecal and non-fecal components. The fecal component includes mainly the Escherichia and Klebsiella genera while the non-fecal component includes mainly the Enterobacter and Citrobacter genera commonly associated with soils and plants (Dufour, 1977).

Neither the multiple tube (MPN) nor the membrane filter (MF) techniques for Total Coliforms (TC) effectively differentiates between the fecal and non-fecal components. The Fecal Coliform (FC) tests (either MPN or MF) provide a better differentiation at the cost of additional labor and time plus more exacting equipment requirements. The tests require either supplemental tests run on TC or incubation at elevated temperatures within precise limits (i.e., $44.5^{o}C \pm 0.2^{o}C$). These more stringent conditions eliminate most of the non-fecal component while still permitting the fecal component to survive. FC represents from 15 to 90 percent of the TC, depending on sample source. Unfortunately, there are major non-fecal sources of FC, most commonly of Klebsiella species (Hendry et al. 1982). Pulp mill wastewater provides a frequent example. Tests for E. coli are even more specific to fecal sources, but again incur further costs for labor and time.

The non-fecal components of the coliforms, especially the Enterobacter and Citrobacter genera, are of limited use in indicating fecal contamination

but do indicate prior contact with soil or plant material. In addition, these genera are capable of regrowth in nutrient-rich natural waters or where surfaces are available for growth.

Fecal streptococci (FS) provide another common indicator of fecal contamination (Clausen et al. 1977). Although all FS belong to the single genus Streptococcus, there are again fecal and non-fecal components. Enterococci and S. faecalis are more specific to fecal sources than the non-enterococcal streptococci. FS and particularly the enterococci are often considered to be able to survive longer in natural waters than either TC or FC. Chamberlin (1982) compared FS (combining TC, FC, and E. coli results) decay rates in cases where the rates were measured in the same experiments and found a high correlation ($r^2 = 0.80$) between the logarithm of the respective rates. In addition, the relationship between the logarithms of the rates had a slope estimated by linear regression that was not significantly different ($p = 0.05$) from 1.0. The intercept was marginally distinguishable from 0.0 at $p = 0.01$ and was estimated as -0.31. This suggests that coliform decay rates were generally twice as large as FS decay rates but that the rates changed generally by equal amounts from one environment to another. According to Geldreich and Kenner (1969), the FC/FS ratio is useful in discriminating between recent human versus animal fecal contamination. If the ratio exceeds approximately 1 (although 4 is often cited as the cut-off value), the source is presumptively human fecal material while if the ratio is less than 1, the source is assumed to be animal feces. But as Dutka and Kwan (1980) have observed, the ratio can change dramatically once the material enters natural waters. They monitored changes from an initial ratio of 2.7 to a low of 0.07 and a high of 22.5 in a single experimental run.

Other proposed fecal indicators have been discussed by Olivieri (1983) and include Clostridium perfringens, yeasts, and RNA coliphages. None of these novel indicators has become generally accepted.

Beyond the selections of a particular indicator or set of indicators, recent work has shown the importance of sublethal stress or injury of influencing observed concentrations in decay studies (Rose et al. 1975;

Bissonette et al. 1977). Rhodes and Kator (1982) and Kapuscinski and Mitchell (1981) have, among others, substantiated these results and have suggested particular mechanisms of injury. Consequently, the decision to use or not use a resuscitation step (e.g., incubation at 35°C in less selective medium for two hours) can have a major impact on the observed decay rates.

8.3 MODELING COLIFORMS

Modeling of coliforms is done for one main reason--establishing the level of fecal and/or soil pollution and potential pathogen contamination. The usual approach is simply to simulate disappearance and to estimate coliform levels as a function of initial loading and the disappearance rate which, in turn, is a function of time or distance of travel from the source and of environmental conditions such as temperatures, salinity, and light intensity.

8.3.1 Factors Affecting Disappearance Rates

Upon discharge to a water body, environmental conditions determine the extent to which coliform regrowth and death occur. Fecal coliforms and streptococci are occasionally observed to increase in numbers, although this may be due to disaggregation of clumps of organisms. Non-fecal organisms may, in fact, increase in numbers in natural waters where conditions are adequate (Lombardo, 1972; Mitchell and Chamberlin, 1978).

Factors can be conveniently classified into three categories: physical, physicochemical, and biochemical-biological. However, note that synergisms (e.g., osmotic effects and photo-oxidation) and interferences (e.g., sedimentation versus photo-oxidation) may exist. Kapuscinski and Mitchell (1980) and Bitton (1980) have reviewed factors that govern virus inactivation in natural waters and present essentially a parallel list to the one given below.

Physical factors that can affect the coliform population in natural waters, resulting in an apparent increase or decrease in the coliform disappearance rate include:

- Photo-oxidation
- Adsorption
- Flocculation
- Coagulation
- Sedimentation
- Temperature

Physicochemical factors include

- Osmotic effects
- pH
- Chemical toxicity
- Redox potential

Biochemical-biological factors include:

- Nutrient levels
- Presence of organic substances
- Predators
- Bacteriophages (viruses)
- Algae
- Presence of fecal matter

8.3.1.1 Physical Factors

Chamberlin and Mitchell (1978) have noted that, although many data have been collected on coliform disappearance rates, mechanisms mediating the rates have historically been poorly understood. According to Chamberlin and Mitchell, however, light is one of the most important factors. They observe that it is difficult to show statistically significant relationships between coliform disappearance rates and many factors usually hypothesized as

influencing those rates. In contrast, significant relationships between light intensity and coliform disappearance rates can be demonstrated. Chamberlin and Mitchell (1978) have shown that field data statistically support the photo-oxidation model (to be discussed), and data presented by Wallis et al. (1977) also appear to implicate incident light. Subsequent work by Sieracki (1980), Kapuscinski and Mitchell (1983), Lantrip (1983), and others has demonstrated that viruses and enteric bacterial pathogens are also sensitive to light but that viruses are generally less sensitive than coliforms.

Chamberlin and Mitchell (1978) have elaborated upon possible mechanisms by which light may increase coliform disappearance rates. They point out that although in many cases of light induced mortality, one or more photosensitizing substances are involved, visible and near ultraviolet (UV) light can kill E. coli in the absence of exogenous photosensitizers. Grigsby and Calkins (1980) have confirmed the significance of the near UV.

One suggested mechanism is that light quanta drive some exogenous or endogenous chromophore to an electronically excited state. The chromophore, in the process of returning to the ground state, transfers its absorbed light energy to another substance to form superoxides (0_2^*), which, in turn, cause damage to cellular components. Alternatively, the activated chromophore may cause damage directly, without the agency of a superoxygenated intermediate. Kapuscinski and Mitchell (1981) observed that injury to the catalase system is the most likely site of damage in E. coli and that the damage can be repaired if the coliforms are transferred to an appropriate recovery medium. Krinsky (1977) has, on the other hand, argued that the "cause of death" may be division-inhibition, mutation, and/or membrane damage.

Substances within coliform and other bacterial cells are effective, near-UV chromophores, including ubiquinones, porphyrins, and tryptophan (Krinsky 1977). Exogenous sources of photo-oxidants include algal pigments, lignins, and humic and fulvic acids. More highly colored and turbid waters have been shown to produce peroxides, singlet oxygen, and hydroxide radicals

at greater rates than well waters (for example, Zepp et al. 1977; Cooper and Zika, 1983).

Adsorption, coagulation, and flocculation may affect coliform disappearance rates, although few quantitative data are available. Adsorption refers to the attachment of coliform organisms to suspended particles. Coagulation refers to the coalescence of bacteria into clumps, and flocculation refers to the formation of soft, loose aggregates incorporating much water.

According to Mitchell and Chamberlin (1978), early investigations by several workers have demonstrated that clays tend to adsorb coliforms more than do silts or sands. This is, of course, commonly the case with sorbed substances. As Mitchell and Chamberlin point out, the nature and stability of coliform aggregates incorporating other particulate matter depends to a very large extent upon the physicochemical nature of the particles. Gannon et al. (1983) found that 90 to 96 percent of the coliforms entering a lake from upland watersheds were associated with 0.45 to 5 μm particles.

Sedimentation involves the settling out of bacterial particles and aggregates. The rate of disappearance may be materially influenced by aggregation and sedimentation, but the magnitude and direction of the change in rate is not well understood. The mechanism of apparent disappearance due to sedimentation is actually simple removal of cells from the water column--that is, transfer of matter from one physical compartment (the water column) to another (the benthos). However simple, sedimentation may sometimes be the predominant mechanism of removal as Gannon et al. (1983) demonstrated in a field study of coliform survival in a lake. Accordingly, modeling coliform disappearance in the water column may give misleading results, particularly where shellfish are harvested for human consumption. Reduction in coliform levels in the water column may simply mean increased numbers in the benthos.

Temperature influences most, if not all, of the the other factors. Bitton (1980) and Lantrip (1983) argue that temperature is the single most important modifier of decay rates, especially in freshwater and in the dark.

8.3.1.2 Physicochemical Factors

Mitchell and Chamberlin (1978) report that physicochemical factors may have significant effects on disappearance rates. Survival rates of E. coli, for example, are inversely proportional to salinity both in natural seawater (due to osmotic and other effects) and in artificial salt solutions. In addition, Sieracki (1980) has observed a synergism with light effects. Work by Zafiriou and True (1979) suggest that nitrite photolysis in seawater may be a partial cause. In general, E. coli have been found to survive longer in lower pH salt solutions (pH < 8) than under alkaline conditions.

Heavy metal toxicity toward microorganisms has been known since the late nineteenth century. A great number of studies have been done on the "oliogodynamic action" of silver and copper salts. According to Mitchell and Chamberlin (1978), heavy metals have been implicated as important mediators of E. coli disappearance rates, and the heavy metal effects may be reduced by addition of chelating agents. Redox potential, through its effect on heavy metals solubilities, also affects disappearance rates. In addition to this, redox may influence disappearance rates in other ways, although data on this are not extensive.

Finally, Kott (1982) has presented evidence that when coliforms undergo the transition from the generally low oxygen environment of sewage to the higher oxygen levels found in seawater, the oxygen shock promotes rapid decay.

8.3.1.3 Biochemical and Biological Factors

Nutrient concentrations may be important in determining disappearance rates under some conditions. In many nutrient studies, the apparent impact of nutrient addition to the coliform culture is due to chelation of heavy metal ions (Mitchell and Chamberlin, 1978). Thus, the apparent decrease in disappearance rate in many cases may not be due to the additional nutrient, but instead to reduce toxicity of the culture medium. Mitchell and Chamberlin (1978) cite the work of Jones (1964) who found that E. coli would

not grow at 37°C in either filter-sterilized natural or synthetic seawater supplemented with glucose, ammonium chloride, and potassium phosphate. Inhibition could be reversed by autoclaving, by addition of very small amount of organic matter, or by addition of metal chelating or complexing agents. Jones demonstrated that two levels of toxic metals would produce the inhibitory effect, and concluded that the apparent influence on disappearance rates was due to naturally occurring trace heavy metals in solution. Furthermore, as Mitchell and Chamberlin (1978) note, other researchers have obtained experimental results implicating heavy metals, and their chelation upon addition of nutrients, in apparent changes in disappearance rates.

In some situations, it appears that nutrient levels influence disappearance rates in ways unrelated to toxic metals availability. Savage and Hanes (1971) and Chamberlin (1977), for example, have reported growth-limiting effects of available BOD or organic matter. Recent work by Dutka and Kwan (1983) indicates that after-growth and long-term persistence is particularly sensitive to nutrient levels. Further, it is possible that the level of nutrients affects coliform predators, thereby influencing rates of grazing on coliforms. Mitchell and Chamberlin (1978) report that predators in natural waters may be significant in reducing coliform populations given high predator levels. They cite three groups of micro-organisms which may be importantly in seawater. These are cell wall-lytic marine bacteria, certain marine amoebae, and marine bacterial parasites similar to Bdellovibrio bacteriovorus. Experiments performed by a number of researchers have implicated predators in disappearance of coliforms in both fresh and seawater, although Lantrip (1983) did not observe a significant predator influence in chamber experiments using freshwater. Bacteriophages, on the other hand, are apparently of minor importance, despite their demonstrated presence in sea water. The relative insignificance of phages, according to Mitchell and Chamberlin (1978), stems from their ineffectiveness in killing E. coli where the bacterial cells are not actively growing and multiplying, and the rapid inactivation of the phages by seawater.

Some forms of phytoplankton produce antibacterial agents which are excreted into the water column. These substances are heat-liable macromolecules, and according to Mitchell and Chamberlin (1978) at least one, a chlorophyllide, is active only if the system is illuminated. The fact that at least one antibacterial agent is activated by light suggests that algae may play a mediating role in the effect of light on disappearance rates. Other mechanisms of algal anti-coliform activity have been suggested. One is that during algal blooms, other organisms which prey on both algae and coliforms may also increase in numbers.

Table 8-1 is a summary of factors influencing coliform disappearance rates.

8.3.2 Modeling Formulations

Traditionally, coliform modeling has only taken into account disappearance, and a simple first-order kinetics approach has been used (Baca and Arnett,1976; Chen, et al., 1975; Chen et al., 1976; U.S. Army Corps of Engineers,1974; Chen and Orlob, 1975; Lombardo, 1973; Lombardo, 1972; Smith, 1978; Anderson et al. 1976; Huber, et al. 1972; Hydroscience, 1971; Chen and Wells, 1975; Tetra Tech, 1976b):

$$\frac{dC}{dt} = -kC \tag{8-1}$$

or

$$C_t = C_o e^{-kt} \tag{8-2}$$

where C = coliform concentration, MPN or count/100 ml
C_o = initial coliform concentration, MPN or count/100 ml
C_t = coliform concentration at time t, MPN or count/100 ml
k = disappearance rate constant, day^{-1} or hr^{-1}
t = exposure time, days or hours.

A summarized listing of values for k is presented in Table 8-2. The data summarize 30 studies of rates measured in situ. Table 8-3 shows values for k from a number of modeling studies. The median rate for the in situ studies is .04 hr^{-1} with 60 percent of the values less than .05 hr^{-1} and 90 percent less than .22 hr^{-1}.

TABLE 8-1. FACTORS AFFECTING COLIFORM DISAPPEARANCE RATES

Factor	Effects
Sedimentation	Important with regard to water column coliform levels, particularly where untreated or primary sewage effluent or stormwater is involved, and under low vertical mixing conditions. May adversely affect shellfish beds by depositing coliforms and fecal matter into benthos.
Temperature	Probably the most generally influential factor modifying all other factors.
Adsorption, Coagulation, Flocculation	Inconclusive.
Solar Radiation	Important; high levels may cause more than 10-fold increase in disappearance rate over corresponding rate in the dark in seawater. Rates also materially increased in freshwater.
Nutrient Deficiencies	Appear to accelerate disappearance. Numerous studies have indicated that increasing nutrient levels of seawater decrease disappearance rates.
Predation	Several species of organisms (bacteria, amoebae) have been shown to attack and destroy E. coli. Importance of predation depends strongly on the concentration of predators.
Bacteriophages	Apparently not important.
Algae	Bactericidal substances are known to be produced by planktonic algae. Substances may be photoactivators, mediating the influence of light on coliform disappearance. This might account for variability of data in studies of light-induced disappearance rates. Another hypothesis is that algal predators with blooms concomitant with algal blooms may produce substances toxic to E. coli or may prey upon them.
Bacterial Toxins	Antibiotic substances produced by indigenous bacteria are not believed important in coliform disappearance.
Physiochemical Factors	Apparently, pH, heavy metals content, and the presence of organic chelating substances mediate coliform disappearance rates. Importance of each, however, is poorly understood at present. Salinity strongly enhances the effect of solar radiation.

A number of researchers have determined values for the half saturation constant (K_s) for E. coli growth, using the Monod expression:

TABLE 8-2. COLIFORM BACTERIA FRESHWATER DISAPPEARANCE RATES MEASURED IN SITU (AFTER MITCHELL AND CHAMBERLIN, 1978)

System	Temperature	k(1/hr)	Reference
Ohio River	Summer (20°C) Winter (5°C	0.049 0.045	Frost and Streeter (1924)
Upper Illinois River	June-September October and May December-March April and November	0.085 0.105 0.024 0.043	Hoskins et al. (1927)
Lower Illinois River	June-September October and May December-March April and November	0.085 0.037 0.026 0.029	Hoskins et al. (1927)
"Shallow Turbulent Stream"		0.63	Kittrell and Kochtitzky (1947)
Missouri River	Winter	0.020	Kittrell and Furfari (1963)
Tennessee River (Knoxville)	Summer	0.043	Kittrell and Furfari (1963)
Tennessee River (Chattanooga)	Summer	0.005	Kittrell and Furfari (1963)
Sacramento River	Summer	0.072	Kittrell and Furfari (1963)
Cumberland River	Summer	0.23	Kittrell and Furfari (1963)
Glatt River		1.1	Wasser et al. (1934)
Groundwater Stream	10°C	0.021	Wuhrmann (1972)
Leaf River (Mississippi)		0.017	Mahloch (1974)
Wastewater Lagoon	7.9-25.5°C	0.00833-0.029	Klock (1971)
Maturation Ponds		0.083	Marais (1974)
	19°C	0.07	
Oxidation Ponds	"T"	$k = 0.108 \cdot (1.19)^{T-20}$	Marais (1974)
Lake Michigan	10-17°C	0.36	Zanoni et al. (1978)
Ford Lake (Ypsilanti, Michigan)	August	0.4	Gannon et al. (1983)
DeGray Reservoir (Arkansas)	October 1976 (15°C) March 1977 (10°C) June 1977 (20°C)	0.052 0.109 and 0.016 0.138 and 0.114	Thornton et al. (1980)

Modified from Mitchell and Chamberlin (1978).

$$\mu = \frac{\mu_M S}{K_s + S} \tag{8-3}$$

where μ = growth rate at nutrient concentrations, day^{-1}

S = concentration of growth limiting nutrient, mg/l

μ_M = maximum growth rate, day^{-1}

K_s = half-saturation constant producing the half-maximal value of μ, mg/l

Table 8-4 shows some reported values for K_s.

However, Gaudy et al. (1971) have shown that the Monod expression (Equation 8-3) is not adequate to describe transient coliform growth behavior. Accordingly, as suggested by Mitchell and Chamberlin (1978), the utility of the K_s value is in evaluating which nutrient may be growth limiting rather than in estimating a growth rate, μ.

TABLE 8-3. VALUES FOR COLIFORM-SPECIFIC DISAPPEARANCE RATES USED IN SEVERAL MODELING STUDIES

System	k @20°C, 1/hr	Reference
North Fork Kings River, California	.042	Chen, et al. (1976)
Various Streams	.0004-.146	Baca and Arnett (1976)
Lake Ontario	.02-.083	U.S. Army Corps of Engineers (1974)
Lake Washington	.02	Chen and Orlob (1975)
Various Streams	.042-.125	Hydroscience (1971)
Boise River, Idaho	.02	Chen and Wells (1975)
San Francisco Bay Estuary	.02	Chen (1970)
Long Island Estuaries, New York	.02-.333	Tetra Tech (1976)

TABLE 8-4. NUTRIENT K_s VALUES FOR ESCHERICHIA COLI (AFTER MITCHELL AND CHAMBERLIN, 1978)

Nutrient	Medium	T °C	K_s Micromoles	Remarks	Reference
Glucose	minimal medium		22.		Monod (1942)
			19.4		
			41.7		Moser (1958)
		30	405.		Schultz and Lipe (1964)
		30	550.		
	seawater	20	44.		Jannasch (1968)
Lactose	seawater	20	50.		Jannasch (1968)
	minimal medium		111.		Monod (1942)
Phosphate	minimal medium		0.7	uptake study	Medveczky and Rosenberg (1970)
	minimal medium	30	17.35		Shehata and Marr (1971)
Glucose		30	0.378		Shehata and Marr (1971)

Work on coliforms in the Ohio River by Frost and Streeter (1924) revealed that the log decay rate for coliforms is nonlinear with time. Accordingly, use of a simple decay expression such as Equation (8-1) with a single value of k is only an approximation to the actual disappearance process. Such an approach must, to some extent as a function of time, overestimate and/or underestimate dC/dt. One approach to solving the problem of a time-variable decay rate is to decompose the death curve into two components, each having its own decay rate (Velz, 1970). This approach is predicated upon typical death rate curves such as those shown in Figure 8-2. These curves have essentially two regions, each with its own characteristic slope, and the coliform concentration as a function of time may be defined as:

$$C_t = C_o e^{-kt} + C_o' e^{-k't} \tag{8-4}$$

where C_t = coliform concentration at time t, MPN or count/100 ml

C_o, C_o' = concentrations of each of the two hypothetical organism types, MPN or count/100 ml

k, k' = decay rates for the two organism types, day^{-1}

Table 8-5 shows values for C_o, C_o', k, and k' for E. coli as estimated by Phelps (1944).

Lombardo (1972), in an effort to more meaningfully model coliforms, has formulated the dynamics of the coliform population plus streptococci with three separate first-order expressions:

$$C_{T_t} = C_{T_o} e^{-k_t t} \tag{8-5}$$

$$C_{F_t} = C_{F_o} e^{-k_f t} \tag{8-6}$$

$$C_{S_t} = C_{S_o} e^{-k_s t} \tag{8-7}$$

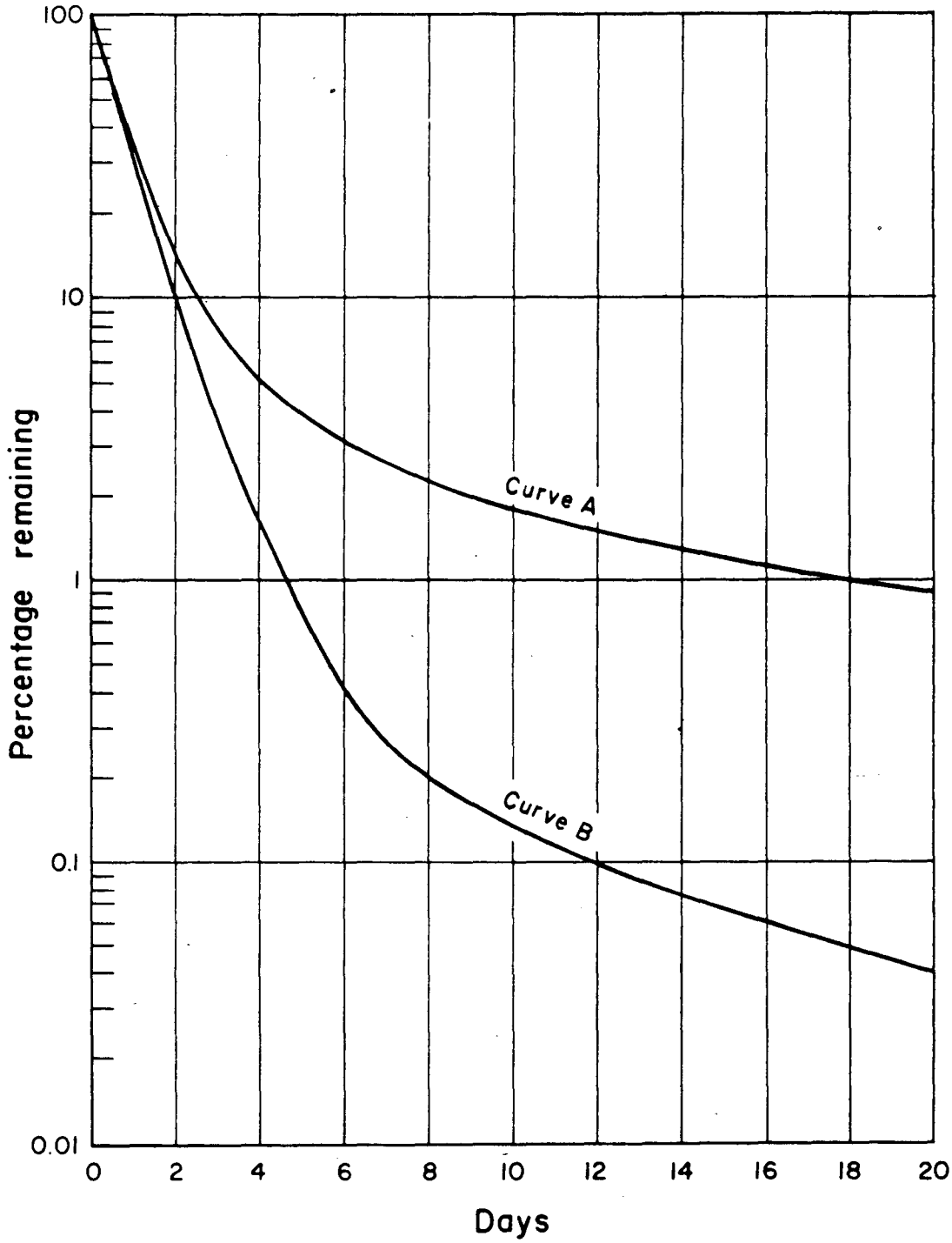

Figure 8-2. Typical mortality curves for coliforms as a function of time. Curve A is for cool weather while curve B represents warm weather decay (redrawn from Velz, 1970).

TABLE 8-5. VALUES OF Co, C', k, AND k' FROM THE OHIO RIVER PHELPS (1944)

Parameter	Warm Weather	Cold Weather
C_o (percent)	99.51	97
k (1/day)	1.075	1.165
Half-life (day)	.64	.59
C_o' (percent)	.49	3.0
k' (1/day)	.1338	.0599
Half-life (day)	5.16	11.5

where C_t = organism concentration at time t, MPN or count/100 ml
C_o = organism concentration at time zero, MPN or count/100 ml

Table 8-6 provides data for k_T, k_S and k_F as summarized from Lombardo (1972).

As discussed earlier, recent studies have suggested that incident light levels strongly affect coliform disappearance rates. Chamberlin and Mitchell (1978) have defined a light level-dependent disappearance rate coefficient as

$$k' = k_\ell \ell_o e^{-\alpha z} \tag{8-8}$$

where k' = the light dependent coliform disappearance rate, 1/hr.
k_ℓ = proportionality constant for the specific organism, cm^2/cal
ℓ_o = incident light energy at the surface, cal/cm^2-hr
α = light attenuation coefficient per unit depth
z = depth in units consistent with α.

TABLE 8-6. SUMMARY OF DECAY RATES OF TC, FC, AND FS, REPORTED BY LOMBARDO (1972)

Indicator	n	Median k (1/hr)	Minimum k (1/hr)	Maximum k (1/hr)
TC	16	0.038	0.010	0.105
FC	13	0.048	0.008	0.130
FS	5	0.007	0.002	0.063

Then, incorporating the vertical dispersion of bacterial cells,

$$\frac{\partial C(z,t)}{\partial t} - V_z \frac{\partial C(z,t)}{\partial z} = E_z \frac{\partial^2 C(z,t)}{\partial_z^2} - k'C(z,t) \qquad (8\text{-}9)$$

where E_z = the vertical dispersion coefficient, cm^2/hr
V_z = the vertical settling velocity, cm/hr

An expression of this kind is useful where the vertical distribution of coliforms is nonuniform over depth and where disappearance is assumed to be solely a function of light intensity. Chamberlin (1977) has presented solutions of Equation 8-2 for various ranges of V_z, E_z, k_ℓ, α, and H (depth of water column) using dimensionless variables.

According to an independent development by Mancini (1978) and Chamberlin and Mitchell (1978), if the bacterial cells can be assumed uniform over depth (i.e., the water column is vertically mixed), then the depth-averaged light intensity and the depth-averaged decay rate, respectively, may be computed:

$$\bar{\ell} = \ell_0 \left(\frac{1-e^{-\alpha H}}{\alpha H} \right) \qquad (8\text{-}10)$$

and

$$\bar{k} = k_{\ell}\bar{\ell} \tag{8-11}$$

where $\bar{\ell}$ = the depth-averaged light intensity, cal/cm^2/hr

H = the depth of the water column in units consistent with α

$\bar{k}$ = the depth-averaged light-dependent disappearance rate, hr^{-1}

The depth-averaged, light-dependent, disappearance rate, $\bar{k}$, may be used in the first order disappearance expression for a vertically mixed water body so that:

$$\frac{dC}{dt} = -\bar{k}C \tag{8-12}$$

It is clear that the use of such a model (Equation (8-12)) might be further refined by computing $\bar{k}$ using a sinusoidal function to estimate light levels and incorporating the influence of such factors as latitude, day of the year, time of day, and atmospheric conditions including cloud cover and dust effects. Table 8-7 presents some values for k_{ℓ}.

Since coliforms and other indicators are known to decay in the dark, Mancini (1978) and Lantrip (1983) have developed decay rate models combining light-dependent and light-independent (i.e., dark) components. The model proposed by Mancini expresses k' as a function of temperature, percent seawater, and depth-averaged light intensity:

$$k' = \frac{(0.8 + 0.006(\%SW))}{24} 1.07^{T-20} + k_{\ell}\bar{\ell} \tag{8-13}$$

where T = water temperature in ^{o}C.

The model coefficients were estimated based on a combination of laboratory, chamber, and field studies. Note that k_{ℓ} is not expressed as a function of either salinity or temperature.

TABLE 8-7. COMPARISON OF k_ℓ ESTIMATES BASED ON CHAMBERLIN AND MITCHELL (1978) WITH ADDITIONAL VALUES

Organism	Study	k_ℓ (cm^2/cal)	Data Source
Coliform Group	14 field studies		Gameson and Gould (1975)
	Mean	0.481	
	5 percentile	0.163	
	95 percentile	1.25	
	24 field studies		Foxworthy and Kneeling (1969)
	Mean	0.168	
	5 percentile	0.068	
	95 percentile	0.352	
	61 laboratory studies		Gameson and Gould (1975)
	Mean	0.136	
	5 percentile	0.062	
	95 percentile	0.244	
	Estimated from diurnal field experiments in SW	0.18 at I = 1.0 cal/cm^2hr 0.07 at I = 0.1 cal/cm^2hr	Bellair *et al.* (1977)
Fecal Coliform	Estimated from compilation of field and laboratory studies, both SW and FW.	0.042	Mancini (1978)
Total Coliforms	22 chamber studies in FW		Lantrip (1982)
	Mean	0.004	
	Minimum	0.000	
	Maximum	0.013	
Fecal Coliforms	22 chamber studies in FW		Lantrip 91982)
	Mean	0.005	
	Minimum	0.000	
	Maximum	0.011	
Escherichia coli	4 field studies		Gameson and Gould (1975)
	Mean	0.362	
	Minimum	0.321	
	Maximum	0.385	
	4 laboratory studies		Gameson and Gould (1975)
	Mean	0.354	
Seratia marcescens	4 field studies		Gameson and Gould (1975)
	Mean	0.192	
	Minimum	0.093	
	Maximum	0.360	
Bacillus subtilis var. niger	1 laboratory study	0.002	Gameson and Gould (1975)
Fecal Streptococci	3 laboratory studies		Gameson and Gould (1975)
	Minimum	0.048	
	Maximum	0.123	
	3 field studies	0.000	Gameson and Gould (1975)
	1 field study	0.007	
	12 field studies, initial rates		Foxworthy and Kneeling (1969)
	Mean	0.091	
	Minimum	0.004	
	Maximum	0.184	
	23 chamber studies in FW		Lantrip (1982)
	Mean	0.008	
	Minimum	0.001	
	Maximum	0.028	
Salmonella typhimurium	2 laboratory studies	1.48 6.40	Eisenstark (1970)

Lantrip (1983) developed a set of temperature and light-dependent models based on a series of chamber studies conducted in freshwater. Separate models were determined for TC, FC, and FS. He used nonlinear regression methods to determine the "best" coefficient values and reported both the "best" estimates and associated standard deviations. The three models have the same form:

$$k' = k_{d,20}\theta^{T-20} + k_{\ell}\bar{\ell} \tag{8-14}$$

where $k_{d,20}$ = "dark" decay rate at 20°C (1/hr)

θ = temperature correction term

The coefficients for the three models are summarized in Table 8-8. Note that Lantrip also considers k_{ℓ} to be independent of temperature.

Finally, many investigators have noted an initially very low decay rate in laboratory and field studies. For example, see Mitchell and Chamberlin (1978), Mancini (1978), and others. Kapuscinski and Mitchell (1983) and Severin et al. (1978) have argued that this "shoulder" in the decay curve is not the consequence of growth or particle breakup but is instead due to the nature of the photo-oxidation process. Severin et al. present two mechanistic models that would produce a "shoulder":

- Multi-target model based on assumption that several targets or sites in the organism must be hit before the organism will be killed:

$$C_t = C_o\left(1 - \left[(1-e^{-k_{\ell}\cdot\ell\cdot t})^{j}\right]\right) \tag{8-15}$$

where j = number of critical sites,

- A series-event model that assumes that the same target must be hit a series of times before inactivation occurs:

$$C_t = C_o e^{-k_\ell \cdot \ell \cdot t} \left(\sum_{i=0}^{n} \frac{(k_\ell \cdot \ell \cdot t)^i}{i!} \right) \qquad (8\text{-}16)$$

where n = event threshold for inactivation

Such models are still novel in engineering applications and have not yet been incorporated into water quality models.

8.3.3 Methods of Measurement

Estimates of the coliform disappearance rate, k, may be obtained in a number of ways in the laboratory chamber studies, or, preferably, in situ. For laboratory estimates, samples of effluent may be taken along with samples of receiving water. Then, under controlled conditions of light, temperature, and dilution, the time rate of disappearance may be determined for various combinations of conditions. Unfortunately "bottle effects" often distort laboratory results as shown by Zanoni and Fleissner (1982),

TABLE 8-8. PARAMETER ESTIMATES FOR LANTRIP (1983) MULTI-FACTOR DECAY MODELS

Indicator		n	Standard Error Regression	$k_{d,20}$ (1/hr)	θ	k_ℓ (cm^2/cal)
TC	Estimate	38	0.0151	0.0301	1.0893	0.0022
	Standard Error			0.0044	0.0208	0.00065
FC	Estimate	41	0.020	0.0305	1.0978	0.00377
	Standard Error			0.0057	0.0280	0.00081
FS	Estimate	38	0.0183	0.0294	1.0859	0.00502
	Standard Error			0.0050	0.0234	0.00076

since enteric bacterial growth is promoted by availability of surfaces for attachment.

In situ k values can be determined whether the flow regime is well defined or not, although there are inherent errors involved in each method. Where there are no flow regime data, or where flows are of a transient nature, a commonly used method (e.g., Zanoni et al. 1978 and Gannon et al. 1983 provide recent examples) is to add a slug of a conservative tracer substance (a dye, rare element, or radioisotope) to the steady-state discharge. Then the discharge plume is sampled, dilution is estimated from concentrations of tracer, and the dilution corrected coliform counts permit k to be estimated. It should be recognized that this technique may give misleading results where the dilution of the tracer is due to mixing with water heavily contaminated with the same discharge. Since the tracer had been introduced as a slug, there is no way to know how much of the surviving coliforms originated in the tracer-dosed effluent and how much came from pre-dosing or post-dosing effluent. However, where the flow regime is sufficiently predictable and stable to assure that dilution occurs essentially with ambient water, and where coliform levels in the ambient water are known, this should not be a problem.

Another method, which is particularly useful where discharge is to a channel, is as follows. First, a base sampling site is established below the discharge where the water column is fully mixed normal to the direction of flow. Then samples are taken at the base site and at several points downstream. Based upon known velocities and the change in coliform concentration with distance (time), k values may be estimated. Clearly, errors will be introduced to the extent that there is incomplete lateral mixing of the stream, nonuniform longitudinal velocities laterally and vertically across the channel, and unknown inflows causing dilution or introducing additional coliforms between sampling sites.

Also, sampling can be done so that the same "parcel" or water is sampled, in case the discharge is not at steady-state. For example, if the first sampling site is one mile below the base site, and the channel flow

has a mean velocity of 2 ft per second, then the first sampling site should be sampled:

$$\frac{5280 \text{ ft}}{\text{mile}} \times \frac{1 \text{ second}}{2 \text{ ft}} \times \frac{1 \text{ hr}}{3600 \text{ seconds}} = .73 \text{ hr}$$

or 44 minutes after sampling at the base site. Clearly, however, this does not account for dispersion, and the 44 minutes is an average figure corresponding to the peak loading. Where possible, dye studies or other techniques should be used to characterize stream dispersion at the sampling location. Then, by integrating under the curve, total surviving coliforms can be estimated. If, on the other hand, discharge and stream conditions are clearly at steady-state, sampling times are of no consequence.

Equation (8-17) may be used to estimate k where a slug dose of tracer has been introduced into the discharge (assuming first-order decay):

$$k = -\ln (C_t F_o / F_t C_o)/t \qquad (8\text{-}17)$$

where F_o = discharge concentration of tracer, mg/l
F_t = observed concentration of tracer, mg/l

If no tracer is used and conditions approximating plug flow exist, then:

$$k = -\ln(C_t/C_o)/t \qquad (8\text{-}18)$$

where C_o = concentration of coliforms at the base sampling site, MPN or count/100 ml

Regardless of the technique used for estimating k, it is important to concurrently quantify, to the extent possible, those variables which influence k. For example, light levels should be measured or at least estimated over the period for which k is estimated. If this is not done, and if the effects of the important parameters are not taken into account in modeling coliforms, serious errors will result. Table 8-9 shows how serious such errors can be. The data show T-90 values for coliforms as a function

TABLE 8-9. EXPERIMENTAL HOURLY T-90 VALUES
(AFTER WALLIS, ET AL., 1977)

Time of Day	T-90 (hours)	Time of Day	T-90 (hours)	Time of Day	T-90 (hours)
0100	40	0900	3.2	1700	5.3
0200	40	1000	2.5	1800	6.7
0300	40	1100	2.3	1900	8.5
0400	40	1200	2.5	2000	11
0500	40	1300	2.9	2100	14
0600	19	1400	3.3	2200	20
0700	8.0	1500	3.9	2300	27
0800	4.6	1600	4.6	2400	34

of incident light. T-90 values are the times required for 90 percent mortality. The associated k values are .058 hr^{-1} in the dark and .1 hr^{-1} at midday. It is clear that estimating a single value for a k could result in greater than order-of-magnitude errors.

8.4 SUMMARY

The coliform group is of interest as an index of potential pathogen contamination in surface waters and has become one of the more commonly modeled water quality parameters. Modeling coliforms usually involves the use of a simple first-order decay expression to describe disappearance. Since regrowth is generally neglected, no growth terms are normally included in the model.

The disappearance rate, k, is a function of a number of variables, the effects of all of which are not well understood. It now appears that light (in the near-UV and visible range) is important as are a number of

physicochemical factors. Rates of disappearance are also sensitive to the salinity of the water which also affects the influence of light on disappearance rates.

8.5 REFERENCES

Anderson, D.R., J.A. Dracup, T.J. Fogarty, and R. Willis, 1976. Water Quality Modeling of Deep Reservoirs, Journal Water Pollution Control Federation, 48(1):134-146.

Baca, R.G. and R.C. Arnett, 1976. A Limnological Model for Eutrophic Lakes and Impoundments. Battelle Pacific Northwest Laboratories, Richland, Washington.

Baross, J.A., F.J. Hanus, R.Y. Morita, 1975. Survival of Human Enteric and Other Sewage Microorganisms Under Simulated Deep-Sea Conditions, Appl. Microbiology, 30(2):309-318.

Bellair, J.T., G.A. Parr-Smith, I.G. Wallis, 1977. Significance of Diurnal Variations in Fecal Coliform disappearance Rates in the Design of Ocean Outfalls, JWPCF, 49:2022-2030.

Bissonette, G.K., J.J. Jezeski, G.A. McFeters, D.G. Stuart, 1977. Evaluation of Recovery Methods to Detect Coliforms in Water, Appl. and Environ. Microbiology, 33:590-595.

Bitton, G., 1980. Introduction to Environmental Virology, John Wiley & Sons, New York, 326 pp.

CDWR (California Department of Water Resources, Sacramento), 1962. Sacramento River Water Pollution Survey, Appendix C: Public Health Aspects, Bulletin No. 111.

Chamberlin, C.E., 1977. A Model of Coliform Bacteria Survival in Seawater, Ph.D. Dissertation, Harvard University, Cambridge, Massachusetts.

Chamberlin, C. and R. Mitchell, 1978. A Decay Model for Enteric Bacteria in Natural Waters, R. Mitchell (ed.), Water Pollution Microbiology, Vol. 2, John Wiley and Sons, New York, pp. 325-348.

Chamberlin, C.E., 1982. Physical Influences on the Survival of Enteric Bacteria in Natural Waters, Symposium on the Survival of Pathogens in the Natural Environment, XIII International Congress of Microbiology, Boston, Massachusetts.

Chen, C.W., 1970. Concepts and Utilities of Ecological Model, ASCE, Journal of the Sanitary Engineering Division, 96, (SA5).

Chen, C.W. and G.T. Orlob, 1975. Ecological Simulation of Aquatic Environments, in Systems Analysis and Simulation in Ecology, Vol. 3,B. C Pattern (ed.), Academic Press, New York, N. Y. pp. 476-588.

Chen, C.W. and J. Wells, 1975. Boise River Water Quality-Ecological Model for Urban Planning Study, Tetra Tech technical report prepared for U.S. Army Engineering District, Walla Walla, Washington, Idaho Water Resources Board, and Idaho Dept. of Environmental and Community Services.

Chen, C. W., M. Lorenzen, D. J. Smith, 1975. A comprehensive Water Quality Ecological Model for Lake Ontario (final report), prepared for National Oceanic and Atmospheric Administration, Tetra Tech, Inc., Lafayette, CA.

Chen, C. W., D. J. Smith and S. S. Lee, 1976a. Documentation of Water Quality Models for the Helms Pumped Storage Project, Prepared for Pacific Gas and Electric Company, Tetra Tech, Inc., Lafayette, CA.

Chojnowski, K.J., J.L. Mancini, J.S. Jeris, 1979. Influence of Light on Coliform Mortality Rates in Fresh Water and Sea Water, JWPCF, 51(10):2538-2539.

Clausen, E.M., B.L. Green, W. Litsky, 1977. Fecal Streptococci: Indicators of Pollution, Bacterial Indicators/Health Hazards Associated with Water, ASTM STP 635, A.W. Hoadley and B.J. Dutka (eds.), American Society for Testing and Materials, pp. 247-264.

Cooper, W.J. and R.G. Zika, 1983. Photochemical Formation of Hydrogen Peroxide in Surface and Ground Waters Exposed to Sunlight, Science, 220:711-712.

Dufour, A.P., 1977. Escherichia coli: the Fecal Coliform, Bacterial Indicators/Health Hazards Associated with Water, ASTM STP 635, A.W. Hoadley and B.J. Dutka (eds.), American Society for Testing and Materials, pp. 48-58.

Dutka, B.J., K.K. Kwan, 1980. Bacterial disappearance and Stream Transport Studies, Water Research, 14:909-915.

Dutka, B.J., K.K. Kwan, 1983. Environmental Studies of Enteric Bacteria Longevity in Membrane Filter Chambers, JAWWA, 75:380-382.

Eisenstark, A., 1970. Mutation Res., 10 (1).

Evans, F.L., E.E. Goldreich, S.R. Weibel, and G.G. Robeck, 1968. Treatment of Urban Stormwater Runoff, Journal Water Pollution Control Federation, 40 (5):R162-170.

Foxworthy, J.E. and H.R. Kneeling, 1969. Eddy Diffusion and Bacterial Reduction in Waste Fields in the Ocean, Univ. Southern California, Los Angeles.

Frost, W.H. and H.W. Streeter, 1924. Public Health Bulletin 143, U.S. Public Health Service, Washington, D.C.

Gameson, A.L.H. and D.J. Gould, 1975. In Proc. Int. Symp. on Discharge of Sewage from Sea Outfalls, Pergamon Press, London.

Gannon, J.J., M.K. Busse, J.E. Schillinger, 1983. Fecal Coliform Disappearance in a River Impoundment, Water Research, 17(11):1595-1601.

Gaudy, A.F., Jr., A. Obayashi, and E.T. Gaudy, 1971. Control of Growth Rate by Initial Substrate Concentration at Values Below Maximum Rate, Applied Microbiology, 22:1041-1047.

Geldreich, E.E. and B.A. Kenner, 1969. Concepts in Fecal Streptococci in Stream Pollution, Journal Water Pollution Control Federation, 41 (8):R336-352.

Gordon, R.W., C.B. Fliermans, 1978. Survival and Viability of Escherichia coli in a Thermally Altered Reservoir, Water Research, 12:343-352.

Grigsby, P., J. Calkins, 1980. The Inactivation of a Natural Population of Coliform Bacteria by Sunlight, Photochemistry and Photobiology, 14:291-294.

Hendry, G.S., S. Janhurst, G. Horsnell, 1982. Some Effects of Pulp and Paper Wastewater on Microbiological Water Quality of a River, Water Research, 16:1291-1295.

Hoskins, J.K. C.C. Ruchhoft, and L.G. Williams, 1927. A Study of the Pollution and Natural Purification of the Illinois River. I. Surveys and Laboratory Studies, Public Health Bulletin No. 171.

Huber, W.C., D.R.F. Harleman, and P.J. Ryan, 1972. Temperature Prediction in Stratified Reservoirs, ASCE, Journal of the Hydraulics Division, 98 (HY4)

Hydroscience, Inc., 1971. Simplified Mathematical Modeling of Water Quality, EPA-Water Programs.

Jannasch, H.W., 1968. Competitive Elimination of Enterobacteriaceae from Seawater, Appl. Microbiol., 16:1616-1618.

Jones, G.E., 1964. Effect of Chelating Agents on the Growth of Escherichia coli in Seawater, J. Bact., 87:483-99.

Kay, D., A. McDonald, 1980. Reduction of Coliform Bacteria in Two Upland Reservoirs: The Significance of Distance Decay Relationships, Water Research, 14:305-318.

Kelch, W.J., J.S. Lee, 1978. Modeling Techniques for Estimating Fecal Coliforms in Estuaries, JWPCF, 50:862-868.

Kapuscinski, R.B. and R. Mitchell, 1980. Processes Controlling Virus Inactivation in Coastal Waters, Water Research, 14:363-371.

Kapuscinski, R.B. and R. Mitchell, 1981. Solar Radiation Induces Sublethal Injury in Escherichia coli in Seawater, Appl. and Env. Microbiology, 41:670-674.

Kapuscinski, R.B. and R. Mitchell, 1983. Sunlight-Induced Mortality of Viruses and Escherichia coli in Coastal Seawater, ES&T, 17(1):1-6.

Kittrell, F.W. and O.W. Kochtitzky, Jr., 1947. Natural Purification Characteristics of a Shallow Turbulent Stream, Sew. Works J., 19:1032-1048.

Kittrell, F.W. and S.A. Furfari, 1963. Observations of Coliform Bacteria in Streams, Journal Water Pollution Control Federation, 35:1361.

Klock, J.W., 1971. Survival of Coliform Bacteria in Wastewater Treatment Lagoons, Journal Water Pollution Control Federation, 43:2071-2083.

Kott, Y., 1982. Chemical Factors, Symposium on the Survival of Pathogens in the Natural Environment, XIII International Congress of Microbiology, Boston, Massachusetts.

Krinsky, N.I., 1977. Cellular Damage Initiated by Visible Light, in T.R.G. Gray, J.R. Postgate (eds.), The Survival of Vegetative Microbes, 26th Symposium of Society for General Microbiology, Cambridge University Press, Cambridge, United Kingdom, pp. 209-239.

Lantrip, B.M., 1983. The Decay of Enteric Bacteria in an Estuary, Doctor of Science Dissertation, School of Hygiene and Public Health, The Johns Hopkins University, Baltimore, Maryland.

Lombardo, P.S., 1972. Mathematical Model of Water Quality in Rivers and Impoundments, technical report, Hydrocomp, Inc.

Lombardo, P.S., 1973. Critical Review of Currently Available Water Quality Models, Hydrocomp, Inc., technical report, Contract No. 14-31-0001-3751.

Mahloch, J.L., 1974. Comparative Analysis of Modeling Techniques for Coliform Organisms in Streams, Appl. Microbiol., 27:340-345.

Mancini, J.L., 1978. Numerical Estimates of Coliform Mortality Rates Under Various Conditions, JWPCF, 50(11):2477-2484.

Marais, V.R., 1974. Faecal Bacterial Kinetics in Stabilization Ponds, Journal of the Environmental Engineering Division, ASCE, 100 (EEI):119-139.

McCambridge, J., T.A. McMeekin, 1981. Effect of Solar Radiation and Predacious Microorganisms on Survival of Fecal and Other Bacteria, Appl. and Env. Microbiology, 41(5):1083-1087.

McFeters, G.A., G.K. Bissonnette, J.J. Jezeski, C.A. Thomson, D.G. Stuart, 1974. Comparative Survival of Indicator Bacteria and Enteric Pathogens in Well Water, Appl. Microbiology, 27(5):823-829.

Medveczky, N. and H. Rosenberg, 1970. The Phosphate Binding Protein of Escherichia coli, Nature, 211:158-168.

Mitchell, R. and C. Chamberlin, 1978. Factors Affecting the Survival of Indicator Organisms in the Aquatic Environment, G. Berg (ed.). Indicators of Enteric Contamination in Natural Waters. Ann Arbor Press, Ann Arbor, Michigan.

Monod, J., 1942. Recherches sur la Croissance des Cultures Bacteriennes, Hermann, Paris.

Morita, R.Y., 1980. Microbial Life in the Deep Sea, Canadian Journal of Microbiology, 26(12):1375-1384.

Moser, H., 1958. Dynamics of Cell Populations, Publications of the Carnegie Instn., No. 614.

Olivieri, V.P., 1983. Measurement of Microbial Quality, Assessment of Microbiology and Turbidity Standards for Drinking Water, P.S. Berger and Y. Argaman (eds.), U.S. Environmental Protection Agency, EPA 570-9-83-001.

Phelps, E.B., 1944. Stream Sanitation, Wiley & Sons, New York, p. 209.

Rhodes, M.W., H.I. Kator, 1982. In Situ Survival of Enteric Bacteria in Estuarine Environments of Different Nutrient Characteristics, prepared for Office of Water Research and Technology, available through National Technical Information Service, Springfield, Virginia 22161, PB83-140038, pp. 47.

Rose, R.E., E.E. Geldreich, W. Litsky, 1975. Improved Membrane Filter Method for Fecal Coliform Analysis, Appl. Microbiology, 29:532-536.

Savage, H.P. and N.B. Hanes, 1971. Toxicity of Seawater to Coliform Bacteria, Journal of the Water Pollution Control Federation, 43:854-861.

Schulze, K.L. and R.S. Lipe, 1964. Relationship Between Substrate Concentration, Growth Rate, and Respiration Rate of E. coli in Continuous Culture, Archiv fur Mikrobiologie, 48:1-20.

Severin, B.F., M.T. Suidan, R.S. Engelbrecht, 1983. Kinetic Modeling of U.V. Disinfection of Water, Water Research, 17(11):1669-1678.

Shehata, T.E. and A.G. Marr, 1971. Effect of Nutrient Concentration on the Growth of Escherichia coli, J. Bact., 107:210-216.

Sieracki, M., 1980. The Effects of Short Exposures of Natural Sunlight on the Decay Rates of Enteric Bacteria and a Coliphage in a Simulated Sewage Outfall Microcosm, M.S. Thesis, University of Rhode Island, Kingston, Rhode Island, 62 pp.

Sobsey, M., B. Olson, 1983. Microbial Agents of Waterborne Disease, Assessment of Microbiology and Turbidity Standards for Drinking Water, P.S. Berger and Y. Argaman (eds.), U.S. Environmental Protection Agency, EPA 570-9-83-001.

Smith, D. J., 1978. Water Quality for River-Reservoir Systems (technical report). U.S. Army Corps of Engineers (Hydrologic Engineering Center), Davis, CA.

Tetra Tech, Inc. 1976. Estuary Water Quality Models, Long Island, New York-User's Guide, technical report prepared for Nassau Suffolk Regional Planning Board, Hauppauge, New York 11787.

Thornton, K.W., J.F. Nix, and J.D. Bragg. 1980. Coliforms and Water Quality: Use of Data in Project Design and Operation. Wat. Res. 16:86-92.

U.S. Environmental Protection Agency, 1984. May, 24, Federal Register, 49: 21988.

Velz, C. J., 1970. Applied Stream Sanitation, Wiley Interscience, New York, pp. 242-246.

Wallis, I.G., J.T. Bellair, and G.A. Parr-Smith, 1977. T-90 Values for Faecal Coliforms in Seawater, prepared for Symposium on Rate Constants, Coefficients, and Kinetics Formulations in Surface Water Modeling held in Concord, California, February 23-25.

Waser, E., W. Husmann, and G. Blochliger, 1934. Ber. Schweiz. Bot. Ges., 43:253.

Whipple, G.C., 1917. State Sanitation, Vols. I and II, Harvard University Press, Cambridge, Massachusetts.

Wuhrmann, K., 1972. Stream Purification, Chapter 6 in R. Mitchell (ed.), Water Pollution Microbiology, Wiley-Interscience, New York, 1972.

Zafiriou, O.C., M.B. True, 1979. Nitrite Photolysis in Seawater by Sunlight, Marine Chemistry, 8:9-32.

Zanoni, A.E., J.T. Fleissner, 1982. Indicator Bacteria Survival under Laboratory Conditions, JWPCF, 54(5):500-503.

Zanoni, A.E., W.J. Katz, H.H. Carter, R.C. Whaley, 1978. An In Situ Determination of the Disappearance of Coliforms in Lake Michigan, JWPCF, 50:321-330.

Zepp, R.G., N.L. Wolfe, G.L. Baughman, R.C. Hollis, 1977. Singlet Oxygen in Natural Waters, Nature 267:421-423.

☆U.S. GOVERNMENT PRINTING OFFICE:1989 -648-163/ 00347